In this Issue

Highlights from this issue of *A&R* | By Lara C. Pullen, PhD

Cytokine Response to Ustekinumab in Psoriatic Arthritis

Many immune cells release interleukin-17A (IL-17A) and IL-17F in response to IL-23. Researchers, therefore, anticipated that inhibition of IL-12/IL-23 with ustekinumab would result in the rapid reduction of IL-17A and IL-17F. p. 1660 In this issue, Siebert et al (p. 1660) evaluate the associations of C-reactive protein (CRP) and circulating Th17-associated cytokine levels with psoriatic arthritis (PsA) disease activity and therapeutic response to ustekinumab.

The investigators measured IL-17A, IL-17F, IL-23, and CRP concentrations in serum samples collected as part of the 2 PSUMMIT phase III studies of ustekinumab in PsA. They used generalized linear models and Pearson's product-moment correlation tests to perform post hoc analyses of the relationships of IL-17A, IL-17F, and CRP at baseline, week 4, and week 24 with baseline skin and joint disease activity and response to therapy. Baseline serum IL-23/IL-17 levels correlated with skin but not joint disease activity in patients with PsA. In addition, the authors found rapid reductions in IL-23/IL-17 following ustekinumab therapy.

While IL-17 and CRP levels reduced significantly following treatment with ustekinumab, neither baseline Th17-associated cytokine levels nor CRP level were predictive of therapeutic response to ustekinumab in the skin or joints. At 24 weeks, ustekinumab-treated patients who had a 75% improvement in the Psoriasis Area and Severity Index score or 20% improvement according to the American College of Rheumatology criteria had greater reductions in CRP level, but not IL-17A or IL-17F levels, than nonresponders. The authors state that the stronger correlation of IL-23/IL-17 levels with the severity of skin disease is consistent with the emerging evidence base suggesting tissue-specific variations in the pathologic drivers within PsA. They also note the implications of their data for clinical and drug development.

Machine Learning Classifier for Assigning Individual SSc Patients to Intrinsic Molecular Subsets

Only certain patients with systemic sclerosis (SSc) respond to any given immunosuppressive therapy. This selective response has created the need for a tool that classifies individual SSc patients into molecular subsets, which would improve both diagnostic accuracy and selective enrollment in clinical trials. p. 1701 The use of high-throughput gene expression profiling of tissue samples from patients with SSc has allowed the identification of 4 "intrinsic" gene expression subsets: inflammatory, fibroproliferative, normal-like, and limited. Unfortunately, this gene expression profiling requires agglomerative clustering of many samples, and therefore the need still exists for a method to assign individual patients to a molecular subset.

In this issue, Franks et al (p. 1701) introduce a novel machine learning classifier as a robust and accurate intrinsic subset predictor. In order to generate their classifier, the researchers used repeated cross-fold validation with multinomial elastic net to identify consistent and discriminative markers. These markers performed with an average classification accuracy of 87.1% and had a high sensitivity and specificity.

When the investigators performed external validation, they found that the classifier achieved an average accuracy of 85.4%. Using the classifier to reanalyze data from a previous study, the authors identified a subset of patients that represented the canonical inflammatory, fibroproliferative, and normal-like subsets. This method can be used to identify intrinsic subsets of SSc patients for clinical trials, as well as help with clinical decision making and the interpretation of heterogeneous molecular information in SSc patients.

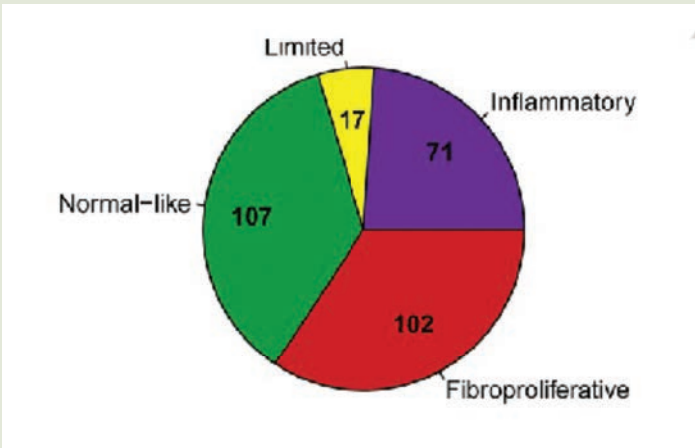

Figure 1. Relative proportion and numbers of intrinsic subsets present in the full merged training data set are shown.

Reducing Versus Maintaining the Dose of Subcutaneous Tocilizumab in Patients With RA in Clinical Remission

In this issue, Sanmarti et al (p. 1616) evaluate the efficacy of increasing the dose interval of subcutaneous tocilizumab (TCZ-SC). Their study is the first randomized trial to compare TCZ dose reduction with a standard regimen. The randomized, open-label trial compared an increase in the dose interval of TCZ-SC to 162 mg every 2 weeks in patients who had achieved sustained clinical remission with a dose interval of 162 mg once weekly. The participants were rheumatoid arthritis (RA) patients with active disease and an inadequate response to conventional synthetic disease-modifying antirheumatic drugs (csDMARDs) or to a biologic agent. These patients were entered into a single-arm treatment phase with 162 mg of TCZ-SC administered once weekly (TCZ-SC 162 mg qw) as monotherapy or in combination with a csDMARD for 24 weeks.

p. 1616

Patients were determined to be in clinical remission if they had a Disease Activity Score in 28 joints (DAS28) of <2.6. Approximately half (45%) of 401 patients in the single-arm phase achieved clinical remission and were randomized to receive TCZ-SC 162 mg qw or to switch to TCZ-SC 162 mg q2w for 24 weeks. At week 48, 90% of patients who received TCZ-SC 162 mg qw remained in clinical remission compared to 73% who received TCZ-SC mg q2w (p=0.004). From other efficacy measures, the only one that was significantly different between the two groups was the mean change from baseline in the DAS28 score at week 48.

The investigators therefore found that increasing the dose interval of TCZ-SC in patients with RA was associated with a lower likelihood of maintaining remission after 24 weeks. Moreover, the increased dose interval was not associated with better tolerability. Nevertheless, the researchers note that most patients were able to sustain remission with a half-dose of TCZ-SC, suggesting that the strategy does deserve further investigation.

Predictors of Development of Rheumatoid Arthritis Can Be Found in ACPA

IgG anti–citrullinated protein antibodies (ACPAs) are the most relevant prognostic and diagnostic biomarker in rheumatoid arthritis (RA). More than 90% of IgG ACPAs have *N*-linked glycans in the antibody variable (V) domain, and the corresponding *N*-glycosylation sites in ACPA V-region sequences result from somatic hypermutation. The fact that this hypermutation is a T cell–dependent process is one of several pieces of evidence that suggest that T cells drive the maturation of the ACPA response prior to arthritis onset.

p. 1626

In this issue, Hafkenscheid et al (p. 1626) investigate whether the presence of glycans in IgG ACPA V domains predicts the transition from predisease autoimmunity to overt RA. They found that a subset of predisposed first-degree relatives (FDRs) of RA patients, originating from an Indigenous North American population, have extensive glycosylation of the IgG ACPA V domain. Moreover, the FDRs who later developed RA exhibited extensive V-domain glycosylation prior to the onset of arthritis.

Specifically, the researchers found that FDR-derived IgG ACPA displayed less than half of the V-domain glycans as compared to IgG ACPA from RA patients. IgG ACPA V-domain glycosylation was strongly associated with future development of RA (hazard ratio 6.07 [95% confidence interval 1.46–25.2]; P = 0.013). Glycosylation of the IgG ACPA V domain represents a predictive marker for RA development in ACPA-positive individuals and may serve to better target prevention measures. The authors note that their data help to refine the understanding of the ACPA immune response and its predisease evolution.

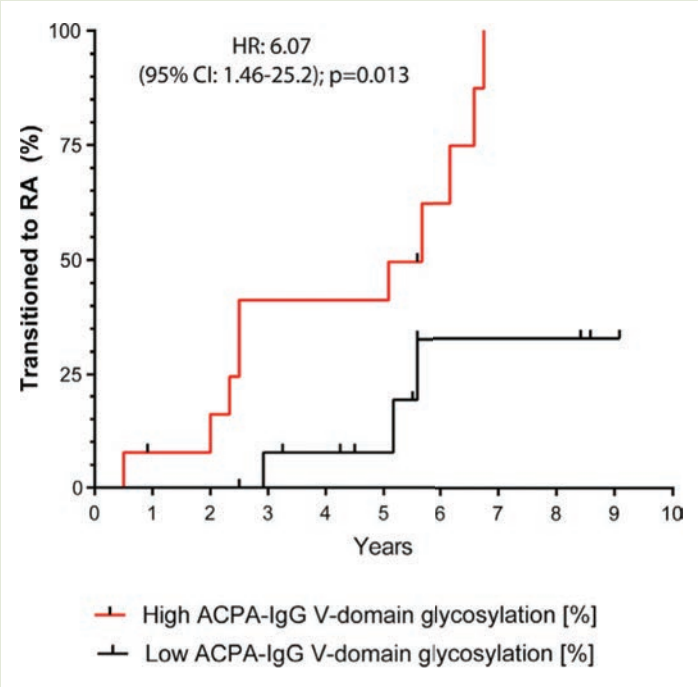

Figure 1. Development of RA in ACPA-positive FDRs, based on degree of IgG ACPA V-domain glycosylation at the first instance of sampling. IgG ACPA V-domain glycosylation levels below and above the 58.5% median are shown. HR = hazard ratio; 95% CI = 95% confidence interval.

Clinical Connections

Induction of Inflammation and Fibrosis by Semaphorin 4A in Systemic Sclerosis

Carvalheiro et al, *Arthritis Rheumatol* 2019;71:1711–1722

CORRESPONDENCE
Samuel García, PhD: S.GarciaPerez@umcutrecht.nl

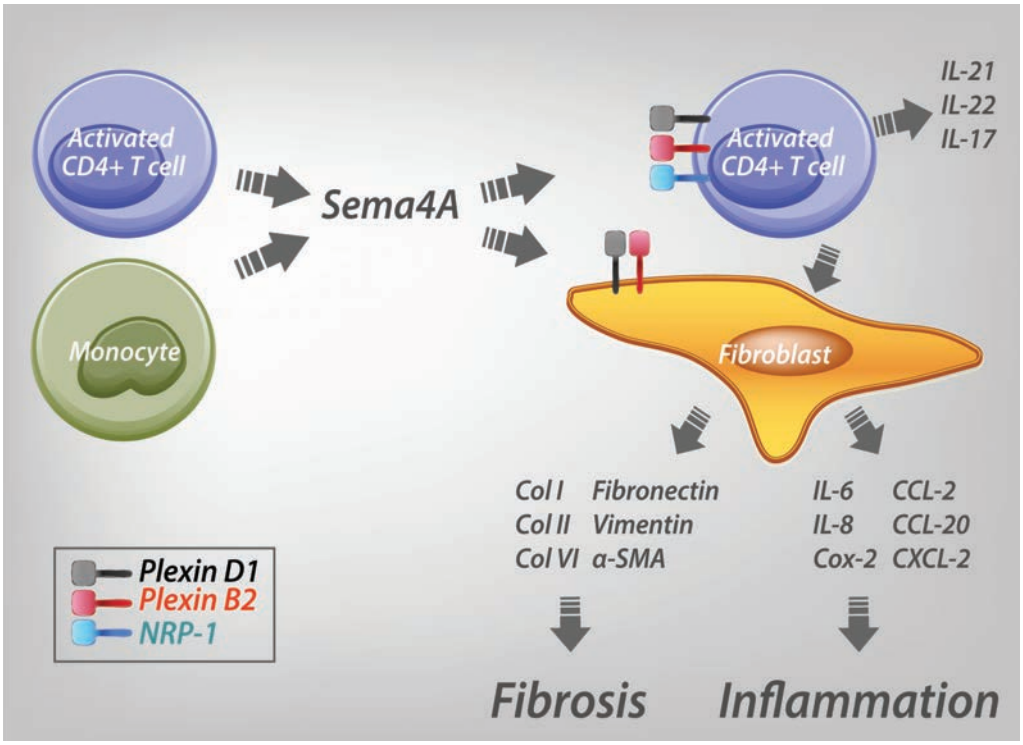

KEY POINTS

- Inflammation and fibrosis are main features of the immunopathology of SSc.
- IL-17 is elevated in SSc patients, but its precise role in the disease is unclear.
- Dermal fibroblasts are key players in the fibrotic processes observed in SSc.
- Sema4A induces IL-17–mediated inflammation and a fibrotic phenotype in dermal fibroblasts, pointing to its potentially central role in SSc pathogenesis.

SUMMARY

Semaphorin 4A (Sema4A) is a transmembrane protein belonging to the semaphorin family. In their study, Carvalheiro et al analyzed the potential role of Sema4A in inflammatory and fibrotic processes involved in the pathology of systemic sclerosis (SSc). Sema4A is elevated in plasma, and in the monocytes and CD4+ T cells of SSc patients, and has an apparent dual role in the pathology of the disease. Sema4A induces the expression of Th17 cytokines (interleukin-17 [IL-17], IL-21, and IL-22) in activated CD4+ T cells, promoting the inflammatory activation of dermal fibroblasts. Additionally, Sema4A directly induces in dermal fibroblasts the expression of extracellular matrix components, such as collagen (Col) family members, fibronectin and vimentin, as well as the myofibroblast marker α-smooth muscle actin (α-SMA). Importantly, these effects are abroggated by the neutralization or silencing of the Sema4A receptors plexin D1, plexin B2, and neuropilin-1 (NRP-1). Sema4A thus appears to play a unifying role in the immunopathology of SSc and may be a potentially attractive therapeutic target.

Regulation of Fatty Acid Oxidation by Twist1 in the Metabolic Adaptation of T Helper Lymphocytes to Chronic Inflammation

Hradilkova et al, *Arthritis Rheumatol* 2019;71:1756–1765

CORRESPONDENCE
Andreas Radbruch, PhD: radbruch@drfz.de

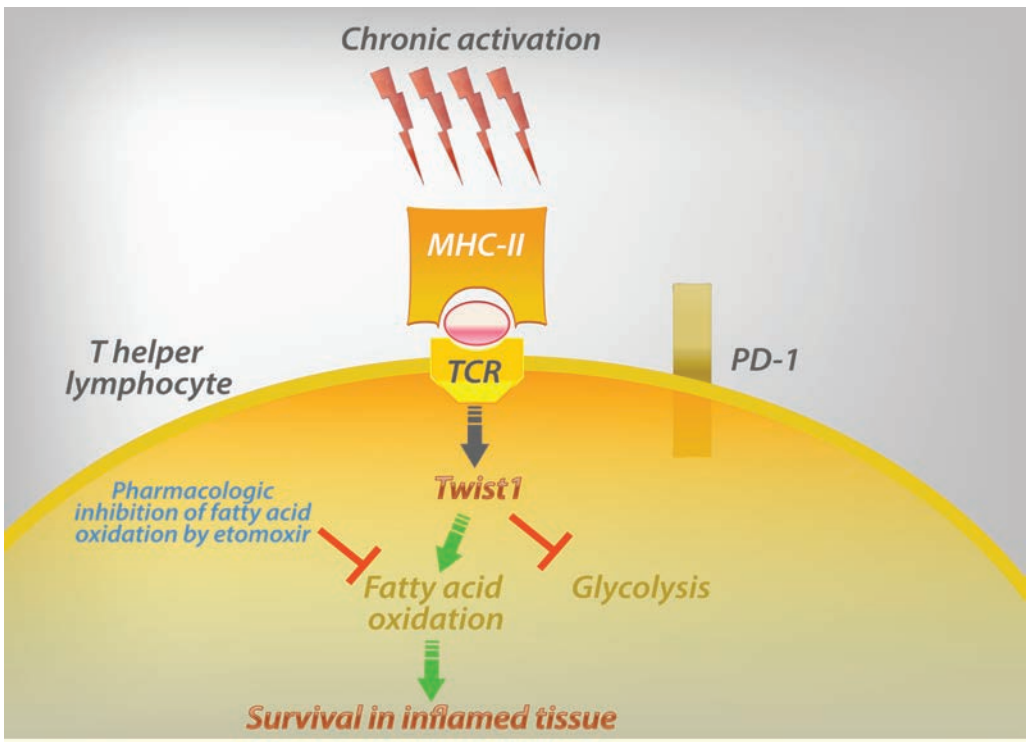

KEY POINTS

- Chronically inflamed tissue is characterized by hypoxia and low glucose levels.
- Despite limiting glucose levels, T helper lymphocytes persist in the inflamed tissue and presumably drive inflammation.
- The transcription factor Twist 1 regulates the switch from glucose dependency to fatty acid oxidation, thereby allowing T helper cells to persist in glucose-poor environments.

SUMMARY

T helper lymphocytes are abundant in the inflamed synovia of patients with rheumatic joint disease despite low levels of ambient oxygen and nutrients such as glucose. T helper lymphocytes expressing the surface marker programmed death 1 (PD-1) have been implicated as a major driver of chronic rheumatic inflammation. In their study, Hradilkova et al identified the E-box–binding transcription factor Twist 1 to be up-regulated in the activated T helper lymphocytes that persist in chronically inflamed tissue. PD-1–positive but not PD-1–negative T helper lymphocytes isolated from the synovial fluid of patients with juvenile idiopathic arthritis express *TWIST1* and die ex vivo when energy metabolism via fatty acid oxidation is inhibited pharmacologically. Murine T helper lymphocytes, repeatedly activated in vitro to mimic activation in chronically inflamed tissue, switch their metabolism from glycolysis to fatty acid oxidation. Murine T helper lymphocytes in which Twist1 has been deleted genetically maintain dependency on glycolysis for their energy supply and die when glucose is lacking. These data establish Twist1 to be a major regulator of the metabolic adaptation of T helper lymphocytes, and offer a mechanism for how chronic inflammation is maintained in rheumatic synovia.

Arthritis & Rheumatology

An Official Journal of the American College of Rheumatology
www.arthritisrheum.org and wileyonlinelibrary.com

Cover design: Todd Machen

This journal is printed on acid-free paper.

Arthritis & Rheumatology

An Official Journal of the American College of Rheumatology
www.arthritisrheum.org and wileyonlinelibrary.com

VOLUME 71 • October 2019 • NO. 10

Cover image: The figure on the cover shows a longitudinal ultrasound view of the carotid artery at the level of the common carotid bifurcation. The oblong density within the lumen of the carotid artery is an atherosclerotic plaque. This issue of *Arthritis & Rheumatology* features a report on the use of carotid ultrasound to detect carotid atherosclerosis in patients with psoriatic disease and the utility of this technique in predicting risk of cardiovascular events in these patients (Sobchak et al, pages 1651–1659). Image courtesy of Lihi Eder, MD, PhD.

Arthritis & Rheumatology
Vol. 71, No. 10, October 2019, pp 1593–1594
DOI 10.1002/art.40882

American College of Rheumatology
Empowering Rheumatology Professionals

EDITORIAL

Trust in Publication: Now More Than Ever

Richard J. Bucala[1] and Daniel H. Solomon[2]

The academic freedom inherent in scientific publication carries with it academic responsibility, although the two concepts are rarely equated (1). For authors, there is the fundamental ethical obligation to publish work that is truthful and scientifically defendable. For reviewers, academic responsibility requires impartiality and fairness while not abusing the privilege of anonymous review, despite professional competition. Ultimately, it is the *Arthritis & Rheumatology* community of contributors and reviewers that not only sustains but expands the foundation of trust that ensures continued research progress. For Editors, it is the duty not only to curate new science but to provide leadership in the highest standards of publication, encompassing both research content and the publication process itself. The product of academic freedom and responsibility gives value to academic publication, as we work collectively to advance discovery, clinical care, and training in rheumatology.

Now more than ever, the readers and the greater public we serve must trust the conduct and publication of science. The stakes to society—in terms of population and individual health, cost of care, and confidence in the professionalism of its physicians and scientists—mandate the highest standards for integrity and transparency in scientific publication. As our editorial board enters its last year of service, we take this opportunity to reflect and share with the American College of Rheumatology our experience with challenges to ethical and professional standards, and we revisit long-accepted obligations of authors, reviewers, and Editors.

For academic authors, as for many practitioners of scholarship, it remains the case that "you are what you publish," and the pressures to publish one's work in a timely and visible manner have never been greater. The acceptance rates for submitted manuscripts at top-tier medical journals are at historic lows, adding to the hurdle of professional recognition and career advancement. Publishers and journals like *A&R* have responded by more actively promoting published content for authors and by opening additional and more specialized publications, including online open-access journals (2).

Unfortunately, increased publication pressures also promote pernicious practices that undermine research integrity. Web-based "watchdog" organizations employ software tools to scour publications for plagiarism and for data and image inconsistencies, whether accidental or from intentional manipulation and deception. In high-profile cases, authors may be unnecessarily impugned in the rush to judgment. Independent research suggests that a significant percentage of published research findings (across all disciplines) are irreproducible or at least significantly and misleadingly overstated (3). A variety of reasons besides careless or deceptive science contribute to this estimation, but the effect on research direction and investment in potentially therapeutic findings is a growing concern for funding agencies and the pharmaceutical industry. Journals have responded with increased data requirements, including more raw data for review, made feasible by the capacity for publication of online-only supplementary material. Unfortunately, rather than facilitating publication, these requirements add burdens to authors and reviewers and can slow publication timelines, which at the same time have become increasingly competitive among journals. These developments around data integrity also have forced journals and their editorial boards to redefine their role in publication, and whether to remain simple conduits for publication or become arbiters of research integrity. *A&R* strives for the highest standards in this evolution, forthrightly addressing integrity concerns and promoting more robust statistical methodologies and enhanced data reporting, especially in the realms of clinical investigation.

The problematic impingement of commercial and for-profit forces on research, which can produce outcomes with significant financial consequences for the health and pharmaceutical industry, continues despite renewed public and regulatory commitments to transparency and conflict-of-interest reporting. Recent examples of physicians obscuring or underreporting

[1]Richard J. Bucala, MD, PhD: Yale School of Medicine, New Haven, Connecticut (Editor-in-Chief, *Arthritis & Rheumatology*); [2]Daniel H. Solomon, MD, MPH: Brigham and Women's Hospital, Boston, Massachusetts (Deputy Editor, *Arthritis & Rheumatology*).

Dr. Bucala is coinventor on patents for anti–macrophage migration inhibitory factor (anti-MIF), anti-MIF receptor, small molecule MIF modulators, MIF genotyping, and fibrocytes, for which he has received licensing and milestone royalties, owns stock or stock options in MIFCOR and Promedior, and has received research support from MIFCOR. Dr. Solomon receives salary support from research contracts to his institution from AbbVie, Amgen, Corrona, Genentech, Janssen, and Pfizer.

Address correspondence to Richard J. Bucala, MD, PhD, Section of Rheumatology, Yale University School of Medicine, New Haven, CT 06520. E-mail: richard.bucala@yale.edu.

Submitted for publication March 5, 2019; accepted March 7, 2019.

commercial entanglements have led to conspicuous cases and professional embarrassment, fueling public cynicism about the medical establishment (4). Current self-reporting standards may be inadequate for publication. Not all authors follow guidelines, there is little meaningful oversight, and it may be sensible to mandate the reporting of all potential conflicts whether considered relevant or not by authors, allowing journal readers to assess the relevance and potential impact of any conflicts or commercial relationships. An argument also can be made for a more robust, centralized, and global database of industry–physician relationships following the one established for manufacturers by the 2010 US Sunshine Act.

It is arguably in the realm of clinical trial reporting and patient-centered studies, where there is an overarching need for transparency and the ethical handling of patient data, that trust and integrity matter most. Clinical trialists and their sponsors exercise a near-monopoly on information from experimental interventions, and the complexity of studies can sometimes encourage post hoc selection of data that oversimplify outcomes and mislead even the most informed readers. Despite the well-recognized need for publicly available clinical trial registries that force investigators to commit to defined protocols and prespecified analytic plans, trial registration is haphazard and sometimes circumvented by the pressures to modify study design or outcomes to accommodate accruing data. *A&R* enforces standards for clinical trial registration and data reporting, as advocated by the International Committee of Medical Journal Editors (5). Rheumatology as a field must conform to the highest standards of clinical investigation, given the trust placed in us by our fellow physicians and by our patients who put themselves in our care.

A&R will undoubtedly face unexpected challenges in the next year and beyond, and our responses will remain anchored in the best interests of the rheumatology community, whom it is both our privilege and our obligation to serve.

REFERENCES

1. Kennedy D. Academic duty. Cambridge: Harvard University Press; 1997.
2. Bucala RJ, Hannan MT. A fresh new look, and a fresh new journal [editorial]. Arthritis Rheumatol 2019;71:1.
3. Reality check on reproducibility [editorial]. Nature 2016;533:437.
4. Thomas K, Ornstein C. The New York Times. Memorial Sloan Kettering's season of turmoil. 2018. URL: https://www.nytimes.com/2018/12/31/health/memorial-sloan-kettering-conflicts.html.
5. Taichman DB, Backus J, Baethge C, Bauchner H, de Leeuw PW, Drazen JM, et al. Sharing clinical trial data: a proposal from the International Committee of Medical Journal Editors [editorial]. Ann Intern Med 2016;164:505–6.

Arthritis & Rheumatology
Vol. 71, No. 10, October 2019, pp 1595–1598
DOI 10.1002/art.40902

American College of Rheumatology
Empowering Rheumatology Professionals

EDITORIAL

Using Machine Learning to Molecularly Classify Systemic Sclerosis Patients

Weiyang Tao, Timothy R. D. J. Radstake, and Aridaman Pandit

Systemic sclerosis (SSc) is an autoimmune disease that is characterized by high molecular complexity (1). SSc patients display tremendous heterogeneity in disease onset manifestations and disease progression, and this heterogeneity has remained a major hindrance in SSc diagnosis, follow-up, and treatment. The past decade has seen a massive growth in high-throughput technologies and advancements in computational methods, which together have enabled us to generate and analyze molecular data at an unprecedented level and at affordable cost. These technological advancements are paving the way for molecular disease classification and thereby for personalized medicine. Molecular classification of SSc collects information from different layers of genetic and epigenetic data with the aim of identifying molecular signatures that can be associated with the patient's pathology. Despite the promising results of molecular disease classification, it has yet to be incorporated into SSc diagnosis and treatment. Therefore, there is a dire need to include molecular disease classification with conventional clinical criteria to improve SSc diagnosis and treatment strategies.

Molecular classification has been successful in identifying signatures that are unique to an individual patient or patient groups in heterogeneous cancers and has improved clinical diagnoses and treatments. For instance, when treatment has been specifically designed for patients using their molecular signatures based on estrogen receptor, progesterone receptor, and human epidermal growth factor receptor 2, there has been a substantial decrease in the mortality rate of breast cancer (2). Similarly, identification of molecularly distinct subsets of non–small cell lung cancer has led to the development of effective and targeted therapy that has largely improved clinical outcomes (3). Given these successful cases, we might ask: Is there any method to automatically stratify patients into different molecular groups and take the first steps toward personalized treatment of a heterogeneous disease like SSc?

The classification criteria for SSc have evolved over time (4,5). According to the 2013 American College of Rheumatology/European League Against Rheumatism criteria, patients are classified as having SSc based on a threshold of an additive point system, which includes scores for skin thickening in fingers, abnormal nailfold capillaries, scleroderma-related autoantibodies, fingertip lesions, and pulmonary arterial hypertension, among others (5). SSc patients are thus clinically classified into 3 subsets, according to the extent of skin involvement: noncutaneous SSc (ncSSc), limited cutaneous SSc (lcSSc), and diffuse cutaneous SSc (dcSSc). When classified based on these clinical criteria, SSc patients display heterogeneous disease phenotypes within each SSc subset. For instance, SSc patients who are classified as having lcSSc based on clinical criteria tend to display distinct molecular phenotypes varying in degree of inflammation and other molecular characteristics. Multiple studies involving molecular data obtained from SSc patients typically classify SSc patients into 4 molecular subsets as follows: normal-like, limited, inflammatory, and fibroproliferative (6–9). Compared to the clinical classification, when patients are molecularly classified into the "limited" subset, they tend to display more homogeneous disease phenotypes.

Molecular classification approaches for SSc have relied on computational methods that cluster or stratify patients based only on their gene expression signatures. In general, 2 different clustering approaches can be used to molecularly stratify patients: 1) the "unsupervised clustering" approach defines patient groups from the molecular signature data without the researcher/user predefining the nature and number of patient groups, and 2) the "supervised clustering" approach matches the patients' molecular signatures with predefined molecular signatures associated with different patient groups. For example, Milano et al developed a molecular stratification method for SSc using an unsupervised hierarchical clustering algorithm on genome-wide gene expression profiles obtained from skin biopsy specimens (6). That and other studies have laid the foundations of molecular classification for

Mr. Tao's work was supported by a China Scholarship Council Fellowship (201606300050). Dr. Pandit's work was supported by The Netherlands Organization for Scientific Research (grant 016.Veni.178.027).

Weiyang Tao, MSc, Timothy R. D. J. Radstake, MD, PhD, Aridaman Pandit, PhD: University Medical Center Utrecht, Utrecht University, Utrecht, The Netherlands.

No potential conflicts of interest relevant to this article were reported.

Address correspondence to Aridaman Pandit, PhD, Heidelberglaan 100, 3584 CX Utrecht, The Netherlands. E-mail: A.Pandit@umcutrecht.nl.

Submitted for publication March 12, 2019; accepted in revised form March 28, 2019.

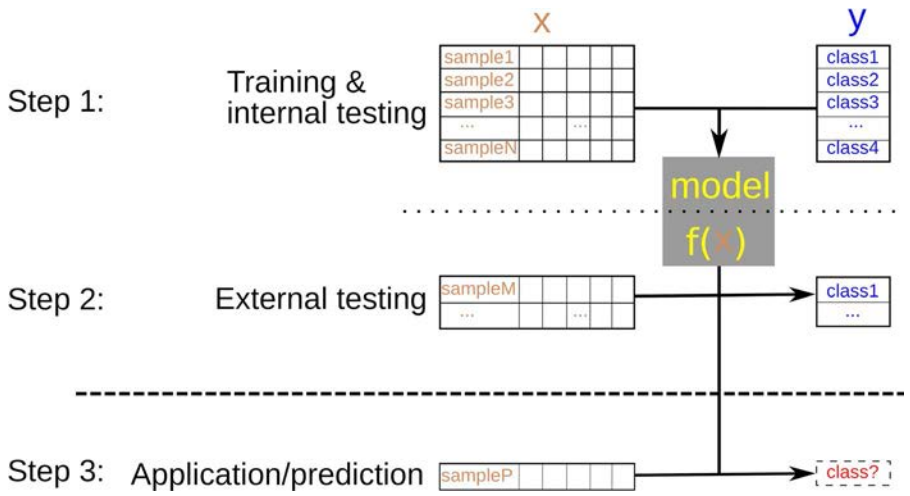

Figure 1. Development of a typical supervised machine learning model.

SSc (10–12). However, unsupervised clustering methods generally require a large cohort, they may over- or understratify patients, and the stratification of patient groups may vary from data set to data set based on the quality of the data set. Therefore, we need studies that can stratify SSc patients into molecular subsets that are robust across many different data sets and thereby can be ultimately implemented to aid clinical decision-making.

In this issue of *Arthritis & Rheumatology*, Franks et al (13) describe a "supervised" model that uses machine learning algorithms to classify individual patients into 4 molecular SSc subsets (normal-like, limited, inflammatory, and fibroproliferative) based on their gene expression patterns. The basic idea of supervised machine learning is that it uses inputs (such as gene expression data) to generate a model that best allows us to determine an output (such as patient classification). Development of a typical supervised machine learning model comprises 2 steps (Figure 1). First, a model is trained using a training data set and iteratively tested by using multiple subsets of the training data set to achieve high model accuracy (internal testing). Second, the model is validated using an independent external test set (Figure 1). Thus, to develop a robust machine learning model, we need a training data set and ≥1 test data set containing the same kind of inputs (gene expression profiles) and outputs (patient groups). Furthermore, different machine learning models can be trained using different machine learning algorithms.

Franks et al studied 6 publicly available DNA microarray data sets from the GEO database, together consisting of more than 400 samples representing a broad spectrum of SSc patients and matched healthy controls. Three of the 6 data sets (together consisting of 297 samples) had clear and definitive intrinsic subset labels and were from the same microarray platform. These samples were delicately combined and were used to train 3 different machine learning models using elastic net (GLMnet), support vector machine, and random forest algorithms. Franks et al applied the repeated cross-validation technique to benchmark these models, which repeatedly splits the original data to test if the machine learning model is sensitive to changes in the data set. The GLMnet model was found to outperform other methods in terms of overall accuracy (average accuracy of 87.1%) and Cohen's kappa coefficient.

Franks et al further validated their best model using the 3 remaining independent and multiplatform data sets. Although the first 2 data sets (10,11) were from a different microarray platform, the model exhibited high performance (concordance of 83–87.5%). The third data set by Assassi et al (12) did not classify the patients into molecular subsets (i.e., normal-like, limited, inflammatory, and fibroproliferative) used by Franks et al; the authors therefore used a network-based prediction of molecular signatures from Assassi et al (12,14) and indirectly demonstrated the robustness of their machine learning model. Thus, taken together, the direct and indirect, as well as the internal and external, validations suggest that the GLMnet-based machine learning classification model is robust and capable of classifying patients from data obtained from different experiments and multiple DNA microarray platforms.

Because of data set splitting and the nature of current machine learning algorithms, training a supervised machine learning model usually requires a large data set (ranging from hundreds to millions of samples, depending on tasks). Too few samples and/or too many input genes can easily make the model overfit to the training data set. As SSc is a rare disease and the gene expression profiling is not performed very often, currently available single data sets are rather small. So the first strength of the study by Franks et al is that they combined multiple data sets to increase the sample size (13). A known drawback of combining gene expression data from multiple studies is that the data get a study/batch-specific bias, also known as "batch effect." The authors did not observe a significant batch effect in their "training" and "test" data sets, and therefore did not use batch effect correction methods while applying their prediction model to different data sets.

The second strength of the study is that it provides an automatic way to perform SSc subset assignment for single patients

high accuracy. For rheumatologists, this could be very useful to classify patients in clinics. And since this model outputs 4 subsets based on molecular signatures (normal-like, limited, inflammatory, and fibroproliferative), it may be more informative than the 3 clinical subsets (ncSSc, lcSSc, and dcSSc). There are several ongoing efforts to develop robust clinical criteria for SSc classification, despite the fact that the classification remains subjective among different clinical experts. Franks and colleagues provide proof-of-principle that molecular signatures can improve patient classification or even directly classify patients into clinically relevant subsets.

Despite these strengths, the study had some limitations. First, although Franks et al used 3 independent data sets from different DNA microarray platforms to externally test their model, the first 2 testing data sets used for validating their model had extremely small sample sizes of 8 and 6 samples, respectively, and the third data set was not directly comparable by prediction model. Thus, this model will require further development and validation before clinical use. The second limitation is a computational/technical issue; to predict a molecular signature in a new patient, one needs to handle batch effect more rigorously, potentially by incorporating some reference genes that can normalize the patient-specific data and make it comparable to the cross-platform training data set used by Franks and colleagues (Figure 1). Third, as noted by the authors, overfitting is one of the greatest concerns in their work. The current model was based on more than 12,000 genes, but the authors do not show if such a high number of genes makes their model overfit to the data. Fourth, the authors used 3 training data sets to train their machine learning model. The patients considered in these 3 training data sets were typically patients with early SSc. Since SSc is a dynamic and heterogeneous disease, underrepresentation of patients with late SSc (lcSSc and dcSSc) requires that the model be further tested on broader SSc patient samples from different stages of disease.

The GLMnet model classifies samples considering expression of genes that are weighted by a coefficient. The coefficient of the genes thus allows us to assess the importance of the genes in the model. Franks et al used these coefficients to identify important/crucial genes as the genes with positive coefficients in their final GLMnet model. Surprisingly, despite laying a strong foundation for molecular SSc classification, these genes did not contain some of the crucial SSc-associated genes, such as *CD247, STAT4*, *TLR8*, *IRF5*, *IRF4*, and *IRF7*. Several recent studies have shown that genetic and epigenetic profiling of specific cell types provides more information on disease mechanisms and phenotypes than whole tissue or peripheral blood mononuclear cell profiling (15–20). For example, *CXCL4* has been shown to be a predictive biomarker for SSc progression and was captured by independent dendritic cell profiling or by proteomic profiling of blood and skin (17,18). Similarly, van der Kroef et al (21) recently showed that SSc patients have altered chromatin marks in their monocytes, which is correlated with their interferon/inflammation signature. However, some of the known biomarker genes, such as *CXCL4*, and inflammatory genes with altered expression and chromatin profiles, such as *MX1* and *OAS1*, were not ranked as important genes in the GLMnet model. In addition, the existence of a fibroproliferative intrinsic SSc subset is still under debate in the SSc community (12). Franks and colleagues found that the genes corresponding to the fibroproliferative intrinsic SSc subset corresponded to metabolic pathways and cellular processes, and not to fibrotic or proliferative processes as one would expect (13). Thus, either the methodology used for identifying important genes needs further exploration or the classification and overlap between fibroproliferative and other intrinsic SSc subsets should be further explored in future studies.

Despite these limitations, the study by Franks et al provides a novel and promising way to better stratify a heterogeneous disease such as SSc into more homogeneous and clinically relevant subgroups. As such, it is an important step toward better diagnostic testing in SSc and toward providing a novel way to better understand the mechanisms in the development of SSc. Such models, along with detailed genetic and epigenetic profiling of SSc patients, may help in further refining molecular classification of SSc, understanding SSc progression and disease mechanisms, and thereby seeding future therapies.

AUTHOR CONTRIBUTIONS

All authors drafted the article, revised it critically for important intellectual content, and approved the final version to be published.

REFERENCES

1. Gabrielli A, Avvedimento EV, Krieg T. Mechanisms of disease: scleroderma. N Engl J Med 2009;360:1989–2003.
2. Carey LA. Directed therapy of subtypes of triple-negative breast cancer. Oncologist 2011;16 Suppl 1:71–8.
3. Kumarakulasinghe NB, van Zanwijk N, Soo RA. Molecular targeted therapy in the treatment of advanced stage non-small cell lung cancer (NSCLC). Respirology 2015;20:370–8.
4. Pope JE, Johnson SR. New classification criteria for systemic sclerosis (scleroderma). Rheum Dis Clin North Am 2015;41:383–98.
5. Van den Hoogen F, Khanna D, Fransen J, Johnson SR, Baron M, Tyndall A, et al. 2013 classification criteria for systemic sclerosis: an American College Of Rheumatology/European League Against Rheumatism collaborative initiative. Arthritis Rheum 2013;65:2737–47.
6. Milano A, Pendergrass SA, Sargent JL, George LK, McCalmont TH, Connolly MK, et al. Molecular subsets in the gene expression signatures of scleroderma skin. PLoS One 2008;3:e2696.
7. Pendergrass SA, Lemaire R, Francis IP, Mahoney JM, Lafyatis R, Whitfield ML. Intrinsic gene expression subsets of diffuse cutaneous systemic sclerosis are stable in serial skin biopsies. J Invest Dermatol 2012;132:1363–73.
8. Hinchcliff M, Huang CC, Wood TA, Mahoney JM, Martyanov V, Bhattacharyya S, et al. Molecular signatures in skin associated with clinical improvement during mycophenolate treatment in systemic sclerosis. J Invest Dermatol 2013;133:1979–89.
9. Mahoney JM, Taroni J, Martyanov V, Wood TA, Greene CS, Pioli PA, et al. Systems level analysis of systemic sclerosis shows a network of immune and profibrotic pathways connected with genetic polymorphisms. PLoS Comput Biol 2015;11:e1004005.

10. Gordon JK, Martyanov V, Magro C, Wildman HF, Wood TA, Huang WT, et al. Nilotinib (Tasigna™) in the treatment of early diffuse systemic sclerosis: an open-label, pilot clinical trial. Arthritis Res Ther 2015;17:213.
11. Chakravarty EF, Martyanov V, Fiorentino D, Wood TA, Haddon DJ, Jarrell JA, et al. Gene expression changes reflect clinical response in a placebo-controlled randomized trial of abatacept in patients with diffuse cutaneous systemic sclerosis. Arthritis Res Ther 2015;17:159.
12. Assassi S, Swindell WR, Wu M, Tan FD, Khanna D, Furst DE, et al. Dissecting the heterogeneity of skin gene expression patterns in systemic sclerosis. Arthritis Rheumatol 2015;67:3016–26.
13. Franks JM, Martyanov V, Cai G, Wang Y, Li Z, Wood TA, et al. A machine learning classifier for assigning individual patients with systemic sclerosis to intrinsic molecular subsets. Arthritis Rheumatol 2019;71:1701–10.
14. Langfelder P, Horvath S. WGCNA: an R package for weighted correlation network analysis. BMC Bioinformatics 2008;9:559.
15. Angiolilli C, Marut W, van der Kroef M, Chouri E, Reedquist KA, Radstake TR. New insights into the genetics and epigenetics of systemic sclerosis. Nat Rev Rheumatol 2018;1:657–73.
16. Broen JC, Radstake TR, Rossato M. The role of genetics and epigenetics in the pathogenesis of systemic sclerosis. Nat Rev Rheumatol 2014;10:671–81.
17. Van Bon L, Affandi AJ, Broen J, Christmann RB, Marijnissen RJ, Stawski L, et al. Proteome-wide analysis and CXCL4 as a biomarker in systemic sclerosis. N Engl J Med 2014;370:433–43.
18. Ah Kioon MD, Tripodo C, Fernandez D, Kirou KA, Spiera RF, Crow MK, et al. Plasmacytoid dendritic cells promote systemic sclerosis with a key role for TLR8. Sci Transl Med 2018;10:eeam8458.
19. Van Bon L, Popa C, Huijbens R, Vonk M, York M, Simms R, et al. Distinct evolution of TLR-mediated dendritic cell cytokine secretion in patients with limited and diffuse cutaneous systemic sclerosis. Ann Rheum Dis 2010;69:1539–47.
20. Chouri E, Servaas NH, Bekker CP, Affandi AJ, Cossu M, Hillen MR, et al. Serum microRNA screening and functional studies reveal miR-483-5p as a potential driver of fibrosis in systemic sclerosis. J Autoimmun 2018;89:162–70.
21. Van der Kroef M, Castellucci M, Mokry M, Cossu M, Garonzi M, Bossini-Castillo LM, et al. Histone modifications underlie monocyte dysregulation in patients with systemic sclerosis, underlining the treatment potential of epigenetic targeting. Ann Rheum Dis 2019;78:529–38.

Arthritis & Rheumatology
Vol. 71, No. 10, October 2019, pp 1599–1613
DOI 10.1002/art.41042

American College of Rheumatology
Empowering Rheumatology Professionals

SPECIAL ARTICLE

2019 Update of the American College of Rheumatology/ Spondylitis Association of America/Spondyloarthritis Research and Treatment Network Recommendations for the Treatment of Ankylosing Spondylitis and Nonradiographic Axial Spondyloarthritis

Michael M. Ward,[1] Atul Deodhar,[2] Lianne S. Gensler,[3] Maureen Dubreuil,[4] David Yu,[5] Muhammad Asim Khan,[6] Nigil Haroon,[7] David Borenstein,[8] Runsheng Wang,[9] Ann Biehl,[1] Meika A. Fang,[10] Grant Louie,[11] Vikas Majithia,[12] Bernard Ng,[13] Rosemary Bigham,[14] Michael Pianin,[15] Amit Aakash Shah,[16] Nancy Sullivan,[17] Marat Turgunbaev,[16] Jeff Oristaglio,[17] Amy Turner,[16] Walter P. Maksymowych,[18] and Liron Caplan[19]

Guidelines and recommendations developed and/or endorsed by the American College of Rheumatology (ACR) are intended to provide guidance for particular patterns of practice and not to dictate the care of a particular patient. The ACR considers adherence to the recommendations within this guideline to be voluntary, with the ultimate determination regarding their application to be made by the health care provider in light of each patient's individual circumstances. Guidelines and recommendations are intended to promote beneficial or desirable outcomes but cannot guarantee any specific outcome. Guidelines and recommendations developed and endorsed by the ACR are subject to periodic revision as warranted by the evolution of medical knowledge, technology, and practice. ACR recommendations are not intended to dictate payment or insurance decisions. These recommendations cannot adequately convey all uncertainties and nuances of patient care.

The American College of Rheumatology is an independent, professional, medical and scientific society that does not guarantee, warrant, or endorse any commercial product or service.

Objective. To update evidence-based recommendations for the treatment of patients with ankylosing spondylitis (AS) and nonradiographic axial spondyloarthritis (SpA).

Methods. We conducted updated systematic literature reviews for 20 clinical questions on pharmacologic treatment addressed in the 2015 guidelines, and for 26 new questions on pharmacologic treatment, treat-to-target strategy, and use of imaging. New questions addressed the use of secukinumab, ixekizumab, tofacitinib, tumor necrosis factor inhibitor (TNFi) biosimilars, and biologic tapering/discontinuation, among others. We used the Grading of Recommendations, Assessment, Development and Evaluation methodology to assess the quality of evidence and formulate recommendations and required at least 70% agreement among the voting panel.

Results. Recommendations for AS and nonradiographic axial SpA are similar. TNFi are recommended over secukinumab or ixekizumab as the first biologic to be used. Secukinumab or ixekizumab is recommended over the use of a second TNFi in patients with primary nonresponse to the first TNFi. TNFi, secukinumab, and ixekizumab are favored over tofacitinib. Co-administration of low-dose methotrexate with TNFi is not recommended, nor is a strict treat-to-target strategy or discontinuation or tapering of biologics in patients with stable disease. Sulfasalazine is recommended only for persistent peripheral arthritis when TNFi are contraindicated. For patients with unclear disease activity, spine or pelvis magnetic resonance imaging could aid assessment. Routine monitoring of radiographic changes with serial spine radiographs is not recommended.

Conclusion. These recommendations provide updated guidance regarding use of new medications and imaging of the axial skeleton in the management of AS and nonradiographic axial SpA.

INTRODUCTION

Axial spondyloarthritis (SpA), comprising ankylosing spondylitis (AS) and nonradiographic axial SpA, is the main form of chronic inflammatory arthritis affecting the axial skeleton (1). AS affects 0.1–0.5% of the population, and is characterized by inflammatory back pain, radiographic sacroiliitis, excess spinal bone formation, and a high prevalence of HLA–B27 (2,3). Although nonradiographic axial SpA shares several features with AS, advanced sacroiliac joint damage and spine ankylosis are absent (4). The severity of arthralgia, stiffness, and limited flexibility varies widely among patients and over the course of axial SpA. Skeletal disease may be accompanied by uveitis, psoriasis, and inflammatory bowel disease (IBD). Axial SpA can impose substantial physical and social burdens on patients, and can interfere with work and schooling (5,6). The goals of treatment are to alleviate symptoms, improve functioning, maintain the ability to work, decrease disease complications, and forestall skeletal damage as much as possible.

In 2015, the American College of Rheumatology (ACR), Spondylitis Association of America (SAA), and Spondyloarthritis Research and Treatment Network (SPARTAN) published recommendations for the treatment of adults with AS and those with nonradiographic axial SpA (7). Recommendations were provided for pharmacologic treatment, rehabilitation, use of surgery, management of selected comorbidities, disease monitoring, patient education, and preventive care. The recommendations were tailored to patients with either active or stable disease and focused on the most common decisions confronting clinicians when treating these patients.

The advent of new medications to treat axial SpA warranted this update. We did not reexamine all of the 2015 recommendations, but rather focused on those questions for which consequential new evidence was present. We added several new recommendations on how the newly available medications should fit in treatment strategies and on the use of imaging. The target populations are adults with AS or nonradiographic axial SpA. The target users of these recommendations are rheumatologists, primary care clinicians, physiatrists, physical therapists, and others providing care to patients with axial SpA.

METHODS

These recommendations followed ACR and Grading of Recommendations, Assessment, Development and Evaluation (GRADE) methodology (8,9), as described in Supplementary Appendix 1, available on the *Arthritis & Rheumatology* web site at http://onlinelibrary.wiley.com/doi/10.1002/art.41042/abstract. Briefly, systematic literature reviews were done for prespecified clinical population, intervention, comparator, outcomes (PICO) questions. The resulting evidence was reviewed, and recommendations formulated and voted on, by an expert voting panel (see Supplementary Appendices 2–5 at http://onlinelibrary.wiley.com/doi/10.1002/art.41042/abstract). Key definitions, including ones for active and stable disease, are provided in Table 1. Clinical trials of ixekizumab became available during the time the manuscript was in preparation, after the voting panel had met (10,11). The data from these trials were provided to the voting panel, and revised recommendations that included ixekizumab were reviewed and voted on by the panel.

This article is published simultaneously in *Arthritis Care & Research.*

The views expressed herein do not necessarily represent those of the National Institutes of Health or the United States Department of Veterans Affairs.

Supported by the American College of Rheumatology, the Spondylitis Association of America, and the Spondyloarthritis Research and Treatment Network. Dr. Ward's work was supported by the NIH (Intramural Research Program grant ZIA-AR-041153 from the National Institute of Arthritis and Musculoskeletal and Skin Diseases).

[1]Michael M. Ward, MD, MPH, Ann Biehl, MS, PharmD, BCPS: National Institute of Arthritis and Musculoskeletal and Skin Diseases, Bethesda, Maryland; [2]Atul Deodhar, MD, MRCP: Oregon Health & Science University, Portland; [3]Lianne S. Gensler, MD: University of California, San Francisco; [4]Maureen Dubreuil, MD, MSc: Boston University School of Medicine, Boston, Massachusetts; [5]David Yu, MD: University of California, Los Angeles; [6]Muhammad Asim Khan, MD, FRCP, MACP: Case Western Reserve University, Cleveland, Ohio; [7]Nigil Haroon, MBBS, MD, DM: University of Toronto, Krembil Research Institute, Toronto Western Hospital, Toronto, Ontario, Canada; [8]David Borenstein, MD: Arthritis & Rheumatism Associates, Washington, DC; [9]Runsheng Wang, MD, MHS: Columbia University Medical Center, New York, New York; [10]Meika A. Fang, MD: VA West Los Angeles Medical Center, Los Angeles, California; [11]Grant Louie, MD, MHS: Arthritis and Rheumatism Associates, Wheaton, Maryland; [12]Vikas Majithia, MD, MPH: University of Mississippi Medical Center, Jackson; [13]Bernard Ng, MD: University of Washington, Seattle; [14]Rosemary Bigham: Seattle, Washington; [15]Michael Pianin, JD: Pianin and Associates, PC, Phoenix, Arizona; [16]Amit Aakash Shah, MD, MPH, Marat Turgunbaev, MD, MPH, Amy Turner: American College of Rheumatology, Atlanta, Georgia; [17]Nancy Sullivan, BA, Jeff Oristaglio, PhD: ECRI Institute, Plymouth Meeting, Pennsylvania; [18]Walter P. Maksymowych, MD, FRCPC: University of Alberta, Edmonton, Alberta, Canada; [19]Liron Caplan, MD, PhD: Rocky Mountain Regional VA Medical Center and University of Colorado, Aurora.

Dr. Deodhar has received consulting fees from AbbVie, Amgen, Boehringer Ingelheim, Bristol-Myers Squibb, GlaxoSmithKline, Galapagos, Janssen, and Pfizer (less than $10,000 each), Eli Lilly and Company, Novartis, and UCB (more than $10,000 each). Dr. Gensler has received consulting fees from AbbVie, Galapagos, Eli Lilly and Company, Novartis, Pfizer, and UCB (less than $10,000 each). Dr. Khan has received consulting fees from Eli Lilly and Company (less than $10,000), and AbbVie, and Novartis (more than $10,000 each). Dr. Haroon has received consulting fees from Amgen, AbbVie, Janssen, Eli Lilly and Company, Novartis, and UCB (less than $10,000 each). Dr. Borenstein has received consulting fees from AbbVie, Pfizer, and Novartis (more than $10,000 each). Dr. Wang has received consulting fees from Novartis and Eli Lilly and Company (less than $10,000 each), and had no conflicts of interest during the time of guideline development, but before publication became a consultant for Novartis, and a member of the medical education advisory board for Eli Lilly. Dr. Louie has received consulting fees from Janssen (less than $10,000). Dr. Majithia has received consulting fees from Novartis (less than $10,000), and had no conflicts of interest during the time of guideline development, but just before publication became the site principal investigator for clinical trials for systemic lupus erythematosus by Bristol-Myers Squibb and Janssen. Dr. Maksymowych has received consulting fees from AbbVie, Boehringer, Celgene, Galapagos, Janssen, Eli Lilly and Company, Novartis, Pfizer, and UCB (less than $10,000 each). No other disclosures relevant to this article were reported.

Address correspondence to Michael M. Ward, MD, MPH, NIAMS/NIH, Building 10 CRC, Room 4-1339, 10 Center Drive, MSC 1468, Bethesda, MD 20892. E-mail: wardm1@mail.nih.gov.

Submitted for publication March 28, 2019; accepted in revised form July 9, 2019.

Table 1. Definitions of key terms*

Term	Definition
Active disease	Disease causing symptoms at an unacceptably bothersome level to the patient and judged by the examining clinician to be due to inflammation.
Stable disease	Disease that was asymptomatic or causing symptoms but at an acceptable level as reported by the patient. A minimum of 6 months was required to qualify as clinically stable.
Primary nonresponse	Absence of a clinically meaningful improvement in disease activity over the 3 to 6 months after treatment initiation, not related to toxicity or poor adherence.
Secondary nonresponse	Recurrence of ankylosing spondylitis activity, not due to treatment interruption or poor adherence, after having a sustained clinically meaningful improvement on treatment (generally, beyond the initial 6 months of treatment).
Conventional synthetic antirheumatic drug	Sulfasalazine, methotrexate, leflunomide, apremilast, thalidomide, pamidronate.
Biosimilar	Biopharmaceuticals that are copies of an original biologic medication and tested to be of the same purity and potency as the original. In these recommendations, we refer only to TNFi biosimilars. Examples include infliximab-dyyb, etanercept-szzs, and adalimumab-atto.
TNFi	Infliximab, etanercept, adalimumab, certolizumab, golimumab, and their biosimilars.
TNFi monoclonal antibodies	Infliximab, adalimumab, certolizumab, golimumab.
Biologics	TNFi, abatacept, rituximab, sarilumab, tocilizumab, ustekinumab, secukinumab, ixekizumab.**
High-quality evidence	Studies that provide high confidence in the effect estimate, and new data from future studies are thought unlikely to change the effect.
Moderate-quality evidence	Studies that provide confidence that the true effect is likely to be close to the estimate but could be substantially different.
Low-quality evidence	Studies that provide limited confidence about the effect, and the true effect may be substantially different from the estimate.
Very low-quality evidence	Studies that provide very little certainty about the effect, and the true effect may be quite different from the estimate.
Strong recommendation	Action should be favored in almost all patients, usually requiring high-quality evidence, high confidence that future research will not alter the conclusion, AND an assessment that the desirable effects of the intervention outweigh the undesirable effects. Should not be taken to imply that the intervention has large clinical benefits.
Conditional recommendation	Action should be followed in only selected cases, often limited by low-quality evidence, OR when the desirable and undesirable consequences of an intervention are more balanced, OR if patients' preferences for the intervention are thought to vary widely.
Patient preferences	Beliefs and expectations regarding potential benefits and harms of treatment and how these relate to an individual's goals for health and life.
Shared decision-making	The process by which a patient and clinician arrive at an individualized treatment decision based on an understanding of the potential benefits and risks of available treatment options and of a patient's values and preferences.

* TNFi = tumor necrosis factor inhibitor.

RESULTS

Here we present the recommendations that were reviewed in this update, whether it was a new recommendation (designated "new") or reevaluation of an existing recommendation. Table 2 and Table 3 provide all current recommendations, including those from the 2015 report that were not newly reviewed. The order of recommendations presented here does not imply priority for use or recommended sequencing of different interventions. PICO numbers following each recommendation can be used to locate related evidence in Supplementary Appendix 6, available on the *Arthritis & Rheumatology* web site at http://onlinelibrary.wiley.com/doi/10.1002/art.41042/abstract.

**Correction added on 26 September 2019, after first online publication: Secukinumab and ixekizumab were omitted in Table 1. They have been restored in this version of the article.

A. Recommendations for the treatment of patients with active AS

In adults with active AS, we conditionally recommend continuous treatment with nonsteroidal antiinflammatory drugs (NSAIDs) over on-demand treatment with NSAIDs (PICO 1).

The efficacy of NSAIDs for symptom improvement in active AS has been established in many controlled trials. Evidence that continuous NSAID use results in slower rates of spinal fusion on radiographs over 2 years compared to on-demand NSAID use is inconsistent, with results of one trial of celecoxib suggesting less progression with continuous use, and one trial of diclofenac indicating no difference in progression (12,13) (See Supplementary Appendix 6, available on the *Arthritis & Rheumatology* web site at http://onlinelibrary.wiley.com/doi/10.1002/art.41042/abstract). Despite the

Table 2. Recommendations for the treatment of adults with AS*

Recommendation	Level of evidence	PICO
RECOMMENDATIONS FOR ADULTS WITH ACTIVE AS		
1. We strongly recommend treatment with NSAIDs over no treatment with NSAIDs.†	Low	2
2. We conditionally recommend continuous treatment with NSAIDs over on-demand treatment with NSAIDs.	Low to moderate	1
3. We do not recommend any particular NSAID as the preferred choice.†	Low to moderate	3
4. In adults with active AS despite treatment with NSAIDs, we conditionally recommend treatment with sulfasalazine, methotrexate, or tofacitinib over no treatment with these medications. Sulfasalazine or methotrexate should be considered only in patients with prominent peripheral arthritis or when TNFi are not available.	Very low to moderate	7
5. In adults with active AS despite treatment with NSAIDs, we conditionally recommend treatment with TNFi over treatment with tofacitinib.	Very low	60
6. In adults with active AS despite treatment with NSAIDs, we strongly recommend treatment with TNFi over no treatment with TNFi.	High	6
7. We do not recommend any particular TNFi as the preferred choice.	Moderate	5
8. In adults with active AS despite treatment with NSAIDs, we strongly recommend treatment with secukinumab or ixekizumab over no treatment with secukinumab or ixekizumab.	High	58
9. In adults with active AS despite treatment with NSAIDs, we conditionally recommend treatment with TNFi over treatment with secukinumab or ixekizumab.	Very low	59
10. In adults with active AS despite treatment with NSAIDs, we conditionally recommend treatment with secukinumab or ixekizumab over treatment with tofacitinib.	Very low	61
11. In adults with active AS despite treatment with NSAIDs and who have contraindications to TNFi, we conditionally recommend treatment with secukinumab or ixekizumab over treatment with sulfasalazine, methotrexate, or tofacitinib.	Low	8
12. In adults with active AS despite treatment with the first TNFi used, we conditionally recommend treatment with secukinumab or ixekizumab over treatment with a different TNFi in patients with primary nonresponse to TNFi.	Very low	10
13. In adults with active AS despite treatment with the first TNFi used, we conditionally recommend treatment with a different TNFi over treatment with a non-TNFi biologic in patients with secondary nonresponse to TNFi.	Very low	10
14. In adults with active AS despite treatment with the first TNFi used, we strongly recommend against switching to treatment with a biosimilar of the first TNFi.	Very low	62
15. In adults with active AS despite treatment with the first TNFi used, we conditionally recommend against the addition of sulfasalazine or methotrexate in favor of treatment with a new biologic.	Very low	9
16. We strongly recommend against treatment with systemic glucocorticoids.†	Very low	4
17. In adults with isolated active sacroiliitis despite treatment with NSAIDs, we conditionally recommend treatment with locally administered parenteral glucocorticoids over no treatment with local glucocorticoids.†	Very low	13
18. In adults with stable axial disease and active enthesitis despite treatment with NSAIDs, we conditionally recommend using treatment with locally administered parenteral glucocorticoids over no treatment with local glucocorticoids. Peri-tendon injections of Achilles, patellar, and quadriceps tendons should be avoided.†	Very low	14
19. In adults with stable axial disease and active peripheral arthritis despite treatment with NSAIDs, we conditionally recommend using treatment with locally administered parenteral glucocorticoids over no treatment with local glucocorticoids.†	Very low	15
20. We strongly recommend treatment with physical therapy over no treatment with physical therapy.†	Moderate	16
21. We conditionally recommend active physical therapy interventions (supervised exercise) over passive physical therapy interventions (massage, ultrasound, heat).†	Very low	17
22. We conditionally recommend land-based physical therapy interventions over aquatic therapy interventions.†	Moderate	18
RECOMMENDATIONS FOR ADULTS WITH STABLE AS		
23. We conditionally recommend on-demand treatment with NSAIDs over continuous treatment with NSAIDs.	Low to moderate	1
24. In adults receiving treatment with TNFi and NSAIDs, we conditionally recommend continuing treatment with TNFi alone compared to continuing both treatments.	Very low	11
25. In adults receiving treatment with TNFi and a conventional synthetic antirheumatic drug, we conditionally recommend continuing treatment with TNFi alone over continuing both treatments.	Very low	12
26. In adults receiving treatment with a biologic, we conditionally recommend against discontinuation of the biologic.	Very low to low	66

(Continued)

Table 2. (*Cont'd*)

Recommendation	Level of evidence	PICO
27. In adults receiving treatment with a biologic, we conditionally recommend against tapering of the biologic dose as a standard approach.	Very low to low	65
28. In adults receiving treatment with an originator TNFi, we strongly recommend continuing treatment with the originator TNFi over mandated switching to its biosimilar.	Very low	63
29. We strongly recommend treatment with physical therapy over no treatment with physical therapy.†	Low	19
RECOMMENDATIONS FOR ADULTS WITH ACTIVE OR STABLE AS		
30. In adults receiving treatment with TNFi, we conditionally recommend against co-treatment with low-dose methotrexate.	Low	64
31. We conditionally recommend advising unsupervised back exercises.†	Moderate	20
32. We conditionally recommend fall evaluation and counseling.†	Very low	51
33. We conditionally recommend participation in formal group or individual self-management education.†	Moderate	48
34. In adults with spinal fusion or advanced spinal osteoporosis, we strongly recommend against treatment with spinal manipulation.†	Very low	21
35. In adults with advanced hip arthritis, we strongly recommend treatment with total hip arthroplasty over no surgery.†	Very low	25
36. In adults with severe kyphosis, we conditionally recommend against elective spinal osteotomy.†	Very low	26
RECOMMENDATIONS FOR ADULTS WITH AS-RELATED COMORBIDITIES		
37. In adults with acute iritis, we strongly recommend treatment by an ophthalmologist to decrease the severity, duration, or complications of episodes.†	Very low	27
38. In adults with recurrent iritis, we conditionally recommend prescription of topical glucocorticoids over no prescription for prompt at-home use in the event of eye symptoms to decrease the severity or duration of iritis episodes.†	Very low	28
39. In adults with recurrent iritis, we conditionally recommend treatment with TNFi monoclonal antibodies over treatment with other biologics.	Low	29
40. In adults with inflammatory bowel disease, we do not recommend any particular NSAID as the preferred choice to decrease the risk of worsening of inflammatory bowel disease symptoms.†	Very low	31
41. In adults with inflammatory bowel disease, we conditionally recommend treatment with TNFi monoclonal antibodies over treatment with other biologics.	Very low	32
DISEASE ACTIVITY ASSESSMENT, IMAGING, AND SCREENING		
42. We conditionally recommend the regular-interval use and monitoring of a validated AS disease activity measure.†	Very low	54
43. We conditionally recommend regular-interval use and monitoring of CRP concentrations or ESR over usual care without regular CRP or ESR monitoring.†	Very low	55
44. In adults with active AS, we conditionally recommend against using a treat-to-target strategy using a target of ASDAS <1.3 (or 2.1) over a treatment strategy based on physician assessment.	Low	67
45. We conditionally recommend screening for osteopenia/osteoporosis with DXA scan over no screening.†	Very low	49
46. In adults with syndesmophytes or spinal fusion, we conditionally recommend screening for osteoporosis/osteopenia with DXA scan of the spine as well as the hips, compared to DXA scan solely of the hip or other non-spine sites.†	Very low	50
47. We strongly recommend against screening for cardiac conduction defects with electrocardiograms.†	Very low	52
48. We strongly recommend against screening for valvular heart disease with echocardiograms.†	Very low	53
49. In adults with AS of unclear activity while on a biologic, we conditionally recommend obtaining a spinal or pelvis MRI to assess activity.	Very low	68
50. In adults with stable AS, we conditionally recommend against obtaining a spinal or pelvis MRI to confirm inactivity.	Very low	69
51. In adults with active or stable AS on any treatment, we conditionally recommend against obtaining repeat spine radiographs at a scheduled interval (e.g., every 2 years) as a standard approach.	Very low	70

* AS = ankylosing spondylitis; PICO = population, intervention, comparison, and outcomes; NSAIDs = nonsteroidal antiinflammatory drugs; TNFi = tumor necrosis factor inhibitor; CRP = C-reactive protein; ESR = erythrocyte sedimentation rate; ASDAS = Ankylosing Spondylitis Disease Activity Score; DXA = dual x-ray absorptiometry; MRI = magnetic resonance imaging.
† These recommendations were from 2015 and were not reviewed in this update. The number preceding the recommendation is the recommendation number and is referenced as bracketed numbers in Figure 1.

Table 3. Recommendations for the treatment of adults with nonradiographic axial SpA*

Recommendation	Level of evidence	PICO
RECOMMENDATIONS FOR ADULTS WITH ACTIVE NONRADIOGRAPHIC AXIAL SpA		
52. We strongly recommend treatment with NSAIDs over no treatment with NSAIDs.†	Very low	34
53. We conditionally recommend continuous treatment with NSAIDs over on-demand treatment with NSAIDs.	Very low	33
54. We do not recommend any particular NSAID as the preferred choice.†	Very low	35
55. In adults with active nonradiographic axial SpA despite treatment with NSAIDs, we conditionally recommend treatment with sulfasalazine, methotrexate, or tofacitinib over no treatment with these medications.	Very low	39
56. In adults with active nonradiographic axial SpA despite treatment with NSAIDs, we strongly recommend treatment with TNFi over no treatment with TNFi.	High	38
57. We do not recommend any particular TNFi as the preferred choice.	Very low	37
58. In adults with active nonradiographic axial SpA despite treatment with NSAIDs, we conditionally recommend treatment with TNFi over treatment with tofacitinib.	Very low	73
59. In adults with active nonradiographic axial SpA despite treatment with NSAIDs, we conditionally recommend treatment with secukinumab or ixekizumab over no treatment with secukinumab or ixekizumab.	Very low	71
60. In adults with active nonradiographic axial SpA despite treatment with NSAIDs, we conditionally recommend treatment with TNFi over treatment with secukinumab or ixekizumab.	Very low	72
61. In adults with active nonradiographic axial SpA despite treatment with NSAIDs, we conditionally recommend treatment with secukinumab or ixekizumab over treatment with tofacitinib.	Very low	74
62. In adults with active nonradiographic axial SpA despite treatment with NSAIDs and who have contraindications to TNFi, we conditionally recommend treatment with secukinumab or ixekizumab over treatment with sulfasalazine, methotrexate, or tofacitinib.	Very low	40
63. In adults with active nonradiographic axial SpA and primary nonresponse to the first TNFi used, we conditionally recommend switching to secukinumab or ixekizumab over switching to a different TNFi.	Very low	42
64. In adults with active nonradiographic axial SpA and secondary nonresponse to the first TNFi used, we conditionally recommend switching to a different TNFi over switching to a non-TNFi biologic.	Very low	42
65. In adults with active nonradiographic axial SpA despite treatment with the first TNFi used, we strongly recommend against switching to the biosimilar of the first TNFi.	Very low	75
66. In adults with active nonradiographic axial SpA despite treatment with the first TNFi used, we conditionally recommend against the addition of sulfasalazine or methotrexate in favor of treatment with a different biologic.	Very low	41
67. We strongly recommend against treatment with systemic glucocorticoids.†	Very low	36
68. In adults with isolated active sacroiliitis despite treatment with NSAIDs, we conditionally recommend treatment with local glucocorticoids over no treatment with local glucocorticoids.†	Very low	45
69. In adults with active enthesitis despite treatment with NSAIDs, we conditionally recommend using treatment with locally administered parenteral glucocorticoids over no treatment with local glucocorticoids. Peri-tendon injections of Achilles, patellar, and quadriceps tendons should be avoided.†	Very low	46
70. In adults with active peripheral arthritis despite treatment with NSAIDs, we conditionally recommend using treatment with locally administered parenteral glucocorticoids over no treatment with local glucocorticoids.†	Very low	47
71. We strongly recommend treatment with physical therapy over no treatment with physical therapy.†	Low	22
72. We conditionally recommend active physical therapy interventions (supervised exercise) over passive physical therapy interventions (massage, ultrasound, heat).†	Very low	23
73. We conditionally recommend land-based physical therapy interventions over aquatic therapy interventions.†	Very low	24
RECOMMENDATIONS FOR ADULTS WITH STABLE NONRADIOGRAPHIC AXIAL SpA		
74. We conditionally recommend on-demand treatment with NSAIDs over continuous treatment with NSAIDs.	Very low	33
75. In adults receiving treatment with TNFi and NSAIDs, we conditionally recommend continuing treatment with TNFi alone compared to continuing both medications.	Very low	43
76. In adults receiving treatment with TNFi and a conventional synthetic antirheumatic drug, we conditionally recommend continuing treatment with TNFi alone over continuing treatment with both medications.	Very low	44
77. In adults receiving treatment with a biologic, we conditionally recommend against discontinuation of the biologic.	Low	79
78. In adults receiving treatment with a biologic, we conditionally recommend against tapering of the biologic dose as a standard approach.	Very low	78
79. In adults receiving treatment with an originator TNFi, we strongly recommend continuation of treatment with the originator TNFi over mandated switching to its biosimilar.	Very low	76

(Continued)

Table 3. (*Cont'd*)

Recommendation	Level of evidence	PICO
RECOMMENDATIONS FOR ADULTS WITH ACTIVE OR STABLE NONRADIOGRAPHIC AXIAL SpA		
80. In adults receiving treatment with TNFi, we conditionally recommend against co-treatment with low-dose methotrexate.	Low	77
DISEASE ACTIVITY ASSESSMENT AND IMAGING		
81. We conditionally recommend the regular-interval use and monitoring of a validated AS disease activity measure.†	Very low	56
82. We conditionally recommend regular-interval use and monitoring of the CRP concentrations or ESR over usual care without regular CRP or ESR monitoring.†	Very low	57
83. In adults with active nonradiographic axial SpA, we conditionally recommend against using a treat-to-target strategy using a target of ASDAS <1.3 (or 2.1) over a treatment strategy based on physician assessment.	Very low	80
84. In adults with nonradiographic axial SpA of unclear activity while on a biologic, we conditionally recommend obtaining a pelvis MRI to assess activity.	Very low	81
85. In adults with stable nonradiographic axial SpA, we conditionally recommend against obtaining a spinal or pelvis MRI to confirm inactivity.	Very low	82
86. In adults with active or stable nonradiographic axial SpA on any treatment, we conditionally recommend against obtaining repeat spine radiographs at a scheduled interval (e.g., every 2 years) as a standard approach.	Very low	83

* SpA = spondyloarthritis; PICO = population, intervention, comparison, and outcomes; NSAIDs = nonsteroidal antiinflammatory drugs; TNFi = tumor necrosis factor inhibitor; AS = ankylosing spondylitis; CRP = C-reactive protein; ESR = erythrocyte sedimentation rate; ASDAS = Ankylosing Spondylitis Disease Activity Score; MRI = magnetic resonance imaging.
† These recommendations were from 2015 and were not reviewed in this update. The number preceding the recommendation is the recommendation number and is referenced as bracketed numbers in Figure 1.

uncertainty regarding potential disease-modifying effects, the committee conditionally favored continuous use of NSAIDs in patients with active AS, primarily for controlling disease activity. The decision to use NSAIDs continuously may vary depending on the severity of symptoms, patient preferences, and comorbidities, particularly gastrointestinal and kidney comorbidities, and cardiovascular disease.

In adults with active AS despite treatment with NSAIDs, we conditionally recommend treatment with sulfasalazine, methotrexate, or tofacitinib over no treatment with these medications (new, PICO 7). Sulfasalazine or methotrexate should be considered only in patients with prominent peripheral arthritis or when tumor necrosis factor inhibitors (TNFi) are not available.

Treatment with sulfasalazine is recommended primarily for patients with prominent peripheral arthritis and few or no axial symptoms. However, TNFi may provide a better option for these patients. Evidence for the efficacy of sulfasalazine is based on 8 older controlled trials that showed benefit for peripheral arthritis (see Supplementary Appendix 6, on the *Arthritis & Rheumatology* web site at http://onlinelibrary.wiley.com/doi/10.1002/art.41042/abstract). Although a recent placebo-controlled trial of sulfasalazine demonstrated improvement in axial symptoms, and modest clinical and imaging responses were seen in a second trial, the preponderance of evidence indicates that sulfasalazine has little benefit for axial symptoms (14,15). Sulfasalazine may have a role in treating patients who have contraindications to TNFi, those who decline treatment with TNFi, or those with limited access to TNFi.

Three trials of methotrexate with negative results tested doses of ≤10 mg weekly, and the lack of benefit may reflect the low doses used (16–18). One uncontrolled study of methotrexate 20 mg weekly showed no improvement in axial symptoms, but a decrease in swollen joint count (19). Treatment with methotrexate may be considered for patients with predominately peripheral arthritis, although among nonbiologics, there is more evidence supporting the use of sulfasalazine.

A phase II study of tofacitinib showed benefit in both clinical and imaging outcomes of axial disease over 12 weeks (20). Use of tofacitinib could be another option, although the results of phase III trials are not available. Leflunomide, apremilast, thalidomide, and pamidronate are not recommended (See Supplementary Appendix 6, available on the *Arthritis & Rheumatology* web site at http://onlinelibrary.wiley.com/doi/10.1002/art.41042/abstract).

In adults with active AS despite treatment with NSAIDs, we strongly recommend treatment with TNFi over no treatment with TNFi (PICO 6).

In adults with active AS despite treatment with NSAIDs, we do not recommend any particular TNFi as the preferred choice (PICO 5).

The efficacy of TNFi in patients with active AS has been demonstrated in 24 randomized controlled trials, most of which were short-term (6 months or shorter) placebo-controlled studies. Improvements were shown in patient-reported outcomes, composite response criteria, and spine and sacroiliac inflammation on magnetic resonance imaging (MRI) (see Supplementary Appendix 6, on the *Arthritis & Rheumatology* web site at http://onlinelibrary.wiley.com/doi/10.1002/art.41042/abstract). The panel judged that the evidence justified a strong recommenda-

tion for use of TNFi in patients whose AS remained active (as defined in Table 1) despite treatment with NSAIDs. The panel recommended that lack of response (or intolerance) to at least 2 different NSAIDs at maximal doses over 1 month, or incomplete responses to at least 2 different NSAIDs over 2 months, would be adequate trials with which to judge NSAID responsiveness prior to escalating to treatment with TNFi.

Indirect comparisons in network meta-analyses of clinical trials have not showed clinically meaningful differences in short-term efficacy among TNFi in the treatment of active AS (see Supplementary Appendix 6, at http://onlinelibrary.wiley.com/doi/10.1002/art.41042/abstract) (21). Direct comparisons among these medications are limited to a trial of infliximab versus its biosimilar, and a very small open-label trial of infliximab versus etanercept (22,23). The panel judged that the evidence did not support preference of 1 TNFi over any other for the typical patient. Important exceptions apply to patients with recurrent uveitis or coexistent IBD (see PICO 29 and PICO 32 below). Patients treated with infliximab may have increased risks of tuberculosis and of infections generally (24,25). TNFi other than infliximab should be considered for patients at higher risk of tuberculosis exposure (either through travel or household contacts) or with a history of recurrent infections. Patient preferences regarding the frequency of dosing and route of administration should be weighed when selecting a specific TNFi.

In adults with active AS despite treatment with NSAIDs, we strongly recommend treatment with secukinumab or ixekizumab over no treatment with secukinumab or ixekizumab (new, PICO 58).

In adults with active AS despite treatment with NSAIDs, we conditionally recommend treatment with TNFi over treatment with secukinumab or ixekizumab (new, PICO 59).

In adults with active AS despite treatment with NSAIDs, we conditionally recommend treatment with TNFi over treatment with tofacitinib (new, PICO 60).

In adults with active AS despite treatment with NSAIDs, we conditionally recommend treatment with secukinumab or ixekizumab over treatment with tofacitinib (new, PICO 61).

The use of secukinumab and ixekizumab in patients with active AS is supported by data from large placebo-controlled trials (see Supplementary Appendix 6, on the *Arthritis & Rheumatology* web site at http://onlinelibrary.wiley.com/doi/10.1002/art.41042/abstract). The panel recommended use of TNFi over secukinumab or ixekizumab based on greater experience with TNFi and familiarity with their long-term safety and toxicity. Similarly, the panel judged that TNFi, secukinumab, or ixekizumab should be used over tofacitinib, given the larger evidence base for TNFi, secukinumab, and ixekizumab. In patients with coexisting ulcerative colitis, if treatment with TNFi is not an option, tofacitinib should be considered over secukinumab or ixekizumab. Interleukin-17 (IL-17) inhibitors have not been shown to be efficacious in IBD, although tofacitinib is an approved treatment for ulcerative colitis (26,27).

In adults with active AS despite treatment with NSAIDs and who have contraindications to TNFi, we conditionally recommend treatment with secukinumab or ixekizumab over treatment with sulfasalazine, methotrexate, or tofacitinib (new, PICO 8).

No studies have directly compared the risks and benefits of treatment alternatives in patients who have contraindications to treatment with TNFi. The panel favored treatment with secukinumab or ixekizumab over treatment with sulfasalazine or methotrexate based on a higher likelihood of benefit, but this recommendation was conditional on the specific contraindication. If the contraindication to TNFi use was the presence of congestive heart failure or demyelinating disease, secukinumab or ixekizumab was preferred, since these medications have not been shown to worsen these conditions. If the contraindication to TNFi use was tuberculosis, other chronic infection, or a high risk of recurrent infections, sulfasalazine was preferred over secukinumab, izekizumab, and tofacitinib. In these cases, efforts to mitigate the infections should be undertaken so that TNFi might safely be used. Treatment with rituximab, abatacept, ustekinumab, or IL-6 inhibitors is not recommended, even in patients with contraindications to TNFi, due to lack of effectiveness.

In adults with active AS despite treatment with the first TNFi used, we conditionally recommend treatment with secukinumab or ixekizumab over treatment with a different TNFi in patients with primary nonresponse to TNFi (new, PICO 10).

In adults with active AS despite treatment with the first TNFi used, we conditionally recommend treatment with a different TNFi over treatment with a non-TNFi biologic in patients with secondary nonresponse to TNFi (new, PICO 10).

In adults with active AS despite treatment with the first TNFi used, we strongly recommend against switching to treatment with a biosimilar of the first TNFi (new, PICO 62).

In adults with active AS despite treatment with the first TNFi used, we conditionally recommend against the addition of sulfasalazine or methotrexate in favor of switching to a new biologic (PICO 9).

Direct comparisons of treatment strategies for patients who do not have or sustain adequate responses to their first TNFi have not been reported, and the recommendations are based on the panel's consideration of indirect comparisons among the available treatment options (see Supplementary Appendix 6, at http://onlinelibrary.wiley.com/doi/10.1002/art.41042/abstract). Data from observational studies suggest that 25–40% of patients who switch from one TNFi to another will have a meaningful response (e.g.,

50% improvement in Bath AS Disease Activity Index) to the second TNFi (28–30). However, not all patients in these studies switched TNFi because of ineffectiveness.

The panel judged that treatment should differ for patients who had a primary nonresponse to TNFi and those with secondary nonresponse to TNFi. Switching to secukinumab or ixekizumab was recommended in most patients who had a primary nonresponse to the first TNFi, under the assumption that TNF was not the key inflammatory mediator in these patients. Continuing treatment with the first TNFi could be considered if additional time was believed important to assess the response fully, or if a higher dose or shorter dosing interval was thought to be beneficial.

In patients who relapse after an initial response (i.e., secondary nonresponse), the panel judged that treatment with a different TNFi held a reasonable prospect of benefit and should be used in most patients, rather than immediately switching to a different class of biologics. Although ixekizumab is efficacious among TNFi nonresponders, trials have not directly compared responses to ixekizumab (or secukinumab) to responses to a second TNFi in patients with a secondary nonresponse to the first TNFi (11). Given that options for biologics are limited, treatment with a second TNFi was recommended in these patients.

In cases of nonresponse (primary or secondary), the panel recommended against switching to the biosimilar of the first TNFi (e.g., switching from originator infliximab to infliximab-dyyb), as the clinical response would not be expected to be different. The panel also recommended against the addition of sulfasalazine or methotrexate to TNFi in cases of nonresponse to TNFi, judging any benefit would likely be marginal. The addition of sulfasalazine could be considered in the rare patient whose axial symptoms are well-controlled with TNFi but who has active peripheral arthritis.

In adults with either active or stable AS on treatment with TNFi, we conditionally recommend against co-treatment with low-dose methotrexate (new, PICO 64).

In rheumatoid arthritis, the likelihood of TNFi discontinuation is lower among patients who receive co-treatment with methotrexate, perhaps by reducing the development of antidrug antibodies (31). In AS, it is less clear whether the duration of TNFi use, and by inference their effectiveness, is similarly prolonged (32). Data from observational studies are conflicting, although some studies, primarily of infliximab, showed longer TNFi treatment when methotrexate was co-administered (see Supplementary Appendix 6 at http://onlinelibrary.wiley.com/doi/10.1002/art.41042/abstract). Clinical responses were not greater among patients who received co-treatment with methotrexate. In the absence of convincing evidence of benefit, and due to greater burden for patients, the panel recommended against routine co-administration of methotrexate with TNFi, although its use could be considered in patients treated with infliximab.

B. Recommendations for the treatment of patients with stable AS

In adults with stable AS, we conditionally recommend on-demand treatment with NSAIDs over continuous treatment with NSAIDs (PICO 1).

This recommendation applies to patients whose AS has been stable while not receiving any pharmacologic treatment. In this group, the panel considered that the potential toxicities of continuous NSAID treatment outweighed the uncertain benefit of less radiographic progression. On-demand treatment should be considered for short-term symptom recurrences (flares).

In adults with stable AS receiving treatment with TNFi and NSAIDs, we conditionally recommend continuing treatment with TNFi alone over continuing both medications (PICO 11).

In adults with stable AS receiving treatment with TNFi and a conventional synthetic antirheumatic drug, we conditionally recommend continuing treatment with TNFi alone over continuing both medications (PICO 12).

No new studies have directly compared outcomes between patients who continued combination treatment and those who discontinued either NSAIDs or a conventional synthetic antirheumatic drug (csARD). The NSAID-sparing potential of etanercept was demonstrated in a recent trial (33). The panel judged these recommendations primarily based on symptom control, rather than on any potential effect of combination therapy on future spinal fusion. In stable patients, a trial of withdrawing either the NSAIDs or the csARD should be considered, due to the likelihood of greater toxicity with the long-term use of more than one medication. However, on-demand NSAID treatment for control of intermittent symptoms is recommended for patients with good responses to previous courses of NSAIDs.

In adults with stable AS receiving treatment with a biologic, we conditionally recommend against discontinuation of the biologic (new, PICO 66).

In adults with stable AS receiving treatment with a biologic, we conditionally recommend against tapering of the biologic dose as a standard approach (new, PICO 65).

Data from several observational studies suggest that discontinuation of TNFi after achieving either remission or low disease activity results in relapses in 60–74% of patients, occasionally within a few weeks to months from discontinuation (see Supplementary Appendix 6, available at http://onlinelibrary.wiley.com/doi/10.1002/art.41042/abstract). Although the data only concerned TNFi discontinuation, the panel judged that a similar recommendation would also apply to other biologics. In general, treatment with a biologic should be planned to be

continued long-term, barring toxicities. Discontinuation might be considered in patients in sustained remission (i.e., several years), with the anticipation that only one-third of patients would not experience relapse. Patient preferences should help guide this decision.

Tapering of TNFi could entail a change in either the dose or frequency of administration. Two controlled unblinded trials of tapering etanercept to 25 mg weekly versus maintaining the dose at 50 mg weekly in patients with stable AS showed that remission or partial remission was somewhat less likely among those in whom etanercept was tapered (34,35). In small observational studies, 53–70% of patients were still receiving their reduced dose at 2 years, but there is little evidence regarding maintenance of long-term remission after tapering of TNFi (see Supplementary Appendix 6, available at http://onlinelibrary.wiley.com/doi/10.1002/art.41042/abstract). Therefore, the panel recommended against tapering of biologics as a standard approach. One condition in which tapering could be considered would be in patients with prolonged stable AS, if the patient and provider engage in shared decision-making.

In adults with stable AS receiving an originator TNFi, we strongly recommend continuing treatment with the originator TNFi over mandated switching to its biosimilar (new, PICO 63).

While the efficacy of originator and biosimilar TNFi is comparable, and although either could be chosen to initiate new courses of TNFi treatment, it was the opinion of the panel to recommend against mandated switching to a biosimilar during the course of treatment, in the absence of evidence of interchangability. Medication changes can increase the risk of destabilizing a patient's condition, and the panel judged that additional data were needed to understand the frequency of potential problems and concerns associated with switching patients who were stable on an originator TNFi to its biosimilar. Given these concerns, the panel judged that there should be a compelling rationale for switching medications, particularly in light of the marginal cost savings apparent for US patients (36).

C. Recommendations for adults with AS-related comorbidities

In adults with AS and recurrent uveitis, we conditionally recommend treatment with TNFi monoclonal antibodies over treatment with other biologics (PICO 29).

Evidence for this recommendation is limited to indirect comparisons of the rates of acute uveitis episodes in clinical trials or observational studies, rather than from direct comparisons (see Supplementary Appendix 6, available at http://onlinelibrary.wiley.com/doi/10.1002/art.41042/abstract). Many reports showed overall rates of uveitis without separately reporting recurrences as opposed to incident episodes (37). The rates were generally lower for adalimumab and infliximab compared to etanercept. For example, a large observational study demonstrated rates of uveitis (per 100 patient-years) in patients receiving adalimumab, infliximab, and etanercept of 13.6, 27.5, and 60.3, respectively, compared to pretreatment rates of 36.8, 45.5, and 41.6, respectively (38). Adalimumab or infliximab are preferred over etanercept for the treatment of AS in patients with recurrent uveitis. Certolizumab or golimumab may also be considered, although supporting data are less substantial (39,40). Data from clinical trials suggest that rates of uveitis flares were not different between patients with AS treated with secukinumab and those treated with placebo, but more evidence is needed. Secukinumab was not efficacious in the treatment of panuveitis or posterior uveitis (41). Rates of uveitis flares among patients treated with ixekizumab have not been well-defined.

In adults with AS and IBD, we conditionally recommend treatment with TNFi monoclonal antibodies over treatment with other biologics (PICO 32).

This recommendation was based on limited indirect evidence on the risks of flares or new onset of IBD among patients with AS during treatment with biologics, and the much larger literature on the treatment of IBD in general. Patients with AS treated with infliximab or adalimumab have lower risks of IBD exacerbations than those treated with etanercept (see Supplementary Appendix 6, on the *Arthritis & Rheumatology* web site at http://onlinelibrary.wiley.com/doi/10.1002/art.41042/abstract). Infliximab, adalimumab, and certolizumab are approved for the treatment of Crohn's disease, and infliximab, adalimumab, and golimumab are approved for the treatment of ulcerative colitis, while etanercept is not approved for either condition (42,43). This evidence is the basis for the recommendation favoring TNFi monoclonal antibody use in patients with AS and coexisting IBD. The choice of the particular TNFi monoclonal antibody should be made in consultation with the patient's gastroenterologist. Secukinumab has been associated with the new onset, or exacerbation, of Crohn's disease (44–46). Increased risks of IBD exacerbation appear to also occur with ixekizumab (47).

D. Recommendations for the treatment of patients with either active or stable nonradiographic axial spondyloarthritis

Parallel questions on pharmacologic treatment were investigated for patients with nonradiographic axial SpA. There were no relevant published data for 19 questions. There was high-quality evidence only for the use of TNFi in nonradiographic axial SpA, which was examined in several clinical trials. Low-quality or very low-quality evidence from single studies suggested no differences in outcomes among different TNFi in nonradiographic axial SpA, high likelihood of relapse following discontinuation of TNFi, and no association between co-treatment with nonbiologics and TNFi persistence (see Supplementary Appendix 6, available at http://onlinelibrary.wiley.com/doi/10.1002/art.41042/abstract).

Therefore, the recommendations for nonradiographic axial SpA were largely extrapolated from evidence in AS (Table 3). The recommendations were identical in both patient groups with 1 notable exception: treatment with secukinumab or ixekizumab was strongly recommended over no treatment with secukinumab or ixekizumab in patients with AS, while use of these medications was conditionally recommended in patients with nonradiographic axial SPA, because trials in nonradiographic axial SPA have not been reported. Evidence on tofacitinib in nonradiographic axial SpA has not been reported.

E. Disease activity assessment and imaging

In adults with active AS, we conditionally recommend against using the treat-to-target strategy, which aims at a target of an Ankylosing Spondylitis Disease Activity Score <1.3 (or 2.1), over a treatment strategy based on physician assessment (new, PICO 67).

The concept of treat-to-target strategies is well-founded in chronic disease management for conditions that have an accurate measure of disease activity (often one that is asymptomatic, as in blood pressure or glycosylated hemoglobin), a tight link between this disease activity measure and future health outcomes, and evidence that maintaining a particular target in the disease activity measure is closely associated with better long-term health (48). The treat-to-target approach in AS is indirectly supported by associations between levels of AS activity and future radiographic progression but lacks robust direct evidence. Because adoption of this strategy would place additional burdens on patients and providers, the panel judged that more convincing evidence of benefit should be present before endorsing this change in practice. There was also concern that focus on a specific target could lead to rapid cycling through all currently available treatments in some patients. As reflected in the 2015 guidelines, quantifying disease activity is important to help guide treatment decisions.

In adults with AS of unclear activity while receiving a biologic, we conditionally recommend obtaining a spinal or pelvis MRI to assess activity (new, PICO 68).

In adults with nonradiographic axial SpA of unclear activity while receiving a biologic, we conditionally recommend obtaining a pelvis MRI to assess activity (new, PICO 81).

Because physical and laboratory measures are often normal despite active axial SpA, and because symptoms may be nonspecific, it may be difficult to know whether a patient is experiencing inflammation that warrants a change in treatment. Limited evidence suggests that knowledge of MRI findings in the spine and sacroiliac joints may alter treatment recommendations. However, the degree of inflammatory change on MRI may not correlate with treatment responses, and the location of inflammation on MRI may not correlate with the location of pain (49) (see Supplementary Appendix 6, available at http://onlinelibrary.wiley.com/doi/10.1002/art.41042/abstract). The panel judged that MRI could provide useful information in cases where the level of disease activity was unclear and where this information would influence treatment decisions. For patients with nonradiographic axial SpA, the imaging should focus on the sacroiliac joints. In interpreting MRI results, it is important to keep in mind the range and frequency of abnormalities, including bone marrow edema lesions, that may occur in individuals without axial SpA and that may not represent inflammation due to axial SpA (50,51). MRI is not recommended in patients in whom disease activity is either clearly clinically active or clinically stable, or when the results of MRI would not be expected to change treatment.

In adults with stable AS, we conditionally recommend against obtaining a spinal or pelvis MRI to confirm inactivity (new, PICO 69).

In adults with stable nonradiographic axial SpA, we conditionally recommend against obtaining a spine or pelvis MRI to confirm inactivity (new, PICO 82).

Because the clinical assessment of inflammation in axial SpA has many limitations, questions may arise about whether subclinical inflammation that could be detected by MRI is being "missed" by either the physical examination, symptoms, or laboratory studies. Given the lack of evidence that obtaining an MRI in stable patients improves clinical outcomes, the only moderate sensitivity and specificity of MRI-defined abnormalities for measurement of activity in axial SpA, the burden of testing, and concern for possible overtreatment, the panel recommended against obtaining an MRI in this setting. MRI could be considered in circumstances where the clinician and patient differ in their assessment of whether the disease is stable.

In adults with active or stable AS receiving any treatment, we conditionally recommend against obtaining repeat spine radiographs at a scheduled interval (e.g., every 2 years) as a standard approach (new, PICO 70).

In adults with active or stable nonradiographic axial SpA on any treatment, we conditionally recommend against obtaining repeat spine radiographs at a scheduled interval (e.g., every 2 years) as a standard approach (new, PICO 83).

Spine radiographs are useful for the diagnosis of axial SpA, in evaluating the extent of spinal fusion, and for investigating new spinal pain in patients with established AS. In research studies, small changes in the extent of spine damage can be detected in 20–35% of patients with AS over a 2-year interval (see Supplementary Appendix 6, available at http://onlinelibrary.wiley.com/doi/10.1002/art.41042/abstract). There is no evidence that monitoring serial changes in

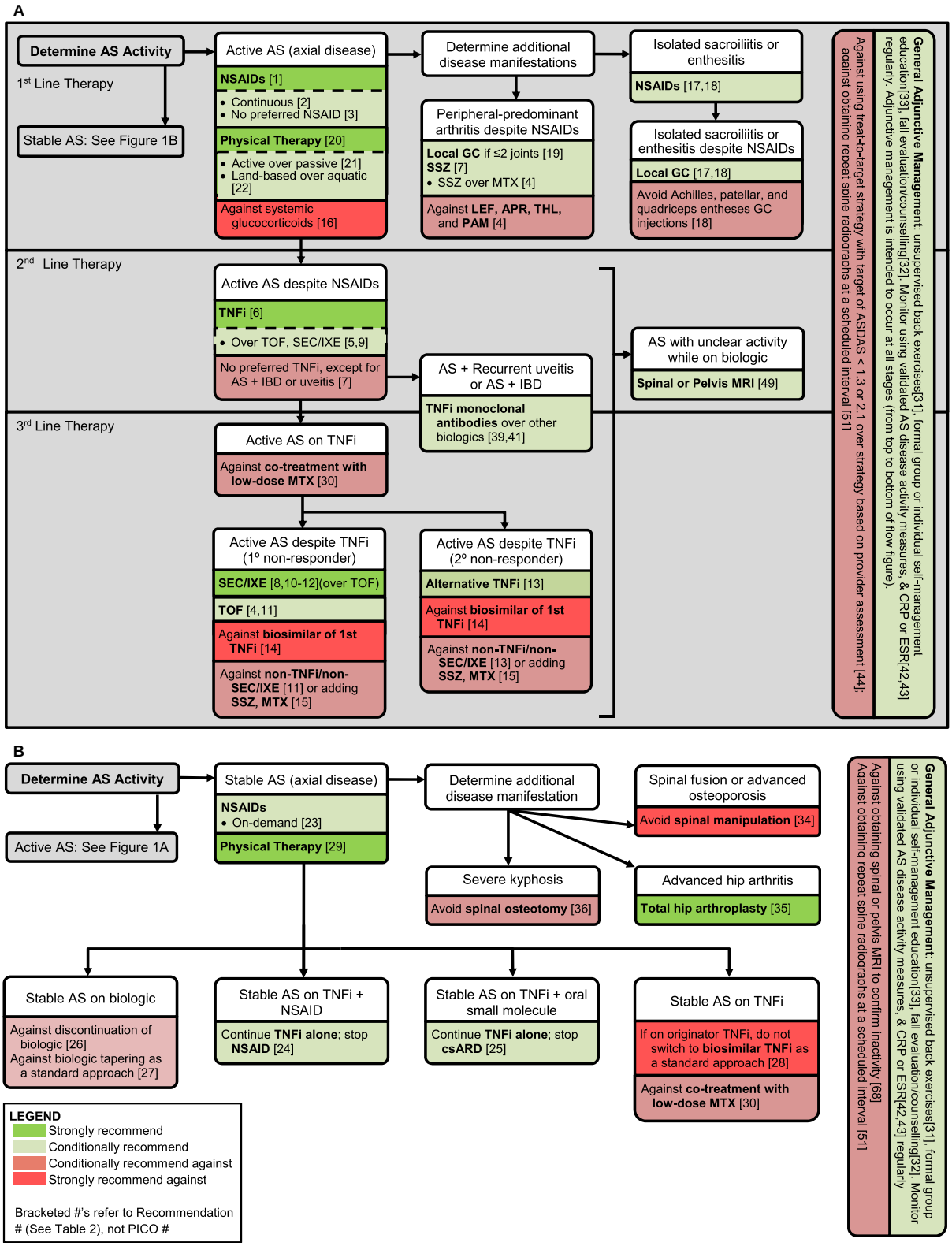

Figure 1. Summary of the main recommendations for the treatment of patients with **A,** active ankylosing spondylitis and **B,** stable ankylosing spondylitis. AS = ankylosing spondylitis; NSAIDs = nonsteroidal antiinflammatory drugs; GC = glucocorticoid; SSZ = sulfasalazine; MTX = methotrexate; LEF = leflunomide; APR = apremilast; THL = thalidomide; PAM = pamidronate; TNFi = tumor necrosis factor inhibitor; TOF = tofacitinib; SEC = secukinumab; IXE = ixekizumab; IBD = inflammatory bowel disease; csARD = conventional synthetic antirheumatic drugs; ESR = erythrocyte sedimentation rate; CRP = C-reactive protein level; ASDAS = Ankylosing Spondylitis Disease Activity Score; MRI = magnetic resonance imaging; PICO = population, intervention, comparison, and outcomes.

spine radiographs at a regular interval leads to better patient outcomes, and data balancing a clinical benefit with the risk of radiation exposure are absent. Therefore, the panel recommended against repeating spine radiographs as a standard approach. In the absence of clinical indications, repeat spine radiographs could be considered on an ad hoc basis for counseling patients on the progression of their disease, which may help in career and life planning.

F. Summary of recommendations

Figure 1 presents a diagram of the main treatment recommendations for active and stable AS, integrating the new recommendations with the 2015 recommendations that were not updated in this review.

DISCUSSION

This update was primarily motivated by the availability of new treatment options, notably secukinumab, ixekizumab, tofacitinib, and TNFi biosimilars, for patients with axial SpA. Providers and patients have questions on where these new medications fit in the pharmacologic strategy, and how originator TNFi, sulfasalazine, and NSAIDs should be used given these new options. Based on the current evidence and the considerations of the panel, NSAIDs and TNFi remain the primary classes of medications for the treatment of AS and nonradiographic axial SpA. Secukinumab or ixekizumab is recommended for patients with active disease who have heart failure or demyelinating disease as a contraindication to TNFi, and in primary nonresponders to TNFi. Secukinumab and ixekizumab are not recommended in patients with IBD or recurrent uveitis, as TNFi monoclonal antibodies are better options. Tofacitinib is a potential second-line option for patients with contraindications to TNFi other than infections. Recommendations regarding tofacitinib may change pending the results of larger clinical trials.

Several of the 2015 recommendations were modified in this update. The current recommendation is conditionally in favor of use of sulfasalazine in limited clinical circumstances, whereas the 2015 recommendations had this as an exception to the general recommendation against the use of conventional synthetic antirheumatic drugs. In the 2015 recommendations, sulfasalazine and pamidronate were suggested as alternatives for the treatment of patients with active disease and contraindications to TNFi, while the current recommendations suggest use of secukinumab or ixekizumab in most of these cases (except patients with high risk of infections). In cases of failure of TNFi, the 2015 guidelines included a conditional recommendation for a trial of a second TNFi and against use of a non-TNFi biologic, whereas the current guidelines differentiate treatment recommendations based on whether there was primary or secondary nonresponse to the TNFi. For the treatment of patients with recurrent uveitis, the previous guidelines specified conditional use of infliximab or adalimumab, while the update broadened this recommendation to include TNFi monoclonal antibodies generally. Similarly, for patients with coexisting IBD, the update includes a conditional recommendation for TNFi monoclonal antibodies over other biologics, rather than over only etanercept. Finally, the recommendation for use of TNFi in patients with active nonradiographic axial SpA was changed from conditional to strong.

New questions on the treatment of patients with stable disease were addressed in this update. Discontinuation of biologics is not recommended due to the likelihood for symptom recurrence. If tapering is considered, patients should be counseled regarding the potential for increased disease activity. Co-treatment with low-dose methotrexate is not generally recommended, but ongoing studies will shed further light on this question. Switching to a biosimilar during the course of treatment with TNFi is also not recommended, echoing the concerns previously expressed by the ACR (52).

Imaging remains a central tool in the diagnosis of axial SpA, but its role in monitoring patients is less well-defined. Spine and/or pelvis MRI could aid in the evaluation of patients in whom the degree of active inflammation is uncertain, and especially in those for whom the findings would change management. MRI is not recommended to seek subclinical inflammation in patients with stable disease (as defined in Table 1). However, MRI could be considered in circumstances where it may inform shared decision-making. We recommend against obtaining spine radiographs on scheduled intervals to monitor progression. This practice entails radiation exposure and would not alter treatment in most cases.

We used the GRADE method to develop these treatment recommendations in a way that was transparent, systematic, and explicit, and that was informed by the medical evidence as well as patient preferences. The major limitation of these guidelines is the very low quality of evidence for many recommendations, which necessitated reliance on the clinical expertise of the panel. For nonradiographic axial SpA, most recommendations were based on extrapolation of results from studies in AS. We tried to identify the most common and consequential treatment questions, so that the recommendations would be useful in guiding clinical decision-making. The low quality of evidence for many questions is an indication that research has not yet tackled many of the most important treatment questions. As more treatment options become available, this problem will grow. Importantly, failure to recommend a particular medication does not imply that it is contraindicated. Key evidence gaps include the comparative effectiveness and safety of different biologics, the optimal sequencing of treatments, and the role of NSAIDs.

This update addressed only a subset of treatment questions. The 2015 recommendations that were not reexamined are to be considered extant. Recommendations are meant to describe the approach to treatment of the typical patient and cannot anticipate all possible clinical scenarios. Application of these recommendations must be individualized, and requires

careful assessment, sound clinical judgment of each patient's circumstances, and consideration of a patient's preferences.

ACKNOWLEDGMENTS

We thank Cassie Shafer and Elin Aslanyan of the SAA for their partnership on this project. We thank SPARTAN for its partnership on this project. We thank our patient representatives for adding valuable perspectives. We thank the ACR staff, including Ms Regina Parker for assistance in organizing the face-to-face meeting and coordinating the administrative aspects of the project, and Ms Robin Lane for assistance in manuscript preparation. We thank Ms Janet Waters for help in developing the literature search strategy and performing the literature search and updates, and Ms Janet Joyce for peer-reviewing the literature search strategy.

AUTHOR CONTRIBUTIONS

All authors were involved in drafting the article or revising it critically for important intellectual content, and all authors approved the final version to be published. Dr. Ward had full access to all of the data in the study and takes responsibility for the integrity of the data and the accuracy of the data analysis.

Study conception and design. Ward, Deodhar, Turner, Caplan.

Acquisition of data. Ward, Deodhar, Shah, Sullivan, Turgunbaev, Oristaglio, Caplan.

Analysis and interpretation of data. Ward, Deodhar, Gensler, Dubreuil, Yu, Khan, Haroon, Borenstein, Wang, Biehl, Fang, Louie, Majithia, Ng, Bigham, Pianin, Shah, Sullivan, Turgunbaev, Oristaglio, Maksymowych, Caplan.

REFERENCES

1. Taurog JD, Chhabra A, Colbert RA. Ankylosing spondylitis and axial spondyloarthritis. N Engl J Med 2016;374:2563–74.
2. Van der Linden S, Valkenburg HA, Cats A. Evaluation of diagnostic criteria for ankylosing spondylitis: a proposal for modification of the New York criteria. Arthritis Rheum 1984;27:361–8.
3. Wang R, Ward MM. Epidemiology of axial spondyloarthritis: an update. Curr Opin Rheumatol 2018;30:137–43.
4. Rudwaleit M, van der Heidje D, Landewé R, Listing J, Akkoc N, Brandt J, et al. The development of the Assessment of SpondyloArthritis international Society classification criteria for axial spondyloarthritis (part II): validation and final selection. Ann Rheum Dis 2009;68:777–83.
5. Boonen A, Sieper J, van der Heijde D, Dougados M, Bukowski JF, Valluri S, et al. The burden of non-radiographic axial spondyloarthritis. Sem Arthritis Rheum 2015;44:556–62.
6. Ward MM. Quality of life in patients with ankylosing spondylitis. Rheum Dis Clin North Am 1998;24:815–27.
7. Ward MM, Deodhar A, Akl EA, Lui A, Ermann J, Gensler LS, et al. American College of Rheumatology/Spondylitis Association of America/Spondyloarthritis Research and Treatment Network 2015 recommendations for the treatment of ankylosing spondylitis and nonradiographic axial spondyloarthritis. Arthritis Care Res 2016;68:151–66.
8. Guyatt G, Oxman AD, Akl EA, Kunz R, Vist G, Brozek J, et al. GRADE guidelines: 1. Introduction—GRADE evidence profiles and summary of findings tables. J Clin Epidemiol 2011;64:383–94.
9. Guyatt GH, Oxman AD, Kunz R, Falck-Ytter Y, Vist GE, Liberati A, et al. Rating quality of evidence and strength of recommendations: going from evidence to recommendations. BMJ 2008;336:1049–51.
10. Van der Heijde D, Wei JC, Dougados M, Mease P, Deodhar A, Maksymowych WP, et al. Ixekizumab, an interleukin-17A antagonist in the treatment of ankylosing spondylitis or radiographic axial spondyloarthritis in patients previously untreated with biological disease-modifying anti-rheumatic drugs (COAST-V): 16 week results of a phase 3 randomised, double-blind, active-controlled and placebo-controlled trial. Lancet 2018;392:2441–51.
11. Deodhar A, Poddubnyy D, Pacheco-Tena C, Salvarani C, Lespessailles E, Rahman P, et al. Efficacy and safety of ixekizumab in the treatment of radiographic axial spondyloarthritis: sixteen-week results from a phase III randomized, double-blind, placebo-controlled trial in patients with prior inadequate response to or intolerance of tumor necrosis factor inhibitors. Arthritis Rheumatol 2019;71:599–611.
12. Wanders A, van der Heijde D, Landewé R, Behier JM, Calin A, Olivieri I, et al. Nonsteroidal antiinflammatory drugs reduce radiographic progression in patients with ankylosing spondylitis: a randomized clinical trial. Arthritis Rheum 2005;52:1756–65.
13. Sieper J, Listing J, Poddubnyy D, Song IH, Hermann KG, Callhoff J, et al. Effect of continuous versus on-demand treatment of ankylosing spondylitis with diclofenac over 2 years on radiographic progression of the spine: results from a randomised multicentre trial (ENRADAS). Ann Rheum Dis 2016;75:1438–43.
14. Khanna Sharma S, Kadiyala V, Naidu G, Dhir V. A randomized controlled trial to study the efficacy of sulfasalazine for axial disease in ankylosing spondylitis. Int J Rheum Dis 2018;21:308–14.
15. Song IH, Hermann KG, Haibel H, Althoff CE, Listing J, Burmester GR, et al. Effects of etanercept versus sulfasalazine in early axial spondyloarthritis on active inflammatory lesions as detected by whole-body MRI (ESTHER): a 48-week randomised controlled trial. Ann Rheum Dis 2011;70:590–6.
16. Altan L, Bingol U, Karakoc Y, Aydiner S, Yurtkuran M, Yurtkuran M. Clinical investigation of methotrexate in the treatment of ankylosing spondylitis. Scand J Rheumatol 2001;30:255–9.
17. Roychowdhury B, Bintley-Bagot S, Bulgen DY, Thompson RN, Tunn EJ, Moots RJ. Is methotrexate effective in ankylosing spondylitis? Rheumatology (Oxford) 2002;41:1330–2.
18. Gonzalez-Lopez L, Garcia-Gonzalez A, Vazquez-Del-Mercado M, Munoz-Valle JF, Gamez-Nava JI. Efficacy of methotrexate in ankylosing spondylitis: a randomized, double blind, placebo controlled trial. J Rheumatol 2004;31:1568–74.
19. Haibel H, Brandt HC, Song IH, Brandt A, Listing J, Rudwaleit M, et al. No efficacy of subcutaneous methotrexate in active ankylosing spondylitis: a 16-week open-label trial. Ann Rheum Dis 2007;66:419–21.
20. Van der Heijde D, Deodhar A, Wei JC, Drescher E, Fleishaker D, Hendrikx T, et al. Tofacitinib in patients with ankylosing spondylitis: a phase II, 16-week, randomised, placebo-controlled, dose-ranging study. Ann Rheum Dis 2017;76:1340–7.
21. Wang R, Dasgupta A, Ward MM. Comparative efficacy of tumor necrosis factor-α inhibitors in ankylosing spondylitis: a systematic review and Bayesian network metaanalysis. J Rheumatol 2018;45:481–90.
22. Park W, Hrycaj P, Jeka S, Kovalenko V, Lysenko G, Miranda P, et al. A randomised, double-blind, multicentre, parallel-group, prospective study comparing the pharmacokinetics, safety, and efficacy of CT-P13 and innovator infliximab in patients with ankylosing spondylitis: the PLANETAS study. Ann Rheum Dis 2013;72:1605–12.
23. Giardina AR, Ferrante A, Ciccia F, Impastato R, Miceli MC, Principato A, et al. A 2-year comparative open label randomized study

of efficacy and safety of etanercept and infliximab in patients with ankylosing spondylitis. Rheumatol Int 2010;30:1437–40.

24. Souto A, Maneiro JR, Salgado E, Carmona L, Gomez-Reino JJ. Risk of tuberculosis in patients with chronic immune-mediated inflammatory diseases treated with biologics and tofacitinib: a systematic review and meta-analysis of randomized controlled trials and long-term extension studies. Rheumatology (Oxford) 2014;53:1872–85.
25. Yun H, Xie F, Delzell E, Chen L, Levitan EB, Lewis JD, et al. Risk of hospitalised infection in rheumatoid arthritis patients receiving biologics following a previous infection while on treatment with anti-TNF therapy. Ann Rheum Dis 2015;74:1065–71.
26. Hueber W, Sands BE, Lewitzky S, Vandemeulebroecke M, Reinisch W, Higgins PD, et al. Secukinumab, a human anti-IL-17A monoclonal antibody, for moderate to severe Crohn's disease: unexpected results of a randomised, double-blind placebo-controlled trial. Gut 2012;61:1693–700.
27. Sandborn WJ, Su C, Sands BE, D'Haens GR, Vermeire S, Schreiber S, et al. Tofacitinib as induction and maintenance therapy for ulcerative colitis. N Engl J Med 2017;376:1723–36.
28. Rudwaleit M, Van den Bosch F, Kron M, Kary S, Kupper H. Effectiveness and safety of adalimumab in patients with ankylosing spondylitis or psoriatic arthritis and history of anti-tumor necrosis factor therapy. Arthritis Res Ther 2010;12:R117.
29. Paccou J, Solau-Gervais E, Houvenagel E, Salleron J, Luraschi H, Philippe P, et al. Efficacy in current practice of switching between anti-tumour necrosis factor-α agents in spondyloarthropathies. Rheumatology (Oxford) 2011;50:714–20.
30. Ciurea A, Exer P, Weber U, Tamborrini G, Steininger B, Kissling RO, et al. Does the reason for discontinuation of a first TNF inhibitor influence the effectiveness of a second TNF inhibitor in axial spondyloarthritis? Results from the Swiss Clinical Quality Management Cohort. Arthritis Res Ther 2016;18:71.
31. Souto A, Maneiro JR, Gomez-Reino JJ. Rate of discontinuation and drug survival of biologic therapies in rheumatoid arthritis: a systematic review and meta-analysis of drug registries and health care databases. Rheumatology (Oxford) 2015;55:523–34.
32. Heiberg MS, Koldingsnes W, Mikkelsen K, Rødevand E, Kaufmann C, Mowinckel P, et al. The comparative one-year performance of anti–tumor necrosis factor α drugs in patients with rheumatoid arthritis, psoriatic arthritis, and ankylosing spondylitis: results from a longitudinal, observational, multicenter study. Arthritis Care Res (Hoboken) 2008;59:234–40.
33. Dougados M, Wood E, Combe B, Schaeverbeke T, Miceli-Richard C, Berenbaum F, et al. Evaluation of the nonsteroidal anti-inflammatory drug-sparing effect of etanercept in axial spondyloarthritis: results of the multicenter, randomized, double-blind, placebo-controlled SPARSE study. Arthritis Res Ther 2014;16:481.
34. Yates M, Hamilton LE, Elender F, Dean L, Doll H, MacGregor AJ, et al. Is etanercept 25 mg once weekly as effective as 50 mg at maintaining response in patients with ankylosing spondylitis? A randomized controlled trial. J Rheumatol 2015;42:1177–85.
35. Cantini F, Niccoli L, Cassara E, Kaloudi O, Nannini C. Duration of remission after halving of the etanercept dose in patients with ankylosing spondylitis: a randomized, prospective, long-term, follow-up study. Biologics 2013;7:1–6.
36. Yazdany J, Dudley RA, Lin GA, Chen R, Tseng CW. Out-of-pocket costs for infliximab and its biosimilar for rheumatoid arthritis under Medicare part D. JAMA 2018;320:931–3.
37. Rudwaleit M, Rødevand E, Holck P, Vanhoof J, Kron M, Kary S, et al. Adalimumab effectively reduces the rate of anterior uveitis flares in patients with active ankylosing spondylitis: results of a prospective open-label study. Ann Rheum Dis 2009;68:696–701.
38. Lie E, Lindström U, Zverkova-Sandström T, Olsen IC, Forsblad-d'Elia H, Askling J, et al. Tumour necrosis factor inhibitor treatment and occurrence of anterior uveitis in ankylosing spondylitis: results from the Swedish biologics register. Ann Rheum Dis 2017;76:1515–21.
39. Rudwaleit M, Rosenbaum JT, Landewé R, Marzo-Ortega H, Sieper J, Van Der Heijde D, et al. Observed incidence of uveitis following certolizumab pegol treatment in patients with axial spondyloarthritis. Arthritis Care Res (Hoboken) 2016;68:838–44.
40. Calvo-Río V, Blanco R, Santos-Gómez M, Rubio-Romero E, Cordero-Coma M, Gallego-Flores A, et al. Golimumab in refractory uveitis related to spondyloarthritis. Multicenter study of 15 patients. Semin Arthritis Rheum 2016;46:95–101.
41. Dick AD, Tugal-Tutkun I, Foster S, Zierhut M, Liew SH, Bezlyak V, et al. Secukinumab in the treatment of noninfectious uveitis: results of three randomized, controlled clinical trials. Ophthalmology 2013;120:777–87.
42. Kornbluth A, Sachar DB. Ulcerative colitis practice guidelines in adults: American College of Gastroenterology practice parameters committee. Am J Gastroenterol 2010;105:501–23.
43. Lichtenstein GR, Loftus EV, Isaacs KL, Regueiro MD, Gerson LB, Sands BE. ACG clinical guideline: management of Crohn's disease in adults. Am J Gastroenterol 2018;113:481–517.
44. Hueber W, Sands BE, Lewitzky S, Vandemeulebroecke M, Reinisch W, Higgins PD, et al. Secukinumab, a human anti-IL-17A monoclonal antibody, for moderate to severe Crohn's disease: unexpected results of a randomised, double-blind placebo-controlled trial. Gut 2012;61:1693–700.
45. Targan SR, Feagan BG, Vermeire S, Panaccione R, Melmed GY, Blosch C, et al. A randomized, double-blind, placebo-controlled study to evaluate the safety, tolerability, and efficacy of AMG 827 in subjects with moderate to severe Crohn's disease. Gastroenterology 2012;143:e26.
46. Baeten D, Sieper J, Braun J, Baraliakos X, Dougados M, Emery P, et al. Secukinumab, an interleukin-17a inhibitor, in ankylosing spondylitis. N Engl J Med 2015;373:2534–48.
47. Reich K, Leonardi C, Langley RG, Warren RB, Bachelez H, Romiti R, et al. Inflammatory bowel disease among patients with psoriasis treated with ixekizumab: a presentation of adjudicated data from an integrated database of 7 randomized controlled and uncontrolled trials. J Am Acad Dermatol 2017;76:441–8.
48. Atar D, Birkeland KI, Uhlig T. 'Treat to target': moving targets from hypertension, hyperlipidaemia and diabetes to rheumatoid arthritis. Ann Rheum Dis 2010;69:629–30.
49. De Hooge M, de Bruin F, de Beer L, Bakker P, van den Berg R, Ramiro S, et al. Is the site of back pain related to the location of magnetic resonance imaging lesions in patients with chronic back pain? Results from the Spondyloarthritis Caught Early Cohort. Arthritis Care Res (Hoboken) 2017;69:717–23.
50. De Winter J, de Hooge M, van de Sande M, de Jong H, van Hoeven L, de Koning A, et al. Magnetic resonance imaging of the sacroiliac joints indicating sacroiliitis according to the Assessment of SpondyloArthritis international Society definition in healthy individuals, runners, and women with postpartum back pain. Arthritis Rheumatol 2018;70:1042–8.
51. De Hooge M, van den Berg R, Navarro-Compán V, Reijnierse M, van Gaalen F, Fagerli K, et al. Patients with chronic back pain of short duration from the SPACE cohort: which MRI structural lesions in the sacroiliac joints and inflammatory and structural lesions in the spine are most specific for axial spondyloarthritis? Ann Rheum Dis 2016;75:1308–14.
52. American College of Rheumatology. Position statement: biosimilars. 2018. URL: www.rheumatology.org/Portals/0/Files/Biosimilars-Position-Statement.pdf.

American College of Rheumatology
Empowering Rheumatology Professionals

Arthritis & Rheumatology
Vol. 71, No. 10, October 2019, pp 1614–1615
DOI 10.1002/art.41053

IN MEMORIAM

Gerald Weissmann, MD, 1930–2019

It is in our genes to understand the universe if we can, to keep trying even if we cannot, and to be enchanted by the act of learning all the way.

Lewis Thomas

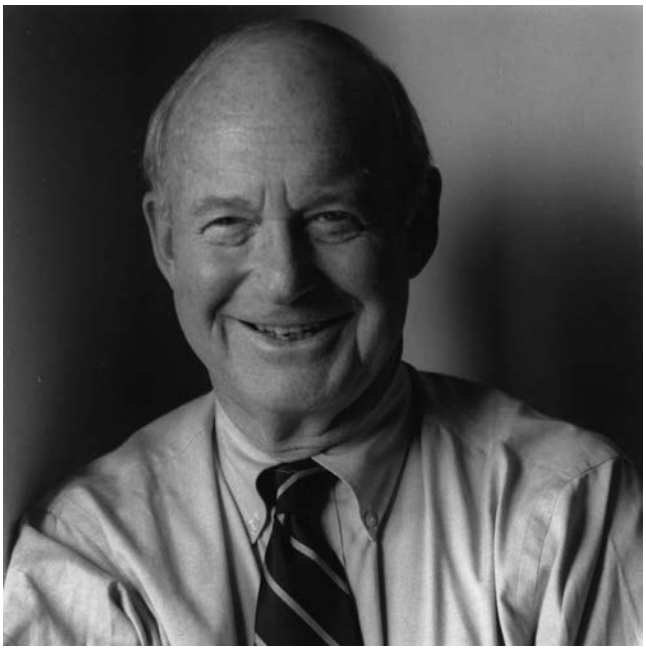

Gerald Weissmann, MD, professor emeritus at New York University School of Medicine and former President of the American College of Rheumatology (1983–1984), who died on July 10, 2019, defined an era of inquiry and accomplishment in rheumatology, contributing enduring benchmarks as a physician, scientist, writer, and mentor.

Dr. Weissmann was born in Vienna in 1930. His family left Austria in 1938, shortly after the rise of Nazism in Europe, and eventually settled in New York City, where his father resumed his practice of medicine. After earning his undergraduate degree from Columbia University, he completed his medical degree at NYU School of Medicine, graduating in 1954. Having completed his residency at Mount Sinai Hospital, Dr. Weissmann returned to NYU where he served as the first chief resident under Lewis Thomas, MD, chairman of medicine, who would later become the dean. Dr. Weissmann never left NYU, continuing on a successful upward trajectory and assuming the directorship of NYU Langone's Division of Rheumatology in 1973, a position he held through 2000. He is survived by his wife, Ann, a true lifetime partner of over 65 years; his daughter, Dr. Lisa Beth Weissmann, of Mount Auburn Hospital in Cambridge, Massachusetts; his grandson, Ben; and his son, Andrew Weissmann, Esq., distinguished senior fellow at NYU School of Law.

Gerald Weissmann was internationally known for his contributions to knowledge of the molecular mechanisms of inflammation and lipid metabolism. He began his education at the Art Students League of New York, where he started out on a career in the arts. His father, a Vienna-trained physician with a strong interest in the rheumatic diseases (before there was such a thing as rheumatology), brought his budding artist son to a lecture on corticosteroids and their potential use in the therapy of rheumatic diseases in the early 1950s, an event that led to a rapid change in his educational orientation. His career as a physician-scientist began in the laboratory of Dr. Thomas, where his interest was further piqued by studies in the area of inflammation. He co-authored one of his first papers with Dr. Thomas, detailing studies on neutrophil lysosomes in the *Journal of Cell Biology* (1964). From these beginnings, Dr. Weissmann launched a career that led him to become a world-renowned scientist, rheumatologist, and mentor. As the son of a practicing physician, he never forgot that patients were at the center of his work. Gerry is best known for presenting evidence that identified rheumatoid arthritis as an immune complex disease, and demonstrating that crises in systemic lupus erythematosus are provoked by intravascular complement activation. He authored pioneering studies in leukocyte activation and the role of salicylates and corticosteroids in cell signaling and adhesion. In the mid-1960s, in an attempt to better understand the antiinflammatory mechanism of corticosteroids, he co-discovered liposomes, lipid vesicles that have become a crucial tool for delivery of substances such as medications and nutrients into tissue and that are widely used in both the laboratory and the clinic.

In his decades as an international leader in medicine, Gerry received numerous distinctions and awards. He was a fellow of the American Association for the Advancement of Science and the Royal Society of Medicine. In 2002, he was elected to Galileo's Accademia Nazionale dei Lincei of Rome, the world's oldest scholarly society. He received two of the American College of Rheumatology's highest honors, the Presidential Gold Medal and the Lifetime Achievement Award. In 2009, Dr. Weissmann was recognized during Dean's Honors Day at NYU School of Medicine as the Master Educator and Mentor. From 1975 to 2001, he served as the founding editor of the journal

Inflammation, and from 2006 to 2016 he was editor-in-chief of *The FASEB Journal*.

Medicine was not Dr. Weissmann's only passion: throughout his career, he wrote and published literary essays. His writing appeared in *The New York Times Book Review*, the *London Review of Books*, and *The New Republic*, among others. His work has been collected in nearly a dozen book-length volumes, including *The Woods Hole Cantata: Essays on Science and Society* (1985), *Darwin's Audubon: Science and The Liberal Imagination* (2002), *Galileo's Gout* (2007), *Mortal and Immortal DNA* (2009), *Epigenetics in the Age of Twitter* (2012), and, most recently, *The Fevers of Reason* (2018).

Although a scientist of the first order, Gerry had an unmatched dedication to educating students. While setting the highest expectations, he always provided encouragement. Despite his own myriad accomplishments, his greatest pride was in the success of those he trained. In the laboratory, he was well known for his phrase, "That's a wow!" when a young investigator would present him with a new observation. At the same time, all those around him appreciated that such nurturing was accompanied by an obligation to publish and achieve, leading to another oft-quoted Gerryism: "Don't tell me about your last idea, tell me about your next paper!" He hand-picked all his fellows, which we often thought might have been influenced by the answers to his query of the latest book we had read. He was a man of influence and every invited speaker to grand rounds, regardless of his or her accomplishments, knew that when Gerry was in the audience, the most challenging of questions would be guaranteed. Gerry taught us all how important neutrophils are, to dissect a research problem down to its bare bones, to write in the Queen's English (never a noun to be used as an adjective), to deliver a masterful speech (hours spent slide by slide, color for color for every ACR presentation), and to appreciate that ear cartilage tells a health story.

Dr. Weissmann ignited a spark in countless lives. In writing to other members of the NYU rheumatology division, the depth of Gerry's influence was evidenced in dozens of e-mails, each more beautifully expressive than the last. This is what Gerry brought out in those he touched. It is hard to imagine that he is not looking down on this writing to offer a way in which to improve the message. He so often chimed in on group e-mails with his own appreciation. For example, in reference to an e-mail about incoming fellows he responded, "The torch burns bright and its carriers look great!" Indeed Gerry profoundly influenced us even in writing this memorial, as we reviewed a beautiful example he wrote in remembrance of one of his highly respected disciples, Ira Goldstein.

For those fortunate enough to grow up under Gerry's strong wings, you will feel as we do that we are missing a major pillar of our foundation and his famous purple magic marker, which highlighted all the ways in which to deliver the significance of one's discoveries in a communication that would be understood by all. Even those who met Gerry only briefly, interviewed for a fellowship, or simply attended his lectures at national meetings appreciated this universal man of grand proportions who enlightened our field of rheumatology for decades.

Steven B. Abramson, MD
Bruce Cronstein, MD
Jill P. Buyon, MD
NYU School of Medicine
NYU Langone Health
New York, NY

American College of Rheumatology
Empowering Rheumatology Professionals

Arthritis & Rheumatology
Vol. 71, No. 10, October 2019, pp 1616–1625
DOI 10.1002/art.40905

Reducing or Maintaining the Dose of Subcutaneous Tocilizumab in Patients With Rheumatoid Arthritis in Clinical Remission: A Randomized, Open-Label Trial

Raimon Sanmarti,[1] Douglas J. Veale,[2] Emilio Martin-Mola,[3] Alejandro Escudero-Contreras,[4] Carlos González,[5] Liliana Ercole,[6] Rocío Alonso,[6] João E. Fonseca,[7] and the ToSpace Study Group

Objective. To evaluate the efficacy and safety of increasing the dose interval of subcutaneous tocilizumab (TCZ-SC) in patients with rheumatoid arthritis (RA) who are in clinical remission.

Methods. RA patients with active disease and an inadequate response to conventional synthetic disease-modifying antirheumatic drugs (csDMARDs) or to a biologic agent were entered into a single-arm treatment phase with 162 mg of TCZ-SC administered once weekly (TCZ-SC 162 mg qw) as monotherapy or in combination with a csDMARD for 24 weeks. Patients who achieved clinical remission at weeks 20 and 24 were randomized to continue with the same regimen or to switch to 162 mg TCZ-SC administered every 2 weeks (TCZ-SC 162 mg q2w) for 24 weeks (open-label). Patients with a Disease Activity Score in 28 joints (DAS28) of <2.6 were considered to be in clinical remission.

Results. In total, 179 (45%) of 401 patients in the single-arm phase achieved clinical remission and were randomized to continue to receive TCZ-SC 162 mg qw (n = 89) or to switch to TCZ-SC 162 mg q2w (n = 90) for 24 weeks. At week 48, significantly more patients treated with TCZ-SC 162 mg qw remained in clinical remission compared to patients who received TCZ-SC 162 mg q2w (90% versus 73%; $P = 0.004$). The results of other efficacy measures revealed greater efficacy with TCZ-SC 162 mg qw, but none of the efficacy outcomes in this group were significantly different from those in patients treated with TCZ-SC 162 mg q2w, except for the mean change from baseline in the DAS28 score at week 48 (mean change −4.07 points [SD 1.29] versus −3.65 points [SD 1.35]; $P = 0.034$). Tolerability and safety parameters were similar between the treatment groups.

Conclusion. Increasing the dose interval of TCZ-SC in patients with RA was associated with a lower likelihood of maintaining remission after 24 weeks and was not associated with better tolerability. However, most patients were able to sustain remission with a half-dose of TCZ-SC, and therefore this strategy deserves further investigation.

INTRODUCTION

The efficacy and safety of biologic disease-modifying antirheumatic drugs (bDMARDs) have been well established in patients with rheumatoid arthritis (RA) who experience an inadequate response to conventional synthetic DMARDs (csDMARDs) such as methotrexate (1,2). A significant proportion of RA patients achieve sustained remission or low disease activity following treatment with bDMARDs, and optimizing their administration after achievement of the therapeutic objective is an attractive option for safety or

ClinicalTrials.gov identifier: NCT01995201; EudraCT database number: 2013-002429-52.

Supported by Roche Pharma SA.

[1]Raimon Sanmarti, MD, PhD: Hospital Clinic of Barcelona and IDIBAPS, Barcelona, Spain; [2]Douglas J. Veale, MD: St. Vincent's University Hospital and University College Dublin, Belfield, Dublin, Ireland; [3]Emilio Martin-Mola, MD, PhD: Hospital Universitario La Paz, Madrid, Spain; [4]Alejandro Escudero-Contreras, MD: Rheumatology Service, Reina Sofia Hospital, Maimonides Institute for Research in Biomedicine of Cordoba, University of Cordoba, Cordoba, Spain; [5]Carlos González, MD, PhD: Hospital Gregorio Marañón, Madrid, Spain; [6]Liliana Ercole, MD, Rocío Alonso, PharmD: Roche Farma, Madrid, Spain; [7]João E. Fonseca, MD, PhD: Universidade de Lisboa and Hospital de Santa Maria CHLN, Lisbon, Portugal. Members of the ToSpace Study Group are listed in Appendix A.

Dr. Sanmarti has received consulting fees from AbbVie, Eli Lilly, Pfizer, Roche, Sanofi, and UCB (less than $10,000 each) and research support from Bristol-Myers Squibb, MSD, and Pfizer. Dr. Veale has received speaking fees from AbbVie, Actelion, BMS, Celgene, Novartis, Pfizer, MSD, Mundipharma, Roche, Regeneron, and Sanofi (less than $10,000 each) and research support from AbbVie, Janssen, MSD, Novartis, Pfizer, and Roche. Dr. Escudero-Contreras has received speaking fees from Pfizer, Eli Lilly, AbbVie, BMS, Roche, Novartis, and Sanofi (less than $10,000 each). Dr. González has received consulting fees and/or honoraria from Janssen, Celgene, MSD, and Novartis (less than $10,000 each) and research support from Roche and Pfizer. Drs. Ercole and Alonso own stock or stock options in Roche. Dr. Fonseca has received speaking fees from AbbVie, Ache, Amgen, Biogen, BMS, Janssen, Eli Lilly, MSD, Novartis, Pfizer, Roche, and UCB (less than $10,000 each) and has received research support from those companies. No other disclosures relevant to this article were reported.

Address correspondence to Raimon Sanmarti, MD, PhD, Hospital Clinic of Barcelona, Arthritis Unit Rheumatology Service, Villarroel, 170, 08036 Barcelona, Spain. E-mail: sanmarti@clinic.cat.

Submitted for publication October 11, 2018; accepted in revised form April 2, 2019.

economic reasons (3). Discontinuation of bDMARDs highly increases the risk of losing remission and experiencing a disease relapse with radiographic progression of RA, and therefore discontinuation of bDMARDs is not recommended as an optimizing strategy (3–5). In contrast, reducing/tapering the dose of bDMARDs may maintain the therapeutic objective in patients with RA and could be considered for a potential strategy in those patients who achieve sustained remission or low disease activity (6). Although information is limited, dose-reduction strategies may also be cost effective (7,8). Thus, bDMARD dose optimization is included in the recommended strategies of the European League Against Rheumatism (EULAR) and the American College of Rheumatology (ACR) for patients with established RA who are in sustained remission or have low disease activity (9,10).

Tocilizumab (TCZ) is the first interleukin-6 inhibitor approved for the treatment of RA. This bDMARD is effective in the treatment of RA in several clinical settings, including for the treatment of csDMARD-naive patients and patients who have shown an inadequate response to csDMARDs or other bDMARDs. TCZ is most commonly administered in combination with methotrexate but is also efficacious as a monotherapy, and it is considered the bDMARD of choice when monotherapy is preferred. TCZ was initially developed as an intravenous formulation, but a subcutaneous (SC) formulation was recently developed (11). The clinical efficacy and safety of TCZ administered subcutaneously (TCZ-SC) has been found to be similar to that of intravenous TCZ (12,13). Findings from a retrospective study suggested the possibility of a dose reduction with intravenous TCZ in a substantial proportion of RA patients without a disease flare (14). However, neither the efficacy nor the safety of a dose reduction of TCZ, either by the intravenous or the SC route of administration, has been evaluated in patients with RA in randomized controlled trials.

Therefore, as part of a multinational project (the TOZURA study) (15), we performed this randomized, open-label trial in patients with RA who achieved sustained clinical remission after having received 24 weeks of TCZ-SC (dose of 162 mg) administered once weekly (TCZ-SC 162 mg qw). In this patient cohort, we assessed the efficacy and safety of continuing with the same weekly regimen (TCZ-SC 162 mg qw) for 24 weeks or switching to TCZ-SC (dose of 162 mg) administered every 2 weeks (TCZ-SC 162 mg q2w).

PATIENTS AND METHODS

Study design. This study was part of an international project (the TOZURA study) comprising 11 studies in 22 countries that was designed as an open-label, single-arm study to evaluate the efficacy and safety of weekly TCZ-SC (162 mg) as monotherapy or in combination with csDMARDs for 24 weeks in patients with moderate-to-severe RA who had an inadequate response to csDMARDs or to tumor necrosis factor inhibitor (TNFi) agents or who were methotrexate naive. The methods and global results of this phase IV study program have been published elsewhere (15).

The present study was a continuation of this single-arm study and was performed at 46 sites in Spain, Ireland, and Portugal between September 2013 and March 2016. The study was performed in accordance with the International Conference on Harmonisation Guidelines for Good Clinical Practice and the ethics principles contained in the Declaration of Helsinki. The ethics committees of each participating site approved the study, and all patients provided their written informed consent to participate. Qualified researchers may request access to individual patient-level data through the clinical study data request platform (https://www.clinicalstudydatarequest.com). Further details on Roche's criteria for eligible studies are available at https://clinicalstudydatarequest.com/Study-Sponsors/Study-Sponsors-Roche.aspx, and further details on Roche's Global Policy on the Sharing of Clinical Information and instructions on how to request access to related clinical study documents are provided at https://www.roche.com/research_and_development/who_we_are_how_we_work/clinical_trials/our_commitment_to_data_sharing.htm.

Patients. Inclusion and exclusion criteria for the initial single-arm phase of the study are described in detail elsewhere (15). Briefly, included patients were patients ages ≥18 years who exhibited active RA, defined according to the 1987 revised ACR criteria for RA or the 2010 ACR/EULAR classification criteria for RA (16,17), and who had demonstrated intolerance to or an inadequate response to csDMARDs or a first-line TNFi. Patients were excluded if they had undergone major surgery within 8 weeks prior to screening or had a major surgery scheduled within 6 months from baseline, exhibited a rheumatic or inflammatory joint disease other than RA, had ACR functional class IV RA (18), or presented other safety issues or had received or were receiving treatments that precluded proper evaluation of drug efficacy. Supplementary Table 1 (available on the *Arthritis & Rheumatology* web site at http://onlinelibrary.wiley.com/doi/10.1002/art.40905/abstract) presents the full set of inclusion and exclusion criteria.

Patients who achieved clinical remission at weeks 20 and 24 of the single-arm phase were included in the randomized continuation phase, which is the focus of the present report.

Interventions, randomization, and masking. All patients in the single-arm phase received 162 mg of TCZ-SC once weekly for 24 weeks on an outpatient basis, administered as monotherapy or in combination with a csDMARD, as clinically indicated. Concomitant treatment with csDMARDs was allowed if the csDMARD was administered at a stable dose for at least 4 weeks prior to the initiation of the single-arm phase. Similarly, patients who were receiving nonsteroidal antiinflammatory drugs (up to the maximum recommended dose) or glucocorticoids (≤10 mg of prednisone or equivalent) were allowed to continue receiving these drugs if they had achieved a stable dose at least 4 weeks prior to the initiation of the single-arm phase. Patients who exhibited an inadequate response to at least 3 months of TNFi therapy had discontinued this drug prior to inclusion in the single-arm phase.

Patients who achieved clinical remission, defined as a Disease Activity Score in 28 joints using the erythrocyte sedimentation rate (DAS28-ESR) of <2.6 (19), at weeks 20 and 24 of the single-arm phase of the study were randomized in a 1:1 ratio to receive, in an open-label manner, continued treatment with TCZ-SC 162 mg qw or to switch to TCZ-SC 162 mg q2w. Randomization was centralized and performed using a computer-generated system, and patients were stratified according to body weight (<60 kg, 60 kg to <100 kg, or >100 kg), Clinical Disease Activity Index (CDAI) score (<10 or ≥10) (20), and type of TCZ-SC regimen in the single-arm phase (monotherapy or in combination with csDMARDs).

Study assessments. Week 0 (i.e., baseline visit) of the single-arm phase was also the baseline evaluation of the randomized phase. Study assessments in this phase were scheduled every 4 weeks for 24 weeks, with an additional 8-week follow-up period.

Efficacy outcome measures in the randomized phase included assessment of the mean change from baseline in the following indices: DAS28, Simplified Disease Activity Index (SDAI) (21), CDAI, tender and swollen joint counts of 28 joints, serum C-reactive protein (CRP) levels, ESR, pain intensity scores (assessed on a 100-mm visual analog scale), patient and physician global health assessments (numeric rating scales of 0–100), and scores on the Health Assessment Questionnaire (HAQ) disability index (DI) (22). Patients with a DAS28 score of <2.6 were considered to be in clinical remission. Treatment response was defined according to the ACR improvement response criteria (levels of at least 20%, 50%, 70%, and 90% improvement in RA disease activity from the baseline visit of the single-arm phase) and EULAR response criteria (no response, moderate response, or good response) (23,24). Low disease activity was defined using the CDAI score (CDAI <10) and SDAI score (SDAI <11). Patients with a HAQ DI score of <0.5 were considered to have no significant functional disability. No radiographic assessments were performed.

Safety assessments included incidence of any adverse events (AEs) as reported in response to an open-ended question and as determined by physical examination and vital signs. AEs of special interest included serious and/or medically significant infections, myocardial infarction/acute coronary syndrome, gastrointestinal perforations, malignancies, anaphylaxis/hypersensitivity reactions, demyelinating disorders, stroke, serious and/or medically significant bleeding events, and serious and/or medically significant hepatic events.

Statistical analysis. We estimated that a sample size of 420 patients would be needed from the participating sites contributing to the combined total of 2,000 patients required for the global project. However, pivotal studies of TCZ-SC have

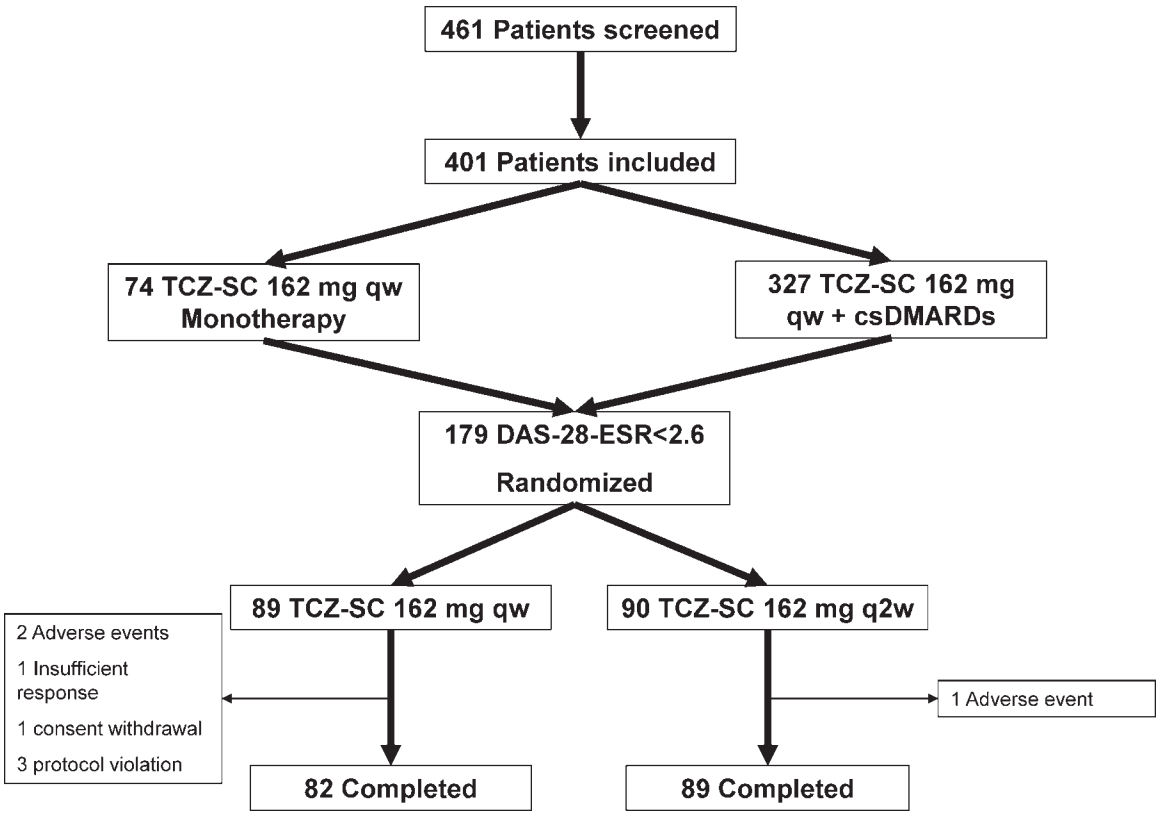

Figure 1. Disposition of the study patients. TCZ-SC = subcutaneous tocilizumab; qw = once weekly; csDMARDs = conventional synthetic disease-modifying antirheumatic drugs; DAS28-ESR = Disease Activity Score in 28 joints using the erythrocyte sedimentation rate; q2w = every 2 weeks.

suggested that one-third of these patients (i.e., 140 patients) would achieve clinical remission in the single-arm phase of the study and would be included in the randomized phase. This sample size was expected to provide an 83% power to detect a between-group difference of 0.6 (i.e., the limit of clinical relevance) in the mean change from baseline in the DAS28.

Efficacy analyses were performed in the full analysis set (FAS) population, which was defined as all patients included in the study who received at least one dose of TCZ-SC. Efficacy analyses were also performed in the per protocol (PP) population, which was defined as patients in the FAS population who exhibited no major protocol violations of the selection criteria and who completed the study without major protocol violations. Missing data were imputed using the last observation carried forward (LOCF) approach. Safety analyses were performed in the FAS population.

Continuous outcomes are presented as the mean ± SD, and categorical outcomes are presented as absolute and relative frequencies. Student's *t*-tests were performed to compare scores and mean changes from baseline in the DAS28 and other quantitative outcomes in paired samples. Categorical outcomes were compared using the chi-square test or Fisher's exact test. All tests were 2-sided and considered significant at *P* values less than 0.05.

Several post hoc analyses were performed. A sensitivity analysis for efficacy outcomes was performed using nonresponder imputation instead of LOCF, in which participant dropouts were assumed to be nonresponders regardless of actual response status at the time of dropout. Logistic regression analysis was performed in the TCZ-SC 162 mg q2w group to further investigate potential factors for maintaining remission. The dependent variable was remission (i.e., a DAS28 score <2.6) at week 48. Independent variables included age, body mass index, disease duration, rheumatoid factor/anti–citrullinated protein antibody (ACPA) status, and DAS28 score at week 24. Treatment-by-subgroup interactions were also analyzed using logistic regression analysis to determine whether the identified factors explained differences between the TCZ-SC 162 mg qw and TCZ-SC 162 mg q2w groups.

In addition, efficacy results were analyzed according to the monotherapy/combination therapy status and the CDAI-defined remission status (i.e., CDAI <2.8 versus CDAI ≥2.8) at the time of randomization. Time to relapse, defined as a DAS28-ESR score of ≥2.6, was analyzed using Kaplan-Meier curves and a univariate Cox proportional hazards model.

All analyses were performed using SAS version 9.2 (SAS Institute).

RESULTS

Disposition and baseline characteristics of the patients. A total of 401 patients of the 461 screened were included in the single-arm phase of the study, and 179 (45%) of these patients exhibited clinical remission at weeks 20 and 24 (Figure 1). The distribution of patients in clinical remission was not significantly different between the TCZ-SC monotherapy group and the group receiving TCZ-SC in combination with csDMARDs. Patients who achieved clinical remission were randomized to continue to receive TCZ-SC 162 mg qw (n = 89) or switched to TCZ-SC 162 mg q2w (n = 90) for 24 weeks. All 179 patients were included in the FAS population.

The demographic and clinical characteristics of the patients at baseline were similar between the 2 treatment groups (Table 1). More than 80% of the patients had received a csDMARD at the time of entry in the randomized phase. The most common csDMARD was methotrexate, which was being taken by 62% of the TCZ-SC 162 mg qw–treated patients and 66% of the TCZ-SC 162 mg q2w–treated patients.

Efficacy results. Significantly more patients treated with TCZ-SC 162 mg qw remained in clinical remission, as evaluated using the DAS28, at week 48 when compared to

Table 1. Demographic and clinical characteristics at study entry in patients who entered the randomized phase of the study*

Characteristic	Tocilizumab 162 mg qw (n = 89)	Tocilizumab 162 mg q2w (n = 90)
Age, mean ± SD years	52.5 ± 12.2	52.6 ± 12.5
Women, no. (%)	72 (80.9)	68 (75.6)
White ethnic origin, no. (%)	85 (95.5)	88 (97.8)
Weight, mean ± SD kg	69.6 ± 13.4	70.1 ± 12.7
Disease duration, mean ± SD years	6.5 ± 7.3	6.4 ± 6.4
Rheumatoid factor positive, no. (%)	71 (79.8)	67 (74.4)
ACPA positive, no. (%)	65 (73.0)	64 (71.1)
CRP, mean ± SD mg/liter	12.2 ± 20.4	11.5 ± 15.9
DAS28-ESR score, mean ± SD	5.62 ± 0.95	5.61 ± 1.01
SDAI score, mean ± SD	41.45 ± 24.9	40.92 ± 21.42
CDAI score, mean ± SD	29.27 ± 10.9	29.64 ± 12.13
HAQ DI score, mean ± SD†	1.21 ± 0.68	1.20 ± 0.7
Glucocorticoid use, no. (%)	52 (58.4)	53 (58.9)
Prednisone or equivalent daily dose, mean ± SD mg/day	5.5 ± 2.1	7.1 ± 5.5
Current treatments, no. (%)		
Any csDMARD	71 (79.8)	76 (84.4)
Methotrexate	55 (61.8)	59 (65.6)
Leflunomide	10 (11.2)	13 (14.4)
Hydroxichloroquine	4 (4.5)	4 (4.4)
Sulfasalazine	2 (2.2)	2 (2.2)

* With the exception of current treatments, which are described at the time of randomization, all characteristics are described at the time of entry into the single-arm phase of the study. ACPA = anti–citrullinated protein antibody; CRP = C-reactive protein; DAS28-ESR = Disease Activity Score in 28 joints using the erythrocyte sedimentation rate; SDAI = Simplified Disease Activity Index; CDAI = Clinical Disease Activity Index; csDMARD = conventional synthetic disease-modifying antirheumatic drug.
† Data on Health Assessment Questionnaire (HAQ) disability index (DI) scores were missing for 1 patient in the subcutaneous tocilizumab every week (qw) group and 1 patient in the subcutaneous tocilizumab every 2 weeks (q2w) group.

patients who received TCZ-SC 162 mg q2w (90% versus 73%, respectively; $P = 0.004$). Post hoc analysis using non-responder imputation in the FAS population yielded similar results with regard to sustained clinical remission (89% versus 73%, respectively; $P = 0.007$). Time to relapse was longer in patients treated with TCZ-SC 162 mg qw than in patients treated with TCZ-SC 162 mg q2w, although the difference was not statistically significant (hazard ratio 0.87, 95% confidence interval [95% CI] 0.54–1.41; log-rank test $P = 0.561$) (see Supplementary Figure 1, available on the *Arthritis & Rheumatology* web site at http://onlinelibrary.wiley.com/doi/10.1002/art.40905/abstract).

The frequency of low disease activity, as determined using the DAS28, was also significantly higher in the TCZ-SC 162 mg qw arm than in the TCZ-SC 162 mg q2w arm. More patients achieved CDAI- or SDAI-defined clinical remission or low disease activity with the weekly dose of TCZ-SC than with TCZ-SC given every 2 weeks, but the differences were not statistically significant (Figure 2). We observed no differences in functional disability as evaluated with the HAQ DI at week 48; the proportion of patients with a HAQ DI score of <0.5 was 55% among those treated with TCZ-SC 162 mg qw and 57% among those treated with TCZ-SC 162 mg q2w ($P = 0.83$).

Furthermore, no significant differences between the 2 treatment groups were observed in the various patient-reported outcomes evaluated. More patients treated with TCZ-SC 162 mg qw achieved ACR improvement responses as compared to patients treated with TCZ-SC 162 mg q2w, but these differences were not statistically significant. Moreover, the EULAR treatment response was significantly better in patients treated with TCZ-SC 162 mg qw compared to patients treated with TCZ-SC 162 mg q2w (see Supplementary Table 2, available on the *Arthritis & Rheumatology* web site at http://onlinelibrary.wiley.com/doi/10.1002/art.40905/abstract).

Evaluation of continuous disease activity outcomes revealed no significant differences between the 2 treatment groups, except for the mean change from baseline in the DAS28. Reductions in the DAS28 score were significantly greater in the TCZ-SC 162 mg qw group compared to the TCZ-SC 162 mg q2w group (mean change in DAS28 –4.07 points [SD 1.29] with TCZ-SC 162 mg qw versus –3.65 points [SD 1.35] with TCZ-SC 162 mg q2w; $P = 0.034$) (Table 2). Patients treated with TCZ-SC 162 mg qw showed a greater reduction of the DAS28-ESR score compared to those treated with TCZ-SC 162 mg q2w (estimated treatment difference –0.386 [95% CI –0.674 to –0.097]). The time course of the changes from baseline in the disease activity measures is

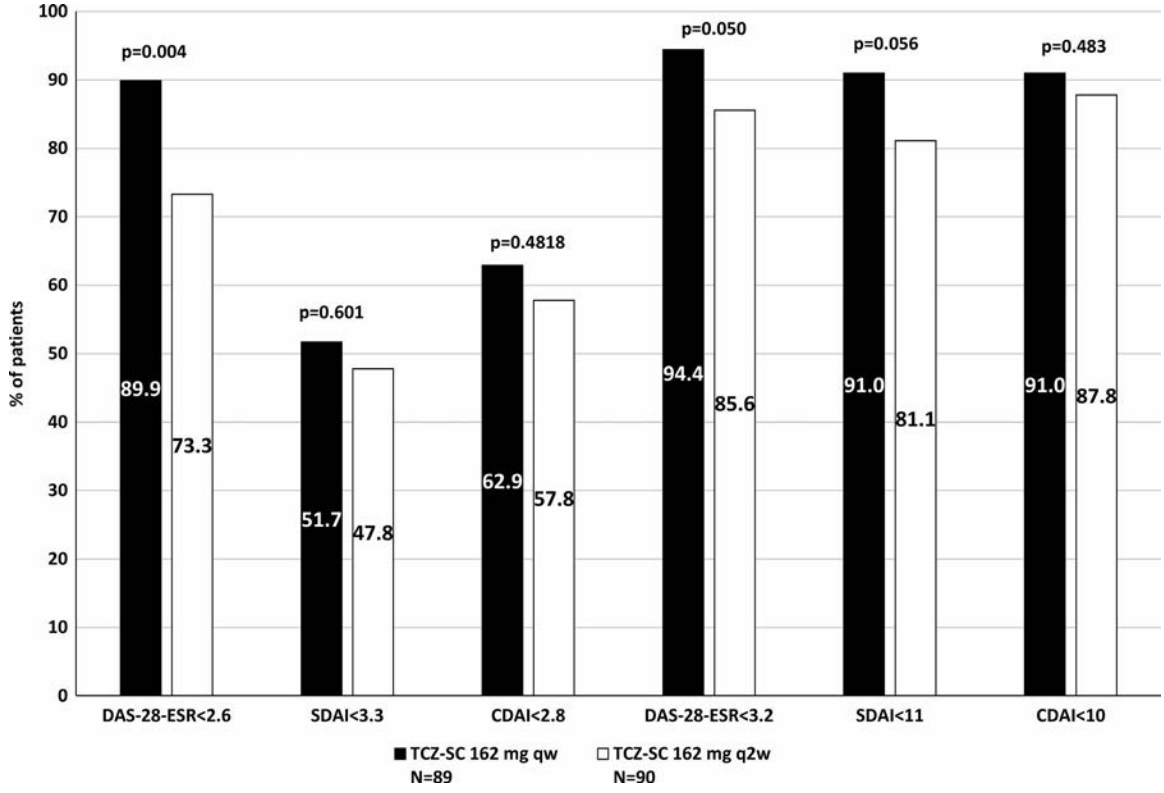

Figure 2. Measures of clinical remission and low disease activity at week 48 in the full analysis set (last observation carried forward) of rheumatoid arthritis patients treated with 162 mg subcutaneous tocilizumab (TCZ-SC) once weekly (qw) or every 2 weeks (q2w) for 24 weeks. DAS28-ESR = Disease Activity Score in 28 joints using the erythrocyte sedimentation rate; SDAI = Simplified Disease Activity Index; CDAI = Clinical Disease Activity Index.

Table 2. Mean change from baseline (week 0) to week 48 in measures of disease activity and function in the full analysis set (last observation carried forward) of patients with rheumatoid arthritis*

Efficacy measure	Tocilizumab 162 mg qw (n = 89)	Tocilizumab 162 mg q2w (n = 90)
DAS28-ESR	−4.07 ± 1.29	−3.65 ± 1.35
SDAI†	−36.93 ± 25.75	−34.69 ± 21.75
CDAI	−25.74 ± 11.29	−24.87 ± 12.67
Tender joint count	−13.96 ± 8.68	−13.27 ± 12.20
Swollen joint count	−8.82 ± 6.51	−8.64 ± 7.33
C-reactive protein†	−7.56 ± 15.60	−7.35 ± 13.82
ESR	−31.19 ± 25.67	−28.47 ± 20.89
Physician global assessment	−50.00 ± 20.55	−50.74 ± 23.59
Patient global assessment	−44.30 ± 24.85	−41.42 ± 26.38
Patient pain score	−42.99 ± 24.71	−39.59 ± 27.66
HAQ DI score†	−0.65 ± 0.66	−0.65 ± 0.58

* Values are the mean ± SD change from week 0 to week 48 in the Disease Activity Score in 28 joints using the erythrocyte sedimentation rate (DAS28-ESR), Simplified Disease Activity Index (SDAI) (scale 0–86), Clinical Disease Activity Index (CDAI) (scale 0–76), tender and swollen joint counts of 28 joints, serum C-reactive protein levels, ESR, physician and patient global assessments of health on 100-mm visual analog scales (VAS), patient assessment of pain on 100-mm VAS, and Health Assessment Questionnaire (HAQ) disability index (DI) scores (range 0–3.0, in 0.125 increments). No significant between-group differences were observed, except in the DAS28-ESR ($P = 0.034$).
† Data were missing as follows: for the SDAI, 1 patient in the subcutaneous tocilizumab (TCZ-SC) every 2 weeks (q2w) group; for C-reactive protein levels, 3 patients in the TCZ-SC q2w group; for the HAQ DI, 1 patient in the TCZ-SC once weekly (qw) group and 1 patient in the TCZ-SC q2w group.

presented in Supplementary Figure 2 (available on the *Arthritis & Rheumatology* web site at http://onlinelibrary.wiley.com/doi/10.1002/art.40905/abstract).

Results of the PP population analysis were in the same direction and magnitude as that in the FAS population (data not shown).

Post hoc analysis of factors predictive of remission at week 48 and their impact on treatment effect. Multiple logistic regression analysis of the TCZ-SC 162 mg q2w group showed that only body mass index and DAS28 scores at week 24 were significantly associated with remission at week 48 (see Supplementary Table 3, available on the *Arthritis & Rheumatology* web site at http://onlinelibrary.wiley.com/doi/10.1002/art.40905/abstract). A 1-point increase in the body mass index was associated with a 12% reduction in the likelihood of remission at week 48. An increase of 1 point in the DAS28 score at week 24 was associated with a 61% reduction in the likelihood of remission.

The multiple logistic regression model performed in the entire sample to investigate treatment-by-subgroup interactions for age, body mass index, disease duration, rheumatoid factor/ACPA status, and DAS28 at week 24 did not reveal any significant interactions, with the exception of the rheumatoid factor/ACPA status (data not shown). The rheumatoid factor/ACPA status could not be investigated, because all patients who were negative for these markers in the TCZ-SC 162 mg qw group were in remission at week 48.

Post hoc subgroup analyses of remission and disease activity measures. The proportion of patients who remained in clinical remission was higher in the TCZ-SC 162 mg qw treatment group than in the TCZ-SC 162 mg q2w treatment group, regardless of the monotherapy/combination therapy status or the CDAI-defined remission status at the time of randomization. In these subgroup analyses, results of other efficacy outcome measures showed a similar trend, in most cases. Better outcomes were observed in patients who were considered to be in remission based on the CDAI score at baseline (see results in Supplementary Table 4, available on the *Arthritis & Rheumatology* web site at http://onlinelibrary.wiley.com/doi/10.1002/art.40905/abstract)

Safety and tolerability results. Overall, the proportion of patients who reported at least 1 treatment-emergent AE (TEAE) was 56% in the TCZ-SC 162 mg qw group and 70% in the TCZ-SC 162 mg q2w group, and the proportion of patients with a TEAE that required dose modification was 17% and 26%, respectively (Table 3). There were 3 serious AEs, none of them considered related to the study drug: 1 patient in the TCZ-SC 162 mg qw group presented with a metastatic malignant melanoma and did not recover by the end of the follow-up, another patient in the TCZ-SC 162 mg qw group had an episode of ileus from which he recovered, and 1 patient in the TCZ-SC 162 mg q2w group presented with a diverticular perforation and fully recovered by the end of the study. Three patients showed TEAEs of special interest: in the TCZ-SC 162 mg qw group, 1 female patient showed a significant increase in the levels of alanine aminotransferase (more than 3 times the upper limit of normal [ULN]) and bilirubin (more than 2 times the ULN), while in the TCZ-SC 162 mg q2w group, 1 patient developed herpes zoster and 1 patient developed varicella infection.

Table 3. Tolerability and safety results*

Parameter	Tocilizumab 162 mg qw (n = 89)	Tocilizumab 162 mg q2w (n = 90)
Any TEAE	50 (56.2)	63 (70.0)
At least 1 TEAE of special interest	1 (1.1)	2 (2.2)
At least 1 serious TEAE	2 (2.2)	1 (1.1)
At least 1 TEAE leading to dose modification	15 (16.9)	23 (25.6)
Al least 1 TEAE leading to discontinuation	1 (1.1)	2 (2.2)

* Values are the number (%) of patients. Qw = once weekly; q2w = every 2 weeks; TEAE = treatment-emergent adverse event.

The results with regard to the frequency of AEs that led to drug discontinuation were similar in both study groups. The most common TEAEs were infections/infestations (28% and 30% in the TCZ-SC 162 mg qw and TCZ-SC 162 mg q2w schedules, respectively), and were primarily upper respiratory infections (10% and 8%, respectively).

Based on the laboratory findings, 42 patients (47%) in the TCZ-SC 162 mg qw group and 33 patients (37%) in the TCZ-SC 162 mg q2w group exhibited neutropenia during this phase of the study; 3 patients in the q2w group showed grade 3 neutropenia (≥10.0 to <50.0 × 10^9/liter). Sixteen patients (18%) in the TCZ-SC 162 mg qw group and 15 patients (17%) in the TCZ-SC 162 mg q2w group had thrombocytopenia; there were no cases of grade 3 or 4 thrombocytopenia. The proportion of patients who exhibited an increase in the serum glutamic oxaloacetic transaminase (SGOT) level was 25 (28%) in the TCZ-SC 162 mg qw group and 14 (16%) in the TCZ-SC 162 mg q2w group; there were 2 cases of a grade 3 SGOT increase (>5 to 20 times the ULN) in the qw group. Finally, 28 patients (31%) in the TCZ-SC 162 mg qw group and 25 patients (28%) in the TCZ-SC 162 mg q2w group showed an increase in the level of serum glutamic pyruvic transaminase (SGPT); 3 patients in the qw group were categorized as having grade 3 SGPT (>5 to 20 times the ULN). There were no relevant findings in the biochemistry analyses (data not shown).

DISCUSSION

This randomized, open-label trial shows that increasing the dose interval of TCZ-SC to 162 mg every 2 weeks in patients who had achieved sustained clinical remission with 162 mg once weekly is associated with a lower likelihood of maintaining remission after 24 weeks compared to continuation with the standard regimen of 162 mg once weekly.

To our knowledge, this is the first study to evaluate the efficacy of increasing the dose interval of TCZ-SC and the first randomized trial to compare TCZ dose reduction with a standard regimen. In 22 RA patients who were receiving 8 mg/kg intravenous TCZ every 4 weeks and had low disease activity (i.e., a DAS28 score of ≤3.2 and/or low disease activity judged by a rheumatologist), van Herwaarden et al (14) retrospectively evaluated the rate of success after reducing the dose of TCZ to 4 mg/kg. This dose reduction was successful (i.e., the patients were maintained on a dose of 4 mg/kg because they still had low disease activity) in 77% of patients at 3 months and 55% of patients at 6 months (14). That retrospective study used quite different criteria to define success, but their findings support the notion that reducing the dose of TCZ in RA patients who are in remission or have low disease activity may be associated with a loss of efficacy in a significant proportion of patients.

Several randomized controlled trials have evaluated the effects of halving the dose of DMARDs, including etanercept (25–27), abatacept (28), rituximab (29), or any DMARD (30). The results of these studies are reviewed in detail elsewhere but suggest that a half-dose of the DMARD in patients who achieved remission at the full dose is a feasible option (6,31). However, our results suggest that continuation with the recommended dose of TCZ-SC is associated with better results, and the results of a recent meta-analysis partially support our findings. Henaux et al (3) meta-analyzed 7 studies that evaluated tapering strategies via dose reduction or spacing strategies. Those authors found that such strategies were associated with a slight, but significant, increased risk of remission loss (risk ratio 1.23, 95% CI 1.06–1.42) but were not associated with an increased risk of low disease activity loss or an increased risk of radiographic progression (3).

Despite these differences in the proportion of patients who maintained remission between the half-dose and full-dose groups, we should remember that ~3 in 4 patients in the half-dose group maintained remission according to the DAS28 score, and no significant differences were found in the rates of remission or low disease activity using other disease activity indices such as the SDAI or CDAI or using ACR response criteria. Therefore, we may consider that this strategy is an interesting option for a substantial proportion of patients who are being treated with TCZ-SC. In fact, the initial dose recommended by the US Food and Drug Administration is 162 mg every 2 weeks, which has demonstrated efficacy in RA, both in combination with csDMARDs (32) or as monotherapy (12).

However, there are several issues to resolve before this strategy may be considered to be a truly feasible option for those patients who have started with the full weekly dose of TCZ-SC. Methods, and especially definitions of success, vary greatly between studies, which makes comparison with our results very difficult. However, the overall rate of remission in our study after 24 weeks with TCZ-SC 162 q2w (73%) was similar to the rates of success reported with a half-dose of DMARDs in other randomized controlled trials, including rates of remission of 44%, 79%, and 82% with etanercept (25–27), a rate of no relapse of 66% with abatacept (28), and a rate of no relapse of 61% with any DMARD (30). Notably, these previous studies used a longer follow-up period (>1 year in all studies). Therefore, our study duration is a limitation and the proportion of patients who remained in remission with a half-dose of TCZ-SC with longer follow-up periods should be further investigated.

Second, we must try to identify those patients receiving treatment with TCZ-SC who are more suitable for a dose reduction. Our post hoc analysis identified some factors that identify candidates for dose reduction; namely, the body mass index and the DAS28 score at week 24. However, another post hoc analysis evaluated the potential interactions between these variables and the treatment strategies tested in our trial, and found no statistically significant interactions, which suggests that in our study, continuation with full doses of TCZ-SC was superior to halving the dose, regardless of these characteristics. Our post hoc subgroup analysis showed that the differences between these 2 dos-

ing strategies with TCZ-SC are not affected by the monotheraphy/combination therapy status at baseline. The challenge of identifying patients who are more suitable for a TCZ-SC dose reduction remains. A recent systematic review found very limited and low-quality information on potential markers for successful dose reduction or discontinuation of biologic agents in RA (33). Some studies with adalimumab have suggested that a higher trough level of adalimumab may be a good marker for reducing the dose; however, in our study, we did not determine drug serum levels (34,35).

Finally, we should ascertain whether patients who experience a relapse after a dose reduction of TCZ-SC can be restarted on full doses of this agent and achieve remission. A retrospective study with intravenous TCZ suggests that it is possible to reduce the dose of this agent and successfully titrate up the dose in patients who experience a flare (14).

Halving the dose of TCZ-SC was not associated with better tolerability or safety as compared with continuing with the full weekly dose. In contrast, a previous small-sized retrospective study of intravenous TCZ found a somewhat better tolerability with a reduced dose (36). That study examined a group of 19 patients treated with 8 mg/kg intravenous TCZ, and the dose was reduced at the investigator's discretion when the patient reached remission or exhibited neutropenia or thrombocytopenia. The rate and severity of infections were lower in that group than in a group of 63 patients who continued to receive 8 mg/kg of intravenous TCZ (36).

In addition to the previously noted short duration of follow-up, the major limitations of our study were the lack of blinding and the lack of radiographic assessment. The lack of blinding may have biased the results against the half-dose group. Patients randomized to receive a half-dose of TCZ may have had negative expectations concerning the outcomes of the intervention and may have exhibited worse results because of this nocebo effect (6). Qualitative studies have demonstrated that RA patients associated a risk of relapse with dose-optimization strategies (6), which supports the nocebo effect. The lack of radiographic data in our study, together with the short duration of follow-up, limited the amount of information on disease progression that we could obtain.

In conclusion, reducing the dose of TCZ-SC to 162 mg every 2 weeks in patients with RA who acheived sustained remission at the recommended dose of 162 mg once per week was associated with a lower likelihood of maintaining remission after 24 weeks when compared to continuing with the standard regimen of this agent. Moreover, dose reduction was not associated with better tolerability. However, most patients did remain in remission with a half-dose of TCZ-SC, and this strategy therefore warrants further investigation in randomized controlled trials with longer follow-up periods and a comparison between a continuation strategy and a strategy that includes dose reduction and restarting of full doses in cases of relapse.

ACKNOWLEDGMENT

The authors thank Ignacio Fernández (Roche Farma, Madrid, Spain) for his statistical advice.

AUTHOR CONTRIBUTIONS

All authors were involved in drafting the article or revising it critically for important intellectual content, and all authors approved the final version to be published. Dr. Sanmarti had full access to all of the data in the study and takes responsibility for the integrity of the data and the accuracy of the data analysis.

Study conception and design. Sanmarti, Veale, Martin-Mola, Fonseca.
Acquisition of data. Sanmarti, Veale, Escudero-Contreras, González, Fonseca.
Analysis and interpretation of data. Sanmarti, Ercole, Alonso.

ROLE OF THE STUDY SPONSOR

Roche Pharma SA was involved in the study design and analysis and collection of the data, and provided support for third-party writing assistance for the manuscript (furnished by Fernando Rico-Villademoros, MD, PhD, of COCIENTE S.L), and reviewed and approved the manuscript prior to submission. The authors independently collected the data, interpreted the results, and had the final decision to submit the manuscript for publication. Publication of this article was not contingent upon approval by Roche Pharma SA.

REFERENCES

1. Nam JL, Takase-Minegishi K, Ramiro S, Chatzidionysiou K, Smolen JS, van der Heijde D, et al. Efficacy of biological disease-modifying antirheumatic drugs: a systematic literature review informing the 2016 update of the EULAR recommendations for the management of rheumatoid arthritis. Ann Rheum Dis 2017;76:1113–36.
2. Ramiro S, Sepriano A, Chatzidionysiou K, Nam JL, Smolen JS, van der Heijde D, et al. Safety of synthetic and biological DMARDs: a systematic literature review informing the 2016 update of the EULAR recommendations for management of rheumatoid arthritis. Ann Rheum Dis 2017;76:1101–36.
3. Henaux S, Ruyssen-Witrand A, Cantagrel A, Barnetche T, Fautrel B, Filippi N, et al. Risk of losing remission, low disease activity or radiographic progression in case of bDMARD discontinuation or tapering in rheumatoid arthritis: systematic analysis of the literature and meta-analysis. Ann Rheum Dis 2018;77:515–22.
4. Jiang M, Ren F, Zheng Y, Yan R, Huang W, Xia N, et al. Efficacy and safety of down-titration versus continuation strategies of biological disease-modifying anti-rheumatic drugs in patients with rheumatoid arthritis with low disease activity or in remission: a systematic review and meta-analysis. Clin Exp Rheumatol 2017;35:152–60.
5. Uhlig T, Moe RH, Kvien TK. The burden of disease in rheumatoid arthritis. Pharmacoeconomics 2014;32:841–51.
6. Verhoef LM, Tweehuysen L, Hulscher ME, Fautrel B, den Broeder AA. BDMARD dose reduction in rheumatoid arthritis: a narrative review with systematic literature search. Rheumatol Ther 2017;4:1–24.
7. Kievit W, van Herwaarden N, van den Hoogen FH, van Vollenhoven RF, Bijlsma JW, van den Bemt BJ, et al. Disease activity-guided dose optimisation of adalimumab and etanercept is a cost-effective strategy compared with non-tapering tight control rheumatoid arthritis care: analyses of the DRESS study. Ann Rheum Dis 2016;75:1939–44.
8. Vanier A, Mariette X, Tubach F, Fautrel B, STRASS Study Group. Cost-effectiveness of TNF-blocker injection spacing for patients with established rheumatoid arthritis in remission: an economic evaluation from the Spacing of TNF-blocker injections in Rheumatoid ArthritiS trial. Value Health 2017;20:577–85.

9. Singh JA, Saag KG, Bridges SL Jr, Akl EA, Bannuru RR, Sullivan MC, et al. 2015 American College Of Rheumatology guideline for the treatment of rheumatoid arthritis. Arthritis Rheumatol 2016;68:1–26.
10. Smolen JS, Landewé R, Bijlsma J, Burmester G, Chatzidionysiou K, Dougados M, et al. EULAR recommendations for the management of rheumatoid arthritis with synthetic and biological disease-modifying antirheumatic drugs: 2016 update. Ann Rheum Dis 2017;76:960–77.
11. Mitchell E, Jones G. Subcutaneous tocilizumab for the treatment of rheumatoid arthritis. Expert Rev Clin Immunol 2016;12:103–14.
12. Ogata A, Tanimura K, Sugimoto T, Inoue H, Urata Y, Matsubara T, et al. Phase III study of the efficacy and safety of subcutaneous versus intravenous tocilizumab monotherapy in patients with rheumatoid arthritis. Arthritis Care Res (Hoboken) 2014;66:344–54.
13. Burmester GR, Rubbert-Roth A, Cantagrel A, Hall S, Leszczynski P, Feldman D, et al. A randomised, double-blind, parallel-group study of the safety and efficacy of subcutaneous tocilizumab versus intravenous tocilizumab in combination with traditional disease-modifying antirheumatic drugs in patients with moderate to severe rheumatoid arthritis (SUMMACTA study). Ann Rheum Dis 2014;73:69–74.
14. Van Herwaarden N, Herfkens-Hol S, van der Maas A, van den Bemt BJ, van Vollenhoven RF, Bijlsma JW, et al. Dose reduction of tocilizumab in rheumatoid arthritis patients with low disease activity. Clin Exp Rheumatol 2014;32:390–4.
15. Choy E, Caporali R, Xavier R, Fautrel B, Sanmarti R, Bao M, et al. Subcutaneous tocilizumab in rheumatoid arthritis: findings from the common-framework phase 4 study programme TOZURA conducted in 22 countries. Rheumatology (Oxford) 2018;57:499–507.
16. Arnett FC, Edworthy SM, Bloch DA, McShane DJ, Fries JF, Cooper NS, et al. The American Rheumatism Association 1987 revised criteria for the classification of rheumatoid arthritis. Arthritis Rheum 1988;31:315–24.
17. Aletaha D, Neogi T, Silman AJ, Funovits J, Felson DT, Bingham CO III, et al. 2010 rheumatoid arthritis classification criteria: an American College of Rheumatology/European League Against Rheumatism collaborative initiative. Arthritis Rheum 2010;62:2569–81.
18. Steinbrocker O, Traeger CH, Batterman RC. Therapeutic criteria in rheumatoid arthritis. JAMA 1949;140:659–62.
19. Prevoo ML, van 't Hof MA, Kuper HH, van Leeuwen MA, van de Putte LB, van Riel PL. Modified disease activity scores that include twenty-eight–joint counts: development and validation in a prospective longitudinal study of patients with rheumatoid arthritis. Arthritis Rheum 1995;38:44–8.
20. Aletaha D, Nell VP, Stamm T, Uffmann M, Pflugbeil S, Machold K, et al. Acute phase reactants add little to composite disease activity indices for rheumatoid arthritis: validation of a clinical activity score. Arthritis Res Ther 2005;7:R796–806.
21. Smolen JS, Breedveld FC, Schiff MH, Kalden JR, Emery P, Eberl G, et al. A Simplified Disease Activity Index for rheumatoid arthritis for use in clinical practice. Rheumatology (Oxford) 2003;42:244–57.
22. Fries JF, Spitz P, Kraines RG, Holman HR. Measurement of patient outcome in arthritis. Arthritis Rheum 1980;23:137–45.
23. Felson DT, Anderson JJ, Boers M, Bombardier C, Furst D, Goldsmith C, et al. American College of Rheumatology preliminary definition of improvement in rheumatoid arthritis. Arthritis Rheum 1995;38:727–35.
24. Van Gestel AM, Prevoo ML, van 't Hof MA, van Rijswijk MH, van de Putte LB, van Riel PL. Development and validation of the European League Against Rheumatism response criteria for rheumatoid arthritis: comparison with the preliminary American College of Rheumatology and the World Health Organization/International League Against Rheumatism criteria. Arthritis Rheum 1996;39:34–40.
25. Raffeiner B, Botsios C, Ometto F, Bernardi L, Stramare R, Todesco S, et al. Effects of half dose etanercept (25 mg once a week) on clinical remission and radiographic progression in patients with rheumatoid arthritis in clinical remission achieved with standard dose. Clin Exp Rheumatol 2015;33:63–8.
26. Smolen JS, Nash P, Durez P, Hall S, Ilivanova E, Irazoque-Palazuelos F, et al. Maintenance, reduction, or withdrawal of etanercept after treatment with etanercept and methotrexate in patients with moderate rheumatoid arthritis (PRESERVE): a randomised controlled trial. Lancet 2013;381:918–29.
27. Van Vollenhoven RF, Østergaard M, Leirisalo-Repo M, Uhlig T, Jansson M, Larsson E, et al. Full dose, reduced dose or discontinuation of etanercept in rheumatoid arthritis. Ann Rheum Dis 2016;75:52–8.
28. Westhovens R, Robles M, Ximenes AC, Wollenhaupt J, Durez P, Gomez-Reino J, et al. Maintenance of remission following 2 years of standard treatment then dose reduction with abatacept in patients with early rheumatoid arthritis and poor prognosis. Ann Rheum Dis 2015;74:564–8.
29. Mariette X, Rouanet S, Sibilia J, Combe B, Le Loët X, Tebib J, et al. Evaluation of low-dose rituximab for the retreatment of patients with active rheumatoid arthritis: a non-inferiority randomised controlled trial. Ann Rheum Dis 2014;73:1508–14.
30. Haschka J, Englbrecht M, Hueber AJ, Manger B, Kleyer A, Reiser M, et al. Relapse rates in patients with rheumatoid arthritis in stable remission tapering or stopping antirheumatic therapy: interim results from the prospective randomised controlled RETRO study. Ann Rheum Dis 2016;75:45–51.
31. Fautrel B, Den Broeder AA. De-intensifying treatment in established rheumatoid arthritis (RA): why, how, when and in whom can DMARDs be tapered? Best Pract Res Clin Rheumatol 2015;29:550–65.
32. Kivitz A, Olech E, Borofsky M, Zazueta BM, Navarro-Sarabia F, Radominski SC, et al. Subcutaneous tocilizumab versus placebo in combination with disease-modifying antirheumatic drugs in patients with rheumatoid arthritis. Arthritis Care Res (Hoboken) 2014;66:1653–61.
33. Tweehuysen L, van den Ende CH, Beeren FM, Been EM, van den Hoogen FH, den Broeder AA. Little evidence for usefulness of biomarkers for predicting successful dose reduction or discontinuation of a biologic agent in rheumatoid arthritis: a systematic review. Arthritis Rheumatol 2017;69:301–8.
34. Chen DY, Chen YM, Hsieh TY, Hung WT, Hsieh CW, Chen HH, et al. Drug trough levels predict therapeutic responses to dose reduction of adalimumab for rheumatoid arthritis patients during 24 weeks of follow-up. Rheumatology (Oxford) 2016;55:143–8.
35. L'Ami MJ, Krieckaert CL, Nurmohamed MT, van Vollenhoven RF, Rispens T, Boers M, et al. Successful reduction of overexposure in patients with rheumatoid arthritis with high serum adalimumab concentrations: an open-label, non-inferiority, randomised clinical trial. Ann Rheum Dis 2018;77:484–7.
36. Fechtenbaum M, Lasselin-Boyard P, Salomon S, Jelin G, Millot F, Grados F, et al. Decrease of tocilizumab dose in patients with rheumatoid arthritis: a pilot study. Pharmacology 2016;98:73–8.

APPENDIX A: THE TOSPACE STUDY GROUP

Members of the ToSpace Study Group are as follows: Cristina Alcañiz, José María Álvaro-Gracia, Alejandro Balsa, José Luis de Pablos, Consuelo Díaz Miguel, and José Manuel Rodríguez (Madrid, Spain); Jose Alves (Amadora, Portugal); Elena Aurrecoechea and Jaime Calvo (Torrelavega, Spain); Joaquín Belzunegui (San Sebastián, Spain); Francisco Blanco (A Coruña, Spain); Rafael Caliz

(Granada, Spain); Javier Calvo and José Román Ivorra (Valencia, Spain); Helena Canhão and Helena Santos (Lisbon, Portugal); Eugenio Chamizo (Mérida, Spain); Javier del Pino (Salamanca, Spain); Concepción Delgado (Zaragoza, Spain); César Díaz (Barcelona, Spain); Antonio Fernández Nebro (Málaga, Spain); Alexander Fraser (Limerick, Ireland); Antonio Gomez (Sabadell, Spain); Blanca Hernández, Federico Navarro, and Juan Povedano (Seville, Spain); Antonio Juan Mas (Palma de Mallorca, Spain); David Kane and Bryan Whelan (Dublin, Ireland); Carlos Marras (Murcia, Spain); Juan Moreno (Cartagena, Spain); José Pérez Venegas (Jerez, Spain); Manuel Pombo (Santiago de Compostela, Spain); Elena Riera (Terrasa, Spain); Antonio Rosas (Las Palmas de Gran Canaria, Spain); John Ryan (Cork, Ireland); José Santos (Toledo, Spain); Maria Santos (Almada, Portugal); Jesús Tornero (Guadalajara, Spain); Juan Víctor Tovar (Elche, Spain); Eduardo Ucar (Bilbao, Spain); Carlos Vasconcelos (Porto, Portugal); Raúl Veiga (Fuenlabrada, Spain); Paloma Vela (Alicante, Spain).

Arthritis & Rheumatology
Vol. 71, No. 10, October 2019, pp 1626–1633
DOI 10.1002/art.40920

American College of Rheumatology
Empowering Rheumatology Professionals

N-Linked Glycans in the Variable Domain of IgG Anti–Citrullinated Protein Antibodies Predict the Development of Rheumatoid Arthritis

Lise Hafkenscheid,[1] Emma de Moel,[1] Irene Smolik,[2] Stacey Tanner,[2] Xiaobo Meng,[2] Bas C. Jansen,[3] Albert Bondt,[1] Manfred Wuhrer,[1] Tom W. J. Huizinga,[1] Rene E. M. Toes,[1] Hani El-Gabalawy,[2] and Hans U. Scherer[1]

Objective. Anti–citrullinated protein antibodies (ACPAs) are disease-specific biomarkers in rheumatoid arthritis (RA). More than 90% of IgG ACPAs harbor *N*-linked glycans in the antibody variable (V) domain. The corresponding *N*-glycosylation sites in ACPA V-region sequences result from somatic hypermutation, a T cell–dependent process. As ample evidence indicates that T cells drive the maturation of the ACPA response prior to arthritis onset, we undertook this study to investigate whether the presence of glycans in IgG ACPA V domains predicts the transition from predisease autoimmunity to overt RA.

Methods. We analyzed 2 independent sets of serum samples obtained from 126 ACPA-positive first-degree relatives (FDRs) of RA patients. Both sets originated from an Indigenous North American population and comprised cross-sectional and longitudinal samples of individuals who did or did not develop inflammatory arthritis. Serum IgG ACPAs were affinity-purified and subjected to ultra high-performance liquid chromatography–based glycan analysis.

Results. In both data sets, FDR-derived IgG ACPA displayed markedly lower levels of V domain glycans (<50%) compared to IgG ACPA from RA patients. Notably, FDRs who later developed RA showed extensive V-domain glycosylation before the onset of arthritis. Moreover, IgG ACPA V-domain glycosylation was strongly associated with future development of RA (hazard ratio 6.07 [95% confidence interval 1.46–25.2]; $P = 0.013$).

Conclusion. Extensive glycosylation of the IgG ACPA V domain is present in a subset of predisposed FDRs of Indigenous North American RA patients. The presence of this feature substantially increases the risk of RA development. Based on these findings, we propose that glycosylation of the IgG ACPA V domain represents a predictive marker for RA development in ACPA-positive individuals and may serve to better target prevention measures.

INTRODUCTION

Rheumatoid arthritis (RA) is a systemic autoimmune disease. Approximately 1% of the global population is affected, but higher prevalence rates have been observed in certain defined populations, such as Indigenous North Americans (1,2). Indigenous North Americans develop RA at a younger age, experience higher disease burden, have a remarkably high prevalence of the major genetic risk factor for RA (HLA class II shared epitope [SE] alleles) (3), and develop RA that is primarily seropositive for RA-associated autoantibodies, particularly anti–citrullinated protein antibodies (ACPAs) (4).

It is now well established that ACPAs can be present for many years without evidence of clinical symptoms of RA (5).

Supported by the Canadian Institutes of Health Research (grant MOP 77700), the Netherlands Organization for Scientific Research (NWO) (projects 435000033 and 91214031), and the Innovative Medicines Initiative funded projects BeTheCure (contract 1151422) and RTCure (contract 777357). Ms Hafkenscheid's work was supported by the Dutch Arthritis Foundation (grant NR 12-2-403). Drs. Bondt and Wuhrer's work was supported by funding from the European Union's Seventh Framework Programme (contract FP7-Health-F5-2011; project HighGlycan; grant 278535). Dr. Scherer's work was supported by the NWO and the Netherlands Organization for Health Research and Development (ZonMW) (NWO-ZonMW VENI grant 91617107, ZonMW Enabling Technology Hotels grant 435002030, and an ZonMW Clinical Fellowship project 90714509) and the Dutch Arthritis Foundation (project 15-2-402).

[1]Lise Hafkenscheid, MSc, Emma de Moel, MD, Albert Bondt, PhD, Manfred Wuhrer, PhD, Tom W. J. Huizinga, MD, PhD, Rene E. M. Toes, PhD, Hans U. Scherer, MD, PhD: Leiden University Medical Center, Leiden, The Netherlands; [2]Irene Smolik, PhD, Stacey Tanner, MD, Xiaobo Meng, PhD, Hani El-Gabalawy, MD: University of Manitoba, Winnipeg, Manitoba, Canada; [3]Bas C. Jansen, PhD: Ludger Ltd., Oxfordshire, UK.

Drs. El-Gabalawy and Scherer contributed equally to this work.

Drs. Huizinga, Toes, and Scherer have submitted a provisional patent application related to research obtained in this study. No other disclosures relevant to this article were reported.

Address correspondence to Hans U. Scherer, MD, PhD, Leiden University Medical Center, PO Box 9600, 2300 RC Leiden, The Netherlands. E-mail: h.u.scherer@lumc.nl.

Submitted for publication November 29, 2018; accepted in revised form April 30, 2019.

Notably, ACPA levels, isotype usage, and the citrullinated antigen recognition profile broaden relatively close to the onset of arthritis (6). Thus, it has been postulated that the development of ACPA-positive disease is a multistep process (7–9), in which tolerance to citrullinated antigens is initially broken, followed by a putative "second hit" that leads to the expansion of the ACPA response and, ultimately, to development of clinically detectable disease. Hence, it has become of considerable interest to understand the drivers of this predisease expansion of the ACPA response and to identify markers that predict the transition from asymptomatic autoimmunity to ACPA-positive inflammatory arthritis (IA). Interestingly, recent immunogenetic evidence indicates that HLA SE alleles might contribute to the expansion of the ACPA response by facilitating the provision of T helper cell activity to ACPA-expressing B cells. This is based on the observation that HLA SE alleles are risk factors for ACPA-positive disease but do not predispose to the development of ACPA positivity in healthy individuals (10,11). Thus, it can be hypothesized that in individuals destined to develop RA, ACPA-expressing B cells receive predisease T cell "help" that initiates and drives B cell maturation, including isotype switching and somatic hypermutation (SHM) (6).

Recently, we found that almost all IgG ACPA molecules carry *N*-glycans in their B cell receptor variable (V) domains (12,13). Notably, all of the consensus *N*-glycosylation sequences (Asn-X [≠Pro]–Ser/Thr) found in these V regions were generated upon SHM and not encoded in the germline genetic repertoire (14). Moreover, we found evidence that the generation of such *N*-glycosylation sites offers an advantage to ACPA-expressing B cells that helps with their escape from selection checkpoints, as these cells acquire extensive somatic mutations despite a lack of avidity maturation. Together, these observations are consistent with the notion that T cells have a pivotal role in the selection and expansion of ACPA-expressing B cells, possibly by facilitating the introduction of *N*-glycosylation sites in IgG ACPA V domains.

Based on these considerations, we hypothesized that the detection of IgG ACPA V-domain glycosylation in ACPA-positive individuals is indicative of maturation of this autoimmune response and could potentially serve as a predictor for the development of ACPA-positive RA. To address this hypothesis, we analyzed IgG ACPA V-domain glycosylation in a longitudinal manner in unaffected ACPA-positive first-degree relatives (FDRs) of RA patients in an Indigenous North American population predisposed to the disease. We determined that there is a heterogeneity of IgG ACPA V-domain glycosylation levels in unaffected FDRs and that high levels, comparable to those seen in most RA patients, serve to substantially increase the risk of future RA development.

PATIENTS AND METHODS

Study population. The current study is nested within a longitudinal research project initiated in 2005 entitled "Early Identification of Rheumatoid Arthritis in First Nations," that was based at the Arthritis Centre at the University of Manitoba. The study and its consenting process were fully approved by the University of Manitoba Research Ethics Board and the Band Councils of the study's participating communities, the latter based on specific study agreements with the communities (15). Sera were sent in 2 sets, in a blinded manner, to Leiden University Medical Center. The first set was collected from a cross-sectional cohort consisting of 10 RA patients and 84 ACPA-positive FDRs. A second set of samples represented a longitudinal cohort of FDRs who had serial visits. As a quality control measure, there was intentional overlap, with 11 FDRs being in both sets (Table 1 and Supplementary Figure 1, on the *Arthritis & Rheumatology* web site at http://onlinelibrary.wiley.com/doi/10.1002/art.40920/abstract). Additional information on study design and IA case definition are available in the Supplementary Methods.

Table 1. Patient characteristics*

	Age, mean ± SD years	Female sex, no. (%)	CCP-3, mean ± SD titer	Follow-up duration, mean ± SD months
Cross-sectional cohort				
RA patients (n = 10)†	50 ± 10	9 (90)	148 ± 71	–
FDRs (n = 84)	38 ± 14	55 (65)	66 ± 68	–
FDRs included based on IgG ACPA QC (n = 15)	36 ± 12	11 (73)	131 ± 124	–
Longitudinal cohort				
Transitioned FDRs (n = 13)‡	34 ± 14	9 (69)	122 ± 120	50 ± 28
Nontransitioned FDRs (n = 19)§	39 ± 15	12 (63)	49 ± 85	64 ± 24
Nontransitioned FDRs included based on IgG ACPA QC (n = 15)	40 ± 18	11 (73)	62 ± 90	45 ± 29

* For relationships between donors, quality control, and number of samples, see Supplementary Figure 1 and Supplementary Methods (http://onlinelibrary.wiley.com/doi/10.1002/art.40920/abstract). CCP-3 = cyclic citrullinated peptide 3.
† Median disease duration of rheumatoid arthritis (RA) patients was 6.8 years (interquartile range 2.9–18.7). After quality control (QC) measures, samples from all 10 RA patients were included for analysis of IgG anti–citrullinated protein antibodies (ACPAs).
‡ After QC measures, samples from all 13 transitioned first-degree relatives (FDRs) were included for analysis of IgG and analysis of IgG ACPA. The mean ± SD follow-up duration for samples included for analysis of IgG ACPA was 46 ± 24 months.
§ After QC measures, samples from all 19 nontransitioned FDRs were included for analysis of IgG.

Isolation of IgG ACPA and of total IgG depleted of ACPA. IgG ACPA and IgG were captured as previously described (16). Briefly, ACPA were purified from 25 µl serum by antigen affinity chromatography using NeutrAvidin Plus UltraLink beads (Thermo Scientific) coated with cyclic citrullinated peptide 2 (CCP-2). Incubation was performed by shaking the plate for 2 hours at room temperature. The flowthrough was collected by centrifugation. Beads were washed with phosphate buffered saline, and ACPAs were eluted with formic acid and immediately neutralized (16). IgG and IgG ACPAs were subsequently isolated in a similar manner using 20 µl Protein G Sepharose (GE Healthcare Life Sciences). Two hundred microliters of ACPA elution or 15 µl of the flowthrough was loaded onto protein G beads and incubated by shaking at room temperature. Elution was performed with formic acid and centrifugation at 50*g* for 1 minute.

Glycan analysis. Glycans were isolated and analyzed as previously described (12). Briefly, IgG and IgG ACPA eluates were dried by vacuum centrifugation. Glycans were released using PNGase F (Roche) and labeled with 2-aminobenzoic acid (2-AA) and 2-picoline borane (Sigma-Aldrich). The 2-AA–labeled glycans were purified via hydrophilic interaction liquid chromatography–solid phase extraction (HILIC-SPE) using multiwell filter plates, as previously described (17,18). HILIC-SPE–purified 2-AA–labeled glycans were diluted in 100% acetonitrile and injected into a UHPLC Dionex Ultimate 3000 (ThermoFisher Scientific) equipped with an Acquity UHPLC BEH Glycan column and a fluorescence detector.

Data analysis. HappyTools was used to align, calibrate, and integrate the raw emissions of the chromatograms exported from Chromeleon, version 7.1.2.1713 (ThermoFisher Scientific) (19). The calibrations list, settings, and quality control measurements are provided in the Supplementary Methods and Supplementary Tables 1 and 2 (http://onlinelibrary.wiley.com/doi/10.1002/art.40920/abstract). V-domain glycosylation was calculated using the following formula: percentage V-domain glycosylation = (V-domain glycans/Fc glycans) × 100, where the V-domain glycans were GP19 plus GP23 plus GP24, and the Fc glycans were GP4 plus GP8 plus GP14. We selected the glycans used for the calculation based on our previous observation of their respective, exclusive presence in either the Fc portion or in the V domain (12,13) (Supplementary Figure 2). IgG ACPA glycan profiles could be obtained for all 10 RA samples from the cross-sectional cohort; 15 of the 84 FDR samples showed IgG ACPA glycan profiles that met the criteria. In the longitudinal cohort, 67 of the 117 samples from the FDRs yielded sufficient signal to determine the IgG ACPA glycan profile (Table 1 and Supplementary Figure 1, http://onlinelibrary.wiley.com/doi/10.1002/art.40920/abstract).

Statistical analysis. In the cross-sectional cohort, the percentage of V-domain glycosylation between RA patients and FDRs was compared by Mann-Whitney U test. In the longitudinal cohort, levels of V-domain glycosylation over time were compared between FDRs who developed RA and those who did not, using linear mixed models with a random intercept and slope. A multivariable Cox proportional hazards regression analysis was performed, with RA diagnosis as outcome and V-domain glycosylation level as predictor. We used V-domain glycosylation at the first moment of sampling, dichotomized as above or below the group median to draw Kaplan-Meier survival curves and estimate risk of developing RA. Receiver operating characteristic curve (ROC) regression was used to calculate diagnostic properties. All analyses in the longitudinal cohort included adjustment for age and sex and were conducted using Stata SE 14.1. All reported percentage values refer to IgG ACPA V-domain glycosylation levels and not to relative changes. Hazard ratios (HRs) and 95% confidence intervals (95% CIs) were calculated.

RESULTS

Lower levels of ACPA V-domain glycosylation in ACPA-positive healthy FDRs compared to RA patients. Previously, we demonstrated that IgG ACPAs, in contrast to other antigen-specific IgG molecules (e.g., IgG against tetanus toxoid), are hyperglycosylated in the V domain in patients with established RA. These glycans are biantennary *N*-linked glycans that are fully galactosylated and sialylated (12,13). Although ACPA can be present before disease onset in individuals who will eventually develop RA, the V-domain glycosylation state of ACPA has not been studied in the predisease phase. To address this question, IgG ACPAs were isolated from the serum of ACPA-positive Indigenous North American patients with RA and their unaffected ACPA-positive FDRs. By analyzing an initial cross-sectional set of samples, we observed that FDR-derived IgG ACPA showed, on average, substantially lower levels of V-domain glycosylation than IgG ACPA from patients with established RA (Supplementary Figure 3A, http://onlinelibrary.wiley.com/doi/10.1002/art.40920/abstract). Notably, the levels of V-domain glycosylation of IgG ACPA isolated from Indigenous North American RA patients were comparable to the levels we previously reported in Dutch RA patients (112% versus 93%, respectively) (12). Additionally, tetanus toxoid–specific IgG in Indigenous North American RA patients did not show the enhanced V-domain *N*-glycosylation observed in IgG ACPA, which is consistent with our previous observations in Dutch RA patients (data not shown) (13,14).

Analysis of a second set of samples derived from longitudinally followed up, unaffected, ACPA-positive FDRs essentially replicated the cross-sectional results, which demonstrated low levels of IgG ACPA V-domain glycosylation compared to those in RA patients (Supplementary Figure 3B, http://onlinelibrary.wiley.com/doi/10.1002/art.40920/abstract). For subsequent group-level analyses, we combined the IgG ACPA V-domain glycosyl-

ation data from the initial cross-sectional cohort with the data from baseline samples from the FDRs included in the longitudinal cohort (Figure 1A). Thus, each individual FDR contributed only once to the analysis, but overall this approach served to increase sample size and statistical power of the analysis.

FDRs displayed heterogeneous levels of IgG ACPA V-domain glycosylation. This observation prompted us to analyze whether FDRs with high levels subsequently developed clinically detectable IA. As depicted in Figure 1B (and in Supplementary Figures 3A and B, http://onlinelibrary.wiley.com/doi/10.1002/art.40920/abstract), FDRs who transitioned to a state of clinically detectable IA later in life had substantially higher levels of IgG ACPA V-domain glycosylation compared to individuals who did not transition during follow-up (89% versus 20%; $P < 0.0001$). Furthermore, a small portion of FDRs reported new arthralgia; these individuals demonstrated higher IgG ACPA V-domain glycosylation levels compared to FDRs who remained asymptomatic (Supplementary Figure 3). Therefore, the initially unaffected FDRs who subsequently developed clinically detectable IA or new-onset arthralgia displayed high levels compared to FDRs who remained in an unaffected or asymptomatic state.

Association of high IgG ACPA V-domain glycosylation levels in FDRs and development of RA. The observation that unaffected FDRs who developed IA later in life had significantly higher IgG ACPA V-domain glycosylation levels than FDRs who did not develop IA (Figure 1B) prompted us to determine the time course of glycosylation in these individuals. Intriguingly, we observed that V-domain glycosylation levels were already increased in some FDRs up to 7 years before the onset of arthritis. Other individuals who developed IA showed an increase in glycosylation ~1–2 years before disease onset (Figure 2A). When all available time points were considered, IgG ACPA V-domain glycosylation was 34% higher (95% CI 7–62%) in FDRs who developed IA compared to FDRs who did not ($P = 0.015$) (Figure 2B). Notably, FDRs with new-onset arthralgia were classified as nontransitioned. Taken together, these data indicate that ACPA-positive individuals who subsequently developed IA displayed a high degree of IgG ACPA V-domain glycosylation in the preclinical phase. The time course for development of IA, however, varied considerably between individuals.

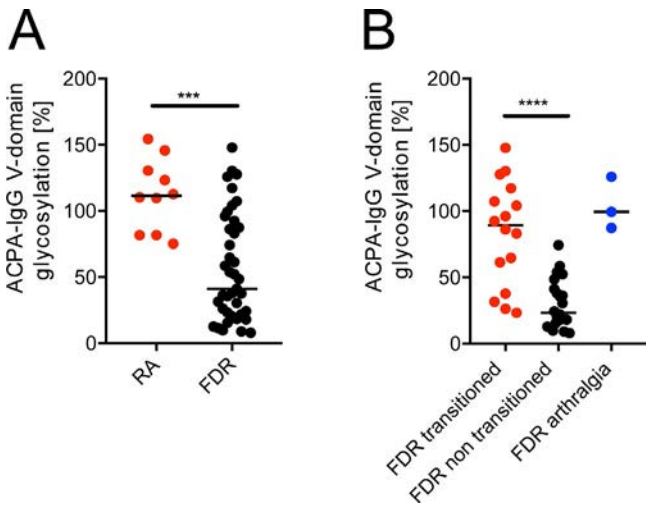

Figure 1. Anti–citrullinated protein antibody (ACPA)–positive first-degree relatives (FDRs) have lower levels of IgG ACPA variable (V)–domain glycosylation than do patients with clinically evident rheumatoid arthritis (RA). Percentages of IgG ACPA V-domain glycosylation in RA patients versus unaffected FDRs (**A**) and in FDRs who transitioned to inflammatory arthritis versus those who did not (**B**) are shown. Symbols represent individual subjects; bars show the median. *** = $P < 0.001$; **** = $P < 0.0001$. Color figure can be viewed in the online issue, which is available at http://onlinelibrary.wiley.com/doi/10.1002/art.40920/abstract.

Absence of elevated V-domain glycosylation in IgG ACPA. The degree of V-domain glycosylation of IgG ACPA is remarkably high compared to other IgG molecules. To date, we have been unable to identify another autoreactive B cell response with comparably high levels of V-domain glycans (12,13). Furthermore, among the Dutch RA population, non-ACPA IgG V-domain glycosylation levels were only 17%. To confirm that non-ACPA IgG V-domain glycosylation is also low in the Indigenous North American population and to investigate a potential association with clinical outcome, we used the flowthrough of the ACPA isolation columns to further purify non-ACPA IgG from FDR-derived sera, followed by glycosylation analysis as it was performed for IgG ACPA. V-domain glycosylation of non-ACPA IgG was as low as 15–25% in these samples, with a mean of 17% for FDRs who did not develop IA and 20% for those who did (P not significant) (Figure 3). These levels are consistent with published data on IgG in healthy individuals (12,20). Moreover, the degree of V-domain glycosylation remained low over time and showed no differences in mean levels between transitioning and nontransitioning FDRs ($P = 0.33$). These data suggest that increased V-domain glycosylation is not a feature of non-ACPA IgG and that this phenomenon is inherent in the citrulline-directed immune response.

Elevated IgG ACPA V-domain glycosylation level as a predictive marker for disease development in ACPA-positive at-risk subjects. Given that FDRs who developed IA had higher levels of IgG ACPA V-domain glycosylation over time compared to those who did not, we attempted to create models of glycosylation as a predictor of IA development. To account for the variance between time points and duration of follow-up of available study subjects, 2 statistical models were established. In the first model, we used the median IgG ACPA V-domain glycosylation level in the cross-sectional analysis (58%) as a cutoff point, thus generating a binary variable. Cox regression analysis, corrected for age and sex, revealed that IgG ACPA V-domain glycosylation levels above the median were associated with development of IA (HR 6.07 [95% CI 1.46–25.2]; $P = 0.013$) (Figure 4). A similar cutoff point was

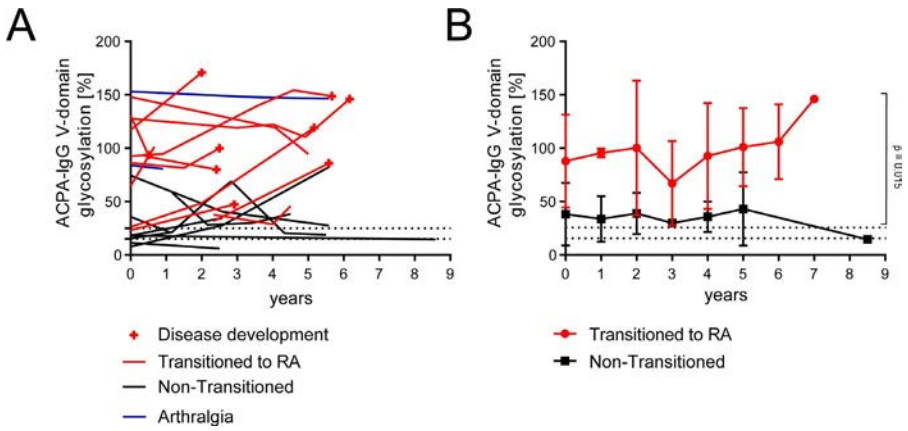

Figure 2. IgG ACPA V-domain glycosylation is elevated in FDRs who transitioned to RA during follow-up. **A**, Longitudinal data on IgG ACPA V-domain glycosylation. Time of RA diagnosis is shown with a red cross; lines without crosses indicate that the patient transitioned to RA but did not have a sample obtained at the time of diagnosis. **B**, Median IgG ACPA V-domain glycosylation levels in FDRs who transitioned to RA versus those who did not. Bars show the median and range. Dotted lines indicate the range of IgG V-domain glycosylation observed in healthy individuals. See Figure 1 for definitions.

created when ROC regression was used to determine the predictive value of high IgG ACPA V-domain glycosylation levels. At this cutoff point, IgG ACPA V-domain glycosylation had a sensitivity of 76.9% (95% CI 46.2–95.0%), a specificity of 78.6% (95% CI 49.2–95.3%), a positive predictive value (PPV) of 76.9% (95% CI 46.2–95.0%), and a negative predictive value (NPV) of 78.6% (95% CI 49.2–95.3%) for IA development.

DISCUSSION

IgG ACPA represents the most relevant prognostic and diagnostic biomarker in RA and is associated with poor prognosis and progressive joint destruction (21). A large body of evidence indicates that early intervention in RA improves clinical outcomes (22,23). Based on these observations, it is hypothesized that intervention at a stage prior to the onset of clinically detectable arthritis may result in better clinical outcomes and possibly even prevent disease (22). Currently, this preclinical phase is identified based on the presence of suggestive joint symptoms such as arthralgia, the detection of RA-associated autoantibodies, especially ACPA, or both of these factors. Imaging studies indicate that this clinical phenotype may also feature subclinical synovitis (22,24). Although arthralgia in conjunction with a broad autoantibody response is a strong predictor of imminent RA onset, a linear progression toward these features has been difficult to demonstrate (25). In particular, the existing longitudinal data suggest that a considerable proportion of individuals with ACPA do not develop RA. Thus, it has become increasingly important to delineate biomarkers that can be used to improve the risk model and that in turn provide actionable clinical information on which interventions can be based (24,26). Our current study demonstrates that the glycosylation state of the IgG ACPA V domain may serve such a purpose. We found that the presence of

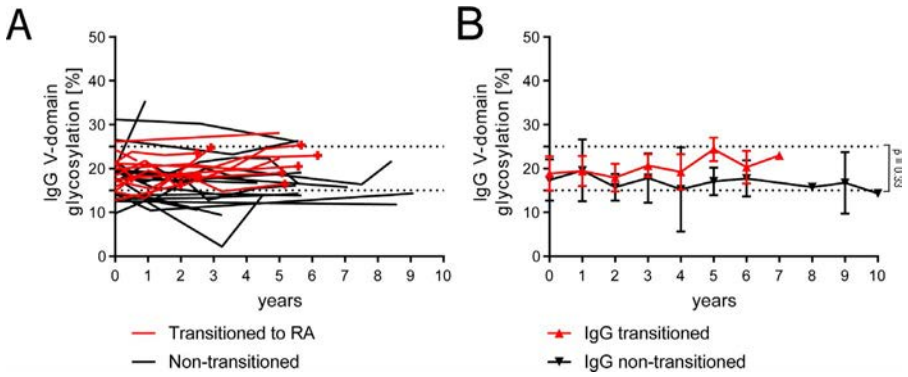

Figure 3. IgG depleted of ACPA does not display enhanced levels of V-domain glycosylation. **A**, Longitudinal data on IgG V-domain glycosylation. Time of RA diagnosis is shown with a red cross; lines without crosses indicate that the patient transitioned to RA but did not have a sample obtained at the time of diagnosis. **B**, Median IgG V-domain glycosylation levels in FDRs who transitioned to RA versus those who did not. Bars show the median and range. Dotted lines indicate the range of IgG V-domain glycosylation observed in healthy individuals. See Figure 1 for definitions.

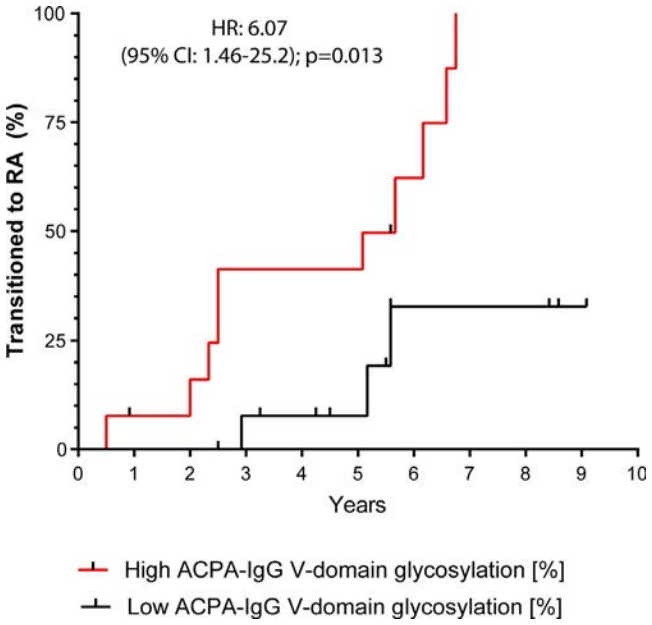

Figure 4. Development of RA in ACPA-positive FDRs, based on degree of IgG ACPA V-domain glycosylation at the first instance of sampling. IgG ACPA V-domain glycosylation levels below and above the 58.5% median are shown. HR = hazard ratio; 95% CI = 95% confidence interval (see Figure 1 for other definitions). Color figure can be viewed in the online issue, which is available at http://onlinelibrary.wiley.com/doi/10.1002/art.40920/abstract.

extensive IgG ACPA V-domain glycosylation in unaffected ACPA-positive individuals is a strong predictor of progression toward disease. Indeed, a high level of IgG ACPA V-domain glycosylation had a PPV of 76.9% and an NPV of 78.6% for predicting the development of IA.

Considering these clinical implications, the present data refine our understanding of the ACPA immune response and its predisease evolution. Conceptually, the development of ACPA-positive RA has been proposed as a multistep process (7,8) in which the break in immune tolerance to citrullinated antigens develops first, followed by expansion and maturation of the autoimmune response, a so-called second hit. Recent evidence suggests that this putative second hit is driven by T helper cells that provide help to ACPA-expressing B cells. This T cell–B cell interaction, which likely mediates the increased usage of isotypes and epitope spreading observed before disease onset, may also be responsible for the introduction of *N*-glycosylation sites in the V domain of IgG ACPA and, therefore, the presence of glycans in this region. This hypothesis is further supported by the observation that the consensus sequences for *N*-glycosylation sites in IgG ACPA V domains are not encoded in their respective germline genes but introduced upon SHM (14). In fact, the presence, frequency, and distribution of these sites suggest a role of the glycans in the selection, development, and activation of the B and plasma cells that express/secrete IgG ACPA.

Notably, the ACPA-positive FDRs examined here exhibited lower levels of IgG ACPA V-domain glycosylation than their relatives with RA, but there was considerable heterogeneity in the population. As a matter of fact, a subset of FDRs had high levels of V-domain glycosylation, which in some cases was detectable years before disease onset. Individuals who exhibited fluctuation between low and normal levels over time (15–25%) rarely transitioned to disease. Given this heterogeneity, we used the available longitudinal samples to develop a kinetic understanding of how IgG ACPA V-domain glycosylation evolves in individuals who ultimately develop IA. Although the data are limited by the small number of those who transitioned to disease, it is clear that there is more than one trajectory and time course for disease development, with some individuals demonstrating a rapid increase in glycosylation and others showing high levels for an extended period of time. These observations suggest that the acquisition of *N*-glycans in the ACPA V domain is a process that requires repeated T cell–dependent B cell hypermutation events, potentially as a result of multiple hits that occur with varying kinetics. Ultimately, these may lead to the persistence, if not the pathogenicity, of the ACPA response.

Our study is limited by the relatively small number of samples with longitudinal follow-up. Also, the number of samples with low-level ACPA that did not pass quality control may have introduced bias. However, except for ACPA levels, the patients who could be included in the analysis had similar baseline characteristics compared to those who had to be excluded because of technical limitations (Table 1). Furthermore, in samples that passed our strict controls, estimates of the predictive value of IgG ACPA V-domain glycosylation were substantial and hold promise for clinical application. Nonetheless, additional studies are necessary to validate and extend these findings.

Finally, our study was conducted exclusively in an Indigenous North American population. Seropositive RA in this population was associated with HLA–DRB1 SE–encoding alleles, as it is in most other populations worldwide. The primary SE allele in the Indigenous North American population is HLA–DRB1*14:02, which is prevalent in the background population and almost unique to Indigenous North Americans. In contrast to other RA-predisposing SE alleles such as HLA–DRB1*04:01, which is seen primarily in white populations, HLA–DRB1*14:02 can accommodate both citrulline and arginine peptides with comparable affinity, but the orientation of citrulline-containing peptides is upright and directly interfaces with the T cell receptor (27,28). It is unclear whether these differences in peptide presentation to T cells impact their capacity to provide help for ACPA-expressing B cells. However, the observation that ACPA V-domain glycosylation patterns are comparable in Indigenous North American and Dutch RA patients suggests that, irrespective of how T cell autoimmunity develops, the T cell–dependent SHM of ACPA B cells is a final common mechanism in the evolution of the ACPA response. Notably, tetanus toxoid–specific IgG did not show enhanced V-domain glycosylation in the Indigenous North American RA patients, in accordance with our previous observations

in Dutch RA patients and with the absence of additional *N*-glycosylation sites in B cell receptors of tetanus toxoid–specific B cells (13,14).

In summary, we have shown that IgG ACPA V-domain glycosylation is a strong predictive biomarker for the development of ACPA-positive RA. Our findings have important implications for assessing the risk of future RA development in unaffected ACPA-positive individuals and, in turn, for stratifying these individuals for intervention studies. The results also provide mechanistic information regarding the evolution of preclinical RA autoimmunity. Future studies in this and other populations will be needed to determine the ultimate clinical utility of these findings.

ACKNOWLEDGMENTS

The authors wish to thank the Indigenous North American people from the Manitoba study communities for their participation and commitment to this longitudinal study. Furthermore, we thank Dr. Jan Wouter Drijfhout (Leiden University Medical Center) for providing the CCP-2 peptide.

AUTHOR CONTRIBUTIONS

All authors were involved in drafting the article or revising it critically for important intellectual content, and all authors approved the final version to be published. Dr. Scherer had full access to all of the data in the study and takes responsibility for the integrity of the data and the accuracy of the data analysis.

Study conception and design. Hafkenscheid, Tanner, Huizinga, Toes, El-Gabalawy, Scherer.

Acquisition of data. Hafkenscheid, Smolik, Tanner, Meng, Wuhrer.

Analysis and interpretation of data. Hafkenscheid, de Moel, Jansen, Bondt, Wuhrer, Huizinga, Toes, El-Gabalawy, Scherer.

ADDITIONAL DISCLOSURES

Author Jansen is an employee of Ludger Ltd.

REFERENCES

1. Ferucci ED, Schumacher MC, Lanier AP, Murtaugh MA, Edwards S, Helzer LJ, et al. Arthritis prevalence and associations in American Indian and Alaska Native people. Arthritis Rheum 2008;59:1128–36.
2. Peschken CA, Esdaile JM. Rheumatic diseases in North America's indigenous peoples. Semin Arthritis Rheum 1999;28: 368–91.
3. El-Gabalawy HS, Robinson DB, Hart D, Elias B, Markland J, Peschken CA, et al. Immunogenetic risks of anti-cyclical citrullinated peptide antibodies in a North American Native population with rheumatoid arthritis and their first-degree relatives. J Rheumatol 2009;36:1130–5.
4. Peschken CA, Hitchon CA, Robinson DB, Smolik I, Barnabe CR, Prematilake S, et al. Rheumatoid arthritis in a North American Native population: longitudinal followup and comparison with a white population. J Rheumatol 2010;37:1589–95.
5. Nielen MM, van Schaardenburg D, Reesink HW, van de Stadt RJ, van der Horst-Bruinsma IE, de Koning MH, et al. Specific autoantibodies precede the symptoms of rheumatoid arthritis: a study of serial measurements in blood donors. Arthritis Rheum 2004;50:380–6.
6. Willemze A, Trouw LA, Toes RE, Huizinga TW. The influence of ACPA status and characteristics on the course of RA. Nat Rev Rheumatol 2012;8:144–52.
7. Kempers AC, Hafkenscheid L, Scherer HU, Toes RE. Variable domain glycosylation of ACPA-IgG: a missing link in the maturation of the ACPA response? Clin Immunol 2018;186:34–7.
8. Koning F, Thomas R, Rossjohn J, Toes RE. Coeliac disease and rheumatoid arthritis: similar mechanisms, different antigens. Nat Rev Rheumatol 2015;11:450–61.
9. Malmström V, Catrina AI, Klareskog L. The immunopathogenesis of seropositive rheumatoid arthritis: from triggering to targeting. Nat Rev Immunol 2017;17:60–75.
10. Wakitani S, Murata N, Toda Y, Ogawa R, Kaneshige T, Nishimura Y, et al. The relationship between HLA-DRB1 alleles and disease subsets of rheumatoid arthritis in Japanese. Br J Rheumatol 1997;36: 630–6.
11. Hensvold AH, Magnusson PK, Joshua V, Hansson M, Israelsson L, Ferreira R, et al. Environmental and genetic factors in the development of anticitrullinated protein antibodies (ACPAs) and ACPA-positive rheumatoid arthritis: an epidemiological investigation in twins. Ann Rheum Dis 2015;74:375–80.
12. Hafkenscheid L, Bondt A, Scherer HU, Huizinga TW, Wuhrer M, Toes RE, et al. Structural analysis of variable domain glycosylation of anti-citrullinated protein antibodies in rheumatoid arthritis reveals the presence of highly sialylated glycans. Mol Cell Proteomics 2017;16:278–87.
13. Rombouts Y, Willemze A, van Beers JJ, Shi J, Kerkman PF, van Toorn L, et al. Extensive glycosylation of ACPA-IgG variable domains modulates binding to citrullinated antigens in rheumatoid arthritis. Ann Rheum Dis 2016;75:578–85.
14. Vergroesen RD, Slot LM, Hafkenscheid L, Koning MT, van der Voort EI, Grooff CA, et al. B-cell receptor sequencing of anti-citrullinated protein antibody (ACPA) IgG-expressing B cells indicates a selective advantage for the introduction of N-glycosylation sites during somatic hypermutation. Ann Rheum Dis 2018;77:956–8.
15. Smolik I, Robinson DB, Bernstein CN, El-Gabalawy HS. First-degree relatives of patients with rheumatoid arthritis exhibit high prevalence of joint symptoms. J Rheumatol 2013;40:818–24.
16. Habets KL, Trouw LA, Levarht EW, Korporaal SJ, Habets PA, de Groot P, et al. Anti-citrullinated protein antibodies contribute to platelet activation in rheumatoid arthritis. Arthritis Res Ther 2015; 17:209.
17. Burnina I, Hoyt E, Lynaugh H, Li H, Gong B. A cost-effective plate-based sample preparation for antibody N-glycan analysis. J Chromatogr A 2013;1307:201–6.
18. Jansen BC, Bondt A, Reiding KR, Scherjon SA, Vidarsson G, Wuhrer M. MALDI-TOF-MS reveals differential N-linked plasma- and IgG-glycosylation profiles between mothers and their newborns. Sci Rep 2016;6:34001.
19. Jansen BC, Hafkenscheid L, Bondt A, Gardner RA, Hendel JL, Wuhrer M, et al. HappyTools: a software for high-throughput HPLC data processing and quantitation. PLoS One 2018;13:e0200280.
20. Van De Bovenkamp FS, Hafkenscheid L, Rispens T, Rombouts Y. The emerging importance of IgG Fab glycosylation in immunity. J Immunol 2016;196:1435–41.
21. Scott DL, Wolfe F, Huizinga TW. Rheumatoid arthritis. Lancet 2010;376:1094–108.
22. Van Steenbergen HW, da Silva JA, Huizinga TW, van der Helm-van Mil AH. Preventing progression from arthralgia to arthritis: targeting the right patients. Nat Rev Rheumatol 2018;14:32–41.
23. Demoruelle MK, Deane KD. Treatment strategies in early rheumatoid arthritis and prevention of rheumatoid arthritis. Curr Rheumatol Rep 2012;14:472–80.

24. Boeters DM, Raza K, vander Helm-van Mil AH. Which patients presenting with arthralgia eventually develop rheumatoid arthritis? The current state of the art. RMD Open 2017;3:e000479.
25. Ten Brinck RM, van Steenbergen HW, van Delft MA, Verheul MK, Toes RE, Trouw LA, et al. The risk of individual autoantibodies, autoantibody combinations and levels for arthritis development in clinically suspect arthralgia. Rheumatology (Oxford) 2017;56:2145–53.
26. Burgers LE, Allaart CF, Huizinga TW, van der Helm-van Mil AH. Clinical trials aiming to prevent rheumatoid arthritis cannot detect prevention without adequate risk stratification: a trial of methotrexate versus placebo in undifferentiated arthritis as an example. Arthritis Rheumatol 2017;69:926–31.
27. Van Heemst J, Jansen DT, Polydorides S, Moustakas AK, Bax M, Feitsma AL, et al. Crossreactivity to vinculin and microbes provides a molecular basis for HLA-based protection against rheumatoid arthritis. Nat Commun 2015;6:6681.
28. Raychaudhuri S, Sandor C, Stahl EA, Freudenberg J, Lee HS, Jia X, et al. Five amino acids in three HLA proteins explain most of the association between MHC and seropositive rheumatoid arthritis. Nat Genet 2012;44:291–6.

DOI 10.1002/art.41014

Clinical Image: Hypertrophic osteoarthropathy in cystic fibrosis

The patient, a 19-year-old man with cystic fibrosis (CF), presented with pain and swelling of both wrists in association with an infective respiratory exacerbation. His CF-related complications included clubbing, multilobar bronchiectasis, chronic infection with *Pseudomonas aeruginosa*, exocrine pancreatic insufficiency, CF-related diabetes mellitus, and low body mass. Examination revealed bilateral wrist swelling and tenderness. Radiography of the hands and wrists demonstrated multi–layered periosteal reactions in the distal ulna and radius bilaterally (**arrows**), consistent with a diagnosis of hypertrophic osteoarthropathy (HOA) (1). While most commonly linked with non–small cell lung cancer, secondary HOA may occur with a range of pulmonary and extrapulmonary pathologies, including CF (2). The pathophysiologic mechanisms remain unclear. In our patient, treatment with intravenous antibiotics and oral corticosteroids was associated with significant improvement in both respiratory and joint symptoms.

1. Turner MA, Baildam E, Patel L, David TJ. Joint disorders in cystic fibrosis. J R Soc Med 1997;90 Suppl 31:13–20.
2. Yap FY, Skalski MR, Patel DB, Schein AJ, White EA, Tomasian A, et al. Hypertrophic osteoarthropathy: clinical and imaging features. Radiographics 2017;37:157–95.

Elizabeth Clarke, MBChB, MRCP
Manchester University NHS Foundation Trust
Wythenshawe Hospital
and University of Manchester
Rowland Bright-Thomas, MBChB, MRCP, MD
Manchester University NHS Foundation Trust
Wythenshawe Hospital
Manchester, UK

24. Boeters DM, Raza K, vander Helm-van Mil AH. Which patients presenting with arthralgia eventually develop rheumatoid arthritis? The current state of the art. RMD Open 2017;3:e000479.
25. Ten Brinck RM, van Steenbergen HW, van Delft MA, Verheul MK, Toes RE, Trouw LA, et al. The risk of individual autoantibodies, autoantibody combinations and levels for arthritis development in clinically suspect arthralgia. Rheumatology (Oxford) 2017;56:2145–53.
26. Burgers LE, Allaart CF, Huizinga TW, van der Helm-van Mil AH. Clinical trials aiming to prevent rheumatoid arthritis cannot detect prevention without adequate risk stratification: a trial of methotrexate versus placebo in undifferentiated arthritis as an example. Arthritis Rheumatol 2017;69:926–31.
27. Van Heemst J, Jansen DT, Polydorides S, Moustakas AK, Bax M, Feitsma AL, et al. Crossreactivity to vinculin and microbes provides a molecular basis for HLA-based protection against rheumatoid arthritis. Nat Commun 2015;6:6681.
28. Raychaudhuri S, Sandor C, Stahl EA, Freudenberg J, Lee HS, Jia X, et al. Five amino acids in three HLA proteins explain most of the association between MHC and seropositive rheumatoid arthritis. Nat Genet 2012;44:291–6.

DOI 10.1002/art.41014

Clinical Image: Hypertrophic osteoarthropathy in cystic fibrosis

The patient, a 19-year-old man with cystic fibrosis (CF), presented with pain and swelling of both wrists in association with an infective respiratory exacerbation. His CF-related complications included clubbing, multilobar bronchiectasis, chronic infection with *Pseudomonas aeruginosa*, exocrine pancreatic insufficiency, CF-related diabetes mellitus, and low body mass. Examination revealed bilateral wrist swelling and tenderness. Radiography of the hands and wrists demonstrated multi–layered periosteal reactions in the distal ulna and radius bilaterally (**arrows**), consistent with a diagnosis of hypertrophic osteoarthropathy (HOA) (1). While most commonly linked with non–small cell lung cancer, secondary HOA may occur with a range of pulmonary and extrapulmonary pathologies, including CF (2). The pathophysiologic mechanisms remain unclear. In our patient, treatment with intravenous antibiotics and oral corticosteroids was associated with significant improvement in both respiratory and joint symptoms.

1. Turner MA, Baildam E, Patel L, David TJ. Joint disorders in cystic fibrosis. J R Soc Med 1997;90 Suppl 31:13–20.
2. Yap FY, Skalski MR, Patel DB, Schein AJ, White EA, Tomasian A, et al. Hypertrophic osteoarthropathy: clinical and imaging features. Radiographics 2017;37:157–95.

Elizabeth Clarke, MBChB, MRCP
Manchester University NHS Foundation Trust
Wythenshawe Hospital
and University of Manchester
Rowland Bright-Thomas, MBChB, MRCP, MD
Manchester University NHS Foundation Trust
Wythenshawe Hospital
Manchester, UK

Arthritis & Rheumatology
Vol. 71, No. 10, October 2019, pp 1634–1641
DOI 10.1002/art.40928

American College of Rheumatology
Empowering Rheumatology Professionals

Causal Factors for Knee, Hip, and Hand Osteoarthritis: A Mendelian Randomization Study in the UK Biobank

Thomas Funck-Brentano,[1] Maria Nethander,[1] Sofia Movérare-Skrtic,[1] Pascal Richette,[2] and Claes Ohlsson[1]

Objective. There is no curative treatment for osteoarthritis (OA), which is the most common form of arthritis. This study was undertaken to identify causal risk factors of knee, hip, and hand OA.

Methods. Individual-level data from 384,838 unrelated participants in the UK Biobank study were analyzed. Mendelian randomization (MR) analyses were performed to test for causality for body mass index (BMI), bone mineral density (BMD), serum high-density lipoprotein cholesterol, low-density lipoprotein cholesterol, and triglyceride levels, type 2 diabetes, systolic blood pressure (BP), and C-reactive protein (CRP) levels. The primary outcome measure was OA determined using hospital diagnoses (all sites, n = 48,431; knee, n = 19,727; hip, n = 11,875; hand, n = 2,330). Odds ratios (ORs) with 95% confidence intervals (95% CIs) were calculated.

Results. MR analyses demonstrated a robust causal association of genetically determined BMI with all OA (OR per SD increase 1.57 [95% CI 1.44–1.71]), and with knee OA and hip OA, but not with hand OA. Increased genetically determined femoral neck BMD was causally associated with all OA (OR per SD increase 1.14 [95% CI 1.06–1.22]), knee OA, and hip OA. Low systolic BP was causally associated with all OA (OR per SD decrease 1.55 [95% CI 1.29–1.87]), knee OA, and hip OA. There was no evidence of causality for the other tested metabolic factors or CRP level.

Conclusion. Our findings indicate that BMI exerts a major causal effect on the risk of OA at weight-bearing joints, but not at the hand. Evidence of causality of all OA, knee OA, and hip OA was also observed for high femoral neck BMD and low systolic BP. However, we found no evidence of causality for other metabolic factors or CRP level.

INTRODUCTION

Osteoarthritis (OA) is the most common form of arthritis in developed countries, representing an increasing health economic burden (1). Patients with knee or hip OA have excess all-cause mortality compared with the general population, and there is no curative treatment for OA (2). Besides age and sex, modifiable factors have been shown to be associated with OA risk, the highest level of evidence being for obesity and joint injury (3,4). Obesity is a major risk factor for OA incidence and progression at the knee, and to a lesser extent, at the hip (5). In addition, the role of obesity is strongly supported by findings of improvement of knee symptoms in patients undergoing weight loss (6,7).

Besides body mass index (BMI), other factors have been described as being associated with either prevalence, incidence or progression of OA. High bone mineral density (BMD) was determined to be associated with increased risk of radiographic hip OA (8) or knee OA (9), and with total joint replacement (10). However, results from prospective studies of incident radiographic OA or OA progression are controversial (11). The concept of a "metabolic OA" phenotype was recently proposed (4). However, as metabolic factors are closely related to BMI, their BMI-independent contribution to the risk of OA is unknown. Previous studies have shown that the presence of the metabolic syndrome and many of its components are associated with the risk of hand and knee OA (12–14). Most associations with each of the metabolic syndrome components, however, become nonsignificant after adjustment for BMI (13,15). In addition, conflicting data regarding type 2 diabetes as a BMI-independent predictor of OA have been reported (16,17). The results from classic epidemiologic studies may be affected by residual confounding or reverse causation. Thus, there is an unmet need for a well-powered study

Supported by the European Commission's Horizon 2020 Framework Programme Marie Skłodowska-Curie Actions (GOTBONE-750579), the French Society of Rheumatology, Vinnova, the Swedish Research Council, the Swedish Foundation for Strategic Research, the ALF/LUA research grant in Gothenburg, the Lundberg Foundation, the Knut and Alice Wallenberg Foundation, the Torsten Söderberg Foundation, and the Novo Nordisk Foundation.

[1]Thomas Funck-Brentano, MD, PhD, Maria Nethander, MSc, Sofia Movérare-Skrtic, PhD, Claes Ohlsson MD, PhD: University of Gothenburg, Gothenburg, Sweden; [2]Pascal Richette, MD, PhD: AP-HP, Hospital Lariboisière, INSERM U1132, Université Paris Diderot, Université de Paris, Paris, France.

No potential conflicts of interest relevant to this article were reported.

Anonymized phenotype and genetic data are available from UK Biobank on application.

Address correspondence to Claes Ohlsson, MD, PhD, Klin Farm Lab, Centre for Bone and Arthritis Research, Vita Stråket 11, SE-41345 Gothenburg, Sweden. E-mail: claes.ohlsson@medic.gu.se.

Submitted for publication November 21, 2018; accepted in revised form May 9, 2019.

to identify causal risk factors of OA. We hypothesized that causal associations may differ by OA site.

Mendelian randomization (MR) can be used to test for a causal association between a risk factor and a particular outcome (18). Two recent MR studies have demonstrated that overweight or high BMI is causally associated with increased risk of OA (19,20). Therefore, to reduce potential bias through genetic associations with confounders, MR analyses of other causal factors should include sensitivity analyses without genetic instrument variables also associated with BMI.

The present study aimed to identify causal risk factors for site-specific OA in the complete UK Biobank data set. Using genetic instrument variables from previously published genome-wide association study (GWAS) meta-analysis, the possible causality of BMI, BMD, serum high-density lipoprotein (HDL) cholesterol, low-density lipoprotein (LDL) cholesterol, and triglyceride levels, type 2 diabetes, systolic blood pressure (BP), and C-reactive protein (CRP) levels in the risk of developing knee, hip, and hand OA was evaluated. The primary outcome measure was hospital diagnosis of OA. In secondary analyses, more severe cases of knee and hip OA, as identified by joint replacement, were also evaluated.

SUBJECTS AND METHODS

UK Biobank study subjects and ethics approval. In this study, conducted using the UK Biobank resource (http://www.ukbiobank.ac.uk/), 502,647 individuals between the ages of 37 and 76 years were recruited from across the UK from 2006 to 2010 (21). Participants provided a range of information regarding health status, demographics, and lifestyle via questionnaires and interviews. In addition, they were physically examined for anthropometric measurements, BP readings, and an estimation of BMD of the heel using a noninvasive method. The full data set was downloaded in April 2018. We included 384,838 unrelated participants of white European descent with valid data on the outcome measure and relevant covariates (age, sex, BMI). Pairs of individuals up to third-degree relatives were identified using the robust estimated kinship coefficients from the King software (22). The UK Biobank has ethical approval from the North West Multi-Centre Research Ethics Committee, and informed consent was obtained from all participants. The present research was approved by the UK Biobank Research and Access Committee (application no. 26952).

Outcome measure definitions. The outcome measure was obtained from the UK Biobank database downloaded in April 2018. The primary outcome measure in the present study was OA as defined by hospital diagnoses (http://biobank.ctsu.ox.ac.uk/crystal/label.cgi?id=2022) using the International Classification of Diseases, Ninth Revision (ICD-9) codes or the Tenth Revision (ICD-10) for all OA (n = 48,431), knee OA (n = 19,727), hip OA (n = 11,875), and hand OA (n = 2,330) (see Supplementary Table 1, available on *Arthritis & Rheumatology* web site at http://onlinelibrary.wiley.com/doi/10.1002/art.40928/abstract). Of the total of 48,731 all OA cases, 11 were identified with ICD-9 codes and 48,420 with ICD-10 codes. In secondary analyses, we evaluated self-reported OA from the UK Biobank questionnaires and more severe cases of OA defined by a history of knee replacement or hip replacement. Patients with valid information from operative procedures summary information for knee replacement (W40-42) or hip replacement (W37-39), according to the Office of Population Censuses and Surveys Classification of Interventions and Procedures, version 4 (http://biobank.ctsu.ox.ac.uk/crystal/label.cgi?id=2025), were included. We excluded patients who had a concomitant diagnosis of chronic inflammatory arthritis or aseptic osteonecrosis at the time of intervention. For hip replacement, we further excluded patients who had concomitantly self-reported hip fracture (Supplementary Table 1, http://onlinelibrary.wiley.com/doi/10.1002/art.40928/abstract). In the UK Biobank, the hospital admissions registers began in 1981 and were updated until February 29, 2016. The last OA case date registered in our data set was February 25, 2016.

As expected, there was a substantial overlap between the different OA outcomes (Supplementary Table 2, http://onlinelibrary.wiley.com/doi/10.1002/art.40928/abstract). Interestingly, among the 11,875 individuals with a hospital diagnosis of hip OA, only 4,445 (37%) were identified in the self-reported OA questionnaire. Therefore, we selected outcome measure definitions using hospital diagnoses for our primary analyses.

Causal associations using MR. To assess causal associations between risk markers and OA, we performed MR analyses. We used genetic instrument variables obtained from selected GWAS as proxies for BMI (23), femoral neck BMD and lumbar spine BMD (24), serum HDL cholesterol, LDL cholesterol, and triglyceride levels (25), type 2 diabetes (26), systolic BP (27), and CRP levels (28) (Supplementary Table 3, http://onlinelibrary.wiley.com/doi/10.1002/art.40928/abstract). As genetic variants are randomly distributed at birth, they are unaffected by confounders. We then regressed the association of these single-nucleotide polymorphisms (SNPs) on the outcome measure, weighing their effect by the magnitude of their effect upon the corresponding exposure.

Our primary MR method was the 2-sample inverse-variance weighting, using the effect estimates for the exposure from the corresponding GWAS. Sensitivity analyses were performed using the MR-Egger method to preclude pleiotropy (29) (Supplementary Figure 1, http://onlinelibrary.wiley.com/doi/10.1002/art.40928/abstract), the weighted median MR method, and the penalized weighted median MR method. When the exposure parameter was available (for BMI, type 2 diabetes, and systolic BP), we also performed 1-sample MR methods using the effect estimates for exposure in the UK Biobank. Power analyses were performed for each exposure and OA outcome (Supplementary Table 4,

http://onlinelibrary.wiley.com/doi/10.1002/art.40928/abstract). Early on we identified a robust causal effect of BMI on the risk of OA and therefore for other candidate causal traits, we performed additional MR sensitivity analyses excluding genetic instrument variables that are also associated ($P < 0.05$) with BMI (Supplementary Tables 5–13, http://onlinelibrary.wiley.com/doi/10.1002/art.40928/abstract). Detailed methods for MR studies are described in Supplementary Methods, http://onlinelibrary.wiley.com/doi/10.1002/art.40928/abstract.

We evaluated 9 candidate causal risk factors, and for all these traits, we first evaluated the association with all OA, as this was the outcome measure with the highest power for the 2-sample inverse-variance weighting method (required Bonferroni-corrected P value <0.0056 [$P = 0.05/9$]). If this threshold was met for all OA, a nominal P value of 0.05 was required for the site-specific analyses of knee, hip, or hand OA. Therefore, 95% confidence intervals (95% CIs) for all OA are presented before and after adjustment for multiple comparisons (n = 9).

Comorbidities and covariates. For BMI, we used the calculated measures of weight/height^2 available in the anthropometrics data at recruitment. Two measures of systolic BP were obtained at the inclusion interview. We used the mean value of the 2 available measures for each individual. Information on the use of antihypertensive medication was collected during the same visit. For the population description at baseline, individuals with prevalent type 2 diabetes were identified using self-reported diabetes at recruitment in combination with a hospital diagnosis of type 2 diabetes by ICD-10 code (E11). For the MR analyses, we included prevalent and incident cases of type 2 diabetes, using any diagnosis of type 2 diabetes by ICD-10 codes in the database. Information on current smoking status (yes or no) was collected at the time of the interview.

RESULTS

The mean age of the 384,838 unrelated individuals of European descent included in the present study was 56.8 years. Patient characteristics and main comorbidities at recruitment are presented in Table 1. Our primary analyses were inverse-variance weighting by 2-sample MR for all OA, and after adjustment for multiple comparisons (9 traits; $P < 0.0056$), causal evidence was observed for high BMI ($P = 3.0 \times 10^{-24}$), high femoral neck BMD ($P = 3.0 \times 10^{-4}$), and low systolic BP ($P = 2.3 \times 10^{-6}$), as shown in Figure 1 (also see Supplementary Table 14, http://onlinelibrary.wiley.com/doi/10.1002/art.40928/abstract). For all OA, there was no clear evidence of pleiotropy, and the MR-Egger intercept demonstrated no significance for any of the tested exposures.

Evidence of a causal association of BMI with knee and hip OA, but not hand OA. The 2-sample MR revealed that an increase in genetically determined BMI was causally associated with all OA (odds ratio [OR] per SD increase 1.57 [95% CI 1.44–1.71; adjusted for 9 comparisons 1.39–1.77]), as shown in Figure 1 and Supplementary Table 14. As individual-level data were available and as the UK Biobank was well-powered for the outcome of all OA, we performed stratified analyses to compare the causal association of BMI in different subgroups. The causal association of genetically determined BMI with all OA was robust and similar in young individuals (below the median age of cases) and older individuals (above the median age of cases), in males and females, as well as in subpopulations stratified by smoking status or type 2 diabetes (Figure 2). Causal associations for BMI were also found at weight-bearing joints (OR per SD increase 1.76 [95% CI 1.56–1.99] in knee OA and 1.52 [95% CI 1.31–1.78] in hip OA), but not at the hand (OR 1.00 [95% CI 0.76–1.31]). Similar results were obtained with the other 2-sample MR methods and 1-sample MR methods (see Supplementary Tables 14–17, http://onlinelibrary.wiley.com/doi/10.1002/art.40928/abstract).

Table 1. Participant characteristics and main comorbidities at recruitment*

All subjects at recruitment	
Age, years	56.8 ± 8.0
Female sex, no. (%)	207,789 (54.0)
Body mass index, kg/m^2	27.4 ± 4.8
Cholesterol-lowering medication users, no. (%)	66,379 (17.3)
Prevalent type 2 diabetes, no. (%)	10,170 (2.6)
Prevalent and incident type 2 diabetes, no. (%)	16,946 (4.4)
Antihypertensive medication users, no. (%)	79,081 (20.6)
Systolic BP, mm Hg	138.0 ± 18.6
Systolic BP, excluding antihypertensive medication users, mm Hg	136.2 ± 18.3
Current smokers, no. (%)	39,840 (10.4)
OA	
All locations combined, no. (%)	
All OA	48,431 (12.6)
Self-reported OA	34,229 (8.9)
Knee, no. (%)	
Knee OA	19,727 (5.1)
Knee replacement	9,716 (2.6)
Hip, no. (%)	
Hip OA	11,875 (3.1)
Hip replacement	9,932 (2.6)
Hand OA, no. (%)	2,330 (0.6)

* The n value for each variable was 384,838, except as follows: for cholesterol-lowering medication users and antihypertensive medication users, n = 384,468; for systolic blood pressure (BP), n = 384,515; for systolic BP, excluding antihypertensive medication users, n = 305,170; for current smokers, n = 383,470; for knee replacement, n = 379,840; and for hip replacement, n = 379,197. Except where indicated otherwise, values are the mean ± SD. OA = osteoarthritis.

Evidence of a causal association of BMD with knee and hip OA. Genetically determined femoral neck BMD was causally associated with all OA (OR per SD increase 1.14 [95% CI 1.06–1.22; adjusted for 9 comparisons 1.03–1.25]; Figure 1). The causal association was found to be of similar magnitude at the knee (OR 1.18 [95% CI 1.05–1.32]) and

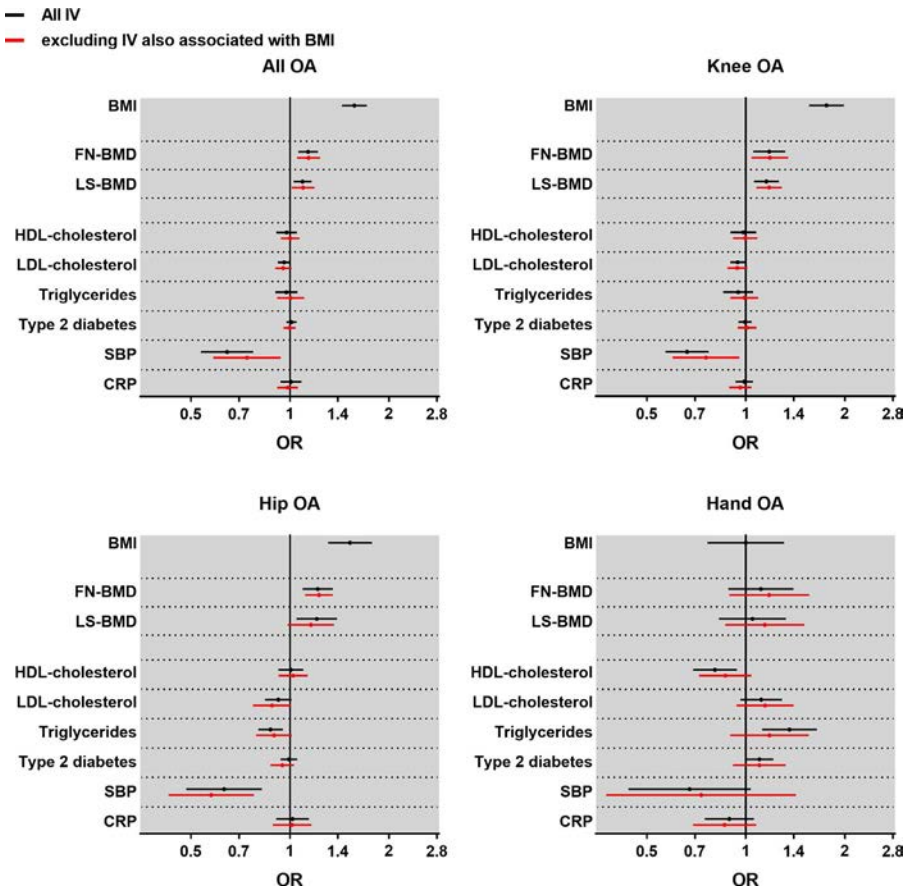

Figure 1. Causal associations between genetically determined risk factors and osteoarthritis (OA) by site. For each site, the odds ratio (OR) and 95% confidence interval for the risk of OA are represented for each factor, as determined using the 2-sample Mendelian randomization inverse-variance weighting method for body mass index (BMI; per SD increase), femoral neck bone mineral density (FN-BMD; per SD increase), lumbar spine BMD (LS-BMD; per SD increase), serum levels of high-density lipoprotein (HDL) cholesterol, low-density lipoprotein (LDL) cholesterol, and triglyceride (per SD increase), systolic blood pressure (SBP; per SD increase), C-reactive protein (CRP) level (per ln[mg/liter] increase), or presence of type 2 diabetes. The total number of subjects is 384,838, with 48,431 all OA, 19,727 knee OA, 11,875 hip OA, and 2,330 hand OA cases. IV = instrument variable.

hip (OR 1.22 [95% CI 1.09–1.35]), but not at the hand (OR 1.11 [95% CI 0.88–1.39]; Figure 1 and Supplementary Table 14). Sensitivity analyses, excluding BMI-associated SNPs (Figure 1), as well as analyses using other MR methods, revealed similar results (Supplementary Table 14). For lumbar spine BMD, the causal association with all OA was less pronounced and only nominally significant. Site-specific analyses demonstrated a causal association of lumbar spine BMD at the knee (OR 1.15 [95% CI 1.06–1.26]), which remained after the exclusion of genetic instrument variables also associated with BMI (Supplementary Table 14).

Evidence of a causal association of systolic BP with hip OA. Systolic BP was causally inversely associated with all OA (OR per SD increase 0.64 [95% CI 0.54–0.77; adjusted for 9 comparisons 0.50–0.83]), knee OA (OR 0.66 [95% CI 0.57–0.77]), and hip OA (OR 0.63 [95% CI 0.48–0.82], Figure 1 and Supplementary Table 14). The associations remained unchanged when subjects receiving antihypertensive medication were excluded from the analyses (see Supplementary Figure 2, http://onlinelibrary.wiley.com/doi/10.1002/art.40928/abstract). Similar results were obtained in sensitivity analyses excluding BMI-associated SNPs, and with other MR methods (Supplementary Tables 14–17, http://onlinelibrary.wiley.com/doi/10.1002/art.40928/abstract).

No evidence of a causal association of other tested metabolic markers or CRP level with OA. No other tested candidate traits (HDL cholesterol, LDL cholesterol, triglyceride level, type 2 diabetes, or CRP level) demonstrated any evidence of a causal association with all OA, knee OA, hip OA, or hand OA that remained after exclusion of genetic instrument variables also associated with BMI or correction for multiple comparisons (Figure 1). Although failing to pass our prespecified threshold for adjustment for multiple comparisons, weak causal inverse associations between LDL cholesterol level and risk of knee OA and hip OA were observed (for knee OA, OR per SD increase 0.94 [95% CI 0.90–0.99] for all SNPs and OR 0.94 [95% CI 0.88–1.01] without BMI SNPs; for hip OA, OR per SD increase 0.92 [95% CI

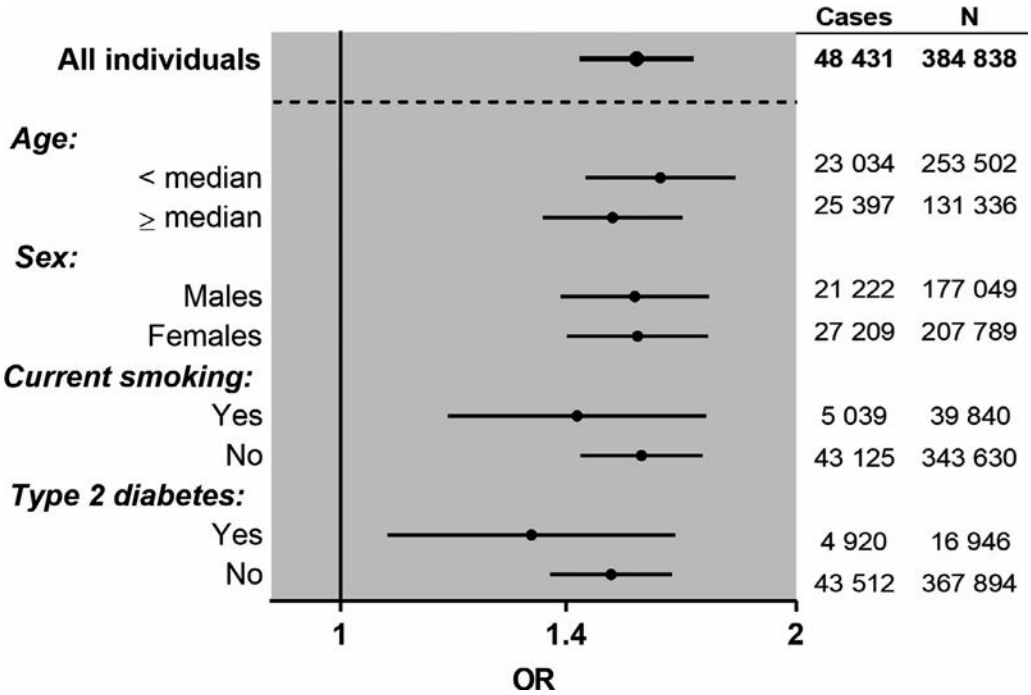

Figure 2. Stratified analyses of the causal associations of body mass index (BMI) with all osteoarthritis (OA). Odds ratios (ORs) and 95% confidence intervals are shown for the causal associations between BMI (per SD increase) and the risk of all OA, as determined using the 2-sample Mendelian randomization inverse-variance weighting method in analyses stratified by age (median of cases), sex, current smoking status, or type 2 diabetes.

0.84–1.01] for all SNPs and OR 0.88 [95% CI 0.77–1.01] without BMI SNPs) (Supplementary Table 14).

Secondary analyses using knee and hip joint replacement as definitions of severe OA. We repeated the analyses using knee or hip replacement definitions of severe OA and found causal associations for genetically determined high BMI (knee replacement: OR per SD increase 2.30 [95% CI 1.93–2.75]; hip replacement: OR per SD increase 1.65 [95% CI 1.41–1.92]), and high femoral neck BMD (knee replacement: OR per SD increase 1.27 [95% CI 1.09–1.48]; hip replacement: OR per SD increase 1.17 [95% CI 1.05–1.31]). Systolic BP was causally inversely associated with joint (knee replacement: OR per SD increase 0.64 [95% CI 0.50–0.83]; hip replacement: OR per SD increase 0.64 [95% CI 0.48–0.85]), which was in accordance with the findings from our primary analyses using hospital diagnoses (Figure 3 and Supplementary Tables 14–17, http://onlinelibrary.wiley.com/doi/10.1002/art.40928/abstract).

DISCUSSION

This study used the largest known data set to date with individual-level clinical, genetic, and outcome data to assess causal factors for OA. In the UK Biobank setting, we found 3 factors (high BMI, high femoral neck BMD, and low systolic BP) that were causally associated with increased risk of OA. High BMI was shown to be causal for knee OA and hip OA, but not hand OA. We also report the first clear evidence of a causal role of high femoral neck BMD, predominantly reflecting cortical bone mass, on the risk of knee OA and hip OA. The most novel finding from this study is that low systolic BP was causally associated with all OA, knee OA, and hip OA. In contrast, the other metabolic factors and CRP levels were not causally associated with the risk of developing OA, after exclusion of the genetic instrument variables that are also associated with BMI.

Weight loss is reported to reduce knee OA symptoms and structural damage (7,30). The causal role of BMI in both knee and hip OA has recently been demonstrated in a previous study using first-release data from the UK Biobank (19). In this study, we replicated these causal BMI associations at weight-bearing joints. In addition, because in the current well-powered study we had access to individual-level data, we also performed stratified analyses, demonstrating that the causal effect of BMI on OA was robust and similar in young and old individuals, in males and females, as well as in subpopulations stratified by smoking status or type 2 diabetes. Importantly, we observed no evidence of a causal effect of BMI on the risk of hand OA. Collectively, these findings demonstrate that it is the body weight–induced loading of the joints that causes the increased risk of OA observed at weight-loaded, but not non–weight-loaded OA sites.

The importance of subchondral bone in the pathophysiology of OA has been extensively debated (31–34). So far, the supposed inverse association between osteoporosis and OA (35,36), and the observation that high bone mass is associated with

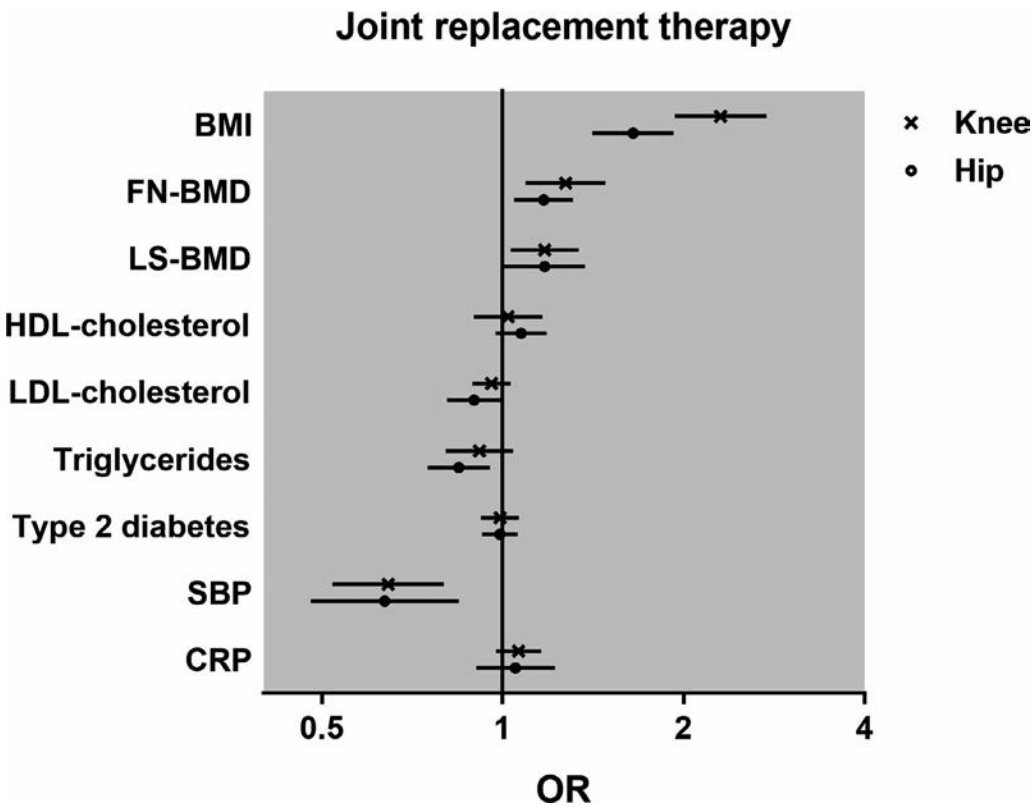

Figure 3. Causal associations between genetically determined risk factors and knee or hip replacement. For each joint replacement osteoarthritis (OA) definition, the odds ratio (OR) and 95% confidence interval for the risk of OA are represented for each factor, as determined using the 2-sample Mendelian randomization inverse-variance weighting method for body mass index (BMI; per SD increase), femoral neck bone mineral density (FN-BMD; per SD increase), lumbar spine BMD (LS-BMD; per SD increase), serum levels of high-density lipoprotein (HDL) cholesterol, low-density lipoprotein (LDL) cholesterol, and triglyceride (per SD increase), systolic blood pressure (SBP; per SD increase), C-reactive protein (CRP) level (per ln[mg/liter] increase), or presence of type 2 diabetes. The total number of subjects is 384,838 (9,716 knee replacement and 9,932 hip replacement cases).

osteophyte volume (37), radiographic OA (8,9), and increased prevalence of joint replacement (10), led to the general hypothesis that increased BMD could be deleterious to the joint. The findings of these observational studies are in accordance with the results from the present MR analyses, which demonstrated a robust causal role of femoral neck BMD on knee and hip OA. We confirmed these associations in sensitivity analyses excluding the genetic instrument variables that were also associated with BMI, to preclude pleiotropy. Similarly, as previously described (19), we observed a modest causal association between lumbar spine BMD and knee OA. The previous lumbar spine BMD MR analyses, performed in an early-released subset of the UK Biobank, did not comply with the MR assumptions that genetic instrument variables should not be associated with the known confounder (BMI). In addition, the previous UK Biobank study was restricted by the phenotypes available in the MR-base platform (http://www.mrbase.org/), and therefore the most powerful lumbar spine BMD GWAS was not used. Also, the femoral neck BMD trait with the most robust causal association in the present study was not available for selection of genetic instrument variables (24).

Our present finding that low systolic BP is causally associated with OA is novel. Previous limited observational studies have evaluated the association between hypertension, defined as a combination of antihypertensive medication use and high BP, and OA. Hypertension was associated with increased risk of radiographic knee OA both in a prospective analysis in the Framingham Osteoarthritis Study (15) and in a large cross-sectional South Korean study (38). However, after adjustment for BMI, hypertension was not significantly associated with incident OA in the Framingham Osteoarthritis Study. It is possible that earlier prospective studies have been underpowered to identify systolic BP as a BMI-independent predictor of OA. Further studies are needed to confirm the causal link between low systolic BP and OA, and to identify the underlying mechanisms.

The previous MR study, which used a less powered subsample from the UK Biobank, indicated that some metabolic factors may display modest, but significant, causal associations with OA (19). However, BMI-associated SNPs were not excluded in those analyses, which therefore most likely were confounded by pleiotropic effects related to the known strong causal effect of BMI on OA. The present study, performing sensitivity analy-

ses with BMI-associated SNPs excluded, did not identify any causal association of metabolic risk factors except for systolic BP. The absence of a causal association for type 2 diabetes on OA in the present study indicates that the results of the previous observational association studies could be biased by remaining confounding factors or by reverse causation. Indeed, low physical activity caused by impaired mobility with knee or hip OA may increase insulin resistance. Finally, the lack of evidence of a causal role of lipids in knee or hip OA is supported by the results of 2 studies that showed no beneficial effect of statin use on OA risk or OA progression (39,40). However, a recent MR analysis in the Malmö Diet and Cancer Study showed that genetically determined increased LDL cholesterol was causally associated with reduced risk of OA (41). This latter MR analysis also confirmed that high BMI is causally associated with increased risk of OA. Although low-grade inflammation has been associated with increased risk of severe OA in observational studies (13), no causal effect of CRP levels was observed in the present study, which is in accordance with the negative results of intervention studies targeting inflammatory cytokines (42).

The major strength of the present study is its large sample size with individual-level data available. With respect to the second and third MR assumptions, we considered possible pleiotropy in sensitivity analyses in addition to the MR-Egger method, by excluding instrument variables that were also associated with BMI, since BMI was early shown to be a strong causative factor for knee and hip OA. We also performed detailed power calculations to ascertain the interpretation of negative results. Finally, we replicated our main analyses using other definitions for severe OA cases, using a joint replacement register that was independent of the ICD-9 and ICD-10 codes and found very similar results.

However, this study has some limitations. As we used hospital diagnoses, we could not assess any radiographic structural progression or pain as is recommended for clinical trials (43). While MR as an approach is appealing to address concerns about confounding, we cannot fully exclude the possibility that the null findings for some of the MR analyses could be due to misclassification of the diagnosis. This limitation may mostly affect hand OA, for which we acknowledge an underestimation of cases. Moreover, for knee OA, posttraumatic OA may be overrepresented when using hospital diagnosis. A hospital contact could also impact the chance of being classified as an OA case. However, we consider that our case definitions, being classified by hospital physicians, reflect symptomatic cases. ICD-10 code validation was not conducted in the present study using the UK Biobank; however, previous validation studies in other cohorts showed good positive predictive value (44,45). Another limitation is that the impact of physical activity could not be analyzed in this study, as no large published GWAS met our criteria to be used as a source of genetic instrument variables. Finally, our conclusions can only apply to a white European population.

In conclusion, BMI exerts a major causal effect on the risk of OA at weight-bearing joints, but not at the hand. Evidence of causality of knee OA and hip OA was observed for high femoral neck BMD and low systolic BP. These results should be considered in the future research of OA and for the elaboration of prevention or therapeutic strategies for the different OA sites.

ACKNOWLEDGMENT

We thank all the participants in the UK Biobank.

AUTHOR CONTRIBUTIONS

All authors were involved in drafting the article or revising it critically for important intellectual content, and all authors approved the final version to be published. Dr. Funck-Brentano had full access to all of the data in the study and takes responsibility for the integrity of the data and the accuracy of the data analysis.

Study conception and design. Funck-Brentano, Nethander, Ohlsson.
Acquisition of data. Nethander.
Analysis and interpretation of data. Funck-Brentano, Nethander, Movérare-Skrtic, Richette, Ohlsson.

REFERENCES

1. Arden N, Nevitt MC. Osteoarthritis: epidemiology. Best Pract Res Clin Rheumatol 2006;20:3–25.
2. Nüesch E, Dieppe P, Reichenbach S, Williams S, Iff S, Jüni P. All cause and disease specific mortality in patients with knee or hip osteoarthritis: population based cohort study. BMJ 2011;342:d1165.
3. Cooper C, Snow S, McAlindon TE, Kellingray S, Stuart B, Coggon D, et al. Risk factors for the incidence and progression of radiographic knee osteoarthritis. Arthritis Rheum 2000;43:995–1000.
4. Bijlsma JW, Berenbaum F, Lafeber FP. Osteoarthritis: an update with relevance for clinical practice. Lancet 2011;377:2115–26.
5. Lohmander LS, Gerhardsson de Verdier M, Rollof J, Nilsson PM, Engström G. Incidence of severe knee and hip osteoarthritis in relation to different measures of body mass: a population-based prospective cohort study. Ann Rheum Dis 2009;68:490–6.
6. Messier SP, Mihalko SL, Legault C, Miller GD, Nicklas BJ, DeVita P, et al. Effects of intensive diet and exercise on knee joint loads, inflammation, and clinical outcomes among overweight and obese adults with knee osteoarthritis: the IDEA randomized clinical trial. JAMA 2013;310:1263–73.
7. Richette P, Poitou C, Garnero P, Vicaut E, Bouillot JL, Lacorte JM, et al. Benefits of massive weight loss on symptoms, systemic inflammation and cartilage turnover in obese patients with knee osteoarthritis. Ann Rheum Dis 2011;70:139–44.
8. Hardcastle SA, Dieppe P, Gregson CL, Hunter D, Thomas GE, Arden NK, et al. Prevalence of radiographic hip osteoarthritis is increased in high bone mass. Osteoarthritis Cartilage 2014;22:1120–8.
9. Hardcastle SA, Dieppe P, Gregson CL, Arden NK, Spector TD, Hart DJ, et al. Individuals with high bone mass have an increased prevalence of radiographic knee osteoarthritis. Bone 2015;71:171–9.
10. Hardcastle SA, Gregson CL, Deere KC, Davey Smith GD, Dieppe P, Tobias JH. High bone mass is associated with an increased prevalence of joint replacement: a case–control study. Rheumatology (Oxford) 2013;52:1042–51.
11. Hardcastle SA, Dieppe P, Gregson CL, Davey Smith G, Tobias JH. Osteoarthritis and bone mineral density: are strong bones bad for joints? [review]. Bonekey Rep 2015;4:624.

12. Sowers M, Karvonen-Gutierrez CA, Palmieri-Smith R, Jacobson JA, Jiang Y, Ashton-Miller JA. Knee osteoarthritis in obese women with cardiometabolic clustering. Arthritis Rheum 2009;61:1328–36.
13. Engström G, Gerhardsson de Verdier M, Rollof J, Nilsson PM, Lohmander LS. C-reactive protein, metabolic syndrome and incidence of severe hip and knee osteoarthritis: a population-based cohort study. Osteoarthritis Cartilage 2009;17:168–73.
14. Berenbaum F, Griffin TM, Liu-Bryan R. Metabolic regulation of inflammation in osteoarthritis. Arthritis Rheumatol 2017;69:9–21.
15. Niu J, Clancy M, Aliabadi P, Vasan R, Felson DT. Metabolic syndrome, its components, and knee osteoarthritis: the Framingham Osteoarthritis Study. Arthritis Rheumatol 2017;69:1194–203.
16. Schett G, Kleyer A, Perricone C, Sahinbegovic E, Iagnocco A, Zwerina J, et al. Diabetes is an independent predictor for severe osteoarthritis: results from a longitudinal cohort study. Diabetes Care 2013;36:403–9.
17. Nielen JT, Emans PJ, Dagnelie PC, Boonen A, Lalmohamed A, de Boer A, et al. Severity of diabetes mellitus and total hip or knee replacement: a population-based case–control study. Medicine (Baltimore) 2016;95:e3739.
18. Burgess S, Butterworth A, Thompson SG. Mendelian randomization analysis with multiple genetic variants using summarized data. Genet Epidemiol 2013;37:658–65.
19. Zengini E, Hatzikotoulas K, Tachmazidou I, Steinberg J, Hartwig FP, Southam L, et al. Genome-wide analyses using UK Biobank data provide insights into the genetic architecture of osteoarthritis. Nat Genet 2018;50:549–58.
20. Panoutsopoulou K, Metrustry S, Doherty SA, Laslett LL, Maciewicz RA, Hart DJ, et al. The effect of FTO variation on increased osteoarthritis risk is mediated through body mass index: a Mendelian randomisation study. Ann Rheum Dis 2014;73:2082–6.
21. Collins R. What makes UK Biobank special? Lancet 2012;379:1173–4.
22. Manichaikul A, Mychaleckyj JC, Rich SS, Daly K, Sale M, Chen WM. Robust relationship inference in genome-wide association studies. Bioinformatics 2010;26:2867–73.
23. Locke AE, Kahali B, Berndt SI, Justice AE, Pers TH, Day FR, et al. Genetic studies of body mass index yield new insights for obesity biology. Nature 2015;518:197–206.
24. Estrada K, Styrkarsdottir U, Evangelou E, Hsu YH, Duncan EL, Ntzani EE, et al. Genome-wide meta-analysis identifies 56 bone mineral density loci and reveals 14 loci associated with risk of fracture. Nat Genet 2012;44:491–501.
25. Willer CJ, Schmidt EM, Sengupta S, Peloso GM, Gustafsson S, Kanoni S, et al. Discovery and refinement of loci associated with lipid levels. Nat Genet 2013;45:1274–83.
26. Morris AP, Voight BF, Teslovich TM, Ferreira T, Segrè AV, Steinthorsdottir V, et al. Large-scale association analysis provides insights into the genetic architecture and pathophysiology of type 2 diabetes. Nat Genet 2012;44:981–90.
27. Ehret GB, Munroe PB, Rice KM, Bochud M, Johnson AD, Chasman DI, et al, for the International Consortium for Blood Pressure Genome-Wide Association Studies. Genetic variants in novel pathways influence blood pressure and cardiovascular disease risk. Nature 2011;478:103–9.
28. Dehghan A, Dupuis J, Barbalic M, Bis JC, Eiriksdottir G, Lu C, et al. Meta-analysis of genome-wide association studies in >80,000 subjects identifies multiple loci for C-reactive protein levels. Circulation 2011;123:731–8.
29. Bowden J, Davey Smith G, Burgess S. Mendelian randomization with invalid instruments: effect estimation and bias detection through Egger regression. Int J Epidemiol 2015;44:512–25.
30. Gersing AS, Schwaiger BJ, Nevitt MC, Joseph GB, Chanchek N, Guimaraes JB, et al. Is weight loss associated with less progression of changes in knee articular cartilage among obese and overweight patients as assessed with MR imaging over 48 months? Data from the Osteoarthritis Initiative. Radiology 2017;284:508–20.
31. Lories RJ, Corr M, Lane NE. To Wnt or not to Wnt: the bone and joint health dilemma. Nat Rev Rheumatol 2013;9:328–39.
32. Funck-Brentano T, Cohen-Solal M. Subchondral bone and osteoarthritis. Curr Opin Rheumatol 2015;27:420–6.
33. Geusens PP, van den Bergh JP. Osteoporosis and osteoarthritis: shared mechanisms and epidemiology. Curr Opin Rheumatol 2016;28:97–103.
34. Felson DT, Neogi T. Osteoarthritis: is it a disease of cartilage or of bone? [editorial]. Arthritis Rheum 2004;50:341–4.
35. Hart DJ, Mootoosamy I, Doyle DV, Spector TD. The relationship between osteoarthritis and osteoporosis in the general population: the Chingford Study. Ann Rheum Dis 1994;53:158–62.
36. Hart DJ, Cronin C, Daniels M, Worthy T, Doyle DV, Spector TD. The relationship of bone density and fracture to incident and progressive radiographic osteoarthritis of the knee: the Chingford Study. Arthritis Rheum 2002;46:92–9.
37. Hardcastle SA, Dieppe P, Gregson CL, Arden NK, Spector TD, Hart DJ, et al. Osteophytes, enthesophytes, and high bone mass: a bone-forming triad with potential relevance in osteoarthritis. Arthritis Rheumatol 2014;66:2429–39.
38. Kim HS, Shin JS, Lee J, Lee YJ, Kim M, Bae YH, et al. Association between knee osteoarthritis, cardiovascular risk factors, and the Framingham risk score in South Koreans: a cross-sectional study. PLoS ONE 2016;11:e0165325.
39. Eymard F, Parsons C, Edwards MH, Petit-Dop F, Reginster JY, Bruyère O, et al. Statin use and knee osteoarthritis progression: results from a post-hoc analysis of the SEKOIA trial. Joint Bone Spine 2018;85:609–14.
40. Michaëlsson K, Lohmander LS, Turkiewicz A, Wolk A, Nilsson P, Englund M. Association between statin use and consultation or surgery for osteoarthritis of the hip or knee: a pooled analysis of four cohort studies. Osteoarthritis Cartilage 2017;25:1804–13.
41. Hindy G, Åkesson KE, Melander O, Aragam KG, Haas ME, Nilsson PM, et al. Cardiometabolic polygenic risk scores and osteoarthritis outcomes: a Mendelian randomization study using data from the Malmö Diet and Cancer Study and the UK Biobank. Arthritis Rheumatol 71:925–34.
42. Chevalier X, Eymard F, Richette P. Biologic agents in osteoarthritis: hopes and disappointments. Nat Rev Rheumatol 2013;9:400–10.
43. Leyland KM, Gates LS, Nevitt M, Felson D, Bierma-Zeinstra SM, Conaghan PG, et al. Harmonising measures of knee and hip osteoarthritis in population-based cohort studies: an international study. Osteoarthritis Cartilage 2018;26:872–9.
44. Rahman MM, Kopec JA, Goldsmith CH, Anis AH, Cibere J. Validation of administrative osteoarthritis diagnosis using a clinical and radiological population-based cohort. Int J Rheumatol 2016;2016:6475318.
45. Turkiewicz A, Petersson IF, Björk J, Hawker G, Dahlberg LE, Lohmander LS, et al. Current and future impact of osteoarthritis on health care: a population-based study with projections to year 2032. Osteoarthritis Cartilage 2014;22:1826–32.

American College of Rheumatology
Empowering Rheumatology Professionals

Arthritis & Rheumatology
Vol. 71, No. 10, October 2019, pp 1642–1650
DOI 10.1002/art.40917

HLA Alleles Associated With Risk of Ankylosing Spondylitis and Rheumatoid Arthritis Influence the Gut Microbiome

Mark Asquith,[†] Peter R. Sternes,[1] Mary-Ellen Costello,[1] Lisa Karstens,[2] Sarah Diamond,[2] Tammy M. Martin,[2] Zhixiu Li,[1] Mhairi S. Marshall,[1] Timothy D. Spector,[3] Kim-Anh le Cao,[4] James T. Rosenbaum,[5] and Matthew A. Brown[1]

Objective. HLA alleles affect susceptibility to more than 100 diseases, but the mechanisms that account for these genotype–disease associations are largely unknown. HLA alleles strongly influence predisposition to ankylosing spondylitis (AS) and rheumatoid arthritis (RA). Both AS and RA patients have discrete intestinal and fecal microbiome signatures. Whether these changes are the cause or consequence of the diseases themselves is unclear. To distinguish these possibilities, we examined the effect of HLA–B27 and HLA–DRB1 RA risk alleles on the composition of the intestinal microbiome in healthy individuals.

Methods. Five hundred sixty-eight stool and biopsy samples from 6 intestinal sites were collected from 107 healthy unrelated subjects, and stool samples were collected from 696 twin pairs from the TwinsUK cohort. Microbiome profiling was performed using sequencing of the 16S ribosomal RNA bacterial marker gene. All subjects were genotyped using the Illumina CoreExome SNP microarray, and HLA genotypes were imputed from these data.

Results. Associations were observed between the overall microbial composition and both the HLA–B27 genotype and the HLA–DRB1 RA risk allele ($P = 0.0002$ and $P = 0.00001$, respectively). These associations were replicated using the stool samples from the TwinsUK cohort ($P = 0.023$ and $P = 0.033$, respectively).

Conclusion. This study shows that the changes in intestinal microbiome composition seen in AS and RA are at least partially due to effects of HLA-B27 and HLA–DRB1 on the gut microbiome. These findings support the hypothesis that HLA alleles operate to cause or increase the risk of these diseases through interaction with the intestinal microbiome and suggest that therapies targeting the microbiome may be effective in preventing or treating these diseases.

INTRODUCTION

HLA molecules affect susceptibility to many diseases, but in the majority of cases the mechanism by which HLA molecules predispose people to disease remains a mystery. The risks of developing ankylosing spondylitis (AS) and rheumatoid arthritis (RA) are primarily driven by genetic effects, with a heritability of >90% for AS (1,2) and 53–68% for RA (3,4). In both diseases, HLA alleles are major susceptibility factors, with AS being strongly associated with HLA–B27 and RA with HLA–DRB1 shared epitope alleles.

Particularly in the disease pathogenesis of AS, there is strong evidence of a role for gut disease. Up to an estimated 70% of AS

Supported by the National Health and Medical Research Council Australia (grant APP1065509). TwinsUK was supported by the Wellcome Trust, Medical Research Council, Chronic Disease Research Foundation, Arthritis Research UK, European Union, and the NIHR-funded Clinical Research Facility and Biomedical Research Centre at Guy's and St. Thomas' NHS Foundation Trust and King's College London (grant WT081878MA). Drs. Asquith and Rosenbaum's work was supported by the Spondylitis Association of America, the Rheumatology Research Foundation, and the NIH (grant R01-EY-029266). Dr. Karstens' work was supported by the NIH (Eunice Kennedy Shriver National Institute of Child Health and Human Development award K12-HD-043488). Dr. Spector's work was supported by the NIHR (Senior Investigator Fellowship). Dr. Rosenbaum's work was supported by the OHSU Foundation (Collins Medical Trust), the William and Mary Bauman Foundation, the Stan and Madelle Family Trust, and Research to Prevent Blindness. Dr. Brown's work was supported by the National Health and Medical Research Council Australia (Senior Principal Research Fellowship).

[1]Peter R. Sternes, PhD, Mary-Ellen Costello, PhD, Zhixiu Li, PhD, Mhairi S. Marshall, MSc, Matthew A. Brown, MBBS, MD: Queensland University of Technology, Brisbane, Queensland, Australia; [2]Lisa Karstens, PhD, Sarah Diamond, PhD, Tammy M. Martin, PhD: Oregon Health & Science University, Portland; [3]Timothy D. Spector, PhD: King's College London, London, UK; [4]Kim-Anh le Cao, PhD: University of Melbourne, Melbourne, Victoria, Australia; [5]James T. Rosenbaum, MD: Oregon Health & Science University and Legacy Devers Eye Institute, Portland.

[†]Dr. Asquith, MD is deceased.

Drs. Rosenbaum and Brown contributed equally to this work.

No potential conflicts of interest relevant to this article were reported.

Address correspondence to Matthew A. Brown, MBBS, MD, Queensland University of Technology, Institute of Health and Biomedical Innovation, Translational Research Institute, Princess Alexandra Hospital, 37 Kent Street, Woolloongabba, QLD 4102 Brisbane, Australia. E-mail: matt.brown@qut.edu.au.

Submitted for publication January 14, 2019; accepted in revised form April 25, 2019.

patients have either clinical or subclinical gut disease, suggesting that intestinal inflammation may play a role in disease pathogenesis (5,6). Increased gut permeability has been demonstrated in both AS patients and their first-degree relatives, compared to unrelated healthy controls (7–11). Crohn's disease (CD) is closely related to AS and has similar prevalence and high heritability. The 2 conditions commonly co-occur, with ~5% of AS patients developing CD and 4–10% of CD patients developing AS (12,13). Strong cofamiliality (14) and the extensive sharing of genetic factors between AS and inflammatory bowel disease (IBD) (15,16) suggests a shared etiopathogenesis. This is consistent with the hypothesis that gut-derived immune cells or microbial products may contribute to spondyloarthritic inflammation (17–19).

Using 16S ribosomal RNA (rRNA) community profiling, we have previously demonstrated that AS patients have a discrete intestinal microbial signature in the terminal ileum compared to healthy controls ($P < 0.001$) (20), a finding that has subsequently been confirmed by other studies (21,22). We have also demonstrated that dysbiosis is an early feature of disease in HLA–B27–transgenic rats, preceding the onset of clinical disease in the gut or joints (23). Similarly, gut dysbiosis has been demonstrated in RA (24,25), and animal models of RA such as collagen-induced arthritis have been shown to be influenced by the gut microbiome (26,27). In these studies, it is difficult to distinguish the potential effects of the gut microbiome on the disease from the effects of immunologic processes in the intestinal wall or the effects of treatments on the intestinal microbiome.

The role of host genetics in shaping intestinal microbial community composition in humans is unclear. In animal models, host gene deletions have been shown to result in shifts in microbiota composition (28). In addition, a recent quantitative trait locus–mapping study in an intercross murine model linked specific genetic polymorphisms to microbial abundances (29). Large-scale studies in twins (n = 1,126 pairs) have demonstrated that of 945 widely shared taxa, 8.8% showed significant heritability, with some taxa having a heritability of >40% (e.g., family *Christensenellaceae*, 42% heritability) (30).

Further studies are needed to determine whether changes in intestinal microbial composition are due to host genetics and how this affects the overall function of the gut microbiome, including how the microbiome subsequently shapes the immune response and influences inflammation. Due to the strong association of AS with HLA–B27, it has been hypothesized that HLA–B27 induces AS through effects on the gut microbiome, in turn driving spondyloarthritis (SpA) and inducing immunologic processes such as interleukin-23 production (31,32). Further experiments comparing the intestinal microbiomes of HLA–B27–negative and HLA–B27–positive patients would shed light on the influence of HLA–B27 on overall intestinal microbiome composition, especially considering the study on HLA–B27–transgenic rats showing that B27 was associated with altered ileal, cecal, colonic, and fecal microbiota (23,33,34). Similar theories have been proposed regarding interaction between the gut microbiome and the immunologic processes that drive RA (35).

In this study, we investigated whether AS- and RA-associated HLA alleles influence the gut microbiome in healthy individuals, which would support the hypothesis that they affect the risk of developing AS and RA through effects on the gut microbiome.

SUBJECTS AND METHODS

Human subjects. A total of 107 subjects who were undergoing routine colorectal cancer screening at Oregon Health & Science University's Center for Health and Healing were included in this study. Subjects were 40–75 years old and typically followed an omnivorous diet (~95%). The majority (~90%) were white. Individuals were excluded if they had a personal history of IBD or colon cancer, prior bowel or intestinal surgery, or were pregnant. All subjects underwent standard polyethylene glycol bowel preparation the day prior to their colonoscopy procedure. During the procedure, biopsy samples were collected from the terminal ileum or other tissue sites, as indicated, for research purposes. Subjects were instructed to collect a stool sample on a sterile swab at home, just prior to starting their bowel preparation procedure. Stool samples were brought to the colonoscopy appointment at room temperature. All samples (biopsy and fecal swabs) were stored at 4°C in the clinic and transported to the laboratory within 2 hours of the colonoscopy procedure, where they were snap-frozen and stored at –80°C prior to processing. Patient samples were obtained over a 24-month period.

Ethical approval for this study was obtained from the Oregon Health & Science University Institutional Review Board (IRB). Written informed consent was obtained from all subjects. This study was performed in accordance with all applicable US federal and state regulations.

TwinsUK. All work involving human subjects was approved by the Cornell University IRB (protocol ID 1108002388). Matched genotypes and stool samples were collected from 1,392 twins. Genotyping, 16S rRNA amplicon sequencing, filtering, and analysis were performed as described by Goodrich et al (36).

Genotyping. DNA was extracted from mucosal biopsy and stool samples and genotyped using Illumina CoreExome single-nucleotide polymorphism (SNP) microarrays according to standard protocols. Bead intensity data were processed and normalized for each sample, and genotypes were called using Genome Studio (Illumina). We imputed HLA–B genotypes using SNP2HLA (37), as previously described (38). The distribution of HLA–B27 and HLA–DRB1 subtypes (risk, protective, and neutral) can be found in Supplementary Table 1 (available on the *Arthritis & Rheumatology* web site at http://onlinelibrary.wiley.com/doi/10.1002/art.40917/abstract).

Amplicon sequencing and analysis of 16S rRNA. Five hundred sixty-eight stool and biopsy samples from 107 individuals were extracted and amplified for the bacterial marker gene 16S rRNA, as previously described (20). Samples were demultiplexed and filtered for quality using the online platform BaseSpace (http://basespace.illumina.com). Paired-end reads were joined, quality-filtered, and analyzed using Quantitative Insights Into Microbial Ecology, version 1.9.1 (39). Operational taxonomy units (OTUs) were picked against a closed reference, taxonomy was assigned using the Greengenes database (gg_13_8) (40), clustered at 97% similarity by UCLUST (41), and low abundance OTUs were removed (<0.01%).

Data visualization and statistical analysis. Multidimensional data visualization was conducted using sparse partial least squares–discriminant analysis (sPLSDA) on centered log-ratio–transformed data, as implemented in R as part of the MixOmics package, version 6.3.1 (42). Association of the microbial composition with metadata of interest was conducted using a permutational multivariate analysis of variance (PERMANOVA) test as part of R-vegan, version 2.4-5 (43), on arcsine square root–transformed data at species level. This process took into account individual identity when multiple sites per individual were coanalyzed, as well as the sources of covariation such as body mass index (BMI) and sex. Alpha diversity was calculated at the species level using the rarefy function in R-vegan, and differences were evaluated using Wilcoxon's rank sum test. The metagenome functional content was predicted using PICRUSt, version 1.1.3 (44), and the resulting predictions were mapped to KEGG pathways using HUMAnN2, version 0.11.1 (45). Differential abundance of bacterial taxa and KEGG pathways was tested for significance using MaAsLin, version 0.0.5 (46).

RESULTS

Profiling of 16S rRNA and SNP array genotyping were successfully completed for 107 individuals (61 female, 46 male), involving a total of 564 biopsy samples (Table 1).

We studied the effect of BMI, sex, and sampling site on the gut microbiome in order to identify relevant covariates for analysis of AS-related genes and their association with the gut microbiome. Striking differences were observed according to sample site, particularly between the stool samples and mucosal samples ($P < 0.0001$) (Figure 1A). When we excluded stool samples from the analysis, marked difference between sites was still observed ($P < 0.0001$). This was mainly driven by differences between the ileal samples and the colonic mucosal samples (left and right colon, cecum, rectum), which largely clustered together (Figure 1B).

Stool samples are much more convenient to obtain than ileal or colonic mucosal samples, which require an endoscopic procedure for collection. Given the prior evidence of primarily ileal inflammation in AS (5), we were interested in the relationship between the ileal and stool microbiomes. In this comparison, marked difference between sites was also observed ($P < 0.0001$), though some overlap was seen on the sPLSDA plot (Supplementary Figure 2, http://onlinelibrary.wiley.com/doi/10.1002/art.40917/abstract).

Among several studies, some showed an increase (47), a decrease (20,21), or no change (48) in alpha diversity metrics for AS patients, and some showed an increase (22) or decrease (49) in alpha diversity for RA patients. In the present study, calculation of rarefied species richness revealed that carriage of HLA–B27 and HLA–DRB1 alleles was not associated with differences in alpha diversity except in stool samples, for which carriage of HLA–DRB1 RA risk alleles was associated with an increased alpha diversity across both cohorts (Figure 2).

With regard to beta diversity assessed via sPLSDA and PERMANOVA, a significant association was observed between BMI category and microbiome composition ($P = 0.0022$) (Supplementary Figure 3A, http://onlinelibrary.wiley.com/doi/10.1002/art.40917/abstract). This appears to be driven particularly by the differences observed in underweight subjects (BMI <18.5) compared to other BMI categories. When the analysis was conducted with the samples from underweight subjects removed, a nonsignificant trend toward

Table 1. Number of samples and status of shared epitope allele by site*

Site	No. of samples			HLA–B27– negative	HLA–B27– positive	HLA–DRB1 RA risk genotype	HLA–DRB1 protective genotype	HLA–DRB1 neutral genotype
	Total	Female	Male					
Cecum	103	59	44	93	10	34	8	47
Ileum	90	51	39	80	10	36	8	45
Left colon	100	57	43	90	10	33	7	47
Rectum	91	53	38	81	10	33	7	41
Right colon	97	57	40	87	10	33	8	45
Stool	83	46	37	73	10	29	8	36

* Subjects had varying numbers of samples obtained, and at no individual site did all subjects have samples obtained. RA = rheumatoid arthritis.

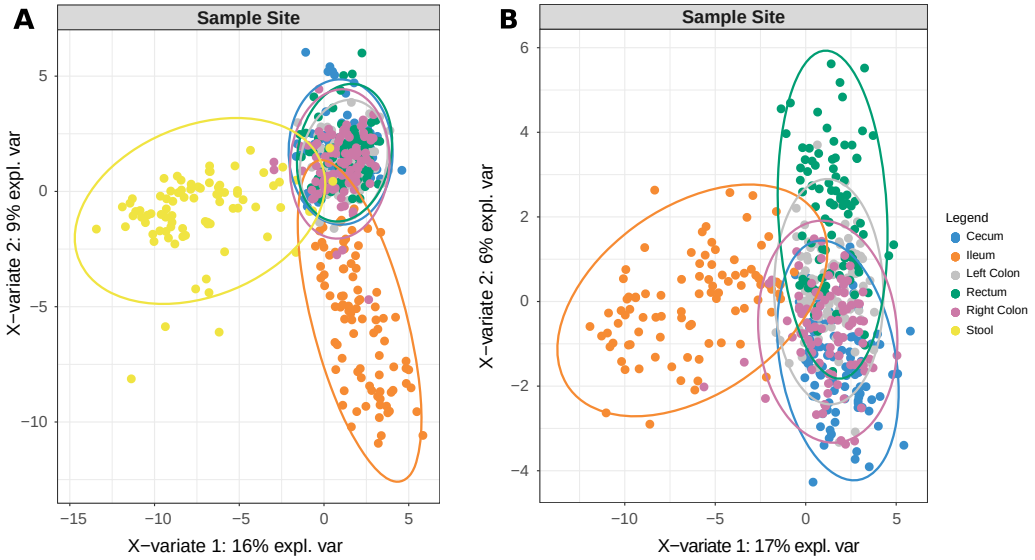

Figure 1. Sparse partial least squares–discriminant analysis comparing the microbiome composition at various sample sites, showing a marked difference at the stool/luminal site compared to all other (mucosal) sites (**A**), and, in the absence of stool samples, the distinction of the ileal site from colonic sites (**B**). A principal components analysis plot of these results is available in Supplementary Figure 1 (http://onlinelibrary.wiley.com/doi/10.1002/art.40917/abstract). Expl. var = explained variance.

association between BMI and microbiome composition was seen (P = 0.078) (Supplementary Figure 3B), which is consistent with previous findings (50–52).

Given that RA and AS affect men and women at unequal rates, and the evidence (in mice) that sex-related hormonal differences are associated with variances in the intestinal microbiome (53,54), we sought to evaluate the influence of sex on the microbiome in this cohort. While substantial overlap in the microbiome profile was evident, significant differences were observed (for all sites combined, P = 0.0004) (Supplementary Figure 4, http://onlinelibrary.wiley.com/doi/10.1002/art.40917/abstract). When indicator species were investigated, a significant reduction in the carriage of *Prevotella* genus was observed among male subjects (P = 0.005).

After controlling for BMI and sex, significant differentiation of the microbiome was identified in individuals carrying HLA–B27 or HLA–DRB1 RA risk alleles (PERMANOVA P = 0.002 and P = 0.0001, respectively) (Figures 3A and B). Despite significant differentiation in terms of beta diversity, there was typically no difference in alpha diversity (Figure 2), indicating that the underlying

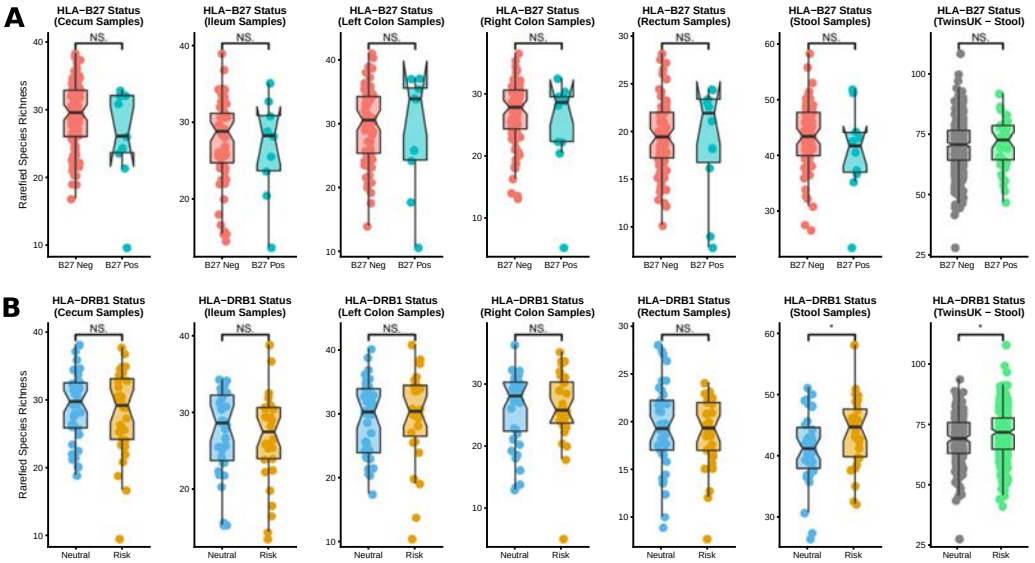

Figure 2. Alpha diversity across each sampling site in the Oregon Health & Science University screening cohort and in stool samples from the TwinsUK cohort. Alpha diversity according to HLA–B27 status (**A**) and HLA–DRB1 status (**B**) is shown, revealing increased alpha diversity in the stool samples from both cohorts. Notched box plots of alpha diversity across each sampling site are shown. * = $P < 0.05$. NS = not significant.

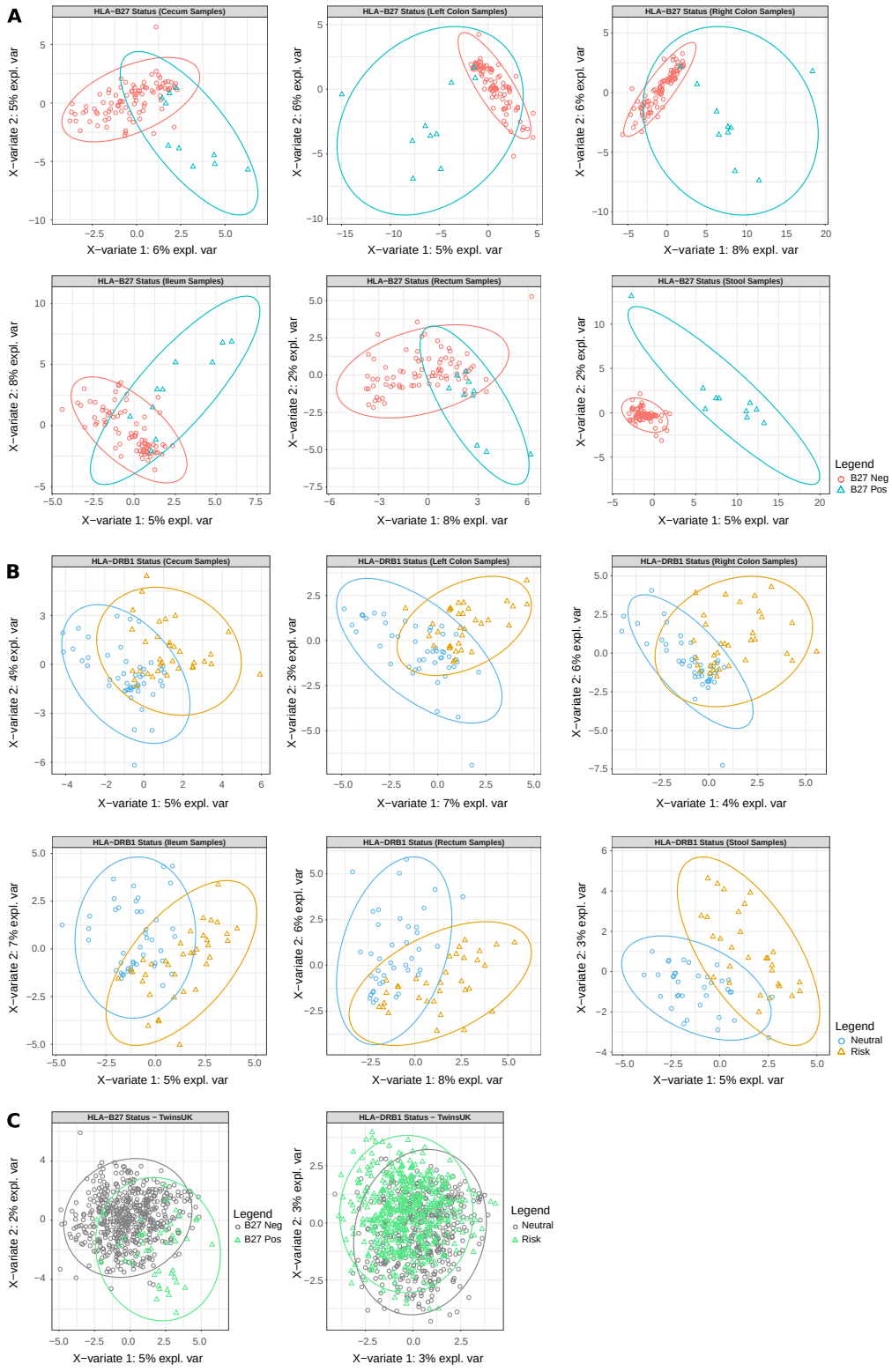

Figure 3. **A**, Sparse partial least squares–discriminant analysis (sPLSDA) comparing the microbiome composition in HLA–B27–positive and –negative subjects across each sampling site. Taking into account all sampling sites and repeated sampling, significant differentiation of the microbiome was observed (permutational multivariate analysis of variance [PERMANOVA] $P = 0.002$). **B**, sPLSDA comparing subjects carrying the HLA–DRB1 rheumatoid arthritis (RA) risk and RA neutral genotypes across each sampling site. Taking into account all sampling sites and repeated sampling, significant differentiation of the microbiome was observed (PERMANOVA $P = 0.0001$). **C**, sPLSDA plot comparing HLA–B27–positive and –negative twins (PERMANOVA $P = 0.023$), and twins with HLA–DRB1 RA risk and neutral genotypes (PERMANOVA $P = 0.033$). A principal components analysis plot of these results is available in Supplementary Figure 5 (http://onlinelibrary.wiley.com/doi/10.1002/art.40917/abstract). Expl. var = explained variance. Color figure can be viewed in the online issue, which is available at http://onlinelibrary.wiley.com/doi/10.1002/art.40917/abstract.

host genetics may affect the overall composition of the microbiome but not the overall species diversity. In the TwinsUK cohort, 1 twin was drawn randomly from each pair and the stool sample was studied. An association of stool microbiome composition with HLA–B27 and with HLA–DRB1 RA risk alleles was observed (P = 0.023 and P = 0.033 respectively, Figure 3C). Study of the sample from the alternate twin from each pair revealed consistent findings. Whether the observed differences in taxonomic and functional composition are consistent between our 2 study cohorts remains to be seen, as they are confounded by differences in experimental approach and surveyed population.

We tested whether HLA–B alleles associated with AS were also associated with gut microbial profiles. The association of HLA–B alleles with AS is complex, with risk associations observed with HLA–B27, B13, B40, B47, and B51, and protective associations observed with HLA–B7 and B57 (55). Of these, only B27 showed a statistically significant association with microbiome profile across both cohorts. Differences in the microbiome composition were more pronounced when comparing risk-associated alleles to protective alleles. For example, when focusing on a subset of data (ileal samples), we observed marginal differentiation of microbiome profiles for B27 (P = 0.16) and no differentiation for B7 (P = 0.61), potentially highlighting sample size constraints. However, a direct comparison of microbiome profiles of B27 to B7 revealed significant differentiation (P = 0.008).

HLA–B27–positive subjects exhibited reduced carriage ($P < 0.05$) of *Bacterioides ovatus* across multiple sites (ileum, cecum, left colon, right colon, and stool), as well as of *Blautia obeum* (left colon and right colon) and *Dorea formicigenerans* (rectum and stool). Increased carriage of a *Roseburia* species was observed across multiple sites (left colon, right colon, rectum, and stool), as was family Neisseriaceae (cecum and ileum). For subjects who showed positivity for HLA–DRB1 RA risk alleles, numerous taxonomic groups were enriched across multiple sites, notably a *Lachnospiraceae* species (ileum, cecum, left colon, right colon, and rectum), a *Clostridiaceae* species (left colon, right colon, rectum, and stool), *Bifidobacterium longum* (cecum, right colon, and rectum), among many others. Enrichment of *Ruminococcus gnavus* was also observed in the ileum of subjects carrying risk alleles. A full list of differentially abundant taxa according to HLA–B27 and HLA–DRB1 status is available in Supplementary Tables 2 and 3 (http://onlinelibrary.wiley.com/doi/10.1002/art.40917/abstract). Interestingly, when accounting for false discovery rate, no single taxon was significantly associated with the investigated genotypes, indicating that community level differences detectable via PERMANOVA may be driven by subtle changes in a high number of taxa, as opposed to marked changes in a select few.

Considering the inferred metabolic profiles for HLA–B27–positive and –negative subjects, we observed significant differences ($P < 0.05$) across multiple sites for numerous KEGG pathways (Supplementary Table 4, http://onlinelibrary.wiley.com/doi/10.1002/art.40917/abstract). Examples include flagellar assembly (ileum, cecum, left colon, right colon, and rectum), alanine metabolism (cecum, ileum, left colon, and right colon), lysine biosynthesis (left and right colon), and degradation (ileum, rectum, and stool) and secondary bile acid biosynthesis (ileum and stool). For the HLA–DRB1 RA risk alleles, numerous differences in KEGG pathways were also observed (Supplementary Table 5, http://onlinelibrary.wiley.com/doi/10.1002/art.40917/abstract). Examples include thiamine metabolism, citric acid cycle, lipopolysaccharide biosynthesis, glycerolipid metabolism biosynthesis of ansamycins, RNA transport, and bacterial chemotaxis, all of which were differentially abundant across every tissue site biopsied.

DISCUSSION

In this study, we have demonstrated for the first time that in the absence of disease or treatment, HLA–B27 and HLA–DRB1 have significant effects on the human gut microbiome. This is consistent with observed associations of HLA–DRB1 with gut microbiome profiles in mice (56) and the effect of HLA–DRB1 alleles on *Prevotella copri* abundance in humans (24). This extends previous observations that AS and RA are characterized by intestinal dysbiosis by confirming that this is due, at least in part, to the effects of the major genetic risk factors for AS and RA: HLA–B27 and HLA–DRB1 risk alleles.

We have demonstrated a clear distinction in microbiome profile between luminal stool samples and mucosal samples, as well as between mucosal samples from different intestinal sites. Notably, marked difference was observed between ileal and stool samples. These findings contrast those of a previous smaller study, in which the failure to demonstrate a difference between ileal and colonic biopsy samples may have been due to sample size considerations (48). Many studies on the influence of gut microbiome focus on stool samples, as they are easier to obtain than mucosal samples. The existence of gut inflammation in AS patients, particularly involving the ileum, has been well documented. Therefore, our findings suggest that studies on the microbiome in AS and RA, particularly in which the aim is to identify the key species or genetic elements driving or protecting against the disease, should use samples that reflect the site of inflammation (i.e., ideally the ileal microbiome in AS). As the microbiome profile of stool samples does not closely correlate with the ileal microbiome, they do not appear to be optimal samples to study, although studying IgA-coated bacteria isolated from stool samples may prove more informative (57,58).

Following our initial study, 3 further studies on the difference in gut microbial composition in AS patients and healthy controls have been reported. In a study of 27 patients with SpA (not necessarily AS) and 15 healthy controls, using 16S rRNA profiling, Tito et al reported an association of the presence of *Dialister* in ileal or colonic mucosal biopsy samples (48) with disease activity assessed by the self-reported Bath Ankylosing Spondylitis Disease Activity Index (BASDAI) (59)

and the Ankylosing Spondylitis Disease Activity Score (60). We did not observe *Dialister* in our study and therefore cannot comment on whether it is associated with HLA–B27 carriage. Tito and colleagues did not observe an association of the gut microbiome with HLA–B27 carriage, but due to the small sample size, particularly of healthy controls, a possible effect (other than a large effect) could not be excluded.

In a Chinese study, Wen et al used shotgun sequencing of stool samples from 97 AS patients and 114 healthy controls and reported significant dysbiosis in the AS patients (21). Breban et al conducted 16S rRNA profiling of the stool microbiome to study 87 patients with axial SpA (42 with AS), 69 healthy controls, and 28 RA patients (22). They also reported evidence of intestinal dysbiosis in the SpA patients, in addition to a correlation of *R gnavus* carriage with BASDAI score. While we did not observe such an association with the carriage of HLA–B27, *R gnavus* was noted to be enriched in the ileum of individuals carrying the HLA–DRB1 RA risk allele (Supplementary Table 3, http://onlinelibrary.wiley.com/doi/10.1002/art.40917/abstract). In a comparison between HLA–B27–positive and –negative siblings (n = 22 and n = 21, respectively), no difference in overall microbial composition was noted, but the HLA–B27–positive siblings had increased carriage of the Micrococcaceae family (including the species *Rothia mucilaginosa* within it), several *Blautia* and *Ruminococcus* species, and *Egerthella lenta* (22). Breban and colleagues also observed a reduced carriage of *Bifidobacterium* and *Odoribacter* species. Of these, we saw a reduction in *Blautia obeum*. Although we did not find dysbiotic changes that co-occurred with these specific taxa, we noted that the enrichment of genera within the Lachospiraceae–Ruminococcaceae grouping in HLA–B27 carriers was a shared feature: *Roseburia* and *Ruminococcus* in the study from Breban et al (22) and *Roseburia*, *Blautia*, *Dorea*, and *Oscillospira* in our current study. These bacteria are known to be enriched within the intestinal mucosa (61) and are plausibly more immunogenic as a result (62).

The differences between these studies may relate to analytical differences such as handling of covariates, disease definition, studied sample site, ethnicity and diet, and the different methods used to profile the microbiome. Our study also confirms the significant effect of sex and BMI category on gut microbial profiles, suggesting that future studies should control for these covariates. Consistent with a recent study that examined the effect of host genetics on the microbiome of 1,046 healthy individuals (63), numerous correlations between specific bacterial taxa and the host's genotype do not remain significant following correction for false discovery rate. This indicates that HLA molecules may have a more generalized effect on microbiome composition as opposed to a marked effect on specific taxa. Despite this, we noted that many of the significant ($P < 0.05$) associations occurred across multiple tissue sites. While the chance of a false-positive result at a single site might be relatively high, the chances of finding the same association across multiple sites decreases exponentially, indicating that the results are less likely to be spurious. Another possibility is that differences in microbial gene content, not necessarily specific taxa, may be more significant. In the present study, the microbiome's predicted gene content was extrapolated from the underlying taxonomy, which indicates that the use of whole-genome sequencing metagenomics (also known as shotgun metagenomics) to directly profile genetic composition may prove fruitful. This will be the focus of subsequent studies.

HLA molecules affect susceptibility to many diseases, most of which are immunologically mediated. In almost all instances, the mechanism that accounts for the predisposition is not known. The microbiome has now been implicated in a long list of diseases, many of which are immunologically mediated. Our findings suggest that HLA molecules could be important factors that contribute to the heterogeneity of the microbiome and operate at least partially through this mechanism in the pathogenesis of many diseases, not just AS and RA. In accordance with this hypothesis, HLA–microbiome associations have been described in reactive arthritis (64), IBD (65), celiac disease (66), and in healthy individuals (24,67).

The metabolic changes imbued by dysbiosis, hypothesized in our current work, are of interest in light of a recent study by our group in an HLA–B27–transgenic rat model of SpA (68). We observed a number of HLA–B27–dependent metabolic changes in this model that include enrichment of bile acid metabolism, lysine metabolism, fatty acid metabolism, and tryptophan metabolism. All of these pathways were predicted to be enriched in HLA–B27–positive individuals in our current study (Supplementary Table 4, http://onlinelibrary.wiley.com/doi/10.1002/art.40917/abstract). Importantly, HLA–B27–dependent dysbiosis can be observed prior to the onset of disease in this model. Thus, our human and rat studies support the hypothesis that HLA–B27–dependent dysbiosis is a preceding event in AS pathogenesis and may not merely be secondary to disease.

In conclusion, this study demonstrates that HLA–B27 and RA-associated HLA–DRB1 allele carriage in humans influences the gut microbiome. The replicated demonstration of intestinal changes in the AS microbiome is consistent with disease models in which HLA molecules interact with the gut microbiome to cause disease. Different models showing how this may occur include effects of HLA–B27 to favor a more inflammatory gut microbiome, increased invasiveness of the gut mucosa in HLA–B27 carriers, and/or aberrant immunologic responses to bacteria in HLA–B27 carriers. Similar hypotheses may explain the role of HLA–DRB1 in driving the immunopathogenesis of RA. Whichever of these models is correct, the data presented here support the need for further research in this field, including investigation of whether manipulation of the gut microbiome may be therapeutic or potentially capable of preventing AS or RA in at-risk subjects.

Addendum. This work is dedicated to the memory of Dr. Mark Asquith, who recently passed away, too early in life: a great young scientist and person, who contributed a lot and will be sorely missed by his friends and colleagues.

ACKNOWLEDGMENTS

We wish to acknowledge Dr. Erica Roberson, MD for her valuable contribution to study design; Patrick Stauffer and Sean Davin for technical assistance; and all OHSU patients and staff whom helped contribute samples for this study.

AUTHOR CONTRIBUTIONS

All authors were involved in drafting the article or revising it critically for important intellectual content, and all authors approved the final version to be published. Dr. Asquith had full access to all of the data in the study and takes responsibility for the integrity of the data and the accuracy of the data analysis.

Study conception and design. Asquith, Rosenbaum, Brown.
Acquisition of data. Asquith, Sternes, Costello, Karstens, Diamond, Martin, Spector, Rosenbaum, Brown.
Analysis and interpretation of data. Asquith, Sternes, Costello, Li, Marshall, le Cao, Rosenbaum, Brown.

REFERENCES

1. Brown MA, Kennedy LG, MacGregor AJ, Darke C, Duncan E, Shatford JL, et al. Susceptibility to ankylosing spondylitis in twins: the role of genes, HLA, and the environment. Arthritis Rheum 1997;40:1823–8.
2. Pedersen OB, Svendsen AJ, Ejstrup L, Skytthe A, Harris JR, Junker P. Ankylosing spondylitis in Danish and Norwegian twins: occurrence and the relative importance of genetic vs. environmental effectors in disease causation. Scand J Rheumatol 2008;37:120–6.
3. MacGregor AJ, Snieder H, Rigby AS, Koskenvuo M, Kaprio J, Aho K, et al. Characterizing the quantitative genetic contribution to rheumatoid arthritis using data from twins. Arthritis Rheum 2000;43:30–7.
4. Van der Woude D, Houwing-Duistermaat JJ, Toes RE, Huizinga TW, Thomson W, Worthington J, et al. Quantitative heritability of anti–citrullinated protein antibody–positive and anti–citrullinated protein antibody–negative rheumatoid arthritis. Arthritis Rheum 2009;60:916–23.
5. Mielants H, Veys EM, Cuvelier C, De Vos M, Botelberghe L. HLA-B27 related arthritis and bowel inflammation. Part 2. Ileocolonoscopy and bowel histology in patients with HLA-B27 related arthritis. J Rheumatol 1985;12:294–8.
6. Ciccia F, Accardo-Palumbo A, Alessandro R, Rizzo A, Principe S, Peralta S, et al. Interleukin-22 and interleukin-22–producing NKp44+ natural killer cells in subclinical gut inflammation in ankylosing spondylitis. Arthritis Rheum 2012;64:1869–78.
7. Martinez-González O, Cantero-Hinojosa J, Paule-Sastre P, Gómez-Magán JC, Salvatierra-Ríos D. Intestinal permeability in patients with ankylosing spondyllitis and their healthy relatives. Br J Rheumatology 1994;33:644–7.
8. Mielants H, De Vos M, Goemaere S, Schelstraete K, Cuvelier C, Goethals K, et al. Intestinal mucosal permeability in inflammatory rheumatic diseases:. II. Role of disease. J Rheumatol 1991;18: 394–400.
9. Morris AJ, Howden CW, Robertson C, Duncan A, Torley H, Sturrock RD, et al. Increased intestinal permeability in ankylosing spondylitis: primary lesion or drug effect? Gut 1991;32:1470–2.
10. Vaile J, Meddings JB, Yacyshyn BR, Russell AS, Maksymowych WP. Bowel permeability and CD45RO expression on circulating CD20+ B cells in patients with ankylosing spondylitis and their relatives. J Rheumatol 1999;26:128–35.
11. Bjarnason I, Helgason KO, Geirsson AJ, Sigthorsson G, Reynisdottir I, Gudbjartsson D, et al. Subclinical intestinal inflammation and sacroiliac changes in relatives of patients with ankylosing spondylitis. Gastroenterology 2003;125:1598–605.
12. Palm O, Moum B, Ongre A, Gran JT. Prevalence of ankylosing spondylitis and other spondyloarthropathies among patients with inflammatory bowel disease: a population study (the IBSEN study). J Rheumatol 2002;29:511–5.
13. Orchard TR, Holt H, Bradbury L, Hammersma J, McNally E, Jewell DP, et al. The prevalence, clinical features and association of HLA-B27 in sacroiliitis associated with established Crohn's disease. Aliment Pharmacol Ther 2009;29:193–7.
14. Thjodleifsson B, Geirsson ÁJ, Björnsson S, Bjarnason I. A common genetic background for inflammatory bowel disease and ankylosing spondylitis: a genealogic study in Iceland. Arthritis Rheum 2007;56:2633–9.
15. Ellinghaus D, Jostins L, Spain SL, Cortes A, Bethune J, Han B, et al. Analysis of five chronic inflammatory diseases identifies 27 new associations and highlights disease-specific patterns at shared loci. Nat Genet 2016;48:510–8.
16. Parkes M, Cortes A, van Heel DA, Brown MA. Genetic insights into common pathways and complex relationships among immune-mediated diseases. Nat Rev Genet 2013;14:661–73.
17. Cua DJ, Sherlock JP. Autoimmunity's collateral damage: gut microbiota strikes 'back'. Nat Med 2011;17:1055–6.
18. Costello ME, Elewaut D, Kenna TJ, Brown MA. Microbes, the gut and ankylosing spondylitis [review]. Arthritis Res Ther 2013;15:214.
19. Rosenbaum JT, Asquith M. The microbiome and HLA-B27-associated acute anterior uveitis. Nat Rev Rheumatol 2018;14:704–13.
20. Costello ME, Ciccia F, Willner D, Warrington N, Robinson PC, Gardiner B, et al. Intestinal dysbiosis in ankylosing spondylitis. Arthritis Rheumatol 2015;67:686–91.
21. Wen C, Zheng Z, Shao T, Liu L, Xie Z, Le Chatelier E, et al. Quantitative metagenomics reveals unique gut microbiome biomarkers in ankylosing spondylitis. Genome Biol 2017;18:142.
22. Breban M, Tap J, Leboime A, Said-Nahal R, Langella P, Chiocchia G, et al. Faecal microbiota study reveals specific dysbiosis in spondyloarthritis. Ann Rheum Dis 2017;76:1614–22.
23. Gill T, Asquith M, Brooks SR, Rosenbaum JT, Colbert RA. Effects of HLA–B27 on gut microbiota in experimental spondyloarthritis implicate an ecological model of dysbiosis. Arthritis Rheumatol 2018;70:555–65.
24. Scher JU, Sczesnak A, Longman RS, Segata N, Ubeda C, Bielski C, et al. Expansion of intestinal Prevotella copri correlates with enhanced susceptibility to arthritis. Elife 2013;2:e01202.
25. Zhang X, Zhang D, Jia H, Feng Q, Wang D, Liang D, et al. The oral and gut microbiomes are perturbed in rheumatoid arthritis and partly normalized after treatment. Nat Med 2015;21:895–905.
26. Jubair WK, Hendrickson JD, Severs EL, Schulz HM, Adhikari S, Ir D, et al. Modulation of inflammatory arthritis in mice by gut microbiota through mucosal inflammation and autoantibody generation. Arthritis Rheumatol 2018;70:1220–33.
27. Rogier R, Evans-Marin H, Manasson J, van der Kraan PM, Walgreen B, Helsen MM, et al. Alteration of the intestinal microbiome characterizes preclinical inflammatory arthritis in mice and its modulation attenuates established arthritis. Sci Rep 2017;7:15613.
28. Spor A, Koren O, Ley R. Unravelling the effects of the environment and host genotype on the gut microbiome. Nat Rev Microbiol 2011;9:279–90.
29. Benson AK, Kelly SA, Legge R, Ma F, Low SJ, Kim J, et al. Individuality in gut microbiota composition is a complex polygenic trait shaped by multiple environmental and host genetic factors. Proc Natl Acad Sci U S A 2010;107:18933–8.
30. Goodrich JK, Davenport ER, Beaumont M, Jackson MA, Knight R, Ober C, et al. Genetic determinants of the gut microbiome in UK twins. Cell Host Microbe 2016;19:731–43.

31. Kenna TJ, Brown MA. Immunopathogenesis of ankylosing spondylitis. Int J Clin Rheumatol 2013;8:265–74.
32. Rosenbaum JT, Davey MP. Time for a gut check: evidence for the hypothesis that HLA–B27 predisposes to ankylosing spondylitis by altering the microbiome. Arthritis Rheum 2011;63:3195–8.
33. Asquith MJ, Stauffer P, Davin S, Mitchell C, Lin P, Rosenbaum JT. Perturbed mucosal immunity and dysbiosis accompany clinical disease in a rat model of spondyloarthritis. Arthritis Rheumatol 2016;68:2151–62.
34. Lin P, Bach M, Asquith M, Lee AY, Akileswaran L, Stauffer P, et al. HLA-B27 and human β2-microglobulin affect the gut microbiota of transgenic rats. PLoS One 2014;9:e105684.
35. Caminer AC, Haberman R, Scher JU. Human microbiome, infections, and rheumatic disease. Clin Rheumatol 2017;36:2645–53.
36. Goodrich JK, Waters JL, Poole AC, Sutter JL, Koren O, Blekhman R, et al. Human genetics shape the gut microbiome. Cell 2014;159:789–99.
37. Jia X, Han B, Onengut-Gumuscu S, Chen WM, Concannon PJ, Rich SS, et al. Imputing amino acid polymorphisms in human leukocyte antigens. PLoS One 2013;8:e64683.
38. Cortes A, Pulit SL, Leo PJ, Pointon JJ, Robinson PC, Weisman MH, et al. Major histocompatibility complex associations of ankylosing spondylitis are complex and involve further epistasis with ERAP1. Nat Commun 2015;6:7146.
39. Caporaso JG, Kuczynski J, Stombaugh J, Bittinger K, Bushman FD, Costello EK, et al. QIIME allows analysis of high-throughput community sequencing data [letter]. Nat Methods 2010;7:335–6.
40. DeSantis TZ, Hugenholtz P, Larsen N, Rojas M, Brodie EL, Keller K, et al. Greengenes, a chimera-checked 16S rRNA gene database and workbench compatible with ARB. Appl Environ Microbiol 2006;72:5069–72.
41. Edgar RC. Search and clustering orders of magnitude faster than BLAST. Bioinformatics 2010;26:2460–1.
42. Lê Cao KA, Costello ME, Lakis VA, Bartolo F, Chua XY, Brazeilles R, et al. MixMC: a multivariate statistical framework to gain insight into microbial communities. PloS One 2016;11:e0160169.
43. Dixon P. VEGAN, a package of R functions for community ecology. J Veg Sci 2003;14:927–30.
44. Langille MG, Zaneveld J, Caporaso JG, McDonald D, Knights D, Reyes JA, et al. Predictive functional profiling of microbial communities using 16S rRNA marker gene sequences. Nat Biotechnol 2013;31:814–21.
45. Abubucker S, Segata N, Goll J, Schubert AM, Izard J, Cantarel BL, et al. Metabolic reconstruction for metagenomic data and its application to the human microbiome. PLoS Comput Biol 2012;8:e1002358.
46. Morgan XC, Tickle TL, Sokol H, Gevers D, Devaney KL, Ward DV, et al. Dysfunction of the intestinal microbiome in inflammatory bowel disease and treatment. Genome Biol 2012;13:R79.
47. Chen Z, Qi J, Zheng X, Wu X, Li X, Gu J. Faecal microbiota study identifies dysbiosis in ankylosing spondylitis patients [abstract]. BMJ 2018;77 Suppl 2:1264.
48. Tito RY, Cypers H, Joossens M, Varkas G, Van Praet L, Glorieus E, et al. Dialister as a microbial marker of disease activity in spondyloarthritis. Arthritis Rheumatol 2017;69:114–21.
49. Wu X, Liu J, Xiao L, Lu A, Zhang G. Alterations of gut microbiome in rheumatoid arthritis [abstract]. Osteoarthritis Cartilage 2017;25:S287–8.
50. Turnbaugh PJ, Bäckhed F, Fulton L, Gordon JI. Diet-induced obesity is linked to marked but reversible alterations in the mouse distal gut microbiome. Cell Host Microbe 2008;3:213–23.
51. Turnbaugh PJ, Hamady M, Yatsunenko T, Cantarel BL, Duncan A, Ley RE, et al. A core gut microbiome in obese and lean twins. Nature 2009;457:480–4.
52. Turnbaugh PJ, Ley RE, Mahowald MA, Magrini V, Mardis ER, Gordon JI. An obesity-associated gut microbiome with increased capacity for energy harvest. Nature 2006;444:1027–31.
53. Markle JG, Frank DN, Mortin-Toth S, Robertson CE, Feazel LM, Rolle-Kampczyk U, et al. Sex differences in the gut microbiome drive hormone-dependent regulation of autoimmunity. Science 2013;339:1084–8.
54. Yurkovetskiy L, Burrows M, Khan AA, Graham L, Volchkov P, Becker L, et al. Gender bias in autoimmunity is influenced by microbiota. Immunity 2013;39:400–12.
55. Cortes A, Maksymowych WP, Wordsworth BP, Inman RD, Danoy P, Rahman P, et al. Association study of genes related to bone formation and resorption and the extent of radiographic change in ankylosing spondylitis. Ann Rheum Dis 2015;74:1387–93.
56. Gomez A, Luckey D, Yeoman CJ, Marietta EV, Berg Miller ME, Murray JA, et al. Loss of sex and age driven differences in the gut microbiome characterize arthritis-susceptible 0401 mice but not arthritis-resistant 0402 mice. PloS One 2012;7:e36095.
57. Palm NW, de Zoete MR, Cullen TW, Barry NA, Stefanowski J, Hao L, et al. Immunoglobulin A coating identifies colitogenic bacteria in inflammatory bowel disease. Cell 2014;158:1000–10.
58. Viladomiu M, Kivolowitz C, Abdulhamid A, Dogan B, Victorio D, Castellanos JG, et al. IgA-coated E. coli enriched in Crohn's disease spondyloarthritis promote T_H17-dependent inflammation. Sci Transl Med 2017;9:eaaf9655.
59. Garrett S, Jenkinson T, Kennedy LG, Whitelock H, Gaisford P, Calin A. A new approach to defining disease status in ankylosing spondylitis: the Bath Ankylosing Spondylitis Disease Activity Index. J Rheumatol 1994;21:2286–91.
60. Lukas C, Landewé R, Sieper J, Dougados M, Davis J, Braun J, et al, for the Assessment of SpondyloArthritis international Society. Development of an ASAS-endorsed disease activity score (ASDAS) in patients with ankylosing spondylitis. Ann Rheum Dis 2009;68:18–24.
61. Nava GM, Friedrichsen HJ, Stappenbeck TS. Spatial organization of intestinal microbiota in the mouse ascending colon. ISME J 2011;5:627–38.
62. Atarashi K, Tanoue T, Ando M, Kamada N, Nagano Y, Narushima S, et al. Th17 cell induction by adhesion of microbes to intestinal epithelial cells. Cell 2015;163:367–80.
63. Rothschild D, Weissbrod O, Barkan E, Kurilshikov A, Korem T, Zeevi D, et al. Environment dominates over host genetics in shaping human gut microbiota. Nature 2018;555:210–5.
64. Manasson J, Shen N, Garcia Ferrer HR, Ubeda C, Iraheta I, Heguy A, et al. Gut microbiota perturbations in reactive arthritis and postinfectious spondyloarthritis. Arthritis Rheumatol 2018;70:242–54.
65. Imhann F, Vich Vila A, Bonder MJ, Fu J, Gevers D, Visschedijk MC, et al. Interplay of host genetics and gut microbiota underlying the onset and clinical presentation of inflammatory bowel disease. Gut 2018;67:108–19.
66. Olivares M, Neef A, Castillejo G, Palma GD, Varea V, Capilla A, et al. The HLA-DQ2 genotype selects for early intestinal microbiota composition in infants at high risk of developing coeliac disease. Gut 2015;64:406–17.
67. Wang J, Thingholm LB, Skiecevičienė J, Rausch P, Kummen M, Hov JR, et al. Genome-wide association analysis identifies variation in vitamin D receptor and other host factors influencing the gut microbiota. Nat Genet 2016;48:1396–1406.
68. Asquith M, Davin S, Stauffer P, Michell C, Janowitz C, Lin P, et al. Intestinal metabolites are profoundly altered in the context of HLA–B27 expression and functionally modulate disease in a rat model of spondyloarthritis. Arthritis Rheumatol 2017;69:1984–95.

Arthritis & Rheumatology
Vol. 71, No. 10, October 2019, pp 1651–1659
DOI 10.1002/art.40925

American College of Rheumatology
Empowering Rheumatology Professionals

Value of Carotid Ultrasound in Cardiovascular Risk Stratification in Patients With Psoriatic Disease

Curtis Sobchak,[1] Shadi Akhtari,[2] Paula Harvey,[3] Dafna Gladman,[4] Vinod Chandran,[4] Richard Cook,[5] and Lihi Eder[3]

Objective. This study aimed to assess whether subclinical atherosclerosis, as evaluated by carotid ultrasound, could predict incident cardiovascular events (CVEs) in patients with psoriatic disease (PsD) and determine whether incorporation of imaging data could improve CV risk prediction by the Framingham Risk Score (FRS).

Methods. In this cohort analysis, patients with PsD underwent ultrasound assessment of the carotid arteries at baseline. The extent of atherosclerosis was assessed using carotid intima-media thickness (CIMT) and total plaque area (TPA). Incident CVEs (new or recurrent) that occurred following the ultrasound assessment were identified. The association between measures of carotid atherosclerosis and the risk of developing an incident CVE was evaluated using Cox proportional hazards models, with adjustment for the FRS.

Results. In total, 559 patients with PsD were assessed, of whom 23 had incident CVEs ascertained. The calculated rate of developing a first CVE during the study period was 1.11 events per 100 patient-years (95% confidence interval [95% CI] 0.74–1.67). When analyzed separately in Cox proportional hazards models that were controlled for the FRS, the TPA (hazard ratio [HR] 3.74, 95% CI 1.55–8.85; $P = 0.003$), mean CIMT (HR 1.21, 95% CI 1.03–1.42; $P = 0.02$), maximal CIMT (HR 1.11, 95% CI 1.01–1.22; $P = 0.03$), and high TPA category (HR 3.25, 95% CI 1.18–8.95; $P = 0.02$) were each predictive of incident CVEs in patients with PsD.

Conclusion. The burden of carotid atherosclerosis is associated with an increased risk of developing future CVEs. Combining vascular imaging data with information on traditional CV risk factors could improve the accuracy of CV risk stratification in patients with PsD.

INTRODUCTION

It is well accepted that patients with psoriasis and psoriatic arthritis (PsA), collectively termed psoriatic disease (PsD), are at an increased risk of cardiovascular events (CVEs) (1–4). This elevated CV risk has been attributed, in part, to traditional CV risk factors (e.g., diabetes and dyslipidemia) but is also related to systemic inflammation (3,5). The systemic inflammation associated with PsD accelerates the development and progression of atherosclerosis and promotes plaque rupture, thus predisposing individuals to increased risk of CV diseases (6–9).

Stratification of CV risk and the management of CV risk factors in patients with PsD are becoming an integral part of patient care. Current treatment guidelines recognize the need to identify patients with PsD who are at high risk of a CVE based on accepted clinical risk scores, such as the Framingham Risk Score (FRS) (10,11). Traditional CV risk score calculation is a cornerstone in the prediction of CVEs (12) and plays an important role in guiding treatment decisions tailored to fit the patient's individual risk factor profile (13). However, the FRS and similar traditional CV risk scores underestimate the CV risk in patients with rheumatic disorders, including PsD (14–17). This is likely because clinical risk scores do not account for the effect of the systemic inflammation that is common to these disorders. As such, these patients are often underdiagnosed and undertreated for CV risk factors (18–20). This has a potential adverse impact on clinical CV outcomes

Parts of this material are based on data and information provided by the Canadian Institute for Health Information. However, the analyses, conclusions, opinions, and statements expressed herein are those of the author and not those of the Canadian Institute for Health Information.

Supported in part by a Young Investigator Operating grant from the Arthritis Society, Canada. Dr. Sobchak's work was supported by a summer studentship award from the Department of Medicine at Women's College Hospital. Dr. Eder's work was supported by a Young Investigator Salary award from the Arthritis Society and the Canadian Association of Psoriasis Patients.

[1]Curtis Sobchak, MD: University of Toronto, Toronto, Ontario Canada; [2]Shadi Akhtari, MD: Women's College Hospital, Toronto, Ontario, Canada; [3]Paula Harvey BMBS, PhD, Lihi Eder, MD, PhD: Women's College Hospital and University of Toronto, Toronto, Ontario Canada; [4]Dafna Gladman, MD, Vinod Chandran, MBBS, MD, DM, PhD: University of Toronto, Krembil Research Institute, and Toronto Western Hospital, Toronto, Ontario, Canada; [5]Richard Cook, PhD: University of Waterloo, Waterloo, Ontario, Canada.

No potential conflicts of interest relevant to this article were reported.

Address correspondence to Lihi Eder, MD, PhD, Women's College Hospital, 76 Grenville Street, Toronto, Ontario M5S 1B2, Canada. E-mail: lihi.eder@wchospital.ca.

Submitted for publication September 1, 2018; accepted in revised form May 7, 2019.

and warrants optimization of CV risk stratification tools that have been designed for use in this population.

Atherosclerosis, the main cause of CVEs, is an inflammatory disorder in which immune mechanisms interact with atherogenic lipid particles to initiate and propagate lesions in the vascular walls (21,22). Inflammation plays a pivotal role in all stages of atherosclerosis. The burden of atherosclerosis in PsD is associated with traditional CV risk factors as well as with measures of disease activity (6,7). Thus, quantification of atherosclerotic plaque burden using vascular imaging could potentially provide a more accurate evaluation of the impact of traditional and nontraditional risk factors on CV risk and may improve precision of CV risk stratification tools for use in patients with PsD. Vascular imaging has been shown to improve the prediction of CVEs both in the general population and in patients with rheumatoid arthritis (RA) (23–25); however, little is known about the role of vascular imaging in improving the prediction of CVEs in PsD.

The aims of the present study were 1) to assess whether subclinical atherosclerosis, as evaluated by carotid ultrasound, could be predictive of incident CVEs in patients with PsD, and 2) to determine whether incorporation of imaging data could improve the prediction of CVEs beyond traditional clinical CV algorithms.

PATIENTS AND METHODS

Patients and setting. In this retrospective analysis of a prospective cohort, we included patients with psoriasis and PsA from the University of Toronto Psoriatic Disease Program. This program includes 2 cohorts, a cohort of PsA patients and a cohort of patients with psoriasis without arthritis (PsC). The PsA cohort was established in 1978 as part of an ongoing prospective study to determine outcomes and prognosis in this disease (26,27). It consists of patients who are referred to the clinic by family doctors and other medical specialists for the management of PsA. Patients are assessed at 6–12-month intervals according to a standard protocol. Patients in the PsA cohort have a rheumatologist-confirmed diagnosis of PsA, and the majority of them meet the CASPAR PsA classification criteria (28).

The PsC cohort was established in 2006 and comprises patients who have a dermatologist's diagnosis of psoriasis and in whom a diagnosis of PsA has been excluded by a rheumatologist. These patients are assessed according to the same protocol as used in the PsA cohort, and participants are followed up annually as part of a longitudinal study until they develop PsA. Patients with PsC are recruited from dermatology clinics, from phototherapy centers, or through advertisement in the local media (27).

As of January 2010, consecutive patients from both of these cohorts have been recruited for participation in a substudy that assesses CV outcomes in patients with PsD. The participants in this substudy undergo a comprehensive CV risk evaluation that includes an assessment of their CV risk factors and an ultrasound of the carotid arteries. Patients with a history of clinical CV disease and those with prior carotid endarterectomy are excluded.

Patients underwent a baseline carotid ultrasound assessment between 2010 and 2015 and were followed up until December 31, 2017. The study was approved by the University Health Network Research Ethics Board. All patients gave their informed consent at the time of assessment.

Assessment of CV risk factors. Information about CV risk factors was collected at the baseline ultrasound assessment and was used to calculate the expected CV risk using the FRS. The use of lipid-lowering agents, antidiabetic medications, and antihypertensive medications was recorded. Participants who reported smoking on a daily basis were considered smokers. Blood pressure was measured with a cuff sphygmomanometer. Blood samples were collected after an overnight fast and analyzed for levels of glucose, total cholesterol, high-density lipoprotein cholesterol, low-density lipoprotein cholesterol, triglycerides, and the erythrocyte sedimentation rate.

To estimate the 10-year risk of CV diseases, we used the formula described by D'Agostino et al (29) to calculate the FRS for each participant. The risk factors included in the score were age, sex, smoking, systolic blood pressure, use of antihypertensive medications, diabetes, total cholesterol, and high-density lipoprotein cholesterol levels. From the Framingham chart, the estimated 10-year risk of CV disease was generated for each patient. Based on that risk, the patient was classified into 1 of the following groups: low risk (<5%), intermediate risk (6–20%), and high risk (>20%) (29).

Carotid ultrasound assessment. A single trained physician (LE) performed all of the ultrasound measurements in accordance with a study protocol that was previously described in detail (30). Scans were performed with MyLab 30 and MyLab 70 XVision scanners with a linear LA523 7–13-MHz transducer (all from Esaote). The scan included detailed B-mode images of both the right and the left common carotid arteries as well as the carotid bulb, internal carotid, and external carotid arteries. All ultrasound scans were saved as video files for later reading. We evaluated 5 measures of atherosclerosis: total plaque area (TPA) (in cm^2), mean carotid intima-media thickness (CIMT) (in μm), maximal CIMT (in μm), plaque category, and TPA category.

Carotid IMT was measured automatically at the far wall of the right and left common carotid arteries (twice at each side) at least 1 cm proximally from the origin of the bulb, using a real-time radiofrequency-based ultrasound system for carotid imaging (QIMT tool; Esaote). The composite mean CIMT was calculated by averaging the common right and left CIMT values. Maximal CIMT was the highest of the 4 measurements of CIMT.

An atherosclerotic plaque was defined as the presence of focal wall thickening that is at least 50% greater than that of the surrounding vessel wall or as a localized intimal thickening exceeding 1 mm that protrudes into the lumen and is distinct

from the adjacent boundary (31). TPA, an independent predictor of clinical CVEs (32), was measured as described by Spence (33). The plane for measurement of each plaque was chosen by reviewing the video of the scan to find the largest extent of plaque as seen in the longitudinal view. The image was then frozen, and the plaque was measured by tracing around the perimeter with a cursor on the screen. The assessor then moved on to the next plaque and repeated the process until all observed plaques in the common, external, and internal carotid arteries were measured. TPA was recorded as the sum of areas of all plaques in the right and left carotid arteries. Due to the lack of accepted cutoff points for TPA, we classified TPA as high and low based on the median value of TPA in our cohort (high TPA >0.21 cm^2). In addition, we considered the presence of plaques in terms of a simpler measure of plaque burden. The plaque category was defined as 1) no plaques, 2) unilateral plaque, or 3) bilateral plaques.

Reading of the scans was performed independent of the scanning and blinded with regard to clinical data. The intraobserver intraclass correlation coefficient for TPA was 0.94.

Definition of CVEs. We considered the major and minor CVEs as outcomes of interest, with major CVEs including myocardial infarction (MI), unstable angina, ischemic stroke, revascularization procedures, or CV-related death, and minor CVEs including stable angina, exacerbation of congestive heart failure (CHF), and transient ischemic attack (TIA). Revascularization procedures included coronary stent insertion, coronary bypass surgery, carotid endarterectomy, or vascular surgery for peripheral vascular disease. We did not include the development of peripheral artery disease as one of the outcomes in our study, since this information has not been routinely collected in our cohort.

Incident potential CVEs were identified by one of the following methods. 1) The cohort database was searched for CVEs that occurred between study visits and were reported by the patients. 2) The provincial hospitalization databases, the Canadian Institute for Health Information Discharge Abstract Database, and the National Ambulatory Care Reporting System were searched. These databases contain detailed information about all inpatient hospital discharges, emergency rooms visits, and same-day surgeries from all hospitals in Ontario, Canada. International Classification of Diseases, Tenth Revision (ICD-10) codes were used to identify hospitalizations due to a CVE (see Supplementary Table 1, available on the *Arthritis & Rheumatology* web site at http://onlinelibrary.wiley.com/doi/10.1002/art.40925/abstract). The accuracy of the CV codes in Canadian databases has been verified in the past (specificities >90% for all codes) (34). 3) The provincial death registry, the Ontario Vital Statistics Death Registry, was searched. This database contains information about all deaths and their primary cause occurring in Ontario, Canada. All deaths due to a CVE (primary cause), based on ICD-10 codes, occurring following the baseline visit were identified (see Supplementary Table 2, available on the *Arthritis & Rheumatology* web site at http://onlinelibrary.wiley.com/doi/10.1002/art.40925/abstract). Using this combined approach, we ensured that all potential CVEs were identified, including in patients who were lost to follow-up.

In order to verify that the recorded CVEs were incident events, we obtained additional details from the medical records (e.g., hospitalization records from acute events, clinic notes from specialists for nonacute events). All medical records were reviewed by a cardiologist (SA) who verified the events and classified them as a minor CVE or a major CVE. For the primary analysis, we used a composite end point of all confirmed CVEs, while the secondary outcome was restricted to major CVEs. Incident CVEs were considered to be the first incident CVE during the follow-up period in patients with no prior CVE at baseline.

Statistical analysis. Continuous variables were summarized as the mean ± SD, and categorical data as the frequency. We used time-to-event analysis to assess the association between measures of carotid atherosclerosis and the occurrence of any CVE. The time from the date of the baseline ultrasound assessment to the date of the first CVE was the response of interest; individuals who were event-free at the date at which they were last known to be alive were censored at that time point. The incidence rate (with 95% confidence interval [95% CI]) was calculated for the composite event of all confirmed CVEs.

We plotted the survival function of patients grouped according to the distribution of plaques (plaque category) using the Kaplan-Meier product limit technique, and used the log-rank statistic to test significance. Cox proportional hazards models were used with any CVE as a primary outcome and major CVE as a secondary outcome. Univariate analysis first included each sonographic measure of atherosclerosis as a single covariate in the regression model. Multivariable regression analyses were then performed by adding the FRS category as a covariate to each of the regression models, in addition to the sonographic measure of atherosclerosis. A sensitivity analysis was then conducted by restricting the analysis to patients with a major CVE.

Since atherosclerotic plaques and CIMT represent 2 separate phenotypes of vessel wall abnormalities, we then performed a multivariable analysis that included TPA and mean CIMT in addition to FRS category in a single regression model to assess the independent predictive value of each one. To assess the predictive ability of the expanded model (vascular imaging data and FRS), we compared it with the base model (FRS alone) using the area under the receiver operating characteristic (ROC) curve (AUC) (with 95% CIs) at 5 years. The timeROC R function in R was used for this calculation.

To measure change in discriminative ability, we assessed the Integrated Discrimination Improvement (IDI). IDI denotes the average increase in absolute CVE risk estimates conferred by the expanded model in individuals who developed CVE outcomes plus the average decrease in absolute risk estimates in those who did not develop CVE outcomes. In addition, Net Reclassifi-

cation Improvement (NRI) was examined to determine the extent to which the expanded risk models reassigned individuals to risk categories that more correctly reflected whether or not that individual developed CV outcomes. The IDI.INF function in the R survIDINRI package was used to calculate the IDI and NRI.

Multiple imputation (using PROC MI and PROC MIANALYZE in SAS) was used to impute missing data, in conjunction with the Cox proportional hazards model. The full conditional specification and predictive mean matching methods were specified as methods of imputation.

RESULTS

Characteristics of the patients. In total, 559 patients with PsD underwent an ultrasound assessment at baseline, between December 11, 2009 and December 9, 2015. These patients were followed up until December 31, 2017. The mean ± SD duration of follow-up was 3.69 ± 1.9 years. The characteristics of the study population are listed in Table 1. After searching the cohort database and the provincial hospitalization and death registries, we identified 42 patients who had experienced a potential CVE during the follow-up period. Of these, 23 patients developed CVEs that were confirmed by a cardiologist (19 events were classified as a major CVE).

The following events were recorded: 10 patients with MI (2 fatal), 5 patients with stroke (1 fatal), 12 patients with revascularization, 3 patients with CHF exacerbation, 7 patients with angina, and 1 with TIA. Some of the patients developed more than 1 event type simultaneously or during several occasions during the follow-up; however, only the first event was considered, and it was classified as either a major CVE or minor CVE according to the most severe type of event in cases in which several types of events occurred simultaneously. Nineteen events were excluded for the following reasons: 13 did not meet the definitions of a

Table 1. Baseline characteristics of the study population by CV outcome*

	Patients with incident CVEs (n = 23)	Patients without CVEs (n = 536)
Age, years	65.9 ± 11	55.8 ± 11.2
Sex, no. (%) male	14 (60.9)	297 (55.4)
PsA, no. (%)	21 (91.3)	355 (66.2)
PsC, no. (%)	2 (8.7)	181 (33.8)
Disease duration, years	33.4 ± 18.4	25.6 ± 14.2
Ethnicity, no. (%) white	21 (91.3)	464 (88.6)
Current smoking, no. (%)	3 (13)	77 (14.4)
FRS category, no. (%)		
Low	3 (13)	304 (56.7)
Intermediate	5 (21.7)	122 (22.8)
High	15 (65.2)	110 (20.5)
Diabetes, no. (%)	5 (21.7)	38 (7.1)
Family history of CVEs, no. (%)	2 (8.7)	26 (4.9)
Use of antihypertensive medications, no. (%)	14 (60.9)	148 (27.6)
Use of antidiabetic medications, no. (%)	3 (13)	37 (6.9)
Use of lipid-lowering medications, no. (%)	10 (43.5)	91 (17)
Tender joint count†	2.5 ± 4.2	3.4 ± 5.9
Swollen joint count†	0.7 ± 1.6	1.1 ± 2.4
Damaged joint count†	12.1 ± 16.5	6.7 ± 11.2
BMI, kg/m^2	29.1 ± 5.8	28.8 ± 5.9
Waist circumference, cm	100.4 ± 13.7	96.1 ± 14.7
PASI	2.4 ± 2.1	3.4 ± 5.0
Total cholesterol, mmoles/liter	5.0 ± 1.3	5 ± 1.0
Total triglycerides, mmoles/liter	1.8 ± 1.2	1.5 ± 0.9
LDL cholesterol, mmoles/liter	2.9 ± 1.1	2.9 ± 0.9
HDL cholesterol, mmoles/liter	1.3 ± 0.4	1.4 ± 0.5
Systolic blood pressure, mm Hg	132 ± 12	122 ± 15
Diastolic blood pressure, mm Hg	78 ± 9	77 ± 9
Use of methotrexate, no. (%)	9 (39.1)	167 (31.2)
Use of nonbiologic DMARDs, no. (%)‡	5 (21.7)	67 (12.5)
Use of TNF inhibitors, no. (%)	6 (26.1)	173 (32.3)

* Except where indicated otherwise, values are the mean ± SD. CV = cardiovascular; CVEs = cardiovascular events; PsC = psoriasis without arthritis; FRS = Framingham Risk Score; BMI = body mass index; PASI = Psoriasis Area and Severity Index; LDL = low-density lipoprotein; HDL = high-density lipoprotein; TNF = tumor necrosis factor.
† Only in patients with psoriatic arthritis (PsA).
‡ Disease-modifying antirheumatic drugs (DMARDs) included methotrexate, leflunomide, sulfasalazine, hydroxychloroquine, cyclosporine, or azathioprine.

CVE after review of the medical records by the cardiologist, 5 events occurred prior to the baseline visit, and 1 event could not be confirmed due to lack of records.

The mean ± SD TPA was 0.18 ± 0.30 cm^2 and mean ± SD CIMT was 639 ± 136 μm. The majority of patients had atherosclerotic plaques at baseline: 27% had unilateral plaques and 31.5% had bilateral plaques. Although no formal comparison was performed, the burden of traditional CV risk factors and atherosclerosis at baseline was higher in patients who developed a CVE compared those who did not develop a CVE (Tables 1 and 2).

The calculated rate of developing a first CVE during the study period was 1.11 events per 100 patient-years (95% CI 0.74–1.67), and was 0.91 events per 100 patient-years (95% CI 0.57–1.43) for the calculated rate of a first major CVE during the study period. The Kaplan-Meier risk estimate showed that the risk of developing a CVE was significantly higher in patients with a higher burden of atherosclerotic plaques at baseline (those with bilateral plaques versus those with unilateral or no plaque) (Figure 1).

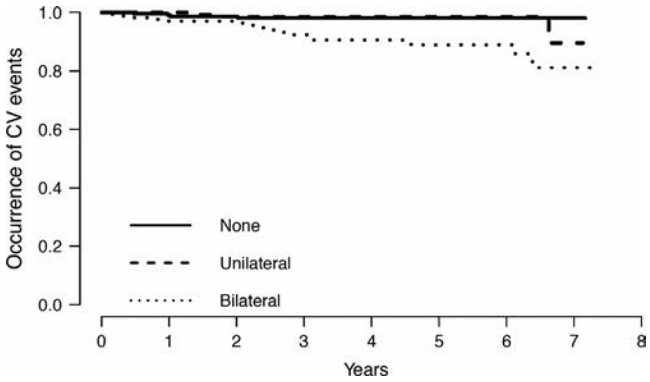

Figure 1. Occurrence of cardiovascular (CV) events by plaque category over time in patients with psoriatic disease.

Association between carotid atherosclerosis and risk of CVEs. The univariate regression analysis that assessed the association between measures of atherosclerosis at baseline and incident CVEs showed a significant association between all measures of atherosclerosis and incident CVEs (Table 3). In the multivariable analysis after adjustment for FRS category, the association between atherosclerosis and incident CVEs was attenuated, but remained statistically significant for most measures of atherosclerosis, including the TPA, maximal CIMT, and high TPA category. Analysis of the secondary study outcome, a major CVE, showed essentially similar results (Table 3).

We then performed a multivariable regression analysis of the association between carotid atherosclerosis and the incident CVEs of TPA and mean CIMT with the addition of the FRS category, to assess the independent predictive value of each of these sonographic measures of atherosclerosis. The effect size was slightly attenuated for both TPA and CIMT. Nevertheless, the association remained statistically significant for the TPA (HR 2.85, 95% CI 1.19–6.82; $P = 0.02$), but was no longer significant for the mean CIMT (HR 1.12, 95% CI 0.93–1.34), suggesting that TPA is a stronger predictor of CVEs than CIMT.

Comparison of the base model and expanded prediction model. To assess whether the addition of imaging data improved the predictive ability of the FRS alone, the estimated AUC of the base model (FRS alone) was compared to that of the expanded model (FRS plus a measure of atherosclerosis) at 5 years. The ROC curves for the base and expanded models are shown in Figure 2. The 5-year model showed a significant difference between the estimated AUC based on a model with FRS alone (AUC 0.81) and the estimated AUC based on an expanded risk model that included the mean IMT plus the FRS (AUC 0.84; $P = 0.046$) and one that included the maximal IMT plus the FRS (AUC 0.84; $P = 0.039$). The difference between the AUC of the base model and that of the expanded models with TPA, plaque category, and TPA category showed statistically nonsignificant trends toward improvement in predictive abilities.

Improvement of the predictive ability of the FRS in the expanded model was further assessed according to its ability to correctly reclassify high-risk patients above the treatment threshold and low-risk patients below the treatment threshold.

Table 2. Carotid ultrasound findings in the study population by CV outcome*

	Patients with incident CVEs (n = 23)	Patients without CVEs (n = 536)	All (n = 559)
TPA, cm^2	0.52 ± 0.61	0.17 ± 0.28	0.18 ± 0.30
Mean CIMT, μm	766 ± 227	633 ± 129	639 ± 136
Maximum CIMT, μm	851 ± 351	681 ± 165	687 ± 180
Plaque category, no. (%)			
No plaques	4 (17.4)	228 (42.5)	232 (41.5)
Unilateral plaque	3 (13)	148 (27.6)	151 (27)
Bilateral plaques	16 (69.6)	160 (29.9)	176 (31.5)
TPA category, no. (%)			
Low (TPA <0.21 cm^2)	8 (34.8)	387 (72.2)	395 (70.6)
High (TPA ≥0.21 cm^2)	15 (65.2)	149 (27.8)	164 (29.3)

* Except where indicated otherwise, values are the mean ± SD. CV = cardiovascular; CVEs = cardiovascular events; TPA = total plaque area; CIMT = carotid intima-media thickness.

Table 3. Association between baseline carotid atherosclerosis and incident CVEs as determined in Cox proportional hazards models*

	Univariate analysis		Adjusted for FRS	
	All CVEs (n = 559; no. events = 23)	Major CVEs (n = 559; no. events = 19)	All CVEs (n = 559; no. events = 23)	Major CVEs (n = 559; no. events = 19)
TPA (in cm^2)	6.79 (3.46–13.34) [<0.001]	6.40 (3.02–13.53) [<0.001]	3.56 (1.60–7.76) [0.002]	3.74 (1.55–8.85) [0.003]
Mean CIMT (in μm)†	1.35 (1.19–1.52) [<0.001]	1.34 (1.17–1.54) [<0.001]	1.20 (1.04–1.39) [0.01]	1.21 (1.03–1.42) [0.02]
Maximal CIMT (in μm)†	1.18 (1.09–1.27) [<0.001]	1.18 (1.08–1.28) [<0.001]	1.11 (1.01–1.21) [0.02]	1.11 (1.01–1.22) [0.03]
Plaque category				
Unilateral vs. none	1.07 (0.24–4.77) [0.93]	1.08 (0.24–4.81) [0.92]	0.74 (0.16–3.32) [0.69]	0.76 (0.17–3.49) [0.73]
Bilateral vs. none	5.36 (1.79–16.02) [0.003]	3.98 (1.28–12.33) [0.02]	2.61 (0.84–8.17) [0.10]	2.07 (0.63–6.75) [0.23]
TPA category, high vs. low	4.83 (2.05–11.41) [<0.001]	5.55 (2.11–14.62) [<0.001]	2.03 (1.03–6.17) [0.04]	3.25 (1.18–8.95) [0.02]

* Values are the hazard ratio (95% confidence interval) [*P*]. FRS = Framingham Risk Score; CVEs = cardiovascular events; TPA = total plaque area; CIMT = carotid intima-media thickness.
† Per 100-unit increase.

We applied the treatment threshold recommended by the Canadian Cardiovascular Society Guidelines for the management of dyslipidemia, which is a treatment threshold of 10% (35). The results are shown in Table 4. The IDI for discriminative ability was significantly improved for the expanded models that included the FRS along with the TPA, mean IMT, or maximal IMT (all $P < 0.05$), while the NRI was improved only for the expanded model that included maximal IMT ($P = 0.03$).

DISCUSSION

This study demonstrates that increased atherosclerotic plaque burden is associated with incident CVEs in patients with PsD. This atherosclerotic burden as estimated by carotid ultrasound can improve the prediction of CVEs in patients with PsD, when combined with the FRS as a prediction tool. Thus, such an approach has the potential to improve CV risk estimation and stratification in this patient population.

The elevated CV risk in patients with PsD is partially attributed to the high prevalence of traditional CV risk factors, but also to the effect of systemic inflammation related to the skin and the joint disease (6–9). As expected, the results of our study support the notion that the presence of atherosclerotic plaque and higher plaque burden is associated with increased CV risk, and that atherosclerosis is one of the primary underlying mechanisms leading to CVEs in patients with PsD (36,37). Therefore, assess-

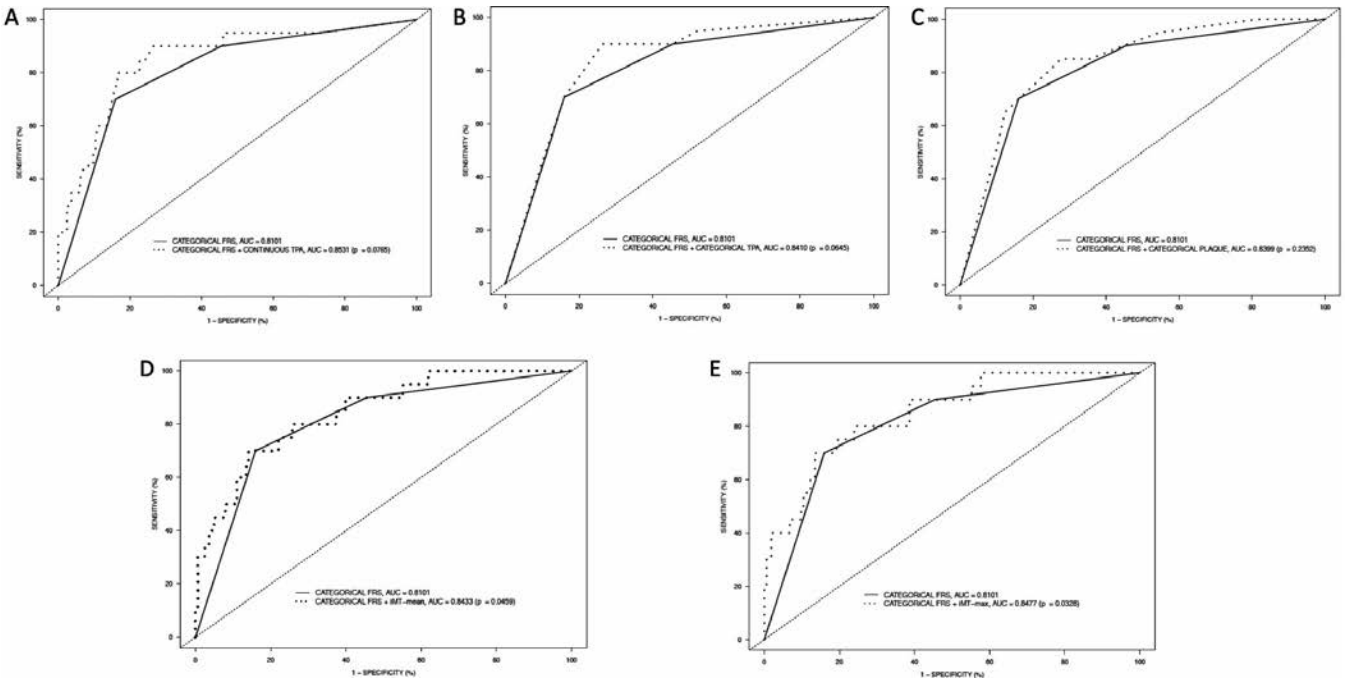

Figure 2. Comparison of the predictive ability of the base model (Framingham Risk Score [FRS] category alone) and expanded model (FRS category plus carotid imaging) for prediction of cardiovascular events in patients with psoriatic disease, including the total plaque area (TPA) (**A**), category of TPA (high versus low, with high defined as >0.21 cm^2) (**B**), plaque category (no plaques, unilateral plaque, or bilateral plaques) (**C**), mean carotid intima-media thickness (IMT) (**D**), and maximal IMT (**E**). AUC = area under the receiver operating characteristics curve.

Table 4. Reclassification properties of each predictor in the 559 patients with psoriatic disease (23 events)*

Predictor, method	Estimate	95% CI	*P* (1-sided)
TPA			
IDI	0.09	0.003, 0.24	0.03
NRI	0.18	−0.12, 0.45	0.15
Mean IMT			
IDI	0.07	0.009, 0.16	0.007
NRI	0.18	−0.02, 0.44	0.07
Maximal IMT			
IDI	0.06	0.02, 0.15	<0.001
NRI	0.29	0.003, 0.47	0.03
Plaque category			
IDI	0.02	−0.004, 0.12	0.11
NRI	0.39	−0.11, 0.59	0.13
TPA category			
IDI	0.007	−0.008, 0.09	0.33
NRI	0.43	−0.32, 0.62	0.23

* 95% CI = 95% confidence interval; TPA = total plaque area; IDI = Integrated Discrimination Improvement; NRI = Net Reclassification Index; IMT = intima-media thickness.

ing the burden of atherosclerosis provides a global estimation of the combined effect of traditional and disease-related factors on the vasculature system, which has a potential of improving CV risk stratification in patients with PsD beyond clinical risk algorithms that rely solely on traditional CV risk factors.

Clinical practice guidelines consider vascular imaging to be a potentially useful way of improving CV risk assessment and serve as a guide for initiating or deferring preventive therapies (38). Although most guidelines refer to quantification of coronary artery calcification in the assessment of CV risk, atherosclerosis in the carotid artery, as evaluated by the presence of plaques, as well as the TPA or the CIMT can also serve as predictors of CVEs in the general population (24,32,39). In general, the burden of atherosclerotic plaques has been found to be a stronger predictor of CVEs than the CIMT, which is in accordance to our findings (40).

There are little data about the predictive utility of carotid ultrasound in estimating CV risk in patients with rheumatic diseases. The largest study thus far conducted evaluated 636 patients with RA (66 events) who were followed up for up to 4 years (25). The presence of unilateral carotid plaque, presence of bilateral carotid plaques, and CIMT were associated with a 2.54-, 5.89-, and 1.31-fold increased risk of developing incident CVEs, respectively, after controlling for traditional CV risk factors. In another smaller study that included 114 patients with RA (17 incident events) who were followed up for 5 years, the presence of bilateral carotid plaques was predictive of CVEs in univariate analysis, but the association was no longer significant after controlling for age, probably because the sample size was small (41). To the best of our knowledge, this is the first study to assess the utility of various measures of carotid atherosclerosis for the prediction of CVEs in patients with psoriasis and PsA. The results of our study are concordant with previous findings in RA and suggest that carotid ultrasound documentation of atherosclerosis could serve as a surrogate measure of clinical CVEs in patients with PsD. Although there is more literature about the ability of carotid ultrasound to predict CVEs in the general population, it is challenging to compare the results of these studies to ours. Some of the limitations include different scanning protocols, various scores used to quantify atherosclerotic plaques, differences in clinical outcomes, and other confounders. Considering these limitations, the effect size found in our study for TPA measurements is within the range reported in large population-based studies from Norway and the US (32,42).

An accurate CV risk algorithm to inform CV risk factor management and enhance primary prevention in PsD is highly desirable. However, traditional algorithms do not consider other factors that may contribute to increased CV risk in patients with rheumatic disease, and tend to underestimate the CV risk (18–20). In RA, attempts to develop a disease-specific clinical prediction score by including measures of disease activity or applying a multiplication factor of 1.5 to the calculated risk have not been proven to significantly improve prediction compared to conventional risk algorithms (43). Another attempt included the development of a disease-specific risk score that combines traditional CV risk factors and measures of disease activity in RA (44). In systemic lupus erythematosus, however, a modified FRS with a multiplier of 2 more accurately predicted coronary artery disease, suggesting that additional variables may enhance risk prediction (45). Similarly, a multiplication factor of 1.5 applied to the calculated risk in patients with PsA was shown to correlate with CV risk as measured by coronary computed tomography angiography (46).

The use of vascular imaging, in particular ultrasound of the carotid arteries, has been proposed as a means to improve CV risk stratification in the recent European League Against Rheumatism recommendations (10). However, this recommendation was restricted to patients with RA, due to a lack of evidence in other rheumatic diseases. The results of our study support the use of carotid ultrasound to improve risk stratification in patients with PsD. The addition of imaging data improved the properties of the prediction model beyond the FRS.

The advantage of ultrasound over other modalities for vascular imaging includes lack of radiation, low cost of the examination, and its widespread use in rheumatology for joint evaluation. Thus, this assessment could potentially be performed "at the bedside" during consultation to provide immediate valuable information to complement clinical data from the medical history review, physical examination, and laboratory data. This strategy may be most useful in patients categorized by traditional scoring algorithms into an intermediate risk group, for whom physicians may be uncertain as to the potential benefit of initiating and/or up-titrating pharmacotherapy for aggressive CV risk factor management. However, it should be noted that only the IMT measurement provided incremental predictive accuracy, as indicated by the AUC and NRI, when compared to a base model that including only the FRS. This may be related to the small number of CVE outcomes.

Our study has several limitations. There was a small number of CVEs (23 events) in the sample, leading to large standard errors for the measures of predictive accuracy (AUC) and leading to improvement in models that included both clinical and imaging data. However, it is important to note that this is the largest study to date to investigate the use of imaging to improve CV risk stratification in the PsD population. Another limitation is the fact that we evaluated only structural aspects of atherosclerosis burden, while other measures, such as plaque vulnerability and vascular inflammation, which may also affect the risk of developing a clinical CVE, were not assessed in this study, although such techniques are likely to have limited clinical utility.

The primary strengths of our study include the careful phenotyping of clinical risk factors and CV outcomes, which were reviewed and confirmed by a cardiologist. We have assessed various phenotypes of atherosclerosis and have provided useful cutoff points for plaque classification, which may assist with CV risk stratification. These will need to be validated, however, in independent cohorts.

In conclusion, the results of this study suggest that the burden of carotid atherosclerosis, as detected and quantified by ultrasound, is predictive of future incident CVEs in patients with PsD independent of a traditional clinical CV risk prediction algorithm. Combining vascular imaging data with clinical and laboratory measures of traditional CV risk factors could improve the accuracy of CV risk stratification in patients with PsD and facilitate earlier initiation of appropriate treatment to reduce CVEs in this population.

AUTHOR CONTRIBUTIONS

All authors were involved in drafting the article or revising it critically for important intellectual content, and all authors approved the final version to be published. Dr. Eder had full access to all of the data in the study and takes responsibility for the integrity of the data and the accuracy of the data analysis.

Study conception and design. Sobchak, Akhtari, Harvey, Gladman, Cook, Eder.

Acquisition of data. Sobchak, Akhtari, Gladman, Chandran, Eder.

Analysis and interpretation of data. Sobchak, Cook, Eder.

REFERENCES

1. Polachek A, Touma Z, Anderson M, Eder L. Risk of cardiovascular morbidity in patients with psoriatic arthritis: a meta-analysis of observational studies. Arthritis Care Res (Hoboken) 2017;69:67–74.
2. Armstrong EJ, Harskamp CT, Armstrong AW. Psoriasis and major adverse cardiovascular events: a systematic review and meta-analysis of observational studies. J Am Heart Assoc 2013;2:e000062.
3. Miller IM, Ellervik C, Yazdanyar S, Jemec GB. Meta-analysis of psoriasis, cardiovascular disease, and associated risk factors. J Am Acad Dermatol 2013;69:1014–24.
4. Mehta NN, Azfar RS, Shin DB, Neimann AL, Troxel AB, Gelfand JM. Patients with severe psoriasis are at increased risk of cardiovascular mortality: cohort study using the General Practice Research Database. Eur Heart J 2010;31:1000–6.
5. Eder L, Jayakar J, Pollock R, Pellett F, Thavaneswaran A, Chandran V, et al. Serum adipokines in patients with psoriatic arthritis and psoriasis alone and their correlation with disease activity. Ann Rheum Dis 2013;72:1956–61.
6. Eder L, Thavaneswaran A, Chandran V, Cook R, Gladman DD. Increased burden of inflammation over time is associated with the extent of atherosclerotic plaques in patients with psoriatic arthritis. Ann Rheum Dis 2015;74:1830–5.
7. Dey AK, Joshi AA, Chaturvedi A, Lerman JB, Aberra TM, Rodante JA, et al. Association between skin and aortic vascular inflammation in patients with psoriasis: a case-cohort study using positron emission tomography/computed tomography. JAMA Cardiol 2017;2:1013–8.
8. Szentpetery A, Healy GM, Brady D, Haroon M, Gallagher P, Redmond CE, et al. Higher coronary plaque burden in psoriatic arthritis is independent of metabolic syndrome and associated with underlying disease severity. Arthritis Rheumatol 2018;70:396–407.
9. Shen J, Wong KT, Cheng IT, Shang Q, Li EK, Wong P, et al. Increased prevalence of coronary plaque in patients with psoriatic arthritis without prior diagnosis of coronary artery disease. Ann Rheum Dis 2017;76:1237–44.
10. Agca R, Heslinga SC, Rollefstad S, Heslinga M, McInnes IB, Peters MJ, et al. EULAR recommendations for cardiovascular disease risk management in patients with rheumatoid arthritis and other forms of inflammatory joint disorders: 2015/2016 update. Ann Rheum Dis 2017;76:17–28.
11. Coates LC, Kavanaugh A, Mease PJ, Soriano ER, Acosta-Felquer ML, Armstrong AW, et al. Group for Research and Assessment of Psoriasis and Psoriatic Arthritis 2015 treatment recommendations for psoriatic arthritis. Arthritis Rheumatol 2016;68:1060–71.
12. Wilson PW, D'Agostino RB, Levy D, Belanger AM, Silbershatz H, Kannel WB. Prediction of coronary heart disease using risk factor categories. Circulation 1998;97:1837–47.
13. Karmali KN, Goff DC Jr, Ning H, Lloyd-Jones DM. A systematic examination of the 2013 ACC/AHA pooled cohort risk assessment tool for atherosclerotic cardiovascular disease. J Am Coll Cardiol 2014;64:959–68.
14. Eder L, Chandran V, Gladman DD. The Framingham Risk Score underestimates the extent of subclinical atherosclerosis in patients with psoriatic disease. Ann Rheum Dis 2014;73:1990–6.
15. Arts EE, Popa C, Den Broeder AA, Semb AG, Toms T, Kitas GD, et al. Performance of four current risk algorithms in predicting cardiovascular events in patients with early rheumatoid arthritis. Ann Rheum Dis 2015;74:668–74.
16. Ernste FC, Sánchez-Menéndez M, Wilton KM, Crowson CS, Matteson EL, Maradit Kremers H. Cardiovascular risk profile at the onset of psoriatic arthritis: a population-based cohort study. Arthritis Care Res (Hoboken) 2015;67:1015–21.
17. Mehta NN, Krishnamoorthy P, Yu Y, Khan O, Raper A, Van Voorhees A, et al. The impact of psoriasis on 10-year Framingham Risk. J Am Acad Dermatol 2012;67:796–8.
18. Kimball AB, Szapary P, Mrowietz U, Reich K, Langley RG, You Y, et al. Underdiagnosis and undertreatment of cardiovascular risk factors in patients with moderate to severe psoriasis. J Am Acad Dermatol 2012;67:76–85.
19. Parsi KK, Brezinski EA, Lin TC, Li CS, Armstrong AW. Are patients with psoriasis being screened for cardiovascular risk factors? A study of screening practices and awareness among primary care physicians and cardiologists. J Am Acad Dermatol 2012;67:357–62.
20. Eder L, Harvey P, Chandran V, Rosen CF, Dutz J, Elder JT, et al. Gaps in diagnosis and treatment of cardiovascular risk factors in patients with psoriatic disease: an international multicenter study. J Rheumatol 2018;45:378–84.

21. Sattar N, McInnes IB. Vascular comorbidity in rheumatoid arthritis: potential mechanisms and solutions. Curr Opin Rheumatol 2005;17:286–92.
22. Hansson GK, Hermansson A. The immune system in atherosclerosis. Nat Immunol 2011;12:204–12.
23. Greenland P, Blaha MJ, Budoff MJ, Erbel R, Watson KE. Coronary calcium score and cardiovascular risk. J Am Coll Cardiol 2018;72:434–47.
24. Mitchell C, Korcarz CE, Gepner AD, Kaufman JD, Post W, Tracy R, et al. Ultrasound carotid plaque features, cardiovascular disease risk factors and events: the Multi-Ethnic Study of Atherosclerosis. Atherosclerosis 2018;276:195–202.
25. Evans MR, Escalante A, Battafarano DF, Freeman GL, O'Leary DH, del Rincón I. Carotid atherosclerosis predicts incident acute coronary syndromes in rheumatoid arthritis. Arthritis Rheum 2011;63:1211–20.
26. Gladman DD, Shuckett R, Russell ML, Thorne JC, Schachter RK. Psoriatic arthritis (PSA): an analysis of 220 patients. Q J Med 1987;62:127–41.
27. Eder L, Chandran V, Shen H, Cook RJ, Shanmugarajah S, Rosen CF, et al. Incidence of arthritis in a prospective cohort of psoriasis patients. Arthritis Care Res (Hoboken) 2011;63:619–22.
28. Taylor W, Gladman D, Helliwell P, Marchesoni A, Mease P, Mielants H, et al. Classification criteria for psoriatic arthritis: development of new criteria from a large international study. Arthritis Rheum 2006;54:2665–73.
29. D'Agostino RB Sr, Vasan RS, Pencina MJ, Wolf PA, Cobain M, Massaro JM, et al. General cardiovascular risk profile for use in primary care: the Framingham Heart Study. Circulation 2008;117:743–53.
30. Eder L, Jayakar J, Shanmugarajah S, Thavaneswaran A, Pereira D, Chandran V, et al. The burden of carotid artery plaques is higher in patients with psoriatic arthritis compared with those with psoriasis alone. Ann Rheum Dis 2013;72:715–20.
31. Spence DJ. Ultrasound measurement of carotid plaque as a surrogate outcome for coronary artery disease. Am J Cardiol 2002;89:10B–15.
32. Johnsen SH, Mathiesen EB, Joakimsen O, Stensland E, Wilsgaard T, Løchen ML, et al. Carotid atherosclerosis is a stronger predictor of myocardial infarction in women than in men: a 6-year follow-up study of 6226 persons: the Tromsø Study. Stroke 2007;38:2873–80.
33. Spence JD. Technology insight: ultrasound measurement of carotid plaque: patient management, genetic research, and therapy evaluation. Nat Clin Pract Neurol 2006;2:611–9.
34. Johnstone DE, Buller CE, National Steering Committees on Quality Indicators and Data Definitions, Canadian Cardiovascular Society. Pan-Canadian cardiovascular data definitions and quality indicators: a status update. Can J Cardiol 2012;28:599–601.
35. Anderson TJ, Grégoire J, Pearson GJ, Barry AR, Couture P, Dawes M, et al. 2016 Canadian Cardiovascular Society guidelines for the management of dyslipidemia for the prevention of cardiovascular disease in the adult. Can J Cardiol 2016;32:1263–82.
36. Karpouzas GA, Malpeso J, Choi TY, Li D, Munoz S, Budoff MJ. Prevalence, extent and composition of coronary plaque in patients with rheumatoid arthritis without symptoms or prior diagnosis of coronary artery disease. Ann Rheum Dis 2014;73:1797–804.
37. Eder L, Gladman DD, Ibañez D, Urowitz MB. The correlation between carotid artery atherosclerosis and clinical ischemic heart disease in lupus patients. Lupus 2014;23:1142–8.
38. Goff DC Jr, Lloyd-Jones DM, Bennett G, Coady S, D'Agostino RB Sr, Gibbons R, et al. 2013 ACC/AHA guideline on the assessment of cardiovascular risk: a report of the American College of Cardiology/American Heart Association Task Force on Practice Guidelines. J Am Coll Cardiol 2014;63:2935–59.
39. Roman MJ, Kizer JR, Best LG, Lee ET, Howard BV, Shara NM, et al. Vascular biomarkers in the prediction of clinical cardiovascular disease: the Strong Heart Study. Hypertension 2012;59:29–35.
40. Spence JD. Carotid plaque measurement is superior to IMT [editorial]. Atherosclerosis 2012;220:34–5.
41. Ajeganova S, de Faire U, Jogestrand T, Frostegård J, Hafström I. Carotid atherosclerosis, disease measures, oxidized low-density lipoproteins, and atheroprotective natural antibodies for cardiovascular disease in early rheumatoid arthritis: an inception cohort study. J Rheumatol 2012;39:1146–54.
42. Mitchell C, Korcarz CE, Gepner AD, Kaufman JD, Post W, Tracy R, et al. Ultrasound carotid plaque features, cardiovascular disease risk factors and events: The Multi-Ethnic Study of Atherosclerosis. Atherosclerosis 2018;276:195–202.
43. Arts EE, Popa CD, Den Broeder AA, Donders R, Sandoo A, Toms T, et al. Prediction of cardiovascular risk in rheumatoid arthritis: performance of original and adapted SCORE algorithms. Ann Rheum Dis 2016;75:674–80.
44. Solomon DH, Greenberg J, Curtis JR, Liu M, Farkouh ME, Tsao P, et al. Derivation and internal validation of an expanded cardiovascular risk prediction score for rheumatoid arthritis: a Consortium of Rheumatology Researchers of North America Registry Study. Arthritis Rheumatol 2015;67:1995–2003.
45. Urowitz MB, Ibañez D, Su J, Gladman DD. Modified Framingham Risk Factor Score for systemic lupus erythematosus. J Rheumatol 2016;43:875–9.
46. Haroon M, Szentpetery A, Dodd JD, Fitzgerald O. Modifications of cardiovascular risk scores, but not standard risk scores, improve identification of asymptomatic coronary artery disease in psoriatic arthritis [letter]. J Rheumatol 2018;45:1329–30.

American College of Rheumatology
Empowering Rheumatology Professionals

Arthritis & Rheumatology
Vol. 71, No. 10, October 2019, pp 1660–1669
DOI 10.1002/art.40921

Responsiveness of Serum C-Reactive Protein, Interleukin-17A, and Interleukin-17F Levels to Ustekinumab in Psoriatic Arthritis: Lessons From Two Phase III, Multicenter, Double-Blind, Placebo-Controlled Trials

Stefan Siebert,[1] Kristen Sweet,[2] Bidisha Dasgupta,[2] Kim Campbell,[2] Iain B. McInnes,[1] and Matthew J. Loza[2]

Objective. To evaluate the associations of C-reactive protein (CRP) and circulating Th17-associated cytokine levels with psoriatic arthritis (PsA) disease activity and therapeutic response to ustekinumab.

Methods. Interleukin-17A (IL-17A), IL-17F, IL-23, and CRP concentrations were measured in serum samples collected as part of the 2 PSUMMIT phase III studies of ustekinumab in PsA (n = 927). In post hoc analyses, relationships of IL-17A, IL-17F, and CRP levels at baseline, week 4, and week 24 with baseline skin and joint disease activity and response to therapy were evaluated using generalized linear models and Pearson's product-moment correlation tests.

Results. Baseline serum levels of IL-17A and IL-17F were positively correlated with baseline skin disease scores (r = 0.39–0.62). IL-23 levels were correlated with skin disease scores to a lesser extent (r = 0.26–0.31). No significant correlations were observed between these cytokine or CRP levels and baseline joint disease activity. There was no significant association of baseline levels of IL-17A, IL-17F, IL-23, or CRP with therapeutic response to ustekinumab in either the skin or joints. Significant reductions from baseline in levels of IL-17A, IL-17F, and CRP were seen in patients treated with ustekinumab compared to those treated with placebo. Ustekinumab-treated patients in whom 75% improvement in the Psoriasis Area and Severity Index score or 20% improvement according to the American College of Rheumatology criteria was achieved after 24 weeks of treatment had greater reductions in CRP level (geometric mean decreases of 51–58% versus 32–33%; $P < 0.05$), but not IL-17A or IL-17F levels, than nonresponders.

Conclusion. Baseline serum IL-23/IL-17 levels correlated with skin, but not joint, disease activity, suggesting tissue-specific variation. However, neither baseline Th17-associated cytokine levels nor CRP level were predictive of therapeutic response to ustekinumab in the skin or joints, despite rapid reductions in their levels following ustekinumab therapy.

INTRODUCTION

Psoriatic arthritis (PsA) is part of the spondyloarthritis spectrum and affects 10–30% of people with psoriasis (1). Patients with PsA may have enthesitis, synovitis, and osteitis, in addition to variable skin involvement, resulting in a highly heterogeneous clinical presentation. Therapeutic options for psoriasis and PsA were limited until the development of biologic drugs, including tumor necrosis factor (TNF) inhibitors, antibodies targeting the interleukin-12 (IL-12)/IL-23/Th17 pathway (including ustekinumab, guselkumab, secukinumab, and ixekizumab), and JAK inhibitors, that facilitated specific immune intervention and transformed disease management and outcomes.

Despite these advances, there remains significant unmet need in the management of PsA, with many patients exhibiting

ClinicalTrials.gov identifiers: NCT01009086 (PSUMMIT 1) and NCT01077362 (PSUMMIT 2).

Supported by Janssen Research and Development, LLC.

[1]Stefan Siebert, MD, PhD, Iain B. McInnes, MD, PhD: University of Glasgow, Glasgow, UK; [2]Kristen Sweet, PhD, Bidisha Dasgupta, PhD, Kim Campbell, PhD, Matthew J. Loza, PhD: Janssen Research and Development LLC, Spring House, Pennsylvania.

Drs. Siebert and Sweet contributed equally to this work.

Dr. Siebert has received consulting fees, speaking fees, and/or honoraria from Novartis, Janssen, Celgene, UCB, Boehringer Ingelheim, and AbbVie (less than $10,000 each) and has received research support from Novartis, Janssen, Celgene, UCB, Boehringer Ingelheim, Bristol-Myers Squibb, and GlaxoSmithKline. Drs. Sweet, Dasgupta, Campbell, and Loza own stock in Johnson & Johnson. Dr. McInnes has received consulting fees, speaking fees, and/or honoraria from Bristol-Myers Squibb, Galvani Bioelectronics, Leo Pharma, UCB, AbbVie, Novartis, Celgene, Pfizer, GlaxoSmithKline, Eli Lilly, and Boehringer (less than $10,000 each) and has received research support from AstraZeneca, Bristol-Myers Squibb, Compugen, GlaxoSmithKline, Janssen, Novartis, Pfizer, and UCB.

Address correspondence to Stefan Siebert, MD, PhD, Sir Graeme Davies Building, 120 University Place, Glasgow G12 8TA, Scotland, UK. E-mail: Stefan.siebert@glasgow.ac.uk.

Submitted for publication February 25, 2019; accepted in revised form May 2, 2019.

no or only partial response to available therapies, or a dichotomous response in the skin and musculoskeletal system. Moreover, no clear predictive biomarkers of response to therapy exist as yet, though clearly they would confer value in defining those patients most likely to benefit from a given intervention.

Clinical trials using targeted biologic therapies offer an opportunity to identify potential theranostic biomarkers and better understand underlying inflammatory processes that drive disease in humans. Two PSUMMIT phase III studies demonstrated the efficacy of ustekinumab, a human IgG1κ monoclonal antibody that binds to the p40 subunit common to both IL-12 and IL-23, for treatment of the cutaneous and musculoskeletal components of PsA (2,3), significant inhibition of radiographic progression of joint damage (4), and improvement in patient-reported outcomes (5). Serum samples were collected as part of these studies to allow the further characterization of Th17-associated cytokines in PsA and the effects of IL-12/IL-23 inhibition with ustekinumab on the levels of these cytokines.

The objective of the analyses reported here was to evaluate the association of serum levels of Th17-associated cytokines with PsA disease activity, the pharmacodynamic impact of ustekinumab on serum levels of these cytokines, and whether this was correlated with therapeutic response.

PATIENTS AND METHODS

Study design and participants. Detailed descriptions of the phase III, multicenter, double-blind, placebo-controlled PSUMMIT 1 (ClinicalTrials.gov identifier: NCT01009086) and PSUMMIT 2 (ClinicalTrials.gov identifier: NCT01077362) study designs, patient populations, and results have been reported elsewhere (2,3). Briefly, in both studies, patients with active PsA were randomly assigned (1:1:1) to receive ustekinumab 45 mg, ustekinumab 90 mg, or placebo at baseline, week 4, and every 12 weeks thereafter. PSUMMIT 1 included only patients who were naive to TNF biologic therapies (n = 615), whereas PSUMMIT 2 included both anti-TNF–naive patients (n = 132) and anti-TNF–exposed patients (n = 180). The primary end point in both studies was the proportion of participants with at least 20% improvement in disease activity according to the American College of Rheumatology response criteria (ACR20) at week 24. Clinical changes in skin disease were evaluated using a week-24 end point of at least 75% improvement in the Psoriasis Area and Severity Index (PASI75). For biomarker analyses, patients in whom less than a 50% improvement in PASI (PASI50) was achieved were considered inadequate responders and were the reference group for comparison to PASI75 responders.

Biomarker assays and analyses. Serum IL-17A and IL-17F protein levels were assayed at weeks 0, 4, and 24 in the PSUMMIT 1 study and at weeks 0 and 4 in the PSUMMIT 2 study. Serum C-reactive protein (CRP) levels were measured at weeks 0, 4, and 24 in both studies. Because of limited available sample volumes, IL-23 was assayed in the PSUMMIT 2 study only. Due to the inability of the assay to distinguish between free IL-23 and IL-23 bound by ustekinumab, only baseline levels of IL-23 were measured. Samples were assayed using Single Molecule Counting Human Immunoassay Kits (MilliporeSigma [formerly Singulex]) for IL-17A, IL-17F, and IL-23 and CardioPhase high-sensitivity CRP assay (performed centrally at Covance) for CRP. Samples from PSUMMIT 1 and PSUMMIT 2 were assayed independently in separate batches.

Statistical analysis. Levels of serum protein biomarkers generally had log-normal distributions and were $\log_2$-transformed for statistical analyses and data display. The significance of the differences between groups was evaluated by generalized linear model analyses, and *P* values less than 0.05 were considered significant. The significance of the correlations between variables was evaluated by Pearson's product-moment correlation test, with significance defined as a *P* value of less than 0.05 and correlation coefficient r of greater than 0.25 or less than –0.25. Data from the 2 studies were analyzed independently.

RESULTS

Correlation between baseline serum cytokine levels and clinical characteristics. The baseline characteristics of the PSUMMIT 1 and PSUMMIT 2 study populations have been reported previously and are shown in Supplementary Table 1, available on the *Arthritis & Rheumatology* web site at http://onlinelibrary.wiley.com/doi/10.1002/art.40921/abstract. Clinical outcomes of the 2 trials are shown in Supplementary Table 2, available on the *Arthritis & Rheumatology* web site at http://onlinelibrary.wiley.com/doi/10.1002/art.40921/abstract. The relationship between serum CRP, IL-17A, IL-17F, and IL-23 levels at the baseline (week 0) study visit (before the first dose of study agent was administered) and the skin and joint scores at that visit was evaluated. Baseline serum levels of IL-17A and IL-17F were positively correlated with clinical skin disease scores, as measured by body surface area and PASI, in both PSUMMIT studies, with correlations ranging from r = 0.39 to r = 0.62 (Table 1). Correlations of IL-23 level with PASI and body surface area were also observed, to a lesser degree (r = 0.26 and r = 0.31, respectively) (Table 1). However, there were no significant correlations observed between the levels of these cytokines and baseline joint disease activity as measured by swollen and tender joint counts (r = –0.04–0.18) (Table 1). Serum CRP levels were not significantly correlated with either baseline joint or skin disease activity (r = 0.04–0.19). As expected for variables with short half-lives, there was no significant correlation of any of these 4 serum biomarkers with the duration of PsA or psoriasis (r = –0.12–0.15).

Table 1. Correlation between baseline clinical characteristics and baseline levels of serum biomarkers in patients with psoriatic arthritis in the PSUMMIT 1 and PSUMMIT 2 studies*

	CRP			IL-17A			IL-17F			IL-23		
	r	*P*	n	r	*P*	n	r	*P*	n	r	*P*	n
PSUMMIT 1 study												
Body surface area	0.06	0.1301	614	0.42†	<0.0001	474	0.57†	<0.0001	237	NA	NA	NA
PASI	0.09	0.0253	615	0.39†	<0.0001	474	0.56†	<0.0001	237	NA	NA	NA
Swollen joint count in 66 joints	0.09	0.0241	615	0.02	0.6025	474	0.07	0.2803	237	NA	NA	NA
Tender joint count in 68 joints	0.05	0.1750	615	0.11	0.0143	474	0.18	0.0044	237	NA	NA	NA
Swollen joint count in 28 joints	0.11	0.0065	615	−0.04	0.3989	474	−0.03	0.6124	237	NA	NA	NA
Tender joint count in 28 joints	0.04	0.2818	615	0.06	0.2232	474	0.09	0.1581	237	NA	NA	NA
Psoriatic arthritis duration	0.07	0.0936	615	0.08	0.0676	474	0.06	0.3505	237	NA	NA	NA
Psoriasis duration	0.00	0.9749	615	0.09	0.0487	474	0.15	0.0204	237	NA	NA	NA
PSUMMIT 2 study												
Body surface area	0.17	0.0025	311	0.56†	<0.0001	310	0.54†	<0.0001	298	0.31†	<0.0001	306
PASI	0.17	0.0025	308	0.62†	<0.0001	307	0.56†	<0.0001	295	0.26†	<0.0001	303
Swollen joint count in 66 joints	0.19	0.0010	312	0.11	0.0579	310	0.15	0.0113	298	0.08	0.1890	306
Tender joint count in 68 joints	0.13	0.0219	312	0.09	0.1110	310	0.12	0.0410	298	−0.01	0.8261	306
Swollen joint count in 28 joints	0.14	0.0134	312	0.00	0.9405	310	0.03	0.5560	298	0.03	0.6298	306
Tender joint count in 28 joints	0.14	0.0161	312	0.05	0.4023	310	0.08	0.1633	298	−0.03	0.5438	306
Psoriatic arthritis duration	0.07	0.2377	312	0.01	0.8152	310	−0.02	0.7728	298	−0.12	0.0406	306
Psoriasis duration	0.08	0.1833	312	0.03	0.5654	310	0.04	0.4830	298	−0.09	0.1005	306

* Correlations were determined by Pearson's product-moment correlation test. CRP = C-reactive protein; IL-17A = interleukin-17A; NA = not applicable; PASI = Psoriasis Area and Severity Index.
† Significant correlation ($r > 0.25$ or $r < -0.25$).

Distributions of the baseline serum biomarker levels did not differ significantly among subclassifications of PsA, including asymmetric peripheral arthritis, distal interphalangeal joint arthritis, polyarticular arthritis, and spondylitis with peripheral arthritis (Supplementary Figure 1, *Arthritis & Rheumatology* web site at http://onlinelibrary.wiley.com/doi/10.1002/art.40921/abstract).

Lack of correlation between baseline serum cytokine levels and response to therapy. The associations of baseline serum levels of IL-17A, IL-17F, IL-23, and CRP with clinical response at week 24 were evaluated. Regardless of whether response was measured by skin improvement (PASI75 responders compared to PASI50 nonresponders at week 24) (Figure 1)

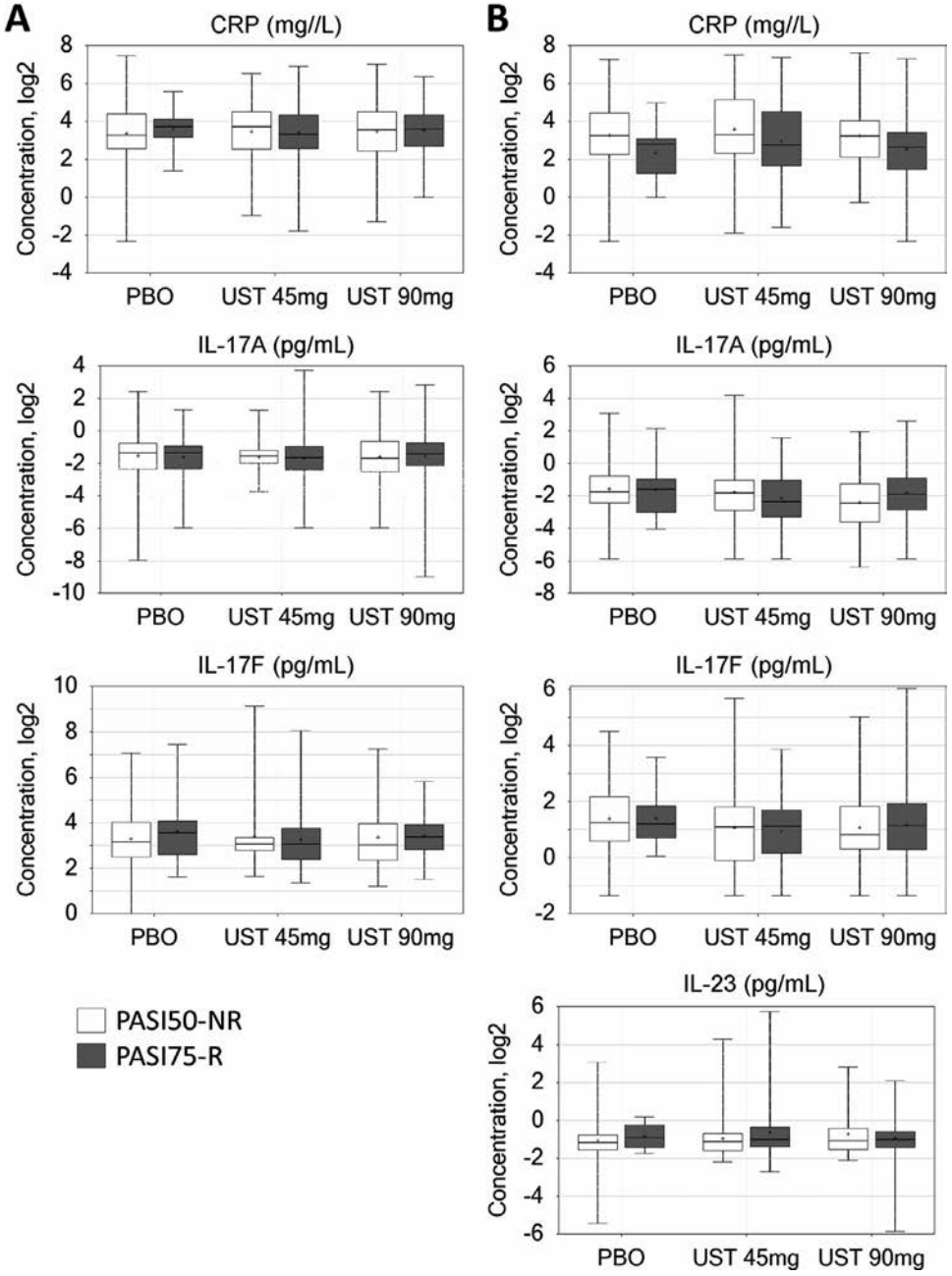

Figure 1. Association of Psoriasis Area and Severity Index (PASI) response at week 24 with baseline serum biomarker levels in patients with psoriatic arthritis treated with placebo (PBO), ustekinumab (UST) 45 mg, or ustekinumab 90 mg and classified as those in whom less than 50% improvement in the PASI was achieved (PASI50 nonresponders [PASI50-NR]) and those in whom at least 75% improvement in the PASI was achieved (PASI75 responders [PASI75-R]). **A**, Baseline (week 0) serum levels of C-reactive protein (CRP), interleukin-17A (IL-17A), and IL-17F in patients in the PSUMMIT 1 trial. **B**, Baseline serum levels of CRP, IL-17A, IL-17F, and IL-23 in patients in the PSUMMIT 2 trial. Data are shown as box plots. Each box represents the upper and lower interquartile range. Lines inside the boxes represent the median. Whiskers represent the range. Symbols inside the boxes represent the mean. Patients with an intermediate response between PASI50 and PASI75 were not included. See Supplementary Table 2, available on the *Arthritis & Rheumatology* web site at http://onlinelibrary.wiley.com/doi/10.1002/art.40921/abstract, for sample sizes.

or joint symptom improvement (ACR20 responders compared to nonresponders at week 24) (Figure 2), there were no significant associations of response to therapy with baseline levels of IL-17A, IL-17F, CRP, or IL-23 in either the ustekinumab or placebo arms.

Pharmacodynamic changes in serum biomarker levels. We next evaluated biomarker concentrations over time after drug exposure. At week 4, there was a significant reduction from baseline in levels of IL-17A, IL-17F, and CRP in the

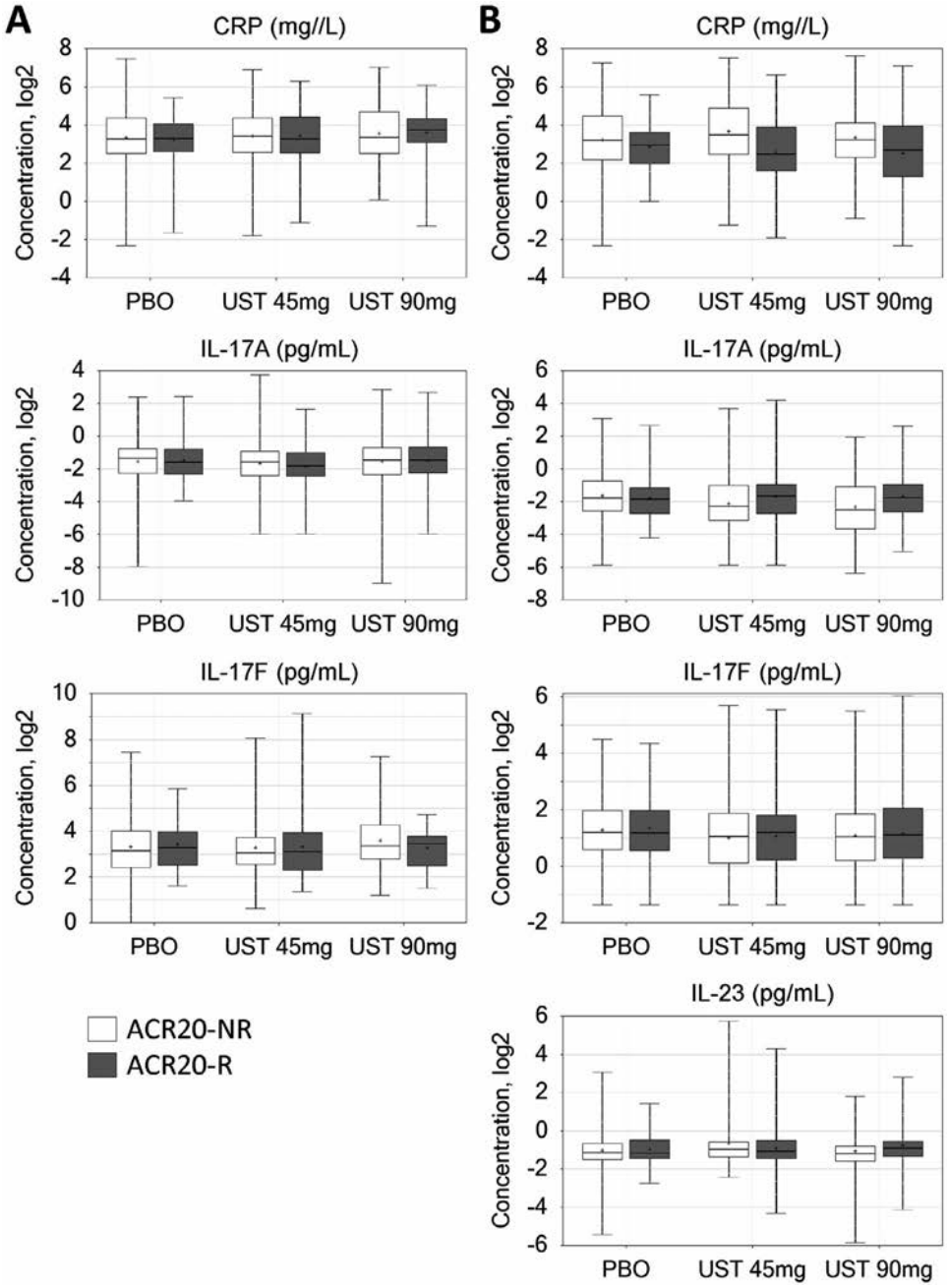

Figure 2. Association of American College of Rheumatology criteria for 20% improvement in disease activity (ACR20) response at week 24 with baseline serum biomarker levels in patients with psoriatic arthritis treated with placebo, ustekinumab 45 mg, or ustekinumab 90 mg and classified as those in whom an ACR20 response was not achieved (ACR20 nonresponders [ACR20-NR]) and those in whom an ACR20 response was achieved (ACR20 responders [ACR20-R]). **A**, Baseline (week 0) serum levels of CRP, IL-17A, and IL-17F in patients in the PSUMMIT 1 trial. **B**, Baseline serum levels of CRP, IL-17A, IL-17F, and IL-23 in patients in the PSUMMIT 2 trial. Data are shown as box plots. Each box represents the upper and lower interquartile range. Lines inside the boxes represent the median. Whiskers represent the range. Symbols inside the boxes represent the mean. See Supplementary Table 2, available on the *Arthritis & Rheumatology* web site at http://onlinelibrary.wiley.com/doi/10.1002/art.40921/abstract, for sample sizes. See Figure 1 for other definitions.

ustekinumab treatment arms compared to the placebo arm in both the PSUMMIT 1 and PSUMMIT 2 studies ($P < 0.05$), with geometric mean decreases ranging from 18% to 35% for CRP level, 24% to 44% for IL-17A level, and 27% to 38% for IL-17F level in the ustekinumab treatment arms (Figure 3 and Supplementary Table 3, available on the *Arthritis & Rheumatology* web site at http://onlinelibrary.wiley.com/doi/10.1002/art.40921/abstract). Further decreases in CRP level were observed at week 24 in both studies, and remained significantly different from changes in the placebo arm ($P < 0.05$). Levels of IL-17A and IL-17F at week 24 (measured in the PSUMMIT 1 study only) remained decreased in both ustekinumab treatment arms, though the difference from the change in the placebo arm was significant only for IL-17F in the ustekinumab 90 mg arm ($P = 0.038$) (Figure 3A). Thus, the p40 pathway is functionally linked to the elaboration of cytokine expression and the acute-phase response in PsA. The extent of changes in IL-17A, IL-17F, and CRP levels after 4 or 24 weeks of treatment with ustekinumab did not differ significantly among subclassifications of PsA (Supplementary Figure 2, available on the *Arthritis & Rheumatology* web site at http://onlinelibrary.wiley.com/doi/10.1002/art.40921/abstract).

Correlation between pharmacodynamic changes in serum biomarker levels and clinical response. We next assessed whether pharmacodynamic changes in serum biomarker levels were distinct in clinical responders in the ustekinumab treatment arms. Because of the reduced sample sizes available in this subgroup analysis and the similar pharmacodynamic changes for both ustekinumab arms, the 45 mg and 90 mg ustekinumab treatment arms were combined to improve statistical power. For ustekinumab-treated subjects in both PSUMMIT studies, CRP level decreased from baseline to week 24 both in patients in whom a PASI75 response was achieved and in those in whom a PASI50 response was not achieved (nonresponders), but with a significantly greater reduction in the PASI75 responders than in the PASI50 nonresponders (geometric mean decreases of 58% versus 33% in the PSUMMIT 1 study and 51% versus 32% in the PSUMMIT 2 study; $P < 0.05$) (Figure 4). This difference between clinical response groups was not apparent at week 4. IL-17A levels were significantly decreased in PASI75 responders versus PASI50 nonresponders at week 4 in the PSUMMIT 2 study (geometric mean decreases of 50% versus 28%; $P = 0.0054$), but not at either week 4 or week 24 in the PSUMMIT 1 study (Figure 4). Changes in IL-17F levels

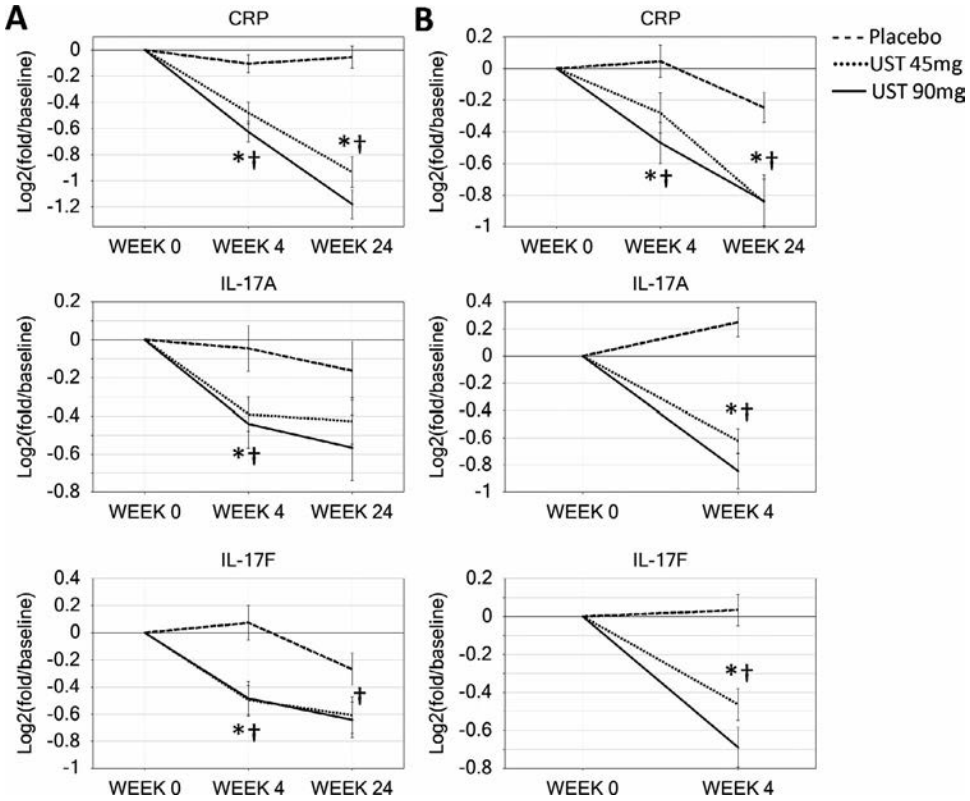

Figure 3. Pharmacodynamic changes in serum biomarker levels in patients with psoriatic arthritis treated with placebo, ustekinumab 45 mg, or ustekinumab 90 mg. **A**, Changes from baseline (week 0) to weeks 4 and 24 in CRP, IL-17A, and IL-17F levels in patients in the PSUMMIT 1 trial. **B**, Changes from baseline to weeks 4 and 24 in CRP level and from baseline to week 4 in IL-17A and IL-17F levels in patients in the PSUMMIT 2 trial. Horizontal lines and error bars show the mean ± SEM. * = $P < 0.05$, ustekinumab 45 mg versus placebo; † = $P < 0.05$, ustekinumab 90 mg versus placebo. See Supplementary Table 3, available on the *Arthritis & Rheumatology* web site at http://onlinelibrary.wiley.com/doi/10.1002/art.40921/abstract, for samples sizes and statistical data. See Figure 1 for definitions.

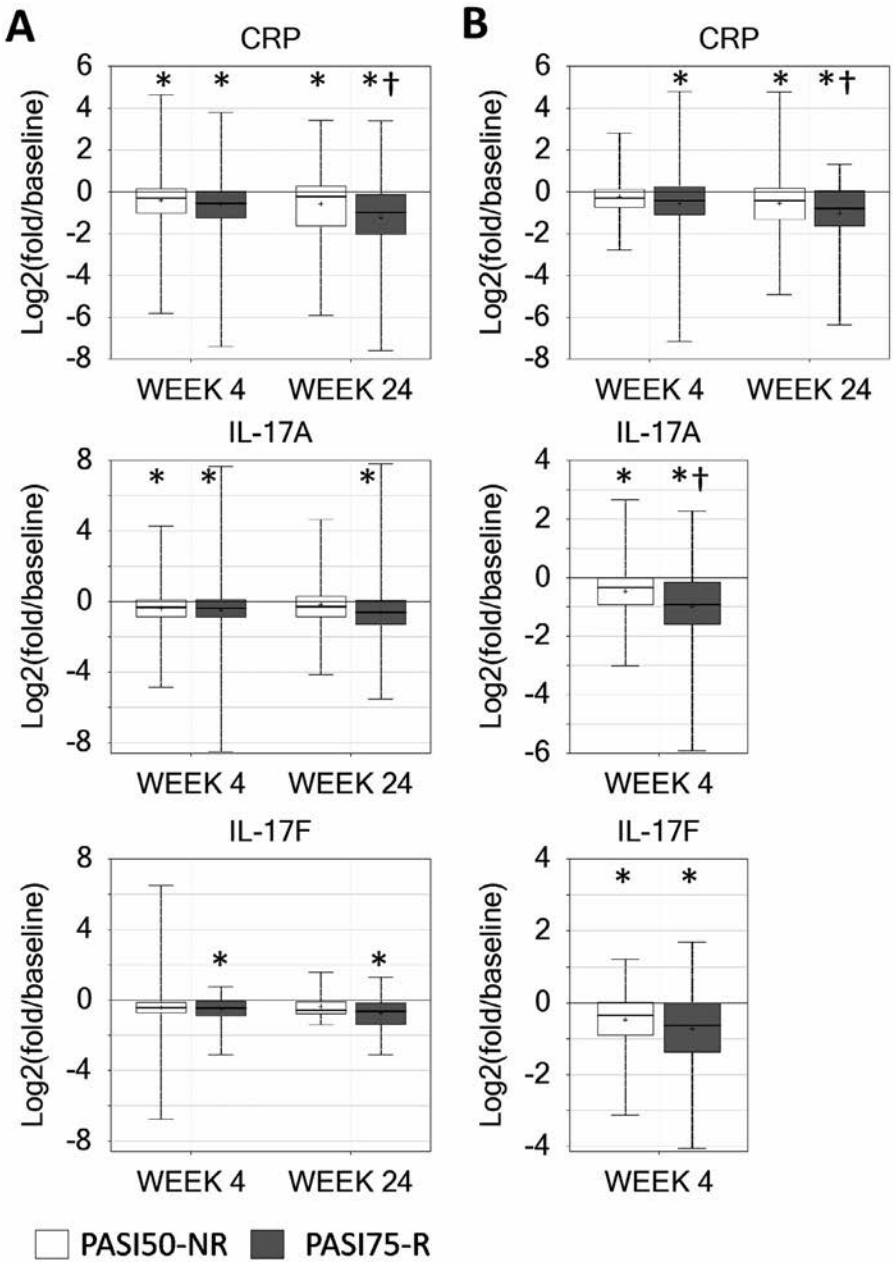

Figure 4. Association of PASI response at weeks 4 and 24 with changes in serum biomarker levels in patients with psoriatic arthritis treated with ustekinumab and classified as those in whom less than 50% improvement in the PASI was achieved (PASI50 nonresponders) and those in whom at least 75% improvement in the PASI was achieved (PASI75 responders). Patients receiving ustekinumab 45 mg and those receiving ustekinumab 90 mg were combined into one group. **A**, Changes from baseline (week 0) to weeks 4 and 24 in CRP, IL-17A, and IL-17F levels in patients in the PSUMMIT 1 trial. **B**, Changes from baseline to weeks 4 and 24 in CRP level and from baseline to week 4 in IL-17A and IL-17F levels in patients in the PSUMMIT 2 trial. Data are shown as box plots. Each box represents the upper and lower interquartile range. Lines inside the boxes represent the median. Whiskers represent the range. Symbols inside the boxes represent the mean. Patients with an intermediate response between PASI50 and PASI75 were not included. See Supplementary Table 4, available on the *Arthritis & Rheumatology* web site at http://onlinelibrary.wiley.com/doi/10.1002/art.40921/abstract, for sample sizes. * = $P < 0.05$ versus 0 (no change) in the same response group at the indicated time point; † = $P < 0.05$ versus PASI50 nonresponders at the same time point. See Figure 1 for definitions.

were not significantly different in PASI75 responders compared to PASI50 nonresponders in either study.

Similarly, ustekinumab-treated subjects in whom an ACR20 response was achieved had significantly greater reductions from baseline in CRP level, compared to ACR20 nonresponders, at week 24 in both studies (geometric mean decreases of 64% versus 38% in the PSUMMIT 1 study and 59% versus 28% in the PSUMMIT 2 study; $P < 0.05$) and at week 4 in the

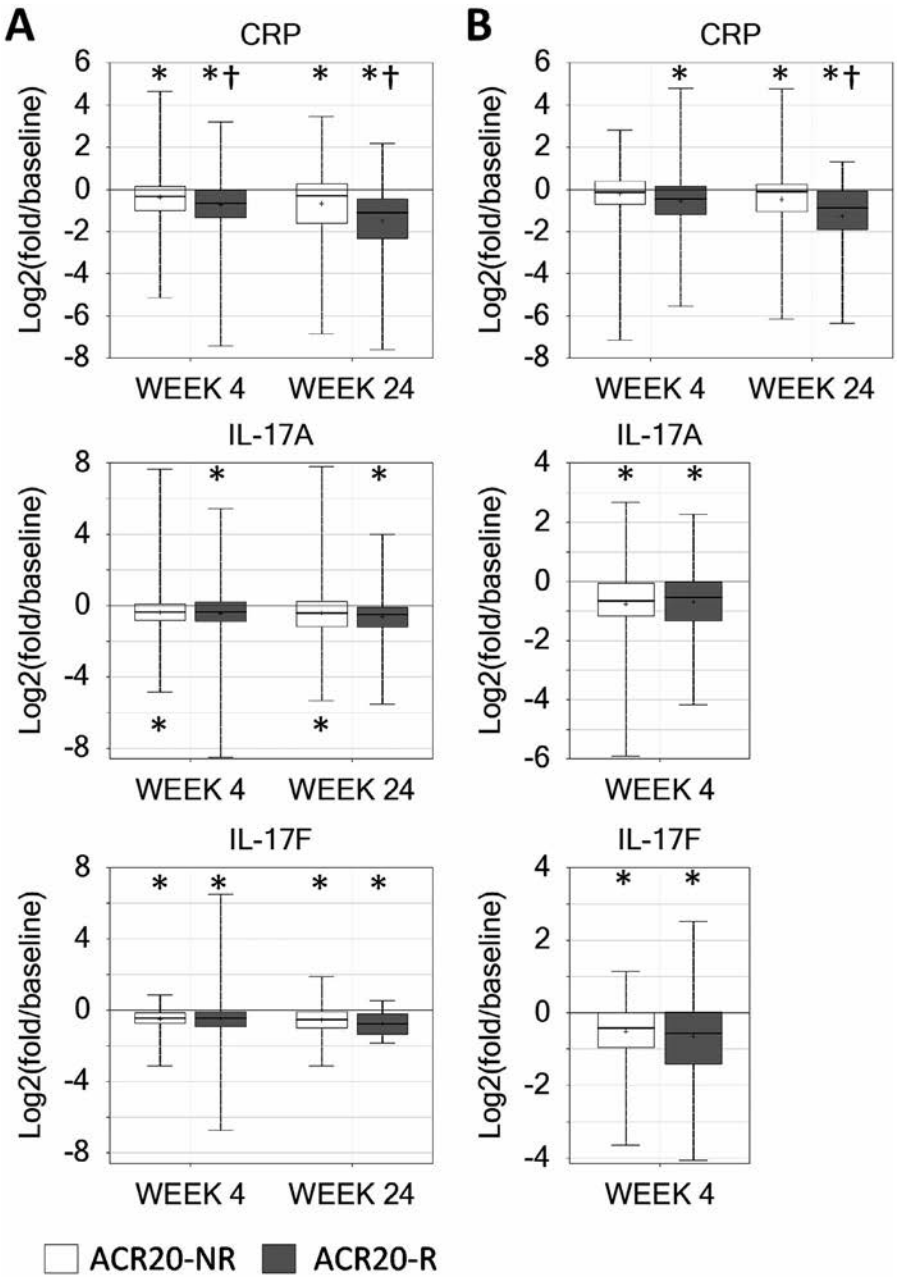

Figure 5. Association of American College of Rheumatology criteria for 20% improvement in disease activity (ACR20) response at weeks 4 and 24 with changes in serum biomarker levels in patients with psoriatic arthritis treated with ustekinumab and classified as those in whom an ACR20 response was not achieved and those in whom an ACR20 response was achieved. Patients receiving ustekinumab 45 mg and those receiving ustekinumab 90 mg were combined into one group. **A**, Changes from baseline (week 0) to weeks 4 and 24 in CRP, IL-17A, and IL-17F levels in patients in the PSUMMIT 1 trial. **B**, Changes from baseline to weeks 4 and 24 in CRP level and from baseline to week 4 in IL-17A and IL-17F levels in patients in the PSUMMIT 2 trial. Data are shown as box plots. Each box represents the upper and lower interquartile range. Lines inside the boxes represent the median. Whiskers represent the range. Symbols inside the boxes represent the mean. See Supplementary Table 4, available on the *Arthritis & Rheumatology* web site at http://onlinelibrary.wiley.com/doi/10.1002/art.40921/abstract, for sample sizes. * = $P < 0.05$ versus 0 (no change) in the same response group at the indicated time point; † = $P < 0.05$ versus ACR20 nonresponders at the same time point. See Figure 1 for other definitions.

PSUMMIT 1 study only (40% versus 24% decrease; $P < 0.05$) (Figure 5). Changes in serum levels of IL-17A and IL-17F were not associated with ACR20 response to ustekinumab in either study (Figure 5).

DISCUSSION

The results presented herein have clinical and drug development implications. While serum IL-17A, IL-17F, and IL-23

levels correlated with baseline severity of skin disease, they did not correlate with clinical assessments of joint disease in patients with active PsA. Neither baseline IL-17A, IL-17F, nor CRP levels predicted response to ustekinumab therapy in the skin or joints, despite rapid reductions (within 4 weeks) in IL-17A, IL-17F, and CRP levels following ustekinumab therapy. Responders to ustekinumab (those in whom a PASI75 or ACR20 response was achieved) had a significant reduction in CRP level at week 24 compared to nonresponders (those in whom a PASI50 or ACR20 response was not achieved), but not in IL-17A or IL-17F levels.

A stronger correlation of IL-23/IL-17 levels with the severity of skin disease is consistent with the emerging evidence base suggesting tissue-specific variations in the pathologic drivers within PsA. Recent pathogenesis and therapeutic studies indicate a dominant role for IL-17–related pathways in the skin in psoriatic disease (6–12). In contrast, the musculoskeletal component of PsA appears more heterogeneous and less clearly defined. Belasco et al (6) reported that while gene expression in PsA synovium was more closely related to gene expression in psoriasis skin lesions than to expression in synovium in other forms of arthritis (including rheumatoid arthritis [RA] and osteoarthritis), PsA synovium and skin gene expression patterns were clearly distinct. Specifically, pathway analysis indicated that the IL-17 gene signature was stronger in the skin than in the synovium in PsA, while TNF and interferon-γ gene signatures were equivalent in both tissue types. However, it should be noted that demonstrating clinical relevance and plausible effector function of an inflammatory pathway does not always translate into therapeutic outcomes, as demonstrated by the failure or limited success of anti–IL-17 monotherapy studies in RA (13–15).

Many immune cells, both Th17 and innate, are known to release IL-17A and IL-17F in response to IL-23, so the rapid reduction in IL-17A and IL-17F levels following inhibition of IL-12/IL-23 with ustekinumab was not unexpected. However, considering the established pathogenic role of IL-17 in PsA, it was somewhat surprising that response to ustekinumab, in skin and/or joints, did not correlate with either baseline levels or changes in circulating IL-17A or IL-17F. The reasons for this finding are unclear. It may be that the changes in IL-17A and IL-17F levels at a target tissue level (skin and joints) in response to ustekinumab are not reflected in the blood, while inhibition of other members of the IL-17 superfamily beyond IL-17A and IL-17F may play a role in treatment response. However, these data indicate that baseline levels of circulating IL-23, IL-17A, and IL-17F and changes in IL-17A and IL-17F levels are not predictive of clinical response to ustekinumab in PsA and, as such, these cytokines cannot serve as theranostic biomarkers in this setting. One limitation of this study is the lack of data from additional therapeutics, which would indicate whether these results are specific to ustekinumab or apply more generally to IL-23 inhibition. It will be interesting to observe changes in IL-23/IL-17 pathway cytokines in response to agents targeting this pathway via different routes, such as p19 IL-23, IL-17 receptor A, or combined IL-17A and IL-17F inhibition, and how these correlate with clinical outcomes.

Finally, while the biomarkers studied in the PSUMMIT program did not translate into therapeutic utility, it is important that relevant biomarker studies associated with phase III clinical trials are published in order to increase our understanding of this complex disease and further dissect the role of the IL-23/IL-17 pathway.

ACKNOWLEDGMENTS

The authors thank Karen Hayden (Janssen Research and Development) for generation of laboratory data and the participants and investigators who participated in the PSUMMIT clinical studies.

AUTHOR CONTRIBUTIONS

All authors were involved in drafting the article or revising it critically for important intellectual content, and all authors approved the final version to be published. Dr. Sweet had full access to all of the data in the study and takes responsibility for the integrity of the data and the accuracy of the data analysis.

Study conception and design. Dasgupta, McInnes.
Acquisition of data. Dasgupta, Campbell, McInnes.
Analysis and interpretation of data. Siebert, Sweet, McInnes, Loza.

ROLE OF THE STUDY SPONSOR

Authors who are current or former employees of Janssen Research & Development, LLC were involved in the study design and in the collection, analysis, and interpretation of the data, the writing of the manuscript, and the decision to submit the manuscript for publication. All authors approved the manuscript for submission. Publication of this article was contingent upon approval by Janssen Research and Development.

REFERENCES

1. Alinaghi F, Calov M, Kristensen LE, Gladman DD, Coates LC, Jullien D, et al. Prevalence of psoriatic arthritis in patients with psoriasis: a systematic review and meta-analysis of observational and clinical studies. J Am Acad Dermatol 2019;80:251–65.
2. McInnes IB, Kavanaugh A, Gottlieb AB, Puig L, Rahman P, Ritchlin C, et al. Efficacy and safety of ustekinumab in patients with active psoriatic arthritis: 1 year results of the phase 3, multicentre, double-blind, placebo-controlled PSUMMIT 1 trial. Lancet 2013;382:780–9.
3. Ritchlin C, Rahman P, Kavanaugh A, McInnes IB, Puig L, Li S, et al. Efficacy and safety of the anti-IL-12/23 p40 monoclonal antibody, ustekinumab, in patients with active psoriatic arthritis despite conventional non-biological and biological anti-tumour necrosis factor therapy: 6-month and 1-year results of the phase 3, multicentre, double-blind, placebo-controlled, randomised PSUMMIT 2 trial. Ann Rheum Dis 2014;73:990–9.
4. Kavanaugh A, Ritchlin C, Rahman P, Puig L, Gottlieb AB, Li S, et al. Ustekinumab, an anti-IL-12/23 p40 monoclonal antibody, inhibits radiographic progression in patients with active psoriatic arthritis: results of an integrated analysis of radiographic data from the phase 3, multicentre, randomised, double-blind, placebo-controlled PSUMMIT-1 and PSUMMIT-2 trials. Ann Rheum Dis 2014;73:1000–6.
5. Rahman P, Puig L, Gottlieb AB, Kavanaugh A, McInnes IB, Ritchlin C, et al. Ustekinumab treatment and improvement of physical function and health-related quality of life in patients with psoriatic arthritis. Arthritis Care Res (Hoboken) 2016;68:1812–22.

6. Belasco J, Louie JS, Gulati N, Wei N, Nograles K, Fuentes-Duculan J, et al. Comparative genomic profiling of synovium versus skin lesions in psoriatic arthritis. Arthritis Rheumatol 2015;67:934–44.
7. Chiricozzi A, Guttman-Yassky E, Suárez-Fariñas M, Nograles KE, Tian S, Cardinale I, et al. Integrative responses to IL-17 and TNF-α in human keratinocytes account for key inflammatory pathogenic circuits in psoriasis. J Invest Dermatol 2011;131:677–87.
8. Langley RG, Elewski BE, Lebwohl M, Reich K, Griffiths CE, Papp K, et al. Secukinumab in plaque psoriasis: results of two phase 3 trials. N Engl J Med 2014;371:326–38.
9. Griffiths CE, Reich K, Lebwohl M, van de Kerkhof P, Paul C, Menter A, et al. Comparison of ixekizumab with etanercept or placebo in moderate-to-severe psoriasis (UNCOVER-2 and UNCOVER-3): results from two phase 3 randomised trials. Lancet 2015;386:541–51.
10. Griffiths CE, Strober BE, van de Kerkhof P, Ho V, Fidelus-Gort R, Yeilding N, et al, for the ACCEPT Study Group. Comparison of ustekinumab and etanercept for moderate-to-severe psoriasis. N Engl J Med 2010;362:118–28.
11. Blauvelt A, Papp KA, Griffiths CE, Randazzo B, Wasfi Y, Shen YK, et al. Efficacy and safety of guselkumab, an anti-interleukin-23 monoclonal antibody, compared with adalimumab for the continuous treatment of patients with moderate to severe psoriasis: results from the phase III, double-blinded, placebo- and active comparator-controlled VOYAGE 1 trial. J Am Acad Dermatol 2017;76:405–17.
12. Reich K, Armstrong AW, Foley P, Song M, Wasfi Y, Randazzo B, et al. Efficacy and safety of guselkumab, an anti-interleukin-23 monoclonal antibody, compared with adalimumab for the treatment of patients with moderate to severe psoriasis with randomized withdrawal and retreatment: results from the phase III, double-blind, placebo- and active comparator-controlled VOYAGE 2 trial. J Am Acad Dermatol 2017;76:418–31.
13. Genovese MC, Durez P, Richards HB, Supronik J, Dokoupilova E, Mazurov V, et al. Efficacy and safety of secukinumab in patients with rheumatoid arthritis: a phase II, dose-finding, double-blind, randomised, placebo controlled study. Ann Rheum Dis 2013;72:863–9.
14. Pavelka K, Chon Y, Newmark R, Lin SL, Baumgartner S, Erondu N. A study to evaluate the safety, tolerability, and efficacy of brodalumab in subjects with rheumatoid arthritis and an inadequate response to methotrexate. J Rheumatol 2015;42:912–9.
15. Blanco FJ, Möricke R, Dokoupilova E, Codding C, Neal J, Andersson M, et al. Secukinumab in active rheumatoid arthritis: a phase III randomized, double-blind, active comparator– and placebo-controlled study. Arthritis Rheumatol 2017;69:1144–53.

American College of Rheumatology
Empowering Rheumatology Professionals

Arthritis & Rheumatology
Vol. 71, No. 10, October 2019, pp 1670–1680
DOI 10.1002/art.40932

Rituximab as Maintenance Treatment for Systemic Lupus Erythematosus: A Multicenter Observational Study of 147 Patients

Matthias A. Cassia,[1] Federico Alberici,[1] Rachel B. Jones,[2] Rona M. Smith,[2] Giovanni Casazza,[3] Maria L. Urban,[4] Giacomo Emmi,[4] Gabriella Moroni,[5] Renato A. Sinico,[6] Piergiorgio Messa,[7] Frances Hall,[8] Augusto Vaglio,[4] Maurizio Gallieni,[9] and David R. Jayne[2]

Objective. The efficacy of rituximab (RTX) in systemic lupus erythematosus (SLE) is a subject of debate. This study was undertaken to investigate the outcomes of RTX treatment in a European SLE cohort, with an emphasis on the role of RTX as a maintenance agent.

Methods. All patients with SLE who were receiving RTX as induction therapy in 4 centers were included. Patients who received a single course of RTX and those who received RTX maintenance treatment (RMT) were followed up after treatment. Disease flares during the follow-up period were defined as an increase in disease activity and the number or dose of immunosuppressive drugs.

Results. Of 147 patients, 27% experienced treatment failure at 6 months. In a multivariate analysis, a low number of previous immunosuppressive therapies ($P = 0.034$) and low C4 levels ($P = 0.008$) reduced the risk of treatment failure. Eighty patients received RMT over a median of 24.5 months during which 85 relapses, mainly musculoskeletal, were recorded (1.06 per patient). At the time of the last RTX course, 84% of the patients were in remission. Twenty-eight (35%) of 80 patients never experienced a flare during RMT and had low damage accrual. Active articular disease at the time of the first RTX administration was associated with a risk of flare during RMT ($P = 0.011$). After RMT, relapse-free survival was similar to that in patients receiving a single RTX course ($P = 0.72$).

Conclusion. RMT is a potential treatment option for patients with difficult-to-treat disease. Relapses occur during RMT and are more likely in those with active articular disease at the time of the first RTX administration. Relapse risk after RMT remains high and apparently comparable to that seen after a single RTX course.

INTRODUCTION

Systemic lupus erythematosus (SLE) is an autoimmune disease characterized by clinical variability and complex pathogenesis (1,2). B cell–depleting strategies have received continued attention in SLE (1) and, although rituximab (RTX) has proven effective in other autoimmune diseases characterized by hyperactivity of the B cell compartment (3), randomized controlled trials (RCTs) of RTX in SLE (4,5) have failed to meet their primary end points.

Sustained remission, although infrequently achieved, is the goal of disease management (6). Improving the management of the maintenance phase of SLE is therefore an unmet need (7), and newer therapeutic options are needed. RTX is frequently used in relapsing and refractory cases (8), and its use is supported by retrospective and prospective nonrandomized studies (1).

Supported by travel grants from the patients' group Associazione Malattie Autoimmuni Mario Rossi ONLUS.

[1]Matthias A. Cassia, MD, Federico Alberici, MD, PhD: ASST Santi Paolo e Carlo and the University of Milan, Milan, Italy; [2]Rachel B. Jones, MD, Rona M. Smith, MD, David R. Jayne, MD: University of Cambridge, Cambridge, UK; [3]Giovanni Casazza, PhD: University of Milan, Milan, Italy; [4]Maria L. Urban, MD, Giacomo Emmi, MD, PhD, Augusto Vaglio, MD, PhD: University of Florence, Florence, Italy; [5]Gabriella Moroni, MD: Fondazione IRCCS Ca' Granda Ospedale Maggiore di Milan, Milan, Italy; [6]Renato A. Sinico, MD: University of Milan Bicocca, Milan, Italy; [7]Piergiorgio Messa, MD: Fondazione IRCCS Ca' Granda Ospedale Maggiore di Milan and University of Milan, Milan, Italy; [8]Frances Hall, MD: Cambridge University Hospital, Cambridge, UK; [9]Maurizio Gallieni, MD: University of Milan and ASST Fatebenefratelli Sacco, Milan, Italy.

Drs. Cassia and Alberici contributed equally to this work.

Dr. Jones has received consulting fees from ChemoCentryx (less than $10,000) and research support from GlaxoSmithKline. Dr. Smith has received speaking fees from Roche (less than $10,000). Dr. Emmi has received consulting fees, speaking fees, and/or honoraria from Novartis, Sobi, Takeda (Baxalta), and GlaxoSmithKline (less than $10,000 each). Dr. Sinico has received speaking fees from Roche (less than $10,000). Dr. Jayne has received consulting fees from AstraZeneca, Boehringer Ingelheim, ChemoCentryx, InflaRx, Insmed, and Takeda (less than $10,000 each) and research support from ChemoCentryx, GlaxoSmithKline, Roche/Genentech, and Genzyme/Sanofi. No other disclosures relevant to this article were reported.

Address correspondence to Federico Alberici, MD, PhD, University of Milan, ASST Santi Paolo e Carlo, San Carlo Borromeo Hospital, 20153 Milan, Italy. E-mail: federico.alberici@gmail.com.

Submitted for publication November 20, 2018; accepted in revised form May 14, 2019.

The discrepancy between the results of RCTs and those observed in real-life settings suggests that solid predictors of response to RTX need to be identified in order to better tailor treatment strategies. Clinical predictors of response to RTX in SLE have been investigated, with heterogeneous results across different cohorts (9). Severe disease, lack of hematologic involvement, or previous treatment with high-dose steroids were associated with a good response in 116 patients (10); younger age and achievement of B cell depletion 6 weeks after treatment with RTX were other favorable characteristics in a different population of 117 patients (11). Among biomarkers, the proportion of plasmablasts 6 months after RTX treatment (11) and a single-nucleotide polymorphism in the *IL2/IL21* area have been associated with response (12). The former has been replicated in 2 different cohorts, while the latter, although it has a strong biologic rationale (13), has so far been replicated only in a cohort of patients with microscopic polyangiitis (14).

Importantly, in RTX-treated patients time to relapse is highly variable (15,16). Relapses are associated with the risk of damage accrual and therefore attention should be focused on flare prevention aiming at the right balance between immunosuppressive drug dosing, risk of toxicity, and disease activity. RTX has a proven role as a maintenance agent in other autoimmune diseases (3), while in SLE, there are few published studies of repeat-dose RTX (17–21). Of note, the cohorts in those studies were small, the number of cycles was low, and the indications for repeating the treatment were heterogeneous, while no study has so far explored the use of RTX as maintenance treatment with the aim of relapse prevention.

In this study, we explore the efficacy and safety of RTX in a cohort of 147 patients with SLE with an emphasis on the subgroup of 80 patients who were re-treated with the drug as a maintenance agent in order to prevent relapses; prognostic factors associated with the response to RTX were also investigated.

PATIENTS AND METHODS

Patients. Data on all patients with a diagnosis of SLE according to the American College of Rheumatology (ACR) or Systemic Lupus International Collaborating Clinics (SLICC) criteria (22,23) who received ≥1 administration of RTX between 2004 and 2016 were collected retrospectively at 4 centers (Addenbrooke's Hospital [Cambridge UK], ASST Santi Paolo e Carlo–San Carlo Borromeo Hospital [Milan, Italy], Policlinico Hospital [Milan, Italy], and Careggi Hospital [Florence, Italy]). Ethics approval was obtained only at the Italian centers; it was not required in the UK center due to the retrospective nature of the work.

Treatment protocol. Patients received either a single RTX course or RTX maintenance treatment (RMT). A single RTX course was any RTX dosing performed within a single month, such as 2 doses of 1 gm each, given 2 weeks apart, or 4 doses of 375 mg/m^2 each, administered once a week for 4 consecutive weeks. Patients who received at least 3 single RTX courses with the aim of relapse prevention and with an interval of 4–8 months between consecutive treatments were classified as receiving RMT. Patients receiving RTX courses that did not meet this definition were censored at the time of re-treatment. Treatment associated with RTX administration and data collected during the follow-up period are reported in the Supplementary Methods, available on the *Arthritis & Rheumatology* web site at http://onlinelibrary.wiley.com/doi/10.1002/art.40932/abstract. This was a retrospective study; therefore, no clear indications for treatment selection or RTX treatment schedule within the maintenance treatment group were provided. Treatment decisions were made by the individual physician.

Assessments of disease severity and response to RTX. Disease activity was assessed using the European Consensus Lupus Activity Measure (ECLAM) score (24), which has been validated for retrospective studies (25), and the physician assessment of disease activity. The type and dose of immunosuppressive therapies was also recorded. The physician assessment of disease activity was scored on a scale of 0–2, where 0 = no signs of active SLE, 1 = mild disease activity, and 2 = severe disease activity.

After 6 months, response to the first RTX course was assessed. A complete response was defined as a physician assessment of disease activity score of 0 or 1, a reduction in the ECLAM score of ≥50%, and a decrease in the dose of immunomodulating agents (including glucocorticoids or immunosuppressants but not antimalarials) of ≥25% from baseline. A partial response was defined as a physician assessment of disease activity score of >0, a reduction in the ECLAM score of 25–50%, and a decrease in the dose of immunomodulating agents of 0–25%. Any other response was defined as a treatment failure. A disease flare during or after RMT as well as after a single RTX course was defined as an increase in at least 2 of the 3 parameters (physician assessment of disease activity, ECLAM score, and number or dose of immunosuppressive agents or glucocorticoids).

Patients were stratified into the following 4 groups according to disease severity: mild, moderate, severe, and drug sparing. The first 3 groups were defined according to the British Society of Rheumatology guidelines (8). The group "drug sparing" included patients with mild or moderate disease to whom RTX was administered with the aim of sparing an ongoing immunosuppressive agent or avoiding an alternative immunosuppressant that was contraindicated in the patient.

The definition of late-onset neutropenia and damage assessment methods are discussed in the Supplementary Methods, available on the *Arthritis & Rheumatology* web site at http://onlinelibrary.wiley.com/doi/10.1002/art.40932/abstract.

Statistical analysis. Statistical analysis was performed using R software (https://www.r-project.org), GraphPad Prism 7, and SAS statistical software (version 9.4; SAS Institute). Results are expressed as the number and percentage for

categorical variables and the median (interquartile range [IQR]) or mean (95% confidence interval [95% CI]) for continuous variables. Methods for comparison of changes in variables and proportions of patients as well as for univariate and multiple logistic regression are listed in the Supplementary Methods. Time to relapse was assessed by Kaplan-Meier survival analysis, and if comparisons between populations were required, the log rank test was used. *P* values less than 0.05 (2-tailed) were considered significant.

RESULTS

Outcome after the first RTX course. The clinical characteristics at the time of the first RTX administration for the whole cohort are shown in Table 1. The mean number of previous immunosuppressive drugs received by patients with mild, moderate, and severe disease and those in the drug-sparing group were 2.92 (95% CI 2.38–3.46), 2.74 (95% CI 1.84–3.64), 2.38 (95% CI 2.04–2.72), and 2.42 (95% CI 1.97–2.87), respectively.

Six months after the first RTX administration, 67 (45%) of the 147 patients had a complete response to therapy and 41 (28%) had a partial response, while 39 (27%) experienced treatment failure. The mean ECLAM score declined from 4 at baseline (95% CI 3.65–4.34) to 1.9 at 6 months (95% CI 1.66–2.14) ($P < 0.0001$); the prednisolone dosage declined from a mean of 15.4 mg/day (95% CI 13.1–17.7) to 8.45 mg/day (95% CI 7.29–9.61) ($P < 0.0001$). In the 4 groups of mild, moderate, and severe

Table 1. Main characteristics of the 147 SLE patients treated with RTX*

	RMT (n = 80)	Single course of RTX (n = 67)	Overall cohort (n = 147)
Age, mean (95% CI) years	45 (42–48)	42 (39–46)	44 (41–46)
Sex, female	71 (89)	63 (94)	134 (91)
Ethnicity, white	74 (93)	62 (93)	136 (93)
Prior disease duration, mean (95% CI) months	154 (100–208)	114 (87–141)	133 (104–161)
RTX given at the time of diagnosis	3 (4)	4 (6)	7 (5)
Organ manifestations at first RTX administration			
Musculoskeletal	52 (65)	35 (53)	87 (59)
Skin	49 (61)	31 (46)	80 (54)
Hematologic	26 (33)	37 (55)	63 (43)
Pulmonary	18 (23)	6 (9)	24 (16)
Renal	15 (19)	37 (55)	52 (36)
Neurologic	14 (18)	8 (12)	22 (15)
Previous therapies			
Mycophenolate mofetil	67 (84)	42 (63)	109 (74)
Hydroxychloroquine	61 (76)	38 (57)	99 (67)
Azathioprine	41 (51)	26 (39)	67 (46)
Methotrexate	26 (33)	13 (19)	39 (27)
Cyclophosphamide	24 (30)	21 (31)	45 (31)
Rituximab	14 (18)	12 (18)	26 (18)
Calcineurin inhibitor	11 (14)	24 (36)	35 (24)
Anti-TNF therapy	6 (8)	3 (4)	9 (6)
Plasma exchange	4 (5)	2 (3)	6 (4)
IV immunoglobulins	4 (5)	6 (9)	10 (7)
Other	10 (13)	9 (13)	19 (13)
No. of previous immunosuppressive therapies, mean (95% CI)†	4.3 (4–4.7)	3.9 (3.5–4.4)	4.1 (3.9–4.4)
Disease severity			
Mild	20 (25)	4 (6)	24 (16)
Moderate	6 (7)	17 (25)	23 (16)
Severe	40 (50)	34 (51)	74 (50)
Drug sparing	14 (18)	12 (18)	26 (18)
Laboratory findings, mean (95% CI)			
Anti-DNA level, IU/ml	67.2 (31.9–104.5)	75.4 (39–111.5)	71 (46–96)
C3, gm/liter	1.1 (1.02–1.21)	0.85 (0.75–94)	1 (0.92–1.07)
C4, gm/liter	0.2 (0.18–0.24)	0.15 (0.12–0.18)	0.18 (0.16–0.2)
Response to RTX at 6 months			
Complete response	32 (40)	35 (52)	67 (45)
Partial response	21 (26)	20 (30)	41 (28)
Treatment failure	27 (34)	12 (18)	39 (27)

* Except where indicated otherwise, values are the number (%). SLE = systemic lupus erythematosus; RTX = rituximab; RMT = RTX maintenance treatment; 95% CI = 95% confidence interval; anti-TNF = anti–tumor necrosis factor; IV = intravenous.
† Including hydroxychloroquine.

disease and drug-sparing, the proportion of patients experiencing treatment failure at 6 months was 65%, 50%, 25%, and 6%, respectively.

In a multivariate analysis, adjusted for the confounding factors number of other immunosuppressive drugs administered and prednisolone dose, the characteristics associated with the risk of experiencing treatment failure were higher C4 levels (odds ratio [OR] 1.76 [95% CI 1.15–2.7], $P = 0.008$) and a greater number of previous immunosuppressive agents received (OR 7.77 [95% CI 1.65–36.6], $P = 0.034$) (Supplementary Table 1, available on the *Arthritis & Rheumatology* web site at http://onlinelibrary.wiley.com/doi/10.1002/art.40932/abstract).

RTX maintenance treatment. Eighty (54%) of the 147 patients received RMT; their characteristics are summarized in Table 1. The median duration of maintenance treatment was 24.5 months (IQR 16–34 months; range 11–99 months), the median cumulative RTX dose was 6 gm (IQR 4.87–9), and the median overall follow-up time was 38 months (IQR 22–54 months). At the time of the first RTX administration, 69 (86%) of the 80 patients were receiving a mean oral prednisolone dosage of 11 mg/day (95% CI 9–13) and 46 (57%) were receiving an immunosuppressive drug (not including hydroxychloroquine). These immunosuppressive drugs included mycophenolate mofetil (n = 28), methotrexate (n = 6), azathioprine (n = 4), cyclophosphamide (n = 4), calcineurin inhibitors (n = 4), intravenous immunoglobulin (n = 3), and other treatments (n = 4). The mean ECLAM score at the first RTX administration was 3.5 (95% CI 3.06–3.93), and the mean number of previous immunosuppressive drugs received by patients in the groups mild disease, moderate disease, severe disease, and drug-sparing was 3.05 (95% CI 2.28–3.82), 3.67 (95% CI 2.7–4.64), 2.42 (95% CI 2.06–2.78), and 2.14 (95% CI 1.64–2.64), respectively. The different protocols used for RTX administration within the RMT group are described in the Supplementary Methods.

After 6 months the mean ECLAM score declined to 1.86 (95% CI 1.52–2.19) ($P < 0.0001$), with a trend toward further reduction/stabilization during maintenance treatment (Figure 1A). At the 6-month assessment 30 (38%) of the 80 patients had a complete response to treatment, and this proportion increased to 40%, 51%, and 48% at the 12-, 18-, and 24-month assessments. The proportion of patients not taking glucocorticoids increased from 14% to 41%, while the mean prednisolone dosage dropped from 11 mg/day at RTX initiation (95% CI 8.9–13) to 3.8 mg/day by the sixth administration (95% CI 1.1–6.4). A trend toward a reduction in the proportion of patients receiving other immunosuppressive drugs was also observed (Figure 1B).

Of the 80 patients receiving RMT, 52 (65%) experienced 85 relapses (1.06 relapses per patient, 53 per 100 patient-years) after a median of 11.5 months (IQR 8–18.25 months). Relapses were more frequent from month 6 to month 12 after the first RTX administration (Supplementary Table 2, available on the *Arthritis & Rheumatology* web site at http://onlinelibrary.wiley.com/doi/10.1002/art.40932/abstract) and more frequently involved the joints (66%) and skin (40%) (Supplementary Table 3, available on the *Arthritis & Rheumatology* web site at http://onlinelibrary.wiley.com/doi/10.1002/art.40932/abstract). At the time of flare, the mean ECLAM score was 2.72 (95% CI 2.42–3.03), and the mean increase in ECLAM score compared to the previous assessment was 1.42 (95% CI 1.11–1.74). Relapses were managed with an increase in prednisolone dosage in 29 (34%) of 85 cases (mean

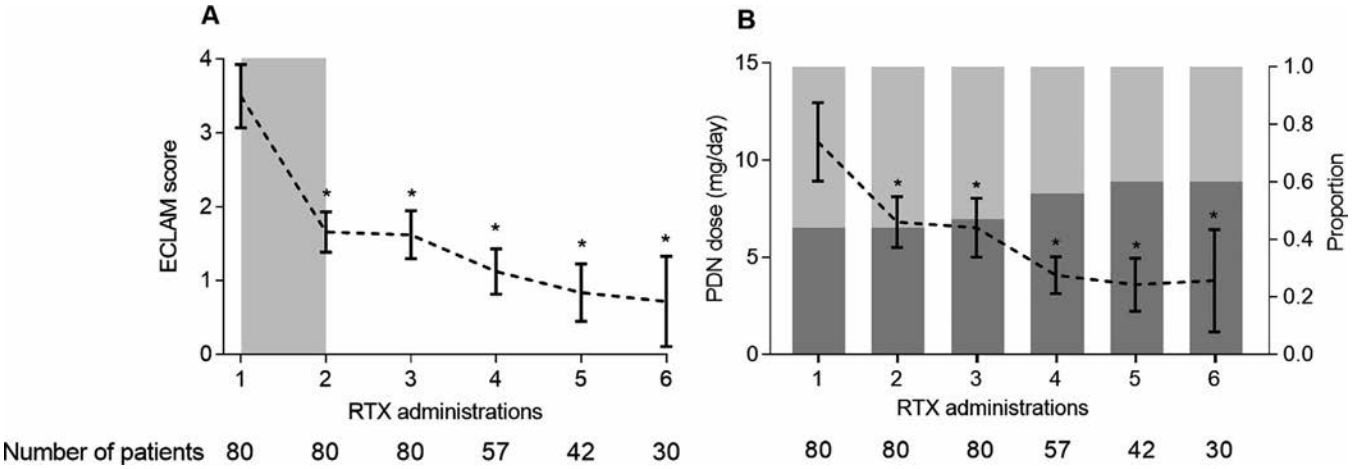

Figure 1. Changes in the European Consensus Lupus Activity Measure (ECLAM) score, prednisolone (PDN) dosage, and immunosuppressive treatment in the 80 patients with systemic lupus erythematosus (SLE) who received maintenance treatment with rituximab (RTX) for relapse prevention. **A**, ECLAM score for the patients with SLE at the time of each RTX administration. Values are the mean and 95% confidence interval. The shaded area represents follow-up after the first RTX administration. **B**, PDN dosage at each RTX administration. Values are the mean and 95% confidence interval. Bars show the proportion of patients who were receiving (light gray) or not receiving (dark gray) other immunosuppressive drugs at the indicated time points. * = $P < 0.05$ versus baseline.

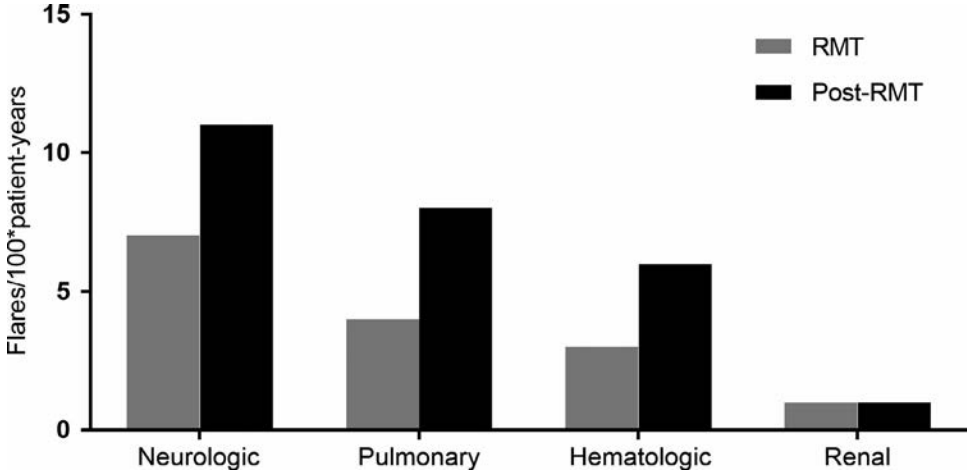

Figure 2. Major organ involvement at the time of flare in patients with systemic lupus erythematosus during and after rituximab maintenance treatment (RMT). Bars show the rate of flares per 100 patient-years.

increase 11.1 mg [95% CI 6.9–15.4]), with a new immunosuppressive drug in 22 (26%), and with an increase in the dose of an ongoing immunosuppressive drug in 12 (14%). In 7 cases (8%), the flare was managed by administering the preplanned RTX infusion earlier than intended, while in 15 (18%) the flare was managed by waiting for the preplanned RTX infusion.

At the time of the last RTX administration, 67 (84%) of the 80 patients were in remission, the mean ECLAM score was 1.5 (95% CI 1.13–1.86), and the mean prednisolone dosage was 6.35 mg/day (95% CI 4.8–7.9).

Outcome after the last RTX infusion. Of the 67 patients who received a single course of RTX, 54 (80%) experienced a complete or partial response by the 6-month assessment and were therefore followed up for posttherapy flare. The median follow-up time after the 6-month assessment was 7.3 months (IQR 3.46–9.78 months). Eighteen (33%) of the patients experienced a disease flare (51.5 flares per 100 patient-years). The mean ECLAM score for the patients who experienced a flare was 2.94 (95% CI 1.97–3.91). The sites showing active disease and the strategies used for flare management are listed in Supplementary Table 4, available on the *Arthritis & Rheumatology* web site at http://onlinelibrary.wiley.com/doi/10.1002/art.40932/abstract. Of the 80 patients receiving RMT, posttreatment follow-up data were available for 57 (71%). The median follow-up time after the last RTX administration was 13 months (IQR 4–22 months). Thirty (53%) of the patients experienced a disease flare (38 flares per 100 patient-years). The mean ECLAM score for patients who experienced a flare was 3.09 (95% CI 2.6–3.58). The sites showing active disease and the strategies used for flare management are listed in Supplementary Table 4.

The rate of flares involving major organs during RMT was 38%; this rate increased to 67% when RMT was discontinued (P = 0.01). In particular, the rate of flares per 100 patient-years

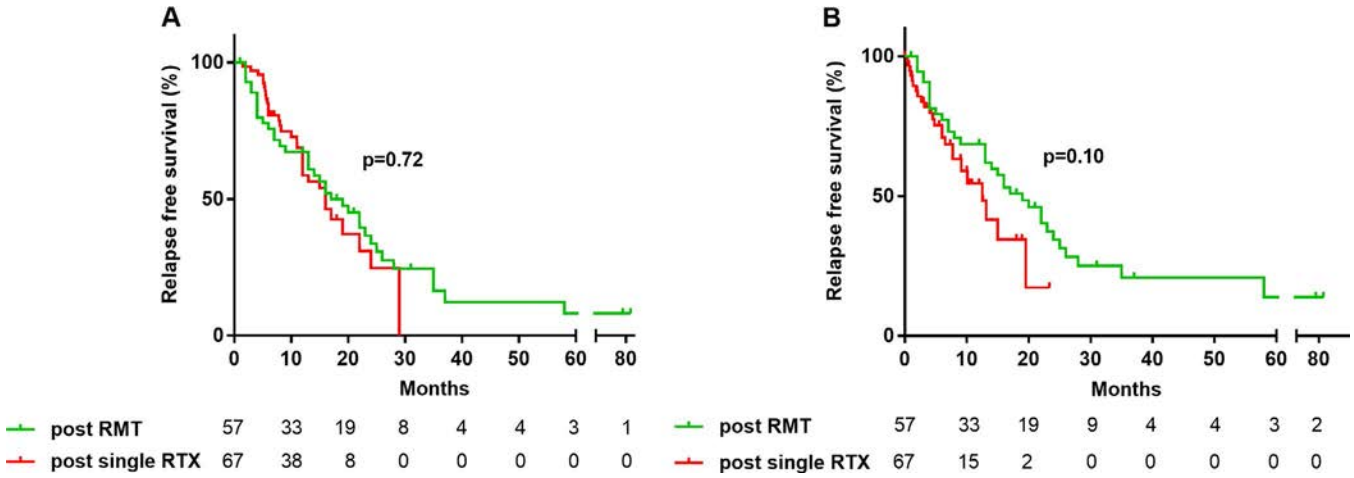

Figure 3. Relapse-free survival in the overall population (**A**) and including only nonmusculoskeletal flares (**B**) after the last rituximab (RTX) administration in patients with systemic lupus erythematosus (SLE) who received RTX maintenance treatment (RMT) and patients with SLE who received a single course of RTX.

increased after RMT compared to during RMT for the neurologic, pulmonary, and hematologic systems, while the rate of renal flares remained stable (Figure 2). Of note, the adjusted number of flares per number of patients at risk remained roughly stable during the follow-up period (see Supplementary Table 5, available on the *Arthritis & Rheumatology* web site at http://onlinelibrary.wiley.com/doi/10.1002/art.40932/abstract).

The median relapse-free survival time after the last RTX infusion was 16 months in the cohort treated with a single course of RTX (IQR 1.2–9 months) and 17 months in the RMT cohort (IQR 4–22 months) (P = 0.72) (Figure 3A). A trend toward a longer relapse-free survival time for the RMT cohort was noted when only nonmusculoskeletal flares were considered, although the difference was not significant (P = 0.10) (Figure 3B).

Sustained responders. Among the 80 patients in the RMT cohort, 28 (35%) did not experience any flares during the maintenance period and were classified as "sustained responders." In a multivariate analysis comparing the sustained responders to those with ≥1 flare, the presence of active articular disease at the time of the first RTX administration was associated with the risk of flare (OR 3.55 [95% CI 1.34–9.37], P = 0.011) (Table 2) even after adjustment of the analyses for disease severity as a potential a priori confounder (OR 3.38 [95% CI 1.25–9.11], P = 0.016).

Post-RMT follow-up data were available for 21 (75%) of the 28 sustained responders. The median follow-up time was 17.5 months (IQR 5.3–23.8 months). Ten (48%) of the 21 patients experienced a flare (27 flares per 100 patient-years). The mean ECLAM score for patients who experienced a flare was 2.45 (95% CI 1.64–3.27). The sites showing active disease at the time of the flare were joints in 5 patients (50%), hematologic system in 4 (40%), renal sites in 2 (20%), central nervous system sites in 2 (20%), and the skin in 1 (10%). Flares were managed by increasing the prednisolone dose in 4 cases (40%), starting a new immunosuppressive drug in 4 (40%), and increasing the dose of an ongoing immunosuppressive drug in 1 (10%). No treatment changes were recorded for 3 patients (30%).

Severe adverse events (SAEs). During the follow-up period, 109 SAEs occurred in 54 patients, with a rate of 30 SAEs per 100 patient-years; in the RMT subgroup the rate was 24, while in the single-course RTX subgroup it was 53

Table 2. Univariate and multivariate analyses of the association between clinical characteristics and the risk of experiencing at least 1 flare during RMT for SLE*

Variable	Univariate analysis		Multivariate analysis	
	OR (95% CI)	*P*	OR (95% CI)	*P*
Sex		0.150	–	–
Female (reference)	1			
Male	4.8 (0.57–40.5)			
No. of immunosuppressive drugs before RTX		0.650	–	–
0–2 (reference)	1			
3–4	1.51 (0.51–4.46)			
>4	0.93 (0.22–4)			
Physician assessment of disease activity at the first administration of RTX		0.501	–	–
0	1			
1	2.81 (0.39–20.4)			
2	3.08 (0.47–20.23)			
Clinical manifestations at the first administration of RTX				
Systemic	2.00 (0.77–5.16)	0.150	–	–
Articular	3.55 (1.34–9.37)	0.011†	3.55 (1.34–9.37)	0.011†
Skin	2.67 (1.04–6.87)	0.042†	–	–
Muscle	0.51 (0.07–3.83)	0.512	–	–
Pulmonary	1.65 (0.53–5.18)	0.390	–	–
CNS	2.18 (0.55–8.58)	0.264	–	–
Renal	0.56 (0.18–1.754)	0.316	–	–
Hematologic	0.64 (0.24–1.70)	0.373	–	–
ECLAM score at the first administration of RTX‡	1.02 (0.80–1.29)	0.887	–	–
Laboratory values at the first administration of RTX				
Anti-DNA titer‡	1.001 (0.997–1.006)	0.615	–	–
C3§	1.02 (0.89–1.17)	0.786	–	–
C4§	1.21 (0.72–2.05)	0.474	–	–
Use of other immunosuppressants with RTX	1 (0.47–2.09)	0.993	–	–
Dose of prednisolone at the first administration of RTX	0.95 (0.91–1.01)	0.079	–	–

* RMT = rituximab maintenance treatment; SLE = systemic lupus erythematosus; 95% CI = 95% confidence interval; RTX = rituximab; CNS = central nervous system; ECLAM = European Consensus Lupus Activity Measure.
† Significant associations.
‡ Odds ratio (OR) with a 1-unit increase in the independent variable.
§ OR with a 0.1-unit increase in the independent variable.

(Supplementary Table 6, available on the *Arthritis & Rheumatology* web site at http://onlinelibrary.wiley.com/doi/10.1002/art.40932/abstract). The incidence of malignant neoplasms was 3% in the overall population and 4% in the RMT group. The cumulative number and the proportions of the different SAEs did not differ between the patients treated with RMT and those treated with a single course of RTX (data not shown).

Sixteen episodes of late-onset neutropenia were recorded during the 452 RTX administrations (4% of administrations) in 9 (11%) of 80 patients, with 4 patients experiencing ≥2 episodes. Ten episodes were grade II neutropenia, 4 were grade III, and 2 were grade IV. In 2 patients the first episode of late-onset neutropenia occurred after the first RTX administration, while in 7 patients the fist episode occurred after one of the subsequent cycles. The median time from the most recent RTX administration to the detection of late-onset neutropenia was 8 months (IQR 5–11 months). Of the 2 patients experiencing grade IV late-onset neutropenia, 1 died of neutropenic sepsis and 1 was admitted for clinical monitoring without experiencing any infection or requiring any specific therapy.

Eleven patients died during the follow-up period, including 2 (3%) of the 67 patients who did not receive RMT and 9 (11.3%) of the 80 patients who did receive RMT. In the latter group 7 died during RMT and 2 after therapy (19 and 35 months after the last RTX infusion). The causes of death are listed in Supplementary Table 7, available on the *Arthritis & Rheumatology* web site at http://onlinelibrary.wiley.com/doi/10.1002/art.40932/abstract).

Damage. At the time of the first RTX administration, the mean SLICC/ACR Damage Index (SDI) score (26) was 1.69 in the overall population (95% CI 1.44–1.94) and 1.8 in the RMT group (95% CI 1.46–2.14). Damage increased during the follow-up period, with a mean SDI at the last available follow-up of 2.14 in the overall population (95% CI 1.83–2.44).

The increase in SDI per patient per year before RTX administration was 0.21, while during RMT it was 0.23; in the sustained responders subgroup, the increase in the SDI per patient per year was 0.17.

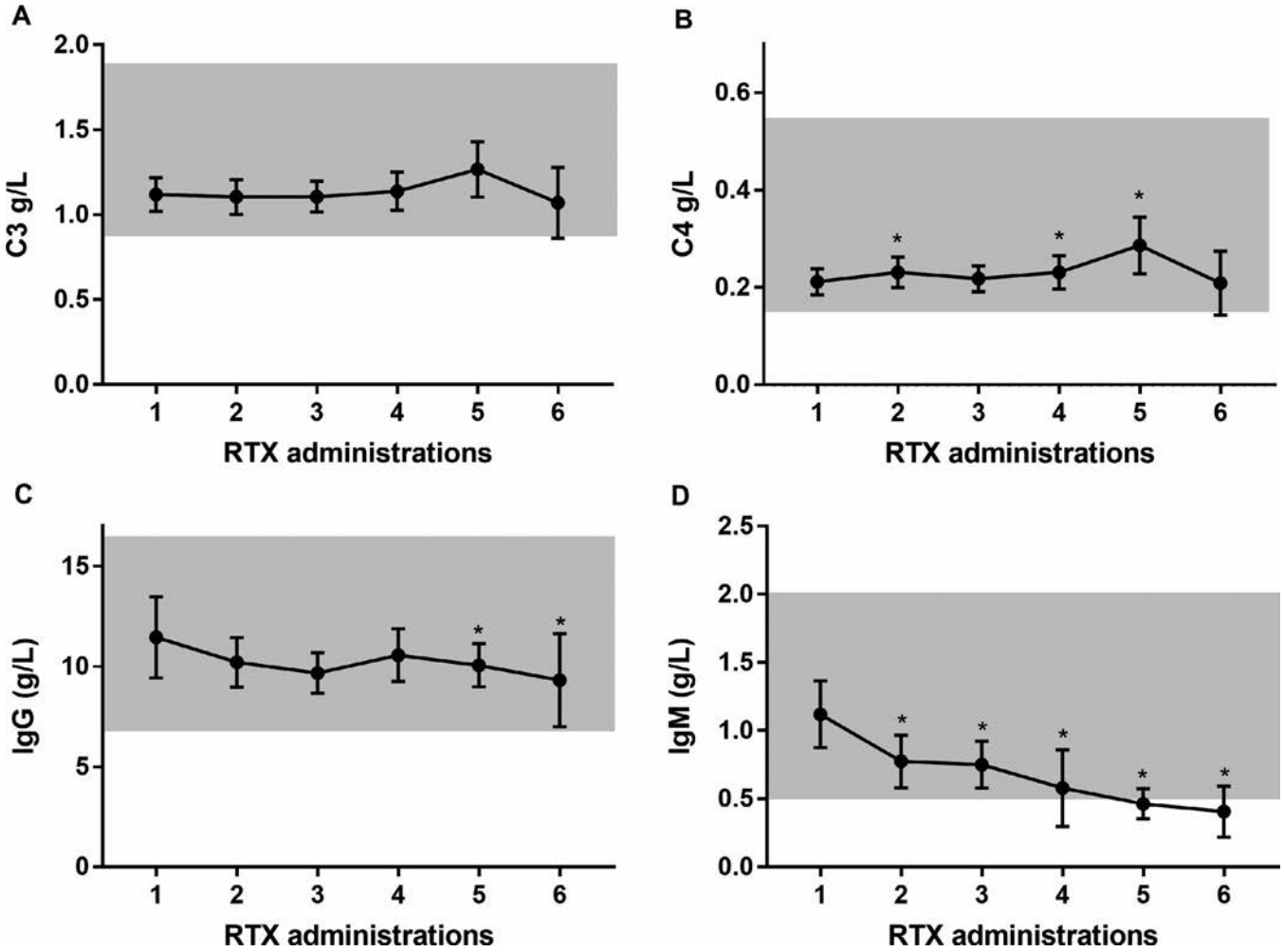

Figure 4. Levels of C3 (**A**), C4 (**B**), IgG (**C**), and IgM (**D**) during follow-up in the cohort of 80 patients with systemic lupus erythematosus (SLE) who received rituximab (RTX) maintenance treatment with the aim of relapse prevention. Values are the mean and 95% confidence interval. The shaded area represents the normal range. * = $P < 0.05$ versus baseline.

Laboratory parameters. During RMT, C3 and C4 levels remained stable if they were normal at the time of the first RTX administration (Figures 4A and B). In the subgroup of patients with reduced levels at the beginning of therapy, the values increased to normal and then stabilized (Supplementary Figure 1, available on the *Arthritis & Rheumatology* web site at http://onlinelibrary.wiley.com/doi/10.1002/art.40932/abstract). IgG levels remained stable during RMT, whereas a trend toward a reduction in IgM levels was noted (Figures 4C and D). Anti-DNA levels assessed by enzyme-linked immunosorbent assay decreased after the first RTX administration to within the normal range and remained stable during RMT (Supplementary Figure 2, available on the *Arthritis & Rheumatology* web site at http://onlinelibrary.wiley.com/doi/10.1002/art.40932/abstract). CD19+ B cells were undetectable in 76% of the patients at the time of the second RTX administration and tended to remain the same during follow-up (Supplementary Figure 3, available on the *Arthritis & Rheumatology* web site at http://onlinelibrary.wiley.com/doi/10.1002/art.40932/abstract).

DISCUSSION

SLE remains a challenging disease characterized by a chronic relapsing course despite the availability of multiple therapies. Although there have been no prospective trials showing the superiority of RTX compared to placebo (4,5), RTX is widely used. Our cohort of 147 patients treated with RTX is one of the largest studied so far (27) and the overall positive response further supports the role of this drug in SLE management. Patients with low C4 levels, those who had received fewer previous immunosuppressive drugs, and those with severe disease were more likely to respond favorably to RTX. This finding suggests that the ideal candidates for RTX may be those with more active disease and without a clear refractory course, which is consistent with the results of other studies (10,11).

Despite the challenges deriving from the management of active SLE, the maintenance phase plays a critical role in the long-term outcome, influencing damage accrual (7). In RTX-treated patients time to relapse is highly variable (15,16), and an RTX-based maintenance treatment at fixed intervals may be attractive. Our study is the first to show that RMT may be an option in SLE. According to our data, during RMT disease activity remains stable over time while allowing for a reduction in the dosage of immunosuppressive drugs; the overall glucocorticoid dose was reduced after the first RTX cycle, and the proportion of patients able to discontinue immunosuppressants at the end of RMT was 41%. However, disease reactivation was common. Flares were generally not severe, mainly involved the musculoskeletal system, and required only minor therapeutic changes. Importantly, during RMT severe flares were rare while these increased when RMT was suspended. In particular, neurologic, pulmonary, and hematologic reactivation doubled.

Interestingly, despite improved disease control with RMT and a reduction in glucocorticoid and immunosuppressive drug dosing, damage accumulated at the same rate as before the RMT phase. Damage in SLE is more likely to increase in patients having already experienced it as well as in those with renal involvement (28); moreover, glucocorticoids may cause late-onset damage (29). Of interest, in a study of 188 patients treated with belimumab in an everyday clinical setting, the damage accrual rate decreased during therapy, although in the context of less severe disease and lower damage at the beginning of therapy than in the present study (mean ± SD SDI 0.85 ± 1.11 compared to 1.8 ± 0.34 in the RMT cohort in the present study) (30). In our RMT cohort, 50% of the patients had severe disease and 20% had active renal disease, with a long disease course and a significant damage burden already recorded at the time of the first RTX administration. In this context further damage progression may not be surprising. It will be of interest to observe whether damage progression also occurs in cohorts treated with RMT but with lower damage at the beginning of therapy, as well as to explore the role of belimumab in damage prevention in patients with a high SDI.

Among the patients treated with RMT in the present study, 35% were classified as sustained responders, since they did not experience any disease reactivation during the maintenance course. This group was characterized by lower damage accumulation compared to the rest of the population and, in multivariate analyses, less frequent articular involvement at the time of the first RTX administration. However, apart from disease severity, no other confounders were considered in the analyses, and this result should therefore be interpreted with caution. No other factors associated with the risk of flares during RMT have been identified, and future studies will need to focus on this particular aspect in patients treated with RMT.

After RMT, relapse-free survival remained the same as that in patients treated with a single course of RTX, even when musculoskeletal flares were excluded. If confirmed, this result would not be consistent with the results of RMT in antineutrophil cytoplasmic antibody–associated vasculitis (31). These data, although of interest, should be interpreted with caution since they are the result of a comparison performed between two heterogeneous, unmatched groups. Moreover, the RMT cohort probably consisted of patients with a more severe disease profile, as suggested by the higher proportion of treatment failure 6 months after the first RTX administration compared to the group receiving a single course of RTX. Importantly, the relapse rate after RMT may have been influenced by the natural course of the disease, which was not adjusted for in our analyses. The role of RMT suspension on post-RMT flares therefore has to be confirmed. However, reassuringly, a clear trend toward an increase in the rate of relapse during follow-up was not identified.

The mortality observed in our cohort is within the high range of what is described in the literature, especially in the RMT group (11.3%). We believe that this may be the consequence of the high-risk profile of this population. Of note, patients with severe comorbidities are usually excluded from RCTs, and the mortality

rate in studies including patients with a similar severity profile is ~8% (32). Reassuringly, cancer risk was similar to that described in the literature.

Importantly, late-onset neutropenia incidence in the RMT group (4% of the RTX administrations in 11% of the patients) was higher than that described in other cohorts of RTX-treated patients with heterogeneous immunologic diseases (2%) (33) but lower than that described in other SLE cohorts (29.9%) (34). Only 2 episodes observed in the RMT group occurred after the first RTX administration, while the remaining 14 were recorded after subsequent administrations, suggesting a possible role of repeat RTX treatments in increasing late-onset neutropenia risk. Four patients experienced 2 or more episodes. Of note, 1 patient in the RMT cohort died of neutropenic sepsis.

Our study was a multicenter, multidisciplinary survey involving a large cohort collected from tertiary care centers with experience in managing SLE. However, when interpreting these results, several observations have to be made. As a retrospective study, some heterogeneity across different centers must be taken into account, as shown by the variability of the treatment protocols during RMT. Only 89% of the population followed a preplanned RTX format of administration, while 9% entered a fixed-interval design within 8 months of the first RTX administration, and 2% were treated irregularly according to changes in symptoms and serologic features. Importantly, 11% of the patients who were supposed to be treated regularly missed at least 1 administration during the first 24 months of treatment. All of these factors, in the context of a highly variable timing of relapse in RTX-treated SLE patients (15,16), may have contributed to the high flare rate observed in our population. Whether this RMT protocol should be considered as a genuine relapse prevention approach rather than repeat induction treatment is unclear, and this will need to be tested in a prospective manner. Importantly, the duration of posttreatment follow-up was relatively short, and the findings of this phase of the study should be interpreted with caution.

Of note, 51 (35%) of the 147 patients had articular and mucocutaneous manifestations as a prominent feature of active SLE at the time of the first RTX administration. All of these patients had previously received glucocorticoids and hydroxychloroquine as well as at least 1 of mycophenolate mofetil, methotrexate (MTX), and azathioprine, with 39% having received 2 of them. Despite the fact that the proportion of patients treated with MTX in our cohort was higher than that in the Study of Belimumab in Subjects with SLE (BLISS) trials (7–21.2%) (35,36), only 50% of the potentially eligible patients with articular disease and 41% of those with mucocutaneous disease in the present study had previously received MTX. This may reflect a more limited experience with this drug of the nephrologists involved in this study as well as safety concerns related to MTX use (37). Moreover, according to the timing of reimbursement approval from the Italian and UK Health Systems, 5% of the patients in our cohort would have been eligible for belimumab but were treated with RTX, which may have been the consequence of a greater experience with RTX of the investigators involved in this study. However, reassuringly, no center effect was noted for RTX, MTX, or belimumab prescription.

The high rate of patients with musculoskeletal and skin involvement may be the reason for the relatively high proportion of patients with mild disease treated with RTX in our population (26%). This group, according to the guidelines of the British Society of Rheumatology (8), should not be treated with RTX. However, it should be noted that for patients with less severe disease, RTX was used in the context of reduced therapeutic options since in this population disease had previously failed to respond to a mean of ~3 immunosuppressive drugs. Another limitation is that for 18% of the patients, a single cycle of RTX had been administered before referral to the centers in this study. At the time of inclusion in our study, however, all of these patients were B cell repopulated. Our population, therefore, might not necessarily reflect that of other centers or current clinical practice, especially since belimumab is more readily available.

The response criteria we used are original and have not been validated. However, the definitions of response in retrospective studies of RTX-treated SLE cohorts have historically been heterogeneous, and the response rates in the present study were consistent with those in the literature (1). Along with the change in a semi-objective score, the ECLAM score, the physician assessment of disease activity was used due to the central role of the physician's judgment in the assessment of a complex disease such as SLE. Reduction in the immunosuppressant dose was also included as part of the response criteria, since in this cohort RTX has frequently been used with the aim of sparing other drugs.

In conclusion, we confirmed in a large, multicenter cohort that RTX may be an option for the treatment of patients with SLE. Its use as maintenance treatment allows glucocorticoid and immunosuppressive drug sparing while stabilizing the overall disease activity. However, it should be noted that musculoskeletal flares were common. Patients without articular involvement at the time of the first RTX administration were less likely to experience relapses during RMT. At the time of drug discontinuation, relapse-free survival remained apparently comparable to that in patients treated with a single course of RTX. An RMT regimen might be considered for patients with severe disease-related complications, for whom waiting for a relapse in order to treat on demand may be risky, and when first-line immunosuppressive options are exhausted.

ACKNOWLEDGMENTS

We gratefully acknowledge Professor Massimiliano Romanelli, Professor Manuela Nebuloni, Professor Giovanna Mantovani, and Professor Nicola Montano (council members of the MD/PhD program of the University of Milan).

AUTHOR CONTRIBUTIONS

All authors were involved in drafting the article or revising it critically for important intellectual content, and all authors approved the final version to be published. Dr. Alberici had full access to all of the data in the study and takes responsibility for the integrity of the data and the accuracy of the data analysis.

Study conception and design. Cassia, Alberici, Jones, Smith, Urban, Emmi, Moroni, Sinico, Messa, Gallieni, Jayne.

Acquisition of data. Cassia, Urban, Emmi, Moroni, Sinico, Hall.

Analysis and interpretation of data. Cassia, Alberici, Casazza, Vaglio, Gallieni, Jayne.

REFERENCES

1. Cassia M, Alberici F, Gallieni M, Jayne D. Lupus nephritis and B-cell targeting therapy. Expert Rev Clin Immunol 2017;13:951–62.
2. Tsokos GC, Lo MS, Costa Reis P, Sullivan KE. New insights into the immunopathogenesis of systemic lupus erythematosus. Nat Rev Rheumatol 2016;12:716–30.
3. Guillevin L, Pagnoux C, Karras A, Khouatra C, Aumaître O, Cohen P, et al. Rituximab versus azathioprine for maintenance in ANCA-associated vasculitis. N Engl J Med 2014;371:1771–80.
4. Rovin BH, Furie R, Latinis K, Looney RJ, Fervenza FC, Sanchez-Guerrero J, et al, for the LUNAR Investigator Group. Efficacy and safety of rituximab in patients with active proliferative lupus nephritis: the Lupus Nephritis Assessment with Rituximab study. Arthritis Rheum 2012;64:1215–26.
5. Merrill JT, Neuwelt CM, Wallace DJ, Shanahan JC, Latinis KM, Oates JC, et al. Efficacy and safety of rituximab in moderately-to-severely active systemic lupus erythematosus: the randomized, double-blind, phase II/III systemic lupus erythematosus evaluation of rituximab trial. Arthritis Rheum 2010;62:222–33.
6. Kim M, Merrill J, Kalunian K, Hahn B, Roach A, Izmirly P, et al. Longitudinal patterns of response to standard of care therapy for systemic lupus erythematosus: implications for clinical trial design. Arthritis Rheumatol 2017;69:785–90.
7. Watson P, Brennan A, Birch H, Fang H, Petri M. An integrated extrapolation of long-term outcomes in systemic lupus erythematosus: analysis and simulation of the Hopkins lupus cohort. Rheumatology (Oxford) 2015;54:623–32.
8. Gordon C, Amissah-Arthur MB, Gayed M, Brown S, Bruce IN, D'Cruz D, et al. The British Society for Rheumatology guideline for the management of systemic lupus erythematosus in adults. Rheumatology (Oxford) 2018;57:e1–45.
9. Pirone C, Mendoza-Pinto C, van der Windt DA, Parker B, O'Sullivan M, Bruce IN. Predictive and prognostic factors influencing outcomes of rituximab therapy in systemic lupus erythematosus (SLE): a systematic review. Semin Arthritis Rheum 2017;47:384–96.
10. Fernández-Nebro A, de la Fuente JL, Carreño L, Izquierdo MG, Tomero E, Rúa-Figueroa I, et al. Multicenter longitudinal study of B-lymphocyte depletion in refractory systemic lupus erythematosus: the LESIMAB study. Lupus 2012;21:1063–76.
11. Md Yusof MY, Shaw D, El-Sherbiny YM, Dunn E, Rawstron AC, Emery P, et al. Predicting and managing primary and secondary non-response to rituximab using B-cell biomarkers in systemic lupus erythematosus. Ann Rheum Dis 2017;76:1829–36.
12. Márquez A, Dávila-Fajardo CL, Robledo G, Rubio JL, de Ramón Garrido E, García-Hernández FJ, et al. IL2/IL21 region polymorphism influences response to rituximab in systemic lupus erythematosus patients. Mol Biol Rep 2013;40:4851–6.
13. Wang S, Wang J, Kumar V, Karnell JL, Naiman B, Gross PS, et al. IL-21 drives expansion and plasma cell differentiation of autoreactive CD11c^{hi}T-bet^{+} B cells in SLE. Nat Commun 2018;9:1758.
14. Alberici F, Smith RM, Fonseca M, Willcocks LC, Jones RB, Holle JU, et al. Association of a TNFSF13B (BAFF) regulatory region single nucleotide polymorphism with response to rituximab in antineutrophil cytoplasmic antibody-associated vasculitis. J Allergy Clin Immunol 2017;139:1684–7.
15. Vital EM, Dass S, Buch MH, Henshaw K, Pease CT, Martin MF, et al. B cell biomarkers of rituximab responses in systemic lupus erythematosus. Arthritis Rheum 2011;63:3038–47.
16. Ng KP, Cambridge G, Leandro MJ, Edwards JC, Ehrenstein M, Isenberg DA. B cell depletion therapy in systemic lupus erythematosus: long-term follow-up and predictors of response. Ann Rheum Dis 2007;66:1259–62.
17. Weide R, Heymanns J, Pandorf A, Köppler H. Successful long-term treatment of systemic lupus erythematosus with rituximab maintenance therapy. Lupus 2003;12:779–82.
18. Turner-Stokes T, Lu TY, Ehrenstein MR, Giles I, Rahman A, Isenberg DA. The efficacy of repeated treatment with B-cell depletion therapy in systemic lupus erythematosus: an evaluation. Rheumatology (Oxford) 2011;50:1401–8.
19. Aguiar R, Araújo C, Martins-Coelho G, Isenberg D. Use of rituximab in systemic lupus erythematosus: a single center experience over 14 years. Arthritis Care Res (Hoboken) 2017;69:257–62.
20. Terrier B, Amoura Z, Ravaud P, Hachulla E, Jouenne R, Combe B, et al. Safety and efficacy of rituximab in systemic lupus erythematosus: results from 136 patients from the French AutoImmunity and Rituximab registry. Arthritis Rheum 2010;62:2458–66.
21. Emmi G, Urban ML, Scalera A, Becatti M, Fiorillo C, Silvestri E, et al. Repeated low-dose courses of rituximab in SLE-associated antiphospholipid syndrome: data from a tertiary dedicated centre. Semin Arthritis Rheum 2017;46:e21–3.
22. Hochberg MC, for the Diagnostic and Therapeutic Criteria Committee of the American College of Rheumatology. Updating the American College of Rheumatology revised criteria for the classification of systemic lupus erythematosus [letter]. Arthritis Rheum 1997;40:1725.
23. Petri M, Orbai AM, Alarcon GS, Gordon C, Merrill JT, Fortin PR, et al. Derivation and validation of the Systemic Lupus International Collaborating Clinics classification criteria for systemic lupus erythematosus. Arthritis Rheum 2012;64:2677–86.
24. Vitali C, Bencivelli W, Isenberg DA, Smolen JS, Snaith ML, Sciuto M, et al. Disease activity in systemic lupus erythematosus: report of the Consensus Study Group of the European Workshop for Rheumatology Research. II. Identification of the variables indicative of disease activity and their use in the development of an activity score. The European Consensus Study Group for Disease Activity in SLE. Clin Exp Rheumatol 1992;10:541–7.
25. Mosca M, Bencivelli W, Vitali C, Carrai P, Neri R, Bombardieri S. The validity of the ECLAM index for the retrospective evaluation of disease activity in systemic lupus erythematosus. Lupus 2000;9:445–50.
26. Gladman D, Ginzler E, Goldsmith C, Fortin P, Liang M, Urowitz M, et al. The development and initial validation of the Systemic Lupus International Collaborating Clinics/American College of Rheumatology Damage Index for systemic lupus erythematosus. Arthritis Rheum 1996;39:363–9.
27. McCarthy EM, Sutton E, Nesbit S, White J, Parker B, Jayne D, et al. Short-term efficacy and safety of rituximab therapy in refractory systemic lupus erythematosus: results from the British Isles Lupus Assessment Group Biologics Register. Rheumatology (Oxford) 2018;57:470–9.
28. Bruce IN, O'Keeffe AG, Farewell V, Hanly JG, Manzi S, Su L, et al. Factors associated with damage accrual in patients with systemic lupus erythematosus: results from the Systemic Lupus International Collaborating Clinics (SLICC) Inception Cohort. Ann Rheum Dis 2015;74:1706–13.

29. Gladman DD, Urowitz MB, Rahman P, Ibañez D, Tam LS. Accrual of organ damage over time in patients with systemic lupus erythematosus. J Rheumatol 2003;30:1955–9.
30. Iaccarino L, Andreoli L, Bocci EB, Bortoluzzi A, Ceccarelli F, Conti F, et al. Clinical predictors of response and discontinuation of belimumab in patients with systemic lupus erythematosus in real life setting: results of a large, multicentric, nationwide study. J Autoimmun 2018;86:1–8.
31. Alberici F, Smith RM, Jones RB, Roberts DM, Willcocks LC, Chaudhry A, et al. Long-term follow-up of patients who received repeat-dose rituximab as maintenance therapy for ANCA-associated vasculitis. Rheumatology (Oxford) 2015;54:1153–60.
32. Doria A, Iaccarino L, Ghirardello A, Zampieri S, Arienti S, Sarzi-Puttini P, et al. Long-term prognosis and causes of death in systemic lupus erythematosus. Am J Med 2006;119:700–6.
33. Salmon JH, Cacoub P, Combe B, Sibilia J, Pallot-Prades B, Fain O, et al. Late-onset neutropenia after treatment with rituximab for rheumatoid arthritis and other autoimmune diseases: data from the AutoImmunity and Rituximab registry. RMD Open 2015;1: e000034.
34. Parodis I, Söder F, Faustini F, Kasza Z, Samuelsson I, Zickert A, et al. Rituximab-mediated late-onset neutropenia in systemic lupus erythematosus: distinct roles of BAFF and APRIL. Lupus 2018;27:1470–8.
35. Navarra SV, Guzmán RM, Gallacher AE, Hall S, Levy RA, Jimenez RE, et al. Efficacy and safety of belimumab in patients with active systemic lupus erythematosus: a randomised, placebo-controlled, phase 3 trial. Lancet 2011;377:721–31.
36. Furie R, Petri M, Zamani O, Cervera R, Wallace DJ, Tegzová D, et al. A phase III, randomized, placebo-controlled study of belimumab, a monoclonal antibody that inhibits B lymphocyte stimulator, in patients with systemic lupus erythematosus. Arthritis Rheum 2011;63:3918–30.
37. Vial T, Patat AM, Boels D, Castellan D, Villa A, Theophile H, et al. Adverse consequences of low-dose methotrexate medication errors: data from French poison control and pharmacovigilance centers. Joint Bone Spine 2019;86:351–5.

Arthritis & Rheumatology
Vol. 71, No. 10, October 2019, pp 1681–1690
DOI 10.1002/art.40931

American College of Rheumatology
Empowering Rheumatology Professionals

Inhibition of EZH2 Ameliorates Lupus-Like Disease in MRL/*lpr* Mice

Dallas M. Rohraff,[1] Ye He,[2] Evan A. Farkash,[1] Mark Schonfeld,[1] Pei-Suen Tsou,[1] and Amr H. Sawalha[3]

Objective. We previously identified a role for EZH2, a transcriptional regulator in inducing proinflammatory epigenetic changes in lupus CD4+ T cells. This study was undertaken to investigate whether inhibiting EZH2 ameliorates lupus-like disease in MRL/*lpr* mice.

Methods. EZH2 expression levels in multiple cell types in lupus patients were evaluated using flow cytometry and messenger RNA expression data. Inhibition of EZH2 in MRL/*lpr* mice was achieved by intraperitoneal 3′-deazaneplanocin (DZNep) administration using a preventative and a therapeutic treatment model. Effects of DZNep on animal survival, anti–double-stranded DNA (anti-dsDNA) antibody production, proteinuria, renal histopathology, cytokine production, and T and B cell numbers and percentages were assessed.

Results. EZH2 expression levels were increased in whole blood, neutrophils, monocytes, B cells, and CD4+ T cells in lupus patients. In MRL/*lpr* mice, inhibition of EZH2 by DZNep was confirmed by significant reduction of EZH2 and H3K27me3 in splenocytes. Inhibiting EZH2 with DZNep treatment before or after disease onset improved survival and significantly reduced anti-dsDNA antibody production. DZNep-treated mice displayed a significant reduction in renal involvement, splenomegaly, and lymphadenopathy. Lymphoproliferation and numbers of double-negative T cells were significantly reduced in DZNep-treated mice. Concentrations of circulating cytokines and chemokines, including tumor necrosis factor, interferon-γ, CCL2, RANTES/CCL5, interleukin-10 (IL-10), keratinocyte-derived chemokine/CXCL1, IL-12, IL-12p40, and CCL4/macrophage inflammatory protein 1β, were decreased in DZNep-treated mice.

Conclusion. EZH2 is up-regulated in multiple cell types in lupus patients. Therapeutic inhibition of EZH2 abrogates lupus-like disease in MRL/*lpr* mice, suggesting that EZH2 inhibitors may be repurposed as a novel therapeutic option for lupus patients.

INTRODUCTION

Systemic lupus erythematosus (SLE), or lupus, is a chronic relapsing autoimmune disease that involves multiple organ systems. Lupus is characterized by the production of autoantibodies directed against nuclear antigens and a dysregulated immune response. The etiology of lupus remains unknown, although both genetic and epigenetic mechanisms have been shown to contribute to disease pathogenesis (1,2).

DNA methylation plays a critical role in the pathogenesis of lupus (3). Abnormal DNA methylation patterns have been described in multiple immune cell types isolated from lupus patients, and a role for genetic–epigenetic interaction in the pathogenesis of lupus has been suggested (4). Furthermore, abnormal DNA methylation patterns in lupus have been shown to contribute to clinical heterogeneity, disease variability between ethnicities, and lupus flare and remission (4).

EZH2 induces H3K27me3 and is the catalytic component of the highly conserved polycomb regressive complex 2. Our group previously demonstrated that increased disease activity in lupus patients is characterized by an early epigenetic shift in naive CD4+ T cells that precedes CD4+ T cell differentiation and effector T cell transcriptional activity (5). We provided evidence that this epigenetic shift is likely induced by EZH2 overexpression as a result of down-regulation of microRNA-101 (miR-101) and miR-26a, in addition to showing that EZH2 overexpression mediates increased T cell adhesion in lupus due to EZH2-induced demethylation and transcrip-

Supported by the Lupus Research Alliance and the National Institute of Allergy and Infectious Diseases (NIAID), NIH (grant R01-AI-097134). Dr. Farkash's work was supported by the NIAID, NIH (grant K23-AI-108951).

[1]Dallas M. Rohraff, BSc, Evan A. Farkash, MD, PhD, Mark Schonfeld, BSc, Pei-Suen Tsou, PhD: University of Michigan, Ann Arbor; [2]Ye He, BSc: University of Michigan, Ann Arbor, and the Second Xiangya Hospital and Central South University, Changsha, China; [3]Amr H. Sawalha, MD: University of Michigan, Ann Arbor, and University of Pittsburgh, Pittsburgh, Pennsylvania.

No potential conflicts of interest relevant to this article were reported.

Address correspondence to Amr H. Sawalha, MD, UPMC Children's Hospital of Pittsburgh, Division of Rheumatology, University of Pittsburgh, 4401 Penn Avenue, Rangos Research Center, Room 7123, Pittsburgh, PA 15224. E-mail: asawalha@pitt.edu.

Submitted for publication December 18, 2018; accepted in revised form May 14, 2019.

tional derepression of the junctional adhesion molecule A (JAM-A) (5,6).

EZH2 overexpression has been linked to increased invasiveness in a number of malignancies, and EZH2 inhibitors are currently being evaluated in clinical trials for cancer therapy (7). Our findings indicate that inhibiting EZH2 might have therapeutic potential in lupus, suggesting the possibility of pharmacologic repurposing of EZH2 inhibitors as a therapeutic option. In this study, we first examined EZH2 expression patterns in other immune cell types isolated in the peripheral blood from lupus patients. We then tested the effects of using 3′-deazaneplanocin (DZNep), an EZH2 inhibitor, in the lupus-prone MRL/*lpr* mouse model. DZNep is an S-adenosylhomocysteine hydrolase inhibitor that inactivates methyltransferase activity through feedback inhibition by accumulation of S-adenosylhomocysteine (8). DZNep has also been shown, by us and others, to decrease EZH2 levels (6,7). In the current study, we utilized both preventative and therapeutic approaches of administering DZNep to MRL/*lpr* mice. Our findings provide robust preclinical evidence supporting the potential use of EZH2 inhibitors in lupus, paving the way for repurposing EZH2 inhibitors in clinical trials.

MATERIALS AND METHODS

EZH2 expression in B cells, monocytes, and neutrophils in lupus patients. We recruited a total of 6 lupus patients (mean ± SEM age 46.2 ± 5.4 years, range 32–61 years) and 6 healthy controls (mean ± SEM age 44.5 ± 5.8 years, range 30–63 years). All lupus patients fulfilled the American College of Rheumatology classification criteria for SLE (9). The mean SLE Disease Activity Index score (10) score for lupus patients was 2, with a median of 1 (range 0–6) (see Supplementary Table 1, on the *Arthritis & Rheumatology* web site at http://onlinelibrary.wiley.com/doi/10.1002/art.40931/abstract). Lupus patients receiving cyclophosphamide or methotrexate were excluded from the study. All subjects provided written informed consent approved by the Institutional Review Board of the University of Michigan.

Peripheral whole blood was collected from each study subject, and erythrocytes in blood samples were lysed with RBC Lysis Buffer (eBioscience). Remaining whole blood cells were incubated with Human Seroblock (Bio-Rad) in Cell Staining Buffer (BioLegend) to block nonspecific Fc receptor binding of Ig, and extracellularly stained with the following antibodies: allophycocyanin (APC)–Cy7–conjugated anti-CD14 (clone 63D3; BioLegend), phycoerythrin (PE)–conjugated mouse anti-human CD16b (clone CLB-gran11.5; BD Biosciences), and APC-conjugated anti-CD19 (clone HIB19; BioLegend). Afterward, cells were fixed with Fixation Buffer (BioLegend), permeabilized with Intracellular Staining Permeabilization Wash Buffer (BioLegend), and subsequently stained with fluorescein isothiocyanate (FITC)–conjugated anti-EZH2 (clone REA907; Miltenyi Biotec) or with corresponding isotype control, REA Control (I) antibody (clone REA293; Miltenyi Biotec). Stained cells were then analyzed by flow cytometry using an iCyt Synergy SY3200 Cell Sorter (Sony Biotechnology) and FlowJo software, version 10.0.7. An example of the gating strategy to determine B cells, monocytes, and neutrophils is shown in Supplementary Figure 1 (http://onlinelibrary.wiley.com/doi/10.1002/art.40931/abstract), based on forward scatter (FSC) versus side scatter (SSC) and positive expression of their respective markers. The expression of EZH2 was measured by the median fluorescence intensity (MFI) of EZH2 antibody minus the MFI of its isotype control.

GEO data analysis. Analysis of EZH2 messenger RNA (mRNA) expression levels between lupus patients and healthy controls (in whole blood cells, CD4+ T cells, and CD19+ B cells) was performed using data sets downloaded from the GEO database (accession nos. GSE72509 and GDS4185). These data sets have previously been described in detail (11,12).

Mice and treatments. Eight-week-old female MRL/*lpr* mice (no. 000485; The Jackson Laboratory) were acclimatized for 2 weeks prior to study commencement and maintained in pathogen-free conditions. There were 2 model types in which DZNep (Cayman Chemical) was administered: a preventative model (DZNep/DZNep) with DZNep treatments that began on day 0 of the study in 10-week-old mice and a therapeutic treatment model (vehicle/DZNep) with DZNep treatments that began on day 28 of the study in 14-week-old mice. A vehicle-only group was also included as control. Mice were treated with either vehicle or DZNep (2 mg/kg) by intraperitoneal injection. DZNep was solubilized in DMSO and diluted in phosphate buffered saline (PBS) prior to injection (final DMSO concentration in PBS was 10%). In the vehicle control group, mice received daily injections of vehicle control for 35 days and were switched to biweekly (Monday and Thursday) dosing until day 98. A similar regimen was used in the DZNep/DZNep prevention model group, in which mice received DZNep once daily from day 0 to day 35 and were then switched to twice-weekly dosing for the remainder of the study. In the vehicle/DZNep therapeutic treatment group, animals received vehicle once daily from day 0 to day 27. On day 28, mice in this group were switched to a daily dose of DZNep until day 63; from day 64 onward, the dosing frequency changed to twice weekly. Animals were monitored and weighed daily throughout the study. This study was performed at Biomodels, an AAALAC-accredited facility, and approved by the Biomodels Institutional Animal Care and Use Committee.

Assessment of lupus nephritis and kidney damage. Kidneys were harvested on day 98 of the study, fixed in formalin, and sections were cut and stained with either hematoxylin and eosin or periodic acid–Schiff (PAS). Glomerulonephritis, crescent formation, and necrosis in kidneys were scored clinically by a pathologist who was blinded with regard to the experimental group. Approximately 125 glomeruli in each PAS-stained slide were counted. Glomeruli were categorized as having crescents,

fibrinoid necrosis, acute glomerulitis, mesangial hypercellularity, segmental glomerulosclerosis, global glomerulosclerosis, or normal architecture. The presence of pseudothrombi, interstitial nephritis, and arteritis was also noted.

Urine was collected every 2 weeks beginning 2 weeks prior to day 0 of the study. Urine albumin and creatinine concentrations were measured using enzyme-linked immunosorbent assay (ELISA) kits from Alpha Diagnostic and R&D Systems, respectively, and were then used to calculate the urine albumin:creatinine ratio.

Quantification of serum and plasma antibodies. Every 2 weeks, serum was collected by retroorbital bleed using serum separator tubes. On day 98 of the study, plasma was collected from all of the animals, while serum was collected in a portion of the DZNep/DZNep-treated mice and all of the vehicle/DZNep-treated mice. Anti–double-stranded DNA (anti-dsDNA) antibody titers in serum or plasma (day 98 only) were determined using ELISA (Alpha Diagnostic).

Spleen and lymph node weight. Spleen and lymph nodes (submaxillary, thoracic, axillary, renal, and mesenteric) were excised on day 98 of the study, trimmed of extra fat and connective tissue, weighed, and photographed. The average weight of all lymph nodes in each mouse was used to represent the average change in lymph node weight between mouse groups.

Flow cytometric analysis of splenocytes. Each spleen was placed in fluorescence-activated cell sorting buffer (0.5% bovine serum albumin, 2 m*M* EDTA in PBS) and processed into single-cell suspension using a gentleMACS Dissociator. Total spleen cell counts were obtained by counting a fraction of the diluted cells by flow cytometry. Red blood cells were lysed using BD Pharm Lyse lysis buffer (BD Biosciences) prior to the addition of mouse FcR Blocking Reagent (Miltenyi Biotec). Cells were stained with the following fluorochrome-conjugated antibodies: VioBlue-conjugated CD3ε (clone 17A2; Miltenyi Biotec), APC–Cy7–conjugated rat anti-mouse CD4 (clone GK1.5; BD Biosciences), PE-conjugated rat anti-mouse CD8a (clone 53-6.7; BD Biosciences), PerCP–Cy5.5–conjugated anti-mouse T cell receptor β chain (TCRβ) (clone H57-597; BioLegend), FITC-conjugated anti-mouse CD19 (clone 6D5; BioLegend), APC-conjugated CD45R (B220) (clone RA3-6B2; Miltenyi Biotec), and PE–Cy7–

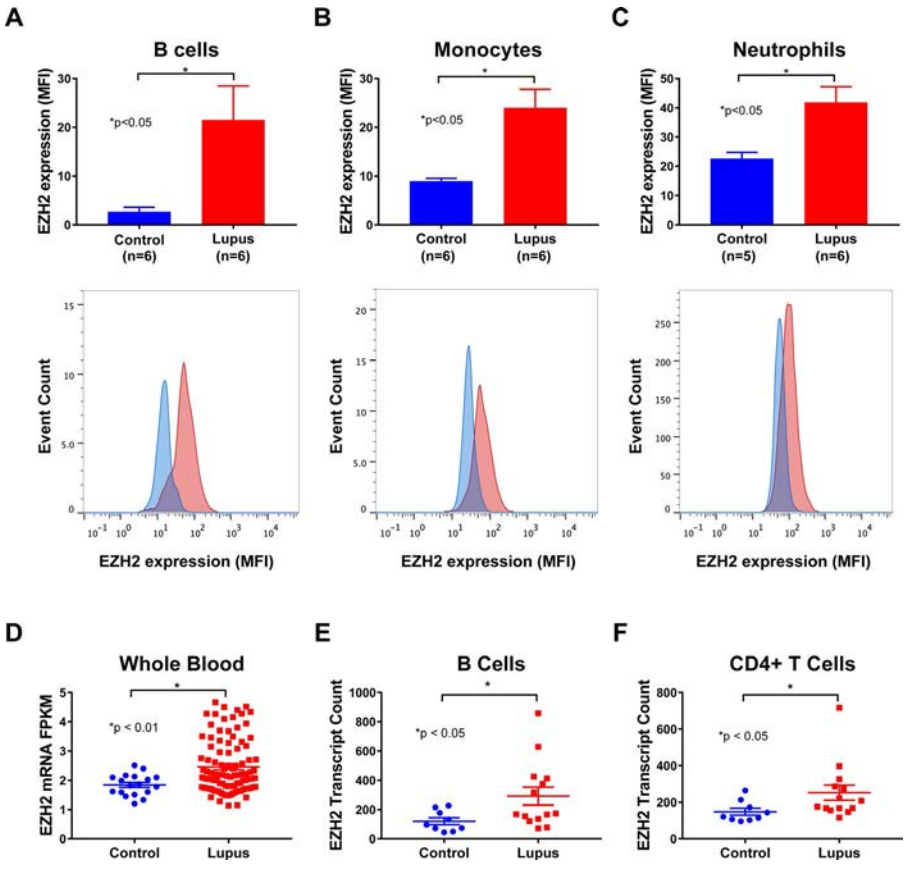

Figure 1. Analysis of EZH2 expression in human peripheral blood cells. **A–C,** EZH2 expression, analyzed by flow cytometry, was elevated in B cells (**A**), monocytes (**B**), and neutrophils (**C**) from lupus patients compared to controls. Values in the upper panels are the mean ± SEM. **D–F,** EZH2 mRNA levels were elevated in whole blood from lupus patients (n = 99) compared to controls (n = 18) (**D**), and were also elevated in B cells (**E**) and CD4+ T cells (**F**) from lupus patients (n = 14) compared to controls (n = 9). Symbols represent individual subjects; bars show the mean ± SEM. MFI = median fluorescence intensity.

conjugated anti-mouse CD11c (clone N418; BioLegend). Stained cells were then analyzed by flow cytometry using a MACSQuant Analyzer 10 (Miltenyi Biotec) and WinList software, version 9 (Verity Software House). The following cell types were gated based on FSC versus SSC and positive expression of their respective markers: B cells (TCRβ–CD19+), total T cells (TCRβ+), CD4+ T cells (TCRβ+CD4+), CD8+ T cells (TCRβ+CD8+), and double-negative T cells (TCRβ+CD4–CD8–). An example of the gating strategy is shown in Supplementary Figure 2 (http://onlinelibrary.wiley.com/doi/10.1002/art.40931/abstract).

EZH2, H3K27me3, and JAM-A expression in splenocytes. To confirm that successful inhibition of EZH2 in mice was achieved by DZNep treatment, EZH2 and H3K27me3 levels in splenocytes were examined using Western blotting. Protein (20 μg) of protein was separated by sodium dodecyl sulfate–polyacrylamide gel electrophoresis before electroblotting onto a nitrocellulose membrane. Blots were probed with anti-EZH2 or anti-H3K27me3 antibodies (both from Cell Signaling Technology). β-actin (Sigma-Aldrich) and H3 (Cell Signaling Technology) were used as loading controls. Since we previously showed that JAM-A is regulated by EZH2 and down-regulated by DZNep in lupus CD4+ T cells (6), we also examined levels of JAM-A (Santa Cruz Biotechnology) in these cells. Densitometry was analyzed using ImageJ.

Cytokine analysis. Cytokine levels in plasma from day 98 of the mouse study were analyzed using a Bio-Plex Pro Mouse Cytokine 23-plex Assay. The cytokines assayed included tumor necrosis factor (TNF), interferon-γ (IFNγ), interleukin-1α (IL-1α), IL-1β, IL-2, IL-3, IL-4, IL-5, IL-6, IL-9, IL-10, IL-12, IL-12p40, IL-13, IL-17A, CCL2, RANTES/CCL5, keratinocyte-derived chemokine (KC)/CXCL1, eotaxin/CCL11, macrophage inflammatory protein 1α (MIP-1α), MIP-1β/CCL4, granulocyte colony-stimulating factor (G-CSF), and granulocyte–macrophage colony-stimulating factor (GM-CSF).

Statistical analysis. Mann-Whitney U tests were used to compare the publicly available data on human EZH2 expression levels in whole blood, B cells, and CD4+ T cells in lupus patients and healthy controls. EZH2 expression , measured by flow cytometry, in B cells, monocytes, and neutrophils from lupus patients versus healthy controls was compared using an

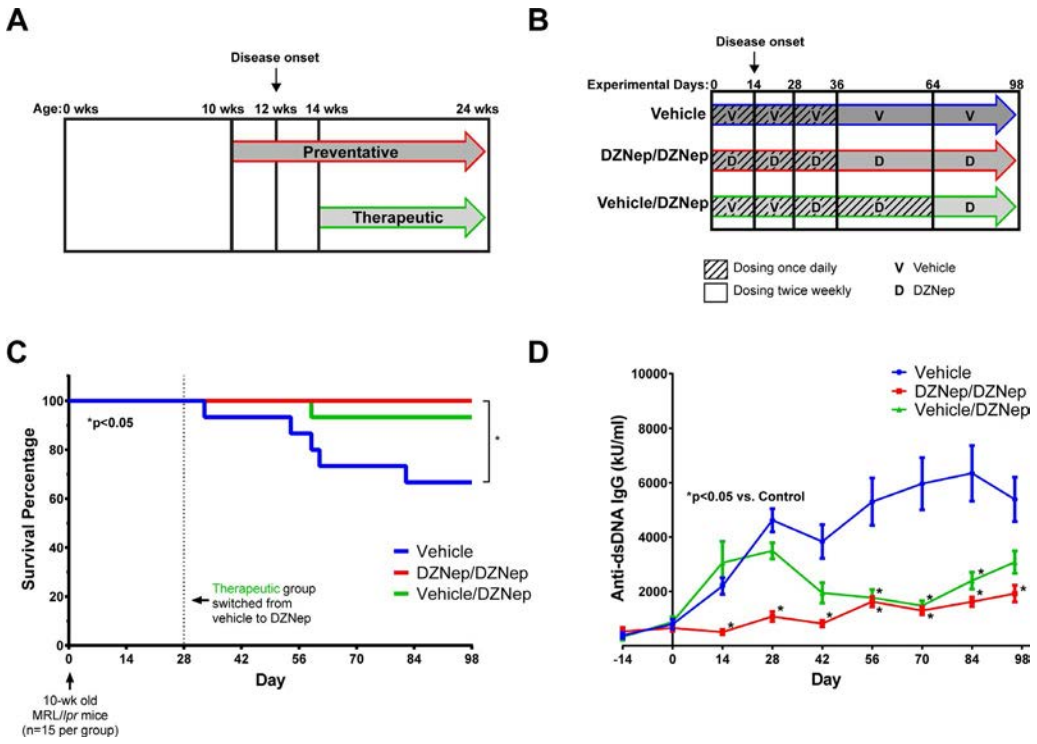

Figure 2. Survival improvement and reduced anti–double-stranded DNA (anti-dsDNA) antibody production in 3′-deazaneplanocin (DZNep)–treated MRL/*lpr* mice. **A**, Schematic representation of preventative and therapeutic treatment models. DZNep treatment in the preventative group (DZNep/DZNep) began when mice were 10 weeks old, 2 weeks prior to typical disease onset. The therapeutic group (vehicle/DZNep) received DZNep treatment 2 weeks after disease onset, when mice were 14 weeks old. **B**, Schematic representation of treatment regimens. The DZNep/DZNep group received DZNep once daily for 35 days and on day 36 was switched to a twice-weekly regimen until the end of the study. The control group was treated at the same times as the DZNep/DZNep group, with vehicle administered instead of DZNep. The vehicle/DZNep group received vehicle once daily for 27 days, then was switched to daily dosing of DZNep from day 28 through day 63. On day 64, DZNep dosing was reduced to twice weekly until the end of the study. **C**, Survival curves of the vehicle, DZNep/DZNep, and vehicle/DZNep groups (n = 15 per group at start). **D**, Anti-dsDNA antibody levels. Values are the mean ± SEM.

unpaired *t*-test, or Mann-Whitney U test when normality could not be assumed. Survival analysis was performed using the Mantel-Cox log-rank test. All other mouse data were evaluated by one-way analysis of variance, or Kruskal-Wallis test when normality could not be assumed, using Dunn's multiple comparison test to compare the preventative and therapeutic groups to the control group. All statistical analyses were performed using GraphPad Prism, version 7. Data are presented as the mean ± SEM. *P* values less than 0.05 were considered significant.

RESULTS

EZH2 expression in lupus. We previously showed that EZH2 is up-regulated in lupus CD4+ T cells and that T cell overexpression of EZH2 plays an important role in lupus (5,6). To examine whether other immune cell types also overexpress EZH2 in lupus, we assessed EZH2 expression using flow cytometry in peripheral blood B cells, monocytes, and neutrophils from lupus patients and compared it to that in healthy controls. EZH2 expression, as measured by MFI, was significantly elevated in B cells, monocytes, and neutrophils of lupus patients compared to matched controls ($P < 0.05$) (Figures 1A–C). Using previously published gene expression profiles available in GEO, we analyzed EZH2 mRNA levels in whole blood (GEO accession no. GSE72509) and freshly isolated lymphocyte subsets (GEO accession no. GDS4185) from lupus patients and healthy controls. EZH2 mRNA levels in whole blood from lupus patients were significantly higher than those in healthy controls ($P < 0.01$) (Figure 1D). Similarly, EZH2 expression was significantly elevated in the freshly isolated B cells and CD4+ T cells from lupus patients compared to controls ($P < 0.05$) (Figures 1E and F).

Effect of EZH2 inhibition on mortality and autoantibody production in MRL/*lpr* mice. To examine whether inhibition of EZH2 is beneficial in lupus-like disease, an EZH2 inhibitor, DZNep, was administered to MRL/*lpr* mice (Figures 2A and B). As shown in Figure 2C, mice that received only vehicle had 33.3% mortality by the end of the study on day 98 (mice were 24 weeks old). Mice in the preventative group had 100% survival, while there was 6.67% mortality in the therapeutic group by the end of the study. There was a significant difference in the mortality rates between the DZNep/DZNep-treated mice and the controls ($P < 0.05$).

Anti-dsDNA antibody levels were significantly lower in the preventative group by day 14, 2 weeks after DZNep treatment began in this group, and anti-dsDNA antibody levels remained significantly lower throughout the duration of the study ($P < 0.001$) (Figure 2D). By day 56, the anti-dsDNA titers were significantly lower in mice in the therapeutic group compared to the vehicle control group ($P < 0.05$) and remained significantly lower for the next 28 days, though there was not a significant difference detected at the final time point (Figure 2D). Although plasma was used instead of serum for quantification of anti-

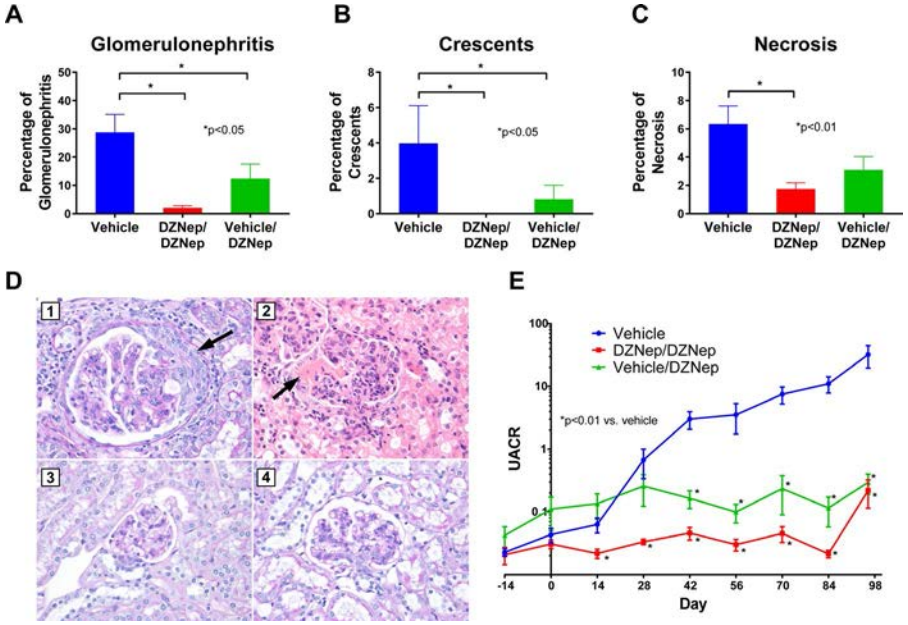

Figure 3. Reduced renal involvement in 3′-deazaneplanocin (DZNep)–treated MRL/*lpr* mice. **A–C,** The percentage of total glomeruli with glomerulonephritis (**A**), crescent formation (**B**), and necrosis (**C**) in the kidneys of mice in the vehicle, DZNep/DZNep, and vehicle/DZNep groups. **D**, Photomicrographic representation of renal damage. D1, Glomerulus with glomerulomegaly and cellular crescent (**arrow**) from a mouse in the control group. D2, Acute global glomerulitis and segmental fibrinoid necrosis (**arrow**) from a mouse in the control group. D3, Normal-appearing glomerulus from a mouse in the DZNep/DZNep group. D4, Glomerulus with mesangial hypercellularity from a mouse in the vehicle/DZNep group. Periodic acid–Schiff stained (D1, D3, and D4) or hematoxylin and eosin stained (D2); original magnification × 400. **E**, Urine albumin:creatinine ratios (UACRs) in the vehicle, DZNep/DZNep, and vehicle/DZNep groups. Values in **A**, **B**, **C**, and **E** are the mean ± SEM.

dsDNA on day 98, the levels were similar to those measured in serum (data not shown). Our results showed that DZNep improved survival in the MRL/*lpr* mice and significantly reduced the production of anti-dsDNA antibodies 2–4 weeks following daily dosing of DZNep.

Effect of DZNep treatment on renal involvement. To assess the effect of DZNep on renal damage, glomerulonephritis, crescent formation, and necrosis were assessed in each mouse on day 98 of the study. Development of glomerulonephritis and crescents was significantly reduced in both the preventative and therapeutic groups compared to the control group ($P < 0.05$) (Figures 3A and B). There also was a significant reduction in glomerular necrosis in the preventative group compared to the control group ($P < 0.01$), but the difference observed between the control group and the therapeutic group was not statistically significant (Figure 3C). Representative photomicrographs of glomeruli from each treatment group are depicted in Figure 3D. Overall, the number of glomeruli with no pathologic abnormality was significantly higher in the preventative group compared to the control group (mean ± SEM 65.8 ± 4.7% versus 31.6 ± 7.2%; $P < 0.01$) (Supplementary Figure 3, http://onlinelibrary.wiley.com/

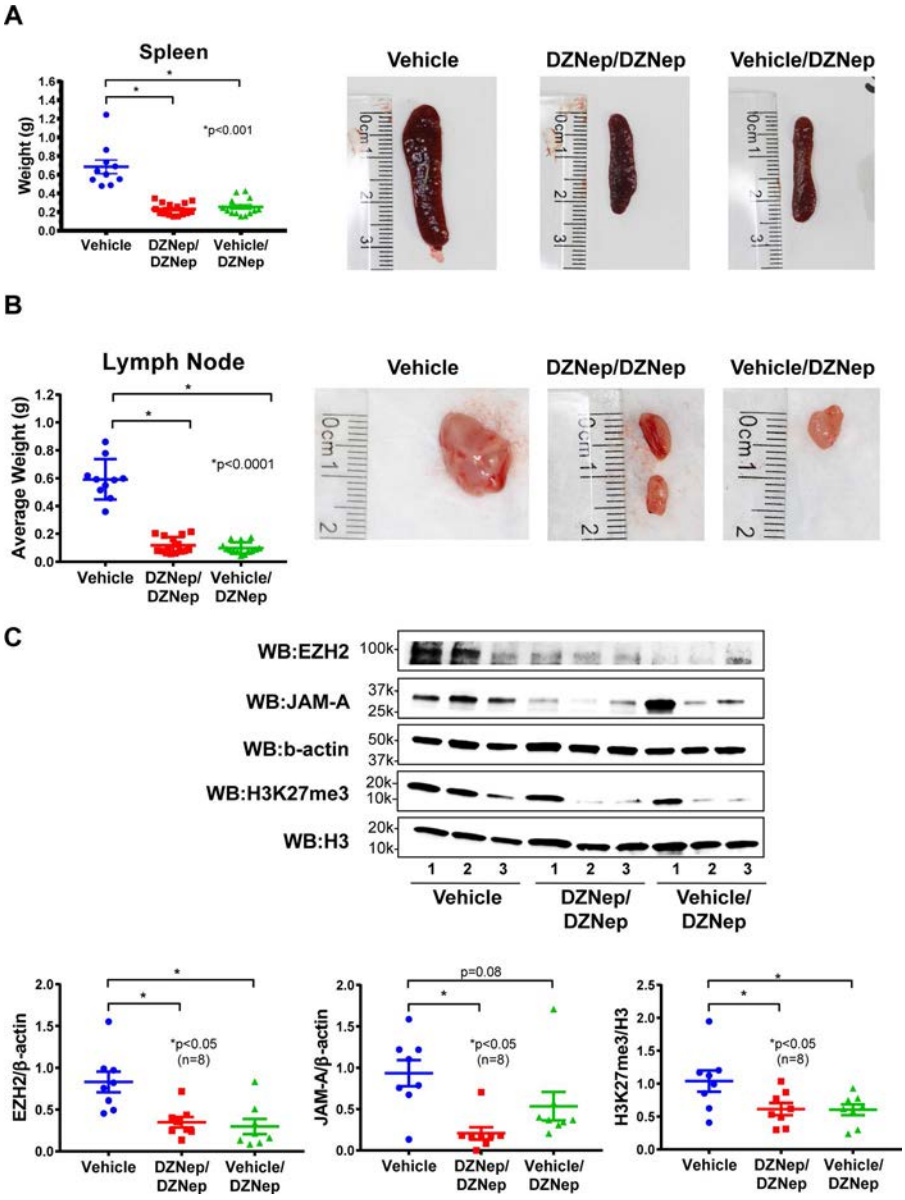

Figure 4. Reduced splenomegaly and lymphadenopathy in 3′-deazaneplanocin (DZNep)–treated MRL/*lpr* mice. **A**, Weight of individual spleens, and representative photographs. **B**, Mean weight of lymph nodes from all sites, and representative photographs of renal lymph nodes. **C**, Expression of EZH2, junctional adhesion molecule A (JAM-A), and H3K27me3 in splenocytes, examined by Western blotting (WB). Representative blots from 3 mice per treatment group are shown. A total of 8 samples per group were analyzed for densitometry. In **A** and **B** (left panels) and **C** (lower panels), symbols represent individual mice; bars show the mean ± SEM.

doi/10.1002/art.40931/abstract). To monitor the progression of kidney involvement, proteinuria was analyzed using albumin:creatinine ratios that were calculated every 2 weeks throughout the study. These ratios were significantly lower in the preventative group (by day 14) and the therapeutic group (by day 42) compared to the control group ($P < 0.01$) (Figure 3E). In both treatment groups, the albumin:creatinine ratio remained significantly lower throughout the remainder of the study. Overall, DZNep treatment, both preventative and therapeutic, significantly reduced lupus nephritis and renal damage in MRL/*lpr* lupus-prone mice.

Reduced splenomegaly and lymphadenopathy with DZNep. MRL/*lpr* mice develop progressive enlargement of the spleen and lymph nodes due to lymphoproliferation that is characteristic of the strain. The spleens from vehicle-treated mice weighed significantly more than those from mice in the preventative and therapeutic groups ($P < 0.001$) (Figure 4A). The mean weight of lymph nodes from all sites (submaxillary, thoracic, axillary, renal, and mesenteric) in both the preventative and therapeutic groups was significantly lower than that of the control group ($P < 0.0001$) (Figure 4B and Supplementary Figure 4, http://onlinelibrary.wiley.com/doi/10.1002/art.40931/abstract). DZNep appeared to be efficacious in reducing the progression of splenomegaly and lymphadenopathy in MRL/*lpr* mice.

Reduced EZH2, H3K27me3, and JAM-A with DZNep. In splenocytes, DZNep treatment in both the preventative and therapeutic groups significantly reduced both EZH2 and H3K27me3 levels, suggesting that the dosing regimen we adopted was effective in inhibiting EZH2 ($P < 0.05$; n = 8) (Figure 4C). In addition, JAM-A levels in splenocytes were significantly reduced in the preventative group ($P < 0.05$), while these reductions were only marginally significant in the therapeutic group due to an outlier ($P = 0.08$). These results suggest that EZH2 regulates JAM-A expression, and manipulation of EZH2 expression by DZNep down-regulates JAM-A, similar to what we previously showed in CD4+ T cells in lupus patients (6).

Reduced lymphoproliferation with DZNep. Using flow cytometry, we further explored the effect of EZH2 inhibition on lymphoproliferation in MRL/*lpr* mice by analyzing differences between groups of T cell and B cell populations. Both the preventative and therapeutic groups showed reduced numbers of total splenocytes, total T cells (TCRβ+), CD8+ T cells (TCRβ+CD8+), and double-negative T cells (TCRβ+CD4–CD8–), compared to the control group ($P < 0.01$) (Figures 5A–C). The total number of CD4+ T cells (TCRβ+CD4+) was significantly decreased in the therapeutic group compared to the control group ($P < 0.01$) (Figure 5C). In addition, DZNep treatment in both the preventative and therapeutic groups significantly reduced the percentage of double-negative T cells, while significantly increasing the percentage of CD4+ and CD8+ T cells by the end of the study, compared to the control group ($P \leq 0.0001$) (Figure 5D). The observed shift in T cell populations and the reduction in total number of T cells suggests that DZNep reduces both T cell hyperproliferation and the generation of pathogenic double-negative T cells in MRL/*lpr* mice.

There was no difference in the total number of B cells (TCRβ–CD19+) between any of the groups (Figure 5E). However, we observed that the B cell percentage among total splenocytes was significantly greater in both the preventative and therapeutic groups compared to the control group ($P \leq 0.0001$) (Figure 5F).

Cytokine levels. To further characterize the effect of EZH2 inhibition in MRL/*lpr* mice, we analyzed the differential expression of plasma cytokine levels on day 98. Levels of IL-3, IL-1β, IL-9, IL-13, IL-6, IL-4, G-CSF, GM-CSF, and MIP-1α were undetectable. No significant differences were observed between DZNep treatment groups and controls for IL-2, IL-5, IL-1α, IL-17A, and eotaxin/CCL11 (data not shown). However, there was a signifi-

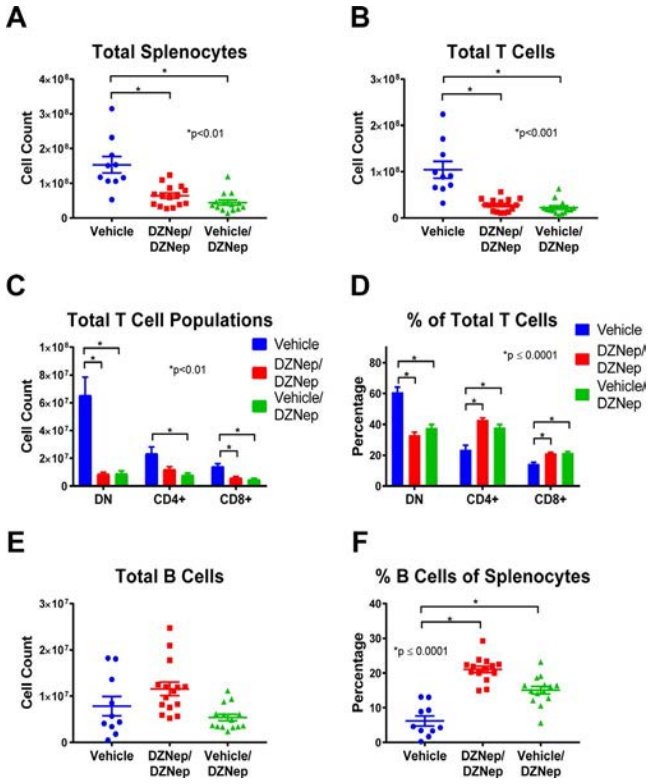

Figure 5. Reduced lymphoproliferation in 3′-deazaneplanocin (DZNep)–treated MRL/*lpr* mice. **A** and **B**, Total numbers of splenocytes (**A**) and T cells (**B**) in the DZNep/DZNep and vehicle/DZNep groups compared to controls. **C** and **D**, Total numbers (**C**) and percentages (**D**) of double-negative (DN) T cells, CD4+ T cells, and CD8+ T cells in mice in each treatment group. Values are the mean ± SEM. **E** and **F**, Total numbers of B cells (**E**) and percentages of B cells among splenocytes (**F**) in mice in each treatment group. In **A**, **B**, **E**, and **F**, symbols represent individual mice; bars show the mean ± SEM.

cant reduction in plasma levels of TNF, IFNγ, CCL2, RANTES/CCL5, IL-10, KC/CXCL1, IL-12, IL-12p40, and MIP-1β/CCL4 in both the preventative and therapeutic groups compared to the control group (Figure 6).

DISCUSSION

Our previous findings suggested that EZH2 plays an important role in lupus (5,6). We have reported that naive CD4+ T cells in lupus patients showed higher expression levels of EZH2 than those in healthy controls, and this up-regulation is critical for T cell adhesion, as inhibition of EZH2 by DZNep can normalize the ability of lupus CD4+ T cells to adhere to endothelial cells (6). In the present study, we further examined the expression of EZH2 in other cell types and showed that EZH2 was significantly up-regulated in B cells, monocytes, and neutrophils in lupus patients. These data prompted us to investigate whether inhibition of EZH2 would be beneficial for lupus treatment. Indeed, in MRL/*lpr* mice, DZNep treatment, administered in either a preventative or a therapeutic protocol, improved survival and reduced autoantibody production. In addition, the therapeutic effects of DZNep appeared rapidly, with lowered anti-dsDNA antibody levels and albumin:creatinine ratio evident 14 days after the first dose.

The improvement in survival observed in DZNep-treated mice is likely due, in part, to a reduction in renal involvement. DZNep treatments appeared to prevent the progression of renal damage, as evidenced by a relatively stable albumin:creatinine ratio in DZNep-treated mice. Renal damage was also assessed at the end of the study by histopathologic examination. We observed a significant reduction in glomerulonephritis and crescent formation in both DZNep treatment groups and a significant reduction in glomerular necrosis in the preventative group (DZNep/DZNep) compared to the control group, by the end of the study. The development of nephritis is indicative of severe disease in lupus patients and is an important predictor of morbidity and mortality. Based on our finding that DZNep treatment effectively reduced renal involvement in MRL/*lpr* mice, an EZH2 inhibitor could prove similarly therapeutic for lupus patients.

The MRL/*lpr* mouse model is a lymphoproliferative model characterized by T cell and B cell dysregulation (13). The infiltration of double-negative T cells, in addition to an overall hyperproliferation of T cell populations, contributes significantly to the

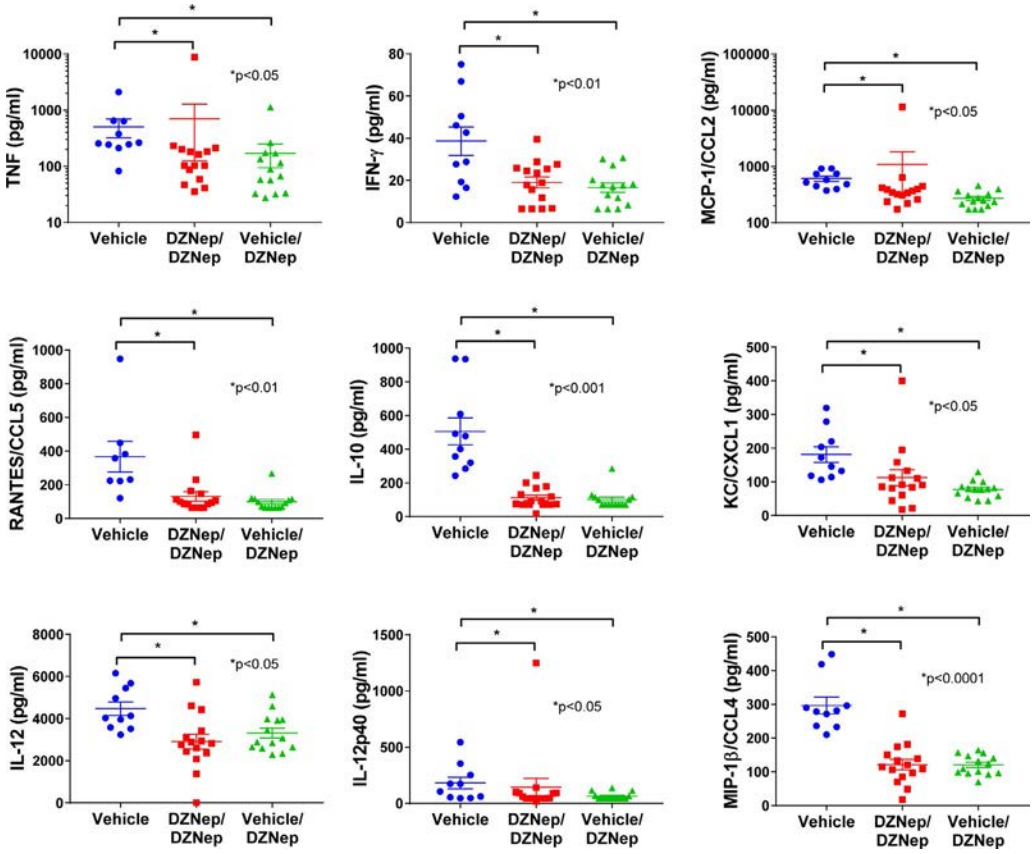

Figure 6. Decreased levels of plasma cytokines in 3′-deazaneplanocin (DZNep)–treated MRL/*lpr* mice. There was a significant reduction in plasma levels of tumor necrosis factor (TNF), interferon-γ (IFNγ), monocyte chemotactic protein 1 (MCP-1)/CCL2, RANTES/CCL5, interleukin-10 (IL-10), keratinocyte-derived chemokine (KC)/CXCL1, IL-12, IL-12p40, and macrophage inflammatory protein 1β (MIP-1β)/CCL4 in both the DZNep/DZNep and vehicle/DZNep groups compared to the control group. Symbols represent individual mice; bars show the mean ± SEM.

observed splenomegaly and lymphadenopathy in MRL/*lpr* mice (13,14). We observed a significant reduction in spleen and lymph node weight in both groups of mice treated with DZNep. A significant decrease in the total number of splenocytes in DZNep-treated groups was also observed, suggesting a reduction in lymphoproliferation. While DZNep treatment in both groups reduced the total number of T cells, CD4+ T cells, and CD8+ T cells, the reduction in CD4−CD8− (double-negative) T cells is of particular interest. Double-negative T cells represent a pathogenic T cell subset in lupus likely derived from CD8+ T cells (15). These cells contribute to the production of autoantibodies, produce significant amounts of inflammatory cytokines including IL-17 and IFNγ, and contribute to renal damage as they accumulate in the kidneys of lupus patients (15–18). Inhibition of EZH2 with DZNep significantly reduced the total number of pathogenic double-negative T cells in MRL/*lpr* mice. Indeed, the significant reduction in double-negative T cell numbers observed with DZNep treatment caused significant elevation in the percentages of single-positive T cells (CD4+ and CD8+ T cells). We speculate that the reduction of pathogenic double-negative T cells in the DZNep-treated groups likely contributed to the observed reduction in renal damage and levels of circulating autoantibodies.

Production of cytokines and chemokines is important in lupus pathogenesis and tissue damage in lupus patients. We observed reduced concentrations of TNF, IFNγ, CCL2, RANTES/CCL5, IL-10, IL-12, IL-12p40, and MIP-1β/CCL4 in the plasma from mice in the DZNep-treated groups compared to controls. All of these cytokines and chemokines have been reported to be elevated in lupus patients (19–23). Chemokines such as RANTES/CCL5, monocyte chemotactic protein 1/CCL2, and MIP-1β/CCL4 contribute to lupus pathogenesis by recruiting leukocytes and other effector cells to inflamed tissues, causing damage (19–21). IL-10 and TNF have been shown to be up-regulated in lupus patients experiencing renal involvement, and their levels correlate with disease activity (19,22). IFNγ has been found to contribute to the development of lupus through promotion of autophagy in lupus T cells, and potentially the persistence of pathogenic T cell subsets (22). Dysregulation of IL-12 has been reported in patients with lupus (24), and promising results were seen in a recent phase II trial in which ustekinumab, which targets IL-12p40, was added to the standard of care in lupus patients (25).

We have previously demonstrated that EZH2 might mediate a pathogenic effect in lupus by altering T cell DNA methylation patterns and up-regulation of the adhesion molecule JAM-A in CD4+ T cells (5,6). In the present study, we showed that DZNep treatment in MRL/*lpr* mice also down-regulates JAM-A in splenocytes, suggesting that its beneficial effect in these animals might be due, in part, to inhibition of lymphocyte adhesion and extravasation. Because the Notch signaling pathway regulates effector T cell survival and function, including cytokine production (26–28), we speculated that another potential mechanism of action for EZH2 in lupus might involve the Notch signaling pathway. EZH2 has been shown to inhibit T cell Notch repressors, promoting Notch activation and thus effector T cell polyfunctionality and survival (29). The Notch pathway is also critical in B cells and monocytes (30–34), which were characterized by EZH2 overexpression in lupus in our study.

Several limitations to this study are worth noting. We utilized a systemic approach to inhibit EZH2. While this approach allowed for assessment of the overall effect of EZH2 inhibition (which would be important if a clinical trial using EZH2 inhibitors were to be conducted in lupus patients), it did not allow for the identification of the specific cell types or pathways mediating the therapeutic effect of EZH2 inhibition in this lupus-prone mouse model. In addition, as noted above, although DZNep is a prototype EZH2 inhibitor, it inhibits methyltransferase activity, and therefore, nonspecific effects of DZNep cannot be ruled out. Future studies focused on characterizing the effects of EZH2 inhibition in specific cell types in vivo and on utilizing other more specific EZH2 inhibitors are warranted.

In summary, we have demonstrated that EZH2 is overexpressed in multiple immune cell types in lupus patients. Inhibition of EZH2 is associated with abrogation of lupus-like disease in MRL/*lpr* mice. Our data suggest that inhibiting EZH2 might provide a novel therapeutic approach for lupus patients.

AUTHOR CONTRIBUTIONS

All authors were involved in drafting the article or revising it critically for important intellectual content, and all authors approved the final version to be published. Dr. Sawalha had full access to all of the data in the study and takes responsibility for the integrity of the data and the accuracy of the data analysis.

Study conception and design. Tsou, Sawalha.
Acquisition of data. Rohraff, He, Schonfeld, Tsou, Sawalha.
Analysis and interpretation of data. Rohraff, Farkash, Tsou, Sawalha.

REFERENCES

1. Weeding E, Sawalha AH. Deoxyribonucleic acid methylation in systemic lupus erythematosus: implications for future clinical practice. Front Immunol 2018;9:875.
2. Deng Y, Tsao BP. Updates in lupus genetics. Curr Rheumatol Rep 2017;19:68.
3. Hedrich CM. Mechanistic aspects of epigenetic dysregulation in SLE. Clin Immunol 2018;196:3–11.
4. Teruel M, Sawalha AH. Epigenetic variability in systemic lupus erythematosus: what we learned from genome-wide DNA methylation studies. Curr Rheumatol Rep 2017;19:32.
5. Coit P, Dozmorov MG, Merrill JT, McCune WJ, Maksimowicz-McKinnon K, Wren JD, et al. Epigenetic reprogramming in naive CD4+ T cells favoring T cell activation and non-Th1 effector T cell immune response as an early event in lupus flares. Arthritis Rheumatol 2016;68:2200–9.
6. Tsou PS, Coit P, Kilian NC, Sawalha AH. EZH2 modulates the DNA methylome and controls T cell adhesion through junctional adhesion molecule A in lupus patients. Arthritis Rheumatol 2018;70:98–108.
7. Gan L, Yang Y, Li Q, Feng Y, Liu T, Guo W. Epigenetic regulation of cancer progression by EZH2: from biological insights to therapeutic potential [review]. Biomark Res 2018;6:10.

8. Glazer RI, Hartman KD, Knode MC, Richard MM, Chiang PK, Tseng CK, et al. 3-deazaneplanocin: a new and potent inhibitor of S-adenosylhomocysteine hydrolase and its effects on human promyelocytic leukemia cell line HL-60. Biochem Biophys Res Commun 1986;135:688–94.
9. Hochberg MC, for the Diagnostic and Therapeutic Criteria Committee of the American College of Rheumatology. Updating the American College of Rheumatology revised criteria for the classification of systemic lupus erythematosus [letter]. Arthritis Rheum 1997;40:1725.
10. Bombardier C, Gladman DD, Urowitz MB, Caron D, Chang DH, and the Committee on Prognosis Studies in SLE. Derivation of the SLEDAI: a disease activity index for lupus patients. Arthritis Rheum 1992;35:630–40.
11. Hutcheson J, Scatizzi JC, Siddiqui AM, Haines GK III, Wu T, Li QZ, et al. Combined deficiency of proapoptotic regulators Bim and Fas results in the early onset of systemic autoimmunity. Immunity 2008;28:206–17.
12. Hung T, Pratt GA, Sundararaman B, Townsend MJ, Chaivorapol C, Bhangale T, et al. The Ro60 autoantigen binds endogenous retroelements and regulates inflammatory gene expression. Science 2015;350:455–9.
13. Cohen PL, Eisenberg RA. Lpr and gld: single gene models of systemic autoimmunity and lymphoproliferative disease. Annu Rev Immunol 1991;9:243–69.
14. Lu LD, Stump KL, Wallace NH, Dobrzanski P, Serdikoff C, Gingrich DE, et al. Depletion of autoreactive plasma cells and treatment of lupus nephritis in mice using CEP-33779, a novel, orally active, selective inhibitor of JAK2. J Immunol 2011;187:3840–53.
15. Crispín JC, Tsokos GC. Human TCR-αβ+ CD4– CD8– T cells can derive from CD8+ T cells and display an inflammatory effector phenotype. J Immunol 2009;183:4675–81.
16. Crispín JC, Oukka M, Bayliss G, Cohen RA, Van Beek CA, Stillman IE, et al. Expanded double negative T cells in patients with systemic lupus erythematosus produce IL-17 and infiltrate the kidneys. J Immunol 2008;181:8761–6.
17. Shivakumar S, Tsokos GC, Datta SK. T cell receptor α/β expressing double-negative (CD4-/CD8-) and CD4+ T helper cells in humans augment the production of pathogenic anti-DNA autoantibodies associated with lupus nephritis. J Immunol 1989;143:103–12.
18. Dean GS, Anand A, Blofeld A, Isenberg DA, Lydyard PM. Characterization of CD3+ CD4- CD8- (double negative) T cells in patients with systemic lupus erythematosus: production of IL-4. Lupus 2002;11:501–7.
19. Lit LC, Wong CK, Tam LS, Li EK, Lam CW. Raised plasma concentration and ex vivo production of inflammatory chemokines in patients with systemic lupus erythematosus. Ann Rheum Dis 2006;65:209–15.
20. Vilá LM, Molina MJ, Mayor AM, Cruz JJ, Ríos-Olivares E, Ríos Z. Association of serum MIP-1α, MIP-1β, and RANTES with clinical manifestations, disease activity, and damage accrual in systemic lupus erythematosus. Clin Rheumatol 2007;26:718–22.
21. Kulkarni O, Pawar RD, Purschke W, Eulberg D, Selve N, Buchner K, et al. Spiegelmer inhibition of CCL2/MCP-1 ameliorates lupus nephritis in MRL-(Fas)lpr mice. J Am Soc Nephrol 2007;18: 2350–8.
22. Pacheco-Lugo L, Sáenz-García J, Navarro Quiroz E, González Torres H, Fang L, Díaz-Olmos Y, et al. Plasma cytokines as potential biomarkers of kidney damage in patients with systemic lupus erythematosus. Lupus 2019;28:34–43.
23. Arriens C, Wren JD, Munroe ME, Mohan C. Systemic lupus erythematosus biomarkers: the challenging quest. Rheumatology (Oxford) 2017;56 Suppl 1:i32–45.
24. Tucci M, Lombardi L, Richards HB, Dammacco F, Silvestris F. Overexpression of interleukin-12 and T helper 1 predominance in lupus nephritis. Clin Exp Immunol 2008;154:247–54.
25. Van Vollenhoven RF, Hahn BH, Tsokos GC, Wagner CL, Lipsky P, Touma Z, et al. Efficacy and safety of ustekinumab, an IL-12 and IL-23 inhibitor, in patients with active systemic lupus erythematosus: results of a multicentre, double-blind, phase 2, randomised, controlled study. Lancet 2018;392:1330–9.
26. Amsen D, Blander JM, Lee GR, Tanigaki K, Honjo T, Flavell RA. Instruction of distinct CD4 T helper cell fates by different notch ligands on antigen-presenting cells. Cell 2004;117:515–26.
27. Ciofani M, Zúñiga-Pflücker JC. Notch promotes survival of pre-T cells at the β-selection checkpoint by regulating cellular metabolism. Nat Immunol 2005;6:881–8.
28. Kryczek I, Zhao E, Liu Y, Wang Y, Vatan L, Szeliga W, et al. Human TH17 cells are long-lived effector memory cells. Sci Transl Med 2011;3:104ra100.
29. Zhao E, Maj T, Kryczek I, Li W, Wu K, Zhao L, et al. Cancer mediates effector T cell dysfunction by targeting microRNAs and EZH2 via glycolysis restriction. Nat Immunol 2016;17:95–103.
30. Cruickshank MN, Ulgiati D. The role of notch signaling in the development of a normal B-cell repertoire. Immunol Cell Biol 2010;88:117–24.
31. Arima H, Nishikori M, Otsuka Y, Kishimoto W, Izumi K, Yasuda K, et al. B cells with aberrant activation of Notch1 signaling promote Treg and Th2 cell-dominant T-cell responses via IL-33. Blood Adv 2018;2:2282–95.
32. Zhang W, Xu W, Xiong S. Blockade of Notch1 signaling alleviates murine lupus via blunting macrophage activation and M2b polarization. J Immunol 2010;184:6465–78.
33. Huang F, Zhao JL, Wang L, Gao CC, Liang SQ, An DJ, et al. MiR-148a-3p mediates Notch signaling to promote the differentiation and M1 activation of macrophages. Front Immunol 2017;8:1327.
34. Martín-Gayo E, González-García S, García-León MJ, Murcia-Ceballos A, Alcain J, García-Peydró M, et al. Spatially restricted JAG1-Notch signaling in human thymus provides suitable DC developmental niches. J Exp Med 2017;214:3361–79.

Arthritis & Rheumatology
Vol. 71, No. 10, October 2019, pp 1691–1700
DOI 10.1002/art.40918

American College of Rheumatology
Empowering Rheumatology Professionals

Validation of the REVEAL Prognostic Equation and Risk Score Calculator in Incident Systemic Sclerosis–Associated Pulmonary Arterial Hypertension

Christopher J. Mullin,[1] Rubina M. Khair,[2] Rachel L. Damico,[2] Todd M. Kolb,[2] Laura K. Hummers,[2] Paul M. Hassoun,[2] Virginia D. Steen,[3] and Stephen C. Mathai,[2] on behalf of the PHAROS Investigators

Objective. A prognostic equation and risk score calculator derived from the Registry to Evaluate Early and Long-term Pulmonary Arterial Hypertension Disease Management (REVEAL) are being used to predict 1-year survival in patients with pulmonary arterial hypertension (PAH), but little is known about the performance of these REVEAL survival prediction tools in systemic sclerosis (SSc)–associated PAH (SSc-PAH).

Methods. Prospectively gathered data from the Johns Hopkins Pulmonary Hypertension Program and Pulmonary Hypertension Assessment and Recognition of Outcome in Scleroderma Registries were used to evaluate the predictive accuracy of the REVEAL models for predicting the probability of 1-year survival in patients with SSc-PAH. Model discrimination was assessed by comparison of the Harrell's C-index, model fit was assessed using multivariable regression techniques, and model calibration was assessed by comparing predicted to observed survival estimates.

Results. The validation cohort consisted of 292 SSc-PAH patients with a 1-year survival rate of 87.4%. The C-index for predictive accuracy of the REVEAL prognostic equation (0.734, 95% confidence interval [95% CI] 0.652–0.816) and for the risk score (0.743, 95% CI 0.663–0.823) demonstrated good discrimination, comparable to that in the model development cohort. The calibration slope was 0.707 (95% CI 0.400–1.014), indicating that the overall model fit was marginal ($P = 0.06$). The magnitude of risk assigned to low distance on the 6-minute walk test (6MWD) and elevated serum levels of brain natriuretic peptide (BNP) was lower in the validation cohort than was originally seen in the REVEAL derivation cohort. Model calibration was poor, particularly for the highest risk groups.

Conclusion. In predicting 1-year survival in patients newly diagnosed as having SSc-PAH, the REVEAL prognostic equation and risk score provide very good discrimination but poor calibration. REVEAL prediction scores should be interpreted with caution in newly diagnosed SSc-PAH patients, particularly those with higher predicted risk of poor 1-year survival resulting from a low 6MWD or a high BNP serum level.

INTRODUCTION

Pulmonary arterial hypertension (PAH) is a chronic disease of the pulmonary vasculature that ultimately leads to right-sided heart failure and death. While rare in the general population, PAH has a lifetime prevalence of 8–14% in patients with systemic sclerosis (SSc) (1,2), and SSc-associated PAH (SSc-PAH) is a leading cause of premature death in this population (3). It is well established that there are differences in clinical characteristics and outcomes between SSc-PAH and other forms of PAH (4). Compared to patients with idiopathic PAH (IPAH), patients with SSc-PAH have less severe hemodynamic

Supported by the NIH (National Heart, Lung, and Blood Institute grant F32-HL-129687 to Dr. Mullin) and the Scleroderma Foundation (grant to Dr. Mathai). The PHAROS registry is supported by the Scleroderma Foundation, the Sibley Hospital Foundation, Actelion, and Gilead.

[1]Christopher J. Mullin, MD, MHS: Warren Alpert Medical School of Brown University, Providence, Rhode Island; [2]Rubina M. Khair, MD, MPH, Rachel L. Damico, MD, PhD, Todd M. Kolb, MD, PhD, Laura K. Hummers, MD, ScM, Paul M. Hassoun, MD, Stephen C. Mathai, MD, MHS: The Johns Hopkins University School of Medicine, Baltimore, Maryland; [3]Virginia D. Steen, MD: Georgetown University, Washington, DC.

Dr. Damico has received honoraria from the Pulmonary Hypertension Association (less than $10,000) and consulting fees from Gerson Lehrman Group and Putman Associates (less than $10,000 each). Ms Steen has received consulting fees from CSL Behring, Bayer, and Reata (less than $10,000 each). Dr. Mathai has received consulting fees, speaking fees, and honoraria from Actelion, Arena, and United Therapeutics (less than $10,000 each). No other disclosures relevant to this article were reported.

Address correspondence to Stephen C. Mathai, MD, MHS, Johns Hopkins University School of Medicine Division of Pulmonary and Critical Care Medicine, 1830 East Monument Street, Baltimore, MD. E-mail: smathai4@jhmi.edu.

Submitted for publication May 2, 2018; accepted in revised form April 30, 2019.

perturbations, yet more impaired right ventricular function at any given afterload, as assessed noninvasively with serum measurements of N-terminal pro–brain natriuretic peptide (NT-proBNP) (5) and invasively by direct measurements of contractility (6). Importantly, survival is worse in SSc-PAH compared to both IPAH (4) and non-SSc connective tissue disease–associated PAH (CTD-PAH) (7,8). Since prediction of survival has become an emerging area of research in PAH and survival prediction tools are being used in clinical practice, it is important to understand whether these tools are valid in clinically important and distinct disease subtypes such as SSc-PAH.

The Registry to Evaluate Early and Long-term PAH Disease Management (REVEAL) prognostic equation and risk score calculator are recently developed tools for predicting 1-year survival in PAH (9,10). The predictive algorithm and risk score were developed using prospectively gathered data from the REVEAL Registry, a multicenter, observational US-based registry established in part to identify predictors of short- and long-term survival in PAH (11). Clinical and hemodynamic variables independently associated with survival were identified using multivariable Cox proportional hazards modeling, and were combined into a prognostic equation and risk score containing 19 parameters (9,10). The prognostic equation results in an estimation of the predicted 1-year survival, whereas the risk score has an integer value between 0 and 22, with higher scores corresponding to a lower predicted probability of 1-year survival.

The cohort of 2,716 patients in the REVEAL Registry used for model development included 648 patients with CTD-PAH (23.9%), of whom 366 (13.5%) had SSc-PAH. The SSc-PAH and non-SSc CTD-PAH groups were reported as having similar risk estimates according to the multivariable Cox proportional hazards survival analysis, and thus these groups were combined together in the final models. In addition, as the REVEAL Registry cohort used for model development included just 13.5% of patients with newly diagnosed PAH, the prognostic equation and risk score were subsequently validated in a supplemental cohort from the REVEAL Registry that consisted of 504 patients with newly diagnosed PAH (10). In this combined REVEAL Registry cohort, only 500 patients had SSc-PAH (15.5% of the combined cohort), of whom 166 were newly diagnosed as having PAH (8). Subsequent studies that have validated the REVEAL models have involved similarly small proportions of SSc-PAH patients in their validation cohorts (12,13).

Given the known clinical differences between SSc-PAH and other PAH subtypes, and the small proportion of patients with incident SSc-PAH in the REVEAL Registry cohort, we hypothesized that the developed predictive algorithm may not be valid in newly diagnosed SSc-PAH. Therefore, we aimed to evaluate the predictive accuracy of the REVEAL prognostic equation and risk score calculator in patients with incident SSc-PAH.

PATIENTS AND METHODS

Validation cohort. Patients in the validation cohort were those with newly diagnosed SSc-PAH from 2 different cohorts, the Johns Hopkins Pulmonary Hypertension Program (JHPHP) Registry, and the multicenter Pulmonary Hypertension Assessment and Recognition of Outcome in Scleroderma (PHAROS) Registry. Patients included from the JHPHP were consecutive patients with SSc who were newly diagnosed as having PAH by right-sided heart catheterization (RHC) from January 1, 2000 until July 1, 2015. The diagnosis of SSc was made by a rheumatologist at the Johns Hopkins Scleroderma Center, with the diagnosis being based on specific criteria, as previously reported (4). The diagnosis of PAH was made based on RHC findings indicating a resting mean pulmonary arterial pressure (mPAP) of ≥25 mm Hg and a pulmonary arterial wedge pressure (PAWP) of ≤15 mm Hg (14). Patients were excluded if they had evidence of either obstructive lung disease (defined as a ratio of forced expiratory volume in 1 second [FEV1] to forced vital capacity [FVC] of <70% predicted, and an FEV1 of <60% predicted) or interstitial lung disease (defined as a total lung capacity [TLC] of <60% predicted or TLC of between 60% and 70% predicted, and chest computed tomography [CT] showing more than mild fibrosis, following a similar methodology as that used by Goh et al [15]). Patients were also excluded if they were diagnosed as having a rheumatic overlap syndrome, were previously treated with active drugs for PH, or were included in the initial REVEAL Registry. Clinical assessment of World Health Organization (WHO) functional class, pulmonary function test results, 6-minute walk test (6MWT) distance (6MWD), chest CT, echocardiogram reports, serum laboratory analyses, vital signs, and hemodynamic measurements from RHC were obtained from the patients' clinical records.

The PHAROS Registry is a North American multicenter, prospective, observational study that was established in 2006 with the aim of understanding the natural history of PH development and progression in SSc (16). Inclusion criteria and patient information collected have been previously published (16). Patients with an established diagnosis of SSc were enrolled if they were diagnosed as having PH within the previous 6 months or if they were classified as being at increased risk for developing PAH based on a reduced lung diffusing capacity for carbon monoxide (DL_{CO}), elevated ratio of FVC to DL_{CO}, or an elevated estimate of right ventricular systolic pressure on echocardiography. Patient data were extracted on May 2, 2016. Patients were excluded if they had a PAWP of >15 mm Hg, a TLC of <60% predicted, or TLC of between 60% and 70% predicted and chest CT showing more than mild fibrosis (as previously described [17]), following a similar methodology as that of Goh et al (15). If the TLC value was missing, then the FVC was used in its place.

As Johns Hopkins is a site in the PHAROS Registry, patients from Johns Hopkins were removed from the PHAROS cohort, since clinical information for these patients was more

complete in the JHPHP Registry than in the PHAROS Registry. It is worth noting that 3 of the 19 parameters in the REVEAL risk score—right atrial pressure (RAP), heart rate, and systolic blood pressure (BP)—are not recorded in the PHAROS Registry. For both cohorts, the estimated glomerular filtration rate (eGFR) was calculated using the Modified Diet in Renal Disease equation (18), and renal dysfunction was defined as an eGFR of <60 ml/minute/1.73 m^2.

Survival analysis. For all patients in the JHPHP cohort, the time at risk began at the date of RHC diagnosis of PAH, as all patients were enrolled in the registry at the time of or before their RHC. Death was determined by clinical records and the Social Security Death Index (SSDI), and all causes of death were included. Patients were administratively censored at 1 year or censored at their last clinical encounter if they were lost to follow-up prior to 1 year. In the PHAROS Registry, the time at risk began at the date of the diagnostic RHC for individuals whose catheterization occurred after their enrollment into the registry. For patients enrolled in the registry after their diagnosis of PAH, the time at risk began at the time of study enrollment, in order to avoid immortal person-time bias. Subjects were administratively censored at 1 year or censored at their last clinical encounter if that occurred before 1 year from the beginning of their time at risk. Death in the PHAROS Registry was assessed by individual study sites using clinical records and the SSDI. Kaplan-Meier curves and estimates were used to assess survival up to and at 1 year.

REVEAL prognostic equation and risk score calculations. The REVEAL prognostic equation and risk score were tabulated for each patient in the validation cohort using the methods described by the REVEAL investigators (9,10). Nineteen parameters were assessed in each patient (Table 1) at the beginning of time at risk or prior to the time at risk. Patients for whom data were missing for a specific parameter were assigned to the reference group, as specified by, and accounted for, in the REVEAL model development (9). Each patient's predicted probability of 1-year survival was calculated as $S_0(1)^{\exp(Z'\beta\gamma)}$, where $S_0(1)$ indicates the baseline survival at 1 year, $S_0(1) = 0.9698$, and $Z'\beta\gamma$ indicates the prognostic index, which is the product of the shrinkage coefficient, $\gamma = 0.939$, and the $Z'\beta$, the sum of all β coefficients of the 19 parameters in the model. Based on the individual's predicted probability of 1-year survival using the prognostic equation, patients were stratified into 5 risk groups: low risk (≥95%), average risk (90 to <95%), moderately high risk (85 to <90%), high risk (70 to <85%), and very high risk (<70%).

The REVEAL risk score is calculated using the same 19 parameters. Each patient begins with a score of 6, and has 1 or 2 points added or subtracted for each parameter (Table 1). Patients are similarly stratified into 5 risk groups: low risk (score of 1–7), average risk (score of 8), moderately high risk (score of 9), high risk (score of 10–11), and very high risk (score of ≥12).

Table 1. Parameters for the REVEAL prognostic equation and risk score*

	Prognostic equation β	Risk score
WHO group I subgroup		
FPAH	+0.7737	+2
APAH-PoPH	+1.2081	+2
APAH-CTD	+0.4624	+1
Demographic, male age >60 years	+0.7779	+2
Comorbidity, renal insufficiency	+0.6422	+1
WHO functional class		
Class I	−0.8740	−2
Class III	+0.3454	+1
Class IV	+1.1402	+2
Vital signs		
Systolic BP <110 mm Hg	+0.5128	+1
Heart rate >92 bpm	+0.3322	+1
6MWD		
≥440 meters	−0.5455	−1
<165 meters	+0.5210	+1
BNP		
<50 pg/ml or NT-proBNP <300 pg/ml	-0.6922	-2
>180 pg/ml or NT-proBNP >1,500 pg/ml	+0.6791	+1
Echocardiography, any pericardial effusion	+0.3014	+1
Pulmonary function test		
DL_{CO} ≥80% predicted	−0.5317	−1
DL_{CO} ≤32% predicted	+0.3756	+1
Right-sided heart catheterization		
RAP >20 mm Hg	+0.5816	+1
PVR >32 Wood units	+1.4062	+2

* For the prognostic equation, the probability of 1-year survival was calculated as $S_0(1)^{\exp(Z'\beta\gamma)}$, where the baseline survival at 1 year, $S_0(1)$, is 0.9698, the shrinkage coefficient, γ, is 0.939, and the $Z'\beta$ is the sum of all β coefficients in the prognostic equation column. The risk score is calculated by beginning with a score of 6 and then summing the points in the risk score column. REVEAL= Registry to Evaluate Early and Long-term Pulmonary Arterial Hypertension Disease Management; WHO = World Health Organization; FPAH = familial pulmonary arterial hypertension; APAH = associated pulmonary arterial hypertension; PoPH = portopulmonary hypertension; CTD = connective tissue disease; BP = blood pressure; bpm = beats per minute; 6MWD= distance on the 6-minute walk test; BNP = brain natriuretic peptide; NT-proBNP = N-terminal pro–brain natriuretic peptide; DL_{CO} = lung diffusing capacity for carbon monoxide; RAP = right atrial pressure; PVR = pulmonary vascular resistance.

Model validation. To assess the predictive accuracy of the model, several analyses were performed to assess model fit, discrimination, and calibration. To evaluate model fit, the Cox proportional hazards regression coefficient of the prognostic index ($Z'\beta\gamma$) was estimated, which is sometimes referred to as the "calibration slope", calculated as $\ln h(t) = \ln h_0(t) + \beta(Z'\beta\gamma)$. A regression coefficient of 1 indicates that discrimination in the validation cohort is equal to that in the derivation cohort, whereas a regression coefficient of >1 or <1 indicates better or poorer discrimination, respectively, in the validation data set (19).

Model fit was assessed by examining the differences in the regression coefficients between the derivation and validation data sets, using a Cox proportional hazards regression on the covariates in the model, with an offset of the prognostic index, calculated as $\ln h(t) = \ln h_0(t) + x'\beta^* + (Z'\beta\gamma)$. Values for the offset coefficients (β^*) in this regression model represent the differences between the

β* coefficients estimated in the model fitted to the derivation data set and those estimated in the model fitted to the validation data set (19). A global test to determine whether all of the β* values equaled zero was performed to assess overall model fit, which can limit the possibility of inflating Type I error by testing each individual β* value of 0. The *P* values resulting from both regression analyses are anticonservative, in that they do not account for the uncertainty in the estimated regression coefficients of the prognostic index (19).

To further assess model discrimination, Harrell's C-index of concordance was calculated for both the prognostic index and the risk score. Harrell's C-index represents the proportion of patient pairs in which the outcome and the predictions are concordant (19). This is analogous to the area under the receiver operating characteristic curve; however, in survival analysis, it accounts for the time to events. The C-index represents the probability that a randomly selected person who dies will have a lower probability of survival than a randomly selected person who is still alive (and not censored) at the time of the death. The C-index was reported both in the derivation of the REVEAL prediction model (9) and in the subsequent validation in patients with newly diagnosed PAH (10); the values are directly comparable.

Kaplan-Meier survival curves were produced for the validation cohort, which was stratified into the 5 risk groups by both the prognostic equation and the risk score. Hazard ratios for each of the 5 risk groups were estimated using a Cox proportional hazards regression, with the low risk group as the reference group.

Model calibration was assessed using 2 types of calibration plots. First, the validation cohort was stratified into the 5 risk groups by both the prognostic equation and the risk score, and Kaplan-Meier estimates of observed 1-year survival were plotted against predicted 1-year survival as estimated by the prognostic equation.

Table 2. Baseline characteristics of the patients from the Johns Hopkins Pulmonary Hypertension Program (JHPHP) and Pulmonary Hypertension Assessment and Recognition of Outcome in Scleroderma (PHAROS) cohorts*

	No. of patients assessed	JHPHP (n = 117)	No. of patients assessed	PHAROS (n = 175)	*P*
Age, mean ± SD years	117	62.3 ± 11.6	171	60 ± 11	0.03
Sex, female	117	95 (81.2)	171	152 (88.9)	0.07
Race	117		170		0.06
White		98 (83.8)		134 (78.8)	
African American		15 (12.8)		20 (11.8)	
Hispanic		0 (0)		11 (6.5)	
Asian/Pacific Islander		1 (0.8)		3 (1.8)	
Other		3 (2.6)		2 (1.1)	
Type of SSc	117		175		0.003
Limited		101 (86.3)		123 (69.9)	
Diffuse		16 (13.7)		45 (25.7)	
Unclassified		0 (0)		7 (4.0)	
WHO functional class	117		170		0.03
Class I		7 (6.0)		24 (14.1)	
Class II		41 (35.0)		69 (40.6)	
Class III		64 (54.7)		66 (38.8)	
Class IV		5 (4.3)		11 (6.5)	
6MWD, median (IQR) meters	77	319.1 (133.5)	137	365.9 (175.0)	0.04
BNP, median (IQR) pg/ml	3	192.1 (222.4)	71	134 (477)	0.65
NT-proBNP, median (IQR) pg/ml	81	942 (1,712)	46	331.5 (2,163)	0.06
Pericardial effusion, any	110	43 (39.1)	162	54 (33.3)	0.33
eGFR <60 ml/minute/1.73m^2	98	43 (43.9)	155	57 (36.8)	0.27
FVC, mean ± SD % predicted	104	84.1 ± 16.7	164	83.6 ± 15.2	0.64
TLC, mean ± SD % predicted	73	88.7 ± 14.9	133	84.8 ± 15.1	0.08
DLco, mean ± SD % predicted	98	51.4 ± 18.5	158	42.5 ± 15.9	0.0002
Systolic BP, mean ± SD mm Hg	106	128 ± 24	–	–	–
Heart rate, mean ± SD bpm	113	79 ± 12	–	–	–
Right atrial pressure, mean ± SD mm Hg	116	8 ± 4	–	–	–
Pulmonary arterial pressure, mean ± SD mm Hg	117	40 ± 12	175	37 ± 10	0.11
Pulmonary arterial wedge pressure, mean ± SD mm Hg	117	10 ± 3	175	10 ± 3	0.87
Cardiac output, mean ± SD liters/minute	117	4.49 ± 1.55	174	5.04 ± 1.68	0.005
Cardiac index, mean ± SD liters/minute/m^2	117	2.51 ± 0.80	–	–	–
PVR, mean ± SD Wood units	117	8.10 ± 5.66	174	6.46 ± 4.51	0.006

* Comparisons between groups were made using Student's *t*-test, Mann-Whitney U test, or chi-square test, where appropriate. Except where indicated otherwise, values are the number (%) of patients. SSc = systemic sclerosis; WHO = World Health Organization; 6MWD = distance on the 6-minute walk test; BNP = brain natriuretic peptide; NT-proBNP = N-terminal pro–brain natriuretic peptide; eGFR = estimated glomerular filtration rate; FVC = forced vital capacity; TLC = total lung capacity; DLco = lung diffusing capacity for carbon monoxide; BP = blood pressure; PVR = pulmonary vascular resistance.

Second, the baseline survival function was estimated in the validation data set, and then smoothed by fitting as a fractional polynomial. Average predicted survival curves were then generated for each risk group and plotted against observed survival points as estimated by the Kaplan-Meier method. Because these calibration plots use the baseline survival function estimated on the validation data set (instead of the derivation data set), this has been termed a partial validation (20).

All statistical analyses were performed using Stata MP, version 12.1 (Stata Statistical Software release 12; StataCorp).

RESULTS

Patient characteristics. A total of 292 patients were included in the validation cohort, 117 from the JHPHP Registry and 175 from the PHAROS Registry. The baseline characteristics of these cohorts are shown in Table 2. In both cohorts, patients were predominantly female and white, and had WHO functional class II or III disease. The mean age was >60 years. There were several key differences between these 2 cohorts; as compared to the PHAROS Registry, the patients in the JHPHP cohort were older, more likely to have limited SSc, had a worse functional class, had a shorter distance on the 6MWT (6MWD), had a higher DL_{CO}, and had worse hemodynamics (lower cardiac output and higher pulmonary vascular resistance [PVR]).

The mean REVEAL risk score was greater in patients in the JHPHP cohort than in the PHAROS Registry cohort (mean ± SD risk score 9 ± 2 versus 8 ± 2; $P = 0.005$). However, as the PHAROS Registry does not record heart rate, systolic BP, or RAP, no patients in the PHAROS Registry received points for these variables. No patients in the JHPHP had a RAP of >20 mm Hg, and no patients in either cohort had a PVR of >32 Wood units (WU).

Results of survival analysis. A total of 36 deaths were observed, and the overall 1-year survival rate was 87.4% (95% CI 82.9–90.7%). Fourteen patients were lost to follow-up before 1 year, 6 in the JHPHP cohort and 8 in the PHAROS Registry. Figure 1 displays the Kaplan-Meier survival curves for the 5 risk groups stratified by the REVEAL prognostic equation (Figure 1A) and the REVEAL risk score (Figure 1B).

Estimates of model validation. The calibration slope, or regression coefficient of the prognostic index (Z'βγ), was 0.707 (95% CI 0.400–1.014), and the test for a coefficient of 1 resulting in a P value of 0.06 indicated a borderline, but acceptable model fit for the prognostic equation. The C-indexes for both the prognostic equation and the risk score are presented in Table 3, along with C-indexes in the REVEAL cohorts and 2 other studies that evaluated REVEAL model performance (12,13). In predicting 1-year survival in patients newly diagnosed as having SSc-PAH, these estimates with the 2 REVEAL survival prediction tools indicated very good discrimination, and demonstrated that the C-indexes in our validation cohort were similar to those in the REVEAL cohorts and the other validation studies.

Hazard ratios for the probability of 1-year survival across the 5 risk groups stratified by the prognostic equation and the risk score are shown in Table 4. Similar to that shown in Figure 1, patients classified into the high risk group by either the prognostic equation or the risk score appeared to have the worst survival, although the hazard ratios had large and overlapping confidence intervals. This suggests that while overall discrimination was very good, discrimination for those patients at higher risk may not be as accurate.

In the regression analysis with the prognostic index offset (data not shown), the joint test, in which the offset coefficients of the 14 covariables included in the model equaled zero, resulted in a chi-square value of 25.22 ($P = 0.03$), indicative of a marginal

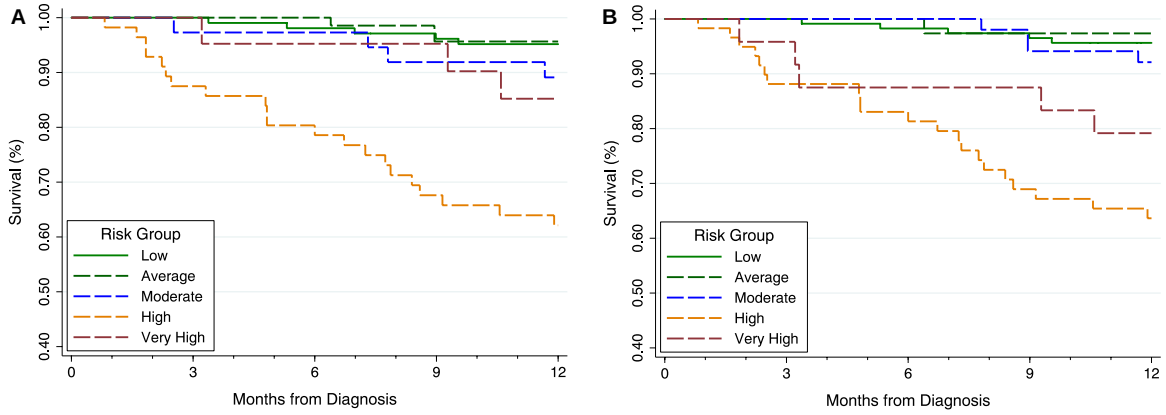

Figure 1. Kaplan-Meier estimates of survival over 1 year in patients with newly diagnosed systemic sclerosis–associated pulmonary arterial hypertension in the validation cohort, stratified by Registry to Evaluate Early and Long-term Pulmonary Arterial Hypertension Disease Management (REVEAL) risk groups according to the REVEAL prognostic equation (**A**) and the REVEAL risk score (**B**). Low risk is defined as a predicted probability of 1-year survival of ≥95%, average risk as predicted survival of 90 to <95%, moderately high risk as predicted survival of 85 to <90%, high risk as predicted survival of 70 to <85%, and very high risk as predicted survival of <70%.

Table 3. Comparison of Harrell's C-index among the derivation and validation cohorts*

Cohort [ref.]	Harrell's C-index (95% CI)	
	Prognostic equation	Risk score
REVEAL (derivation) [9]	0.744	0.735
REVEAL (supplemental) [10]	0.726	0.724
FPHN [13]	–	0.73 (0.69–0.77)
UCSF [12]	0.765 (0.565–0.965)	–
JHPHP	0.727 (0.618–0.836)	0.720 (0.612–0.828)
PHAROS	0.722 (0.593–0.850)	0.748 (0.624–0.872)
Combined	0.734 (0.652–0.816)	0.743 (0.663–0.823)

* Harrell's C-index represents the proportion of patient pairs in which the outcome and the predictions are concordant, and is analogous to the area under the receiver operating characteristic curve, except that it accounts for time to events. 95% CI = 95% confidence interval; REVEAL= Registry to Evaluate Early and Long-term Pulmonary Arterial Hypertension Disease Management; FPHN = French Pulmonary Hypertension Network; UCSF = University of Caliifornia San Francisco; JHPHP = Johns Hopkins Pulmonary Hypertension Program; PHAROS = Pulmonary Hypertension Assessment and Recognition of Outcome in Scleroderma.

model fit. The β* for a 6MWD of <165 meters was 1.8012 (95% CI –3.3216 to –0.2808; P = 0.02), and the β* for a high BNP serum level (BNP >180 pg/ml or NT-proBNP >1,500 pg/ml) was 1.2763 (95% CI –2.1262 to –0.4263; P = 0.003). These were the only 2 covariables whose individual β* values significantly differed from 0 in the offset regression model, indicating that the model fit of these 2 variables in the validation cohort was poor. In both cases, these coefficients were negative, meaning that the hazard assigned to these covariables in the original model was not seen in this validation data set. Put another way, a lower distance on the 6MWT and a higher serum level of BNP or NT-proBNP were not as strongly associated with poorer survival in the multivariable model in our validation cohort as they were in the REVEAL model development cohort.

Calibration curves are presented in Figure 2. Observed versus predicted survival rates at 1 year are shown for each of the risk groups stratified by the prognostic index (Figure 2A) and the risk score (Figure 2B). These, along with the "partial validation" plots of observed and predicted survival rates (Figures 2C and D), show that observed survival was lower than predicted for the high risk group, but higher than predicted for the very high risk group. These findings are consistent with the hazard ratios across groups (Table 4), suggesting that both model discrimination and calibration were not as accurate for the patients in the highest risk groups.

DISCUSSION

Our results show that when applied to a cohort of patients with newly diagnosed SSc-PAH, the REVEAL prognostic equation and risk score for the probability of 1-year survival offer similar measures of overall discrimination as they did in the original model development cohort. However, discrimination and calibration appear to be less accurate in patients in the highest risk groups, indicating that the REVEAL prediction model may not perform adequately in separating and predicting survival in the newly diagnosed SSc-PAH patients with high-risk features and the lowest predicted probabilities of 1-year survival.

Compared to the REVEAL cohort of SSc-PAH patients (both newly and previously diagnosed) (8), our validation cohort of patients with newly diagnosed SSc-PAH was similar in age, sex, WHO functional class, and 6MWD, but had a higher prevalence of renal dysfunction. Our cohort had a lower average mPAP, lower PVR, and higher cardiac output than the REVEAL SSc-PAH patients. Although these differences may be explained by the fact that a population of newly diagnosed PAH patients was compared to one with both newly and previously diagnosed PAH patients, the 1-year survival in our cohort was demonstrably higher than that of the newly diagnosed SSc-PAH patients in the REVEAL Registry (87% versus 76% [8]). There are several possible explanations for this, including earlier diagnosis of PAH in SSc, differences in treatment of PAH (21,22), or better exclusion of interstitial lung disease (ILD) in our cohort compared to the REVEAL Registry cohort. While all of the subjects in our cohort had chest CT scans, only 72% of the scans were interpreted using the Goh criteria. Thus, it is possible that some patients with significant ILD were included. However, with the exclusion criteria for ILD employed in the current study, our cohort had a higher FVC, on average, than

Table 4. Hazard ratios for probability of 1-year survival across REVEAL risk groups*

Risk group	Prognostic equation		Risk score	
	No. of patients	Hazard ratio (95% CI)	No. of patients	Hazard ratio (95% CI)
Low	105	Referent	116	Referent
Average	73	0.90 (0.21–3.75)	41	0.60 (0.07–5.12)
Moderate	37	2.30 (0.62–8.57)	52	1.79 (0.48–6.68)
High	56	9.89 (3.73–26.25)	59	10.30 (3.88–27.34)
Very high	21	3.15 (0.75–13.18)	24	5.27 (1.53–18.21)

* Using the low risk group as the referent, Cox proportional hazard ratios were calculated for each of the risk groups determined by both the prognostic equation and the risk score. REVEAL = Registry to Evaluate Early and Long-term Pulmonary Arterial Hypertension Disease Management; 95% CI = 95% confidence interval.

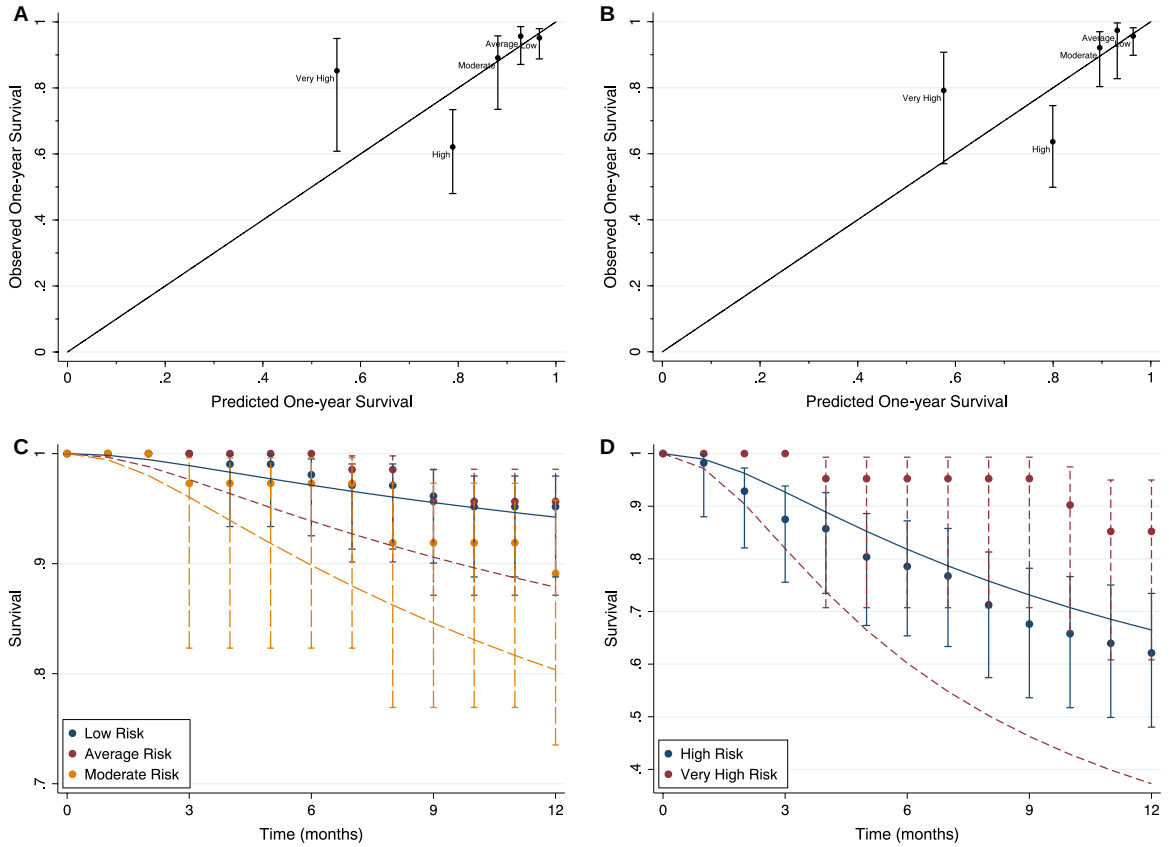

Figure 2. Calibration plots of observed versus predicted survival at 1 year in each of the 5 risk groups stratified by the Registry to Evaluate Early and Long-term Pulmonary Arterial Hypertension Disease Management (REVEAL) prognostic index (**A**) and REVEAL risk score (**B**), and in the partial validation data sets of low, average, and moderate risk groups (**C**) and high and very high risk groups (**D**). Predicted survival curves were estimated using the baseline hazard function of the validation cohort and smoothed as a fractional polynomial, and average predicted survival curves (dashed lines) were generated for each risk group defined by the REVEAL prognostic equation. Observed survival, as estimated using Kaplan-Meier methods, is plotted at every month for each of the 5 risk groups. Low risk is defined as a predicted probability of 1-year survival of ≥95%, average risk as predicted survival of 90 to <95%, moderately high risk as predicted survival of 85 to <90%, high risk as predicted survival of 70 to 85%, and very high risk as predicted survival of <70%. Color figure can be viewed in the online issue, which is available at http://onlinelibrary.wiley.com/doi/10.1002/art.40918/abstract.

the SSc-PAH REVEAL cohort (mean ± SD predicted FVC 84 ± 16% versus 72 ± 18% [8]). As survival is worse in SSc patients with PH related to ILD than in patients with SSc-PAH (23), inclusion of SSc patients with ILD in REVEAL may partly explain this difference in survival.

Other strengths of our study include the exclusion of patients with obstructive lung disease, and our criteria for defining SSc. We used the FEV1:FVC ratio to exclude patients with obstructive lung disease, which was reported in >20% of patients in the REVEAL Registry (24). In our validation cohort, the diagnosis of SSc was established by rheumatologists using internationally accepted diagnostic criteria. The PHAROS Registry was developed and is maintained by rheumatologists, and requires diagnosis of SSc based on fulfillment of either the American College of Rheumatology (ACR) criteria for SSc or the LeRoy definitions of limited cutaneous or diffuse cutaneous SSc (16). All patients in the JHPHP cohort were diagnosed using the ACR criteria by a rheumatologist at the Johns Hopkins Scleroderma Center. Given the differences in survival between patients with SSc-PAH and other forms of non-SSc CTD-PAH (7,8), establishment of a correct rheumatologic diagnosis is important for survival prediction.

In general, validating a prognostic model means establishing that the model works satisfactorily for patients other than those from which the model was derived (25). However, rather than considering validation as a test by which a model passes or fails, some have proposed that it is more helpful to view validation as an unbiased estimate of the prediction error in a model (25,26). Instead of asking, "Are the REVEAL prediction models valid in newly diagnosed SScPAH?", it may be more insightful to ask, "What are the errors in prediction for the REVEAL models when applied to an external cohort of patients with newly diagnosed SScPAH?" When viewed through this lens, the results of our statistical validation, particularly that of model fit, may be explained by some of the clinical differences between SSc-PAH and other forms of PAH.

Assessment of model fit showed that the risk assigned in the REVEAL prediction models to a low 6MWD and a high BNP/NT-proBNP serum level was not seen in our validation cohort. Patients with SSc can have exercise limitations in the absence of known pulmonary involvement (27), and the 6MWD has been shown to be correlated with disease activity and quality of life in SSc (28). The minimal clinically important difference for change in the 6MWD is smaller in CTD-PAH than in other forms of PAH (29). Given that there are differences in the 6MWT between types of PAH, and that SSc patients can have limitations on the 6MWT related to musculoskeletal involvement, it is not surprising that the risk assigned to a low 6MWD is different in SSc-PAH than in PAH in general.

Similarly, there are differences in the serum levels of NT-proBNP between SSc-PAH and other types of PAH. Compared to patients with IPAH, patients with SSc-PAH have higher NT-proBNP levels despite less severe hemodynamics (30), and therefore it is perhaps not unexpected that an elevated NT-proBNP serum level did not carry the same risk in our validation cohort as it did in the REVEAL derivation cohort. Of the 21 patients in the very high risk group (based on the prognostic equation), 19 had an elevated BNP/NT-proBNP serum level, and 9 of the 19 patients with a low 6MWD were in the very high risk group. Thus, the lower-than-predicted mortality seen in the very high risk group may be partly attributable to the fact that a low 6MWD and high BNP/NT-proBNP serum level were driving the categorization of very high risk.

There are a few limitations of our study. First, there were important differences in the use of BNP versus NT-proBNP between the REVEAL, JHPHP, and PHAROS cohorts. The REVEAL Registry was designed to use BNP, for which NT-proBNP was substituted only for patients who had missing data on BNP levels. In the original derivation cohort, 1,340 patients (49.3%) had data on BNP levels, and only 208 patients (7.7%) had data on NT-proBNP levels. In the JHPHP, NT-proBNP levels are used preferentially over BNP, and thus only 3 patients (2.6%) in the JHPHP cohort had data on BNP levels, and NT-proBNP levels were used in 81 patients (69.1%). In the PHAROS cohort, 71 patients (40.3%) had data on BNP levels, and NT-proBNP levels were used in 37 patients (21.0%). The more frequent use of NT-proBNP in our cohort could explain some of the model performance, particularly since the coefficient for a high BNP/NT-proBNP serum level indicated a poor model fit. However, we used the REVEAL model as intended and developed, and thus this is likely to be more a limitation of the REVEAL model performance than of our validation study.

Second, while current guidelines use PVR in the definition of PAH (31,32), we included all patients with an mPAP of ≥25 mm Hg and a PAWP of ≤15 mm Hg, regardless of PVR. Our validation cohort included 54 patients (18.5%) with a PVR of <3 WU. A sensitivity analysis to assess model validation in only those patients with a PVR of >3 WU demonstrated similar C-indexes, as well as similar model fit and model calibration. As the REVEAL and PHAROS Registries completed enrollment before the use of PVR in the definition of PAH, we elected to include all patients who otherwise met the diagnostic criteria for PAH apart from PVR.

Third, there were issues with missing data in our validation cohort, the most concerning of which was the complete absence of 3 parameters (RAP, heart rate, and systolic BP) in the PHAROS cohort. An RAP of >20 mm Hg was not seen in any patients in the JHPHP cohort, and as a rather extreme cutoff, its absence is much less problematic than the absences of heart rate and systolic BP. All 3 of these variables are associated with an increased risk, so it is possible that their systematic absence may have biased predictions toward a lower predicted mortality in the PHAROS cohort. As a sensitivity analysis, heart rate and systolic BP values were imputed into the PHAROS cohort based on data from the JHPHP cohort. With this, there was no significant change in the calibration slope or the C-indexes for either the prognostic equation or the risk score. Similarly, there were no differences in model fit, the hazard ratios across risks groups, or visual inspection of calibration plots with imputed heart rate and systolic BP values. Thus, missing data likely did not contribute to model performance, mostly because the REVEAL prediction models were developed to account for missing data by including patients with missing data in the reference group for every parameter.

Furthermore, the calibration plots (shown in Figure 3) used the baseline survival function from the validation cohort to generate the predicted survival curves. It is possible that the baseline survival functions were different between this validation cohort and the REVEAL derivation cohort. That being said, this method provided a similar depiction of predicted survival compared to the calibration plots of predicted versus observed survival at 1 year (see Figures 2A and B).

Finally, this validation was performed only for patients newly diagnosed as having SSc-PAH, and examined survival to 1 year. Further investigation would be necessary to assess the model's performance for longer-term outcomes or in assessing 1-year survival from any given time point in prevalent SSc-PAH.

In addition to the REVEAL prediction models, a risk assessment tool was proposed in the 2015 European pulmonary hypertension guidelines (32), and this tool has been validated in several cohorts (33–36), of which 2 comprised exclusively patients with SSc-PAH (35,36). This European Respiratory Society/European Society of Cardiology prediction tool differs from the REVEAL models in that it was not as rigorously derived, there is no prescribed way to implement overall risk stratification, and it does not provide predicted survival probabilities.

In summary, the REVEAL prognostic equation and risk score calculator provided measures of overall discrimination in predicting 1-year survival in a cohort of newly diagnosed SSc-PAH patients with results similar to those in the REVEAL cohort. However, model performance was marginal for patients in the highest risk groups,

which is partly explained by poor model fit for the risk attributed to a low 6MWD and a high BNP/NT-proBNP serum level. Use of the REVEAL prediction models for estimating the probability of 1-year survival in patients with SSc-PAH should be done with these caveats in mind, and further investigation to better predict survival in this unique and distinct disease subtype is warranted.

AUTHOR CONTRIBUTIONS

All authors were involved in drafting the article or revising it critically for important intellectual content, and all authors approved the final version to be published. Dr. Mathai had full access to all of the data in the study and takes responsibility for the integrity of the data and the accuracy of the data analysis.

Study conception and design. Mullin, Mathai.

Acquisition of data. Mullin, Khair, Damico, Kolb, Hummers, Hassoun, Steen, Mathai.

Analysis and interpretation of data. Mullin, Mathai.

REFERENCES

1. Hachulla E, Gressin V, Guillevin L, Carpentier P, Diot E, Sibilia J, et al. Early detection of pulmonary arterial hypertension in systemic sclerosis: a French nationwide prospective multicenter study. Arthritis Rheum 2005;52:3792–800.
2. Hunzelmann N, Genth E, Krieg T, Lehmacher W, Melchers I, Meurer M, et al. The registry of the German Network for Systemic Scleroderma: frequency of disease subsets and patterns of organ involvement. Rheumatology (Oxford) 2008;47:1185–92.
3. Steen VD, Medsger TA. Changes in causes of death in systemic sclerosis, 1972–2002. Ann Rheum Dis 2007;66:940–4.
4. Fisher MR, Mathai SC, Champion HC, Girgis RE, Housten-Harris T, Hummers L, et al. Clinical differences between idiopathic and scleroderma-related pulmonary hypertension. Arthritis Rheum 2006;54:3043–50.
5. Mathai SC, Bueso M, Hummers LK, Boyce D, Lechtzin N, Le Pavec J, et al. Disproportionate elevation of N-terminal pro-brain natriuretic peptide in scleroderma-related pulmonary hypertension. Eur Respir J 2010;35:95–104.
6. Tedford RJ, Mudd JO, Girgis RE, Mathai SC, Zaiman AL, Housten-Harris T, et al. Right ventricular dysfunction in systemic sclerosis-associated pulmonary arterial hypertension. Circ Hear Fail 2013;6:953–63.
7. Condliffe R, Kiely DG, Peacock AJ, Corris PA, Gibbs JS, Vrapi F, et al. Connective tissue disease-associated pulmonary arterial hypertension in the modern treatment era. Am J Respir Crit Care Med 2009;179:151–7.
8. Chung L, Farber HW, Benza R, Miller DP, Parsons L, Hassoun PM, et al. Unique predictors of mortality in patients with pulmonary arterial hypertension associated with systemic sclerosis in the REVEAL Registry. Chest 2014;146:1494–504.
9. Benza RL, Miller DP, Gomberg-Maitland M, Frantz RP, Foreman AJ, Coffey CS, et al. Predicting survival in pulmonary arterial hypertension: insights from the Registry to Evaluate Early and Long-Term Pulmonary Arterial Hypertension Disease Management (REVEAL). Circulation 2010;122:164–72.
10. Benza RL, Gomberg-Maitland M, Miller DP, Frost A, Frantz RP, Foreman AJ, et al. The REVEAL Registry risk score calculator in patients newly diagnosed with pulmonary arterial hypertension. Chest 2012;141:354–62.
11. McGoon MD, Krichman A, Farber HW, Barst RJ, Raskob GE, Liou TG, et al. Design of the REVEAL Registry for US patients with pulmonary arterial hypertension. Mayo Clin Proc 2008;83:923–31.
12. Cogswell R, Kobashigawa E, McGlothlin D, Shaw R, De Marco T. Validation of the Registry to Evaluate Early and Long-Term Pulmonary Arterial Hypertension Disease Management (REVEAL) pulmonary hypertension prediction model in a unique population and utility in the prediction of long-term survival. J Heart Lung Transplant 2012;31:1165–70.
13. Sitbon O, Benza RL, Badesch DB, Barst RJ, Elliott CG, Gressin V, et al. Validation of two predictive models for survival in pulmonary arterial hypertension. Eur Respir J 2015;46:152–64.
14. Simonneau G, Gatzoulis MA, Adatia I, Celermajer D, Denton C, Ghofrani A, et al. Updated clinical classification of pulmonary hypertension. J Am Coll Cardiol 2013;62 Suppl:D34–41.
15. Goh NS, Desai SR, Veeraraghavan S, Hansell DM, Copley SJ, Maher TM, et al. Interstitial lung disease in systemic sclerosis: a simple staging system. Am J Respir Crit Care Med 2008;177:1248–54.
16. Hinchcliff M, Fischer A, Schiopu E, Steen VD, for the PHAROS Investigators. Pulmonary Hypertension Assessment and Recognition of Outcomes in Scleroderma (PHAROS): baseline characteristics and description of study population. J Rheumatol 2011;38:2172–9.
17. Fischer A, Swigris JJ, Bolster MB, Chung L, Csuka ME, Domsic R, et al. Pulmonary hypertension and interstitial lung disease within PHAROS: impact of extent of fibrosis and pulmonary physiology on cardiac haemodynamic parameters. Clin Exp Rheumatol 2014;32 Suppl 86:S109–14.
18. Levey AS, Stevens LA, Schmid CH, Zhang YL, Castro AF III, Feldman HI, et al. A new equation to estimate glomerular filtration rate. Ann Intern Med 2009;150:604–12.
19. Royston P, Altman DG. External validation of a Cox prognostic model: principles and methods. BMC Med Res Methodol 2013;13:33.
20. Royston P. Tools for checking calibration of a Cox model in external validation: approach based on individual event probabilities. Stata J 2014;14:738–55.
21. Lammi MR, Mathai SC, Saketkoo LA, Domsic RT, Bojanowski C, Furst DE, et al. Association between initial oral therapy and outcomes in systemic sclerosis–related pulmonary arterial hypertension. Arthritis Rheumatol 2016;68:740–8.
22. Coghlan JG, Galiè N, Barberà JA, Frost AE, Ghofrani HA, Hoeper MM, et al. Initial combination therapy with ambrisentan and tadalafil in connective tissue disease-associated pulmonary arterial hypertension (CTD-PAH): subgroup analysis from the AMBITION trial. Ann Rheum Dis 2017;76:1219–27.
23. Mathai SC, Hummers LK, Champion HC, Wigley FM, Zaiman A, Hassoun PM, et al. Survival in pulmonary hypertension associated with the scleroderma spectrum of diseases: impact of interstitial lung disease. Arthritis Rheum 2009;60:569–77.
24. Badesch DB, Raskob GE, Elliott CG, Krichman AM, Farber HW, Frost AE, et al. Pulmonary arterial hypertension: baseline characteristics from the REVEAL Registry. Chest 2010;137:376–87.
25. Altman DG, Royston P. What do we mean by validating a prognostic model? Stat Med 2000;19:453–73.
26. Miller ME, Hui SL, Tierney WM. Validation techniques for logistic regression models. Stat Med 1991;10:1213–26.
27. De Oliveira NC, dos Santos Sabbag LM, Ueno LM, de Souza RB, Borges CL, de Sá Pinto AL, et al. Reduced exercise capacity in systemic sclerosis patients without pulmonary involvement. Scand J Rheumatol 2007;36:458–61.
28. Deuschle K, Weinert K, Becker MO, Backhaus M, Huscher D, Riemekasten G. Six-minute walk distance as a marker for disability and complaints in patients with systemic sclerosis. Clin Exp Rheumatol 2011;29 Suppl 65:S53–9.
29. Mathai SC, Puhan MA, Lam D, Wise RA. The minimal important difference in the 6-minute walk test for patients with pulmonary arterial hypertension. Am J Respir Crit Care Med 2012;186:428–33.

30. Mathai SC, Bueso M, Hummers LK, Boyce D, Lechtzin N, Le Pavec J, et al. Disproportionate elevation of N-terminal pro-brain natriuretic peptide in scleroderma-related pulmonary hypertension. Eur Respir J 2010;35:95–104.
31. Hoeper MM, Bogaard HJ, Condliffe R, Frantz R, Khanna D, Kurzyna M, et al. Definitions and diagnosis of pulmonary hypertension. J Am Coll Cardiol 2013;62 Suppl:D42–50.
32. Galiè N, Humbert M, Vachiery JL, Gibbs S, Lang I, Torbicki A, et al. 2015 ESC/ERS guidelines for the diagnosis and treatment of pulmonary hypertension. Eur Respir J 2015;46:879–82.
33. Boucly A, Weatherald J, Savale L, Jaïs X, Cottin V, Prevot G, et al. Risk assessment, prognosis and guideline implementation in pulmonary arterial hypertension. Eur Respir J 2017;50:1700889.
34. Kylhammar D, Kjellström B, Hjalmarsson C, Jansson K, Nisell M, Söderberg S, et al. A comprehensive risk stratification at early follow-up determines prognosis in pulmonary arterial hypertension. Eur Heart J 2018;39:4175–81.
35. Weatherald J, Boucly A, Launay D, Cottin V, Prévot G, Bourlier D, et al. Haemodynamics and serial risk assessment in systemic sclerosis associated pulmonary arterial hypertension. Eur Respir J 2018;52:1800678.
36. Mercurio V, Diab N, Peloquin G, Housten-Harris T, Damico R, Kolb TM, et al. Risk assessment in scleroderma patients with newly diagnosed pulmonary arterial hypertension: application of the ESC/ERS risk prediction model. Eur Respir J 2018;18;52:1800497.

Arthritis & Rheumatology
Vol. 71, No. 10, October 2019, pp 1701–1710
DOI 10.1002/art.40898

American College of Rheumatology
Empowering Rheumatology Professionals

A Machine Learning Classifier for Assigning Individual Patients With Systemic Sclerosis to Intrinsic Molecular Subsets

Jennifer M. Franks,[1] Viktor Martyanov,[2] Guoshuai Cai,[3] Yue Wang,[2] Zhenghui Li,[2] Tammara A. Wood,[2] and Michael L. Whitfield[1]

Objective. High-throughput gene expression profiling of tissue samples from patients with systemic sclerosis (SSc) has identified 4 "intrinsic" gene expression subsets: inflammatory, fibroproliferative, normal-like, and limited. Prior methods required agglomerative clustering of many samples. In order to classify individual patients in clinical trials or for diagnostic purposes, supervised methods that can assign single samples to molecular subsets are required. We undertook this study to introduce a novel machine learning classifier as a robust accurate intrinsic subset predictor.

Methods. Three independent gene expression cohorts were curated and merged to create a data set covering 297 skin biopsy samples from 102 unique patients and controls, which was used to train a machine learning algorithm. We performed external validation using 3 independent SSc cohorts, including a gene expression data set generated by an independent laboratory on a different microarray platform. In total, 413 skin biopsy samples from 213 individuals were analyzed in the training and testing cohorts.

Results. Repeated cross-fold validation identified consistent and discriminative markers using multinomial elastic net, performing with an average classification accuracy of 87.1% with high sensitivity and specificity. In external validation, the classifier achieved an average accuracy of 85.4%. Reanalyzing data from a previous study, we identified subsets of patients that represent the canonical inflammatory, fibroproliferative, and normal-like subsets.

Conclusion. We developed a highly accurate classifier for SSc molecular subsets for individual patient samples. The method can be used in SSc clinical trials to identify an intrinsic subset on individual samples. Our method provides a robust data-driven approach to aid clinical decision-making and interpretation of heterogeneous molecular information in SSc patients.

INTRODUCTION

Systemic sclerosis (SSc) is a complex autoimmune connective tissue disease characterized by skin fibrosis, internal organ dysfunction, vascular damage, and immunologic abnormalities. Patients are classified clinically, according to the extent of skin involvement, into limited cutaneous SSc (lcSSc) and diffuse cutaneous SSc (1).

To further characterize disease heterogeneity and pathogenesis, transcriptomics has elucidated common biologic processes in subsets of SSc patients using intrinsic gene expression analysis. Four intrinsic molecular subsets, identified through gene expression profiling in skin samples, are characterized by distinct molecular signatures and have been validated in multiple studies (2–5). The subset is consistent across the different skin biopsy sites within a single patient, regardless of clinically affected or unaffected status, thereby demonstrating the systemic nature of the disease (2–4,6). These subsets have also been found across organ systems in analyses of multiple tissues (7,8). The inflammatory subset is defined by enrichment in immune system response, inflammatory response, and vascular development (3). The fibropro-

Supported by the Scleroderma Research Foundation, Burroughs-Wellcome Big Data in the Life Sciences Training Program, the NIH (Big Data to Knowledge project 5T32LM012204-03), and the Dr. Ralph and Marian Falk Medical Research Trust Catalyst and Transformational Awards.

[1]Jennifer M. Franks, PhD, Michael L. Whitfield, PhD: Geisel School of Medicine at Dartmouth, Department of Molecular and Systems Biology, Hanover and Lebanon, New Hampshire; [2]Viktor Martyanov, PhD, Yue Wang, PhD, Zhenghui Li, PhD, Tammara A. Wood, MS: Geisel School of Medicine at Dartmouth, Hanover, New Hampshire; [3]Guoshuai Cai, PhD: Arnold School of Public Health at University of South Carolina, Columbia.

Dr. Whitfield has received consulting fees from Bristol-Myers Squibb, Boehringer Ingelheim, Corbus Pharmaceuticals, and Third Rock Ventures (less than $10,000 each) and from Celdara Medical and UCB (more than $10,000 each). No other disclosures relevant to this article were reported.

Address correspondence to Michael L. Whitfield, PhD, Geisel School of Medicine at Dartmouth, Department of Molecular and Systems Biology, 7400 Remsen, Hanover, NH 03755. E-mail: michael.whitfield@dartmouth.edu.

Submitted for publication August 2, 2018; accepted in revised form March 21, 2019.

liferative subset is characterized by increased expression of proliferative processes, including cell cycle, mitosis, and chromosome segregation. The normal-like subset is composed of samples from SSc patients whose gene expression most closely resembles that of healthy controls. This subset has previously been characterized by fatty acid metabolism and lipid metabolism, although not consistently (5,9). The limited subset consists exclusively of lcSSc patients and is the least characterized in terms of unique molecular signatures. Importantly, lcSSc patients can also be assigned to the inflammatory and normal-like subsets.

To date, there are no Food and Drug Administration–approved disease-modifying treatments for SSc (10). Although overall survival and treatment strategies for SSc are improving, the power in clinical trials is often compromised by patient heterogeneity. Following a clinical diagnosis of SSc, immunotherapeutic treatment regimens are often intensive and exploratory; in addition to delayed relief, patients risk adverse side effects throughout this experimental approach. Only recently have clinical trials begun to consider molecular heterogeneity in the interpretation of outcomes, which may explain improvement in a subset of SSc patients and may identify patients who will improve naturally as part of their disease course (11). Thus, SSc is an ideal example of a disease in which outcomes may be improved by tools that will aid personalized medicine, especially in the context of molecular subsets.

The inflammatory intrinsic gene expression subset has been associated with response to immunomodulating therapies. For example, Hinchcliff et al showed that 4 of 7 patients treated with mycophenolate mofetil improved, and all 4 were classified as being in the inflammatory subset at baseline (4). Additionally, 4 of 5 improvers in a placebo-controlled study of abatacept were assigned to the inflammatory subset (12). Gordon et al demonstrated that transitions between intrinsic subsets correlated strongly with clinical improvements in a randomized, double-blind, placebo-controlled trial of belimumab with mycophenolate mofetil background therapy (13). Specifically, movement from the inflammatory or fibroproliferative subsets to the normal-like subset strongly correlated with decreases in the modified Rodnan skin thickness score (14). The use of genomic data and intrinsic subsets may help improve patient outcomes by identifying therapies with higher potential for success in each individual patient. Furthermore, longitudinal tracking of intrinsic subset assignment may provide insight into SSc pathogenesis and overall disease trajectory.

Landmark studies that first assigned intrinsic subsets in SSc used agglomerative methods, including intrinsic gene analysis and unsupervised clustering algorithms to determine the number of intrinsic subsets and each sample's membership in a subset (2–4,15,16). There are several limitations with these methods. First, intrinsic gene analysis requires paired samples from each individual (e.g., forearm and back skin biopsies). Paired skin samples are often not available in the setting of clinical trials. Second, the most "intrinsic" genes are agnostically derived from the samples in each data set, and often the exact list differs between studies, although some genes are commonly found and biologic processes are consistent (5). Third, unsupervised clustering algorithms rely on the assumption that at least 2 intrinsic subsets are represented in the data set. This often requires a large number of samples (i.e., n ≥70) for all 4 intrinsic subsets to arise and be distinguishable in a data set.

In order to classify patients in pilot clinical trials or for diagnostic purposes, supervised methods that can assign an individual sample to an intrinsic molecular subset are required. We have developed a method to assign single samples to intrinsic gene expression subsets according to carefully curated and defined criteria using machine learning. The method utilizes a multinomial elastic net classifier and an optimized set of genes for assigning samples to intrinsic gene expression subsets using objective molecular genomic data.

MATERIALS AND METHODS

Training data set curation and preprocessing. DNA microarray data (2–4) (described in Table 1) were collected with at least 80% probes passing filter, analyzed as $\log_2$ lowess-normalized Cy5:Cy3 ratios, and multiplied by –1 to convert them to $\log_2$(-Cy3:Cy5) ratios. Each data set was processed separately using the following pipeline from GenePattern (17): missing values were imputed using the k-nearest neighbors algorithm with default settings, the CollapseDataset module was run using median collapse

Table 1. Studies included in the analysis*

Data set	GEO accession no.	Samples, no.	Platform	Arrays excluded, no.	Arrays included, no.	Purpose
Milano et al, 2008 (2)	GSE9285	75	Agilent (4 × 44K)	13	62	Training
Pendergrass et al, 2012 (3)	GSE32413	89	Agilent (4 × 44K)	13	76	Training
Hinchcliff et al, 2013 (4)	GSE59787	165	Agilent (4 × 44K)	6	159	Training
Chakravarty et al, 2015 (12)	GSE66321	16	Agilent (8 × 60K)	8	8	Testing
Gordon et al, 2015 (25)	GSE65405	12	Agilent (8 × 60K)	6	6	Testing
Assassi et al, 2015 (26)	GSE58095	102	Illumina HT-12 v4	0	102	Testing

* Arrays were excluded if no subset classification was done in the original analysis or if the patient was diagnosed as having morphea and/or eosinophilic fasciitis.

mode, and genes were median centered. Data sets were combined using only genes present in all 3 sets. Arrays from morphea and eosinophilic fasciitis patients were excluded, as well as any arrays that were not assigned to a subset in the original analyses. All gene expression data have previously been published on Gene Expression Omnibus. Altogether, 413 samples, collected from 213 unique individuals, were used to train and test the classifier.

Classifier training and evaluation. The KernSmooth (18), GLMnet (19), random forest (RF) (20), and caret (21) packages implemented in R were used to train supervised classifiers. The support vector machine (SVM) was trained with a linear kernel. GLMnet and RF were run with default parameters. Repeated cross-validation (×10, 3-fold) was used to train the model and simultaneously assess robustness. Accuracy metrics were measured across all repeated cross-validated folds.

External validation. We compared subset assignments made by our model to those reported in the studies described in Table 1. The data sets GSE65405 and GSE66321 were profiled using Agilent 8 × 60K array technology, an updated version of the platform used in the studies to train the classifier. We calculated concordance and Cohen's kappa coefficient based on the intrinsic subset assignment determined by the classifier and compared to the intrinsic subset information from the original publication. Data set GSE58095 was generated using Illumina HT-12, version 4. We downloaded data set GSE58095 from the NCBI GEO. GenePattern (17) was used to impute missing values in the data set using the k-nearest neighbors algorithm and collapse probes to genes using a Chip description file for Illumina HT-12, version 4.

SSc subset molecular signatures. Ranked genes with positive, non-zero coefficients in the final model for each molecular subtype were analyzed with g:Profiler using default g:SCS threshold (22). To further validate the gene signatures, we identified modules (groups of coexpressed genes) using weighted gene coexpression network analyses (WGCNA). We identified modules associated with molecular subsets using biweight midcorrelation with the bicor function in WGCNA R package (23). Modules were annotated with significant biologic processes identified through g:Profiler. The entire workflow is shown in Figure 1.

RESULTS

Data set curation. Our goal for this study was to create the first validated classifier for the intrinsic molecular subsets of SSc using supervised machine learning algorithms. In order to train a broadly applicable classifier, we identified large gene expression data sets from 3 independent studies (Table 1) and developed a machine learning classifier using an optimized scheme (Figure 1).

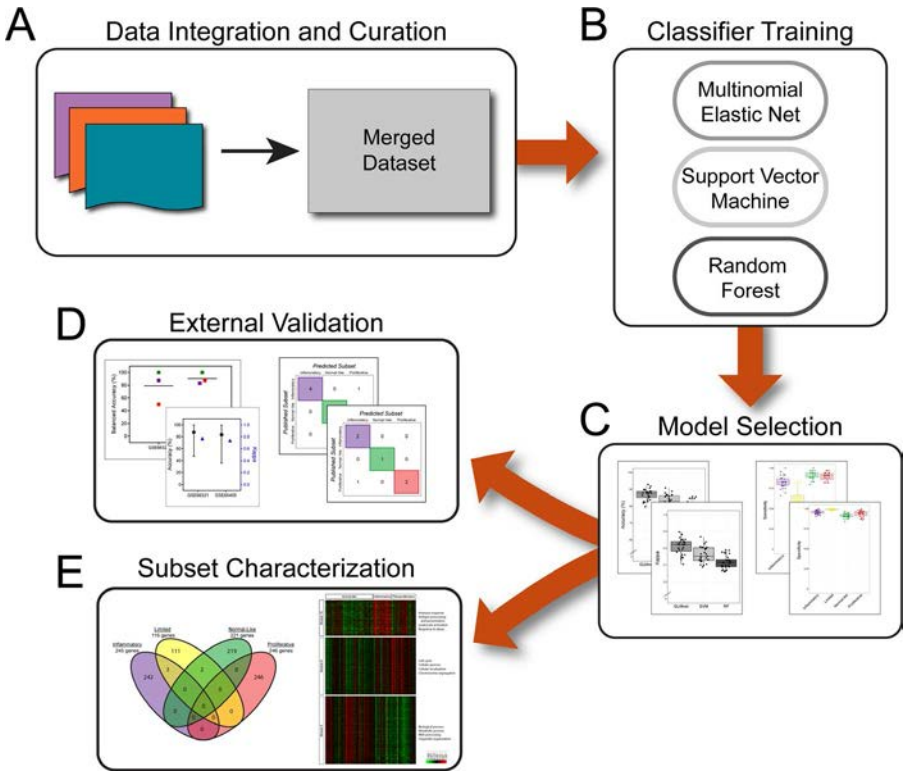

Figure 1. Schematic depiction of the overall study. Gene expression data from 3 independent studies (**A**) were merged into a single data set used to train a variety of machine learning classifiers (**B**). A final model was selected (**C**) and externally validated on other published gene expression data (**D**), then used to further characterize the intrinsic subsets (**E**).

Many clinical studies are characterized by unique and specific inclusion criteria, and these criteria lead to limitations for generalization. While increasing the reliability of results, these criteria often result in a data set of patients that does not represent the full spectrum of disease. By merging data from 3 studies, we are confident that our training data set reflects a broad spectrum of SSc (Figure 2). We only included samples with definitive intrinsic subset labels, as determined in each respective original analysis (Supplementary Table 1, available on the *Arthritis & Rheumatology* web site at http://onlinelibrary.wiley.com/doi/10.1002/art.40898/abstract). Our final training data set contained gene expression data for 11,430 genes across 297 microarrays from 102 unique patients. These arrays represent all 4 intrinsic gene expression subsets (Figure 2A and Supplementary Figure 1, available on the *Arthritis & Rheumatology* web site at http://onlinelibrary.wiley.com/doi/10.1002/art.40898/abstract), although the limited intrinsic subtype is somewhat underrepresented. The other 3 intrinsic subsets are well-balanced in the number of samples: 71 inflammatory, 102 fibroproliferative, and 107 normal-like. The 107 samples in the normal-like intrinsic subset represent both healthy controls (n = 49) and SSc patients (n = 58) who had a normal-like subset label. The patients in our cohort represent a diverse group based on age, sex, disease duration, and extent of skin involvement (Figures 2B and C and Supplementary Table 2, available on the *Arthritis & Rheumatology* web site at http://onlinelibrary.wiley.com/doi/10.1002/art.40898/abstract). We used guided principal components analysis (gPCA) to determine if a significant batch effect existed as a result of combining 3 independent studies (24), and we did not see a significant study bias (P = 0.993 by gPCA) (Figure 2D).

Training machine learning classifiers. We trained supervised classifiers, including multinomial elastic net (GLMnet), SVM, and RF, because they represent a popular and diverse set of machine learning algorithms. Initial evaluation of the classifiers was done using the performance over repeated cross-validation. We found that GLMnet outperformed SVM and RF in iterations of training in both average accuracy and kappa (Figures 3A and B). The overall accuracy and kappa were 87.1% and 0.81 for GLMnet, 83.8% and 0.76 for SVM, and 81.1% and 0.72 for RF. Therefore, we selected GLMnet as the primary classifier to further validate SSc intrinsic subsets using DNA microarray data.

GLMnet displayed high overall sensitivity and specificity for all intrinsic subsets (Figures 3C and D). Sensitivity and specificity for each intrinsic subset in the cross-validation of SVM and RF are shown in Supplementary Figure 2 (available on the *Arthritis & Rheumatology* web site at http://onlinelibrary.wiley.com/doi/10.1002/art.40898/abstract). Specifically, GLMnet attained 83.3% sensitivity and 95.8% specificity for the inflammatory subset and 89.7% sensitivity and 94.1% specificity for

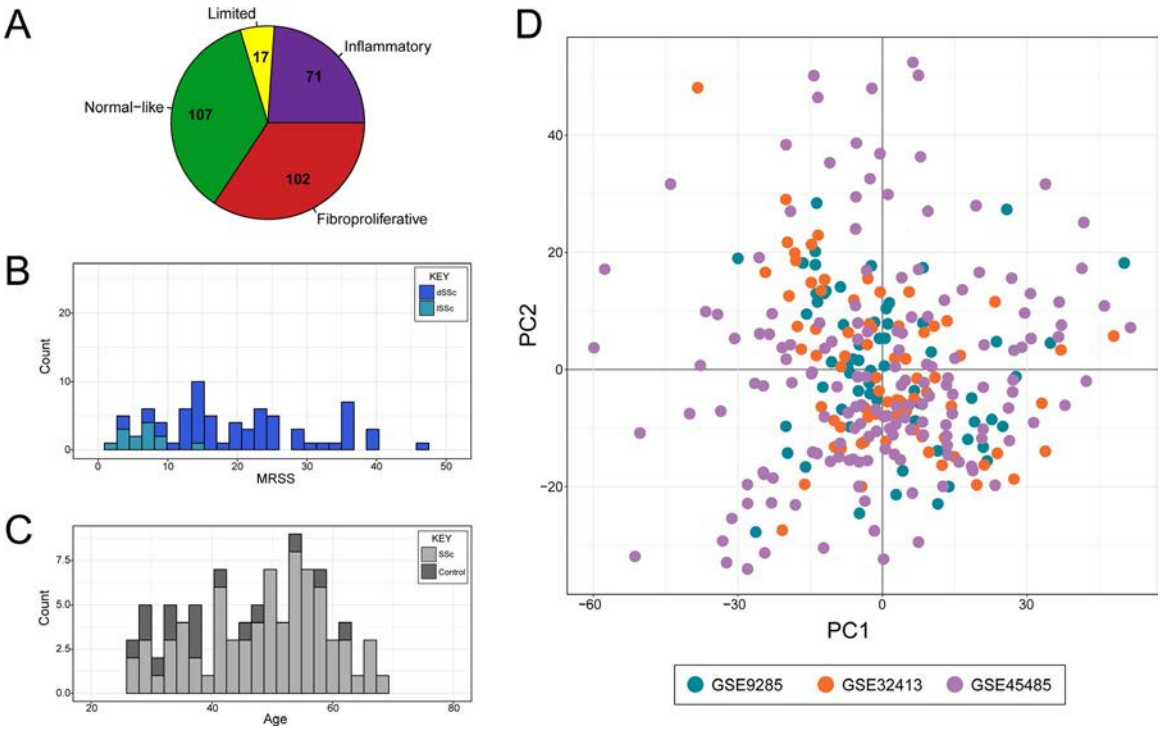

Figure 2. Merge of training data sets. **A**, Relative proportion and numbers of intrinsic subsets present in the full merged training data set. **B** and **C**, Representative data showing the range in skin score severity as designated by the modified Rodnan skin thickness score (MRSS) for diffuse cutaneous systemic sclerosis (dSSc) and limited cutaneous SSc (lSSc) (**B**) and a wide range of age for both SSc patients and controls (**C**). **D**, First and second dimensions of a principal components (PC) analysis, plotted and colored by data set of origin. Symbols represent individual samples.

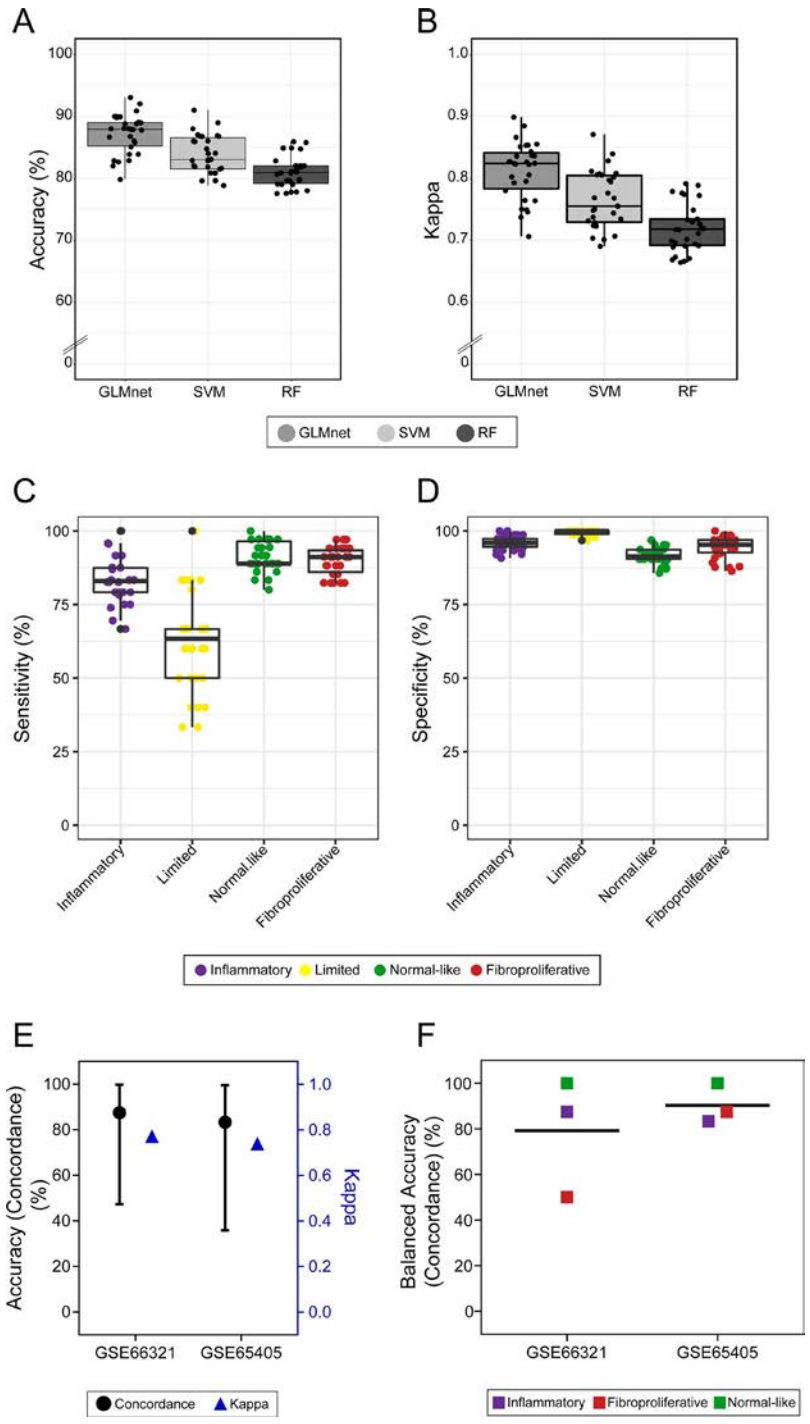

Figure 3. Model selection and validation. **A** and **B**, Accuracy (**A**) and Cohen's kappa (**B**) were calculated for each model during repeated cross-fold validation. **C** and **D**, Sensitivity (**C**) and specificity (**D**) for all 4 intrinsic SSc subsets are plotted from repeated cross-fold validation for the final model. Data in **A**–**D** are presented as box plots, where the horizontal line inside the box shows the median, the box shows the 25th and 75th percentiles, and bars outside the box show the range. Symbols represent a single cross-fold validation from training. In **C** and **D**, symbols shown beyond the bars represent statistical outliers. **E**, In external validations, concordance of intrinsic subset assignment between the original publications and the current analysis is plotted in black, and Cohen's kappa in blue. Bars represent the 95% confidence interval from a 1-sided binomial test that assesses whether the accuracy attained is higher than the no-information rate, as calculated by the confusionMatrix function in caret (see ref. 21). **F**, Balanced accuracy (concordance) is shown for each of the intrinsic subsets represented in each data set. Lines show the mean. SVM = support vector machine; RF = random forest.

the fibroproliferative subset. In contrast to the other subsets, the limited subset showed a greater range in classification sensitivity during training (Figure 3C). This is most likely due to the presence of fewer samples from this subset in the training set. Additionally, the limited subset has not been consistently associated with specific outcomes in SSc clinical trials and represents only a very small proportion of lcSSc patients, because lcSSc patients can also be classified as inflammatory or normal-like. Thus, the variable classification power for the limited subset is neither surprising nor of great importance. Interestingly, SVM was slightly more sensitive in detecting the limited intrinsic subset (Supplementary Figure 2) than GLMnet and RF, but we ultimately selected GLMnet as the best model for DNA microarray data due to superior performance in the remaining 3 subsets. Notably, the SVM had slightly better performance on RNA sequencing (RNA-Seq) data using a small testing set (Supplementary Table 3, available on the *Arthritis & Rheumatology* web site at http://onlinelibrary.wiley.com/doi/10.1002/art.40898/abstract).

Characterizing molecular signatures. GLMnet, through rigorous training, selects the most consistent and discriminative genes to assign intrinsic subsets across multiple cohorts. We identified those genes that were important for prediction of SSc intrinsic subsets by selecting genes with positive non-zero coefficients from the final model (Table 2 and Supplementary Table 4, available on the *Arthritis & Rheumatology* web site at http://onlinelibrary.wiley.com/doi/10.1002/art.40898/abstract). These gene lists were used to determine the significant biological processes for discriminating SSc molecular subsets.

A total of 245 genes were positively associated with prediction of the inflammatory subset and were annotated to Gene Ontology biological processes of immune system response, response to stress, and inflammatory response. Importantly, fibrotic processes such as angiogenesis, cell adhesion, and response to wounding were also up-regulated in the inflammatory subset, consistent with typical clinical presentations of early and active SSc. A total of 246 genes were positively associated with prediction of the fibroproliferative subset. Functional terms including metabolic pathways and cellular process were up-regulated in the fibroproliferative subset. Although the fibroproliferative subset gene signature was not significantly enriched in proliferative processes, it still successfully identified samples previously assigned to this subtype. In the normal-like subset, housekeeping processes such as electron transport chain and cellular respiration were highly expressed. These results validate earlier characterizations of each respective subset. We observed very few genes that overlapped gene lists for each molecular subset (Supplementary Figure 3 (available on the *Arthritis & Rheumatology* web site at http://onlinelibrary.wiley.com/doi/10.1002/art.40898/abstract). This further implies that the SSc molecular subsets represent distinct biologic states.

External validation of SSc molecular subset classifier. In order to test the predictive accuracy of our classifier, we sought validation using additional published DNA microarray data from SSc skin samples with assigned molecular subsets (Table 1). The studies by Chakravarty et al (12) and Gordon et al (25) were small investigator-initiated clinical trials, in which intrinsic subset was determined by calculating Spearman's correlations between each sample's gene expression and the centroid of gene signature associated with each intrinsic subset from the study by Milano et al (2). Unfortunately, the subset labels in these publications do not represent a true gold standard for assessing classifier accuracy. Thus, for the present study, we used concordance of samples being assigned to the same subset as a substitute measure of accuracy. We also report Cohen's kappa coefficient as a robust measure of performance, which takes into account multiple classes and the possibility of agreement by chance.

The study by Chakravarty et al (12) was an investigator-initiated pilot clinical trial of abatacept and contained gene expression data (accession no. GSE66321) with intrinsic subset assignments for 8 SSc patients. Because it is not completely understood how abatacept therapy affects intrinsic subset assignment, we included only the baseline samples for each patient. Additionally, the accuracy metrics from baseline samples are the most relevant in the context of analyses for clinical trials and intrinsic subsets as potential diagnostic and/or prognostic biomarkers. No significant study bias existed between the original training data set and the new data (P = 0.989 by gPCA); therefore, no batch correction measures were taken. We then assigned intrinsic subset labels to each baseline sample using GLMnet and compared these to the intrinsic subset labels reported in the original publication (Supplementary Table 5 and Supplementary Figure 4A, available

Table 2. Genes for profiling molecular pathways enriched in each intrinsic subset*

Subset	Summary of significant biological processes (g:SCS corrected P < 0.05; g:Profiler)	Select genes
Inflammatory	Response to stress, response to wounding, immune system process, inflammatory response, defense response, angiogenesis	*CD33, CD52, CXCL2, CXCR4, CXCR3, CTGF, FN1, IL6, THBS1, COL11A1, COL8A2, VCAM1, SYK, SPHK1*
Fibroproliferative	Metabolic process, cellular metabolic process, noncoding RNA metabolic process, mitochondrial gene expression	*CENPV, CXCL1, COMP, POLR1B, SPIN2B, MTOR, ALAD, TSFM, ELAC2*
Normal-like	Electron transport chain, cellular respiration	*SP5, COX5B, NDUFV3, GPD2, ETFA*
Limited	Actin filament depolymerization	*FBLN1, STAT6, TRIM46, SPTBN1, GSN, VILL*

* Genes were selected using the ranked positive non-zero coefficients in the final model.

on the *Arthritis & Rheumatology* web site at http://onlinelibrary.wiley.com/doi/10.1002/art.40898/abstract). We found that only 1 sample was classified differently with a change in subset from inflammatory to fibroproliferative, giving an overall concordance of 87.5% and a kappa of 0.7714 (Figure 3E). The balanced accuracy for each class was very high for inflammatory (87.5%) and normal-like (100%) intrinsic subsets and was lower for the fibroproliferative subset (50.0%) in this external validation because only 1 patient was classified as in the fibroproliferative subset (Figure 3F).

For a second validation data set, the study by Gordon et al, an investigator-initiated clinical trial of nilotinib that contained gene expression data (accession no. GSE65405) and intrinsic subsets for 6 SSc patients (25), was used. Again, there was no study bias between the testing and training data ($P = 1.00$ by gPCA). We found an overall concordance of 83.33% and a kappa of 0.7391 (Figure 3E). Only 1 sample was classified differently from the original analysis, with a change in subset from fibroproliferative to inflammatory (Supplementary Table 6 and Supplementary Figure 4B, available on the *Arthritis & Rheumatology* web site at http://onlinelibrary.wiley.com/doi/10.1002/art.40898/abstract). There was high balanced accuracy among the 3 intrinsic subsets present in this data set (inflammatory, 83.3%; fibroproliferative, 87.5%; and normal-like, 100%) (Figure 3F). Overall, GLMnet performed consistently well, despite small sample sizes and unbalanced classes. Averaging the results from the first and second data sets, the external validation classification accuracy of GLMnet was 85.4%.

SSc molecular subsets from a different DNA microarray platform. We further tested the predictive power of our algorithm by classifying samples with gene expression data generated by an independent laboratory using a different DNA microarray platform, from the study by Assassi et al (26). This gene expression data set (accession no. GSE58095) contains 102 samples from 97 individuals. The original study identified subsets of patients in this cohort, which they labeled as "keratin," "fibro-inflammatory," and "normal-like" using a different subsetting approach. GLMnet assigned intrinsic subsets to each of the 102 samples; 22 samples were classified as inflammatory, 27 samples were fibroproliferative, and 53 samples were normal-like. Of the 36 healthy control samples, 29 were correctly classified as normal-like, giving an accuracy of 80.6%. Additionally, this data set contained paired early and late samples from 5 patients. For these longitudinal samples, 3 SSc patients were assigned to the same intrinsic subset at both time points, and 2 SSc patients changed from inflammatory or fibroproliferative to normal-like (Supplementary Table 7, available on the *Arthritis & Rheumatology* web site at http://onlinelibrary.wiley.com/doi/10.1002/art.40898/abstract). This change to the normal-like subset over time may represent natural disease process or response to therapy, but more samples and additional studies are needed to understand this variation in subset assignment.

Because there were no gold standard intrinsic subset assignments for the Assassi et al cohort with which to compare the GLMnet classifier labels for a final validation of accuracy, we undertook an independent data-driven procedure to infer the underlying structure of the raw data. In this analysis, we wanted to identify the major gene expression signatures associated with each intrinsic subset in order to evaluate agreement with the previous characterizations of the canonical intrinsic gene expression subsets. First, we used WGCNA to identify modules of co-expressed genes as previously described (5,8,23). Then, the GLMnet molecular classifier was used to assign each sample in the data set to an intrinsic subset. We identified gene modules associated with each intrinsic subset using biweight midcorrelation of the module eigengenes. Further results of this analysis and additional details are shown in Supplementary Figure 5 (available on the *Arthritis & Rheumatology* web site at http://onlinelibrary.wiley.com/doi/10.1002/art.40898/abstract).

We found that several modules correlated significantly with the intrinsic subsets and represented the previously defined distinct biologic processes (Figure 4). Module 10 correlated highly with the inflammatory intrinsic subset, and the module eigenvalues were significantly higher for the inflammatory samples compared to the other subsets ($P = 6.433 \times 10^{-9}$ by Wilcoxon rank sum test). This module contained 739 genes, enriched in Gene Ontology biological processes such as inflammatory response, leukocyte activation, and response to stress. Many of the genes in module 10 have been shown to be important for inflammatory processes and in SSc, including *COL4A1*, *TGFB3*, *HLA–DRA*, *COMP*, and *IL10RB* (27–29). Module 6 was highly correlated with the fibroproliferative subset, and the module eigenvalues were significantly higher for samples labeled fibroproliferative compared to the other subsets ($P = 1.124 \times 10^{-5}$ by Wilcoxon rank sum test). Module 6 showed enrichment for biological processes including cell cycle, cellular process, and chromosome segregation. Among this module's 1,431 genes are *CDC20*, *STAT3*, *CDK10*, *APOE*, *IRF3*, *USP4*, *MYST1*, *CYC1*, and *FBRS*. Module 5 was highly correlated with the normal-like subset, and the module eigenvalues were significantly higher for the normal-like samples compared to the other subsets ($P = 1.458 \times 10^{-9}$ by Wilcoxon rank sum test). This module was enriched for general cellular processes including organelle organization, RNA processing, and metabolic process. These results corroborate the findings of Mahoney et al, who showed that the most consistent biologic processes relevant to SSc were enriched in genes with increased expression in SSc that were significantly correlated with the inflammatory and fibroproliferative subsets (5).

Additionally, we performed unsupervised hierarchical clustering using the genes from the GLMnet classifier (Supplementary Figure 6, available on the *Arthritis & Rheumatology* web site at http://onlinelibrary.wiley.com/doi/10.1002/art.40898/abstract). The clustering showed distinct gene expression signatures associated with the intrinsic subset calls. Interestingly, there were some samples (particularly in the fibroproliferative subset) that appeared

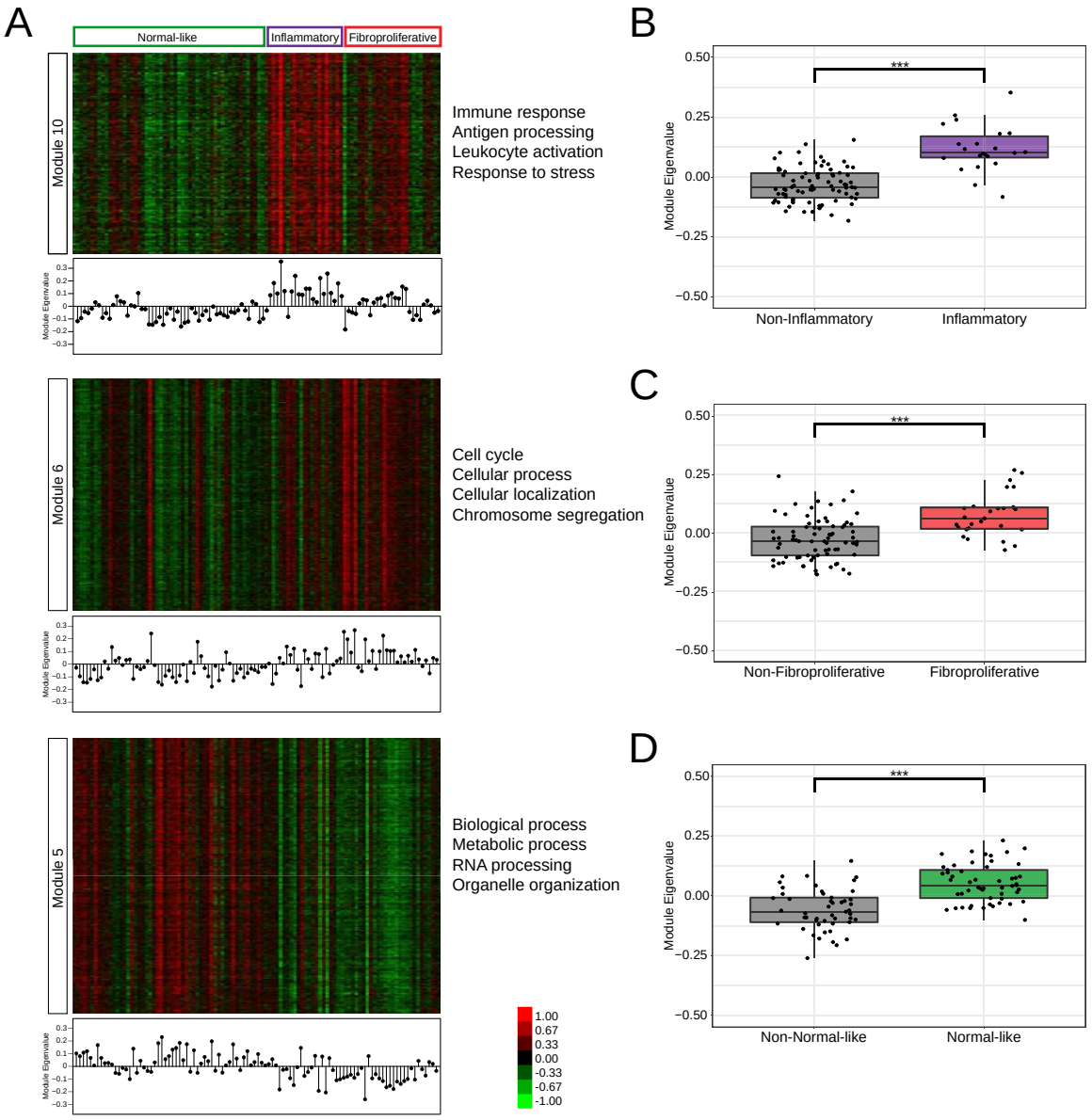

Figure 4. Module analysis of Assassi et al (26). **A**, Expression values are shown for genes annotated to modules 10, 6, and 5. The module eigengene of each module is shown in a stem plot below each heatmap. **B**–**D**, Module eigenvalues were further compared for the inflammatory samples versus all others (**B**), fibroproliferative samples versus all others (**C**), and normal-like samples versus all others (**D**). Data are presented as box plots, where the horizontal line inside the box shows the median, the box shows the 25th and 75th percentiles, and bars outside the box show the minimum and maximum of the samples. Symbols represent individual samples, and the symbols shown beyond the bars indicate statistical outliers. *** = $P < 0.0005$ by Wilcoxon rank sum test.

to also have up-regulated inflammatory signatures, which is consistent with the findings of Assassi et al (26) and with our results from earlier studies.

Finally, we mapped the GLMnet genes to the gene modules identified in the WGCNA analysis (Supplementary Figure 7, available on the *Arthritis & Rheumatology* web site at http://onlinelibrary.wiley.com/doi/10.1002/art.40898/abstract). The GLMnet genes were fairly evenly dispersed throughout many modules. This indicates that the genes selected in the model provide a whole-genome summary of gene expression and include important genes with nonredundant information.

Overall, these analyses result in a GLMnet classification method that is reproducible across multiple DNA microarray platforms and experiments, by which we can assign intrinsic gene expression subsets to SSc patients in clinical trials or for diagnostic purposes. This tool will allow for the identification of the patients most likely to respond to a given therapy using molecular measures.

DISCUSSION

To our knowledge, this is the first published classifier for the intrinsic molecular subsets in SSc. This study represents

improvement over previous approaches that required paired samples from many individuals and rigorous computational analyses through unsupervised clustering algorithms to identify intrinsic gene expression subsets. Moreover, previous studies relied on the assumption that multiple intrinsic subsets were present in the cohort. Our classifier uses defined criteria based on gene expression signatures trained from a large compendium of curated data. It accurately classifies single samples and does not make the assumption that all intrinsic subsets are present in all data sets. This is particularly important for small, pilot clinical trials in SSc.

In the context of immunosuppressive therapy, molecular heterogeneity may explain improvement in select SSc patients (11). Representing distinct pathway signatures, the intrinsic subsets are a logical and meaningful way to interpret the overall picture of global gene expression in patients with SSc. Our validated model accurately classifies single samples and will ultimately improve the speed and reproducibility of computational analyses and guide interpretation of clinical response in the context of intrinsic subsets.

The ability to classify a single sample from individual patients, as needed, is key to implementing such methods in routine clinical care. Performing genomic assays and assigning subsets in a rigorously controlled Clinical Laboratory Improvement Amendments–certified laboratory is also needed to carefully oversee all aspects of the process and ensure that accurate results are generated. We believe the classification model we have developed here may allow personalized medicine in SSc by using intrinsic subsets to help guide the treatment and management of SSc. Our classification model is already being applied in SSc clinical trials, and results for each trial will be published separately as part of those consortia. The method has been designed to work on a wide range of genomic platforms so that it is possible to classify any SSc patient with genomic-level messenger RNA expression data (see below). We have previously shown that an SSc intrinsic subset can predict response in small investigator-initiated clinical trials (4,12,13), and we are further testing this prediction in large, randomized placebo-controlled clinical trials. If an intrinsic subset is shown to predict therapeutic response for a particular treatment in a rigorously controlled clinical trial, then intrinsic subset assignment could be done early in a patient's disease course to determine the patients most likely to benefit from certain therapies. This could have the benefit of getting patients started early with the most effective treatment, ultimately leading to faster and improved patient outcomes. It may be most impactful for therapies that have significant adverse side effects or that are very expensive (e.g., stem cell transplant and biologics agents).

Over time, updates in gene expression profiling technology have improved overall data detection and quality. Namely, RNA-Seq enables detection of novel transcripts as well as better detection of highly and lowly expressed transcripts, which leads to increased sensitivity and specificity. However, due to differences in methods of transcript quantification, there are significant differences in data distributions, which violate statistical assumptions important for machine learning methods. Thus, several considerations should be made in applying our methods to data generated from a different platform. Data should be examined for the existence of platform-related batch effects. We recommend feature specific quantile normalization (FSQN) for eliminating platform-based bias and increasing the comparability between 2 platforms (30). FSQN is a powerful and robust method that allows for highly accurate intrinsic subtype classification even in small data sets, which is an important factor for SSc analyses. Additionally, the SVM described in this report, which retains all genes in the model, may provide more accurate results when assigning samples to intrinsic subsets from RNA-Seq data. For additional details, see Supplementary Table 3 and Supplementary Discussion (available at http://onlinelibrary.wiley.com/doi/10.1002/art.40898/abstract).

Intrinsic molecular subsets are a reproducible feature of SSc skin gene expression (2–5), and this study further validates the previously defined subsets through analysis of an independent gene expression data set generated on a different DNA microarray platform. Our study is the first to build a classification model for accurate intrinsic subset classification of single samples from SSc skin. Although most bioinformatics efforts have focused on profiling the gene expression in SSc skin, there is substantial evidence to suggest that the intrinsic subsets and the immune–fibrotic axis span multiple affected SSc organs (7,8). Further efforts are needed to explore molecular heterogeneity and intrinsic subsets in other tissues and particularly in peripheral blood, given its accessibility. The results of our study are proof of principle that it is feasible to identify a common set of genes sufficient for SSc subset classification. As with many rare diseases, the amount of gene expression data is quite limited, and identifying a smaller set of genes for a biomarker panel is very difficult. With many more features than samples, overfitting the training data is of great concern. Additional work, including the integration of more gene expression data, will be necessary to further refine a gene expression–based biomarker panel for SSc intrinsic subset classification. In conclusion, this body of work represents an important step toward more precise diagnostic testing and treatment in SSc.

ACKNOWLEDGMENTS

The authors wish to thank Jaclyn Taroni and Diana Toledo for helpful discussions.

AUTHOR CONTRIBUTIONS

All authors were involved in drafting the article or revising it critically for important intellectual content, and all authors approved the final version to be submitted for publication. Ms Franks had full access to all the data in the study and takes responsibility for the integrity of the data and the accuracy of the data analysis.

Study conception and design. Franks, Martyanov, Cai, Whitfield.
Acquisition of data. Franks, Li, Wood, Whitfield.
Analysis and interpretation of data. Franks, Martyanov, Wang, Whitfield.

REFERENCES

1. Varga J, Denton CP, Wigley FM, Alanore Y, Kuwana M, editors. Scleroderma: from pathogenesis to comprehensive management. 2nd ed. New York: Springer; 2017.
2. Milano A, Pendergrass SA, Sargent JL, George LK, McCalmont TH, Connolly MK, et al. Molecular subsets in the gene expression signatures of scleroderma skin. PLoS One 2008;3:e2696.
3. Pendergrass SA, Lemaire R, Francis IP, Mahoney JM, Lafyatis R, Whitfield ML. Intrinsic gene expression subsets of diffuse cutaneous systemic sclerosis are stable in serial skin biopsies. J Invest Dermatol 2012;132:1363–73.
4. Hinchcliff M, Huang CC, Wood TA, Mahoney J, Martyanov V, Bhattacharyya S, et al. Molecular signatures in skin associated with clinical improvement during mycophenolate treatment in systemic sclerosis. J Invest Dermatol 2013;133:1979–89.
5. Mahoney JM, Taroni J, Martyanov V, Wood TA, Greene CS, Pioli PA, et al. Systems level analysis of systemic sclerosis shows a network of immune and profibrotic pathways connected with genetic polymorphisms. PLoS Comput Biol 2015;11:e1004005.
6. Whitfield ML, Finlay DR, Murray JI, Troyanskaya OG, Chi JT, Pergamenschikov A, et al. Systemic and cell type-specific gene expression patterns in scleroderma skin. Proc Natl Acad Sci U S A 2003;100:12319–24.
7. Taroni JN, Martyanov V, Huang CC, Mahoney JM, Hirano I, Shetuni B, et al. Molecular characterization of systemic sclerosis esophageal pathology identifies inflammatory and proliferative signatures. Arthritis Res Ther 2015;17:194.
8. Taroni JN, Greene CS, Martyanov V, Wood TA, Christmann RB, Farber HW, et al. A novel multi-network approach reveals tissue-specific cellular modulators of fibrosis in systemic sclerosis. Genome Med 2017;9:27.
9. Johnson ME, Mahoney JM, Taroni J, Sargent JL, Marmarelis E, Wu MR, et al. Experimentally-derived fibroblast gene signatures identify molecular pathways associated with distinct subsets of systemic sclerosis patients in three independent cohorts. PLoS One 2015;10:e0114017.
10. Denton CP, Khanna D. Systemic sclerosis. Lancet 2017;390:1685–99.
11. Martyanov V, Whitfield ML. Molecular stratification and precision medicine in systemic sclerosis from genomic and proteomic data. Curr Opin Rheumatol 2016;28:83–8.
12. Chakravarty EF, Martyanov V, Fiorentino D, Wood TA, Haddon DJ, Jarrell JA, et al. Gene expression changes reflect clinical response in a placebo-controlled randomized trial of abatacept in patients with diffuse cutaneous systemic sclerosis. Arthritis Res Ther 2015;17:159.
13. Gordon JK, Martyanov V, Franks JM, Bernstein EJ, Szymonifka J, Magro C, et al. Belimumab for the treatment of early diffuse systemic sclerosis: results of a randomized, double-blind, placebo-controlled, pilot trial. Arthritis Rheumatol 2018;70:308–16.
14. Clements P, Lachenbruch P, Seibold J, White B, Weiner S, Martin R, et al. Inter and intraobserver variability of total skin thickness score (modified Rodnan TSS) in systemic sclerosis. J Rheumatol 1995;22:1281–5.
15. Sørlie T, Perou CM, Tibshirani R, Aas T, Geisler S, Johnsen H, et al. Gene expression patterns of breast carcinomas distinguish tumor subclasses with clinical implications. Proc Natl Acad Sci U S A 2001;98:10869–74.
16. Perou CM, Sørlie T, Eisen MB, van de Rijn M, Jeffrey SS, Rees CA, et al. Molecular portraits of human breast tumours. Nature 2000;406:747–52.
17. Reich M, Liefeld T, Gould J, Lerner J, Tamayo P, Mesirov JP. GenePattern 2.0 [letter]. Nat Genet 2006;38:500–1.
18. Wand MP, Jones MC. KernSmooth: functions for kernel smoothing supporting Wand & Jones (1995). 2015. URL: https://stat.ethz.ch/R-manual/R-devel/library/KernSmooth/html/00Index.html.
19. Friedman J, Hastie T, Tibshirani R. Regularization paths for generalized linear models via coordinate descent. J Stat Softw 2010;33:1–22.
20. Liaw A, Wiener M. Classification and regression by randomForest. R News 2002;2–3:18–22. URL: https://cran.r-project.org/doc/Rnews/Rnews_2002-3.pdf.
21. Kuhn M. Building predictive models in R using the caret package. J Stat Softw 2008;28:1–26.
22. Reimand J, Arak T, Adler P, Kolberg L, Reisberg S, Peterson H, et al. G:Profiler—a web server for functional interpretation of gene lists (2016 update). Nucleic Acids Res 2016;44:W83–9.
23. Langfelder P, Horvath S. WGCNA: an R package for weighted correlation network analysis. BMC Bioinformatics 2008;9:559.
24. Reese SE, Archer KJ, Therneau TM, Atkinson EJ, Vachon CM, de Andrade M, et al. A new statistic for identifying batch effects in high-throughput genomic data that uses guided principal component analysis. Bioinformatics 2013;29:2877–83.
25. Gordon JK, Martyanov V, Magro C, Wildman HF, Wood TA, Huang WT, et al. Nilotinib (Tasigna™) in the treatment of early diffuse systemic sclerosis: an open-label, pilot clinical trial. Arthritis Res Ther 2015;17:213.
26. Assassi S, Swindell WR, Wu M, Tan FD, Khanna D, Furst DE, et al. Dissecting the heterogeneity of skin gene expression patterns in systemic sclerosis. Arthritis Rheumatol 2015;67:3016–26.
27. Lafyatis R. Transforming growth factor β: at the centre of systemic sclerosis. Nat Rev Rheumatol 2014;10:706–19.
28. Hesselstrand R, Kassner A, Heinegård D, Saxne T. COMP: a candidate molecule in the pathogenesis of systemic sclerosis with a potential as a disease marker. Ann Rheum Dis 2008;67:1242–8.
29. Hikami K, Ehara Y, Hasegawa M, Fujimoto M, Matsushita M, Oka T, et al. Association of IL-10 receptor 2 (IL10RB) SNP with systemic sclerosis. Biochem Biophys Res Commun 2008;373:403–7.
30. Franks JM, Cai G, Whitfield ML. Feature specific quantile normalization enables cross-platform classification of molecular subtypes using gene expression data. Bioinformatics 2018;34:1868–74.

Arthritis & Rheumatology
Vol. 71, No. 10, October 2019, pp 1711–1722
DOI 10.1002/art.40915

American College of Rheumatology
Empowering Rheumatology Professionals

Induction of Inflammation and Fibrosis by Semaphorin 4A in Systemic Sclerosis

Tiago Carvalheiro,[1] Alsya J. Affandi,[1] Beatriz Malvar-Fernández,[1] Ilse Dullemond,[1] Marta Cossu,[1] Andrea Ottria,[1] Jorre S. Mertens,[1] Barbara Giovannone,[1] Femke Bonte-Mineur,[2] Marc R. Kok,[2] Wioleta Marut,[1] Kris A. Reedquist,[1] Timothy R. Radstake,[1] and Samuel García[1]

Objective. To analyze the potential role of semaphorin 4A (Sema4A) in inflammatory and fibrotic processes involved in the pathology of systemic sclerosis (SSc).

Methods. Sema4A levels in the plasma of healthy controls (n = 11) and SSc patients (n = 20) were determined by enzyme-linked immunosorbent assay (ELISA). The expression of Sema4A and its receptors in monocytes and CD4+ T cells from healthy controls and SSc patients (n = 6–7 per group) was determined by ELISA and flow cytometry. Th17 cytokine production by CD4+ T cells (n = 5–7) was analyzed by ELISA and flow cytometry. The production of inflammatory mediators and extracellular matrix (ECM) components by dermal fibroblast cells (n = 6) was analyzed by quantitative polymerase chain reaction, ELISA, Western blotting, confocal microscopy, and ECM deposition assay.

Results. Plasma levels of Sema4A, and Sema4A expression by circulating monocytes and CD4+ T cells, were significantly higher in SSc patients than in healthy controls ($P < 0.05$). Inflammatory mediators significantly up-regulated the secretion of Sema4A by monocytes and CD4+ T cells from SSc patients ($P < 0.05$ versus unstimulated SSc cells). Functional assays showed that Sema4A significantly enhanced the expression of Th17 cytokines induced by CD3/CD28 in total CD4+ T cells as well in different CD4+ T cell subsets ($P < 0.05$ versus unstimulated SSc cells). Finally, Sema4A induced a profibrotic phenotype in dermal fibroblasts from both healthy controls and SSc patients, which was abrogated by blocking or silencing the expression of Sema4A receptors.

Conclusion. Our findings indicate that Sema4A plays direct and dual roles in promoting inflammation and fibrosis, 2 main features of SSc, suggesting that Sema4A might be a novel therapeutic target in SSc.

INTRODUCTION

Systemic sclerosis (SSc) is a severe autoimmune inflammatory disease of unknown etiology with high morbidity and mortality rates, characterized by activation of the immune system, vascular abnormalities, and fibrosis. The resultant skin thickening and stiffness and loss of internal organ function leads to profound disability and premature death (1,2). Fibrosis is marked by the excessive deposition of extracellular matrix (ECM) proteins, as well as increased numbers of fibroblasts expressing the contractile protein α-smooth muscle actin (α-SMA) (3,4). Accumulating evidence has also shown that immune responses are deregulated in SSc patients, contributing to pathology (5,6). One consequence of this immune deregulation is the alteration of T cell homeostasis, with an elevated frequency of Th17 cells in SSc patient peripheral blood and skin (7–11). Interleukin-17 (IL-17) is a cytokine involved in many pathologic features contributing to SSc pathology, including proinflammatory cytokine secretion, monocyte recruitment, and granulocyte–macrophage colony-stimulating factor production (12–14).

The semaphorin family is a large group of proteins initially described as axonal guidance molecules, but now appreciated for their roles in other physiologic and pathologic processes,

Supported by the Dutch Arthritis Association (project grant NR15-3-101 to Dr. García). Dr. Carvalheiro's work was supported by the Portuguese National Funding Agency for Science, Research, and Technology (FCT grant SFRH/BD/93526/2013). Dr. Affandi's work was supported by the Dutch Arthritis Association (grant NR10-1-301) and the Netherlands Organization for Scientific Research (Mosaic grant 017.008.014).

[1]Tiago Carvalheiro, MSc, Alsya J. Affandi, PhD, Beatriz Malvar-Fernández, BSc, Ilse Dullemond, BSc, Marta Cossu, MD, PhD, Andrea Ottria, MSc, MD, Jorre S. Mertens, MSc, MD, Barbara Giovannone, PhD, Wioleta Marut, PhD, Kris A. Reedquist, PhD, Timothy R. Radstake, MD, PhD, Samuel García, PhD: University Medical Center Utrecht, University of Utrecht, Utrecht, The Netherlands; [2]Femke Bonte-Mineur, MD, Marc R. Kok, MD, PhD: Maasstad Hospital Rotterdam, Rotterdam, The Netherlands.

Mr. Carvalheiro and Dr. Affandi contributed equally to this work. Drs. Radstake and García contributed equally to this work.

No potential conflicts of interest relevant to this article were reported.

Address correspondence to Samuel García, PhD, University Medical Center Utrecht, University of Utrecht, Department of Rheumatology and Clinical Immunology and Laboratory of Translational Immunology, Heidelberglaan 100, 3584 CX Utrecht, The Netherlands. E-mail: S.GarciaPerez@umcutrecht.nl.

Submitted for publication October 16, 2018; accepted in revised form April 18, 2019.

including the regulation of immune responses, angiogenesis, cell migration, and tissue invasion (15,16). Semaphorin 4A (Sema4A) is a transmembrane protein that can also be cleaved and released into circulation. Both transmembrane and soluble Sema4A bind to multiple receptors, the best characterized of which are plexin B2, plexin D1, and neuropilin 1 (NRP-1) (17,18). Sema4A is a key molecule in the regulation of T cell homeostasis, activation, and Th1/2/17 differentiation (18–20). Sema4A deficiency or inhibition reduces disease severity in murine models of multiple sclerosis (MS) and autoimmune myocarditis, but enhances the severity of experimental asthma due to impaired Th1/Th17 differentiation and skewing towards a Th2 polarization (19,21–23). Reciprocally, serum levels of Sema4A are increased in MS patients and positively associated with Th17 skewing (23). Thus, Sema4A may play a suppressive role in Th2-driven disease while driving Th1- and Th17-dependent diseases. Sema4A might also play a direct role in fibrosis, inducing collagen contraction by SSc patient lung fibroblasts (24). In this study, we examined whether Sema4A signaling might serve to connect altered Th17 behavior with fibrotic processes in SSc.

MATERIALS AND METHODS

Patients. Blood from patients and sex- and age-matched healthy controls was obtained from the University Medical Center Utrecht and Maasstad Hospital Rotterdam. All subjects provided written informed consent approved by the local institutional medical ethics review boards prior to inclusion in this study. Samples and clinical information were treated anonymously immediately after collection. Patients fulfilled the American College of Rheumatology/European League Against Rheumatism 2013 classification criteria for SSc (25), and the demographic and clinical characteristics of the patients are detailed in Supplementary Tables 1–3, available on the *Arthritis & Rheumatology* web site at http://onlinelibrary.wiley.com/doi/10.1002/art.40915/abstract.

Cell isolation. Peripheral blood mononuclear cells (PBMCs) from healthy controls and SSc patients were isolated by Ficoll gradient (GE Healthcare). Cells were processed for further isolation using magnetic beads and an AutoMACS Pro Separator for monocytes and CD4+ T cells, according to the manufacturer's instructions (Miltenyi Biotec). Purity was routinely >95% for CD4+ T cells and >90% for monocytes, as assessed by flow cytometry. Total CD4+ T cells were stained with allophycocyanin (APC)–eFluor 780–conjugated anti-CD4 (eBioscience), BV-510–conjugated anti-CD27 (BioLegend), phycoerythrin (PE)–conjugated anti-CD25, Alexa Fluor 647–conjugated anti-CD127, and PE–Cy7–conjugated anti-CD45RO (BD Biosciences) antibodies. Cell sorting was performed on a BD FACSAria III cell sorter (BD Bioscience) to obtain pure populations of naive CD4+CD25–CD27+CD45RO–, effector memory CD4+CD25–CD27–CD45RO+, and central memory CD4+CD25–CD27+CD45RO+ T cells (>99% purity).

Flow cytometric analysis. PBMCs were stained with Fixable Viability Dye (for dead cell exclusion) (eBioscience), antibodies to PE-Cy7–conjugated CD19 (Beckman Coulter), APC-conjugatedCD1c,APC–eFluor780–conjugatedCD4,PerCP–Cy5.5–conjugated CD303, BV785-conjugated CD14, Alexa Fluor 700–conjugated CD3 (BioLegend), BV605-conjugated HLA–DR, BV711-conjugated CD141, V500-conjugated CD8, PE–CF594–conjugated CD56 (BD Biosciences), fluorescein isothiocyanate (FITC)–conjugated CD16 (BioConnect), and PE-conjugated Sema4A and its isotype control (R&D Systems). For intracellular staining, PBMCs were first fixed and permeabilized using a FoxP3/Transcription Factor Staining Buffer set (eBioscience). Cells were acquired on an LSRFortessa (BD Biosciences).

CD4+ T cells were stained with Fixable Viability Dye and antibodies to PE-conjugated NRP-1 (Miltenyi Biotec), FITC-conjugated plexin D1, APC-conjugated plexin B2, and their respective isotype controls (R&D Systems). Alternatively, cells were fixed and permeabilized using a FoxP3/Transcription Factor Staining Buffer set, and stained with FITC-conjugated IL-17A, APC-conjugated IL-22, PerCP–Cy5.5–conjugated interferon-γ (IFNγ) (all from eBioscience), BV711-conjugated IL-4, PE-conjugated IL-21, and BV421-conjugated tumor necrosis factor (TNF; all from BD Biosciences). All data were acquired on an LSRFortessa (BD Biosciences). After excluding debris, doublets, and dead cells, cell populations were analyzed using FlowJo software (Tree Star). (See Supplementary Table 4, available on the *Arthritis & Rheumatology* web site at http://onlinelibrary.wiley.com/doi/10.1002/art.40915/abstract, for gating strategy). All flow cytometry data are presented as the percentage of positive cells or the change in median fluorescence intensity (ΔMFI), where ΔMFI = MFI of positive staining – MFI of isotype staining.

Monocyte stimulation. Monocytes were cultured for 30 minutes in RPMI GlutaMax (ThermoFisher Scientific) supplemented with 10% fetal bovine serum (FBS; BioWest) and 10,000 IU penicillin–streptomycin (ThermoFisher Scientific), and then left unstimulated or stimulated with lipopolysaccharide (LPS; 100 ng/ml), R848 (1 μg/ml), high molecular weight poly(I-C) (5 μg/ml) (all from InvivoGen), or CXCL4 (5 μg/ml; PeproTech) for 24 hours. Cells were lysed for messenger RNA (mRNA) expression analysis and cell-free tissue culture supernatants were harvested for cytokine analysis.

CD4+ T cell stimulation. CD4+ total, naive, central memory, or effector memory T cells were activated with Dynabeads Human T-Activator CD3/CD28 (ThermoFisher Scientific) at a bead-to-cell ratio of 1:5 in the absence or presence of recombinant human Sema4A (200 ng/ml; R&D Systems) for 2–7 days. Alternatively, CD4+ T cells were preincubated for 1 hour with neutralizing antibodies to anti–plexin D1 or NRP-1 (R&D Systems) before cell activation and stimulation with Sema4A, as described above, for 5 days. For intracellular cytokine staining,

phorbol 12-myristate 13-acetate (1 μg/ml), ionomycin (50 ng/ml) (both from Sigma-Aldrich) and BD GolgiStop (BD Biosciences) were added for the final 4 hours of stimulation. For proliferation analysis, CD4+ T cells were labeled with CellTrace Violet (1.5 μ*M*; ThermoFisher Scientific) prior to culture.

CD4+ T cell transfection. CD4+ T cells were transfected by electroporation using a Neon Transfection System (ThermoFisher Scientific). CD4+ T cells were activated with Dynabeads Human T-Activator CD3/CD28 at a bead-to-cell ratio of 1:5 for 48 hours. Before transfection, Dynabeads were removed, and activated CD4+ T cells were transfected with plexin B2–specific or scrambled (Sc) nontargeting small interfering RNAs (siRNAs) (50 n*M*; Thermo Scientific) in RPMI GlutaMax containing 10% FBS in the presence of Dynabeads (bead-to-cell ratio of 1:5) for 24 hours, and experiments were performed 4 days after transfection. The efficiency of the transfection was >60% for both healthy control and SSc CD4+ T cells (Supplementary Figures 1A and B, available on the *Arthritis & Rheumatology* web site at http://onlinelibrary.wiley.com/doi/10.1002/art.40915/abstract).

Dermal fibroblast culture and stimulation. SSc dermal fibroblasts (n = 6) were isolated from 3–4-mm skin biopsy sections obtained from a clinically affected area. Healthy control dermal fibroblasts (n = 6) were obtained from skin biopsy sections as resected material after cosmetic surgery. Dermal fibroblast isolation was performed using a whole skin dissociation kit (Miltenyi Biotec) following the manufacturer's instructions, and fibroblasts were routinely maintained in Dulbecco's modified Eagle's medium (DMEM; Invitrogen) supplemented with 10% FBS and 10,000 IU penicillin–streptomycin. Cells were used for experiments between passages 3 and 5, and stimulations were performed after overnight starvation in medium containing 0.1% FBS. Fibroblasts were left unstimulated or preincubated for 1 hour with neutralizing antibodies to anti–plexin D1 or NRP-1 and afterward left unstimulated or stimulated with Sema4A (200 ng/ml) for 24–72 hours. Alternatively, conditioned medium from CD4+ T cells was preincubated for 1 hour at 37°C in the presence of a neutralizing anti–IL-17A antibody (secukinumab 100 ng/ml; kindly provided by Dr. Erik Lubberts, Erasmus Medical Center, Rotterdam, The Netherlands) or its isotype control (IgG1κ; eBioscience) and applied to fibroblasts for 24 hours.

Dermal fibroblast transfection. Dermal fibroblasts were transfected using Dharmafect 1 (Thermo Scientific). Plexin B2–specific or Sc nontargeting siRNAs (50 n*M*; Thermo Scientific) were mixed with Dharmafect 1 prior to transfection for 24 hours. Experiments were performed 48–72 hours after transfection. The efficiency of the silencing was >60% (Supplementary Figures 1C and D).

Cytokine measurement. Sema4A (Biomatik), IL-6, IL-8 (Sanquin), and IL-17A (eBioscience) were measured by enzyme-linked immunosorbent assay in cell-free supernatants and plasma from healthy controls and SSc patients, according to the manufacturer's instructions.

Immunoblotting. Dermal fibroblasts were lysed in Laemmli buffer, and protein content was quantified with a BCA Protein Assay Kit (Pierce). Equivalent amounts of total protein lysate were subjected to electrophoresis on NuPAGE 4–12% Bis-Tris protein gels (ThermoFisher Scientific) and proteins were transferred to PVDF membranes (Millipore). Membranes were incubated overnight at 4°C with primary antibodies specific for α-SMA (Sigma), vimentin, histone 3 (Cell Signaling Technology), type III collagen (Millipore), type VI collagen, and plexin B2 (Abcam). Membranes were then washed and incubated in Tris buffered saline–Tween containing horseradish peroxidase–conjugated secondary antibody. Protein was detected with Lumi-Light Plus Western blotting substrate (Roche Diagnostics) using a ChemiDoc MP System (Bio-Rad). Densitometric analysis was performed with Image J software. Relative protein expression was normalized to histone H3 expression.

Reverse transcriptase–polymerase chain reaction (PCR) and quantitative PCR. RNA from monocytes, CD4+ T cells, and dermal fibroblasts was isolated using an RNeasy kit and RNase-Free DNase set (Qiagen). Total RNA was reverse-transcribed using an iScript cDNA Synthesis kit (Bio-Rad). Duplicate PCR reactions were performed using SYBR Green (Applied Biosystems) with a StepOnePlus Real-Time PCR system (Applied Biosystems). Complementary DNA was amplified using specific primers (Invitrogen) (see Supplementary Table 5, available on the *Arthritis & Rheumatology* web site at http://onlinelibrary.wiley.com/doi/10.1002/art.40915/abstract). Relative levels of gene expression were normalized to the housekeeping genes *B2M* (for monocytes and CD4+ T cells) and *GAPDH* (for fibroblasts). The relative quantity of mRNA was calculated using the formula $2^{-\Delta Ct} \times 1{,}000$.

Confocal microscopy. Nunc Lab-Tek II chamber slides (ThermoFisher Scientific) were precoated with 0.001% poly-L-lysine (Sigma-Aldrich), washed with phosphate buffered saline (PBS), and air-dried. Dermal fibroblasts were seeded in DMEM containing 10% FBS for 24 hours and then incubated overnight in DMEM containing 0.1% FBS. Cells were then stimulated with Sema4A (200 ng/ml) in DMEM containing 2% FBS and 50 μg/ml of L-ascorbic acid, and refreshed 48 hours later. After 72 hours, cells were fixed with 4% paraformaldehyde, washed with PBS–1% bovine serum albumin (BSA), and blocked in 5% normal donkey serum/1% BSA. Cells were incubated with primary antibodies specific for type I collagen (SouthernBiotech), type VI collagen (Abcam), and fibronectin (R&D Systems) for 1 hour at

room temperature, washed, and incubated with secondary antibodies conjugated with Alexa Fluor 488, Alexa Fluor 594, and Alexa Fluor 647 (ThermoFisher Scientific) for 30 minutes at room temperature. Finally, cells were incubated with DAPI (Sigma-Aldrich Chemie) and slides mounted with Mowiol (Sigma-Aldrich Chemie). Imaging data were acquired on a Zen2009 LSM 710 confocal microscope (Zeiss).

Extracellular matrix deposition assay. Black/clear flat-bottomed imaging plates (96 wells each; Corning) were coated with 0.2% gelatin solution for 1 hour at 37°C, washed with Dulbecco's PBS containing 1 m*M* $Ca2^+$ and 1 m*M* $Mg2^+$ (DPBS+), and incubated with 1% glutaraldehyde for 30 minutes at room temperature. Plates were washed again with DPBS+ and incubated for 30 minutes at room temperature with 1*M* ethanolamine. After washing, dermal fibroblasts were seeded, incubated for 24 hours in complete medium, and starved overnight in DMEM containing 0.1% FBS. Cells were then stimulated with Sema4A (200 ng/ml) in DMEM containing 2% FBS and 50 μg/ml of L-ascorbic acid and refreshed 48 hours later. After 72 hours, cells were lysed with 0.5% volume/volume Triton X-100 containing 20 m*M* NH_4OH in PBS, and plates were kept at 4°C overnight. Cellular debris was removed, and wells were fixed in ice-cold 100% methanol. After washing, the ECM was blocked at room temperature with 1% normal donkey serum (Jackson ImmunoResearch) and incubated with primary antibodies specific for type I collagen, type IV collagen, and fibronectin. Afterward, wells were washed, and secondary antibodies (IRDye 800CW and IRDye 680RD; Li-Cor) were added for 1 hour at room temperature. Plates were measured using an Odyssey Sa Infrared Imaging System (Li-Cor Biotechnology).

Statistical analysis. Correlations were analyzed by Spearman's correlation analysis using SPSS software, version 25. Statistical analysis was performed using Windows GraphPad Prism 6 software. Potential differences between experimental groups were analyzed by nonparametric test, Wilcoxon's test, Mann-Whitney test, Kruskal-Wallis test, or Friedman's test, as appropriate. *P* values less than 0.05 were considered significant.

RESULTS

Elevated expression of Sema4A in plasma and immune cells from SSc patients. Plasma levels of Sema4A were significantly higher in SSc patients than in healthy controls and, interestingly, positively correlated with the severity of skin thickening (r = 0.529, *P* = 0.016) (Figures 1A and B). Since Sema4A is a transmembrane protein that can be cleaved and released into the circulation (23), we analyzed the intracellular expression of Sema4A in monocytes, dendritic cells, and B and T cells from healthy control and SSc patient peripheral blood, to determine if circulating white blood cells might contribute to the increased Sema4A expression observed in SSc patients. Sema4A expression was significantly higher in monocytes from SSc patients compared to healthy controls, as was the percentage of monocytes expressing Sema4A (Figures 1C and D and Supplementary Figure 2A, available on the *Arthritis & Rheumatology* web site at http://onlinelibrary.wiley.com/doi/10.1002/art.40915/abstract). We observed similar results in CD4+ T cells, but expression of Sema4A in T cells was much lower than that in monocytes. We did not find differences in Sema4A expression in the other cell subsets analyzed (Supplementary Figures 2B and C). We also analyzed the cellular surface expression of Sema4A and found that the percentage of Sema4A-positive monocytes was higher in SSc patients than in healthy controls. However, CD4+ T cells did not express Sema4A on the cell surface and no differences in expression were found in the other cell populations (Supplementary Figures 2D and E).

Next, we analyzed whether Sema4A expression was regulated in monocytes by different inflammatory mediators involved in the pathogenesis of SSc, namely Toll-like receptor (TLR) agonists and CXCL4 (5,26). LPS and R848 did not modulate the expression of Sema4A (data not shown), but poly(I-C) and CXCL4 significantly induced the secretion of Sema4A by monocytes from SSc patients (Figure 1E). CD3/CD28-induced CD4+ T cell activation also induced Sema4A secretion in both healthy controls and SSc patients, albeit at lower levels compared to monocytes (Figure 1F). Importantly, and consistent with the results of intracellular staining, both basal and stimulated secretion of Sema4A were significantly higher in monocytes and CD4+ T cells from SSc patients than those from healthy controls. Taken together, these data demonstrate that Sema4A expression is deregulated in SSc patient monocytes and, to a lesser extent, CD4+ T cells.

Increased frequency of CD4+ T cells expressing plexin B2 in SSc patients. Since Sema4A plays a key role in the homeostasis and activation of CD4+ T cells (19,20), we determined the expression of the best-characterized Sema4A receptors in healthy control and SSc patient CD4+ T cells. NRP-1 was not expressed by CD4+ T cells (data not shown) and plexin D1 expression was similar between healthy controls and SSc patients. However, the percentage of CD4+ T cells expressing plexin B2 protein was significantly higher in SSc patients (Figure 1G). CD4+ T cells comprise different cell subsets (naive, effector, effector memory, and central memory CD4+ T cells) and, consistent with previous observations (27), frequencies of naive and central memory subsets were significantly altered in SSc patients (Supplementary Figures 3A and B, available on the *Arthritis & Rheumatology* web site at http://onlinelibrary.wiley.com/doi/10.1002/art.40915/abstract). Therefore, we analyzed the expression of Sema4A receptors in these cell populations. Again, NRP-1 was not expressed in any population (data not shown) and we did not find differences in the expression of plexin D1. However, we observed a higher frequency

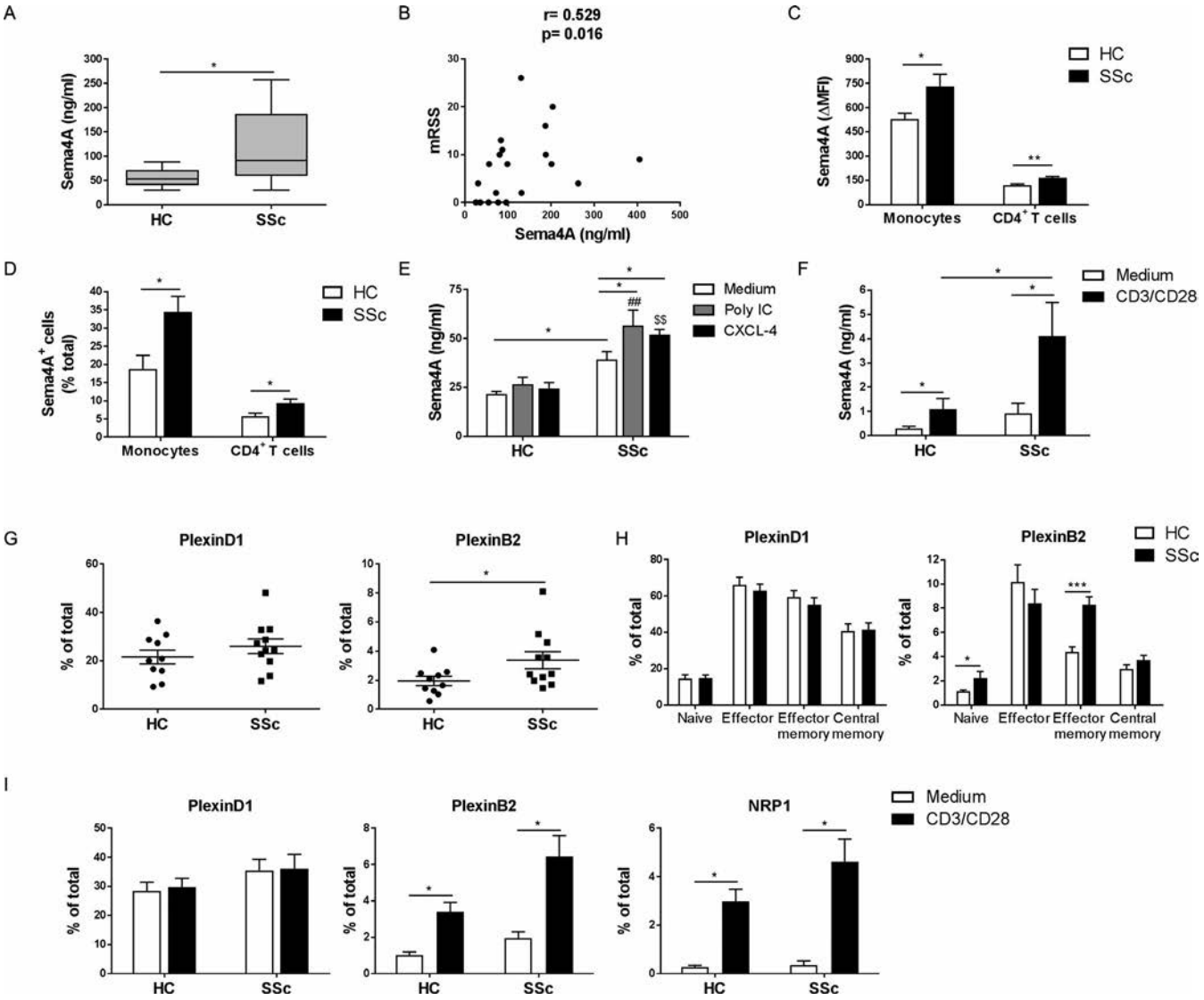

Figure 1. Semaphorin 4A (Sema4A) is elevated in plasma, monocytes, and CD4+ T cells from patients with systemic sclerosis (SSc) and is induced by inflammatory stimuli. **A**, Sema4A levels in plasma from healthy controls (HC; n = 11) and SSc patients (n = 20). Data are shown as box plots. Each box represents the 25th to 75th percentiles. Lines inside the boxes represent the median. Lines outside the boxes represent the 10th and 90th percentiles. **B**, Correlation between Sema4A plasma levels and the modified Rodnan skin thickness score (MRSS). **C** and **D**, Intracellular Sema4A expression in monocytes and CD4+ T cells from healthy controls (n = 6) and SSc patients (n = 6). Data are shown as the change in median fluorescence intensity (ΔMFI) (**C**) or the percentage of positive cells (**D**). **E**, Expression of Sema4A protein by monocytes from healthy controls and SSc patients (n = 6 per group). Cells were stimulated with poly(I-C) or CXCL4 for 48 hours. **F**, Expression of Sema4A protein by CD4+ T cells from healthy controls and SSc patients (n = 6 per group). Cells were stimulated with CD3/CD28 Dynabeads for 5 days. **G**, Surface expression of plexin D1 and plexin B2 in CD4+ T cells from healthy controls and SSc patients. Circles represent individual subjects; horizontal lines and error bars show the mean ± SEM. **H**, Surface expression of plexin D1 and plexin B2 in CD4+ T cell subsets from healthy controls and SSc patients (n = 7 per group). **I**, Surface expression of plexin D1, plexin B2, and neuropilin 1 (NRP-1) in total CD4+ T cells from healthy controls and SSc patients (n = 7 per group). Cells were stimulated with CD3/CD28 Dynabeads. In **C–F**, **H**, and **I**, bars show the mean ± SEM. * = $P < 0.05$; ** = $P < 0.01$; *** = $P < 0.001$ for the indicated comparisons. ## = $P < 0.05$ versus healthy control samples stimulated with poly(I-C); $$ = $P < 0.05$ versus healthy control samples stimulated with CXCL4.

of plexin B2–positive cells in the naive and effector memory CD4+ T cell populations (Figure 1H).

We next determined the effect of CD4+ T cell activation on the expression of the Sema4A receptors. CD3/CD28 stimulation did not affect the expression of plexin D1, but significantly increased the percentage of cells expressing plexin B2 and NRP-1 (Figures 1I and Supplementary Figures 3C and D). Additionally, we found a trend toward a higher frequency of plexin B2–positive and NRP-1–positive cells in SSc patients compared to healthy controls, although the differences were not significant. The induction of plexin B2 and NRP-1 was not specific to any of the CD4+ T cell subsets (Supplementary Figure 3E).

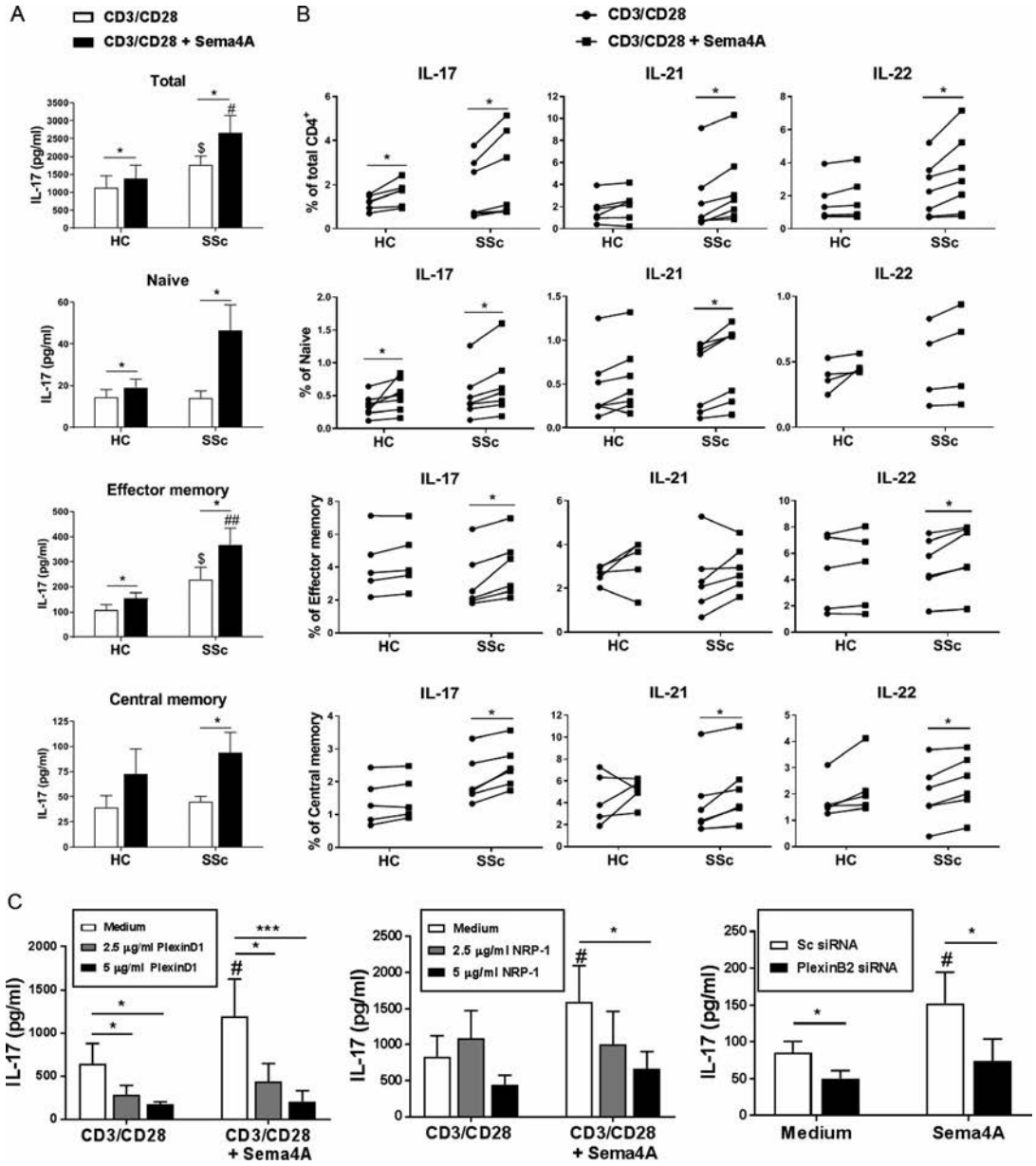

Figure 2. Semaphorin 4A (Sema4A)–induced Th17 cytokine production in CD4+ T cells. **A** and **B**, Interleukin-17 (IL-17) secretion (**A**) and intracellular levels of IL-17, IL-21, and IL-22 (**B**) in total CD4+ T cells and different CD4+ T cell subsets from healthy controls (HCs) and patients with systemic sclerosis (SSc). Cells were activated with CD3/CD28 Dynabeads in the absence or presence of Sema4A for 5 days (for total CD4+ T cells), 7 days (for naive CD4+ T cells), or 2 days (for effector memory and central memory CD4+ T cells). **C**, Secretion of IL-17 by total CD4+ T cells from SSc patients following 5 days of activation with CD3/CD28 Dynabeads in the absence or presence of Sema4A, which had previously been incubated for 1 hour with increasing concentrations of blocking anti–plexin D1 or anti–neuropilin 1 (anti–NRP-1) antibodies or after plexin B2 silencing. In **A** and **C**, bars show the mean ± SEM of 5–7 independent experiments. In **B**, symbols represent individual subjects. * = $P < 0.05$; *** = $P < 0.001$ for the indicated comparisons. $ = $P < 0.05$ versus CD3/CD28-activated cells from healthy controls; # = $P < 0.05$; ## = $P < 0.01$, versus CD3/CD28-activated, Sema4A-treated cells from healthy controls in **A** and versus medium or scrambled (Sc) small interfering RNA (siRNA) in **C**.

Sema4A enhances production of Th17 cytokines by CD4+ T cells. Mouse studies have shown that Sema4A is involved in Th17 skewing (21–23). We therefore analyzed the functional consequences of Sema4A ligation on the human production of Th17 cytokines. Sema4A did not affect cell viability or proliferation in response to CD3/CD28 stimulation of CD4+ T cells from either healthy controls or SSc patients (Supplementary Figures 4A and B, available on the *Arthritis & Rheumatology* web site at http://onlinelibrary.wiley.com/doi/10.1002/art.40915/abstract). However, in both healthy controls and SSc patients, Sema4A enhanced IL-17 secretion induced by CD3/CD28 stimulation, as well the frequency of IL-17–positive, IL-21–positive,

and IL-22–positive cells (Figures 2A and B and Supplementary Figure 4C). In contrast, Sema4A did not regulate the expression of Th1 and Th2 cytokines (Supplementary Figure 5, available on the *Arthritis & Rheumatology* web site at http://onlinelibrary.wiley.com/doi/10.1002/art.40915/abstract). Effects of Sema4A on T cell cytokine production were not due to differences in healthy control and SSc patient T cell subset frequencies, since Sema4A enhanced the secretion of the production of IL-17, IL-21, and IL-22 induced by CD3/CD28 in naive, effector memory, and central memory T cell subsets from healthy controls and SSc patients (Figures 2A and B), while not affecting the production of Th1 and Th2 cytokines (Supplementary Figure 5). Importantly, the production of IL-17 was significantly higher in total, naive, and effector memory CD4+ T cells from SSc patients than in those from healthy controls.

We next determined the effect of blocking the expression of Sema4A receptors on Sema4A-induced production of Th17 cytokines in total CD4+ T cells from healthy controls and SSc patients. The blocking of plexin D1 and NRP-1 with specific antibodies, and the silencing of plexin B2 expression with siRNA, significantly reduced Sema4A-induced secretion of IL-17, as well Sema4A-enhanced frequency of IL-17–positive, IL-21–positive, and IL-22–positive cells in both healthy controls and SSc patients (Figure 2C and Supplementary Figures 6 and 7, available on the *Arthritis & Rheumatology* web site at http://onlinelibrary.wiley.com/doi/10.1002/art.40915/abstract). Notably, this reduction was also observed in the absence of exogenous Sema4A. Since antibody blocking and cell transfection did not affect CD4+ T cell viability or proliferation (data not shown), this effect is likely due to the endogenous secretion of Sema4A by CD4+ T cells (Figure 1F).

Sema4A directs fibroblast activation via IL-17 production by CD4+ T cells. Several studies have implicated IL-17 in SSc inflammatory and fibrotic processes (7–11). To determine if the enhanced IL-17 production induced by Sema4A was sufficient to induce biologic responses, we stimulated dermal fibroblasts from healthy controls with the conditioned medium of CD4+ T cells, previously preincubated with an anti–IL-17 antibody or its isotype control, and analyzed fibroblast expression of mRNA for ECM components and inflammatory mediators. Compared to the conditioned medium of unstimulated CD4+ T cells, the conditioned medium of CD4+ T cells stimulated with CD3/CD28 alone or in combination with Sema4A did not modulate the expression of mRNA for *COL1A1*, *COL3A1*, or *FN1* (Figure 3A). However, the conditioned medium of activated CD4+ T cells significantly induced expression of mRNA for *IL6*, *IL8*, *PTGS2*, *CCL2*, *CCL20*, and *CXCL2*, and the secretion of IL-6 and IL-8 proteins, compared to the conditioned medium of unstimulated cells. Importantly, the

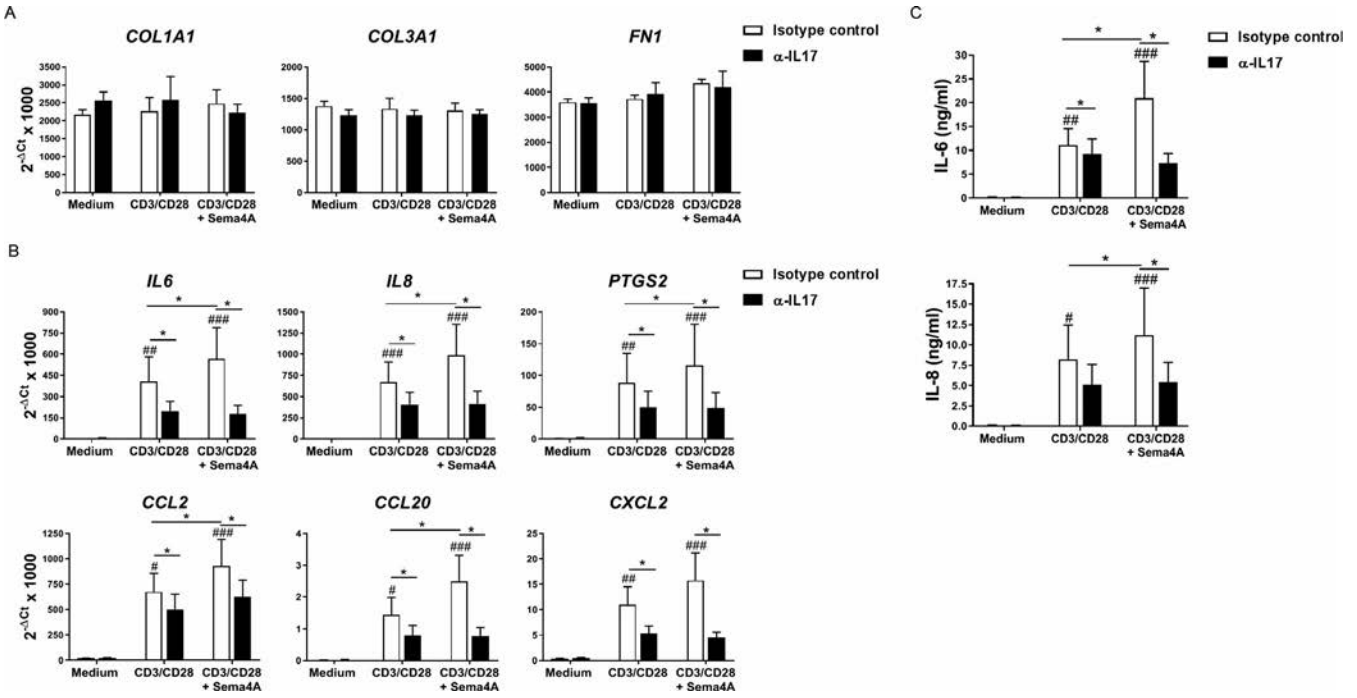

Figure 3. Semaphorin 4A (Sema4A) orchestrates fibroblast activation via interleukin-17 (IL-17) production by CD4+ T cells. **A** and **B**, Expression of mRNA for extracellular matrix components (**A**) and inflammatory mediators (**B**) in skin fibroblasts from healthy controls. Cells were incubated for 24 hours with conditioned medium of activated CD4+ T cells in the absence or presence of Sema4A, which had previously been incubated for 1 hour with an anti–IL-17 antibody or its isotype control. **C**, Expression of IL-6 and IL-8 protein (ng/ml) by skin fibroblasts from healthy controls. Cells were incubated for 24 hours with conditioned medium of activated CD4+ T cells in the absence or presence of Sema4A, which had previously been incubated for 1 hour with an anti–IL-17 antibody or its isotype control. Bars show the mean ± SEM of 7 independent experiments. * = $P < 0.05$ for the indicated comparisons. # = $P < 0.05$; ## = $P < 0.01$; ### = $P < 0.001$ versus medium.

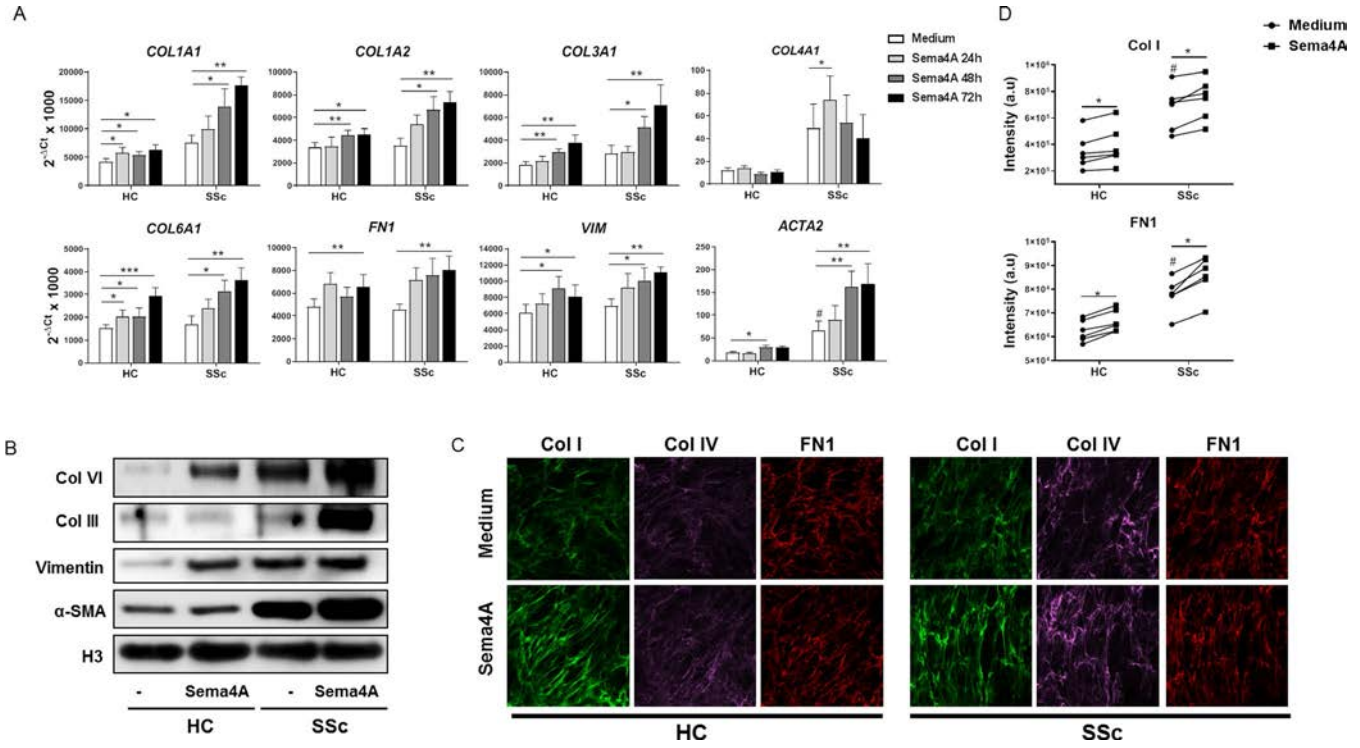

Figure 4. Semaphorin 4A (Sema4A)–induced expression and deposition of extracellular matrix (ECM) components. **A**, Expression of mRNA for ECM components by skin fibroblasts from healthy controls (HCs) and patients with systemic sclerosis (SSc). Cells were stimulated with Sema4A (200 ng/ml) for 24, 48, or 72 hours. Bars show the mean ± SEM of 6 independent experiments. **B**, Representative immunoblots showing expression of type VI collagen (Col VI), type III collagen, vimentin, and α-smooth muscle actin (α-SMA) protein in skin fibroblasts from healthy controls and SSc patients. Cells were stimulated with Sema4A for 72 hours. **C** and **D**, Type I collagen, type IV collagen, and fibronectin 1 (FN1) production (**C**) and deposition (**D**) by skin fibroblasts from healthy controls and SSc patients. Cells were stimulated with Sema4A for 7 days. Images in **C** are representative of 4 independent experiments. Original magnification × 20. Symbols in **D** represent individual subjects. * = $P < 0.05$; ** = $P < 0.01$; *** = $P < 0.001$ for the indicated comparisons. # = $P < 0.05$ versus unstimulated healthy control fibroblasts.

expression of these mediators was significantly enhanced by the conditioned medium of CD4+ T cells activated in the presence of Sema4A and was significantly inhibited when supernatants were preincubated with anti–IL-17 antibody (Figures 3B and C). Taken together, these results suggest that Sema4A-induced IL-17 expression by T cells is partially responsible for dermal fibroblast expression of inflammatory mediators.

Sema4A induces a profibrotic phenotype in dermal fibroblasts. Since Sema4A can modulate collagen contraction by lung fibroblasts (24), we analyzed the potential profibrotic effect of Sema4A on skin fibroblasts. Sema4A up-regulated, in a time-dependent manner, the expression of mRNA for various ECM components involved in fibrotic processes, such as *COL1A1*, *COL1A2*, *COL3A1*, *COL4A1*, *COL6A1, VIM*, *FN1,* and *ACTA2*, the gene that encodes the myofibroblast marker α-SMA, in fibroblasts from both healthy controls and SSc patients (Figure 4A). Protein analysis confirmed these results, as Sema4A induced the expression of type III collagen, type VI collagen, vimentin, and α-SMA (Figure 4B). Sema4A also induced the production of type I collagen, type IV collagen, and fibronectin by both healthy control and SSc dermal fibroblasts (Figure 4C). ECM deposition analysis confirmed these findings and also demonstrated that the deposition of type I collagen and fibronectin was significantly higher in SSc fibroblasts than healthy control fibroblasts (Figure 4D).

Finally, we analyzed the effect of the inhibition of Sema4A signaling on the production of ECM components by SSc fibroblasts. Neutralization of NRP-1 did not affect the expression of mRNA for these components in Sema4A-stimulated fibroblasts (Supplementary Figure 8, available on the *Arthritis & Rheumatology* web site at http://onlinelibrary.wiley.com/doi/10.1002/art.40915/abstract). However, plexin D1 neutralization or plexin B2 silencing significantly suppressed expression of mRNA for *COL1A1*, *COL1A2*, *COL3A1*, *COL6A1, VIM*, *FN1,* and *ACTA2* (Figures 5A and D), and the expression of type III collagen, type VI collagen, vimentin, and α-SMA protein in SSc patient fibroblasts (Figures 5B, C, E, and F). The lack of effect of NRP-1 was not due to differences in the expression levels of plexin D1, plexin B2, and NRP-1, as all 3 receptors were detected in dermal fibroblasts from both healthy controls and SSc patients. We did not find differences in the expression of mRNA for these receptors between healthy con-

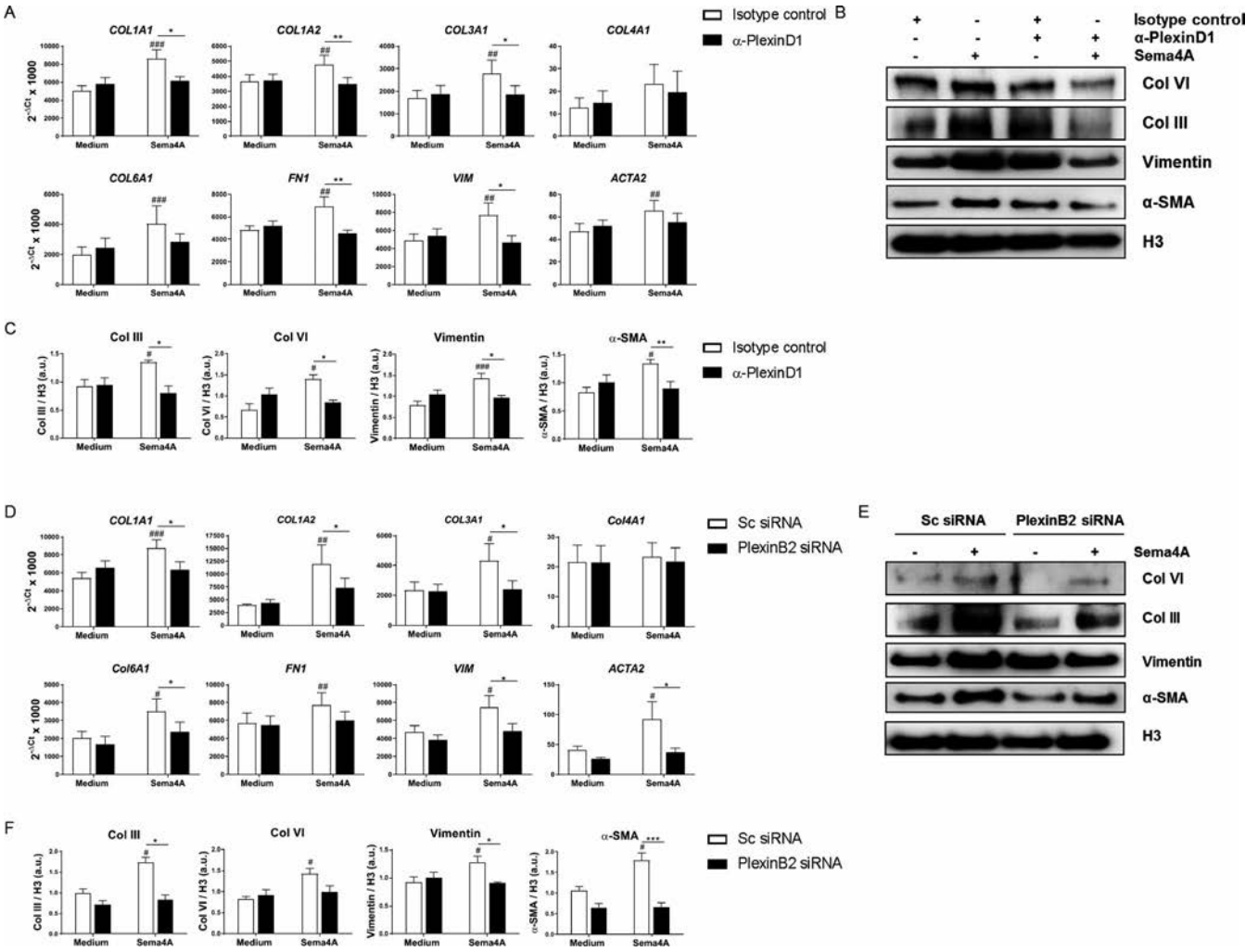

Figure 5. Plexin D1 blocking and plexin B2 silencing abrogate semaphorin 4A (Sema4A)–induced expression of extracellular matrix (ECM) components. **A** and **B**, Expression of mRNA for ECM components (**A**) and representative immunoblots showing expression of type VI collagen (Col VI), type III collagen, vimentin, and α-smooth muscle actin (α-SMA) protein (**B**) by skin fibroblasts from patients with systemic sclerosis (SSc). Cells were stimulated with Sema4A for 72 hours after 1 hour of preincubation with blocking anti–plexin D1 antibody or its isotype control. **C**, Densitometric analysis of type III collagen, type VI collagen, vimentin, and α-SMA protein expression. Data were normalized to histone H3 expression. **D** and **E**, Expression of mRNA for ECM components (**D**) and representative immunoblots showing expression of type VI collagen, type III collagen, vimentin, and α-SMA protein (**E**) by skin fibroblasts from SSc patients. Cells were stimulated with Sema4A for 72 hours after plexin B2 silencing. **F**, Densitometric analysis of type III collagen, type VI collagen, vimentin, and α-SMA protein expression. Data were normalized to histone H3 expression. In **A**, **C**, **D**, and **F**, bars show the mean ± SEM of 5–6 independent experiments. In **B** and **E**, results are representative of 5–6 independent experiments. * = $P < 0.05$; ** = $P < 0.01$; *** = $P < 0.001$ for the indicated comparisons. # = $P < 0.05$; ## = $P < 0.01$; ### = $P < 0.001$, versus isotype control or unstimulated scrambled (Sc) small interfering RNA (siRNA)–transfected cells.

trols and SSc patients, but Sema4A up-regulated the expression of mRNA for *PLXND1*, *PLXNB2,* and *NRP1* in fibroblasts from both healthy controls and SSc patients (Supplementary Figure 9, available on the *Arthritis & Rheumatology* web site at http://onlinelibrary.wiley.com/doi/10.1002/art.40915/abstract), suggesting that Sema4A might further enhance its profibrotic effect via the up-regulation of its receptors. Taken together, these data demonstrate that Sema4A directly induces profibrotic gene expression in healthy control and SSc dermal fibroblasts, dependent on signaling mediated by plexin D1 and plexin B2.

DISCUSSION

Herein, we demonstrated that Sema4A plays an essential role in inflammation and fibrosis, 2 main aspects of SSc pathology. Sema4A induces inflammation in an IL-17–dependent manner and directly induces a profibrotic phenotype in dermal fibroblasts (Figure 6). Abnormal activation of monocytes and T cells contributes to the ongoing inflammation observed in SSc patients (1,5,6,28,29). We found that plasma levels of Sema4A were elevated in SSc patients, similar to other autoimmune diseases such as rheumatoid arthritis and MS (23,30), and identified periph-

eral blood monocytes and CD4+ T cells as potential sources of Sema4A in SSc patients. Importantly, poly(I-C), a TLR-3 agonist, (31) and CXCL4, both important to the pathology of SSc (26), induced Sema4A secretion by circulating monocytes. CD3/CD28-mediated activation of CD4+ T cells also induced the secretion of Sema4A, as well as the surface expression of its receptors plexin B2 and NRP-1. Taken together, these results demonstrate that regulated expression of Sema4A and its receptors is disrupted in circulating SSc patient immune cells.

Previous mouse studies have demonstrated that Sema4A mediates Th17 skewing, and elevated serum levels of Sema4A in MS patients are positively associated with Th17 skewing (21–23). In this study we directly demonstrated a requisite role for Sema4A in the production of Th17, but not Th1 or Th2 cytokines, by human CD4+ T cells. In contrast with our observation, Sema4A was recently reported to induce proliferation and Th2 polarization in human CD4+ T cells (32). These differences may be attributed to the different recombinant Sema4A protein used, the different manner of CD4+ T cell activation and proliferation, and the use of CD4+ T cells from adult blood buffy coats. The effect of Sema4A on Th17 cytokine production was not considered in that study and therefore cannot be directly compared with our results. The effect of Sema4A on Th17 cytokine production was not restricted to a specific CD4+ T cell population, as we observed a similar induction of Th17 cytokines in naive, central memory, and effector memory populations. Importantly, Sema4A-induced IL-17 secretion was significantly higher in SSc patients, likely due to elevated expression of the receptors plexin B2 and NRP-1 by resting and activated SSc patient CD4+ T cells.

Inhibition of Sema4A signaling, through the blocking of the receptors NRP-1 and plexin D1, or the silencing of plexin B2, drastically reduced Th17 cytokine secretion. Notably, this effect was also observed in the absence of exogenous Sema4A, suggesting that CD4+ T cell production of Sema4A induces the expression of Th17 cytokines in an autocrine/paracrine manner. Sema4A can bind to different receptors in a cell type–dependent manner. Plexin D1 is the Sema4A receptor in macrophages, while Sema4A binds to plexin B2 in CD8+ T cells and to NRP-1 in Treg cells (33–35). Our results show that all 3 of these receptors are involved in Sema4A signaling in CD4+ T cells, although the highest inhibition of Sema4A-induced Th17 cytokine production was observed after the blocking of plexin D1. This finding might be explained simply by the fact that the percentage of CD4+ T cells expressing plexin D1 is much higher than those expressing plexin B2 and NRP-1, but we cannot rule out the potential differential blocking efficiency of antibodies used, residual expression of plexin B2 following gene silencing, or involvement of immunoglobulin-like transcript 4, a recently identified Sema4A receptor in CD4+ T cells (32).

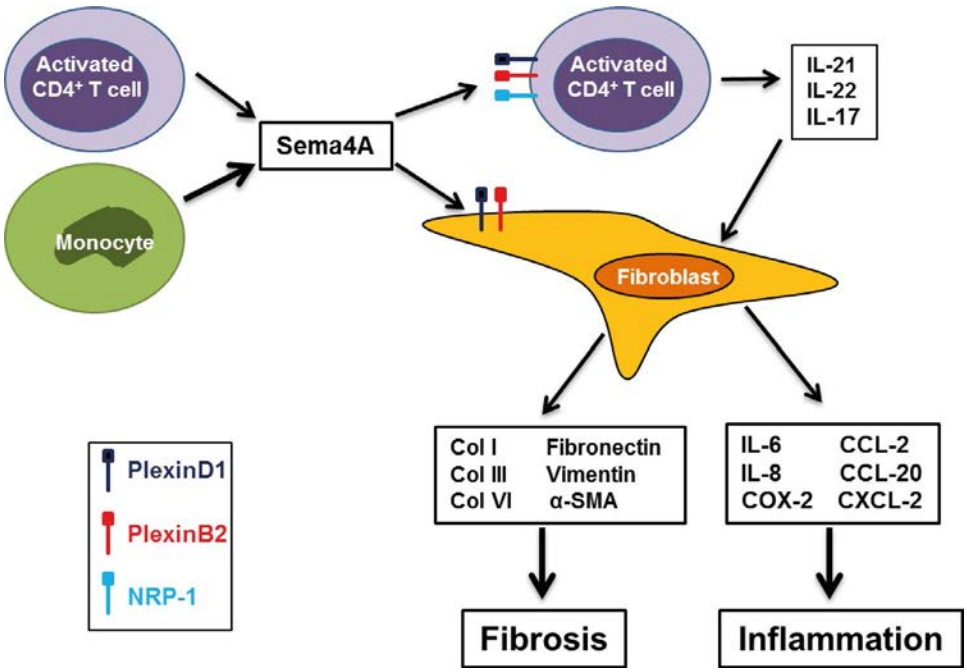

Figure 6. Schematic overview of the inflammatory and fibrotic roles of semaphorin 4A (Sema4A) in the pathogenesis of systemic sclerosis (SSc). Sema4A is elevated in the plasma of SSc patients, due to increased production by monocytes and, to a lesser extent, CD4+ T cells. In CD4+ T cells, Sema4A enhances the production of Th17 cytokines induced by CD3/CD28, and secreted interleukin-17 (IL-17) induces the production of inflammatory mediators and chemokines in dermal fibroblasts. Sema4A also plays a direct role in fibrosis by inducing the production of extracellular matrix components and the expression of the myofibroblast marker α-smooth muscle actin (α-SMA) in dermal fibroblasts. NRP-1 = neuropilin 1; Col I = type I collagen; COX-2 = cyclooxygenase 2.

To date, the role of IL-17 in SSc fibrotic processes has been uncertain, as mouse studies have shown that IL-17 plays a profibrotic role that was not observed in isolated human fibroblasts (36–39). In this study, we observed that IL-17 failed to modulate fibroblast expression of the ECM components examined, confirming that IL-17 does not induce a fibrotic phenotype in SSc fibroblasts. Instead, IL-17 can enhance dermal fibroblast expression of inflammatory mediators that are elevated in SSc patients and play an important role in disease pathology, including IL-6, IL-8, cyclooxygenase 2 (COX-2), CCL2, CCL20, and CXCL2 (1,40,41). Neutralization of IL-17 did not completely abrogate fibroblast production of inflammatory mediators in response to conditioned T cell supernatants, suggesting that other T cell cytokines are also involved in fibroblast activation. In this regard, IL-22 enhances TNF-induced expression of chemokines by healthy control and SSc dermal fibroblasts (42,43). Also, other mediators not regulated by Sema4A, such as TNF and IFNγ, are strong activators of dermal fibroblasts (43–45). However, this effect was not due to the Sema4A present in the supernatants, as the blocking of plexin D1 did not influence the expression of inflammatory mediators (Supplementary Figure 10, available on the *Arthritis & Rheumatology* web site at http://onlinelibrary.wiley.com/doi/10.1002/art.40915/abstract).

Our results suggest that Sema4A plays a role in SSc pathology, through the induction of IL-17 by CD4+ T cells, which promote fibroblast expression of inflammatory mediators. Fibroblasts are also key contributors to fibrosis in SSc, and their activation in affected tissue leads to their differentiation into α-SMA–expressing myofibroblasts and excessive deposition of ECM components (4,46–48). In the present study, we found that Sema4A induced the expression of ECM components and α-SMA by healthy control and SSc patient dermal fibroblasts, effects mediated by the receptors plexin D1 and plexin B2. In conclusion, in this study we have identified Sema4A as a key mediator of Th17 production and fibrosis, and blocking Sema4A signaling might suppress both pathologic processes in SSc, a complex and heterogeneous disease for which currently available therapies can only treat organ manifestations and no antifibrotic drugs have yet to be approved (49,50).

AUTHOR CONTRIBUTIONS

All authors were involved in drafting the article or revising it critically for important intellectual content, and all authors approved the final version to be published. Dr. García had full access to all of the data in the study and takes responsibility for the integrity of the data and the accuracy of the data analysis.

Study conception and design. Carvalheiro, Affandi, Marut, Reedquist, Radstake, García.

Acquisition of data. Carvalheiro, Affandi, Malvar-Fernández, Dullemond, Cossu, Ottria, Mertens, Giovannone, Bonte-Mineur, Kok, García.

Analysis and interpretation of data. Carvalheiro, Affandi, Malvar-Fernández, García.

REFERENCES

1. Gabrielli A, Avvedimento EV, Krieg T. Scleroderma. N Engl J Med 2009;360:1989–2003.
2. Denton CP, Khanna D. Systemic sclerosis. Lancet 2017;390:1685–99.
3. Pattanaik D, Brown M, Postlethwaite BC, Postlethwaite AE. Pathogenesis of systemic sclerosis. Front Immunol 2015;6:272.
4. Ebmeier S, Horsley V. Origin of fibrosing cells in systemic sclerosis. Curr Opin Rheumatol 2015;27:555–62.
5. Van Bon L, Cossu M, Radstake TR. An update on an immune system that goes awry in systemic sclerosis. Curr Opin Rheumatol 2011;23:505–10.
6. Lafyatis R, York M. Innate immunity and inflammation in systemic sclerosis. Curr Opin Rheumatol 2009;21:617–22.
7. Radstake TR, van Bon L, Broen J, Hussiani A, Hesselstrand R, Wuttge DM, et al. The pronounced Th17 profile in systemic sclerosis (SSc) together with intracellular expression of TGFβ and IFNγ distinguishes SSc phenotypes. PLoS One 2009;4:e5903.
8. Rodríguez-Reyna TS, Furuzawa-Carballeda J, Cabiedes J, Fajardo-Hermosillo LD, Martínez-Reyes C, Díaz-Zamudio M, et al. Th17 peripheral cells are increased in diffuse cutaneous systemic sclerosis compared with limited illness: a cross-sectional study. Rheumatol Int 2012;32:2653–60.
9. Zhou Y, Hou W, Xu K, Han D, Jiang C, Mou K, et al. The elevated expression of Th17-related cytokines and receptors is associated with skin lesion severity in early systemic sclerosis. Hum Immunol 2015;76:22–9.
10. Truchetet ME, Brembilla NC, Montanari E, Lonati P, Raschi E, Zeni S, et al. Interleukin-17A+ cell counts are increased in systemic sclerosis skin and their number is inversely correlated with the extent of skin involvement. Arthritis Rheum 2013;65:1347–56.
11. Yang X, Yang J, Xing X, Wan L, Li M. Increased frequency of Th17 cells in systemic sclerosis is related to disease activity and collagen overproduction. Arthritis Res Ther 2014;16:R4.
12. Fossiez F, Djossou O, Chomarat P, Flores-Romo L, Ait-Yahia S, Maat C, et al. T cell interleukin-17 induces stromal cells to produce proinflammatory and hematopoietic cytokines. J Exp Med 1996;183:2593–603.
13. Onishi RM, Gaffen SL. Interleukin-17 and its target genes: mechanisms of interleukin-17 function in disease. Immunology 2010;129:311–21.
14. Gonçalves RS, Pereira MC, Dantas AT, de Almeida AR, Marques CD, Rego MJ, et al. IL-17 and related cytokines involved in systemic sclerosis: perspectives. Autoimmunity 2018;51:1–9.
15. Worzfeld T, Offermanns S. Semaphorins and plexins as therapeutic targets. Nat Rev Drug Discov 2014;13:603–21.
16. Nishide M, Kumanogoh A. The role of semaphorins in immune responses and autoimmune rheumatic diseases. Nat Rev Rheumatol 2018;14:19–31.
17. Nkyimbeng-Takwi E, Chapoval SP. Biology and function of neuroimmune semaphorins 4A and 4D. Immunol Res 2011;50:10–21.
18. Ito D, Kumanogoh A. The role of Sema4A in angiogenesis, immune responses, carcinogenesis, and retinal systems. Cell Adh Migr 2016;10:692–9.
19. Kumanogoh A, Marukawa S, Suzuki K, Takegahara N, Watanabe C, Ch'ng E, et al. Class IV semaphorin Sema4A enhances T-cell activation and interacts with Tim-2. Nature 2002;419:629–33.
20. Kumanogoh A, Shikina T, Suzuki K, Uematsu S, Yukawa K, Kashiwamura SI, et al. Nonredundant roles of Sema4A in the immune system: Defective T cell priming and Th1/Th2 regulation in Sema4A-deficient mice. Immunity 2005;22:305–16.
21. Makino N, Toyofuku T, Takegahara N, Takamatsu H, Okuno T, Nakagawa Y, et al. Involvement of Sema4A in the progression of experimental autoimmune myocarditis. FEBS Lett 2008;582:3935–40.

22. Morihana T, Goya S, Mizui M, Yasui T, Prasad DV, Kumanogoh A, et al. An inhibitory role for Sema4A in antigen-specific allergic asthma. J Clin Immunol 2013;33:200–9.
23. Nakatsuji Y, Okuno T, Moriya M, Sugimoto T, Kinoshita M, Takamatsu H, et al. Elevation of Sema4A implicates Th cell skewing and the efficacy of IFN-β therapy in multiple sclerosis. J Immunol 2012;188:4858–65.
24. Peng HY, Gao W, Chong FR, Liu HY, Zhang JI. Semaphorin 4A enhances lung fibrosis through activation of Akt via PlexinD1 receptor. J Biosci 2015;40:855–62.
25. Van Den Hoogen F, Khanna D, Fransen J, Johnson SR, Baron M, Tyndall A, et al. 2013 classification criteria for systemic sclerosis: an American College of Rheumatology/European League Against Rheumatism collaborative initiative. Arthritis Rheum 2013;65: 2737–47.
26. Van Bon L, Affandi AJ, Broen J, Christmann RB, Marijnissen RJ, Stawski L, et al. Proteome-wide analysis and CXCL4 as a biomarker in systemic sclerosis. N Engl J Med 2014;370:433–43.
27. Papp G, Horvath IF, Barath S, Gyimesi E, Sipka S, Szodoray P, et al. Altered T-cell and regulatory cell repertoire in patients with diffuse cutaneous systemic sclerosis. Scand J Rheumatol 2011;40:205–10.
28. Chizzolini C, Brembilla NC, Montanari E, Truchetet ME. Fibrosis and immune dysregulation in systemic sclerosis. Autoimmun Rev 2011;10:276–81.
29. Brembilla NC, Chizzolini C. T cell abnormalities in systemic sclerosis with a focus on Th17 cells. Eur Cytokine Netw 2012;23:128–39.
30. Wang L, Song G, Zheng Y, Tan W, Pan J, Zhao Y, et al. Expression of semaphorin 4A and its potential role in rheumatoid arthritis. Arthritis Res Ther 2015;17:227.
31. Farina GA, York MR, Di Marzio M, Collins CA, Meller S, Homey B, et al. Poly(I:C) drives type I IFN- and TGFβ-mediated inflammation and dermal fibrosis simulating altered gene expression in systemic sclerosis. J Invest Dermatol 2010;130:2583–93.
32. Lu N, Li Y, Zhang Z, Xing J, Sun Y, Yao S, et al. Human semaphorin-4A drives Th2 responses by binding to receptor ILT-4. Nat Commun 2018;9:742.
33. Ito D, Nojima S, Nishide M, Okuno T, Takamatsu H, Kang S, et al. MTOR complex signaling through the Sema4A–plexin B2 axis is required for optimal activation and differentiation of $CD8^+$ T cells. J Immunol 2015;195:934–43.
34. Meda C, Molla F, De Pizzol M, Regano D, Maione F, Capano S, et al. Semaphorin 4A exerts a proangiogenic effect by enhancing vascular endothelial growth factor-A expression in macrophages. J Immunol 2012;188:4081–92.
35. Delgoffe GM, Woo SR, Turnis ME, Gravano DM, Guy C, Overacre AE, et al. Stability and function of regulatory T cells is maintained by a neuropilin-1-semaphorin-4A axis. Nature 2013;501:252–6.
36. Brembilla NC, Montanari E, Truchetet ME, Raschi E, Meroni P, Chizzolini C. Th17 cells favor inflammatory responses while inhibiting type I collagen deposition by dermal fibroblasts: differential effects in healthy and systemic sclerosis fibroblasts. Arthritis Res Ther 2013;15:R151.
37. Lei L, Zhao C, Qin F, He ZY, Wang X, Zhong XN. Th17 cells and IL-17 promote the skin and lung inflammation and fibrosis process in a bleomycin-induced murine model of systemic sclerosis. Clin Exp Rheumatol 2016;34 Suppl 100:14–22.
38. Park MJ, Moon SJ, Lee EJ, Jung KA, Kim EK, Kim DS, et al. IL-1-IL-17 signaling axis contributes to fibrosis and inflammation in two different murine models of systemic sclerosis. Front Immunol 2018;9:1611.
39. Braun RK, Ferrick C, Neubauer P, Sjoding M, Sterner-Kock A, Kock M, et al. IL-17 producing γδ T cells are required for a controlled inflammatory response after bleomycin-induced lung injury. Inflammation 2008;31:167–79.
40. O'Reilly S, Cant R, Ciechomska M, van Laar JM. Interleukin-6: a new therapeutic target in systemic sclerosis? Clin Transl Immunology 2013;2:e4.
41. Distler JH, Akhmetshina A, Schett G, Distler O. Monocyte chemoattractant proteins in the pathogenesis of systemic sclerosis. Rheumatology (Oxford) 2009;48:98–103.
42. Xing R, Yang L, Jin Y, Sun L, Li C, Li Z, et al. Interleukin-21 induces proliferation and proinflammatory cytokine profile of fibroblast-like synoviocytes of patients with rheumatoid arthritis. Scand J Immunol 2016;83:64–71.
43. Brembilla NC, Dufour AM, Alvarez M, Hugues S, Montanari E, Truchetet ME, et al. IL-22 capacitates dermal fibroblast responses to TNF in scleroderma. Ann Rheum Dis 2016;75:1697–705.
44. Larsen CG, Anderson AO, Oppenheim JJ, Matsushima K. Production of interleukin-8 by human dermal fibroblasts and keratinocytes in response to interleukin-1 or tumour necrosis factor. Immunology 1989;68:31–6.
45. Antonelli A, Fallahi P, Ferrari SM, Giugglioli D, Colaci M, Di Domenicoantonio A, et al. Systemic sclerosis fibroblasts show specific alterations of interferon-γ and tumor necrosis factor-α-induced modulation of interleukin 6 and chemokine ligand 2. J Rheumatol 2012;39:979–85.
46. Gilbane AJ, Denton CP, Holmes AM. Scleroderma pathogenesis: a pivotal role for fibroblasts as effector cells [review]. Arthritis Res Ther 2013;15:215.
47. Hinz B, Phan SH, Thannickal VJ, Galli A, Bochaton-Piallat ML, Gabbiani G. The myofibroblast: one function, multiple origins. Am J Pathol 2007;170:1807–16.
48. Schulz JN, Plomann M, Sengle G, Gullberg D, Krieg T, Eckes B. New developments on skin fibrosis: essential signals emanating from the extracellular matrix for the control of myofibroblasts. Matrix Biol 2018;522–32.
49. Van Rhijn-Brouwer FC, Gremmels H, Fledderus JO, Radstake TR, Verhaar MC, van Laar JM. Cellular therapies in systemic sclerosis: recent progress. Curr Rheumatol Rep 2016;18:12.
50. Bruni C, Praino E, Allanore Y, Distler O, Gabrielli A, Iannone F, et al. Use of biologics and other novel therapies for the treatment of systemic sclerosis. Expert Rev Clin Immunol 2017;13:469–82.

Arthritis & Rheumatology
Vol. 71, No. 10, October 2019, pp 1723–1726
DOI 10.1002/art.40919

American College of Rheumatology
Empowering Rheumatology Professionals

BRIEF REPORT

Use of Proprotein Convertase Subtilisin/Kexin Type 9 Inhibitors in Statin-Associated Immune-Mediated Necrotizing Myopathy: A Case Series

Eleni Tiniakou,[1] Erika Rivera,[1] Andrew L. Mammen,[2] and Lisa Christopher-Stine[1]

Objective. To determine the safety of proprotein convertase subtilisin/kexin type 9 (PCSK9) inhibitors in patients with statin-associated anti–3-hydroxy-3-methlyglutaryl coenzyme A reductase (anti-HMGCR)–positive immune-mediated necrotizing myopathy (IMNM).

Methods. Muscle strength was assessed in anti-HMGCR–positive patients at each visit before and after initiation of PCSK9 inhibitors. The trends in creatine kinase (CK) levels and serum anti-HMGCR antibody titers were monitored over time.

Results. Among 122 anti-HMGCR–positive patients, we identified 8 patients who were receiving PCSK9 inhibitors for hyperlipidemia. Patients were followed up for an average of 1.5 years (range 3–37 months), and none exhibited reduction in muscle strength. The mean ± SD CK level prior to the initiation of PCSK9 inhibitors was 956 ± 1,137 IU/liter, which was reduced to 419 ± 393 IU/liter at their last visit. Anti-HMGCR antibody titers followed a similar trend. Notably, in 2 patients, the initiation of the lipid-lowering medication was followed by unanticipated spontaneous clinical improvement and reduction in immunosuppression.

Conclusion. PCSK9 inhibitors are safe for long-term use as a cholesterol-lowering agent in patients with statin-associated IMNM.

INTRODUCTION

Statins, which reduce cholesterol levels by inhibiting 3-hydroxy-3-methlyglutaryl coenzyme A reductase (HMGCR), are the cornerstone of current lipid-lowering strategies. Although musculoskeletal side effects occur in some statin-treated patients, these are typically mild and reversible with discontinuation of the medication. However, immune-mediated necrotizing myopathy (IMNM) has been known to develop in statin-treated patients in rare cases (1,2). This form of myositis is associated with proximal muscle weakness, elevated creatine kinase (CK) levels, and the presence of autoantibodies recognizing HMGCR. Since statins are known to up-regulate HMGCR expression, it has been proposed that the overexpression of HMGCR may play a role in breaking tolerance and initiating autoimmunity (2). Statin-associated IMNM can be successfully treated by discontinuing the statin and starting immunosuppressive therapy. However, reintroduction of statins is avoided as this may lead to disease flares, possibly by the up-regulation of HMGCR levels (3,4).

As patients with statin-triggered IMNM commonly have a high risk for cardiovascular disease, physicians face a conundrum on how to manage the cholesterol levels in these patients. Proprotein convertase subtilisin/kexin type 9 (PCSK9) inhibitors have been shown to effectively lower cholesterol levels by increasing the cellular uptake of low-density lipoprotein (LDL) (5). Since these agents may actually lower HMGCR levels (6,7), we hypothesized that they might be tolerated by patients with statin-triggered IMNM.

Dr. Tiniakou's work was supported by the Rheumatology Research Foundation Scientist Development Award and the Jerome L. Greene Foundation. Dr. Mammen's work was supported by the NIH National Institute of Arthritis and Musculoskeletal and Skin Diseases Intramural Research Program. Dr. Christopher-Stine's work was supported by the Huayi and Siuling Zhang Discovery Fund.

[1]Eleni Tiniakou, MD, Erika Rivera, MD, Lisa Christopher-Stine, MD: Johns Hopkins University School of Medicine, Baltimore, Maryland; [2]Andrew L. Mammen, MD, PhD: National Institute of Arthritis and Musculoskeletal and Skin Diseases, NIH, Bethesda, Maryland, and Johns Hopkins University School of Medicine, Baltimore, Maryland.

Drs. Mammen and Christopher-Stine hold a patent on a commercial test for anti–hydroxymethylglutaryl-coenzyme A reductase antibodies. Dr. Christopher-Stine receives royalties from Inova Diagnostics. No other disclosures relevant to this article were reported.

Address correspondence to Lisa Christopher-Stine, MD, The Johns Hopkins University, Division of Rheumatology, 5200 Eastern Avenue, MFL Center Tower Suite 4500, Baltimore, MD 21224. E-mail: lchrist4@jhmi.edu.

Submitted for publication March 19, 2019; accepted in revised form April 30, 2019.

Table 1. Demographic and clinical characteristics of the 8 patients with statin-associated anti-HMGCR immune-mediated necrotizing myopathy receiving PCSK9 inhibitors*

Characteristic	Patient 1	Patient 2	Patient 3	Patient 4	Patient 5	Patient 6	Patient 7	Patient 8
Sex	F	F	F	M	F	F	F	M
Race	AA	White	White	White	AA	White	White	White
Age, years								
At start of statin	50	55	43	64	65	54	57	56
At start of muscle-related symptoms	54	57	58	66	66	67	60	71
At start of PCSK9i	70	68	69	75	68	68	69	71
Years between beginning of disease and initiation of PCSK9i	16	11	11	9	2	1	9	0
PCKS9i medication	Evocolumab	Alirocumab	Evocolumab	Alirocumab	Alirocumab	Evocolumab	Evocolumab	Evocolumab
Other lipid-lowering medications	Ezetimibe, fenofibrate	Colesevelam	Ezetimibe, colesevelam	Ezetimibe	–	Fenofibrate	Omega-3 fatty acids	Omega-3 fatty acids
Months between initiation of PCSK9i and most recent evaluation	17	14	15	26	37	32	3	3
Strength								
Arm abductors								
Before PCSK9i	5	5	4	4	4	4	4+	4+
After PCSK9I	5	5	4	4+	4	5	4+	4+
Most recent evaluation	5	5	4–	5	4–	5	–	–
Hip flexors								
Before PCSK9i	2	4+	3	4–	4	2	4+	4
After PCSK9I	2	4+	3	4–	4	2	4+	4
Most recent evaluation	2	4+	4	4+	3	2+	–	–
Creatine kinase, IU/liter								
Before PCSK9i	1,141	585	98	981	68	3,507	67	1,205
After PCSK9I	927	670	151	441	72	3,539	121	1,088
Most recent evaluation	962	677	108	75	43	651	–	–
Anti-HMGCR antibody titer, NAU								
Before PCSK9i	1.369	1.313	1.195	1.654	1.095	–	0.722	0.876
After PCSK9i	1.353	1.204	1.346	–	1.159	–	0.832	0.947
Most recent evaluation	1.346	–	1.096	1.04	–	1.645	–	–
LDL, mg/dl								
Before PCSK9i	180	123	–	106	–	133	–	–
Most recent evaluation	57	64	–	60	–	88	–	–
Medications								
Before PCSK9i	MTX 22.5 mg/week, prednisone 5 mg/day	IVIG 2 gm/kg every 2 weeks	MTX 20 mg/week, prednisone 5 mg/day, IVIG 2 gm/kg every 8 weeks	AZA 100 mg/day	MTX 20 mg/week, prednisone 5 mg/day	MTX 15 mg/week, prednisone 60 mg/day	Prednisone 7 mg/day, IVIG 2 gm/kg every 4 weeks	Prednisone 70 mg/day
Most recent evaluation	Stable	Stable	Stable	None	MTX 17.5 mg/week (following hiatus)	MTX 10 mg/week, AZA 150 mg/day, IVIG 2 gm/kg every 4 weeks	Stable	Prednisone 4 mg/day

* Anti-HMGCR = anti–3-hydroxy-3-methlyglutaryl coenzyme A; PCSK9i = proprotein convertase subtilisin/kexin type 9 inhibitor; AA = African American; NAU = normalized absorbance units; LDL = low-density lipoprotein; MTX = methotrexate; IVIG = intravenous immunoglobulin; AZA = azathioprine.

PATIENTS AND METHODS

Patients included in this study were enrolled in the longitudinal cohort at the Johns Hopkins Myositis Center. All patients provided written informed consent as approved by the Johns Hopkins Institutional Review Board. Among the 122 anti-HMGCR–positive patients available from the cohort, 8 were receiving PCSK9 inhibitors for hyperlipidemia. Arm abduction and hip flexion strength were evaluated using the Medical Research Council Muscle scale, which has a range of 0 to 5 for each muscle group. Data on serum CK levels were available from the most proximal visits before and after the initiation of PCSK9 inhibitors. Serum titers of anti-HMGCR were measured by specific enzyme-linked immunosorbent assay, as described previously (8).

RESULTS

Among 122 patients with anti-HMGCR IMNM evaluated at the Johns Hopkins Myositis Center, we identified 8 patients with severe cardiovascular disease and/or diabetes who began treatment with a PCSK9 inhibitor (Table 1). One patient (patient 3) had previously been rechallenged with a statin, leading to a disease flare. The mean age at initiation of PCSK9 inhibitors was 69.75 years, and the mean ± SD duration of statin-associated anti-HMGCR myositis was 7 ± 5.73 years. Five patients were started on evolocumab, and 3 were started on alirocumab. The average duration of follow-up with PCSK9 inhibitor treatment was 18 months (range 3–37 months).

In 1 patient (patient 6), the initiation of PCSK9 inhibitor treatment was concurrent with the escalation of immunosuppressive regimens due to active disease; the remaining patients were receiving stable doses of immunosuppressive agents. The mean ± SD CK level prior to the initiation of PCSK9 inhibitors was 956 ± 1,137 IU/liter, which had declined to 876 ± 1,140 IU/liter at the next follow-up visit and which, at the most recent evaluation, was further reduced to 419 ± 393 IU/liter. During the follow-up period, there was no decrease in hip flexion or arm abductor muscle strength, except in 1 patient who was not receiving immunosuppressive treatment due to noncompliance. Remarkably, 1 patient receiving PCSK9 inhibitors exhibited CK and muscle strength improvement without the addition of immunosuppressive agents (patient 4), and in another patient, prednisone monotherapy could be tapered from 70 mg to 4 mg (patient 8).

DISCUSSION

While there are 2 previous case reports addressing the role of statin use in IMNM (9,10), our case series represents the largest cohort of patients with statin-associated anti-HMGCR–positive IMNM with the longest time of follow-up. In addition, we provide longitudinal data on HMGCR autoantibody titers. We present data on 8 patients with statin-associated IMNM who received PCSK9 inhibitors, with 1 patient experiencing a myositis flare upon statin rechallenge. All patients tolerated this class of cholesterol-lowering agent without exacerbation of their underlying myopathy. Of interest, 2 patients had unanticipated spontaneous clinical improvement following initiation of PCSK9 inhibitor treatment, which allowed tapering of immunosuppressive therapy. Although the mechanism underlying clinical improvement in myositis features remains unclear, we postulate that PCSK9 inhibitors may ameliorate autoimmunity in these patients by reducing HMGCR levels.

This study is limited by its retrospective nature. Nonetheless, our experience to date suggests that PCSK9 inhibitors are safe in anti-HMGCR–positive IMNM patients who would benefit from cholesterol-lowering therapy due to high cardiovascular risk.

ACKNOWLEDGMENTS

We would like to thank the research coordinators and rheumatology fellows of the Johns Hopkins Myositis Center for their invaluable support in obtaining the patients' samples and gathering the data. We would also like to thank all the patients of the Johns Hopkins Myositis Center who participated in the study.

AUTHOR CONTRIBUTIONS

All authors were involved in drafting the article or revising it critically for important intellectual content, and all authors approved the final version to be submitted for publication. Dr. Tiniakou had full access to all of the data in the study and takes responsibility for the integrity of the data and the accuracy of the data analysis.

Study conception and design. Tiniakou, Christopher-Stine.
Acquisition of data. Tiniakou, Rivera, Christopher-Stine.
Analysis and interpretation of data. Tiniakou, Mammen, Christopher-Stine.

REFERENCES

1. Christopher-Stine L, Casciola-Rosen LA, Hong G, Chung T, Corse AM, Mammen AL. A novel autoantibody recognizing 200-kd and 100-kd proteins is associated with an immune-mediated necrotizing myopathy. Arthritis Rheum 2010;62:2757–66.
2. Mammen AL, Chung T, Christopher-Stine L, Rosen P, Rosen A, Doering KR, et al. Autoantibodies against 3-hydroxy-3-methylglutaryl-coenzyme A reductase in patients with statin-associated autoimmune myopathy. Arthritis Rheum 2011;63:713–21.
3. Mammen AL. Statin-associated autoimmune myopathy [review]. N Engl J Med 2016;374:664–9.
4. Tiniakou E, Christopher-Stine L. Immune-mediated necrotizing myopathy associated with statins: history and recent developments. Curr Opin Rheumatol 2017;29:604–11.
5. Bergeron N, Phan BA, Ding Y, Fong A, Krauss RM. Proprotein convertase subtilisin/kexin type 9 inhibition: a new therapeutic mechanism for reducing cardiovascular disease risk. Circulation 2015;132:1648–66.
6. Lan H, Pang L, Smith MM, Levitan D, Ding W, Liu L, et al. Proprotein convertase subtilisin/kexin type 9 (PCSK9) affects gene expression

pathways beyond cholesterol metabolism in liver cells. J Cell Physiol 2010;224:273–81.
7. Zhang L, McCabe T, Condra JH, Ni YG, Peterson LB, Wang W, et al. An anti-PCSK9 antibody reduces LDL-cholesterol on top of a statin and suppresses hepatocyte SREBP-regulated genes. Int J Biol Sci 2012;8:310–27.
8. Tiniakou E, Pinal-Fernandez I, Lloyd TE, Albayda J, Paik J, Werner JL, et al. More severe disease and slower recovery in younger patients with anti-3-hydroxy-3-methylglutaryl-coenzyme A reductase-associated autoimmune myopathy. Rheumatology (Oxford) 2017;56:787–94.
9. De Dios García-Díaz J, Corral-Bueno IM, Mesa-Latorre JM, Lozano-Durán C, Hernández-Ahijado C. Proprotein convertase subtilisin/kexin type 9 antibody and statin-associated autoimmune myopathy. Ann Intern Med 2019;171:68–9.
10. Brannick B, Childress R. A case of HMGCR-antibodies causing statin-associated autoimmune necrotizing myopathy [abstract]. J Clin Lipidol 2017;11:824.

DOI 10.1002/art.41033

Clinical Images: Takotsubo and Takayasu—a reason to rhyme?

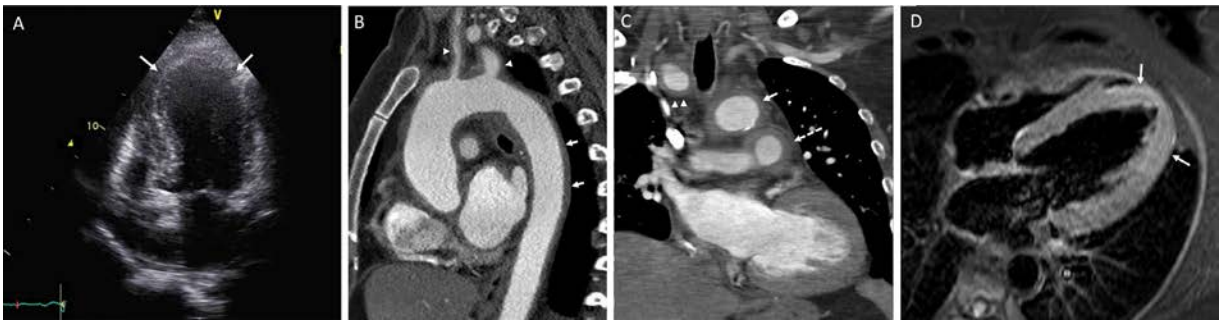

The patient, a 51-year-old Chinese woman with asthma, presented with sudden-onset chest pain and shortness of breath. An early diastolic murmur was auscultated over the precordium. Twelve-lead electrocardiography revealed ST segment elevation in V2–V4. Emergency cardiac catheterization showed no coronary artery abnormality. Echocardiography revealed a left ventricular (LV) ejection fraction of 50%, akinesia, ballooning of the apex (**arrows** in **A**) with hyperkinesia of the basal segments suggestive of takotsubo cardiomyopathy (TC), and dilated aortic root and ascending aorta with moderate aortic regurgitation (AR) (1). Computed tomography angiography of the aorta was performed, revealing abnormal diffuse concentric wall thickening involving the thoracic aorta (**arrows** in **B** and **C**), and right brachiocephalic trunk, left common carotid, left subclavian (**arrowheads** in **B** and **C**), and main and bilateral pulmonary arteries (**broken arrow** in **C**) with areas of stenosis and aneurysm formation, suggestive of Takayasu arteritis (TAK). The patient had decreased left brachial pulse and a blood pressure (BP) difference of >10 mm Hg (in systolic BP between arms), fulfilling the 1990 classification criteria for TAK (2). The erythrocyte sedimentation rate (ESR) was elevated (67 mm/hour), but the C-reactive protein level was normal. Despite the patient's age and elevated ESR, the absence of polymyalgia and cranial symptoms made a diagnosis of giant cell arteritis with large vessel involvement unlikely (3). Cardiovascular magnetic resonance imaging later revealed resolution of LV apical ballooning, with faint myocardial edema at the LV apical segments (**arrows** in **D**), compatible with temporal evolution of TC. TAK was evident in the diffuse wall thickening of the imaged aorta, arch vessels, and main and proximal branch pulmonary arteries. Inflammatory ascending aortitis with secondary aortic annular dilatation resulted in severe AR. Symptoms improved after initiation of treatment with valsartan (for TC), prednisolone, and pulse cyclophosphamide (for the multifaceted cardiac involvement in TAK). To our knowledge, coexistence of TC and TAK has not been reported previously (4).

1. Ghadri JR, Wittstein IS, Prasad A, Sharkey S, Dote K, Akashi YJ, et al. International expert consensus document on takotsubo syndrome. Part I. Clinical characteristics, diagnostic criteria, and pathophysiology. Eur Heart J 2018;39:2032–46.
2. Arend WP, Michel BA, Bloch DA, Hunder GG, Calabrese LH, Edworthy SM, et al. The American College of Rheumatology 1990 criteria for the classification of Takayasu arteritis. Arthritis Rheum 1990;33:1129–34.
3. Koster MJ, Matteson EL, Warrington KJ. Large-vessel giant cell arteritis: diagnosis, monitoring and management. Rheumatology (Oxford) 2018;57 Suppl 2:ii32–42.
4. Cavalli G, Tomelleri A, Di Napoli D, Baldissera E, Dagna L. Prevalence of Takayasu arteritis in young women with acute ischemic heart disease. Int J Cardiol 2018;252:21–3.

Shir Lynn Lim, MBBS, MRCP
National University Heart Centre
Ching Ching Ong, MBBS, FRCR, MMed
D. P. S. Dissanayake, MBBS, MD, MRCP
Lynette Li San Teo, MBChB, FRCR
Sen Hee Tay, MBBS, MRCP
National University Health System
Singapore, Singapore

pathways beyond cholesterol metabolism in liver cells. J Cell Physiol 2010;224:273–81.
7. Zhang L, McCabe T, Condra JH, Ni YG, Peterson LB, Wang W, et al. An anti-PCSK9 antibody reduces LDL-cholesterol on top of a statin and suppresses hepatocyte SREBP-regulated genes. Int J Biol Sci 2012;8:310–27.
8. Tiniakou E, Pinal-Fernandez I, Lloyd TE, Albayda J, Paik J, Werner JL, et al. More severe disease and slower recovery in younger patients with anti-3-hydroxy-3-methylglutaryl-coenzyme A reductase-associated autoimmune myopathy. Rheumatology (Oxford) 2017;56:787–94.
9. De Dios García-Díaz J, Corral-Bueno IM, Mesa-Latorre JM, Lozano-Durán C, Hernández-Ahijado C. Proprotein convertase subtilisin/kexin type 9 antibody and statin-associated autoimmune myopathy. Ann Intern Med 2019;171:68–9.
10. Brannick B, Childress R. A case of HMGCR-antibodies causing statin-associated autoimmune necrotizing myopathy [abstract]. J Clin Lipidol 2017;11:824.

DOI 10.1002/art.41033

Clinical Images: Takotsubo and Takayasu—a reason to rhyme?

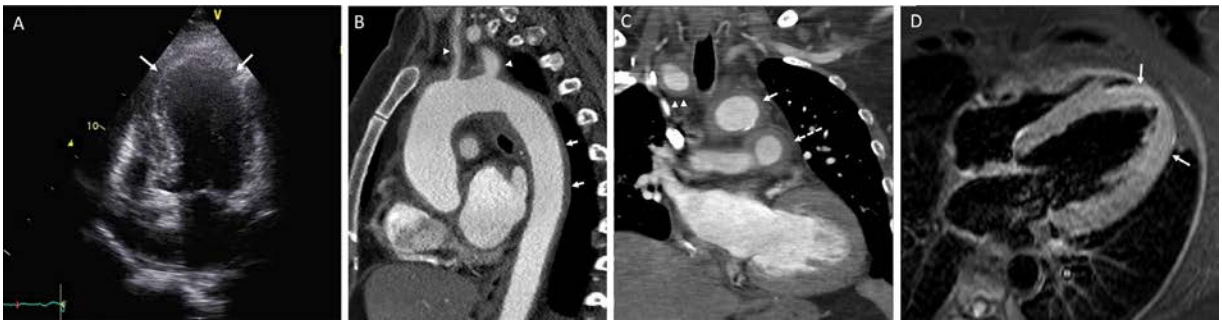

The patient, a 51-year-old Chinese woman with asthma, presented with sudden-onset chest pain and shortness of breath. An early diastolic murmur was auscultated over the precordium. Twelve-lead electrocardiography revealed ST segment elevation in V2–V4. Emergency cardiac catheterization showed no coronary artery abnormality. Echocardiography revealed a left ventricular (LV) ejection fraction of 50%, akinesia, ballooning of the apex (**arrows** in **A**) with hyperkinesia of the basal segments suggestive of takotsubo cardiomyopathy (TC), and dilated aortic root and ascending aorta with moderate aortic regurgitation (AR) (1). Computed tomography angiography of the aorta was performed, revealing abnormal diffuse concentric wall thickening involving the thoracic aorta (**arrows** in **B** and **C**), and right brachiocephalic trunk, left common carotid, left subclavian (**arrowheads** in **B** and **C**), and main and bilateral pulmonary arteries (**broken arrow** in **C**) with areas of stenosis and aneurysm formation, suggestive of Takayasu arteritis (TAK). The patient had decreased left brachial pulse and a blood pressure (BP) difference of >10 mm Hg (in systolic BP between arms), fulfilling the 1990 classification criteria for TAK (2). The erythrocyte sedimentation rate (ESR) was elevated (67 mm/hour), but the C-reactive protein level was normal. Despite the patient's age and elevated ESR, the absence of polymyalgia and cranial symptoms made a diagnosis of giant cell arteritis with large vessel involvement unlikely (3). Cardiovascular magnetic resonance imaging later revealed resolution of LV apical ballooning, with faint myocardial edema at the LV apical segments (**arrows** in **D**), compatible with temporal evolution of TC. TAK was evident in the diffuse wall thickening of the imaged aorta, arch vessels, and main and proximal branch pulmonary arteries. Inflammatory ascending aortitis with secondary aortic annular dilatation resulted in severe AR. Symptoms improved after initiation of treatment with valsartan (for TC), prednisolone, and pulse cyclophosphamide (for the multifaceted cardiac involvement in TAK). To our knowledge, coexistence of TC and TAK has not been reported previously (4).

1. Ghadri JR, Wittstein IS, Prasad A, Sharkey S, Dote K, Akashi YJ, et al. International expert consensus document on takotsubo syndrome. Part I. Clinical characteristics, diagnostic criteria, and pathophysiology. Eur Heart J 2018;39:2032–46.
2. Arend WP, Michel BA, Bloch DA, Hunder GG, Calabrese LH, Edworthy SM, et al. The American College of Rheumatology 1990 criteria for the classification of Takayasu arteritis. Arthritis Rheum 1990;33:1129–34.
3. Koster MJ, Matteson EL, Warrington KJ. Large-vessel giant cell arteritis: diagnosis, monitoring and management. Rheumatology (Oxford) 2018;57 Suppl 2:ii32–42.
4. Cavalli G, Tomelleri A, Di Napoli D, Baldissera E, Dagna L. Prevalence of Takayasu arteritis in young women with acute ischemic heart disease. Int J Cardiol 2018;252:21–3.

Shir Lynn Lim, MBBS, MRCP
National University Heart Centre
Ching Ching Ong, MBBS, FRCR, MMed
D. P. S. Dissanayake, MBBS, MD, MRCP
Lynette Li San Teo, MBChB, FRCR
Sen Hee Tay, MBBS, MRCP
National University Health System
Singapore, Singapore

Arthritis & Rheumatology
Vol. 71, No. 10, October 2019, pp 1727–1732
DOI 10.1002/art.40912

American College of Rheumatology
Empowering Rheumatology Professionals

Long-Term Outcome of Ustekinumab Therapy for Behçet's Disease

Adrien Mirouse,[1] Stéphane Barete,[2] Anne-Claire Desbois,[1] Cloé Comarmond,[1] Damien Sène,[3] Fanny Domont,[1] Bahram Bodaghi,[4] Yasmina Ferfar,[1] Patrice Cacoub,[1] and David Saadoun,[1] for the French Behçet's Network

Objective. Oral ulcers, the hallmark lesion of Behçet's disease (BD), can be disabling and resistant to conventional treatment, and there is a need for safe and effective treatment. We undertook this study to investigate the long-term safety and efficacy of ustekinumab therapy for BD-related oral ulcers that are resistant to colchicine.

Methods. This multicenter, prospective, open-label study included 30 patients who fulfilled the criteria of the International Study Group for BD and who were diagnosed as having active oral ulcers resistant to colchicine. Patients were treated subcutaneously with ustekinumab 90 mg at inclusion, at week 4, and then once every 12 weeks. Each patient was assessed longitudinally for the presence and number of oral ulcers, and median numbers of oral ulcers (with interquartile range [IQR]) were calculated. The primary efficacy end point was the proportion of patients at week 12 who experienced complete response, defined as having no oral ulcers.

Results. The median number of oral ulcers per patient during ustekinumab therapy was significantly lower at week 12 compared to baseline (0 [IQR 0–1] versus 2 [IQR 2–3]; $P < 0.0001$). Complete response was achieved in 60.0% and 88.9% of patients at weeks 12 and 24, respectively. The median Behçet's Syndrome Activity Score (in which higher scores indicate more active disease) was significantly lower at weeks 12 and 24 (17.5 [IQR 10–42.5] and 10 [IQR 8–11], respectively) versus baseline (70 [IQR 50–70]; $P < 0.0001$). After a median follow-up of 12 months (IQR 6–16 months), 26 patients (86.7%) were still receiving ustekinumab treatment. Reasons for ustekinumab discontinuation included BD flare (n = 3) and side effects (n = 1). Seven patients (23.3%) experienced adverse events, including headaches (n = 4) and asthenia (n = 2), with no serious side effects.

Conclusion. Ustekinumab seems to be effective in treating BD-related oral ulcers that are resistant to treatment with colchicine.

INTRODUCTION

Behçet's disease (BD) is a form of vasculitis of unknown etiology, characterized by mucocutaneous, ocular, articular, vascular, and central nervous system (CNS) manifestations (1,2). Mucocutaneous lesions of BD include oral ulcers, genital ulcers, and papulopustular and nodular lesions. Recurrent oral ulcers can be disabling and have a substantial effect on quality of life. If topical therapy alone is unsuccessful, colchicine treatment is recommended, though there is not clear evidence for its efficacy in managing oral ulcers (3). Immunosuppressive drugs such as azathioprine, thalidomide, interferon-α (IFNα), and tumor necrosis factor (TNF) inhibitors may be used. However, these drugs may be associated with some serious adverse events. There is still an unmet need for an efficient, safe, and well-tolerated treatment for mucocutaneous manifestations of BD. Recently, apremilast proved effective in treating BD-related oral ulcers in a phase II controlled study (4).

Ustekinumab is a humanized monoclonal antibody against interleukin 12 (IL-12) and IL-23 (5). IL-23 is critical for the differentiation of Th17 lymphocytes, and previous studies have demonstrated the key role of Th1 and Th17 in the pathogenesis of BD and the correlation of these cytokines with disease activity (6–8). Genome-wide association studies conducted in Japan and Turkey showed *IL23R* and *IL12RB2* loci variations to be associated

[1]Adrien Mirouse, MD, Anne-Claire Desbois, MD, PhD, Cloé Comarmond, MD, PhD, Fanny Domont, MD, Yasmina Ferfar, MD, Patrice Cacoub, MD, PhD, David Saadoun, MD, PhD: Sorbonne Université, Centre National de Référence Maladies Auoimmunes Systémiques Rares, Centre National de Référence Maladies Autoinflammatoires et Amylose Inflammatoire, INSERM 959, Groupe Hospitalier Pitié-Salpêtrière, AP-HP, Paris, France; [2]Stéphane Barete, MD, PhD: Groupe Hospitalier Pitié-Salpêtrière, AP-HP, and Département Hospitalo-Universitaire Inflammation-Immunopathologie-Biotherapie, Paris, France; [3]Damien Sène, MD, PhD: Hôpital Lariboisière, AP-HP, Paris, France; [4]Bahram Bodaghi, MD, PhD: Groupe Hospitalier Pitié-Salpêtrière, AP-HP, Paris, France.

Drs. Cacoub and Saadoun contributed equally to this work.

No potential conflicts of interest relevant to this article were reported.

Address correspondence to David Saadoun, MD, PhD, Hôpital Pitié-Salpêtrière, Department of Internal Medicine and Clinical Immunology, 83 Boulevard de l'Hôpital, 75013 Paris, France. E-mail: david.saadoun@aphp.fr.

Submitted for publication November 11, 2018; accepted in revised form April 16, 2019.

with BD (9,10). Taken together, these findings provide a strong rationale for the use of ustekinumab in BD. We have previously reported that ustekinumab treatment is safe and is associated with a decrease in circulating IL-12 and IL-17 levels in a small cohort of patients with BD-related oral ulcers (11).

The purpose of the present study was to further investigate the therapeutic efficacy of ustekinumab in a cohort of 30 BD patients with refractory oral ulcers, including those described in our earlier report (11). This study examined clinical features, therapeutic tolerance, and long-term findings in patients with BD.

PATIENTS AND METHODS

Patients. We conducted an open-label, multicenter, prospective study between 2014 and 2018. All patients were adults residing in France who met the criteria of the International Study Group for Behçet's Disease (12) and had ≥1 oral ulcer within 28 days before inclusion and ≥2 oral ulcers at the time of inclusion despite colchicine treatment. The study was performed according to the Declaration of Helsinki, and informed consent was obtained from all patients. Demographic features and past medical history of BD were recorded. Data on the number of oral ulcers and other BD manifestations including genital ulcers, skin manifestations, vasculitis, uveitis, and vascular and CNS manifestations were collected. Joint involvement was assessed using tender and swollen joint counts. Behçet's disease activity was determined using the Behçet's Syndrome Activity Score (BSAS), a scale that ranges from 0 to 100, with higher scores indicating more active disease (13). Clinical parameters, safety assessment, daily steroid use, and laboratory findings were collected at inclusion, at week 4, at week 12, and then once every 12 weeks until treatment discontinuation or end of follow-up.

Design. Enrolled patients received 90 mg of ustekinumab subcutaneously at weeks 0 and 4 and then once every 12 weeks, as recommended in France for maintenance therapy in Crohn's disease (French Ministry of Health approval, November 2015). The ustekinumab injection interval could be reduced to once every 8 weeks in the case of end-of-dose effect, as has been described in Crohn's disease and psoriasis (14–16). Prednisone, colchicine, and other immunosuppressive therapies could be taken simultaneously, if given at a stable dose during the month prior to inclusion and during the study period. Patients who needed temporary increases in prednisone dose or any additional immunomodulatory therapy during the study period were considered to be nonresponders to ustekinumab.

End points. The primary efficacy end point was the proportion of patients with a complete response (i.e., no oral ulcers) at week 12. Secondary end points at week 12 included 1) proportion of patients with a partial response (those who had a reduction of ≥50% in the number of oral ulcers); 2) proportion of nonresponders (patients who had neither partial nor complete responses and/or patients who needed a temporary increase in prednisone dose or additional immunomodulatory therapy during the study period); 3) efficacy of ustekinumab for other BD manifestations (i.e., genital ulcers, pyoderma gangrenosum, pseudofolliculitis, and articular, ocular, vascular, neurologic, or gastrointestinal tract involvement); 4) BSAS score between day 0 and week 12; 5) relapse rate while receiving ustekinumab; 6) steroid-sparing effect of ustekinumab between day 0 and week 12; and 7) safety, as all adverse events were recorded prospectively during follow-up.

Statistical analysis. Data are presented as the median (interquartile range [IQR]) for continuous variables and as a percentage for qualitative variables. Wilcoxon's test was used to compare continuous variables and Fisher's exact test to compare categorical variables. *P* values less than 0.05 were considered significant. Statistical analyses were performed using GraphPad Prism 6.0.

RESULTS

Characteristics of the BD patients. During the study period, we included 30 patients (16 men) from 3 French centers. Baseline characteristics are summarized in Table 1. The median age at treatment initiation was 39 years (IQR 33–45 years). All patients had refractory oral ulcers with for which colchicine treatment was ineffective. The most common previous manifestations of BD were genital ulcers (90%), joint involvement (73%), pseudofolliculitis (50%), deep vein thrombosis (DVT) (20%), uve-

Table 1. Demographic and clinical features of the enrolled patients (n = 30)*

Age, median (IQR) years	39 (33–45)
Male sex	16 (53)
Disease duration, median (IQR) years	8 (1–16)
BD manifestations at inclusion	
Oral ulcers	30 (100)
No. of lesions, median (IQR)	2 (2–3)
Genital ulcers	8 (27)
Joint involvement	16 (53)
Tender joint count, median (IQR)	6 (4–8)
Swollen joint count, median (IQR)	0 (0–0.3)
Pseudofolliculitis	8 (27)
Thrombosis	0 (0)
Uveitis	2 (7)
CNS involvement	0 (0)
BSAS at baseline, median (IQR)	70 (50–70)
Previous treatments	
Steroids	23 (77)
Colchicine	30 (100)
No. of DMARDs, median (IQR)†	1 (1–2)
No. of biologic agents, median (IQR)‡	0 (0–1)

* Except where indicated otherwise, values are the number (%) of patients. IQR = interquartile range; BD = Behçet's disease; CNS = central nervous system; BSAS = Behçet's Syndrome Activity Score.
† Disease-modifying antirheumatic drugs (DMARDs) included thalidomide, hydroxychloroquine, methotrexate, cyclophosphamide, azathioprine, mycophenolate mofetil, and everolimus.
‡ Biologics agents included apremilast, tumor necrosis factor inhibitors, tocilizumab, and interleukin-1inhibitors.

Table 2. Efficacy of ustekinumab for BD-related oral ulcers*

	Baseline (n = 30)	Week 12 (n = 30)	Week 24 (n = 27)†	Week 36 (n = 20)	Week 48 (n = 16)	End of follow-up (n = 26)†
Active lesions	30 (100)	12 (40)	3 (11)	1 (5)	1 (6)	3 (12)
No. of lesions, median (IQR)	2 (2–3)	0 (0–1)	0 (0–0)	0 (0–0)	0 (0–0)	0 (0–0)
Response						
Complete	–	18 (60)	24 (89)	19 (95)	15 (94)	23 (88)
Partial	–	9 (30)	3 (11)	1 (5)	1 (6)	3 (12)
None	–	3 (10)	0 (0)	0 (0)	0 (0)	0 (0)

* Except where indicated otherwise, values are the number (%) of patients. BD = Behçet's disease; IQR = interquartile range.
† Patients who discontinued ustekinumab treatment were removed from the analysis.

itis (20%), and CNS involvement (13%). In addition to colchicine treatment, 23 patients (77%) had already been treated with steroids for BD. Before ustekinumab treatment, patients received a median of 1 course of disease-modifying antirheumatic drugs (IQR 1–2) and 0 courses of biologics agents (IQR 0–1).

During the 6 months prior to inclusion, the median number of oral ulcers was 3 (IQR 2–3). At inclusion, the median numbers of oral and genital ulcers were 2 (IQR 2–3) and 0 (IQR 0–1) per patient, respectively (Table 1). Joint manifestations were present in 16 patients (53%) at inclusion, with a median tender and swollen joint count of 6 (IQR 4–8) and 0 (IQR 0–0.3), respectively. The median BSAS at inclusion was 70 (IQR 50–70).

All patients received ustekinumab treatment as scheduled. At inclusion, 16 patients (53%) were receiving a stable steroid dose, with a median daily dose of 11 mg (IQR 10–16). Colchicine treatment was continued in 15 patients (50%). A patient with pyoderma gangrenosum was also undergoing adjunctive therapy with tocilizumab, and another patient with heart allograft was taking mycophenolate mofetil and everolimus.

Efficacy. *Oral ulcers*. Twelve weeks after treatment initiation, 18 patients (60%) met the complete response criteria, 9 (30%) met the partial response criteria, and 3 (10%) had no response (Table 2). The median number of oral ulcers declined from 2 (IQR 2–3) to 0 (IQR 0–1) between day 0 and week 12 ($P < 0.0001$). After a median follow-up of 12 months (IQR 6–16 months), 23 patients fulfilled the complete response criteria, and 3 patients fulfilled the partial response criteria. No patient met the no response criteria.

Other BD manifestations and disease activity. The number of patients with genital ulcers at baseline compared to week 12 decreased from 8 (27%) to 2 (7%) (Table 3). At week 12, arthralgia was reported in 9 patients (30%), with a median tender joint count of 4 (IQR 3–4). Four patients (25%) were able to discontinue steroid treatment. Median BSAS at week 12 was 17.5 (IQR 10–42.5), compared to 70 (IQR 50–70) at inclusion ($P < 0.0001$) , and the median BSAS at week 24 was 10 (IQR 8–11).

At the end of follow-up, 1 patient (4%) still had a genital ulcer. Four patients (15%) still reported arthralgia, with a median tender joint count of 2 (IQR 1–2). No patient experienced arthritis during the treatment period. One patient was able to discontinue morphine treatment for arthralgia during ustekinumab treatment. Of the 16 patients receiving prednisone at inclusion, 6 (38%) were able to discontinue it by the end of follow-up ($P = 0.006$) (Table 4). The median prednisone daily dose decreased significantly between baseline and end of follow-up (11 mg [IQR 10–16] and 7.5 mg [IQR 5–10]; $P = 0.04$) (Table 4).

Safety. While receiving treatment, 7 patients (23.3%) reported adverse events. The most common adverse event was headache after treatment injection, reported in 4 patients (13.3%). Other adverse events are listed in Table 5. There were

Table 3. Efficacy of ustekinumab for BD-related skin and joint involvement*

	Baseline (n = 30)	Week 12 (n = 30)	Week 24 (n = 27)†	Week 36 (n = 20)	Week 48 (n = 16)	End of follow-up (n = 26)†
Genital ulcers	8 (27)	2 (7)	1 (4)	1 (5)	0 (0)	1 (4)
Joint involvement	16 (53)	9 (30)	6 (22)	2 (10)	0 (0)	4 (15)
Tender joint count, median (IQR)	6 (4–8)	4 (3–4)	2 (1–4)	1.5 (1.25–1.75)	–	2 (1–2)
Swollen joint count, median (IQR)	0 (0–0.3)	0 (0–0)	0 (0–0)	0.5 (0.25–0.75)	–	0 (0–0)
Pseudofolliculitis	8 (27)	2 (7)	0 (0)	1 (5)	0 (0)	1 (4)
BSAS, median (IQR)	70 (50–70)	17.5 (10–43)	10 (8–11)	10 (10–23)	10 (5–10)	10 (5–10)

* Except where indicated otherwise, values are the number (%) of patients. See Table 1 for definitions.
† Patients who discontinued ustekinumab treatment were removed from the analysis.

Table 4. Use of steroids and DMARDs during ustekinumab therapy*

	Baseline (n = 30)	Week 12 (n = 30)	Week 24 (n = 27)†	End of follow-up (n = 26)†	*P*‡
Prednisone	16 (53)	12 (40)	10 (37)	10 (38)	0.006
Prednisone dose, median (IQR) mg	11 (10–16)	10 (8–13)	10 (7–15)	7.5 (5–10)	0.04
Colchicine	15 (50)	15 (50)	15 (56)	15 (58)	0.60
Adjunctive therapy§	5 (17)	5 (17)	3 (11)	3 (12)	0.71

* Except where indicated otherwise, values are the number (%) of patients. DMARDs = disease-modifying antirheumatic drugs; IQR = interquartile range.
† Four patients discontinued ustekinumab due to side effects (n = 1) or inefficacy (n = 3).
‡ Wilcoxon's test was used to compare continuous variables, and Fisher's exact test was used for categorical variables, between inclusion (baseline) and the end of follow-up.
§ Adjunctive therapy included azathioprine (n = 2), tocilizumab (n = 1), mycophenolate mofetil (n = 2), and everolimus (1 patient with heart allograft).

no serious adverse events. One patient stopped ustekinumab treatment because of headaches (Figure 1). At the end of follow-up, 26 patients (86.7%) were still receiving ustekinumab. Four patients stopped ustekinumab treatment prior to study completion, at a median of 3 months (IQR 1.8–4.5) after inclusion. Reasons for treatment discontinuation included adverse events in 1 patient (headaches) and a BD flare during treatment in 3 patients (scleritis [n = 1], DVT [n = 1], and pseudofolliculitis and arthralgia [n = 1]) (Figure 1).

End-of-dose effect. End-of-dose effect was reported in 4 patients (13.3%), which included development of oral ulcers (n = 1) and arthralgia (n = 3) 8–10 weeks after the most recent ustekinumab injection. Ustekinumab injection intervals were shortened in these patients, resulting in better disease control (Figure 1).

DISCUSSION

In this prospective study, we investigated the long-term outcome of ustekinumab treatment in BD patients with active oral ulcers that were resistant to colchicine. The main conclusions of this study are as follows: 1) ustekinumab seems to be effective, as complete response had been achieved in 60% and 88.9% of patients at weeks 12 and 24, respectively; 2) ustekinumab seems to be efficacious in treating BD joint manifestations; and 3) ustekinumab is safe, with no serious adverse effects reported.

Table 5. Adverse events during ustekinumab therapy*

≥1 adverse event	7 (23)
Serious adverse events	0 (0)
Events leading to treatment discontinuation	1 (3)
Reported events	
Headaches	4 (13)
Asthenia	2 (7)
Nausea	1 (3)
Diarrhea	1 (3)
Local reaction	1 (3)

* Values are the number (%) of patients (n = 30).

Oral ulcerations represent the hallmark lesion of BD. In this study, ustekinumab proved effective in achieving 95% complete remission of refractory ulcers at weeks 36 and 48. It had a significant steroid-sparing effect, allowing treatment withdrawal in more than one-third of cases. BD activity dramatically improved, with a 7-fold reduction in median BSAS. Onset of action was quick, as 60% of patients showed complete remission at week 12 (i.e., after 2 injections of ustekinumab). After a median follow-up of 12 months, 23 patients were still complete responders and 86.7% were still receiving ustekinumab. However, we observed an end-of-dose effect in 13.3% of patients. These relapses appeared 8–10 weeks after ustekinumab injection. Similar effects have been reported in other diseases treated with ustekinumab, including Crohn's disease (15,16). With dose interval reduction, treatment response was restored in all BD cases.

Although this study was not designed to analyze drug efficacy for BD manifestations other than oral ulcers, we observed improvement in BD-related joint involvement. This is likely to be clinically meaningful, since the main symptom

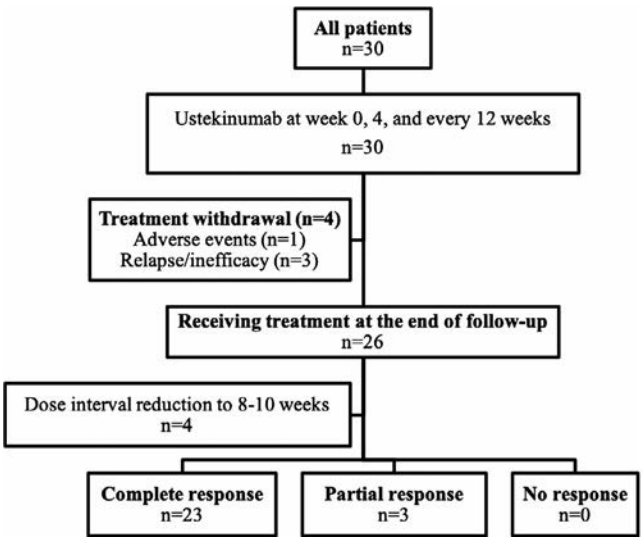

Figure 1. Disposition of the patients.

cluster in BD involves both skin and joints (17). The disease distribution with this cluster was confirmed in a study comparing BD patients who had family members with BD to those who did not, which showed a significantly higher frequency of the papulopustular lesion and joint involvement cluster in the familial group versus the nonfamilial group (39.2% versus 21.5%; $P < 0.001$) (18). Treatment of BD-related joint involvement is challenging and has mainly focused on colchicine, steroids, and sometimes immunosuppressive drugs (3). In psoriatic arthritis, ustekinumab treatment has already been reported to be effective compared to placebo, with better achievement of response according to the American College of Rheumatology criteria for 20% improvement and with less radiographic progression (19–21). Ustekinumab was additionally reported to be effective in treating a patient with Crohn's disease and knee arthritis who also had psoriasis, and in a patient with BD, psoriasis, and distal interphalangeal joint arthritis (22,23). In contrast, in a recent phase III placebo-controlled trial, ustekinumab did not demonstrate significant efficacy in treating spondyloarthritis (24).

Psoriasis and BD share common inflammatory pathways, including IL-23 receptor gene polymorphisms (9,10,25). Ustekinumab is a therapy targeting the p40 IL-12 and IL-23 subunit. These cytokines and the associated Th17 pathway play a central role in BD. Targeting the Th17 pathway with other treatments for BD-related oral ulcers (e.g., apremilast) has been reported as effective (4). Apremilast has also been shown to be effective in treating psoriasis and psoriatic arthritis by increasing intracellular cAMP levels, which results in an antiinflammatory state by inhibiting the activity of TNF, IFNγ, IL-12, and IL-23 (26). However, its efficacy in treating other BD manifestations, including articular manifestations, remains unknown, and arthralgia has been reported as an adverse event with apremilast treatment (27).

In the present study, the main adverse event was headache after ustekinumab injection. There were no serious adverse events. Only 1 patient had to stop the treatment because of headaches. Due to the limited number of patients in our study, less frequent adverse events might have been missed. In a larger controlled study of psoriasis and Crohn's disease, adverse events included headaches (3–16%), upper respiratory tract infections (7.6–16%), and injection site erythema (0.5–2%), with no differences compared to the placebo group (14,15,28).

Our study had several limitations. This was an open-label study, and treatment was not compared to placebo. As the natural course of BD includes exacerbations and remissions of disease activity, a decrease in oral ulcers could simply be part of this normal course. However, oral ulceration flares during the 6 months prior to inclusion were recorded, and the decrease in oral ulcerations was maintained during long-term follow-up in our study. Although steroids, colchicine, and immunosuppressive therapies were allowed, they were given at stable doses during the month prior to inclusion and during the study period. The number of patients in this study was limited, and there is a need to confirm these results in larger studies.

In conclusion, ustekinumab seems to be an effective and safe treatment option for BD patients with colchicine-resistant oral ulcers. Further prospective, placebo-controlled studies are warranted.

AUTHOR CONTRIBUTIONS

All authors were involved in drafting the article or revising it critically for important intellectual content, and all authors approved the final version to be published. Dr. Mirouse had full access to all of the data in the study and takes responsibility for the integrity of the data and the accuracy of the data analysis.

Study conception and design. Mirouse, Cacoub, Saadoun.

Acquisition of data. Mirouse, Barete, Desbois, Comarmond, Sène, Domont, Bodaghi, Ferfar, Cacoub, Saadoun.

Analysis and interpretation of data. Mirouse, Cacoub, Saadoun.

REFERENCES

1. Sakane T, Takeno M, Suzuki N, Inaba G. Behçet's disease. N Engl J Med 1999;341:1284–91.
2. Yazici H, Yurdakul S, Hamuryudan V. Behçet disease. Curr Opin Rheumatol 2001;13:18–22.
3. Hatemi G, Christensen R, Bang D, Bodaghi B, Celik AF, Fortune F, et al. 2018 update of the EULAR recommendations for the management of Behçet's syndrome. Ann Rheum Dis 2018;77:808–18.
4. Hatemi G, Melikoglu M, Tunc R, Korkmaz C, Turgut Ozturk B, Mat C, et al. Apremilast for Behçet's syndrome: a phase 2, placebo-controlled study. N Engl J Med 2015;372:1510–8.
5. Reddy M, Davis C, Wong J, Marsters P, Pendley C, Prabhakar U. Modulation of CLA, IL-12R, CD40L, and IL-2Rα expression and inhibition of IL-12- and IL-23-induced cytokine secretion by CNTO 1275. Cell Immunol 2007;247:1–11.
6. Touzot M, Cacoub P, Bodaghi B, Soumelis V, Saadoun D. IFN-α induces IL-10 production and tilt the balance between Th1 and Th17 in Behçet disease. Autoimmun Rev 2015;14:370–5.
7. Habibagahi Z, Habibagahi M, Heidari M. Raised concentration of soluble form of vascular endothelial cadherin and IL-23 in sera of patients with Behçet's disease. Mod Rheumatol 2010;20:154–9.
8. Gheita TA, Gamal SM, Shaker I, El Fishawy HS, El Sisi R, Shaker OG, et al. Clinical significance of serum interleukin-23 and A/G gene (rs17375018) polymorphism in Behçets disease: relation to neuro-Behçet, uveitis and disease activity [letter]. Joint Bone Spine 2015;82:213–5.
9. Remmers EF, Cosan F, Kirino Y, Ombrello MJ, Abaci N, Satorius C, et al. Genome-wide association study identifies variants in the MHC class I, IL10, and IL23R-IL12RB2 regions associated with Behçet's disease. Nat Genet 2010;42:698–702.
10. Mizuki N, Meguro A, Ota M, Ohno S, Shiota T, Kawagoe T, et al. Genome-wide association studies identify IL23R-IL12RB2 and IL10 as Behçet's disease susceptibility loci. Nat Genet 2010;42:703–6.
11. Mirouse A, Barete S, Monfort JB, Resche-Rigon M, Bouyer AS, Comarmond C, et al. Ustekinumab for Behçet's disease. J Autoimmun 2017;82:41–6.
12. International Team for the Revision of the International Criteria for Behçet's Disease (ITR-ICBD). The International Criteria for Behçet's Disease (ICBD): a collaborative study of 27 countries on the sensitivity and specificity of the new criteria. J Eur Acad Dermatol Venereol 2014;28:338–47.
13. Yilmaz S, Simsek I, Cinar M, Erdem H, Kose O, Yazici Y, et al. Patient-driven assessment of disease activity in Behçet's syndrome:

cross-cultural adaptation, reliability and validity of the Turkish version of the Behçet's Syndrome Activity Score. Clin Exp Rheumatol 2013;31:77–83.

14. Leonardi CL, Kimball AB, Papp KA, Yeilding N, Guzzo C, Wang Y, et al. Efficacy and safety of ustekinumab, a human interleukin-12/23 monoclonal antibody, in patients with psoriasis: 76-week results from a randomised, double-blind, placebo-controlled trial (PHOENIX 1). Lancet 2008;371:1665–74.
15. Sandborn WJ, Feagan BG, Fedorak RN, Scherl E, Fleisher MR, Katz S, et al. A randomized trial of ustekinumab, a human interleukin-12/23 monoclonal antibody, in patients with moderate-to-severe Crohn's disease. Gastroenterology 2008;135:1130–41.
16. Kopylov U, Afif W, Cohen A, Bitton A, Wild G, Bessissow T, et al. Subcutaneous ustekinumab for the treatment of anti-TNF resistant Crohn's disease: the McGill experience. J Crohns Colitis 2014;8:1516–22.
17. Diri E, Mat C, Hamuryudan V, Yurdakul S, Hizli N, Yazici H. Papulopustular skin lesions are seen more frequently in patients with Behçet's syndrome who have arthritis: a controlled and masked study. Ann Rheum Dis 2001;60:1074–6.
18. Karaca M, Hatemi G, Sut N, Yazici H. The papulopustular lesion/arthritis cluster of Behçet's syndrome also clusters in families. Rheumatology (Oxford) 2012;51:1053–60.
19. Felson DT, Anderson JJ, Boers M, Bombardier C, Furst D, Goldsmith C, et al. American College of Rheumatology preliminary definition of improvement in rheumatoid arthritis. Arthritis Rheum 1995;38:727–35.
20. McInnes IB, Kavanaugh A, Gottlieb AB, Puig L, Rahman P, Ritchlin C, et al. Efficacy and safety of ustekinumab in patients with active psoriatic arthritis: 1 year results of the phase 3, multicentre, double-blind, placebo-controlled PSUMMIT 1 trial. Lancet 2013;382:780–9.
21. Kavanaugh A, Ritchlin C, Rahman P, Puig L, Gottlieb AB, Li S, et al. Ustekinumab, an anti-IL-12/23 p40 monoclonal antibody, inhibits radiographic progression in patients with active psoriatic arthritis: results of an integrated analysis of radiographic data from the phase 3, multicentre, randomised, double-blind, placebo-controlled PSUMMIT-1 and PSUMMIT-2 trials. Ann Rheum Dis 2014;73:1000–6.
22. Baerveldt EM, Kappen JH, Thio HB, van Laar JA, van Hagen PM, Prens EP. Successful long-term triple disease control by ustekinumab in a patient with Behçet's disease, psoriasis and hidradenitis suppurativa [letter]. Ann Rheum Dis 2013;72:626–7.
23. Matsumoto S, Mashima H. Efficacy of ustekinumab against infliximab-induced psoriasis and arthritis associated with Crohn's disease. Biologics 2018;12:69–73.
24. Deodhar A, Gensler LS, Sieper J, Clark M, Calderon C, Wang Y, et al. Three multicenter, randomized, double-blind, placebo-controlled studies evaluating the efficacy and safety of ustekinumab in axial spondyloarthritis. Arthritis Rheumatol 2019;71:258–70.
25. Cargill M, Schrodi SJ, Chang M, Garcia VE, Brandon R, Callis KP, et al. A large-scale genetic association study confirms IL12B and leads to the identification of IL23R as psoriasis-risk genes. Am J Hum Genet 2007;80:273–90.
26. Schafer PH, Parton A, Gandhi AK, Capone L, Adams M, Wu L, et al. Apremilast, a cAMP phosphodiesterase-4 inhibitor, demonstrates anti-inflammatory activity in vitro and in a model of psoriasis. Br J Pharmacol 2010;159:842–55.
27. Hatemi G, Mahr A, Takeno M, Kim DY, Melikoglu M, Cheng S, et al. OP0082 Apremilast for Behçet's syndrome: a phase III randomised, placebo-controlled, double-blind study (RELIEF) [abstract]. Ann Rheum Dis 2018;77 Suppl 2:91–2.
28. Papp KA, Langley RG, Lebwohl M, Krueger GG, Szapary P, Yeilding N, et al. Efficacy and safety of ustekinumab, a human interleukin-12/23 monoclonal antibody, in patients with psoriasis: 52-week results from a randomised, double-blind, placebo-controlled trial (PHOENIX 2). Lancet 2008;371:1675–84.

Arthritis & Rheumatology
Vol. 71, No. 10, October 2019, pp 1733–1738
DOI 10.1002/art.41007

American College of Rheumatology
Empowering Rheumatology Professionals

BRIEF REPORT

Associations of Gout and Baseline Serum Urate Level With Cardiovascular Outcomes: Analysis of the Coronary Disease Cohort Study

Lisa K. Stamp,[1] Christopher Frampton,[2] Jill Drake,[2] Robert N. Doughty,[3] Richard W. Troughton,[2] and A. Mark Richards[2]

Objective. To determine whether gout and serum urate (SU) levels are associated with increased risk of death, time to first readmission for any cardiovascular event, or incident heart failure in individuals with cardiovascular disease.

Methods. Individuals presenting with an acute coronary syndrome (ACS) were enrolled in the Coronary Disease Cohort Study. Clinical data were collected from the medical records at the index hospital admission, and clinical, echocardiographic, and biochemical data were collected postdischarge. Gout was defined by self-report, use of urate-lowering therapy, or use of colchicine with evidence of gout on review of the medical record. The primary end points were all-cause mortality, time to readmission for a cardiac ischemic event, and time to readmission for heart failure.

Results. Data from 1,514 participants were available. During the follow-up period, 53 of 160 participants with gout (33.1%) and 298 of 1,354 participants without gout (22.0%) died. After adjustment for other factors known to be associated with mortality, there was no gout-specific increase in risk of mortality (adjusted hazard ratio 0.98 [95% confidence interval 0.69–1.38]). Time to readmission for heart failure was significantly briefer in those with, compared to those without, gout (adjusted hazard ratio 1.42 [95% confidence interval 1.02–1.97]). Irrespective of whether a participant had gout or not, as SU level increased, there was an increased risk of death and readmission for either a cardiovascular event or heart failure.

Conclusion. Survival post-ACS is similar with and without the presence of gout. People with gout are at an increased risk of readmission for heart failure and have longer hospital stays. Risk of these events increases in parallel with increases in SU levels.

INTRODUCTION

It has long been recognized that there is an association between serum urate (SU) level, gout, and cardiovascular disease (CVD). However, whether there is a cause-and-effect relationship between these features is difficult to assess due to confounding by shared comorbidities. Mendelian randomization studies have confirmed that SU level is a causal factor in gout (1), but there is currently no consistent evidence available using this method indicating that increased SU is causal of coronary heart disease (1–3). In individuals with an acute coronary syndrome (ACS), increasing SU levels have been associated with an elevated risk of CV events over 1 year, irrespective of whether there is a concomitant diagnosis of gout (4). There is some evidence that hyperuricemia may contribute to worse outcomes in CVD (5). Gout has also been associated with increased risk of death, primarily due to CVD (6). The risk of death in persons with gout and coexisting CVD has been highlighted in the recent Cardiovascular Safety of Febuxostat and Allopurinol in Patients with Gout and Cardiovascular Morbidities (CARES) clinical trial (7).

Supported by the Health Research Council of New Zealand.

[1]Lisa K. Stamp, MBChB, FRACP, PhD: University of Otago and Christchurch Hospital, Christchurch, New Zealand; [2]Christopher Frampton, PhD, Jill Drake, BN, Richard W. Troughton, MBChB, FRACP, PhD, A. Mark Richards, MD, FRACP, PhD: University of Otago, Christchurch, New Zealand; [3]Robert N. Doughty, MBBS, MD, FRCP, FRACP, FCSANZ, FESC: University of Auckland, Auckland, New Zealand.

Dr. Stamp has received speaking fees from Amgen (less than $10,000). No other disclosures relevant to this article were reported.

Address correspondence to Lisa K. Stamp, MBChB, FRACP, PhD, University of Otago, Christchurch, Department of Medicine, PO Box 4345, Christchurch, New Zealand. E-mail: lisa.stamp@cdhb.health.nz.

Submitted for publication January 30, 2019; accepted in revised form May 30, 2019.

However, the absence of a placebo arm in that study made interpretation challenging due to the lack of comparison with background risk in an untreated population or a population treated with a uricosuric agent.

In individuals with an ACS, a number of specific CV variables, including brain natriuretic peptide (BNP), N-terminal pro–brain BNP (NT-proBNP), and left ventricular ejection fraction (LVEF), have previously been associated with poorer outcomes (8). Whether gout and SU levels are associated with worse outcomes in individuals with an ACS independent of these and other demographic, clinical, and CV variables has not been examined.

The aims of this study were to determine whether gout and SU levels are associated with an increased risk of death, time to first readmission for a CV event, or time to first readmission for heart failure independent of other established CV risk factors in individuals with CVD.

PATIENTS AND METHODS

Study participants and data collection. Individuals presenting with an ACS (see Supplementary Materials, available

Table 1. Baseline demographic and clinical features in subjects with and subjects without gout*

	Total (n = 1,514)	Subjects without gout (n = 1,354)	Subjects with gout (n = 160)	*P*
Age, years	67.9 ± 12.1	67.6 ± 12.1	71.0 ± 11.2	0.001
Male sex, no. (%)	1,063 (70.2)	930 (68.7)	133 (83.1)	<0.001
Ethnicity, no. (%)				<0.001
NZ European	1,360 (89.8)	1,220 (90.1)	140 (87.5)	
Maori	37 (2.4)	23 (1.7)	14 (8.8)	
Pacific Island	6 (0.4)	4 (0.3)	2 (1.3)	
Asian	10 (0.7)	10 (0.7)	0 (0)	
Other	101 (6.7)	97 (7.2)	4 (2.5)	
Admission reason, no. (%)				0.004
NSTEMI	767 (50.7)	676 (49.9)	91 (56.9)	
STEMI	289 (19.1)	274 (20.2)	15 (9.4)	
Unstable angina	458 (30.3)	404 (29.8)	54 (33.8)	
Comorbidities, no. (%)†				
Hypertension	800 (53.3)	689 (51.3)	111 (70.7)	<0.001
CVA	208 (13.8)	167 (12.4)	41 (25.8)	<0.001
Heart failure	166 (11.0)	127 (9.4)	39 (24.5)	<0.001
Lung disease	296 (19.6)	261 (19.3)	35 (21.9)	0.44
Type 2 diabetes	243 (16.1)	201 (14.9)	42 (26.3)	<0.001
Treatment, no. (%)				
Diuretic	471 (31.2)	389 (28.8)	82 (51.3)	<0.001
ACE inhibitor/ARB	900 (59.4)	788 (58.2)	112 (70.0)	0.004
Allopurinol	156 (10.3)	0 (0)	156 (97.5)	<0.001
Colchicine	19 (1.25)	3 (0.2)	16 (10)	<0.001
SU level, mmoles/liter	0.37 ± 0.10	0.37 ± 0.09	0.42 ± 0.13	<0.001
SU level, no. (%)				<0.001
<0.36 mmoles/liter	584 (38.6)	535 (39.5)	49 (30.6)	
0.36–0.42 mmoles/liter	319 (21.1)	299 (22.1)	20 (12.5)	
0.43–0.55 mmoles/liter	272 (17.9)	227 (16.6)	45 (28.1)	
>0.55 mmoles/liter	63 (4.2)	43 (3.2)	20 (12.5)	
Creatinine, ml/minute	98.7 ± 41.8	96.3 ± 38.3	119.6 ± 60.9	<0.001
eGFR, ml/minute/1.73 m^2 (n = 1,470)	70.2 ± 17.9	71.2 ± 17.3	61.5 ± 20.7	<0.001
Troponin T, ng/liter	1.8 ± 0.40	1.80 ± 0.40	1.76 ± 0.43	0.16
NT-BNP, pmoles/liter	141 ± 192	138 ± 190	170 ± 212	0.009
CRP, mg/liter	27.3 ± 52.0	28.6 ± 54.3	20.5 ± 37.4	0.47
LVEF, %	56.2 ± 12.1	56.8 ± 11.6	51.3 ± 14.3	<0.001
E/e'	12.3 ± 6.41	12.2 ± 6.07	13.1 ± 8.83	0.12

* Except where indicated otherwise, values are the mean ± SD. NZ European = New Zealand European; NSTEMI = non–ST-segment elevation myocardial infarction; ACE = angiotensin-converting enzyme; ARB = angiotensin receptor blocker; SU = serum urate; eGFR = estimated glomerular filtration rate; NT-BNP = N-terminal pro–brain natriuretic peptide; CRP = C-reactive protein; LVEF = left ventricular ejection fraction.
†For hypertension, data were available for 1,501 subjects (1,344 without gout and 157 with gout). For cerebrovascular accident (CVA), data were available for 1,509 subjects (1,350 without gout and 159 with gout). For heart failure, data were available for 1,508 subjects (1,349 without gout and 159 with gout).

on the *Arthritis & Rheumatology* web site at http://onlinelibrary.wiley.com/doi/10.1002/art.41007/abstract) were enrolled in the Coronary Disease Cohort Study (CDCS) (ANZCTR no.: ACTRN12605000431628) at Christchurch or Auckland city hospitals (New Zealand). Participants were divided into groups by those with ST-segment elevation myocardial infarction (STEMI), non–STEMI (NSTEMI), or unstable angina. The study was approved by the New Zealand Multi-Region Ethics Committee, and all participants provided written, informed consent. Details of the CDCS design have been previously published (9) and are briefly summarized in the Supplementary Materials, available at http://onlinelibrary.wiley.com/doi/10.1002/art.41007/abstract.

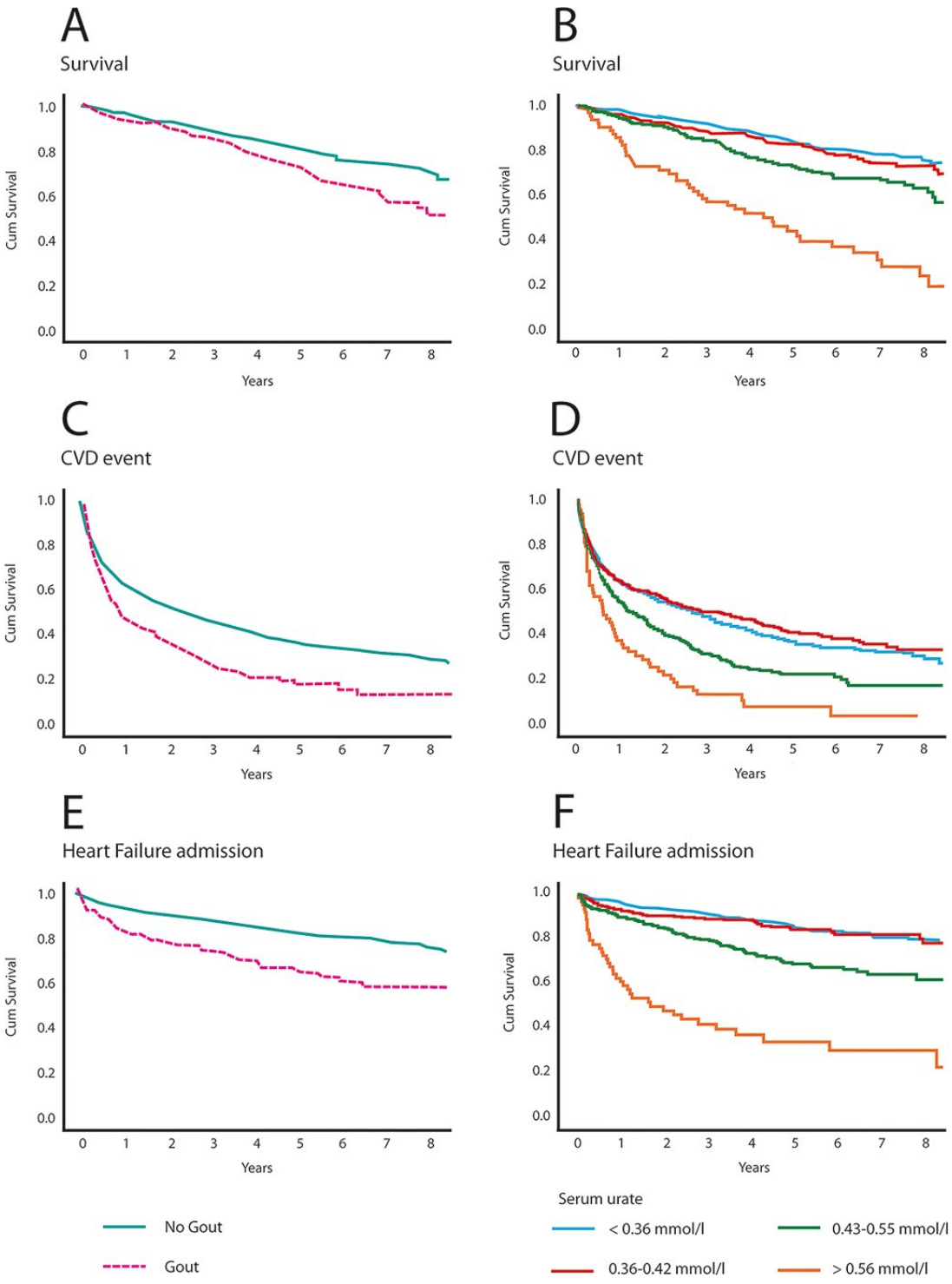

Figure 1. Effect of gout (**A**, **C**, and **E**) and different levels of serum urate (**B**, **D**, and **F**) on cumulative (cum) survival (**A** and **B**), cardiovascular disease (CVD) events (**C** and **D**), and heart failure–related hospital admissions (**E** and **F**).

Table 2. Effect of different serum urate concentrations on cardiovascular disease (CVD) outcomes*

Serum urate, mmoles/liter	All-cause mortality		Heart failure		Any CVD	
	Unadjusted	Adjusted	Unadjusted	Adjusted	Unadjusted	Adjusted
<0.36	1 (reference)	1 (reference)	1 (reference)	1 (reference)	1 (reference)	1 (reference)
0.36–0.42	1.13 (0.84–1.54)	0.99 (0.72–1.38)	1.04 (0.73–1.46)	0.79 (0.54–1.16)	0.91 (0.77–1.09)	0.88 (0.74–1.05)
0.43–<0.55	1.81 (1.36–2.93)	1.11 (0.81–1.51)	2.23 (1.65–3.01)	1.22 (0.86–1.72)	1.44 (1.21–1.70)	1.23 (1.03–1.47)
>0.55	5.04 (3.53–7.20)	2.03 (1.34–3.08)	7.65 (5.24–11.18)	2.29 (1.43–3.66)	2.25 (1.70–2.99)	1.42 (1.04–1.94)

* Values are the hazard ratio (95% confidence interval).

Clinical data were collected from the index hospital admission, and comprehensive clinical, echocardiographic, biochemical, and neurohormonal data were collected at a postdischarge visit (baseline visit; median of 32 days post-ACS). Baseline was deliberately delayed post-ACS per protocol to allow assessment of markers during the post-acute phase. Baseline data included blood pressure; height; weight; family and personal medical history; alcohol, exercise, and smoking history; medications; creatinine level; and SU level. Standardized transthoracic echocardiography was performed using a GE Vivid 3 Ultrasound System (GE Medical Systems). Circulating BNP and NT-proBNP were assayed as previously described (9). Estimated glomerular filtration rate (eGFR) was calculated using the Modification of Diet in Renal Disease Study equation. Troponin T was assayed using Roche fourth-generation kits.

For the present analysis, the primary end points were all-cause mortality, time to readmission for a cardiac ischemic event, or heart failure. Gout was defined by self-report, use of urate-lowering therapy, or use of colchicine with evidence of gout on review of the medical record.

Statistical analysis. Demographic characteristics and clinical features at index admission were compared between individuals with gout and those without gout, using *t*-tests and chi-square tests as appropriate. Cox proportional regression models were used to generate hazards ratios (HRs) with 95% confidence intervals (95% CIs) for the 3 time-to-event outcomes: time to death, time to first readmission for a CV event, and time to first readmission for heart failure. HRs were estimated to compare the outcomes between individuals with and those without gout and between those with SU levels of <0.36 mmoles/liter and those with SU levels of 0.36–0.42 mmoles/liter (upper limit of normal in the Canterbury Health Laboratory assay), 0.43–0.55 mmoles/liter, and >0.55 mmoles/liter. Kaplan-Meier curves were used to portray the time to each of these outcomes according to gout and baseline SU groups. Adjusted HRs were also generated comparing the group with and the group without gout after adjustment for other risk factors for each of the 3 outcomes. These factors included age; sex; baseline eGFR; LVEF; the ratio of early diastolic transmitral velocity to septal annular relaxation velocity (E/e′, a marker of LV diastolic function); NT-proBNP; troponin T; and a history of myocardial infarction, heart failure, type 2 diabetes, cerebrovascular accident, pulmonary disease, or hypertension, and/or treatment with a diuretic or angiotensin-converting enzyme (ACE) inhibitor. *P* values (2-sided) less than 0.05 were considered significant.

RESULTS

Of the 2,129 individuals enrolled in the CDCS, data from 1,514 (71.1%) enrolled at Christchurch Hospital were available. The median follow-up was 4.93 years (interquartile range 3.65–6.74). Of these 1,514 individuals, 160 (10.6%) had gout. Those with gout were older, had more comorbidities, and had higher SU and creatinine levels than those without gout (Table 1). There was a significant difference in diuretic and ACE inhibitor use between the groups with and without gout (Table 1), but no significant difference in use of statins ($P = 0.44$) or beta blockers ($P = 0.95$). In addition, the group with gout had higher NT-proBNP levels and lower LVEF at baseline (Table 1). The majority of those with gout were receiving allopurinol; no other urate-lowering therapies were used.

Association of gout with survival, time to readmission for first CVD-related event, and time to readmission for heart failure. During the follow-up period, 53 of 160 individuals with gout (33.1%) and 298 of 1,354 without gout (22.0%) died. There was an increase in all-cause mortality among the group with gout compared to those without (unadjusted HR 1.63 [95% CI 1.22–2.18]) (Figure 1A). However, this effect was lost after adjustment for other factors known to be associated with mortality (adjusted HR 0.98 [95% CI 0.69–1.38]). Time to readmission for a CV event was shorter among the group with gout compared to those without gout in the unadjusted model (HR 1.62 [95% CI 1.34–1.95]) (Figure 1C), but not in the adjusted model (HR 1.22 [95% CI 0.99–1.51]). Time to readmission for heart failure was shorter among those with gout compared to those without gout in both the unadjusted model (HR 2.21 [95% CI 1.64–2.96]) (Figure 1E) and the adjusted model (adjusted HR 1.42 [95% CI 1.02–1.97]). Participants with gout had more days in hospital due to any cause over the follow-up period compared to those without gout (median 12 days versus 7 days; $P = 0.001$). Similarly, participants with gout had more days in hospital due to CV events over the follow-up period compared to those without gout (median 7 days versus 3 days; $P < 0.001$).

Effect of baseline SU level on all-cause mortality. Baseline SU values are presented in Table 1. Irrespective of

whether a participant had gout or not, as baseline SU level increased there was an increased risk of death (Figure 1B) and readmission for either a CV event (Figure 1D) or heart failure (Figure 1F), in adjusted and unadjusted analyses (Table 2). Using the adjusted model, for every 0.1-mmole increase in SU level, the HR of death was 1.18 (95% CI 1.05–1.33).

DISCUSSION

Herein, we have shown that survival post-ACS is similar between individuals with gout and those without gout. However, those with gout are at increased risk of readmission for a CV event or heart failure and have longer hospital stays.

It is of interest to note that all study participants with gout (except 4) were receiving allopurinol. The effect of urate-lowering therapies and, in particular, the xanthine oxidase inhibitors allopurinol and febuxostat, on CV events has been the subject of much investigation. A recent meta-analysis of the results of randomized controlled trials of xanthine oxidase inhibitors versus placebo or no treatment (10) included 10,684 patients with 6,434 patient-years and showed no reduced risk of major adverse CV events (MACEs) (Peto odds ratio [OR_p] 0.71 [95% CI 0.46–1.09]) or death (OR_p 0.89 [95% CI 0.59–1.33]). However, there was a reduced risk of MACEs in those with previous ischemic events (OR_p 0.42 [95% CI 0.23–0.76]), and allopurinol reduced the risk of myocardial infarction (OR_p 0.38 [95% CI 0.17–0.83]) (10). In the recent CARES clinical trial, 6,190 participants with gout and CVD were randomized to receive either allopurinol or febuxostat (7). There was no increased risk with febuxostat compared to allopurinol for the primary end point (composite of MACEs: CVD-related death, nonfatal myocardial infarction, nonfatal stroke, and unstable angina with urgent revascularization) (HR 1.03 [95% CI 0.87–1.23]). However, the prespecified secondary analyses revealed an increased risk of death from any cause and an increased risk of CVD-related death with febuxostat (7). Whether this represents a protective effect of allopurinol or a true increased risk with febuxostat remains unclear. The risk of death in the CARES study was lower than in our study, which may be due to difference in study design and the period in which the studies were undertaken. Due to the small number of subjects with gout who were not receiving urate-lowering therapy in our cohort, whether allopurinol was protective cannot be determined from our data.

Further, irrespective of whether an individual has gout, there is an increased risk of adverse outcomes as the SU level increases. Currently, there are insufficient data to support treating hyperuricemia in those without clinical manifestations of gout (11). Whether urate-lowering therapy reduces the risk of CV events remains to be determined. However, our data would suggest that the lower the SU level, the lower the risk of CV events, and if allopurinol is shown to reduce the risk of CVD, a specific target SU level may need to be achieved. The literature examining the relationships between gout, SU level, and CVD is conflicting.

The strengths of this study include the prospective study design in contrast to many other studies, which had retrospective or case-controlled designs (12). In addition, we have included multiple specific CV variables known to affect outcomes in the models, including LVEF, the ratio of early diastolic transmitral velocity to septal annular relaxation velocity (E/e′, a marker of LV diastolic function), NT-proBNP, and troponin T, which have not previously been included in outcome models for individuals with gout. Further, the clear association between post-ACS SU levels and outcomes provides strong evidence that a target SU level may be required. Data from current interventional trials will hopefully be able to answer this question.

There are also some limitations to this study. First, ascertainment of gout cases was based on self-report, use of urate-lowering therapy, or use of colchicine with evidence of gout in the medical record. It is possible that some individuals with gout not receiving urate-lowering therapy or colchicine were missed. Second, the majority of those with gout were receiving allopurinol, so we are unable to comment on the background mortality of untreated gout. For those with gout, management using the treat-to-target urate strategy was not part of the study protocol, and gout management was undertaken by the participant's primary care physician. We do not have serial data on urate concentrations to determine whether there was a change over the study period. However, as noted above, there is not currently a CVD-specific SU target level. Finally, this is a survivor cohort, which was designed as such to determine outcomes in those who survived an ACS-related event.

In conclusion, gout is common in individuals with CVD. Survival post-ACS is similar among individuals with gout and those without. However, those with gout are at increased risk of readmission for heart failure and have longer hospital stays. Risk of these events increases in parallel with SU level, regardless of whether gout is present. Whether urate-lowering treatment improves these outcomes remains to be determined.

AUTHOR CONTRIBUTIONS

All authors were involved in drafting the article or revising it critically for important intellectual content, and all authors approved the final version to be submitted for publication. Dr. Stamp had full access to all of the data in the study and takes responsibility for the integrity of the data and the accuracy of the data analysis.

Study conception and design. Stamp, Frampton, Doughty, Troughton, Richards.

Acquisition of data. Stamp, Drake, Doughty, Troughton, Richards.

Analysis and interpretation of data. Stamp, Frampton, Doughty, Troughton, Richards.

REFERENCES

1. Keenan T, Zhao W, Rasheed A, Ho WK, Malik R, Felix JF, et al. Causal assessment of serum urate levels in cardiometabolic diseases through a Mendelian randomization study. J Am Coll Cardiol 2016;67:407–16.

2. Palmer TM, Nordestgaard BG, Benn M, Tybjærg-Hansen A, Davey Smith G, Lawlor DA, et al. Association of plasma uric acid with ischaemic heart disease and blood pressure: Mendelian randomisation analysis of two large cohorts. BMJ 2013;347: f4262.
3. White J, Sofat R, Hemani G, Shah T, Engmann J, Dale C, et al. Plasma urate concentration and risk of coronary heart disease: a Mendelian randomisation analysis. Lancet Diabetes Endocrinol 2016;4:327–36.
4. Pagidipati NJ, Hess CN, Clare RM, Akerblom A, Tricoci P, Wojdyla D, et al. An examination of the relationship between serum uric acid level, a clinical history of gout, and cardiovascular outcomes among patients with acute coronary syndrome. Am Heart J 2017;187:53–61.
5. Kleber ME, Delgado G, Grammer TB, Silbernagel G, Huang J, Krämer BK, et al. Uric acid and cardiovascular events: a Mendelian randomization study. J Am Soc Nephrol 2015;26:2831–8.
6. Choi HK, Curhan G. Independent impact of gout on mortality and risk for coronary heart disease. Circulation 2007;116:894–900.
7. White WB, Saag KG, Becker MA, Borer JS, Gorelick PB, Whelton A, et al. Cardiovascular safety of febuxostat or allopurinol in patients with gout. N Engl J Med 2018;378:1200–10.
8. Richards AM, Nicholls MG, Yandle TG, Frampton C, Espiner EA, Turner JG, et al. Plasma N-terminal pro-brain natriuretic peptide and adrenomedullin: new neurohormonal predictors of left ventricular function and prognosis after myocardial infarction. Circulation 1998;97:1921–9.
9. Prickett TC, Doughty RN, Troughton RW, Frampton CM, Whalley GA, Ellis CJ, et al. C-type natriuretic peptides in coronary disease. Clin Chem 2017;63:316–24.
10. Bredemeier M, Lopes LM, Eisenreich MA, Hickmann S, Bongiorno GK, d'Avila R, et al. Xanthine oxidase inhibitors for prevention of cardiovascular events: a systematic review and meta-analysis of randomized controlled trials. BMC Cardiovasc Disord 2018;18:24.
11. Stamp L, Dalbeth N. Urate-lowering therapy for asymptomatic hyperuricaemia: a need for caution. Semin Arthritis Rheum 2017;46:457–64.
12. Abeles AM, Pillinger MH. Gout and cardiovascular disease: crystallized confusion. Curr Opin Rheumatol 2019;31:118–24.

Arthritis & Rheumatology
Vol. 71, No. 10, October 2019, pp 1739–1746
DOI 10.1002/art.40929

American College of Rheumatology
Empowering Rheumatology Professionals

Effects of Allopurinol Dose Escalation on Bone Erosion and Urate Volume in Gout: A Dual-Energy Computed Tomography Imaging Study Within a Randomized, Controlled Trial

Nicola Dalbeth,[1] Karen Billington,[2] Anthony Doyle,[3] Christopher Frampton,[4] Paul Tan,[1] Opetaia Aati,[1] Jordyn Allan,[1] Jill Drake,[4] Anne Horne,[1] and Lisa K. Stamp[4]

Objective. To examine whether allopurinol dose escalation to achieve serum urate (SU) target can influence bone erosion or monosodium urate (MSU) crystal deposition, as measured by dual-energy computed tomography (DECT) in patients with gout.

Methods. We conducted an imaging study of a 2-year randomized clinical trial that compared immediate allopurinol dose escalation to SU target with conventional dosing for 1 year followed by dose escalation to target, in gout patients who were receiving allopurinol and who had an SU level of ≥0.36 mmoles/liter. DECT scans of feet and radiographs of hands and feet were obtained at baseline, year 1, and year 2 visits. DECT scans were scored for bone erosion and urate volume.

Results. Paired imaging data were available for 87 patients (42 in the dose-escalation group and 45 in the control group). At year 2, the progression in the CT erosion score was higher in the control group than in the dose-escalation group (+7.8% versus +1.4%; $P = 0.015$). Changes in plain radiography erosion or narrowing scores did not differ between groups. Reductions in DECT urate volume were observed in both groups. At year 2, patients in the control group who had an SU level of <0.36 mmoles/liter and patients in the dose-escalation group had reduced DECT urate volume (–27.6 to –28.3%), whereas reduction in DECT urate volume was not observed in control group patients with an SU level of ≥0.36 mmoles/liter (+1.5%) ($P = 0.023$).

Conclusion. These findings provide evidence that long-term urate-lowering therapy using a treat-to-SU-target strategy can influence structural damage and reduce urate crystal deposition in gout.

INTRODUCTION

Monosodium urate (MSU) crystal deposition is the central pathologic feature of gout (1). MSU crystals can deposit in joints or soft tissue structures and induce an acute inflammatory arthritis (gout flare) (2) or present as tophi, which represent organized collections of MSU crystals with surrounding chronic granulomatous inflammatory tissue (3). MSU crystals also contribute to the development of bone erosion in tophaceous gout; advanced imaging studies have demonstrated a very close relationship between tophi and bone erosion in patients with gout (4–7), and laboratory studies have demonstrated that MSU crystals can influence bone cells (osteoclasts, osteoblasts, and osteocytes), both directly and indirectly, toward a proresorptive state (8–10).

Dual-energy computed tomography (DECT) represents a major advance in gout imaging; this technique uses a specific display algorithm that assigns different colors to various materials of

ACTRN: 12611000845932.

Supported by the Health Research Council of New Zealand (grants 09-111D, 11-203, and 15-576).

[1]Nicola Dalbeth, MD, FRACP, Paul Tan, BSc (Hons), Opetaia Aati, MHSc, Jordyn Allan, BSc, Anne Horne, MB, ChB: University of Auckland, Auckland, New Zealand; [2]Karen Billington, MB, BCh, BAO: Auckland District Health Board: Auckland, New Zealand; [3]Anthony Doyle, FRANZCR: Auckland District Health Board and University of Auckland, Auckland, New Zealand; [4]Christopher Frampton, PhD, Jill Drake, RN, Lisa K. Stamp, PhD, FRACP: University of Otago Christchurch, Christchurch, New Zealand.

Dr. Dalbeth has received speaking fees from Pfizer, Janssen, Horizon, and AbbVie (less than $10,000 each), consulting fees from Horizon, Dyve Biosciences, Hengrui, AstraZeneca, and Kowa Pharmaceuticals (less than $10,000 each), and research support from Amgen and AstraZeneca. Dr. Stamp has received consulting fees from AstraZeneca (less than $10,000). No other disclosures relevant to this article were reported.

Address correspondence to Nicola Dalbeth, MD, FRACP, University of Auckland, Department of Medicine, Faculty of Medical and Health Sciences, 85 Park Road, Grafton, Auckland, New Zealand. E-mail: n.dalbeth@auckland.ac.nz.

Submitted for publication October 18, 2018; accepted in revised form May 9, 2019.

chemical composition (11). A protocol has been developed that color-codes urate based on its typical spectral dual-energy properties. DECT has excellent reproducibility in the assessment of MSU crystal burden in people with gout (12). Through visualization of conventional CT images generated at the time of scanning, DECT also provides gold standard visualization of bone erosion (5,13).

Previous clinical and ultrasound observational studies have demonstrated that long-term urate-lowering therapy to a target serum urate (SU) level of <0.36 mmoles/liter (6 mg/dl) can lead to the dissolution of deposited MSU crystals (14–17). The effects of urate-lowering therapy on structural joint damage and on MSU crystal deposition, detected using DECT, have not been previously tested in a randomized clinical trial setting. The aim of this study was to examine whether dose escalation of urate-lowering therapy to achieve a target SU level can influence bone erosion or MSU crystal deposition, as measured by DECT, in gout patients.

PATIENTS AND METHODS

We conducted a prespecified imaging study within the "Safety and Efficacy of High Dose Allopurinol in the Management of Gout" trial. Detailed methods and results of the full trial have been previously reported (18,19). Briefly, this was a 2-year randomized clinical trial that included 183 patients with gout and an SU level of ≥0.36 mmoles/liter and compared conventional allopurinol dosing with dose escalation to a target SU level (ACTRN: 12611000845932). The dose-escalation group received an immediate dose escalation of allopurinol in order to achieve and maintain the target SU level of <0.36 mmoles/liter. The control group had no change in allopurinol dose in year 1 and then received a dose escalation to achieve and maintain SU <0.36 mmoles/liter in year 2. All of the 125 patients at 1 of the 2 study sites (Auckland) were invited to participate in the imaging study, which included DECT scans of both feet and plain radiographs of the hands and feet at the baseline, year 1, and year 2 visits. Ethical approval for the clinical trial, including the imaging study, was obtained from the Multi-Regional Ethics Committee, New Zealand. Written informed consent was obtained from each participant.

DECT of the feet was performed on a Somatom Definition Flash, a dual–X-ray tube 128–detector row scanner (Siemens) (20). Patients were positioned feet-first in a supine position, with the feet in a plantar-flexed position. The scan was acquired in a craniocaudal direction, starting ~5 cm from the ankle joint to the distal big toe. Both ankles and feet were scanned axially in 1 acquisition at 128 × 0.6 mm, field of view 30 cm, and pitch of 0.7. X-ray tube 1 was operated at 80 kV/260 mA and tube 2 at 140 kV/130 mA. The images were reconstructed on a bone algorithm, 512-pixel matrix, to a 0.75-mm slice with 0.5-mm increment. The images were viewed as both 0.75-mm slices and reconstructed 3-mm slices on a picture archiving and communication system. All imaging data were analyzed at the end of the study by 2 independent readers who were blinded with regard to each other's scores and treatment allocation (paired scans from baseline, year 1, and year 2 visits, with order known).

The conventional CT images were scored for bone erosion volume according to a gout CT bone erosion scoring method based on the Rheumatoid Arthritis Magnetic Resonance Imaging Score system for erosion (21) and validated for gout (22) by 2 musculoskeletal radiologists (KB and AD). The gout CT bone erosion scoring system included the following 7 bones for erosion on a semiquantitative scale (0–10, maximum score 140): 1st metatarsal (MT) head, 2nd–4th MT base, cuboid, middle cuneiform, and distal tibia. The interreader intraclass correlation coefficient (ICC) for CT bone erosion score was 0.89. The minimum measurable difference was a score of 1, representing a 10% difference in bone volume in 1 of 140 bones.

DECT urate volume in both feet was measured by 2 independent experienced readers (OA and ND) using automated volume assessment on a Siemens workstation with proprietary software (syngo MMWP VE 36A) (23). Nail bed, skin, submillimeter, motion, and beam-hardening artifacts were excluded from the analysis and from volume measurement (24). For the 80-kV images, fluid was set at 50 HU, the ratio for urate at 1.36, minimum HU of 150, and smoothing range 4. For the 140-kV images, fluid was set at 50 HU, and a maximum HU of 500. DECT urate volume for both feet was measured using automated assessment software on the volume application of the Siemens workstation, with an upper evaluation limit of –1 HU and lower evaluation limit of –1024 HU (Figure 1). The minimum recorded volume was 0.01 cm^3. The interreader ICC for DECT urate volume was 0.99.

Plain radiographs of the hands and feet were scored by an experienced rheumatologist (ND) and musculoskeletal radiologist (KB). The films were scored for erosion and joint space narrowing using a modification of the Sharp/van der Heijde scoring method (25) that was validated for gout (26). The interreader ICC for plain radiography erosion score was 0.90 and for plain radiography joint space narrowing was 0.76.

The prespecified primary end point of the imaging study was change from baseline in CT bone erosion score measured at years 1 and 2. Secondary end points included change from baseline in MSU crystal burden using automated DECT volume assessment software, change from baseline in plain radiography erosion score, and change from baseline in plain radiography joint space narrowing score. All patients with paired imaging results at baseline and year 2 were included in the analysis. The mean score from both readers for each end point was used in the analysis. All dependent variables were $\log_e$-transformed prior to analysis to normalize distributions. The dose-escalation and control groups were compared by analysis of covariance (ANCOVA). For ANCOVA, the dependent variable was change from baseline, the randomized group was a fixed factor, and baseline level was included as a covariate in the analysis. A further fixed factor based on achievement of the target SU level (<0.36 mmoles/liter) at the corresponding study visit was included in additional prespecified

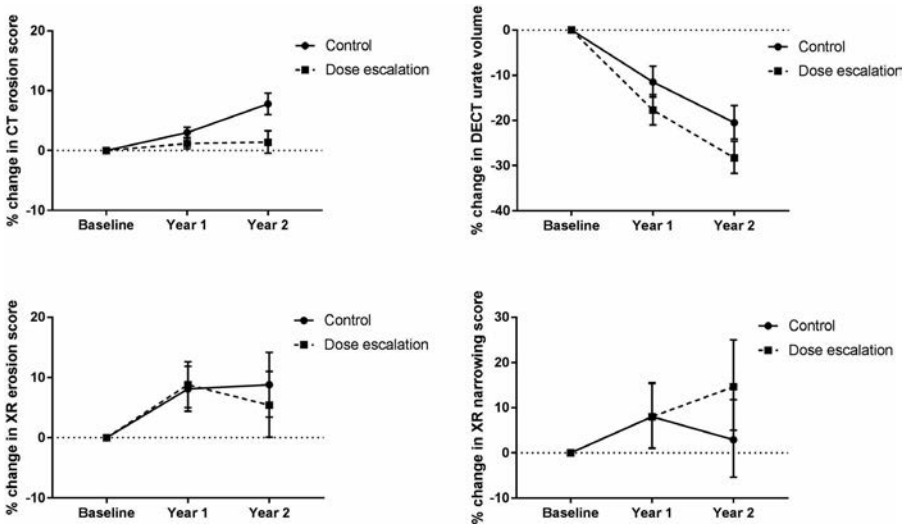

Figure 1. Percentage change in imaging scores according to randomization group. Bars show the mean ± SEM. CT = computed tomography; DECT = dual-energy computed tomography; XR = radiographic.

analyses. The interaction between this factor and the randomized group was tested as part of these analyses and in the presence of testing of the main effects. In unplanned exploratory analyses, a lower target SU level of <0.30 mmoles/liter was included as a fixed factor, and the relationships of gout flares with different measures of joint damage and urate burden were analyzed using Pearson's correlation coefficients. All tests were 2-tailed, and *P* values less than 0.05 were considered significant, with no adjustment for multiple comparisons.

RESULTS

Patient characteristics. Of the 125 patients recruited at the Auckland site, 87 (70%) consented to participate in the imaging study and had paired imaging data at the baseline and year 2 visits. Of those 87 patients, 85 also had imaging assessments at the year 1 visit. The clinical characteristics of these patients at baseline and during the study period are shown in Table 1. The baseline clinical characteristics of patients at the study site who were and were not included in the imaging study analysis are shown in Supplementary Table 1 (available on the *Arthritis & Rheumatology* web site at http://onlinelibrary.wiley.com/doi/10.1002/art.40929/abstract). Participants were predominantly middle-aged men with a mean disease duration of >15 years. Patients in the dose-escalation group received higher allopurinol doses and had lower SU concentrations at year 1, compared with the control group. Both groups had similar allopurinol doses and SU concentrations at year 2.

CT erosion scores. CT erosion scores obtained at each study visit are shown in Table 2. Overall, there was an increase in CT erosion scores over time (*P* = 0.001 from baseline to year 2). Examples of bones with increased CT erosion scores during the 2-year study period are shown in Supplementary Figure 1 (http://onlinelibrary.wiley.com/doi/10.1002/art.40929/abstract). No difference between the randomized groups was observed for CT erosion scores from baseline to year 1 (*P* = 0.16). However, differences between groups were observed from baseline to year 2; over the 2-year study period, the progression of CT erosion scores was higher in the control group compared with that

Table 1. Characteristics of the gout patients in the study*

	Control group (n = 45)	Dose-escalation group (n = 42)
Age, years	61 ± 13	60 ± 13
Male sex, no. (%)	41 (91)	39 (93)
Ethnicity, no. (%)		
Asian	2 (4)	0 (0)
European	20 (44)	16 (38)
Māori	7 (16)	7 (17)
Pacific Island	16 (36)	19 (45)
Disease duration, years	21 ± 12	17 ± 13
≥1 subcutaneous tophus, no. (%)	19 (42)	14 (33)
Allopurinol dose, mg/day		
Baseline	301 ± 122	265 ± 108
Year 1	303 ± 142	400 ± 135
Year 2	370 ± 152	404 ± 159
SU level, mmoles/liter		
Baseline	0.40 ± 0.09	0.42 ± 0.09
Year 1	0.38 ± 0.10	0.33 ± 0.06
Year 2	0.33 ± 0.07	0.33 ± 0.07
SU level <0.36 mmoles/liter, no. (%)		
Year 1	23 (51)	30 (71)
Year 2	31 (69)	31 (74)
SU level <0.30 mmoles/liter, no. (%)		
Year 1	6 (13)	15 (36)
Year 2	14 (31)	15 (36)

* Except where indicated otherwise, values are the mean ± SD. SU = serum urate.

Table 2. Imaging results according to randomized group*

Imaging feature and time point	Control group (n = 45)		Dose-escalation group (n = 42)	
	Geometric mean (95% CI)	Mean change from baseline, % (95% CI)	Geometric mean (95% CI)	Mean change from baseline, % (95% CI)
CT erosion score				
Baseline	4.8 (3.4, 6.5)	–	5.6 (3.9, 7.9)	–
Year 1	5.2 (3.7, 7.2)	3.0 (1.3, 4.8)	5.6 (3.9, 7.9)	1.2 (−0.5, 3.0)
Year 2	5.5 (4.0, 7 .4)	7.8 (4.3, 11.5)	5.6 (3.9, 7.9)	1.4 (−2.2, 5.1)†
DECT urate volume, cm^3				
Baseline	0.64 (0.28, 1.11)	–	0.67 (0.23, 1.26)	–
Year 1	0.50 (0.23, 0.84)	−11.5 (−18.0, −4.5)	0.36 (0.12, 0.64)	−17.7 (−24.0, −10.8)
Year 2	0.36 (0.17, 0.58)	−20.5 (−27.5, −12.7)	0.22 (0.07, 0.40)	−28.3 (−35.0, −20.8)
Plain radiography erosion score				
Baseline	13.5 (8.9, 20.3)	–	10.7 (6.9, 16.4)	–
Year 1	15.3 (10.1, 22.8)	8.1 (0.9, 15.9)	12.3 (7.9, 18.8)	8.8 (1.4, 16.6)
Year 2	14.9 (9.9, 22.3)	8.8 (−1.6, 20.0)	11.9 (7.7, 18.2)	5.4 (−4.8, 16.9)
Plain radiography joint space narrowing score				
Baseline	13.5 (9.5, 19.2)	–	10.4 (6.9, 15.3)	–
Year 1	14.8 (10.3, 20.9)	8.0 (−5.4, 23.2)	12.6 (8.9, 17.5)	8.0 (−5.5, 23.4)
Year 2	13.5 (9.2, 19.6)	2.8 (−12.9, 21.6)	13.4 (9.4, 18.8)	14.6 (−3.6, 36.2)

* 95% CI = 95% confidence interval; CT = computed tomography; DECT = dual-energy computed tomography.
† P = 0.015 versus control group, by analysis of covariance.

in the dose-escalation group (+7.8% versus +1.4%; P = 0.015) (Figure 1 and Table 2). Consistent with the changes observed in CT erosion scores over time, plain radiography erosion scores also increased during the study period (P = 0.021 from baseline to year 2). However, significant differences between randomized groups were not observed in plain radiography erosion scores or plain radiography joint space narrowing scores (Figure 1 and Table 2).

In an analysis that included the area under the curve (AUC) of the SU time-plot from baseline to year 2, the differences between groups in CT erosion scores were observed (P = 0.023 for comparison between randomized groups, P = 0.47 for urate AUC). Similarly, when the groups were subdivided according to achievement of target SU level (<0.36 mmoles/liter) at the corresponding study visit, changes in CT erosion scores did not differ depending on the SU target (P = 0.15), and no interaction was observed between randomized groups and subgroups according to target SU level (P = 0.47) (Figure 2, Table 3, and Supplementary Table 2, http://onlinelibrary.wiley.com/doi/10.1002/art.40929/abstract). Similar findings were observed when the lower target SU (<0.30 mmoles/liter) was included in the analysis (P = 0.023 for randomized groups, P = 0.55 for target SU level, P = 0.88 for interaction between randomized group and target SU level) (Supplementary Table 3, http://onlinelibrary.wiley.com/doi/10.1002/art.40929/abstract).

DECT urate volume. DECT urate volumes at each study visit are shown in Table 2. Overall, there were substantial reductions in DECT urate volume over time (P < 0.001 from baseline to year 2). Examples of scans with reduced DECT urate volume during the 2-year study period are shown in Supplementary Figure 2 (http://onlinelibrary.wiley.com/doi/10.1002/art.40929/abstract). Differences in DECT urate volume between randomized groups were not observed from baseline to year 1 or from baseline to year 2 (P > 0.13). During the study period, the reduction in DECT urate volume was similar in the control group and the dose-escalation group (–20.5% versus –28.3%, respectively; P = 0.14) (Figure 1 and Table 2).

When the randomized groups were subdivided based on achievement of target SU, patients who reached the target level at year 2 had significantly greater reduction in

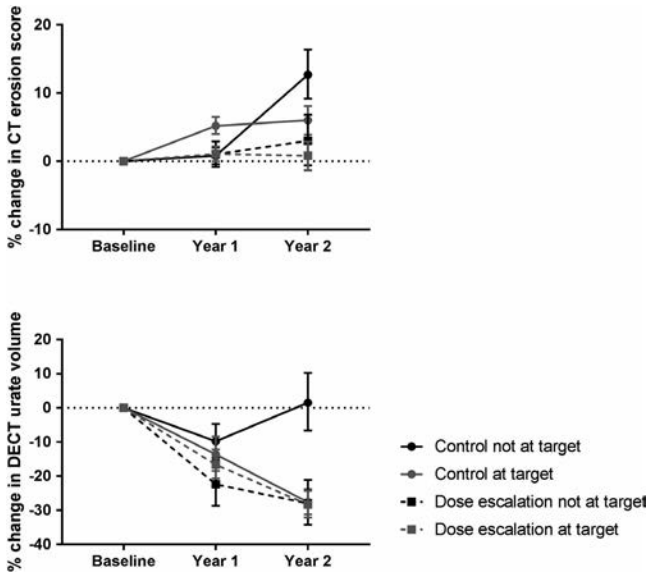

Figure 2. Percentage change in imaging scores according to randomization group and target serum urate level (<0.36 mmoles/liter) at each time point. Bars show the mean ± SEM. See Figure 1 for definitions.

Table 3. Percentage change from baseline according to randomized group and SU target group*

Imaging feature, SU level, and group	Year 1 (n = 85) mean change from baseline, % (95% CI)	Year 2 (n = 87) mean change from baseline, % (95% CI)	Year 1 *P* for randomization/ *P* for urate/*P* for urate × randomization interaction, by ANCOVA	Year 2 *P* for randomization/ *P* for urate/*P* for urate × randomization interaction, by ANCOVA
CT erosion score			0.17/0.11/0.13	0.014/0.15/0.47
SU level <0.36 mmoles/liter				
Control group	5.2 (2.7, 7.8)	6.0 (1.9, 10.2)		
Dose-escalation group	1.1 (−1.0, 3.3)	0.8 (−3.3, 5.1)		
SU level ≥0.36 mmoles/liter				
Control group	0.8 (−1.5, 3.2)	12.7 (5.8, 20.2)		
Dose-escalation group	1.0 (−2.6, 4.7)	3.0 (−4.0, 10.6)		
DECT urate volume			0.16/0.83/0.37	0.017/0.020/0.023
SU level <0.36 mmoles/liter				
Control group	−13.6 (−23.1, −2.9)	−27.6 (−24.7, −19.8)		
Dose-escalation group	−16.6 (−24.6, −7.6)	−28.3 (−35.7, −20.1)		
SU level ≥0.36 mmoles/liter				
Control group	−9.8 (−19.1, 0.7)	1.5 (−14.0, 19.8)		
Dose-escalation group	−22.4 (−34.5, −7.9)	−28.0 (−39.9, −13.7)		
Radiography erosion score			0.49/0.16/0.12	0.30/0.57/0.23
SU level <0.36 mmoles/liter				
Control group	8.9 (−1.4, 20.1)	6.8 (−4.9, 20.1)		
Dose-escalation group	3.6 (−4.9, 12.8)	8.4 (−4.1, 22.5)		
SU level ≥0.36 mmoles/liter				
Control group	7.9 (−2.2, 19.1)	12.6 (−6.3, 35.3)		
Dose-escalation group	22.4 (5.3, 42.4)	−6.2 (−23.2, 14.8)		
Radiography joint space narrowing score			0.23/0.32/0.11	0.52/0.78/0.24
SU level <0.36 mmoles/liter				
Control group	11.0 (−6.9, 32.1)	−2.5 (−19.0, 17.4)		
Dose-escalation group	6.4 (−8.3, 23.5)	23.2 (1.8, 49.3)		
SU level ≥0.36 mmoles/liter				
Control group	4.4 (−12.2, 24.1)	17.6 (−12.0, 57.2)		
Dose-escalation group	28.0 (6.0, 79.8)	9.9 (−19.9, 50.7)		

* SU = serum urate (see Table 2 for other definitions).

DECT urate volume during the study period ($P = 0.020$). There was a significant interaction between the SU level and randomized group in the year 2 analysis ($P = 0.023$) (Figure 2, Table 3, Supplementary Table 2, http://onlinelibrary.wiley.com/doi/10.1002/art.40929/abstract). This interaction was largely a consequence of the patients in the control group who had both an SU level above the target at year 2 and an increased DECT urate volume of +1.5%, compared with ≤–25% in the 3 other groups. No difference between groups was observed when subdivided according to the binary variable of the lower SU target (<0.30 mmoles/liter versus ≥0.30 mmoles/liter) (Supplementary Table 3).

Relationship between DECT urate volume, radiographic damage scores, and gout flares. Additional unplanned correlation analyses showed that at all study visits, DECT urate volume correlated with measures of CT and plain radiographic joint damage (Supplementary Table 4, http://onlinelibrary.wiley.com/doi/10.1002/art.40929/abstract). Overall, there was a higher correlation between DECT urate volume and CT erosion scores (r = 0.58–0.65, $P < 0.001$ for all visits) and between DECT urate volume and plain radiography erosion scores (r = 0.54–0.57, $P < 0.001$ for all visits), compared with the correlation between DECT urate volume and plain radiography joint space narrowing (r = 0.25–0.38, $P < 0.02$ for all visits). There were no significant correlations between change in DECT urate volume and change in CT erosion scores, plain radiography erosion scores, or plain radiography joint space narrowing scores at the year 1 or year 2 visits (r < 0.12, $P > 0.17$ for all comparisons) (Supplementary Table 5, http://onlinelibrary.wiley.com/doi/10.1002/art.40929/abstract). There was no relationship between gout flares and imaging findings at year 1. However, at the year 2 visit, patients who had experienced a gout flare in the preceding year showed higher CT erosion scores, DECT urate volume, and plain radiography erosion (Supplementary Table 6).

DISCUSSION

Our imaging study of a randomized controlled trial has demonstrated that an allopurinol dose-escalation strategy to achieve a target SU level of <0.36 mmoles/liter (6 mg/dl) can prevent CT erosion progression in patients with gout during a 2-year

period. This is the first randomized controlled trial to show that structural modification can be achieved in people with gout. The trial also demonstrated that intensive SU lowering with allopurinol leads to substantial reductions in MSU crystal volume as measured by DECT.

Although significant differences in CT erosion progression were observed between randomized groups, it is noteworthy that the changes over time were small, a finding consistent with those of prior studies describing structural damage progression in gout (27–29). The effects of the allopurinol dose-escalation strategy on CT erosion were observed only after 2 years of treatment, which supports the need for long-term therapy to achieve clinical benefit in gout management. No differences in plain radiography erosion or joint space narrowing scores were observed between groups. These findings highlight the challenges of studies in structural joint damage in gout due to slow rates of change as well as the role of advanced imaging tools with greater sensitivity to change. Although the study showed improvements in CT erosion progression with allopurinol dose escalation, the long-term clinical relevance of these findings with regard to outcomes such as patient function or the need for joint surgery has not been determined, and large studies of longer duration will be needed to understand the impact on these outcomes.

In contrast to our previous case series of gout patients receiving pegloticase, which demonstrated that very intensive SU lowering led to improvement in plain radiography erosion scores (30), allopurinol dose escalation led to prevention of CT erosion progression, rather than improvement in CT erosion scores or plain radiography erosion scores. The mean SU level following allopurinol dose escalation was 0.33 mmoles/liter, in contrast to the undetectable levels observed in pegloticase responders (31). Taken together, these findings suggest that even lower SU levels may be needed to reverse, rather than arrest progression of, bone erosion in people with gout.

In this study, substantial reductions in DECT urate volume were observed during the 2-year study period. Improvements in urate volume were observed in patients in the dose-escalation group and those in the control group who had achieved the target SU level at year 2. These findings are consistent with those of prospective studies of gout patients receiving urate-lowering therapy (32–34), but ours is the first clinical trial to demonstrate that a treat-to-SU-target approach has clinical benefit on MSU crystal burden measured by DECT. Patients in the dose-escalation group experienced a reduction in DECT urate volume irrespective of whether they had reached the target SU level at the relevant time point; some patients may have had SU levels very close to the treatment target at the relevant time point or may have had a low SU level in the prior year but not at the year 1 or year 2 visit. Although substantial reductions in DECT urate deposits were observed with SU level lowering to a target <0.36 mmoles/liter, some crystal deposition persisted even after 2 years of therapy.

It is noteworthy that the slowing of CT erosion progression observed in the allopurinol dose-escalation group was not restricted to patients who had achieved an SU level of <0.36 mmoles/liter at the yearly imaging assessment time points, and that these differences were observed even after including the AUC of the SU time curve in the analysis. There are a number of potential explanations for this observation. The study may not have been powered to detect a true difference in these subgroups (if present). Some patients may have experienced an SU level close to the target at the yearly imaging assessment time point or had a mean SU level below it at various times prior to the yearly visit. It is also possible that allopurinol at higher doses may have benefits for bone remodeling, regardless of achieving the target SU level in this time frame. Recent experimental studies have shown that allopurinol and oxypurinol can promote osteoblast differentiation and increase bone formation (35).

Patients in the control group who received allopurinol dose escalation in the second year of the study had ongoing CT erosion progression at the year 2 visit, despite improvements in DECT urate volume. Furthermore, despite strong correlations between erosion scores and urate volume at each time point, consistent with findings of prior studies (36), there was little correlation between the change in radiologic damage scores (erosion or joint space narrowing) and the change in DECT urate volume. Overall, the reductions in urate volume were large, compared with stabilization of CT erosion progression in the dose-escalation group. These findings suggest a lag between MSU crystal dissolution and stabilization or improvement of radiographic damage.

The main limitation of our study was incomplete participation. It is possible that patients who declined participation in the imaging study differed from those who completed it. Nevertheless, the clinical features of patients who participated in the imaging study were broadly similar to the patients at the same study site who did not complete the imaging study. The data offer a unique opportunity to fully explore DECT assessments and SU data over an extended period within the robust structure of a randomized controlled trial. We acknowledge that the findings are largely hypothesis-generating and will require further validation in other studies. The sample size may not have allowed detection of small differences between subgroups. The target SU level for all patients undergoing dose escalation was <0.36 mmoles/liter, and few patients had an SU level of <0.30 mmoles/liter at either time point. Clinical improvement in joint space narrowing was not observed in any of the groups; joint space narrowing is a nonspecific finding and may not be amenable to change with urate-lowering therapy, even when the SU level is very low (31). Strengths of our study include the relatively high number of Māori and Pacific Island participants, blinded scoring using imaging instruments that had been validated for gout, assessment of both joint damage and urate volume during a long study duration, and systematic imaging assessments within a randomized controlled trial setting.

In summary, this is the first randomized controlled trial to demonstrate that progression of bone erosion can be slowed and potentially prevented using a treat-to–SU-target strategy. The study has also demonstrated that achieving a target SU level of <0.36 mmoles/liter and dose escalation of urate-lowering therapy leads to substantial reduction of MSU crystal burden, as measured by DECT. These findings support the concept that long-term urate-lowering therapy using a treat-to–SU-target strategy can influence structural damage in gout.

AUTHOR CONTRIBUTIONS

All authors were involved in drafting the article or revising it critically for important intellectual content, and all authors approved the final version to be published. Dr. Dalbeth had full access to all of the data in the study and takes responsibility for the integrity of the data and the accuracy of the data analysis.

Study conception and design. Dalbeth, Doyle, Frampton, Stamp.
Acquisition of data. Dalbeth, Billington, Doyle, Tan, Aati, Allan, Drake, Horne, Stamp.
Analysis and interpretation of data. Dalbeth, Frampton, Stamp.

REFERENCES

1. McCarty DJ. A historical note: Leeuwenhoek's description of crystals from a gouty tophus. Arthritis Rheum 1970;13:414–8.
2. Faires JS, McCarty DJ Jr. Acute arthritis in man and dog after intrasynovial injection of sodium urate crystals. Lancet 1962;280:682–5.
3. Dalbeth N, Pool B, Gamble GD, Smith T, Callon KE, McQueen FM, et al. Cellular characterization of the gouty tophus: a quantitative analysis. Arthritis Rheum 2010;62:1549–56.
4. Dalbeth N, Clark B, Gregory K, Gamble G, Sheehan T, Doyle A, et al. Mechanisms of bone erosion in gout: a quantitative analysis using plain radiography and computed tomography. Ann Rheum Dis 2009;68:1290–5.
5. Towiwat P, Doyle AJ, Gamble GD, Tan P, Aati O, Horne A, et al. Urate crystal deposition and bone erosion in gout: 'inside-out' or 'outside-in'? A dual-energy computed tomography study. Arthritis Res Ther 2016;18:208.
6. Dalbeth N, Aati O, Kalluru R, Gamble GD, Horne A, Doyle AJ, et al. Relationship between structural joint damage and urate deposition in gout: a plain radiography and dual-energy CT study. Ann Rheum Dis 2015;74:1030–6.
7. Sapsford M, Gamble GD, Aati O, Knight J, Horne A, Doyle AJ, et al. Relationship of bone erosion with the urate and soft tissue components of the tophus in gout: a dual energy computed tomography study. Rheumatology (Oxford) 2017;56:129–33.
8. Dalbeth N, Smith T, Nicolson B, Clark B, Callon K, Naot D, et al. Enhanced osteoclastogenesis in patients with tophaceous gout: urate crystals promote osteoclast development through interactions with stromal cells. Arthritis Rheum 2008;58:1854–65.
9. Chhana A, Callon KE, Pool B, Naot D, Watson M, Gamble GD, et al. Monosodium urate monohydrate crystals inhibit osteoblast viability and function: implications for development of bone erosion in gout. Ann Rheum Dis 2011;70:1684–91.
10. Chhana A, Pool B, Callon KE, Tay ML, Musson D, Naot D, et al. Monosodium urate crystals reduce osteocyte viability and indirectly promote a shift in osteocyte function towards a proinflammatory and proresorptive state. Arthritis Res Ther 2018;20:208.
11. Choi HK, Al-Arfaj AM, Eftekhari A, Munk PL, Shojania K, Reid G, et al. Dual energy computed tomography in tophaceous gout. Ann Rheum Dis 2009;68:1609–12.
12. Choi HK, Burns LC, Shojania K, Koenig N, Reid G, Abufayyah M, et al. Dual energy CT in gout: a prospective validation study. Ann Rheum Dis 2012;71:1466–71.
13. Perry D, Stewart N, Benton N, Robinson E, Yeoman S, Crabbe J, et al. Detection of erosions in the rheumatoid hand: a comparative study of multidetector computerized tomography versus magnetic resonance scanning. J Rheumatol 2005;32:256–67.
14. Li-Yu J, Clayburne G, Sieck M, Beutler A, Rull M, Eisner E, et al. Treatment of chronic gout. Can we determine when urate stores are depleted enough to prevent attacks of gout? J Rheumatol 2001;28:577–80.
15. Pascual E, Sivera F. Time required for disappearance of urate crystals from synovial fluid after successful hypouricaemic treatment relates to the duration of gout. Ann Rheum Dis 2007;66:1056–8.
16. Perez-Ruiz F, Martin I, Canteli B. Ultrasonographic measurement of tophi as an outcome measure for chronic gout. J Rheumatol 2007;34:1888–93.
17. Ottaviani S, Gill G, Aubrun A, Palazzo E, Meyer O, Dieudé P. Ultrasound in gout: a useful tool for following urate-lowering therapy. Joint Bone Spine 2015;82:42–4.
18. Stamp LK, Chapman PT, Barclay M, Horne A, Frampton C, Tan P, et al. Allopurinol dose escalation to achieve serum urate below 6 mg/dL: an open-label extension study. Ann Rheum Dis 2017;76:2065–70.
19. Stamp LK, Chapman PT, Barclay ML, Horne A, Frampton C, Tan P, et al. A randomised controlled trial of the efficacy and safety of allopurinol dose escalation to achieve target serum urate in people with gout. Ann Rheum Dis 2017;76:1522–8.
20. Dalbeth N, Aati O, Gao A, House M, Liu Q, Horne A, et al. Assessment of tophus size: a comparison between physical measurement methods and dual-energy computed tomography scanning. J Clin Rheumatol 2012;18:23–7.
21. Østergaard M, Edmonds J, McQueen F, Peterfy C, Lassere M, Ejbjerg B, et al. An introduction to the EULAR-OMERACT rheumatoid arthritis MRI reference image atlas. Ann Rheum Dis 2005;64 Suppl 1:i3–7.
22. Dalbeth N, Doyle A, Boyer L, Rome K, Survepalli D, Sanders A, et al. Development of a computed tomography method of scoring bone erosion in patients with gout: validation and clinical implications. Rheumatology (Oxford) 2011;50:410–6.
23. Rajan A, Aati O, Kalluru R, Gamble GD, Horne A, Doyle AJ, et al. Lack of change in urate deposition by dual-energy computed tomography among clinically stable patients with long-standing tophaceous gout: a prospective longitudinal study. Arthritis Res Ther 2013;15:R160.
24. Mallinson PI, Coupal T, Reisinger C, Chou H, Munk PL, Nicolaou S, et al. Artifacts in dual-energy CT gout protocol: a review of 50 suspected cases with an artifact identification guide. AJR Am J Roentgenol 2014;203:W103–9.
25. Van der Heijde DM, van Leeuwen MA, van Riel PL, Koster AM, van 't Hof MA, van Rijswijk MH, et al. Biannual radiographic assessments of hands and feet in a three-year prospective followup of patients with early rheumatoid arthritis. Arthritis Rheum 1992;35:26–34.
26. Dalbeth N, Clark B, McQueen F, Doyle A, Taylor W. Validation of a radiographic damage index in chronic gout. Arthritis Rheum 2007;57:1067–73.
27. Dalbeth N, Aati O, Gamble GD, Horne A, House ME, Roger M, et al. Zoledronate for prevention of bone erosion in tophaceous gout: a randomised, double-blind, placebo-controlled trial. Ann Rheum Dis 2014;73:1044–51.
28. Eason A, House ME, Vincent Z, Knight J, Tan P, Horne A, et al. Factors associated with change in radiographic damage scores in gout: a prospective observational study. Ann Rheum Dis 2016;75:2075–9.

29. McCarthy GM, Barthelemy CR, Veum JA, Wortmann RL. Influence of antihyperuricemic therapy on the clinical and radiographic progression of gout. Arthritis Rheum 1991;34:1489–94.
30. Dalbeth N, Doyle AJ, McQueen FM, Sundy J, Baraf HS. Exploratory study of radiographic change in patients with tophaceous gout treated with intensive urate-lowering therapy. Arthritis Care Res (Hoboken) 2014;66:82–5.
31. Sundy JS, Baraf HS, Yood RA, Edwards NL, Gutierrez-Urena SR, Treadwell EL, et al. Efficacy and tolerability of pegloticase for the treatment of chronic gout in patients refractory to conventional treatment: two randomized controlled trials. JAMA 2011;306:711–20.
32. Zhang Z, Zhang X, Sun Y, Chen H, Kong X, Zhou J, et al. New urate depositions on dual-energy computed tomography in gouty arthritis during urate-lowering therapy. Rheumatol Int 2017;37:1365–72.
33. Neogi T, Jansen TL, Dalbeth N, Fransen J, Schumacher HR, Berendsen D, et al. 2015 gout classification criteria: an American College of Rheumatology/European League Against Rheumatism collaborative initiative. Arthritis Rheumatol 2015;67:2557–68.
34. Bayat S, Aati O, Rech J, Sapsford M, Cavallaro A, Lell M, et al. Development of a dual-energy computed tomography scoring system for measurement of urate deposition in gout. Arthritis Care Res (Hoboken) 2016;68:769–75.
35. Orriss IR, Arnett TR, George J, Witham MD. Allopurinol and oxypurinol promote osteoblast differentiation and increase bone formation. Exp Cell Res 2016;342:166–74.
36. Dalbeth N, Nicolaou S, Baumgartner S, Hu J, Fung M, Choi HK. Presence of monosodium urate crystal deposition by dual-energy CT in patients with gout treated with allopurinol. Ann Rheum Dis 2018;77:364–70.

Arthritis & Rheumatology
Vol. 71, No. 10, October 2019, pp 1747–1755
DOI 10.1002/art.40913

American College of Rheumatology
Empowering Rheumatology Professionals

Identification of Novel Adenosine Deaminase 2 Gene Variants and Varied Clinical Phenotype in Pediatric Vasculitis

Kristen M. Gibson,[1] Kimberly A. Morishita,[1] Paul Dancey,[2] Paul Moorehead,[2] Britt Drögemöller,[1] Xiaohua Han,[1] Jinko Graham,[3] Robert E. W. Hancock,[4] Dirk Foell,[5] Susanne Benseler,[6] Rashid Luqmani,[7] Rae S. M. Yeung,[8] Susan Shenoi,[9] Marek Bohm,[10] Alan M. Rosenberg,[11] Colin J. Ross,[1] David A. Cabral,[1] and Kelly L. Brown,[1] on behalf of the PedVas Investigators Network

Objective. Individuals with deficiency of adenosine deaminase 2 (DADA2), a recently recognized autosomal recessive disease, present with various systemic vascular and inflammatory manifestations, often with young age at disease onset or with early onset of recurrent strokes. Their clinical features and histologic findings overlap with those of childhood-onset polyarteritis nodosa (PAN), a primary "idiopathic" systemic vasculitis. Despite similar clinical presentation, individuals with DADA2 may respond better to biologic therapy than to traditional immunosuppression. The aim of this study was to screen an international registry of children with systemic primary vasculitis for variants in *ADA*2.

Methods. The coding exons of *ADA*2 were sequenced in 60 children and adolescents with a diagnosis of PAN, cutaneous PAN, or unclassifiable vasculitis (UCV), any chronic vasculitis with onset at age 5 years or younger, or history of stroke. The functional consequences of the identified variants were assessed by ADA2 enzyme assay and immunoblotting.

Results. Nine children with DADA2 (5 with PAN, 3 with UCV, and 1 with antineutrophil cytoplasmic antibody–associated vasculitis) were identified. Among them, 1 patient had no rare variants in the coding region of *ADA*2 and 8 had biallelic, rare variants (minor allele frequency <0.01) with a known association with DADA2 (p.Gly47Arg and p.Gly47Ala) or a novel association (p.Arg9Trp, p.Leu351Gln, and p.Ala357Thr). The clinical phenotype varied widely.

Conclusion. These findings support previous observations indicating that DADA2 has extensive genotypic and phenotypic variability. Thus, screening *ADA*2 among children with vasculitic rash, UCV, PAN, or unexplained, early-onset central nervous system disease with systemic inflammation may enable an earlier diagnosis of DADA2.

INTRODUCTION

Deficiency of adenosine deaminase 2 (DADA2) is a recently characterized autosomal recessive genetic disease that was first reported in 2 independent cohorts of children with early-onset vasculopathy resembling polyarteritis nodosa (PAN) (1,2). All children in the described cohorts harbored rare, biallelic variants in the adenosine deaminase 2 (*ADA2*) locus (formerly known as Cat Eye Syndrome candidate region 1, or *CECR1*), which encodes the enzymatic protein ADA2. The absence of ADA activity in the plasma of all patients substantiated the notion of a damaging effect of the identified variants.

Supported by a Canadian Institute of Health Research (CIHR) grant for the PedVas Initiative (TR2-119188 to Dr. Cabral). Dr. Cabral's work was supported by The Arthritis Society (TAS) Canada through the Ross Petty Arthritis Society Chair. Dr. Brown's work was supported by the Michael Smith Foundation for Health Research and a Cassie & Friends Society Scholar Award. Dr. Drögemöller's work was supported by a CIHR Postdoctoral Fellowship and the Michael Smith Foundation for Health Research Trainee Award.

[1]Kristen M. Gibson, BSc, Kimberly A. Morishita, MD, Britt Drögemöller, PhD, Xiaohua Han, BSc, Colin J. Ross, PhD, David A. Cabral, MBBS, Kelly L. Brown, PhD: University of British Columbia and BC Children's Hospital, Vancouver, British Columbia, Canada; [2]Paul Dancey, MD, Paul Moorehead, MD: Janeway Children's Hospital and Rehabilitation Centre, Saint John's, Newfoundland and Labrador, Canada; [3]Jinko Graham, PhD: Simon Fraser University, Burnaby, British Columbia, Canada; [4]Robert E. W. Hancock, PhD: University of British Columbia, Vancouver, British Columbia, Canada; [5]Dirk Foell, MD: University Hospital Muenster, Muenster, Germany; [6]Susanne Benseler, MD, PhD: Alberta Children's Hospital, Calgary, Alberta, Canada; [7]Rashid Luqmani, MD; University of Oxford, Oxford, UK; [8]Rae S. M. Yeung, MD, PhD: Hospital for Sick Children, Toronto, Ontario, Canada; [9]Susan Shenoi, MD: Seattle Children's Hospital, Seattle, Washington; [10]Marek Bohm, MD: Leeds General Infirmary, Leeds Teaching Hospitals Trust, Leeds, UK; [11]Alan M. Rosenberg, MD: Royal University Hospital and University of Saskatchewan, Saskatoon, Saskatchewan, Canada.

No potential conflicts of interest relevant to this article were reported.

Address correspondence to David Cabral, MBBS, BC Children's Hospital, Room K4-119, 4480 Oak Street, Vancouver, BC V6H 3V4, Canada. E-mail: dcabral@cw.bc.ca.

Submitted for publication September 28, 2018; accepted in revised form April 16, 2019.

The most prevalent mutation in the first reports of DADA2 was the p.Gly47Arg variant, having an estimated carrier frequency of 10% in the Georgian-Jewish population—a population known to have high rates of PAN (1). More than 60 disease-causing variants, mostly missense single-nucleotide variants, have now been described across the entire coding region of *ADA2*, including the catalytic, dimerization, and secretion domains (3). The most frequently reported variants, in addition to p.Gly47Arg, are p.Gly47Ala, p.Arg169Gln, Tyr453Cys, and p.Thr360Ala, with the latter being most common in Italian patients (4).

Despite conservation across species (5), there is considerable variation within the human *ADA2* locus. In parallel, there is large phenotypic heterogeneity associated with DADA2. Initial cases were notable for early-onset disease as well as recurrent strokes, fever, and livedo reticularis rash associated with vasculopathy; more recent case descriptions have been extended to include an autoimmune phenotype (6–8), bone marrow deficiencies (4,9), and adult-onset disease (2,10,11). With accumulating reports, the characteristic phenotypic spectrum of DADA2 is widening and there appears to be little correlation between these widening phenotypic clinical features and *ADA2* genotype (4). Patients with DADA2, including those with life-threatening disease, may respond more favorably to treatment with anti–tumor necrosis factor (anti-TNF) blocking agents (12) than with the "traditional" treatments for chronic primary vasculitides (CPVs). It is critical to distinguish patients with DADA2 from those with other types of CPV to enable earlier and more effective interventions; identifying all of the deleterious *ADA2* gene variants and the associated pathogenic mechanisms may further guide both prognostication and therapy.

Because vasculitis remains a predominant feature in most cases of DADA2 described to date (3), we retrospectively and selectively screened an international cohort of children with CPV for DADA2 by targeted Sanger sequencing and assessment of ADA2 enzyme activity in the patients' serum. We identified 9 children with DADA2 with known pathogenic and novel variants in *ADA2*. Based on our observations, we propose additional clinical features that should be considered in screening criteria for DADA2.

PATIENTS AND METHODS

Participants. Patients described in this study were enrolled in the Pediatric Vasculitis Initiative (PedVas), an international study on pediatric CPV. Eligibility criteria for PedVas have been described previously (13). The study protocol was approved by the Children's and Women's Research Ethics Board of the University of British Columbia (approval no. H12-00894) and the respective ethics committees or IRBs at participating PedVas sites. Written informed consent was obtained between February 2013 and July 2018 from children or adolescents age 18 years and younger who were diagnosed as having a systemic CPV, including PAN, cutaneous PAN (cPAN), granulomatosis with polyangiitis (GPA), microscopic polyangiitis, eosinophilic granulomatosis with polyangiitis, Takayasu arteritis, unclassified vasculitis (UCV), or suspected DADA2. Study visits coincided with times of routine clinical care (13). Healthy children with sleep apnea (n = 4), who were enrolled in the BCCH BioBank, were used as pediatric controls for the ADA2 activity assay (approval no. H13-03111).

Clinical data. At each study visit, as described previously, patients contributed data that included demographics, clinical features, medical history, diagnostic data, treatment, and clinical laboratory results (14). Data were entered by participating sites into A Registry of Childhood Vasculitis (ARChiVe), the RedCap (15) data collection platform for PedVas. Clinical data were reviewed in Vancouver for errors and completeness. Patients were formally classified into CPV subtypes by the on-site rheumatologist as well as by using a pediatric-modified algorithm of the European Medicines Agency. Generation of a pediatric vasculitis activity score (PVAS) (16) was a component of data entry to ARChiVe; active and inactive disease was defined as a PVAS of >2 and PVAS of ≤2, respectively.

Biosample collection and processing. Participants contributed blood in serum separation tubes and/or K2 EDTA vacutainers (BD Biosciences) and Tempus RNA tubes (Applied Biosystems). RNA tubes and serum/plasma aliquots were stored at –80°C upon receipt in Vancouver. DNA was isolated from whole blood (collected in K2 EDTA tubes) or saliva (collected in OG-500, OG-575, or OCR-100 Oragene•DNA collection kits; DNA Genotek Inc.) using QIAsymphony SP, in accordance with the manufacturer's protocol (Qiagen). Isolated DNA was quantitated using a Quant-iT PicoGreen double-stranded DNA assay kit (ThermoFisher) and stored at –20°C prior to sequencing.

Sanger sequencing of *ADA2*. Targeted Sanger sequencing was implemented for the coding exons of *ADA2* (exons 2–10) (for primer sequences, see Supplementary Table 1, available on the *Arthritis & Rheumatology* web site at http://onlinelibrary.wiley.com/doi/10.1002/art.40913/abstract). Total genomic DNA (50 ng) was combined with 1× AmpliTaq Gold 360 buffer, 2.0 m*M* magnesium chloride, 3 μl of 360 GC Enhancer, 200 μ*M* dNTPs, 0.5 μ*M* forward primer, 0.5 μ*M* reverse primer, and 0.625 units/reaction AmpliTaq Gold 360 DNA Polymerase in a total volume of 20 μl in a 96-well plate. Initial denaturation was at 95°C for 5 minutes, followed by 40 cycles at 95°C for 50 seconds, 59°C for 35 seconds, 72°C for 60 seconds, and a final extension step at 72°C for 7 minutes. Polymerase chain reaction products were cleaned with ExoSAP-IT Express (ThermoFisher) and analyzed using an ABI Genetic Analyzer (Applied Biosystems). Sequences were aligned to the *ADA2* transcript (ENST00000399839.1, Ensembl GRCh37) and analyzed using CodonCode Aligner version 3.03.

Assay for ADA2 enzyme activity. Extracellular ADA2 enzyme activity was quantified in the patients' serum (patients 1, 2, 4, 6, 7, 8, 10, and 11) and plasma (patient 3) using an ADA assay (Diazyme Laboratories) with some modification to the manufacturer's protocol. Briefly, 10 µl of serum/plasma was incubated with 5 µl of an ADA1-specific inhibitor, erythro-9-(2-hydroxy-3-nonyl) adenine-HCl (100 µ*M*; Millipore Sigma), for 5 minutes at 37°C. Reagent 1 (180 µl) and Reagent 2 (90 µl) were added (reaction volume of 285 µl), and the absorbance at 556 nm was read every 10 minutes over 3 hours, using an Infinite M200 microplate reader and Magellen analysis software (TECAN).

ADA2 enzyme activity in the samples was calculated using a calibrator of known ADA activity and using 0.9% saline as a blank. ADA2 activity in patient 9 was quantified at the local site, using a dried plasma spot analysis. No serum samples were reserved from patient 5 prior to death.

Western blot analysis of ADA2 protein. ADA2 protein in the patients' serum (patients 1, 2, 4, 6, 7, 8, 10, and 11) and plasma (patient 3) was analyzed by immunoblotting. Briefly, nonreduced samples (1:50 dilution) and prestained protein ladder (no. 26619; PageRulerPlus) were resolved on a 10% NuPage sodium dodecyl sulfate–polyacrylamide electrophoresis gel. Separated proteins were transferred to a 0.45-µm PVDF membrane (Immobilon-P; Millipore Sigma) that was blocked with phosphate buffered saline/5% skim milk and probed with an anti-*CECR1* polyclonal antibody (1/1,000 dilution, PA5-30635) followed by a horseradish peroxidase–conjugated goat anti-rabbit IgG (H+L) antibody (1/10,000 dilution, A16104) and SuperSignal West Pico PLUS Chemiluminescent Substrate. The membrane was exposed to autoradiography film (Diamed) and imaged with an Alphalmager 2200 (Alpha Innotech). All reagents were from ThermoFisher, unless specified otherwise.

Statistical analysis. Analysis of variance, followed by a 2-tailed Tukey's test, was used to analyze group differences, and the results were analyzed using GraphPad Prism statistical software version 7.0. For all analyses, 95% confidence intervals were used, and *P* values less than or equal to 0.05 were considered significant.

RESULTS

Identification of novel and rare variants in *ADA2*. Among 542 pediatric CPV patients in our ARChiVe registry, DNA was available from 138 individuals. Of these, Sanger sequencing for variants in the splice-site and coding regions (exons 2–10) of *ADA2* was performed on samples from 60 patients classified as having PAN, cPAN, or UCV (n = 44), suspected DADA2 (n = 2), a disease onset at age ≤5 years (n = 22), and/or stroke-like episodes (n = 7) (see Supplementary Table 2, available on the *Arthritis & Rheumatology* web site at http://onlinelibrary.wiley.com/doi/10.1002/art.40913/abstract). For 3 individuals (patients 5, 6, and 9), *ADA2* variants were identified by whole exome sequencing that was initiated at their respective health care center, and results in 2 samples (patients 6 and 9) were confirmed by Sanger sequencing. Eight individuals carried novel or rare variants in *ADA2* with a minor allele frequency

Table 1. Pediatric vasculitis patients with rare *ADA2* mutations*

Patient	Ethnicity†	Sex	Age at onset‡	Age at diagnosis§	Initial diagnosis	*ADA2* mutation (coding sequence)
1	South Asian	F	11 years	12 years	PAN	c.[139G>C];[139G>C]
2	South Asian	F	11 years	12 years	PAN	c.[139G>A];[139G>A]
3	East Asian	M	16 years	16 years	Unclassified vasculitis	c.[25C>T];[140G>C]¶
4	South Asian	M	11 years	12 years	PAN	c.[1069G>A];[1069G>A]¶
5	White	F	1 week	NA#	Undiagnosed	c.[1052T>A];[1052T>A]¶
6	White	F	10 months	3 years#	Undiagnosed (suspected DADA2)	c.[1052T>A];[1052T>A]¶
7	East Asian	F	4 years	4 years	PAN	c.[139G>A];[139G>A]
8	South Asian	F	3 years	5 years	GPA	No identified variants in coding or splice-site regions
9	White	F	6 months	8 months	Unclassified vasculitis	c.[139G>C]; deletion
10	South Asian	M	11 years	11 years	cPAN	c.927G>A
11	White	F	2 years	NA	Undiagnosed	c.1252G>T

* PAN = polyarteritis nodosa; NA = not applicable; GPA = granulomatosis with polyangiitis; cPAN = cutaneous PAN.
† Self-reported.
‡ At first associated symptoms.
§ At diagnosis of systemic vasculitis.
¶ Variant showing a novel association with deficiency of adenosine deaminase 2 (DADA2).
# In sibling patients 5 and 6, a diagnosis of systemic vasculitis was not made; the diagnosis of DADA2 was made at age 3 years in patient 6 and postmortem in patient 5.

of <0.01, as defined by the Exome Aggregation Consortium (Tables 1 and 2, and Supplementary Figure 1 available on the *Arthritis & Rheumatology* web site at http://onlinelibrary.wiley.com/doi/10.1002/art.40913/abstract).

Three patients (patients 1, 2, and 7) carried the known pathogenic variant within the dimerization domain of *ADA2*, p.Gly47Arg. Patient 3 was compound heterozygous (confirmed by targeted sequencing of the affected exons in the parents) for a known pathogenic variant, p.Gly47Ala, and a variant showing a novel association with DADA2, p.Arg9Trp, that is located in the signal sequence domain of *ADA2* (see Supplementary Figures 1 and 2 at http://onlinelibrary.wiley.com/doi/10.1002/art.40913/abstract). Patient 4 was homozygous for a variant of novel association, p.Ala357Thr, within the catalytic domain of ADA2 (Supplementary Figure 2). Patients 5 and 6 were siblings; in patient 5, whole exome sequencing (GeneDx) identified a novel variant of unknown significance, p.Leu351Gln, that was subsequently identified in patient 6 through this study. Both parents were heterozygous for the p.Leu351Gln variant (Supplementary Figure 1). Patient 8 had no rare variants in the splice-site or coding regions of *ADA2*. Patient 9 was compound heterozygous (confirmed by trio sequencing [data not shown]) for the known pathogenic variant, p.Gly47Arg, and for a deletion that has not yet been fully characterized. Patients 10 and 11 were heterozygous for rare variants, a known one, p.Met309Ile, and one predicted to be pathogenic, p.Val418Leu. The identified variants showing a novel association with DADA2 (p.Arg9Trp, p.Leu351Gln, and p.Ala357Thr) were predicted to be damaging, by computational modeling (Table 2).

Compromising effects of biallelic *ADA2* variants on ADA2 enzyme activity. The impact of the identified variants on ADA2 enzyme function was quantified in the patients' serum (patients 1, 2, 4, 6, 7, 8, 10, and 11) and plasma (patient 3) using an ADA assay. Samples obtained from patients with rare, biallelic *ADA2* variants (patients 1, 2, 3, 4, 6, and 7) had a significant loss of ADA2 enzyme activity (Figure 1B) compared to healthy children (n = 4; $P < 0.0001$) and other children with vasculitis that met *ADA2* screening criteria but did not carry rare *ADA2* variants, which included children with PAN (n = 4; $P < 0.0001$) and children with Takayasu arteritis (n = 7; $P < 0.0001$), a large-vessel vasculitis that may or may not be associated with stroke (Figure 1A). ADA2 enzyme activity was also diminished in patient 8 despite a lack of rare variants in the coding and splice-site regions of *ADA2,* suggesting that this patient may harbor damaging noncoding or structural variants. ADA2 enzyme activity in the serum from patients with a single, rare, known pathogenic variant (patient 10) or a single, rare, predicted pathogenic variant (patient 11) was similar to that in the control groups (Figures 1A and B).

To confirm that ADA2 protein was present in patient samples (thereby confirming that loss of ADA2 enzyme activity could not be attributable to the absence of ADA2 protein), samples of

Table 2. Characteristics of the identified *ADA2* variants and the predicted consequence in silico*

rsID	Coding sequence	Predicted consequence	ExAC MAF	ExAC GMAF	CADD	PolyPhen predicted consequence	ClinVar annotation
rs202134424	c.139 G>C	Missense (p.Gly47Arg)	0.001	<0.01	26	Probably damaging	Pathogenic
rs202134424	c.139G>A	Missense (p.Gly47Arg)	7.40×10^{-5}	<0.01	26	Probably damaging	Pathogenic
rs200930463	c.140G>C	Missense (p.Gly47Ala)	6.60×10^{-5}	<0.01	26	Probably damaging	Pathogenic
rs753994372	c.25C>T†	Missense (p.Arg9Trp)	8.20×10^{-6}	<0.01	18	Benign	NA
rs374974565	c.1069G>A†	Missense (p.Ala357Thr)	1.20×10^{-4}	<0.01	31	Probably damaging	NA
NA	c.1052>A†	Missense (p.Leu351Gln)	NA	NA	25	Probably damaging	NA
rs146597836	c.927G>A	Missense (p.Met309Ile)	0.002	<0.01	3	Benign	Pathogenic in Behçet's syndrome; likely benign in PAN
rs142726959	c.1252G>T	Missense (p.Val418Leu)	7.52×10^{-5}	<0.01	29	Probably damaging	NA

* For each variant, the predicted consequence is shown, along with the following characteristics: ethnicity-matched minor allele frequency (MAF) as reported by the Exome Aggregation Consortium (ExAC), global MAF (GMAF) as reported by the ExAC, combined annotation-dependent depletion score (CADD) based on the conservation and consequence of the affected amino acid, consequence of the amino acid substitution as predicted by PolyPhen, and the ClinVar annotation. NA = not applicable; PAN = polyarteritis nodosa.
† Variant showing a novel association with deficiency of adenosine deaminase 2 (DADA2).

patients' serum/plasma were resolved by gel electrophoresis, and ADA2 protein was detected by immunoblotting. ADA2 protein in all serum/plasma samples was detected at levels similar to those in a patient without variants in ADA2 (a patient with PAN) and was detected in the dimeric form (~120 kd), even in those patients carrying pathogenic variants in the dimerization domain (patients 1–3 and patient 7) (Figure 1C). Furthermore, using paired serum samples from patients with PAN who were negative for rare *ADA2* variants (n = 3), we confirmed that disease activity did not influence the results, as ADA2 activity was similar in samples obtained at a time when the disease was active (PVAS scores of 7, 12, and 17 in the 3 patients) and in samples obtained when it was inactive (PVAS scores of 0 in each patient) (P = 0.2324) (data not shown).

Variation in clinical phenotypes associated with rare, biallelic *ADA2* variants. The age range at the time of symptom onset in patients in our cohort with rare or novel *ADA2* variants was 1 week to 16 years (Table 1). Clinical manifestations in the 9 patients with DADA2 are summarized in Table 3. Cutaneous involvement was present in 8 of the 9 patients and included livedo reticularis/racemosa, nodular lesions, soft tissue/subcutaneous edema, and ulcers. Neurologic involvement, a common cardinal feature that has been reported in other DADA2 patient cohorts (1,2,4), was also present in 8 of 9 patients. Five of these patients had central nervous system (CNS) involvement in the form of stroke (patients 3, 4, 6, 7, and 9) and 1 had stroke along with diffuse cerebral atrophy (patient 5) (Figure 2A), while 4 had peripheral nervous system (PNS) involvement, of whom 1 had mononeuritis multiplex (patient 2) and 3 had cranial nerve involvement (patients 6, 7, and 9).

Sibling patients 5 and 6 had severe disease. Both had gastrointestinal disease resulting in bowel perforations, and significant hematologic disease. Patient 5 at age 1 week was diagnosed as having presumed Diamond-Blackfan anemia, but subsequent testing excluded the diagnosis. She later developed severe neutropenia, with the absence of neutrophils on a complete blood cell count, and had a bone marrow biopsy that showed no neutrophils or precursors (Figure 2B). She died at the age of 17 months due to complications of the bowel perforation. Patient 6, the older sister of patient 5, was treated for urosepsis at age 4 months and was noted to have persisting, unexplained elevated liver transaminase levels. At age 10 months, she developed a third nerve palsy. She was asymptomatic until age 3 years, when she presented, shortly after the death of her younger sibling, with fevers, raised levels of inflammation markers, neutropenia, and evidence of prior stroke.

Four patients had low IgM levels despite having normal levels of IgA and IgG. Blurred vision (defined in the registry as "altered measurement of best visual acuity from previous or baseline, requiring specialist opinion for further evaluation") was noted in 4 patients, in the absence of other diagnoses such as ocular inflammation (uveitis, scleritis, episcleritis) or any underlying retinal pathology. No patient with PAN who was not later diagnosed as having DADA2 had this symptom. All patients were negative for antinuclear antibodies. One patient (patient 8) who was positive for antineutrophil cytoplasmic antibodies (ANCAs), specifically anti–proteinase 3 ANCAs, was diagnosed as having GPA (fulfilling classification criteria), having both multiple pulmonary nodules

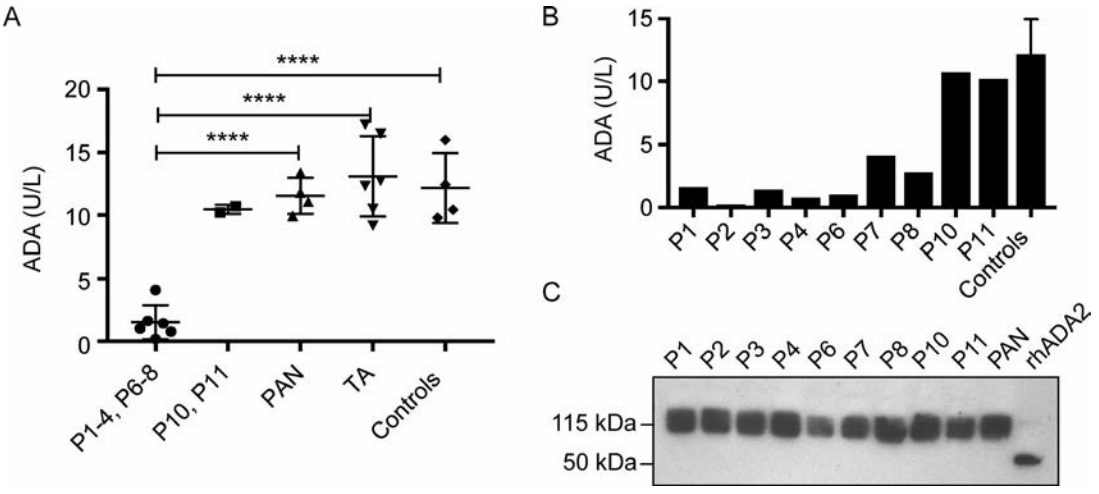

Figure 1. **A**, Adenosine deaminase 2 (ADA2) activity (measured in units/liter) in the serum or plasma of healthy children (controls; n = 4), children with vasculitis and overlapping clinical symptoms (polyarteritis nodosa [PAN] n = 4; Takayasu arteritis [TA] n = 6), and children with biallelic variants in *ADA2* (patients P1–4 and P6–8; n = 7) or with single, heterozygous variants in *ADA2* (patients P10 and P11; n = 2). **B**, ADA2 activity in the serum or plasma of children with biallelic variants in *ADA2* (patients P1–P4, P6, and P7), children with no identified variants in *ADA2* (patient P8), children with a single variant in *ADA2* (patients P10 and P11), and pediatric controls (n = 4). Results in **A** and **B** are the mean ± SD. **C**, Immunoblot analysis of ADA2 protein in the serum of pediatric patients with diminished ADA2 enzyme activity (patients P1–4, P6–8, P10, and P11) compared to a pediatric patient with PAN who had no rare *ADA2* variants and to 10 ng recombinant human ADA2 (rhADA2). **** = $P < 0.0001$.

Table 3. Clinical manifestations in the patients with deficiency of adenosine deaminase 2

	Fever	Cutaneous	Nervous system	Other organ systems	Vascular imaging	Hypogammaglobulinemia
Patient 1	No	Nodules; livedo reticularis	None	Blurred vision; anemia	Microaneurysms (hepatic and splenic artery)	Not determined
Patient 2	Yes	Nodules; diffuse finger and toe swelling	Motor mononeuritis multiplex	Oral ulcers; abdominal pain	Microaneurysms (splanchnic vessels)	Not determined
Patient 3	Yes	Painful subcutaneous nodules	Meningitis/encephalitis; brainstem infarct	None	No abnormal findings	Not determined
Patient 4	Yes	Ulcers; livedo reticularis; superficial infarctions	Midbrain infarcts	Blurred vision	Aneurysms (renal, splanchnic, vertebral arteries)	Low IgM
Patient 5	Yes	Livedo racemosa or cutis marmorata (age 1 week)	Diffuse cerebral atrophy	Oral ulcers; bloody diarrhea; perforated bowel; anemia; neutropenia	No abnormal findings	Low IgM
Patient 6	Yes	None	Stroke; cranial nerve involvement	Blurred vision; chronic liver disease; perforated bowel; neutropenia	No abnormal findings	Low IgM
Patient 7	Yes	Subcutaneous edema; nodules	Stroke; cranial nerve involvement	Blurred vision	Restricted diffusion on left thalamus	Low IgM
Patient 8	Yes	Subcutaneous edema; polymorphous rash	Decreased tendon reflexes	Oral ulcers; anal fissures; saddle nose deformity; glomerulonephritis	No vascular imaging performed	Normal
Patient 9	Yes	Livedo reticularis; Raynaud's phenomenon	Oculomotor nerve involvement; lacunar cerebral infarctions	Oculomotor palsy; ileitis; splenic infarction; hypertension	Decreased diameter of thoracic aorta and right radial artery; irregularities of the abdominal aorta	Not determined

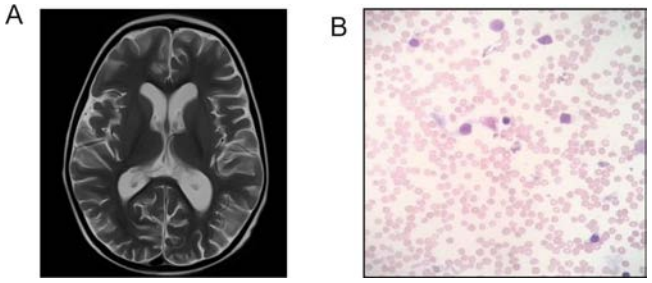

Figure 2. P5 magnetic resonance imaging of the brain (**A**) and bone marrow aspirate (**B**) from representative children with deficiency of adenosine deaminase 2 (DADA2). **A**, T2-weighted axial image of the brain of a patient with DADA2 demonstrates diffuse white matter volume loss. The myelination pattern is appropriate for the age of the patient, indicating no evidence of dysmyelination or demyelination. **B**, Bone marrow aspirate from a patient with DADA2 at age 17 months, in whom the complete white blood cell count was 1.5×10^9/liter, with a neutrophil count of 0.0×10^9/liter and monocyte count of 0.0×10^9/liter, the hemoglobin level was 88 gm/liter (with hypochromia and microcytosis), and the platelet count was 901×10^9/liter. The aspirate is dilute and aparticulate, with a marked decrease in granulopoiesis.

on imaging and renal histopathologic findings showing necrotizing fibrinoid necrosis and pauci-immune glomerulonephritis with crescents.

Variation in the clinical treatment response. Disease severity at presentation ranged from mild and limited to the skin, to severe and lethal. All patients were initially treated with immune-suppressing medications and glucocorticoids (GCs). Initial treatments and the response to treatments are summarized in Table 4. Patients 1 and 2 had the mildest phenotype, with primarily skin disease. Patient 1 responded well to treatment with GCs, methotrexate, and colchicine. Patient 2 was treated with GCs, methotrexate, and intravenous (IV) immunoglobulin; IV cyclophosphamide was added at 6 months for ongoing disease activity. Five patients had moderate-to-severe disease: patient 3 had mild stroke, patient 4 had ulcerating skin disease and aneurysms of the vertebral and splanchnic arteries, patient 7 had stroke and cranial nerve involvement, patient 8 had renal disease, and patient 9 had stroke and cranial nerve involvement. Patient 3 was treated with GCs and 1 dose of rituximab, and then switched to etanercept 1 month later when DADA2 was diagnosed. He responded well to etanercept. Patient 4 and patient 7 were treated with GCs and IV cyclophosphamide. Patient 4 switched to mycophenolate mofetil after 6 months due to poor response. Patient 8 responded well to GCs and methotrexate. Patient 9 was treated with GCs and azathioprine but switched to IV cyclophosphamide due to lack of response. After several years of poorly controlled disease, the patient was started on etanercept, achieving an excellent response.

As previously described, sibling patients 5 and 6 had very severe disease. Patient 5 was initially treated successfully with GCs for the presumed Diamond-Blackfan anemia. At age 14 months, she developed fevers, severe neutropenia, anemia, elevated levels of inflammation markers, and transient rash. GCs and etanercept were initiated after the diagnosis of DADA2 was made; however, she died (due to bowel perforation) after receiving only 1 dose of etanercept. Pathologic examination of a section of the bowel revealed multifocal ischemia with severe bacterial overgrowth, suggesting neutropenic enterocolitis but no definitive evidence of vasculitis. A complete autopsy was

Table 4. Initial treatment and response*

	Initial treatment	Response to treatment
Patient 1	GC, methotrexate, colchicine	Improved on initial treatment; flared at 12 months and restarted on GCs
Patient 2	GC, methotrexate, IVIG	IV cyclophosphamide added 6 months after diagnosis due to ongoing disease activity; improved on cyclophosphamide
Patient 3	GC, rituximab (one dose)	Switched to etanercept 1 month after presentation (after diagnosis of DADA2 was made); inactive disease at 6 months without GC treatment
Patient 4	GC, IV cyclophosphamide	Switched to mycophenolate mofetil at 6 months due to ongoing disease activity and difficult IV access
Patient 5	GC	Etanercept started 1 year after presentation (when diagnosis of DADA2 was made); only received 1 dose of etanercept prior to death
Patient 6	GC, etanercept	Good response to initial treatment; relapse at 4 months; anakinra added to no benefit; underwent bone marrow transplantation
Patient 7	GC, IV cyclophosphamide	Improved on initial treatment; inactive disease at postinduction visit (6 months after diagnosis); switched to azathioprine for maintenance
Patient 8	GC, methotrexate	Improved on initial treatment
Patient 9	GC, azathioprine	Switched to IV cyclophosphamide 3 months after diagnosis, for ongoing disease activity; poor disease control for several years until etanercept started 5 years after diagnosis, with prompt and stable response to etanercept

* GC = glucocorticoid; IVIG = intravenous immumoglobulin; DADA2 = deficiency of adenosine deaminase 2.

declined by the family. Patient 6 was diagnosed as having DADA2 shortly after the death of her sibling and was promptly treated with GCs and etanercept, achieving a good response. After 4 months, the disease relapsed with a recurrence of the fevers and severe neutropenia. As she continued to deteriorate despite an increase in the GC dose and the addition of anakinra to the etanercept regimen, a hematopoietic stem cell transplantation was performed. Currently, at 6 months post-transplantation, she requires only low-dose GCs for treatment of mild graft-versus-host disease.

DISCUSSION

Herein we describe 9 patients with DADA2, of whom 8 had rare, biallelic variants in *ADA2* and 1 had abrogated ADA2 enzymatic activity but no rare variants in the splice-site or coding regions of *ADA2*. The identified variants included 2 variants showing a novel association with DADA2, Arg9Trp (c.25C>T) and Ala357Thr (c.1069G>A), and 1 novel variant, Leu351Gln (c.1052>A). An additional 2 patients carried a single, rare variant in *ADA2.* ADA2 enzyme activity assay and immunoblotting confirmed that patients with biallelic variants had circulating ADA2 protein with severely compromised enzyme activity as compared to that in patients with a single variant, in whom the ADA2 enzyme activity was similar to that in healthy children and children with other vasculitides. These data are consistent with the autosomal recessive mode of inheritance for DADA2 (1,2).

The clinical phenotype of the earliest described cohorts of DADA2 patients included young age at disease onset, early-onset stroke, and livedo reticularis/racemosa rash (1,2). Similarly, vasculitic skin rash (especially livedo reticularis and nodular lesions) and an initial diagnosis of PAN was characteristic of most of our cohort. In contrast, 4 of 9 patients were older than age 10 years at the time of symptom onset. In view of this onset of disease in adolescence and the high frequency of the disease (1 in 8) among the PAN cohort, DADA2 should be considered in the differential diagnosis of patients of all ages with a PAN phenotype. Our data also suggest that DADA2 should be considered in the differential diagnosis of patients outside of the PAN phenotype. The siblings were the youngest patients in our cohort and had the most severe disease, although there were no signs of overt clinical vasculitis (for example, persistent skin rash). Patient 6 had a history of early-onset stroke, while patient 5 had cerebral atrophy without evidence of stroke. Both patients had evidence of a systemic inflammatory response (fever, elevated levels of inflammation markers). Given the disease severity in these patients, DADA2 should be considered in the differential diagnosis of all patients with unexplained early-onset CNS disease (not limited to stroke) with systemic inflammatory features, even in the absence of "vasculitic" rash.

The earlier diagnosis of DADA2 in patient 5 may have been life-saving, and in patient 6, the earlier diagnosis may have enabled earlier treatment with etanercept or hematopoietic stem cell transplantation. Even patients in our cohort with predominantly skin disease required treatment with immune-suppressing medications and GCs—earlier diagnosis of DADA2 in such patients may have prompted alternative, more effective treatments and might have reduced the need for GCs. Several of the patients in our cohort required medication changes due to ongoing disease or flares of disease. Caorsi et al described a similar poor or partial response to conventional immunosuppression in their cohort of DADA2 patients, while patients who received anti-TNF therapy had high rates of remission (17). In our cohort, anti-TNF treatment was used in only 4 patients (patients 3, 5, 6, and 9), in whom disease onset, persisting disease activity, or flare occurred after the DADA2 entity was uncovered (Table 4). In 2 patients (patients 3 and 9), there was an excellent response. Patient 5 died but had only received 1 dose of anti-TNF medication, and patient 6 had an initial response followed by disease relapse. Both patient 5 and patient 6 had severe neutropenia and IgM immunodeficiency, and there is recent evidence that patients with DADA2 who have this phenotype may respond better to hematopoietic stem cell transplantation (18).

As reports of DADA2 cases accumulate, the clinical phenotype continues to evolve and expand. In our cohort, 3 patients were of South Asian descent and 1 was of East Asian descent. Few cohorts have described DADA2 patients of these ethnicities, and it is possible that they are underdiagnosed and underreported. The symptom of blurred vision in 4 patients is interesting. Other patients with PAN in our cohort did not have this reported symptom. The etiology of the blurred vision (either ocular, neurologic, or perhaps thrombotic) remains unclear, as no other ocular diagnoses were reported in any of these patients, no other neurologic abnormalities were identified in 2 of the patients, and none had thromboses at other sites. Additional retrospective elucidation in these patients is not feasible; however, prospective surveillance of this symptom in other patients may clarify its significance.

As the spectrum of DADA2 manifestations unfolds and the age range at the time of disease presentation is clarified, it will likely be increasingly included in the differential diagnosis for a spectrum of unexplained "vasculopathies" and systemic inflammatory diseases with CNS and PNS manifestations beyond the PAN phenotype. Our current inability to correlate genotype to phenotype and the absence of an identifiable genetic abnormality in 1 patient suggest that other factors are involved in the pathogenesis of DADA2, which may include modifying alleles, epigenetic modifications, or environmental exposures. For DADA2 patients with an autoimmune or bone marrow–deficient phenotype, hematopoietic stem cell transplantation may be an effective therapy (18,19). In addition, there is clinical evidence that patients with DADA2 elicit a positive response to biologic therapy, particularly anti-TNF therapy (2), but there is little mechanistic evidence for particular treatment choices. A deeper understanding of all of the factors contributing to the pathogenesis of DADA2 will be crucial to predict its disease course in individuals, inform clinical treat-

ment decisions, and improve the outcomes in patients with DADA2.

AUTHOR CONTRIBUTIONS

All authors were involved in drafting the article or revising it critically for important intellectual content, and all authors approved the final version to be published. Drs. Cabral and Brown had full access to all of the data in the study and takes responsibility for the integrity of the data and the accuracy of the data analysis.

Study conception and design. Gibson, Morishita, Dancey, Drögemöller, Graham, Hancock, Foell, Ross, Cabral, Brown.

Acquisition of data. Gibson, Dancey, Moorehead, Han, Benseler, Luqmani, Yeung, Shenoi, Bohm, Rosenberg, Cabral.

Analysis and interpretation of data. Gibson, Morishita, Dancey, Moorehead, Drögemöller, Ross, Cabral, Brown.

REFERENCES

1. Navon Elkan P, Pierce SB, Segel R, Walsh T, Barash J, Padeh S, et al. Mutant adenosine deaminase 2 in a polyarteritis nodosa vasculopathy. N Engl J Med 2014;370:921–31.
2. Zhou Q, Yang D, Ombrello AK, Zavialov AV, Toro C, Zavialov AV, et al. Early-onset stroke and vasculopathy associated with mutations in ADA2. N Engl J Med 2014;370:911–20.
3. Meyts I, Aksentijevich I. Deficiency of adenosine deaminase 2 (DADA2): updates on the phenotype, genetics, pathogenesis, and treatment. J Clin Immunol 2018;38:569–78.
4. Van Montfrans JM, Hartman EA, Braun KP, Hennekam EA, Hak EA, Nederkoorn PJ, et al. Phenotypic variability in patients with ADA2 deficiency due to identical homozygous R169Q mutations. Rheumatology (Oxford) 2016;55:902–10.
5. Maier SA, Galellis JR, McDermid HE. Phylogenetic analysis reveals a novel protein family closely related to adenosine deaminase. J Mol Evol 2005;61:776–94.
6. Alsultan A, Basher E, Alqanatish J, Mohammed R, Alfadhel M. Deficiency of ADA2 mimicking autoimmune lymphoproliferative syndrome in the absence of livedo reticularis and vasculitis. Pediatr Blood Cancer 2018;65:e26912.
7. Skrabl-Baumgartner A, Plecko B, Schmidt WM, König N, Hershfield M, Gruber-Sedlmayr U, et al. Autoimmune phenotype with type I interferon signature in two brothers with ADA2 deficiency carrying a novel CECR7 mutation. Pediatr Rheumatol Online J 2017;15:67.
8. Uettwiller F, Sarrabay G, Rodero MP, Rice GI, Lagrue E, Marot Y, et al. ADA2 deficiency: case report of a new phenotype and novel mutation in two sisters. RMD Open 2016;2:e000236.
9. Ben-Ami T, Revel-Vilk S, Brooks R, Shaag A, Hershfield MS, Kelly SJ, et al. Extending the clinical phenotype of adenosine deaminase 2 deficiency. J Pediatr 2016;177:316–20.
10. Bras J, Guerreiro R, Santo GC. Mutant ADA2 in vasculopathies. N Engl J Med 2014;371:478–80.
11. Schepp J, Bulashevska A, Mannhardt-Laakmann W, Cao H, Yang F, Seidl M, et al. Deficiency of adenosine deaminase 2 causes antibody deficiency. J Clin Immunol 2016;36:179–86.
12. Caorsi R, Penco F, Schena F, Gattorno M. Monogenic polyarteritis: the lesson of ADA2 deficiency [review]. Pediatr Rheumatol Online J 2016;14:51.
13. Cabral DA, Canter DL, Muscal E, Nanda K, Wahezi DM, Spalding SJ, et al. Comparing presenting clinical features in 48 children with microscopic polyangiitis to 183 children who have granulomatosis with polyangiitis (Wegener's): an ARChiVe cohort study. Arthritis Rheumatol 2016;68:2514–26.
14. Cabral DA, Uribe AG, Benseler S, O'Neil KM, Hashkes PJ, Higgins G, et al. Classification, presentation, and initial treatment of Wegener's granulomatosis in childhood. Arthritis Rheum 2009;60:3413–24.
15. Harris PA, Taylor R, Thielke R, Payne J, Gonzalez N, Conde JG. Research Electronic Data Capture (REDCap): a metadata-driven methodology and workflow process for providing translational research informatics support. J Biomed Inform 2009;42:377–81.
16. Dolezalova P, Price-Kuehne FE, Özen S, Benseler SM, Cabral DA, Anton J, et al. Disease activity assessment in childhood vasculitis: development and preliminary validation of the Paediatric Vasculitis Activity Score (PVAS). Ann Rheum Dis 2013;72:1628–33.
17. Caorsi R, Penco F, Grossi A, Insalaco A, Omenetti A, Alessio M, et al. ADA2 deficiency (DADA2) as an unrecognised cause of early onset polyarteritis nodosa and stroke: a multicentre national study. Ann Rheum Dis 2017;76:1648–56.
18. Hashem H, Kumar AR, Müller I, Babor F, Bredius R, Dalal J, et al. Hematopoeitic stem cell transplant rescues the hematological, immunological, and vascular phenotype in DADA2. Blood 2017;130:2682–8.
19. Van Eyck L Jr, Hershfield MS, Pombal D, Kelly SJ, Ganson NJ, Moens L, et al. Hematopoietic stem cell transplantation rescues the immunologic phenotype and prevents vasculopathy in patients with adenosine deaminase 2 deficiency. J Allergy Clin Immunol 2015;135:283–7.

Arthritis & Rheumatology
Vol. 71, No. 10, October 2019, pp 1756–1765
DOI 10.1002/art.40939

American College of Rheumatology
Empowering Rheumatology Professionals

Regulation of Fatty Acid Oxidation by Twist 1 in the Metabolic Adaptation of T Helper Lymphocytes to Chronic Inflammation

Kristyna Hradilkova,[1] Patrick Maschmeyer,[1] Kerstin Westendorf,[1] Heidi Schliemann,[1] Olena Husak,[1] Anne Sae Lim von Stuckrad,[2] Tilmann Kallinich,[2] Kirsten Minden,[3] Pawel Durek,[1] Joachim R. Grün,[1] Hyun-Dong Chang,[1] and Andreas Radbruch[1]

Objective. Inflamed tissue is characterized by low availability of oxygen and nutrients. Yet CD4+ T helper lymphocytes persist over time in such tissue and probably contribute to the chronicity of inflammation. This study was undertaken to analyze the metabolic adaptation of these cells to the inflamed environment.

Methods. Synovial and blood CD4+ T cells isolated ex vivo from patients with juvenile idiopathic arthritis (JIA) and murine CD4+ T cells were either stimulated once or stimulated repeatedly. Their dependency on particular metabolic pathways for survival was then analyzed using pharmacologic inhibitors. The role of the transcription factor Twist 1 was investigated by determining lactate production and oxygen consumption in *Twist1*-sufficient and *Twist1*-deficient murine T cells. The dependency of these murine cells on particular metabolic pathways was analyzed using pharmacologic inhibitors.

Results. Programmed death 1 (PD-1)+ T helper cells in synovial fluid samples from patients with JIA survived via fatty acid oxidation (mean ± SEM survival of 3.4 ± 2.85% in the presence of etomoxir versus 60 ± 7.08% in the absence of etomoxir on day 4 of culture) ($P < 0.0002$; n = 6) and expressed the E-box–binding transcription factor *TWIST1* (2–14-fold increased expression) ($P = 0.0156$ versus PD-1– T helper cells; n = 6). Repeatedly restimulated murine T helper cells, which expressed *Twist1* as well, needed *Twist1* to survive via fatty acid oxidation. In addition, *Twist1* protected the cells against reactive oxygen species.

Conclusion. Our findings indicate that *TWIST1* is a master regulator of metabolic adaptation of T helper cells to chronic inflammation and a target for their selective therapeutic elimination.

INTRODUCTION

CD4+ T lymphocytes are considered a driving force and relevant therapeutic target in chronic inflammatory rheumatic diseases. In the inflamed synovial tissue of patients, CD4+ T lymphocytes persist despite low levels of oxygen and nutrients, and they are refractory to conventional immunosuppressive therapies (1,2). With respect to nutrients qualifying as a metabolic energy source, there is little glucose (3) and glutamine (4) in inflamed tissue, while fatty acids are readily available (5,6). Herein, we describe the metabolic adaptation of CD4+ T lymphocytes to this inflamed environment.

Among the CD4+ T lymphocytes present in inflamed tissues, CD4+ T cells expressing programmed death 1 (PD-1) protein (7) are a subpopulation of potential relevance for pathogenesis (8). In this study, we show that PD-1+ Th1 cells isolated from the synovial

Supported by the European Research Council Advanced Grant IMMEMO (project ERC-2010-AdG.20100317; grant 268987 to Dr. Radbruch), Deutsche Forschungsgemeinschaft (grant SFB 650 to Drs. Chang and Radbruch), the Innovative Medicines Initiative 2 Joint Undertaking under grant agreement no. 777357, the Rheumastiftung (to Dr. Chang), and the Leibniz ScienceCampus Chronic Inflammation. Dr. Hradilkova's work was supported by the BSRT graduate school. Dr. Maschmeyer's work was supported by the state of Berlin and the European Regional Development Fund (ERDF 2014-2020 and EFRE 1.8/11 to Deutsches Rheuma-Forschungszentrum) and by EUTRAIN, a Seventh Framework Programme Marie Curie Initial Training Network for Early Stage Researchers funded by the European Union (FP7-PEOPLE-2011-ITN-289903).

[1]Kristyna Hradilkova, PhD, Patrick Maschmeyer, PhD, Kerstin Westendorf, PhD, Heidi Schliemann, PhD, Olena Husak, MSc, Pawel Durek, PhD, Joachim R. Grün, PhD, Hyun-Dong Chang, PhD, Andreas Radbruch, PhD: Deutsches Rheuma-Forschungszentrum Berlin, Berlin, Germany; [2]Anne Sae Lim von Stuckrad, MD, Tilmann Kallinich, MD: Charité–Universitätsmedizin Berlin, Berlin, Germany; [3]Kirsten Minden, MD: Deutsches Rheuma-Forschungszentrum Berlin and Charité–Universitätsmedizin Berlin, Berlin, Germany.

Drs. Chang and Radbruch contributed equally to this work.

No potential conflicts of interest relevant to this article were reported.

Address correspondence to Andreas Radbruch, PhD, Deutsches Rheuma-Forschungszentrum Berlin (DRFZ), a Leibniz Institute, Charitéplatz 1, 10117 Berlin, Germany. E-mail: radbruch@drfz.de.

Submitted for publication November 1, 2018; accepted in revised form May 21, 2019.

fluid of patients with juvenile idiopathic arthritis (JIA) are dependent on fatty acid oxidation for survival. Their survival is blocked by the carnitine palmitoyltransferase 1 inhibitor etomoxir (9), which inhibits the transport of fatty acids from the cytoplasm into the mitochondria. We show that CD4+ PD-1+ T cells in inflamed synovia express the E-box–binding transcription factor *TWIST1*, a hallmark of T lymphocytes persisting in chronically inflamed human tissue (2).

Twist1 expression is selective for repeatedly activated murine Th1 cells, as compared to other types of T helper cells and Th1 cells activated only once. *Twist1* expression by murine Th1 cells has been shown to dampen immunopathology in an autoregulatory, cell-intrinsic manner (2). At the same time, *Twist1* supports the persistence of repeatedly activated Th1 cells by inducing expression of microRNA-148a (miR-148a), which in turn regulates expression of the proapoptotic protein Bim (10). We previously demonstrated that selective depletion of *Twist1*-expressing Th1 cells through blockade of miR-148a, a *Twist1*-induced miRNA, in vivo with antagomirs ameliorates inflammation, identifying *Twist1*-expressing T helper cells as those driving inflammation (11). Conditional inactivation of *Twist1* in repeatedly activated Th1 lymphocytes relieves their dependency on fatty acid oxidation and allows them to survive alternatively on glycolysis, demonstrating that *Twist1* forces T helper cells into fatty acid oxidation, and thus regulates their proinflammatory activity (12,13). *Twist1* thus qualifies as an essential regulator of the metabolism of T helper lymphocytes in chronic inflammation, inhibiting glycolysis, and thus limiting immunopathology, while at the same time stimulating fatty acid oxidation, allowing the cells to persist in and contribute to the chronification of inflammation.

MATERIALS AND METHODS

Mice. C57BL/6J mice were purchased from Charles River. OT-II × Twist1$^{fl/fl}$ × CD4Cre$^{+/-}$ and OT-II × Twist1$^{wt/wt}$ × CD4Cre$^{+/-}$, Twist1$^{fl/fl}$ × CD4Cre$^{+/-}$, and Twist1$^{wt/wt}$ × CD4Cre$^{+/-}$ mice were bred in the Deutsches Rheuma-Forschungszentrum animal facility under specific pathogen–free conditions in individually ventilated cages. Mice were handled in accordance with good animal practice as defined by the German animal welfare bodies, and killed by cervical dislocation. All experiments were approved by the State Office for Health and Social Affairs (Berlin, Germany).

Human patient samples. Peripheral blood and synovial fluid samples were collected at the Department of Pediatrics, Pediatric Rheumatology Section of Charité–Universitätsmedizin Berlin as approved by the ethics committee of Charité–Universitätsmedizin Berlin (approval no. EA2/069/15).

Human T cell phenotyping and cultivation. Mononuclear cells from peripheral blood were isolated by Ficoll density-gradient centrifugation. Synovial fluid cells were depleted of CD14+ granulocytes by magnetic cell sorting using CD14 microbeads (Miltenyi Biotec). CD4+ T helper lymphocytes were isolated using CD4 microbeads (Miltenyi Biotec). For analysis of cytokine expression, synovial CD4+ T cells were stimulated with phorbol 12-myristate 13-acetate (PMA) (10 ng/ml) and ionomycin (1 μg/ml) (both from Sigma-Aldrich) for a total of 5–6 hours in medium. After 1 hour, 5 μg/ml brefeldin A (BioLegend) was added to block the secretion of cytokines. Cells were fixed with Cytofix/Cytoperm (BD Biosciences) for 20 minutes at 4°C and stained intracellularly with anti–interferon-γ (anti-IFNγ) (4SB3; BioLegend), anti–interleukin-17a (anti–IL-17a) (BL168; BioLegend), anti–tumor necrosis factor (anti-TNF) (cA2; Miltenyi Biotec), anti–IL-2 (MQ1-17H12; BioLegend), anti–IL-10 (JES3-9D7; Miltenyi Biotec), anti–IL-4 (8D48; BioLegend), and anti–IL-21 (7H20-I19-M3; BioLegend) according to published guidelines (14). For intracellular T-bet staining (4B10; BioLegend), cells were additionally permeabilized with 0.01% Triton X-100 for 10 minutes on ice. PD-1+ and PD-1– CD3+CD4+CD14–CD45RO+ T lymphocytes were sorted by fluorescence-activated cell sorting (FACS) using a FACSAria cell sorter (BD Biosciences) and plated in RPMI medium containing human AB serum (Sigma), 100 units/ml penicillin, and 100 μg/ml streptomycin (Life Technologies). Etomoxir was added to the final concentrations as indicated. The numbers of viable CD4+ T cells were monitored over time by flow cytometry, using DAPI to exclude dead cells.

In vitro cultivation and differentiation of murine T helper cells. Murine CD4+CD62L+ (naive) T helper cells were isolated as previously described (15) and cultured at a concentration of 2.5 × 10^6 cells/5 ml in 6-well plates in RPMI medium supplemented with 10% fetal calf serum (Merck), 300 μg/ml glutamine (Invitrogen), 100 units/ml penicillin, 100 μg/ml streptomycin (Life Technologies), and 50 μ*M* β-mercaptoethanol (Sigma-Aldrich) at 37°C in 5% CO_2 and 4.2% oxygen. The T helper cells were stimulated polyclonally with plate-bound anti-CD3 antibody (145-2C11; 3 μg/ml) and soluble anti-CD28 antibody (37.51; 1.5 μg/ml). For Th1 polarization, 5 ng/ml recombinant IL-12, 10 ng/ml recombinant IL-2, and 10 μg/ml anti–IL-4 antibody (11B11) was added. To induce Th17 polarization, 10 μg/ml anti-IFNγ (AN18.17.24), 10 μg/ml anti–IL-4 (11B11), 20 ng/ml recombinant IL-6, 20 ng/ml recombinant IL-23, and 1 ng/ml recombinant transforming growth factor β (all from R&D Systems) were added. After 48 hours of stimulation, the cells were removed from the antibody-coated culture dishes and cultured for an additional 3–4 days. T cell receptor–transgenic OT-II lymphocytes were activated with 1 μg/ml of ovalbumin 327–339 peptide in the presence of irradiated (30 Gy) CD90-depleted splenocytes from C57BL/6 mice. For repeated activation, viable T helper cells were isolated using Ficoll density-gradient centrifugation and stimulated again under the original conditions.

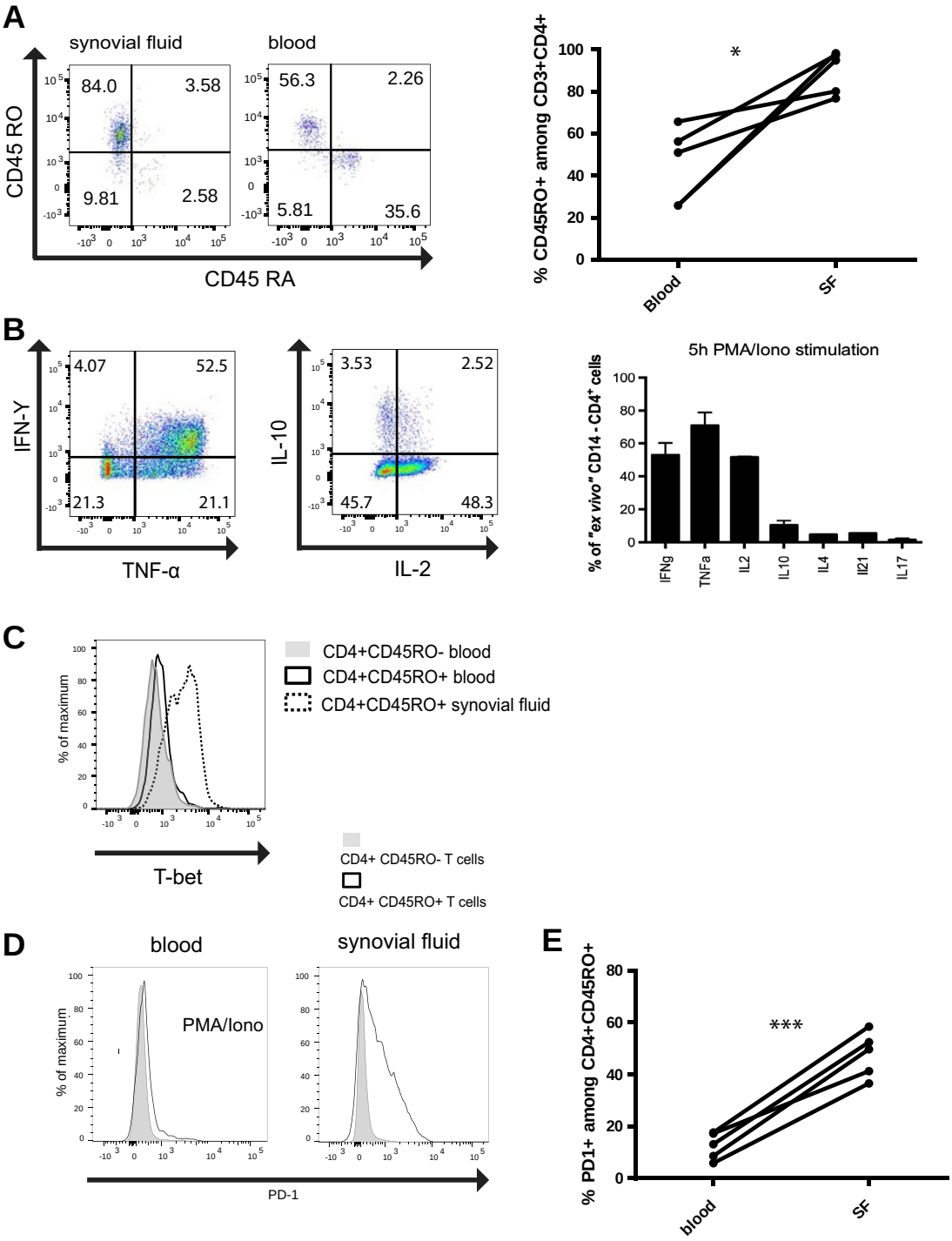

Figure 1. Synovial fluid (SF) T cells from patients with juvenile idiopathic arthritis (JIA) have a Th1 phenotype and express programmed death 1 (PD-1). **A**, Left, Flow cytometric analysis indicating the frequencies of CD45RA+ and CD45RO+ cells among CD3+CD4+ T cells in synovial fluid and blood from patients with JIA. Results are representative of 5 experiments. Right, Percentage of CD3+CD4+ cells expressing CD45RO in blood and synovial fluid from patients with JIA (n = 5). * = $P < 0.05$ by 2-tailed *t*-test. **B**, Left, Expression of interferon-γ (IFNγ), tumor necrosis factor (TNF), interleukin-10 (IL-10), and IL-2 in ex vivo-isolated synovial T cells after stimulation with phorbol 12-myristate 13-acetate (PMA) and ionomycin (iono), as analyzed by intracellular cytokine staining. Results are representative of 5 experiments. Right, Frequencies of synovial fluid CD4+ T cells expressing IFNγ, TNF, IL-2, IL-10, IL-4, IL-21, and IL-17A after 5 hours of restimulation with PMA and ionomycin. Bars show the mean ± SEM (n = 5). **C**, T-bet expression in CD4+CD45RO– and CD4+CD45RO+ T cells in blood and CD4+CD45RO+ T cells in synovial fluid from a patient with JIA. Results are representative of 3 experiments. **D**, PD-1 expression in CD4+CD45RO– and CD4+CD45RO+ T cells isolated from blood stimulated with PMA and ionomycin and synovial fluid from a patient with JIA. Results are representative of 5 experiments. **E**, Percentage of CD4+CD45RO+ cells expressing PD-1 in blood and synovial fluid from patients with JIA (n = 5). *** = $P < 0.001$ by 2-tailed *t*-test. Color figure can be viewed in the online issue, which is available at http://onlinelibrary.wiley.com/doi/10.1002/art.40939/abstract.

Quantitative RNA expression analysis. Total RNA was isolated using an RNeasy kit (Qiagen) or a Direct-zol RNA kit (Zymo Research) according to the manufacturer's instructions. RNA concentration and quality were determined by NanoDrop spectrometry. RNA (200 ng to 1 μg) was reverse transcribed using a TaqMan Reverse Transcription kit (ThermoFisher Scientific) according to the manufacturer's recommendations. Real-time quantitative polymerase chain reaction was used to quantify the messenger RNA of interest with the following primer sets (TIB Molbiol Berlin): for murine hypoxanthine guanine phosphoribosyltransferase (Hprt), forward 5′-TCCTCCTCAGACCGCTTTT-3′ and reverse 5′-CATAA CCTGGTTCATCATCGC-3′; for human HPRT, forward 5′-ACCC TTTCCAAATCCTCAGC-3′ and reverse 5′-GTTATGGCGACC CGCAG-3′; for murine *Twist1*, forward 5′-CGCACGCAGTCGC TGAACG-3′ and reverse 5′-GACGCGGACATGGACCAGG-3′; for human *TWIST1*, forward 5′-GGCACCCAGTCGCTGAACG-3′ and reverse 5′-GACGCGGACATGGACCAGG-3′; for murine *Pdcd1*, forward 5′-CGTCCCTCAGTCAAGAGGAG-3′ and reverse 5′-GTCCCTAGAAGTGCCCAACA-3′. Prior to *Twist1* analysis, cultured cells were restimulated with PMA (10 ng/ml) and ionomycin (1 μg/ml) for 5 hours.

Glucose uptake assay. Murine naive CD4+ T helper cells were stimulated with 3 μg/ml of plate-bound anti-CD3 and 1.5 μg/ml of soluble anti-CD28 antibodies at 3×10^5 cells per well under Th1-inducing conditions for 5 hours. Medium was then aspirated, and 100 μl of glucose-free medium with 1.5 μg/ml of soluble anti-CD28 antibody was added to the cells. Following incubation for 60 minutes, 100 μl of glucose-free RPMI with 300 μ*M* 2-([7-nitro-2,1,3-benzoxadiazol-4-yl]amino)-2 deoxyglucose (2-NBDG) was added to the well, to reach a final concentration of 150 μ*M* 2-NBDG. Cultures with no 2-NBDG added and cultures with 150 μ*M* 2-NBDG and 30 μ*M* cytochalasin B were used as controls. Cells were incubated for 30 minutes at 37°C. After incubation, cells were washed twice in cold phosphate buffered saline (PBS) and maintained at 4°C. Uptake of 2-NBDG was determined by flow cytometry using a MACSQuant analyzer. Dead cells were excluded by propidium iodide staining.

Determination of lactate production and oxygen consumption. Glycolysis, as determined by extracellular acidification, and oxidative phosphorylation, as determined by oxygen consumption, were measured using a Seahorse XP analyzer (Agilent). Prior to the assay, T lymphocytes were starved in glucose-free RPMI assay medium and equilibrated in 5% CO_2 at 37°C, under normoxic conditions.

T cell survival assay. CD4+ T helper cells were seeded in a 96-well plate coated with 3 μg/ml anti-CD3 antibodies and 1.5 μg/ml soluble anti-CD28 antibodies under Th1- or Th17-polarizing conditions. The inhibitors 2-deoxy-D-glucose (2-DG; 2 m*M*), 6-diazo-5-oxo-L-norleucine (50 μ*M*), oligomycin (2 μ*M*), or etomoxir (150 μ*M*) were added. Dead cells were excluded by staining with 100 ng/ml propidium iodide or 100 ng/ml DAPI. Numbers of viable cells were determined by flow cytometry using a MACSQuant analyzer.

Lipid peroxidation. BODIPY 581/591 C11 was added to CD4+ T lymphocytes in a 96-well plate at a final concentration of 3 μ*M* in RPMI without serum and 2-mercaptoethanol. Cells were incubated for 40 minutes at 37°C and then washed with PBS/bovine serum albumin. Viable cells were quantified using a MACSQuant analyzer, and dead cells were excluded by DAPI staining.

RESULTS

Survival of PD-1+CD4+ T helper lymphocytes in inflamed synovia via fatty acid oxidation. CD4+ T helper lymphocytes were isolated from the synovial fluid of patients with JIA. More than 70% of the CD3+CD4+ cells were CD45RO+CD45RA– (Figure 1A). Upon stimulation with PMA and ionomycin ex vivo, ~50% of them expressed IFNγ, 70% expressed TNF, 50% expressed IL-2, and 10% expressed IL-10. IL-4, IL-17, and IL-21 were each expressed by <10% of the cells (Figure 1B). Consistent with the cytokine expression pattern, almost all JIA synovial T helper cells expressed the T-box–binding transcription factor T-bet, identifying them as bona fide Th1 cells (Figure 1C). A significantly higher proportion of synovial T helper cells than peripheral blood T helper cells expressed PD-1 (Figures 1D and E).

PD-1+ and PD-1– synovial T helper cells were separated by FACS (Figure 2A and Supplementary Figure 1, available on the *Arthritis & Rheumatology* web site at http://onlinelibrary.wiley.com/doi/10.1002/art.40939/abstract), and their dependency on fatty acid oxidation was analyzed. CD4+CD45RO+ T cells isolated from the blood of healthy donors did not survive when cultured in vitro under hypoxic conditions (4.2% O_2), with >90% of them dying within 2 days. Of the PD-1– T helper cells isolated from synovial fluid, a mean ± SEM of 24.6 ± 2.29% survived until day 2 of culture and 19 ± 1.31% survived until day 4. Their survival was not affected by the addition of etomoxir, an inhibitor of fatty acid oxidation. In the presence of etomoxir, 20% of the cells survived until day 2 and 15.6 ± 4.5% survived until day 4 (Figure 2B). Of the PD-1+ synovial T helper cells, 39.85 ± 7.35% survived until day 2, and these surviving cells expanded again to 60 ± 7.08% of the original number on day 4. Survival and expansion of these cells was entirely dependent on fatty acid oxidation, since they could be blocked with etomoxir, reducing cell numbers to a mean ± SEM of 3.4 ± 2.85% on day 4 (Figure 2B).

We have previously shown that the E-box–binding transcription factor *TWIST1* is a hallmark of T helper lymphocytes isolated from the inflamed joints of patients with rheumatic diseases (2). In this study, we found that PD-1+ synovial T cells isolated from the inflamed joints of patients with JIA expressed significantly higher

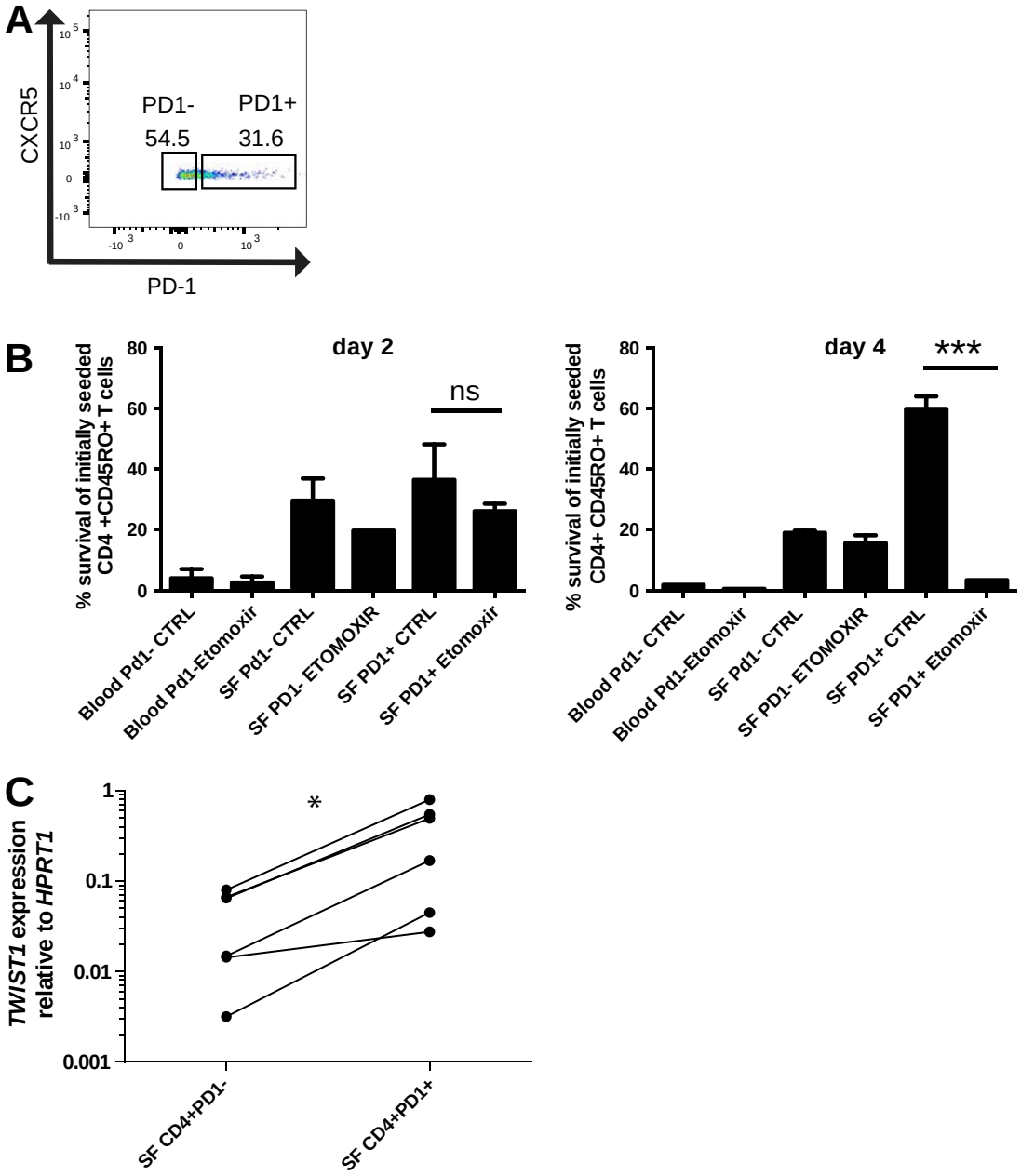

Figure 2. Survival of synovial CD4+CD45RO+PD-1+ T cells in patients with JIA is dependent on fatty acid oxidation. **A**, Representative gating strategy for sorting PD-1+ and PD-1– CD4+CD45RO+ T cells from synovial fluid and blood. **B**, Frequency of viable cells relative to the number of initially seeded cells determined on day 2 and day 4 after stimulation with anti-CD3 and anti-CD28 antibodies in the presence or absence (control) of 200 μ*M* etomoxir. Bars show the mean ± SEM. Data were pooled from 2 experiments (n = 3 blood and synovial fluid samples per experiment). *** = $P < 0.0002$ by unpaired 2-tailed *t*-test. NS = not significant. **C**, *TWIST1* mRNA expression relative to *HPRT* in PD-1+ and PD-1– CD4+CD45RO+ T cells directly isolated from synovial fluid from patients with JIA (n = 6). * = $P = 0.016$ by Wilcoxon's 1-tailed paired rank test. See Figure 1 for other definitions. Color figure can be viewed in the online issue, which is available at http://onlinelibrary.wiley.com/doi/10.1002/art.40939/abstract.

levels of *TWIST1* than PD-1– T helper cells isolated from the same synovia (Figure 2C).

Upon repeated activation, murine Th1 cells shift from glycolysis to fatty acid oxidation. To investigate the role of *Twist1* in the regulation of the metabolism of T helper lymphocytes, we used a murine model of repeatedly activated Th1 lymphocytes, which was previously used as a model to study transcriptional adaptations of chronic activation and in which we had previously demonstrated up-regulated *Twist1* expression (2). Naive CD4+CD62L+ T cells were stimulated with anti-CD3 and anti-CD28 antibodies 4 times at 6-day inter-

vals. We then compared the capacity of these cells to take up glucose and perform glycolysis, the latter reflected by the production of lactate, as outlined in Figure 3A. Uptake of the fluorescent glucose analog 2-NBDG was monitored by flow cytometry. Repeatedly activated mouse Th1 cells took up 2.3-fold less 2-NBDG than mouse Th1 cells that were activated one time (Figure 3B).

Repeatedly activated murine Th1 cells were also less efficient in glycolysis, compared to Th1 cells activated once. Murine Th1 cells activated once produced 1.4-fold more lac-

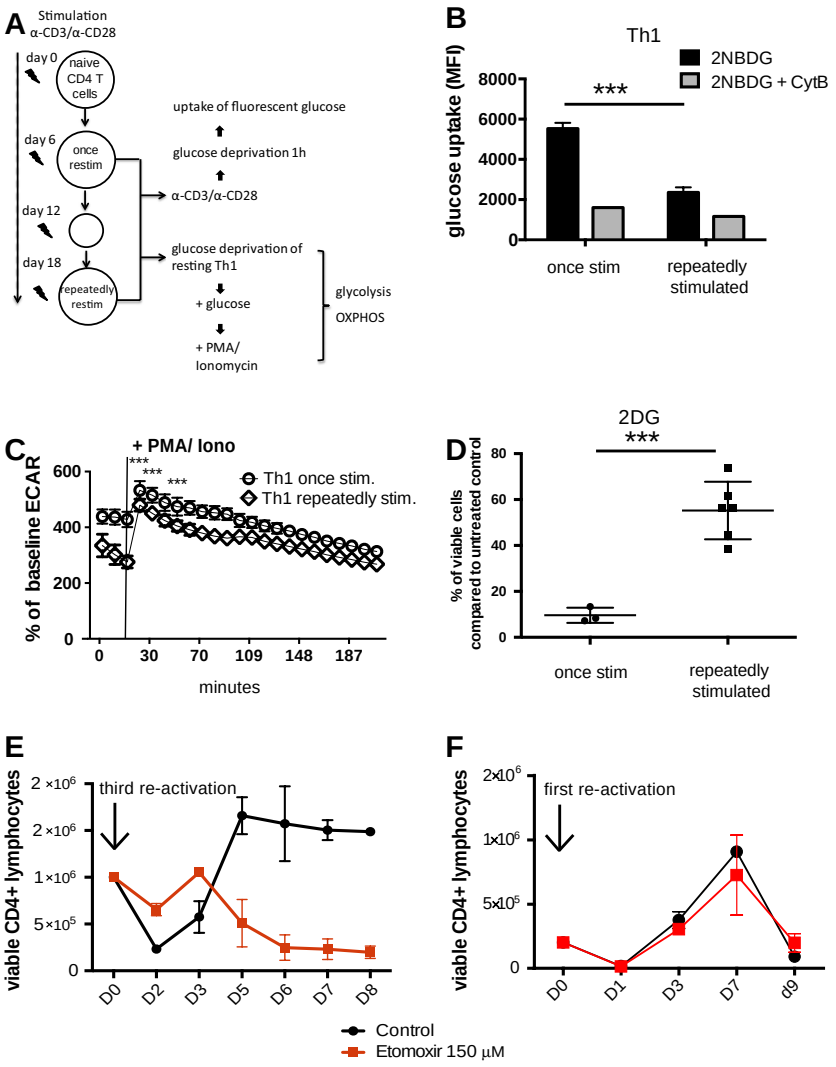

Figure 3. Repeatedly stimulated (stim) murine Th1 cells switch their metabolism from glycolysis to fatty acid oxidation. **A**, Experimental design. Naive CD4+CD62L+ T cells isolated from C57BL/6 mice were stimulated once or stimulated 2 additional times at 6-day intervals with anti-CD3/anti-CD28 antibodies under Th1-differentiating conditions. Cells were analyzed for energy metabolism. OXPHOS = oxidative phosphorylation. **B**, Glucose uptake in murine Th1 cells stimulated once and repeatedly stimulated murine Th1 cells, measured by flow cytometry using the fluorescent glucose analog 2-([7-nitro-2,1,3-benzoxadiazol-4-yl]amino)-2 deoxyglucose (2-NBDG). Th1 cells were restimulated for 6 hours with anti-CD3 and anti-CD28 antibodies prior to analysis. Cytochalasin B (CytB) was used to determine background fluorescence. Bars show the mean ± SEM. Results are representative of 3 independent experiments. *** = $P < 0.0006$ by Mann-Whitney 2-tailed test. **C**, Glycolytic activity, measured by extracellular acidification rate (ECAR), in murine Th1 cells stimulated once and repeatedly stimulated murine Th1 cells before and after restimulation with phorbol 12-myristate 13-acetate (PMA) and ionomycin (iono). Values are the mean ± SEM (n = 4 samples per group). *** = $P < 0.0001$ at 14 minutes, $P = 0.0027$ at 30 minutes, and $P = 0.0027$ at 50 minutes after glucose addition, by 2-tailed *t*-test. **D**, Frequency of viable murine CD4+ T cells stimulated once and murine CD4+ T cells stimulated repeatedly after restimulation with anti-CD3/anti-CD28 antibodies in the presence of the glycolysis inhibitor 2-deoxy-D-glucose (2-DG; 2 m*M*) for 72 hours, relative to cells cultivated without inhibitor (untreated control). Symbols represent individual samples; horizontal lines and error bars show the mean ± SEM. *** = $P = 0.0005$ by *t*-test. **E** and **F**, Absolute number of repeatedly stimulated murine Th1 cells (**E**) and murine Th1 cells stimulated once (**F**) and restimulated with anti-CD3/anti-CD28 antibodies in the presence or absence of 150 µ*M* etomoxir. Viability and cell count were determined by propidium iodide exclusion using flow cytometry. Values are the mean ± SEM. Results are representative of 3 experiments. MFI = mean fluorescence intensity.

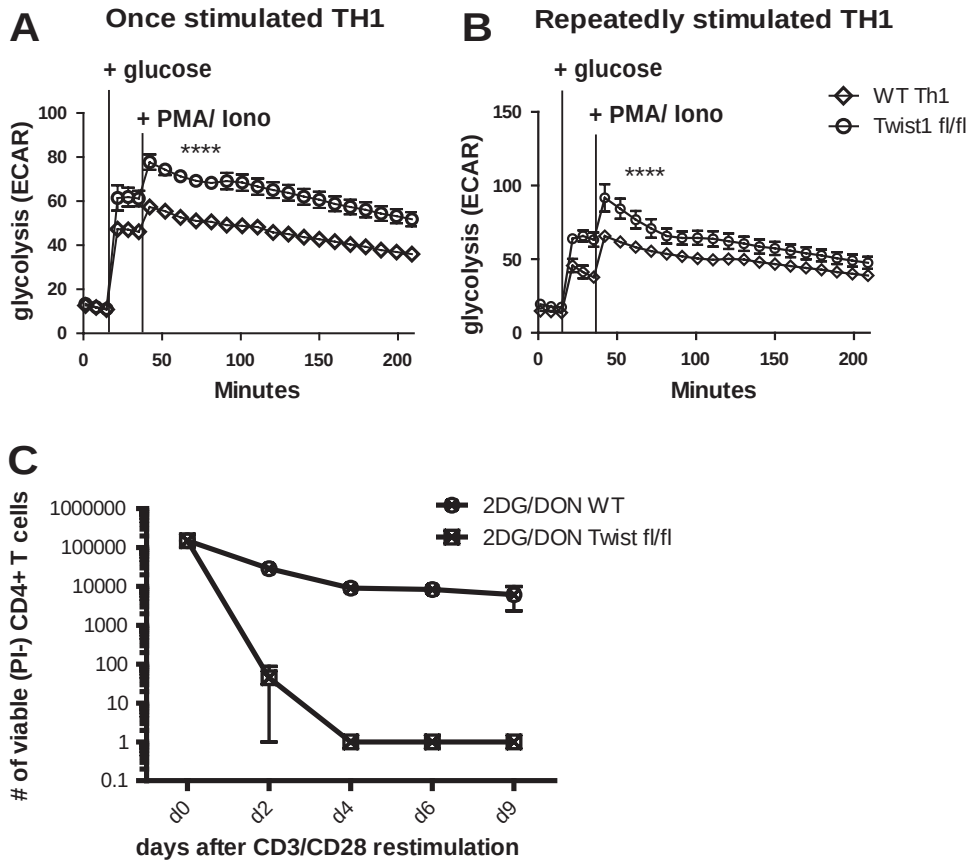

Figure 4. Twist 1 inhibits glycolysis in murine Th1 cells stimulated once and murine Th1 cells stimulated repeatedly. **A** and **B**, Glycolytic activity, measured by extracellular acidification rate (ECAR) of *Twist1*-deficient (Twist1$^{fl/fl}$) and *Twist1*-sufficient (wild-type [WT]) OT-II TCR-transgenic mouse Th1 cells stimulated once (**A**) or stimulated repeatedly (**B**) with ovalbumin peptide before and after the addition of glucose and restimulation with 12-myristate 13-acetate (PMA) and ionomycin (iono). **** = $P < 0.0001$ at all time points following glucose addition in **A** and at all time points from glucose addition to 120 minutes in **B**, by paired *t*-test. **C**, Absolute number of viable repeatedly stimulated *Twist1*-deficient and *Twist1*-sufficient mouse Th1 cells treated with inhibitors of glycolysis (2-deoxy-D-glucose [2-DG]) and glutaminolysis (6-diazo-5-oxo-L-norleucine [DON]). Viable cells were determined every 2 days by propidium iodide (PI) exclusion using flow cytometry. Values are the mean ± SEM. Results are representative of 2 experiments.

tate than repeatedly activated murine Th1 cells in the presence of glucose, before and after stimulation with PMA and ionomycin (Figure 3C). Lactate production remained significantly lower in repeatedly activated murine Th1 cells thereafter. Of the Th1 cells that had been activated once, inhibition of glycolysis with 2-DG killed 85% within 72 hours after activation, suggesting that such Th1 cells were dependent on glycolysis. In contrast, 50% of the repeatedly stimulated murine Th1 cells survived when glycolysis was inhibited by 2-DG (Figure 3D), demonstrating that repeatedly stimulated T helper cells have alternative metabolic options, i.e., fatty acid oxidation. Blocking fatty acid oxidation with etomoxir for up to 8 days after a third reactivation showed that repeatedly stimulated murine Th1 cells use and are dependent on fatty acid oxidation, in particular in the late phase of expansion, between days 3 and 5 (Figure 3E). This was not the case for murine Th1 cells during the first week after the first reactivation (Figure 3F), which survived and proliferated even in the presence of etomoxir. The metabolism of repeatedly restimulated murine Th1 cells thus corresponds to that of PD-1^{high} human T helper cells isolated from inflamed synovia, in that they are dependent on fatty acid oxidation.

Inhibition of glycolysis of Th1 lymphocytes by *Twist1*. To analyze the role of *Twist1* in regulating the metabolism of T helper cells functionally, we used mice with a conditional, cell type–specific knockout of *Twist1* (CD4Cre × *Twist1*$^{fl/fl}$) (10) (Supplementary Figure 2, available on the *Arthritis & Rheumatology* web site at http://onlinelibrary.wiley.com/doi/10.1002/art.40939/abstract). Both the *Twist1*-deficient mouse Th1 cells that had been stimulated once and those that had been stimulated repeatedly showed an increased rate of glycolysis, as reflected by an increased production of lactate, when compared to their wild-type counterparts (Figures 4A and B), indicating that *Twist1* inhibits glycolysis. *Twist1* selectively regulated the glycolysis of Th1, but not of repeatedly stimulated Th17 cells (Supplementary Figure 3,

available on the *Arthritis & Rheumatology* web site at http://onlinelibrary.wiley.com/doi/10.1002/art.40939/abstract).

Requirement of *Twist1* for the survival of Th1 lymphocytes via fatty acid oxidation. *Twist1* is indispensable for the survival of repeatedly stimulated Th1 cells via fatty acid oxidation. When glycolysis and glutaminolysis were blocked by 2-DG and 6-diazo-5-oxo-L-norleucine, respectively, *Twist1*-deficient mouse T helper cells did not survive (Figure 4C). In this situation, when fatty acid oxidation is the only metabolic pathway available, the competence to survive on this pathway depends on *Twist1*.

***Twist1* protects Th1 cells against reactive oxygen species (ROS).** Consistent with fatty acid oxidation being the major energy source for repeatedly stimulated murine Th1 cells, these cells show a higher degree of oxidative phosphorylation than murine Th1 cells stimulated once, both in the resting phase and after reactivation ex vivo (Figure 5A). Oxidative phosphorylation is associated with the generation of ROS. ROS promote peroxidation of lipids in cell membranes, an effect that has been suggested to be involved in the pathogenesis of rheumatoid arthritis (16,17). In T helper lymphocytes, lipid peroxides of the membrane, as detected by BODIPY C11 staining, were more abundant in T helper cells that had been stimulated 3 times, 8 days after reactivation, compared to T helper cells that had been stimulated once (Figure 5B). Compared to *Twist1*-deficient mouse Th1 cells, *Twist1*-sufficient (wild-type) mouse Th1 cells, both those stimulated once and those stimulated repeatedly, showed significantly reduced lipid peroxidation ($P = 0.002$ for cells stimulated once and $P = 0.0323$ for cells stimulated repeatedly) (Figure 5B). These data suggest that in addition to promoting oxidative phosphorylation through fatty acid oxidation, *Twist1* protects murine Th1 cells against harmful lipid peroxides, presumably by enhancing lipid peroxide scavenging.

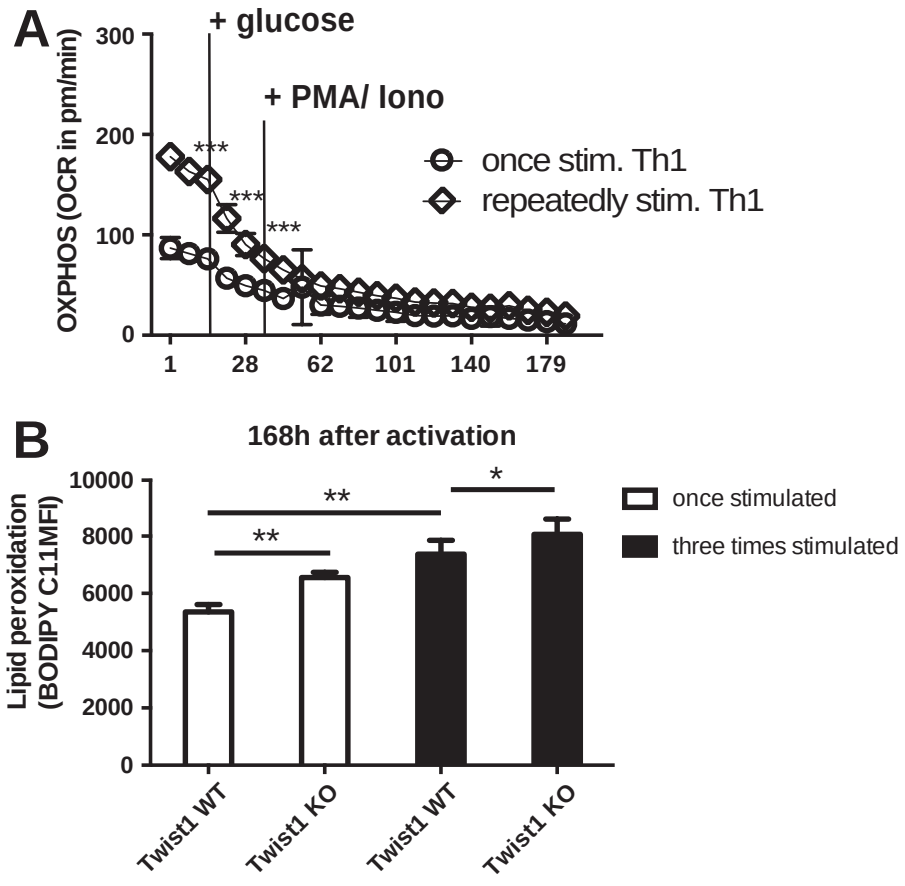

Figure 5. Repeatedly stimulated Th1 cells have increased oxidative phosphorylation. **A**, Oxidative phosphorylation (OXPHOS), measured by oxygen consumption rate (OCR) in Th1 cells stimulated once and Th1 cells stimulated repeatedly, before and after addition of glucose and restimulation with 12-myristate 13-acetate (PMA) and ionomycin (iono). Values are the mean ± SEM. *** = $P < 0.0001$ at 15 minutes; $P = 0.0009$ at 28 minutes; and $P = 0.64$ at 52 minutes, by paired *t*-test. Results are representative of 3 independent experiments. **B**, Levels of lipid peroxides in wild-type (WT) and *Twist1*-deficient (knockout [KO]) mouse Th1 cells stimulated once or stimulated repeatedly. Levels were determined by BODIPY 581/591 C11 (2 μ*M*) staining 7 days after the last reactivation with anti-CD3/anti-CD28 antibodies. Bars show the mean ± SEM. * = $P = 0.0323$; ** = $P = 0.002$, by paired 2-tailed *t*-test. MFI = mean fluorescence intensity.

DISCUSSION

Acute, protective immune reactions are characterized by the apparent elimination of the antigen triggering them. The lymphocytes involved are either eliminated as well, or they develop into memory lymphocytes, resting in terms of activation and proliferation (18–20). Persistent antigens, whether they be pathogens, tumor antigens, or autoantigens, are a challenge to the immune system. Lymphocytes involved in chronic immune responses have to adapt to chronic inflammation and in doing so may become refractory to physiologic and conventional immunosuppression, resulting in chronic inflammatory diseases. CD4+ T helper lymphocytes in chronic inflammation express the E-box–binding transcription factor *TWIST1*, which limits their ability to induce immunopathology (2) and promotes their resistance to apoptosis (10). In this study, we demonstrated that T helper lymphocytes in chronic inflammation also adapt their metabolism to become entirely dependent on fatty acid oxidation. These findings are consistent with the findings of ^{13}C-glucose tracing studies showing that chronically activated splenocytes in mice with lupus, and also chronically activated human T cells, have reduced lactate production, i.e., down-regulate their glycolysis rate (21).

Reasoning that persistent antigen would lead to repeated restimulation of the T lymphocytes recognizing it, we previously compared the transcriptomes of murine T helper lymphocytes activated once with those activated 3 or 4 times. We identified transcription factors like Hopx (22) and Twist 1 (2) and miRNAs like miR-182 and miR-148a (10,23) as selectively expressed in repeatedly activated T helper cells. Of particular interest is the E-box–binding transcription factor *Twist1*, originally identified as an anticachectic gene, with a strong dose dependency (24), since mice that are haploinsufficient for *Twist1* and its isologue *Twist2* are already prone to die young of cachexia (24). Expression of *Twist1* is induced in activated T helper lymphocytes by STAT4 signaling, and thus a characteristic of Th1 lymphocytes, and its expression increases upon subsequent reactivations (2). The comparison of *Twist1*-deficient and -sufficient, repeatedly activated T helper cells shows that *Twist1* controls the ability of the cells to survive on fatty acid oxidation.

We previously showed that up-regulation of the expression of *Twist1*, upon restimulation ex vivo, is a hallmark of CD4+ T lymphocytes isolated from the inflamed joints of patients with inflammatory rheumatic diseases, or from the inflamed intestinal mucosa of patients with inflammatory bowel diseases (2). *Twist1* expression apparently is a hallmark of pathogenic CD4+ T cells, as selective targeting of such cells via the *Twist1*-induced miR-148a ameliorates inflammation without affecting memory CD4+ T cells induced by vaccination (11). In this study we confirm the observation that *TWIST1* is highly expressed in CD4+ T lymphocytes isolated from the synovia of patients with JIA. We compared PD-1^{high} and PD-1^{low} synovial T helper cells, since PD-1 expression by these cells has been invoked as a correlate of their involvement in chronic inflammation (7,25–28). PD-1^{high} cells from the synovial fluid of patients with JIA indeed showed a significant up-regulation of expression of *TWIST1*, directly ex vivo. Like the repeatedly activated murine Th1 cells, the PD-1^{high} synovial human T helper cells were dependent on fatty acid oxidation for their survival, as evidenced by the fact that they could be killed by etomoxir, an inhibitor of fatty acid oxidation, unlike their PD-1^{low} synovial counterparts. This result points to an interesting therapeutic option to ablate PD-1^{high} CD4+ T lymphocytes selectively in chronic inflammatory diseases. Moreover, in preclinical models this would allow the determination of whether these cells indeed are the driving force of chronic inflammation, substantiating evidence that is thus far only correlative.

ACKNOWLEDGMENTS

We thank Toralf Kaiser, Jenny Kirsch, and Ana Teichmüller for support at the flow cytometry core facility, and Patrick Thiemann and Manuela Ohde for assistance with animal care.

AUTHOR CONTRIBUTIONS

All authors were involved in drafting the article or revising it critically for important intellectual content, and all authors approved the final version to be published. Drs. Chang and Radbruch had full access to all of the data in the study and take responsibility for the integrity of the data and the accuracy of the data analysis.

Study conception and design. Hradilkova, Chang, Radbruch.

Acquisition of data. Hradilkova, Maschmeyer, Westendorf, Schliemann, Husak, von Stuckrad, Kallinich, Minden.

Analysis and interpretation of data. Hradilkova, Durek, Grün, Chang, Radbruch.

REFERENCES

1. Maciolek JA, Pasternak JA, Wilson HL. Metabolism of activated T lymphocytes. Curr Opin Immunol 2014;27:60–74.
2. Niesner U, Albrecht I, Janke M, Doebis C, Loddenkemper C, Lexberg MH, et al. Autoregulation of Th1-mediated inflammation by Twist1. J Exp Med 2008;205:1889–901.
3. Ciurtin C, Cojocaru VM, Miron IM, Preda F, Milicescu M, Bojincă M, et al. Correlation between different components of synovial fluid and pathogenesis of rheumatic diseases. Rom J Intern Med 2006;44:171–81.
4. Sido B, Seel C, Hochlehnert A, Breitkreutz R, Dröge W. Low intestinal glutamine level and low glutaminase activity in Crohn's disease: a rational for glutamine supplementation? Dig Dis Sci 2006;51:2170–9.
5. Bole GG, Peltier DF. Synovial fluid lipids in normal individuals and patients with rheumatoid arthritis. Arthritis Rheum 1962;5:589–601.
6. Leimer EM, Pappan KL, Nettles DL, Bell RD, Easley ME, Olson SA, et al. Lipid profile of human synovial fluid following intra-articular ankle fracture. J Orthop Res 2017;35:657–66.
7. Hatachi S, Iwai Y, Kawano S, Morinobu S, Kobayashi M, Koshiba M, et al. CD4+ PD-1+ T cells accumulate as unique anergic cells in rheumatoid arthritis synovial fluid. J Rheumatol 2003;30:1410–9.
8. Rao DA, Gurish MF, Marshall JL, Slowikowski K, Fonseka CY, Liu Y, et al. Pathologically expanded peripheral T helper cell subset drives B cells in rheumatoid arthritis. Nature 2017;542:110–4.

9. Horn CC, Ji H, Friedman MI. Etomoxir, a fatty acid oxidation inhibitor, increases food intake and reduces hepatic energy status in rats. Physiol Behav 2004;81:157–62.
10. Haftmann C, Stittrich AB, Zimmermann J, Fang Z, Hradilkova K, Bardua M, et al. MiR-148a is upregulated by Twist1 and T-bet and promotes Th1-cell survival by regulating the proapoptotic gene Bim. Eur J Immunol 2015;45:1192–205.
11. Maschmeyer P, Petkau G, Siracusa F, Zimmermann J, Zügel F, Kühl AA, et al. Selective targeting of pro-inflammatory Th1 cells by microRNA-148a-specific antagomirs in vivo. J Autoimmun 2018;89:41–52.
12. Chang CH, Curtis JD, Maggi LB Jr, Faubert B, Villarino AV, O'Sullivan D, et al. Posttranscriptional control of T cell effector function by aerobic glycolysis. Cell 2013;153:1239–51.
13. Millet P, Vachharajani V, McPhail L, Yoza B, McCall CE. GAPDH binding to TNF-α mRNA contributes to posttranscriptional repression in monocytes: a novel mechanism of communication between inflammation and metabolism. J Immunol 2016;196:2541–51.
14. Cossarizza A, Chang HD, Radbruch A, Akdis M, Andrä I, Annunziato F, et al. Guidelines for the use of flow cytometry and cell sorting in immunological studies. Eur J Immunol 2017;47:1584–797.
15. Lexberg MH, Taubner A, Förster A, Albrecht I, Richter A, Kamradt T, et al. Th memory for interleukin-17 expression is stable in vivo. Eur J Immunol 2008;38:2654–64.
16. Seven A, Güzel S, Aslan M, Hamuryudan V. Lipid, protein, DNA oxidation and antioxidant status in rheumatoid arthritis. Clin Biochem 2008;41:538–43.
17. Dingjan I, Verboogen DR, Paardekooper LM, Revelo NH, Sittig SP, Visser LJ, et al. Lipid peroxidation causes endosomal antigen release for cross-presentation. Sci Rep 2016;6:22064.
18. Manz RA, Thiel A, Radbruch A. Lifetime of plasma cells in the bone marrow. Nature 1997;388:133–4.
19. Tokoyoda K, Zehentmeier S, Hegazy AN, Albrecht I, Grün JR, Löhning M, et al. Professional memory CD4+ T lymphocytes preferentially reside and rest in the bone marrow. Immunity 2009;30:721–30.
20. Siracusa F, Alp ÖS, Maschmeyer P, McGrath M, Mashreghi MF, Hojyo S, et al. Maintenance of $CD8^+$ memory T lymphocytes in the spleen but not in the bone marrow is dependent on proliferation. Eur J Immunol 2017;47:1900–5.
21. Wahl DR, Petersen B, Warner R, Richardson BC, Glick GD, Opipari AW. Characterization of the metabolic phenotype of chronically activated lymphocytes. Lupus 2010;19:1492–501.
22. Albrecht I, Niesner U, Janke M, Menning A, Loddenkemper C, Kühl AA, et al. Persistence of effector memory Th1 cells is regulated by Hopx. Eur J Immunol 2010;40:2993–3006.
23. Stittrich AB, Haftmann C, Sgouroudis E, Kühl AA, Hegazy AN, Panse I, et al. The microRNA miR-182 is induced by IL-2 and promotes clonal expansion of activated helper T lymphocytes. Nat Immunol 2010;11:1057–62.
24. Šošić D, Richardson JA, Yu K, Ornitz DM, Olson EN. Twist regulates cytokine gene expression through a negative feedback loop that represses NF-kB activity. Cell 2003;112:169–80.
25. De Jager W, Hoppenreijs EP, Wulffraat NM, Wedderburn LR, Kuis W, Prakken BJ. Blood and synovial fluid cytokine signatures in patients with juvenile idiopathic arthritis: a cross-sectional study. Ann Rheum Dis 2007;66:589–98.
26. Murray KJ, Luyrink L, Grom AA, Passo MH, Emery H, Witte D, et al. Immunohistological characteristics of T cell infiltrates in different forms of childhood onset chronic arthritis. J Rheumatol 1996;23:2116–24.
27. Li S, Liao W, Chen M, Shan S, Song Y, Zhang S, et al. Expression of programmed death-1 (PD-1) on CD4+ and CD8+ T cells in rheumatoid arthritis. Inflammation 2014;37:116–21.
28. Patsoukis N, Bardhan K, Chatterjee P, Sari D, Liu B, Bell LN, et al. PD-1 alters T-cell metabolic reprogramming by inhibiting glycolysis and promoting lipolysis and fatty acid oxidation. Nat Commun 2015;6:6692.

American College of Rheumatology
Empowering Rheumatology Professionals

Arthritis & Rheumatology
Vol. 71, No. 10, October 2019, pp 1766–1767
DOI 10.1002/art.40934

CONCISE COMMUNICATION

DOI 10.1002/art.40934

Senescence signature in skin biopsies from systemic sclerosis patients treated with senolytic therapy: potential predictor of clinical response?

Accumulation of senescent cells has been implicated in the pathogenesis of organ fibrosis and might be therapeutically targeted using senolytic agents. A recent first-in-humans, open-label trial of senolytic therapy using dasatinib plus quercetin in idiopathic pulmonary fibrosis (IPF) showed that functional clinical improvement was associated with reduced levels of circulating proteins, microRNAs, and cytokines related to senescence-associated secretory phenotype (SASP) (1). Similarly to IPF, systemic sclerosis (SSc) is commonly complicated by fibrotic interstitial lung disease (ILD) and presently lacks approved therapies. To address the potential pathogenic role of cellular senescence in SSc-associated ILD (SSc-ILD), we reexamined our results from a recent single-arm clinical trial of dasatinib (2), in which 12 patients with SSc-ILD received treatment for 169 days. We sought to investigate changes in skin SASP gene signature across clinical improvers (defined as a decrease of >5 points or >20% from baseline in the modified Rodnan skin thickness score (3), a validated measure of SSc skin involvement) and in non-improvers.

For this analysis, we retrieved a set of 77 genes annotated to SASP from Reactome (4), 66 of which were present in our skin biopsy–based gene expression data set. While a hallmark database (5) was previously used, in the present analysis we used the Reactome as a more appropriate database, since the former does not contain SASP and senescence gene sets. Despite using different databases, we found that the SASP gene set significantly overlapped (false discovery rate [FDR] <5%) with several hallmarks we identified previously, such as HYPOXIA, TNFA_SIGNALING_VIA_NFKB, P53_PATHWAY, INFLAMMATORY_RESPONSE, PI3K_AKT_MTOR_SIGNALING, and IL6_JAK_STAT3_SIGNALING. For each gene from the Reactome SASP gene set, we created its centroid by averaging its expression across baseline and posttreatment biopsies from 3 dasatinib improvers and 9 non-improvers. The results showed that the SASP gene signature was significantly decreased from baseline in dasatinib-treated improvers; in marked contrast, no change

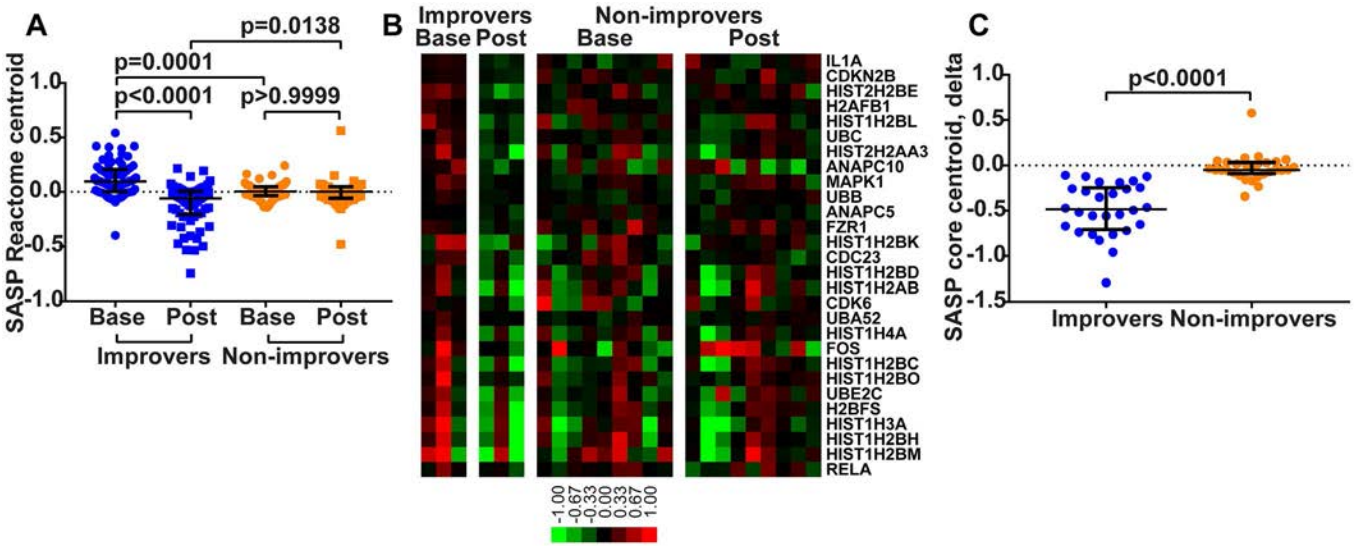

Figure 1. Skin senescence-associated secretory phenotype (SASP) gene signature across dasatinib improvers and non-improvers. **A**, Centroids of genes in the Reactome SASP gene set, created by averaging expression values for component genes across baseline (base) and posttreatment (post) biopsy samples from improvers and non-improvers. *P* values were determined by Kruskal-Wallis test with Dunn's multiple comparison test. **B**, Gene expression heatmap of 28 SASP pathway genes that significantly contributed to SASP enrichment in baseline biopsy samples from improvers. Genes are ordered by rank metric score (i.e., IL1A was the largest contributor to SASP enrichment). Color bar shows the $\log_2$-transformed median-centered fold change represented by each color in the heatmap. **C**, Comparison of the degree of change (calculated as posttreatment minus baseline expression level) for 28 SASP pathway core enrichment genes between improvers and non-improvers. *P* value was determined by Mann-Whitney test. In **A** and **C**, each symbol represents a specific gene; bars show the median and interquartile range.

from baseline was seen in non-improvers. We also found that SASP levels were significantly higher at baseline, and significantly lower posttreatment, in improvers compared to non-improvers (Figure 1A). Among the 66 SASP signature genes, 53 (80.3%) showed a decrease in expression posttreatment in improvers, compared to only 35 (53.0%) in non-improvers (P = 0.0015 by Fisher's exact test).

Next, in order to characterize whole-genome transcriptional changes in an unbiased manner, we performed a gene set enrichment analysis (GSEA) (6,7) using the entire Reactome pathway gene set database. The SASP gene set was significantly enriched in baseline biopsy samples (FDR 1.5%; top 3 result in terms of statistical significance), and decreased posttreatment in improvers. Core enrichment genes from SASP (28 of 66) followed the same trends as the overall SASP pathway (Figure 1B), and their degree of change (calculated as posttreatment minus baseline expression level) was significantly lower in improvers compared to non-improvers (Figure 1C).

Four additional senescence-related gene sets were significantly enriched in baseline biopsy samples from improvers and decreased posttreatment (cellular senescence, DNA damage/telomere stress–induced senescence, oncogene-induced senescence, and oxidative stress–induced senescence; all FDRs <5%). In fact, these gene sets were overrepresented among gene sets significantly enriched in improvers at baseline, compared to all other gene sets enriched in improvers (5 of 23 gene sets with FDR <5% versus 0 of 755 gene sets with FDR > 5%; $P < 0.0001$ by Fisher's exact test). In contrast, we found that in non-improvers the senescence-related gene sets showed no change from baseline to posttreatment (lowest FDR for senescence-related gene set 26.9%, FDR for SASP 78.0%). Baseline GSEA comparison between improvers and non-improvers revealed that while SASP was nonsignificantly enriched in baseline biopsy specimens from improvers (FDR 11.7%), the DNA damage/telomere stress-induced senescence gene set was very significantly enriched in improvers compared to non-improvers (FDR 0.6%; top 2 result in terms of statistical significance).

In summary, a reanalysis of the results from a recent open-label trial of the senolytic agent dasatinib in patients with SSc-ILD demonstrated that a decrease in skin expression of SASP and other senescence-related gene sets was associated with treatment, and correlated with clinical improvement. Additionally, baseline skin biopsy specimens from clinical improvers showed higher expression of these senescence-associated gene sets. These results can be viewed as consistent with a clinically beneficial senolytic effect, suggesting that dasatinib-mediated clearance of pathogenic senescent cells in lesional tissue and consequent reduction in the systemic senescence burden may have mitigated the fibrotic process and led to clinical improvement. Indeed, this mechanistic scenario closely parallels recent experimental observations in an animal model of bleomycin-induced lung fibrosis, where pharmacologic clearance of senescent cells using dasatinib plus quercetin resulted in functional attenuation of the lung fibrosis (8). While the potential of a tissue SASP gene signature as a biomarker of clinical response to antifibrosis therapy requires further study, the present results provide conceptual support for senolytic therapy in SSc-ILD.

Drs. Martyanov and Whitfield's work was supported by grant P50-AR-060780 from the National Institute of Arthritis and Musculoskeletal and Skin Diseases and a grant from the Scleroderma Research Foundation. No other disclosures relevant to this article were reported.

Viktor Martyanov, PhD
Michael L. Whitfield, PhD
Geisel School of Medicine at Dartmouth
Hanover, NH
John Varga, MD
Northwestern University
Chicago, IL

AUTHOR CONTRIBUTIONS

All authors were involved in drafting the article or revising it critically for important intellectual content, and all authors approved the final version to be published. Dr. Martyanov had full access to all of the data in the study and takes responsibility for the integrity of the data and the accuracy of the data analysis.

Study conception and design. Martyanov, Whitfield, Varga.
Acquisition of data. Martyanov, Whitfield, Varga.
Analysis and interpretation of data. Martyanov, Whitfield, Varga.

1. Justice JN, Nambiar AM, Tchkonia T, LeBrasseur NK, Pascual R, Hashmi SK, et al. Senolytics in idiopathic pulmonary fibrosis: results from a first-in-human, open-label, pilot study. EBioMedicine 2019;40:554–63.
2. Martyanov V, Kim GJ, Hayes W, Du S, Ganguly BJ, Sy O, et al. Novel lung imaging biomarkers and skin gene expression subsetting in dasatinib treatment of systemic sclerosis-associated interstitial lung disease. PLoS One 2017;12:e0187580.
3. Clements P, Lachenbruch P, Siebold J, White B, Weiner S, Martin R, et al. Inter and intraobserver variability of total skin thickness score (modified Rodnan TSS) in systemic sclerosis. J Rheumatol 1995;22:1281–5.
4. Fabregat A, Jupe S, Matthews L, Sidiropoulos K, Gillespie M, Garapati P, et al. The Reactome Pathway Knowledgebase. Nucleic Acids Res 2018;46:D649–55.
5. Liberzon A, Birger C, Thorvaldsdottir H, Ghandi M, Mesirov JP, Tamayo P. The Molecular Signatures Database (MSigDB) hallmark gene set collection. Cell Syst 2015;1:417–25.
6. Mootha VK, Lindgren CM, Eriksson KF, Subramanian A, Sihag S, Lehar J, et al. PGC-1α-responsive genes involved in oxidative phosphorylation are coordinately downregulated in human diabetes. Nat Genet 2003;34:267–73.
7. Subramanian A, Tamayo P, Mootha VK, Mukherjee S, Ebert BL, Gillette MA, et al. Gene set enrichment analysis: a knowledge-based approach for interpreting genome-wide expression profiles. Proc Natl Acad Sci USA 2005;102:15545–50.
8. Schafer MJ, White TA, Iijima K, Haak AJ, Ligresti G, Atkinson EJ, et al. Cellular senescence mediates fibrotic pulmonary disease. Nat Commun 2017;8:14532.

American College of Rheumatology
Empowering Rheumatology Professionals

Arthritis & Rheumatology
Vol. 71, No. 10, October 2019, pp 1768–1772

LETTERS

DOI 10.1002/art.41002

Overrepresentation of elderly subjects in a population-based study of antiphospholipid syndrome: comment on the article by Duarte-García et al

To the Editor:

Duarte-García and colleagues conducted an epidemiologic study of antiphospholipid syndrome (APS) in Olmsted County, Minnesota, focusing on annual incidence, prevalence, and mortality (1). They estimated a prevalence of 50 per 100,000 inhabitants and an overall annual incidence of 2 per 100,000. Certainly, as the authors noted, there is a lack of studies evaluating the "real" prevalence of APS in a community setting. Durcan and Petri, for example, reported an annual incidence of APS of ~5 per 100,000 individuals and a prevalence of 40–50 cases per 100,000 individuals (2). Most published information about the prevalence and mortality of APS is from studies of patients at academic medical centers, collaborative multicenter studies (3–5), and systematic reviews (6).

We believe the information provided by Duarte-García et al is relevant but should be interpreted with caution. The data are significantly influenced by the fact that patients >75 years of age constituted 25% of the cohort. This large proportion of older individuals cannot be explained by the demographic distribution of the population of Olmsted County; according to the most recent census data, persons ≥65 years of age comprise only 15% of its population (United States Census Bureau; online at http://www.census.gov/quickfacts/olmstedcounty.minnesota).

Although the authors used the current Sydney criteria for the classification of APS (7), antiphospholipid antibody (aPL) testing was performed at a centralized laboratory, and the presence of either venous or arterial thrombosis was confirmed using medical records, the clinical picture in 10 of the 40 patients >75 years of age included in the study is not typical of the APS seen in clinical inpatient and outpatient settings in different parts of the world.

The Olmsted County APS cohort was predominantly white (97%) and mostly included patients with primary APS (82%); the mean ± SD age was 55.7 ± 19 years. The Euro-Phospholipid cohort was also predominantly white and consisted of 1,000 patients (3); the mean ± SD age at diagnosis was 34 ± 13 years, and primary APS accounted for 53% of cases. In that cohort, only 12.7% of patients were >50 years of age. In a multicenter cohort of patients with primary APS followed up at 4 different centers, the median age was 42 years (range 16–79) (4). Further, in a cohort of patients with aPL associated with malignancies, the mean ± SD age was 56 ± 17 years (8).

To the best of our knowledge, only Grimaud and colleagues have examined the clinical characteristics of elderly-onset APS (9). They evaluated a cohort of 44 elderly-onset APS patients from different French centers. Sixty-eight percent of the patients were women, 72% were diagnosed as having primary APS, and the mean age ± SD at diagnosis was 68.7 ± 7 years. Clinically, elderly-onset patients did not differ from the general Euro-Phospholipid cohort, except for having a higher proportion of male patients and a higher frequency of primary APS.

As Duarte-García et al noted, their data are not generalizable to more diverse populations because the large majority of the population studied was white and most patients had primary APS. More data are needed from other regions with different race/ethnic backgrounds (especially African American, Hispanic, and Asian populations) and different socioeconomic characteristics.

The prevalence of aPL positivity increases with age, especially among elderly patients with chronic disease(s), with up to 50% of elderly individuals reported as being positive for aPL (10). In addition, elderly individuals have a higher prevalence of other traditional cardiovascular risk factors for arterial and venous thrombosis, explaining in part why this group accounts for a high proportion of cases in the cohort analyzed by Duarte-García and colleagues.

In conclusion, we suggest that new prevalence estimates are needed and that at least a subgroup analysis excluding those patients >75 years of age would be helpful in future studies of APS prevelance.

Dr. Gómez-Puerta has received consulting fees, speaking fees, and/or honoraria from AbbVie, GlaxoSmithKline, Eli Lilly, Pfizer, and Roche (less than $10,000 each). No other disclosures relevant to this article were reported.

Jose A. Gómez-Puerta, MD, PhD, MPH
Department of Rheumatology
Hospital Clínic
Ricard Cervera, MD, PhD, FRCP
Department of Autoimmune Diseases
Hospital Clínic
Barcelona, Spain
Graciela S. Alarcón, MD, MPH
School of Medicine,
University of Alabama at Birmingham

1. Duarte-García A, Pham MM, Crowson CS, Amin S, Moder KG, Pruthi RK, et al. The epidemiology of antiphospholipid syndrome: a population-based study. Arthritis Rheumatol 2019;71:1545–52.
2. Durcan L, Petri M. Epidemiology of the antiphospholipid syndrome. In: Handbook of systemic autoimmune diseases. Amsterdam: Elsevier; 2016. p. 17–30.
3. Cervera R, Piette JC, Font J, Khamashta MA, Shoenfeld Y, Camps MT, et al. Antiphospholipid syndrome: clinical and immunologic manifestations and patterns of disease expression in a cohort of 1,000 patients. Arthritis Rheum 2002;46:1019–27.
4. Gómez-Puerta JA, Martín H, Amigo MC, Aguirre MA, Camps MT, Cuadrado MJ, et al. Long-term follow-up in 128 patients with

primary antiphospholipid syndrome: do they develop lupus? Medicine (Baltimore) 2005;84:225–30.
5. Ames PR, Merashli M, Chis Ster I, D'Andrea G, Iannaccone L, Marottoli V, et al. Survival in primary antiphospholipid syndrome: a single-centre cohort study. Thromb Haemost 2016;115:1200–8.
6. Chighizola CB, Andreoli L, de Jesus GR, Banzato A, Pons-Estel GJ, Erkan D. The association between antiphospholipid antibodies and pregnancy morbidity, stroke, myocardial infarction, and deep vein thrombosis: a critical review of the literature. Lupus 2015;24:980–4.
7. Miyakis S, Lockshin MD, Atsumi T, Branch DW, Brey RL, Cervera R, et al. International consensus statement on an update of the classification criteria for definite antiphospholipid syndrome (APS). J Thromb Haemost 2006;4:295–306.
8. Gómez-Puerta JA, Cervera R, Espinosa G, Aguiló S, Bucciarelli S, Ramos-Casals M, et al. Antiphospholipid antibodies associated with malignancies: clinical and pathological characteristics of 120 patients. Semin Arthritis Rheum 2006;35:322–32.
9. Grimaud F, Yelnik C, Pineton de Chambrun M, Amoura Z, Arnaud L, Costedoat Chalumeau N, et al. Clinical and immunological features of antiphospholipid syndrome in the elderly: a retrospective national multicentre study. Rheumatology (Oxford) 2019;58:1006–10.
10. Manoussakis MN, Tzioufas AG, Silis MP, Pange PJ, Goudevenos J, Moutsopoulos HM. High prevalence of anti-cardiolipin and other autoantibodies in a healthy elderly population. Clin Exp Immunol 1987;69:557–65.

DOI 10.1002/art.41000

Reply

To the Editor:

We thank Dr. Gómez-Puerta and colleagues for their interest in our study on the epidemiology of APS. Gómez-Puerta et al state that 25% of our population-based APS inception cohort was >75 years of age. This figure is taken from our secondary analysis; in fact, the primary analysis was performed using the Sydney classification criteria (1), in which ~20% of the subjects were >75 years of age. There are several reasons why the results of our population-based study differ from findings based on referral cohorts.

Gómez-Puerta et al argue that the age distribution in our study is not the same as the one encountered in specialized centers. Cases identified in a clinic or hospital, particularly those that specialize in a specific condition, are not representative of the general population. Those patients have undergone selection by referring physicians and patients themselves (2). As a consequence, patients seen in tertiary care centers differ significantly from population-based studies of incident cases. This type of selection is known as referral bias or Berkson's bias (3).

Patients seen in tertiary care centers generally have more severe forms of the disease of interest. Additionally, older patients are underrepresented in studies based at tertiary care centers, and therefore subjects in population-based studies have a higher mean age than subjects in referral center studies (4). Another example of this underrepresentation is seen in lupus studies. Compared to referral center–based cohorts, the mean age at incidence of lupus in US Centers for Disease Control and Prevention–funded population-based inception cohorts was consistently higher (in some racial/ethnic groups, by close to 10 years) (5–8). Population studies including all patients with the disease of interest are much less likely to be affected by referral bias since they include all of the individuals with the disease of interest in a defined geographic area, across the care continuum.

APS, like other autoimmune conditions, has systemic manifestations that can be heterogeneous. Classification criteria were designed to identify a homogeneous group of patients using a standardized definition of a disease that will capture subjects with the basic features of the disease of interest (9). In our study, we stringently applied the Sydney criteria. These criteria do not have an age restriction, but the authors noted, "the association of aging and of common risk factors for cardiovascular disease with thrombosis may cause classification bias. No published data provides a valid estimation of an age boundary for diagnosing APS" (1). Our study provides evidence that the classification criteria capture older patients.

The results of our study provide useful information about the epidemiology of APS using an accepted disease definition rather than relying on physician identification of disease features for diagnostic criteria that may vary from clinician to clinician. If the current accepted definition is considered insufficient, then new criteria for disease classification and diagnosis need to be developed. For this reason, we have chosen to present results using the accepted Sydney criteria and not undertake a reestimation of epidemiologic parameters. Further population-based studies in other settings using comparable criteria are needed to gain a better understanding of the demographic characteristics and clinical features of APS.

Ali Duarte-García, MD
Cynthia S. Crowson, PhD
Kenneth J. Warrington, MD
Eric. L. Matteson, MD, MPH
Mayo Clinic College of Medicine and Science
Rochester, MN

1. Miyakis S, Lockshin MD, Atsumi T, Branch DW, Brey RL, Cervera R, et al. International consensus statement on an update of the classification criteria for definite antiphospholipid syndrome (APS). J Thromb Haemost 2006;4:295–306.
2. Salive ME. Referral bias in tertiary care: the utility of clinical epidemiology [editorial]. Mayo Clinic Proc 1994;69:808–9.
3. Berkson J. Limitations of the application of fourfold table analysis to hospital data. Biometrics 1946;2:47–53.
4. Kokmen E, Özsarfati Y, Beard CM, O'Brien PC, Rocca WA. Impact of referral bias on clinical and epidemiological studies of Alzheimer's disease. J Clin Epidemiol 1996;49:79–83.
5. Somers EC, Marder W, Cagnoli P, Lewis EE, DeGuire P, Gordon C, et al. Population-based incidence and prevalence of systemic lupus erythematosus: the Michigan Lupus Epidemiology and Surveillance program. Arthritis Rheumatol 2014;66:369–78.
6. Izmirly PM, Wan I, Sahl S, Buyon JP, Belmont HM, Salmon JE, et al. The incidence and prevalence of systemic lupus erythematosus in New York County (Manhattan), New York: the Manhattan Lupus Surveillance Program. Arthritis Rheumatol 2017;69:2006–17.

primary antiphospholipid syndrome: do they develop lupus? Medicine (Baltimore) 2005;84:225–30.
5. Ames PR, Merashli M, Chis Ster I, D'Andrea G, Iannaccone L, Marottoli V, et al. Survival in primary antiphospholipid syndrome: a single-centre cohort study. Thromb Haemost 2016;115:1200–8.
6. Chighizola CB, Andreoli L, de Jesus GR, Banzato A, Pons-Estel GJ, Erkan D. The association between antiphospholipid antibodies and pregnancy morbidity, stroke, myocardial infarction, and deep vein thrombosis: a critical review of the literature. Lupus 2015;24:980–4.
7. Miyakis S, Lockshin MD, Atsumi T, Branch DW, Brey RL, Cervera R, et al. International consensus statement on an update of the classification criteria for definite antiphospholipid syndrome (APS). J Thromb Haemost 2006;4:295–306.
8. Gómez-Puerta JA, Cervera R, Espinosa G, Aguiló S, Bucciarelli S, Ramos-Casals M, et al. Antiphospholipid antibodies associated with malignancies: clinical and pathological characteristics of 120 patients. Semin Arthritis Rheum 2006;35:322–32.
9. Grimaud F, Yelnik C, Pineton de Chambrun M, Amoura Z, Arnaud L, Costedoat Chalumeau N, et al. Clinical and immunological features of antiphospholipid syndrome in the elderly: a retrospective national multicentre study. Rheumatology (Oxford) 2019;58:1006–10.
10. Manoussakis MN, Tzioufas AG, Silis MP, Pange PJ, Goudevenos J, Moutsopoulos HM. High prevalence of anti-cardiolipin and other autoantibodies in a healthy elderly population. Clin Exp Immunol 1987;69:557–65.

DOI 10.1002/art.41000

Reply

To the Editor:

We thank Dr. Gómez-Puerta and colleagues for their interest in our study on the epidemiology of APS. Gómez-Puerta et al state that 25% of our population-based APS inception cohort was >75 years of age. This figure is taken from our secondary analysis; in fact, the primary analysis was performed using the Sydney classification criteria (1), in which ~20% of the subjects were >75 years of age. There are several reasons why the results of our population-based study differ from findings based on referral cohorts.

Gómez-Puerta et al argue that the age distribution in our study is not the same as the one encountered in specialized centers. Cases identified in a clinic or hospital, particularly those that specialize in a specific condition, are not representative of the general population. Those patients have undergone selection by referring physicians and patients themselves (2). As a consequence, patients seen in tertiary care centers differ significantly from population-based studies of incident cases. This type of selection is known as referral bias or Berkson's bias (3).

Patients seen in tertiary care centers generally have more severe forms of the disease of interest. Additionally, older patients are underrepresented in studies based at tertiary care centers, and therefore subjects in population-based studies have a higher mean age than subjects in referral center studies (4). Another example of this underrepresentation is seen in lupus studies. Compared to referral center–based cohorts, the mean age at incidence of lupus in US Centers for Disease Control and Prevention–funded population-based inception cohorts was consistently higher (in some racial/ethnic groups, by close to 10 years) (5–8). Population studies including all patients with the disease of interest are much less likely to be affected by referral bias since they include all of the individuals with the disease of interest in a defined geographic area, across the care continuum.

APS, like other autoimmune conditions, has systemic manifestations that can be heterogeneous. Classification criteria were designed to identify a homogeneous group of patients using a standardized definition of a disease that will capture subjects with the basic features of the disease of interest (9). In our study, we stringently applied the Sydney criteria. These criteria do not have an age restriction, but the authors noted, "the association of aging and of common risk factors for cardiovascular disease with thrombosis may cause classification bias. No published data provides a valid estimation of an age boundary for diagnosing APS" (1). Our study provides evidence that the classification criteria capture older patients.

The results of our study provide useful information about the epidemiology of APS using an accepted disease definition rather than relying on physician identification of disease features for diagnostic criteria that may vary from clinician to clinician. If the current accepted definition is considered insufficient, then new criteria for disease classification and diagnosis need to be developed. For this reason, we have chosen to present results using the accepted Sydney criteria and not undertake a reestimation of epidemiologic parameters. Further population-based studies in other settings using comparable criteria are needed to gain a better understanding of the demographic characteristics and clinical features of APS.

Ali Duarte-García, MD
Cynthia S. Crowson, PhD
Kenneth J. Warrington, MD
Eric. L. Matteson, MD, MPH
Mayo Clinic College of Medicine and Science
Rochester, MN

1. Miyakis S, Lockshin MD, Atsumi T, Branch DW, Brey RL, Cervera R, et al. International consensus statement on an update of the classification criteria for definite antiphospholipid syndrome (APS). J Thromb Haemost 2006;4:295–306.
2. Salive ME. Referral bias in tertiary care: the utility of clinical epidemiology [editorial]. Mayo Clinic Proc 1994;69:808–9.
3. Berkson J. Limitations of the application of fourfold table analysis to hospital data. Biometrics 1946;2:47–53.
4. Kokmen E, Özsarfati Y, Beard CM, O'Brien PC, Rocca WA. Impact of referral bias on clinical and epidemiological studies of Alzheimer's disease. J Clin Epidemiol 1996;49:79–83.
5. Somers EC, Marder W, Cagnoli P, Lewis EE, DeGuire P, Gordon C, et al. Population-based incidence and prevalence of systemic lupus erythematosus: the Michigan Lupus Epidemiology and Surveillance program. Arthritis Rheumatol 2014;66:369–78.
6. Izmirly PM, Wan I, Sahl S, Buyon JP, Belmont HM, Salmon JE, et al. The incidence and prevalence of systemic lupus erythematosus in New York County (Manhattan), New York: the Manhattan Lupus Surveillance Program. Arthritis Rheumatol 2017;69:2006–17.

7. Reveille JD, Moulds JM, Ahn C, Friedman AW, Baethge B, Roseman J, et al. Systemic lupus erythematosus in three ethnic groups: I. The effects of HLA class II, C4, and CR7 alleles, socioeconomic factors, and ethnicity at disease onset. Arthritis Rheum 1998;41:1161–72.
8. Gladman DD, Ibañez D, Urowitz MB. Systemic lupus erythematosus disease activity index 2000. J Rheumatol 2002;29:288–91.
9. Aggarwal R, Ringold S, Khanna D, Neogi T, Johnson SR, Miller A, et al. Distinctions between diagnostic and classification criteria? Arthritis Care Res (Hoboken) 2015;67:891–7.

DOI 10.1002/art.41015

Where does denosumab stand in the treatment of glucocorticoid-induced osteoporosis? Comment on the article by Saag et al

To the Editor:

We read with interest the article by Dr. Saag et al in which they compared the efficacy and safety of denosumab versus risedronate in glucocorticoid-induced osteoporosis (GIOP) (1). Osteoporosis in the setting of GIOP can be challenging to treat because of issues with drug adherence (due to pill burden) and the presence of multiple comorbidities. Denosumab is a welcome addition to the treatment regimens for this disease due to its once per 6 months dosing schedule, which is associated with better adherence than bisphosphonates (2), and its renal safety (3). However, certain clarifications may further help readers to understand its applicability when choosing it as an alternative therapy.

First, the basis of using risedronate as an active comparator in the study by Saag et al is not clear. According to the available data on different bisphosphonates, risedronate appears to be less effective than alendronate in treating vertebral fractures (36% versus 44%) and hip fractures (26% versus 40%) per a recent meta-analysis (3). The results of the current study may be partially biased due to the utilization of a weak comparator. Indeed, alendronate remains the gold-standard oral bisphosphonate for most physicians.

Second, the primary concern regarding the use of denosumab is postwithdrawal rebound decline in bone mineral density and increased risk of multiple and severe vertebral fractures (4), which was not addressed in the study by Saag and colleagues.

Third, the external validity of the study may be limited in the young population, few of whom were included, as was also the case for patients with systemic lupus erythematosus.

Fourth, of particular concern is the long-term use of denosumab on a background of other multiple immunosuppressive drugs. Denosumab is known to affect various aspects of the immune system. RANK/RANKL is linked with generation and induction of T cell tolerance (5). A significant concern is the numerically higher incidence of malignancy in the study by Saag et al. As in most randomized controlled trials, the study was not powered for adverse events, and hence, long-term postmarketing surveillance will be important.

Finally, despite significant bone mineral density changes at 24 months, the occurrence of nonvertebral fractures was numerically higher in the denosumab-treated group. It would be of interest to know the sites of these nonvertebral fractures, which was previously provided by Saag and colleagues in their 12-month follow-up data (6).

Arghya Chattopadhyay, MD
Shefali K. Sharma, MD
Aman Sharma, MD
Sanjay Jain, MD, DM
Varun Dhir, MD, DM
PGIMER
Chandigarh, India

1. Saag KG, Pannacciulli N, Geusens P, Adachi JD, Messina OD, Morales-Torres J, et al. Denosumab versus risedronate in glucocorticoid-induced osteoporosis: final results of a twenty-four–month randomized, double-blind, double-dummy trial. Arthritis Rheumatol 2019;71:1174–84.
2. Kendler DL, McClung MR, Freemantle N, Lillestol M, Moffett AH, Borenstein J, et al. Adherence, preference, and satisfaction of postmenopausal women taking denosumab or alendronate. Osteoporos Int 2011;22:1725–35.
3. Eastell R, Rosen CJ, Black DM, Cheung AM, Murad MH, Shoback D. Pharmacological management of osteoporosis in postmenopausal women: an Endocrine Society clinical practice guideline. J Clin Endocrinol Metab 2019;104:1595–622.
4. Brown JP, Roux C, Torring O, Ho PR, Beck Jensen JE, Gilchrist N, et al. Discontinuation of denosumab and associated fracture incidence: analysis from the Fracture Reduction Evaluation of Denosumab in Osteoporosis Every 6 Months (FREEDOM) trial. J Bone Miner Res 2013;28:746–52.
5. Cheng ML, Fong L. Effects of RANKL-targeted therapy in immunity and cancer [review]. Front Oncol 2014;3:329.
6. Saag KG, Wagman RB, Geusens P, Adachi JD, Messina OD, Emkey R, et al. Denosumab versus risedronate in glucocorticoid-induced osteoporosis: a multicentre, randomised, double-blind, active-controlled, double-dummy, non-inferiority study. Lancet Diabetes Endocrinol 2018;6:445–54.

DOI 10.1002/art.41016

Bisphosphonates as a first-line treatment for glucocorticoid-induced osteoporosis: comment on the article by Saag et al

To the Editor:

We read with interest the article by Dr. Saag and colleagues (1). This 24-month randomized trial demonstrated the efficacy and safety of denosumab compared with risedronate. The discussion did not address 3 major concerns regarding denosumab discontinuation that could affect the conclusions reached in the study.

First, in postmenopausal women with osteoporosis, denosumab discontinuation is associated with a severe rebound effect that lasts <2 years (2–4), which combines an increase in bone turnover markers, complete loss of gained bone density, and an increased risk (from ≥1% to <10%) of multiple vertebral fractures. In 70 women with multiple vertebral fractures after denosumab discontinuation, the median number of vertebral fractures was 5 within 7–20 months following the last denosumab injection (4). The post hoc analysis of the Fracture Reduction Evaluation of Denosumab in Osteoporosis Every 6 Months (FREEDOM) trial evaluated

1,001 women 9–12 months after the last denosumab injection (5). The annualized risk of vertebral fractures was 7.1%, of which 60.7% were multiple vertebral fractures. This risk was likely an underestimate due to insufficient follow-up in relation to duration of the rebound effect. In the FREEDOM trial placebo group, the annualized risk of radiologic vertebral fractures was between 2.22 and 3.15% (6). The majority of these vertebral fractures were isolated and without clinical consequence. The multiple vertebral fractures after denosumab discontinuation negatively affects quality of life and should have been addressed in Saag and colleagues' analysis.

Second, treatment with a potent bisphosphonate (alendronate, zoledronic acid) is mandatory for 2 years following denosumab discontinuation (4,5). This strategy reduces bone loss but whether it prevents vertebral fractures is not known. Thus, the benefit of denosumab may be attenuated, with a partial loss of bone density increase obtained with denosumab.

Third, glucocorticoid treatment and denosumab discontinuation are both major risk factors for vertebral fractures. The increased vertebral fracture risk associated with glucocorticoids persists 1 year after discontinuation. The vertebral fracture risk after denosumab discontinuation may rise further if a severe increase in rebound effect–related bone turnover markers occurs with the glucocorticoid effect.

Two conclusions can be reached. First, bisphosphonates remain the first-line treatment for glucocorticoid-induced osteoporosis, due to the uncertainty regarding denosumab discontinuation. Second, studies with denosumab should include a 2-year follow-up after its discontinuation before conclusions can be made in terms of bone density or fracture risk.

Elena Gonzalez-Rodriguez, MD, PhD
Bérengère Aubry-Rozier, MD
Delphine Stoll, MD
Olivier Lamy, MD
Lausanne University Hospital
Lausanne, Switzerland

1. Saag KG, Pannacciulli N, Geusens P, Adachi JD, Messina OD, Morales-Torres J, et al. Denosumab versus risedronate in glucocorticoid-induced osteoporosis: final results of a twenty-four–month randomized, double-blind, double-dummy trial. Arthritis Rheumatol 2019;71:1174–84.
2. Bone HG, Bolognese MA, Yuen CK, Kendler DL, Miller PD, Yang YC, et al. Effects of denosumab treatment and discontinuation on bone mineral density and bone turn-over markers in postmenopausal women with low bone mass. J Clin Endocrinol Metab 2011;96:972–80.
3. Anastasilakis AD, Polyzos SA, Makras P, Aubry-Rozier B, Kaouri S, Lamy O. Clinical features of 24 patients with rebound-associated vertebral fractures after denosumab discontinuation: systematic review and additional cases. J Bone Miner Res 2017;32:1291–6.
4. Lamy O, Stoll D, Aubry-Rozier B, Gonzalez-Rodriguez E. Stopping denosumab. Curr Osteoporos Rep 2019;17:8–15.
5. Cummings SR, Ferrari S, Eastell R, Gilchrist N, Jensen JB, McClung M, et al. Vertebral fractures after discontinuation of denosumab: a post hoc analysis of the randomized placebo-controlled FREEDOM trial and its extension. J Bone Miner Res 2018;33:190–8.
6. Bone HG, Wagman RB, Brandi ML, Brown JP, Chapurlat R, Cummings SR, et al. 10 years of denosumab treatment in postmenopausal women with osteoporosis: results from the phase 3 randomised FREEDOM trial and open-label extension. Lancet Diabetes Endocrinol 2017;5:513–23.

DOI 10.1002/art.41013

Reply

To the Editor:

We thank Drs. Chattopadhyay, Gonzalez-Rodriguez, and their respective colleagues for their interest in defining optimal treatment approaches in GIOP. They noted previous findings of increased bone turnover and heightened fracture risk upon discontinuation of denosumab in postmenopausal women enrolled in the FREEDOM extension study following 3–10 years of denosumab treatment (1,2). Patients in our study on denosumab versus risedronate in GIOP did not have an extended follow-up after the study to inform this question directly. The circumstance in GIOP is somewhat different because many patients receive denosumab only during concomitant use of glucocorticoids, leading to a potentially shorter course of denosumab.

A phase II study of individuals with rheumatoid arthritis receiving denosumab therapy (3) included a subgroup of patients (n = 82) who were also receiving glucocorticoids at baseline and were followed up for 12 months after denosumab discontinuation. In a recent subgroup analysis of these patients, investigators secondarily examined the effects of denosumab cessation on bone turnover and bone mineral density (4). In that analysis of short-term denosumab use, bone turnover was reduced with denosumab and gradually returned to baseline upon discontinuation, without a clear increase to above-baseline levels in the off-treatment period. However, the study was underpowered to address the question comprehensively, and there are very limited data available overall to inform treatment after limited denosumab doses, such as for patients concurrently receiving glucocorticoids. It is nonetheless prudent to have an "exit strategy" when initiating denosumab in all indications.

Questions were also raised about the best timing to initiate treatment with an alternate antiresorptive agent after denosumab is stopped. There may be differences in timing the initiation of a pulsatile bisphosphonate such as zoledronic acid (which, possibly, would be initiated at least a few months after the next denosumab dose would have been due) compared with alendronate (which likely should begin immediately after stopping denosumab) (5).

Chattopadhyay et al questioned the use of risedronate as the active comparator in our study. We noted this limitation in the original report describing 12-month primary outcome data (6), and we agree that additional comparisons of denosumab with other bis-

phosphonates or osteoporosis therapies are warranted in future studies. At the time of our study design, the goal was to conduct a study similar to the zoledronic acid GIOP trial, which also used risedronate as the active comparator (7).

Regarding the generalizability of our findings to younger patients receiving glucocorticoids, no past GIOP studies have included large populations of these patients due to difficulties of finding such patients, who often have more severe and active inflammatory diseases. In relatively small studies with only 2 years of observation such as ours, trying to disentangle differences between treatment arms in a small number of low-prevalence adverse events of interest is very difficult. Larger, more pragmatic designs or postmarketing pharmacovigilance provide alternate approaches to safety questions in general. While there were no significant differences in fracture rates between treatment arms in our study, numerical imbalances were noted both for vertebral fractures (fewer with denosumab) and nonvertebral fractures (fewer with risedronate). Nonvertebral fracture locations are summarized in Table 1. Conclusions cannot be drawn on preferential benefit or risk of such fracture events by study arms; such a comparison would require a much larger sample size to have adequate power to detect very small differences in fracture incidence in an active comparator trial.

Malignancies were numerically imbalanced between the treatment arms, but no particular cancer type explained this difference. There was a small numerical imbalance in basal cell skin cancers, with events occurring in 4 patients receiving denosumab and 0 patients receiving risedronate.

Gonzalez-Rodriguez and colleagues recommend that bisphosphonates be used first in the treatment of GIOP. We agree with this recommendation for many (if not most) patients, and this is consistent with the American College of Rheumatology GIOP guidelines (8), which were prepared before we published the results of our study (6). However, some patients have contraindications to (oral) bisphosphonates, poor adherence to such regimens, or are at severe risk for osteoporosis, leading to a clinical decision to first use drugs such as teriparatide or denosumab that have been shown to have better efficacy in GIOP compared with an oral bisphosphonate (6,9). As Chattopadhyay et al note, and we strongly echo, it is always helpful to have an expanded therapeutic armamentarium in a disease state, since one size does not fit all in our collective efforts toward more personalized medicine.

Table 1. Number of nonvertebral fractures occurring though month 24, by site

Site	Risedronate 5 mg/day (n = 397)	Denosumab 60 mg every 6 months (n = 398)
Total	16	24
Sternum	1	0
Rib	3	7
Humerus	3	3
Radius	2	1
Pelvis	2	4
Hip	1	2
Fibula	2	1
Femur distal	0	1
Tibia	1	0
Foot	1	3
Metatarsus	0	2

Dr. Saag has received consulting fees and/or honoraria from AbbVie, Ironwood/AstraZeneca, Bayer, Gilead, Horizon, Kowa, Radius, Sobi, and Teijin (less than $10,000 each) and from Amgen, Roche/Genentech, and Takeda (more than $10,000 each) and has received research support from Amgen and Radius. Dr. Geusens has received honoraria from Amgen and Eli Lilly (less than $10,000 each) and research support from Abbott, Amgen, Bristol-Myers Squibb, Celgene, Janssen, Eli Lilly, MSD, Novartis, Pfizer, Roche, UCB, and Will-Pharma. Dr. Lems has received consulting fees, speaking fees, and/or honoraria from Amgen, MSD, Pfizer, and Eli Lilly (less than $10,000 each).

Kenneth G. Saag, MD, MSc
University of Alabama at Birmingham
Piet Geusens, MD, PhD
Maastricht University
Maastricht, The Netherlands
Willem F. Lems, MD, PhD
VU University Medical Center
Amsterdam, The Netherlands

1. Cummings SR, Ferrari S, Eastell R, Gilchrist N, Jensen JB, McClung M, et al. Vertebral fractures after discontinuation of denosumab: a post hoc analysis of the randomized placebo-controlled FREEDOM trial and its extension. J Bone Miner Res 2018;33:190–8.
2. Bone HG, Wagman RB, Brandi ML, Brown JP, Chapurlat R, Cummings SR, et al. 10 years of denosumab treatment in postmenopausal women with osteoporosis: results from the phase 3 randomised FREEDOM trial and open-label extension. Lancet Diabetes Endocrinol 2017;5:513–23.
3. Dore RK, Cohen SB, Lane NE, Palmer W, Shergy W, Zhou L, et al. Effects of denosumab on bone turnover in patients with rheumatoid arthritis receiving concurrent glucocorticoids or bisphosphonates. Ann Rheum Dis 2010;69:872–5.
4. Saag KG, McDermott MT, Adachi J, Lems W, Lane NE, Geusens P, et al. Effect of discontinuation of denosumab in subjects with rheumatoid arthritis treated with glucocorticoids. Ann Rheum Dis 2019;78 Suppl 2:A931.
5. Chapurlat R. Effects and management of denosumab discontinuation. Joint Bone Spine 2018;85:515–7.
6. Saag KG, Wagman RB, Geusens P, Adachi JD, Messina OD, Emkey R, et al. Denosumab versus risedronate in glucocorticoid-induced osteoporosis: a multicentre, randomised, double-blind, active-controlled, double-dummy, non-inferiority study. Lancet Diabetes Endocrinol 2018;6:445–54.
7. Reid DM, Devogelaer JP, Saag K, Roux C, Lau CS, Reginster JY, et al. Zoledronic acid and risedronate in the prevention and treatment of glucocorticoid-induced osteoporosis (HORIZON): a multicentre, double-blind, double-dummy, randomised controlled trial. Lancet 2009;373:1253–63.
8. Buckley L, Guyatt G, Fink HA, Cannon M, Grossman J, Hansen KE, et al. 2017 American College of Rheumatology guideline for the prevention and treatment of glucocorticoid-induced osteoporosis. Arthritis Rheumatol 2017;69:1521–37.
9. Saag KG, Shane E, Boonen S, Marín F, Donley DW, Taylor KA, et al. Teriparatide or alendronate in glucocorticoid-induced osteoporosis. N Engl J Med 2007;357:2028–39.

ACR Announcements

AMERICAN COLLEGE OF RHEUMATOLOGY
2200 Lake Boulevard NE, Atlanta, Georgia 30319-5312
www.rheumatology.org

ACR Meetings

ACR/ARP Annual Meeting
November 8–13, 2019, Atlanta
November 6–11, 2020, Washington, DC
Winter Rheumatology Symposium
January 25–31, 2020, Snowmass
State-of-the-Art Clinical Symposium
March 27–29, 2020, New Orleans

Download the ACR Publications App

Search "ACR Publications" in the Apple Store or the Google Store to download the ACR Publications Mobile App. Members can log into the ACR Publications app for complete access to full text of all articles published in *Arthritis & Rheumatology* (*A&R*) and *Arthritis Care & Research* (*AC&R*). In addition, both members and nonmembers can access *A&R* and *AC&R* article abstracts, full text of articles published more than one year ago, select open-access articles published recently, as well as all issues of *ACR Open Rheumatology* (*ACROR*) and *The Rheumatologist*. Save your favorite articles for quick and easy access, including offline, share articles with colleagues or students, and utilize the full-screen figure and table viewer. The ACR Publications app offers an entirely new browsing and reading experience and the opportunity to better keep up-to-date with the most important developments in rheumatology research and practice.

Follow the ACR Journals on Twitter

On Twitter, follow @ACR_Journals, the official social media feed of *A&R*, *AC&R*, and *ACROR*, to engage with authors and other rheumatology professionals about current research, enjoy special features and updates about the field of rheumatology and related disciplines, and stay up-to-date with first looks at recently accepted content in *A&R*, *AC&R*, and *ACROR*.

Education Programs

6th Systemic Sclerosis World Congress. March 5–7, 2020, Prague, Czech Republic. The Systemic Sclerosis World Congress boasts an eclectic mix of interactive opportunities for attendees, including hands-on workshops; lectures, and discussions between physicians, medical staff, and patients; oral presentations; and satellite sessions. Lectures will be given in English but will be translated into major audience languages, and some topics will be covered in different languages in smaller groups. The broad scope of the Congress includes, among other topics, developments in scleroderma treatments, an update on major research projects, and how to treat pain in digital ulcers. Smaller groups will examine more specific topics, including juvenile scleroderma and the impact of scleroderma on sexual life. Registration fees are €700 (early; until December 2), €760 (December 3–February 17), and €830 (February 18–onsite) for physicians; €240 (early; until December 2), €300 (December 3–February 17), and €365 (February 18–onsite) for fellows, basic scientists, and health professionals, and €120 (early; until December 2), €180 (December 3–February 17), and €240 (February 18–onsite) for students. For additional information, e-mail worldsclerodermafoundation@gmail.com or visit the web site http://worldsclerofound.org/systemic-sclerosis-world-congress/.